1996TS921

THE SILURIAN-DEVONIAN SUCCESSION IN NORTHEASTERN GASPE BASIN: RESERVOIR POTENTIAL-HYDROCARBON CHARGE AND TECTONIC HISTORY - PHASE 1

96TS921

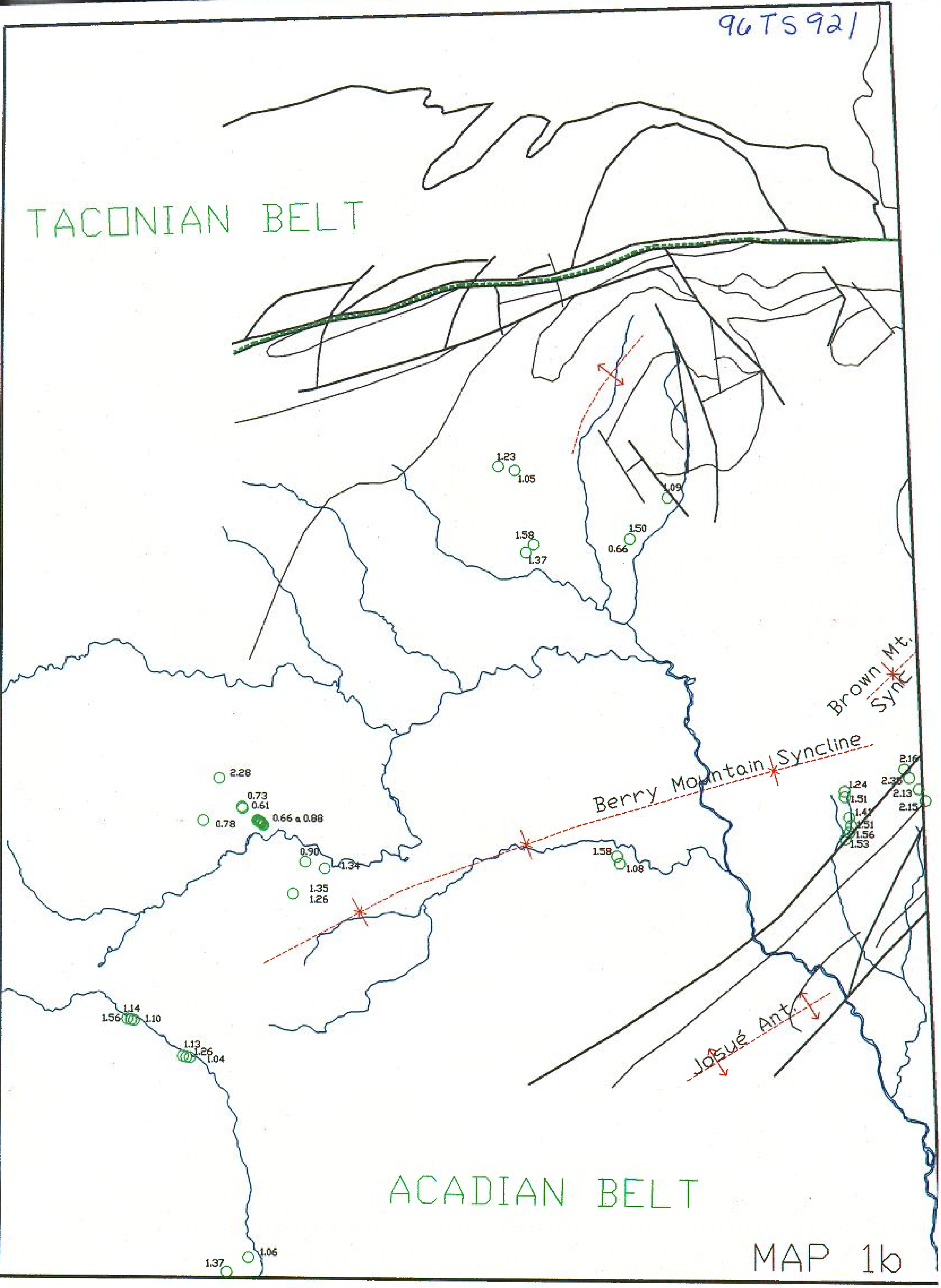

MAP 1b

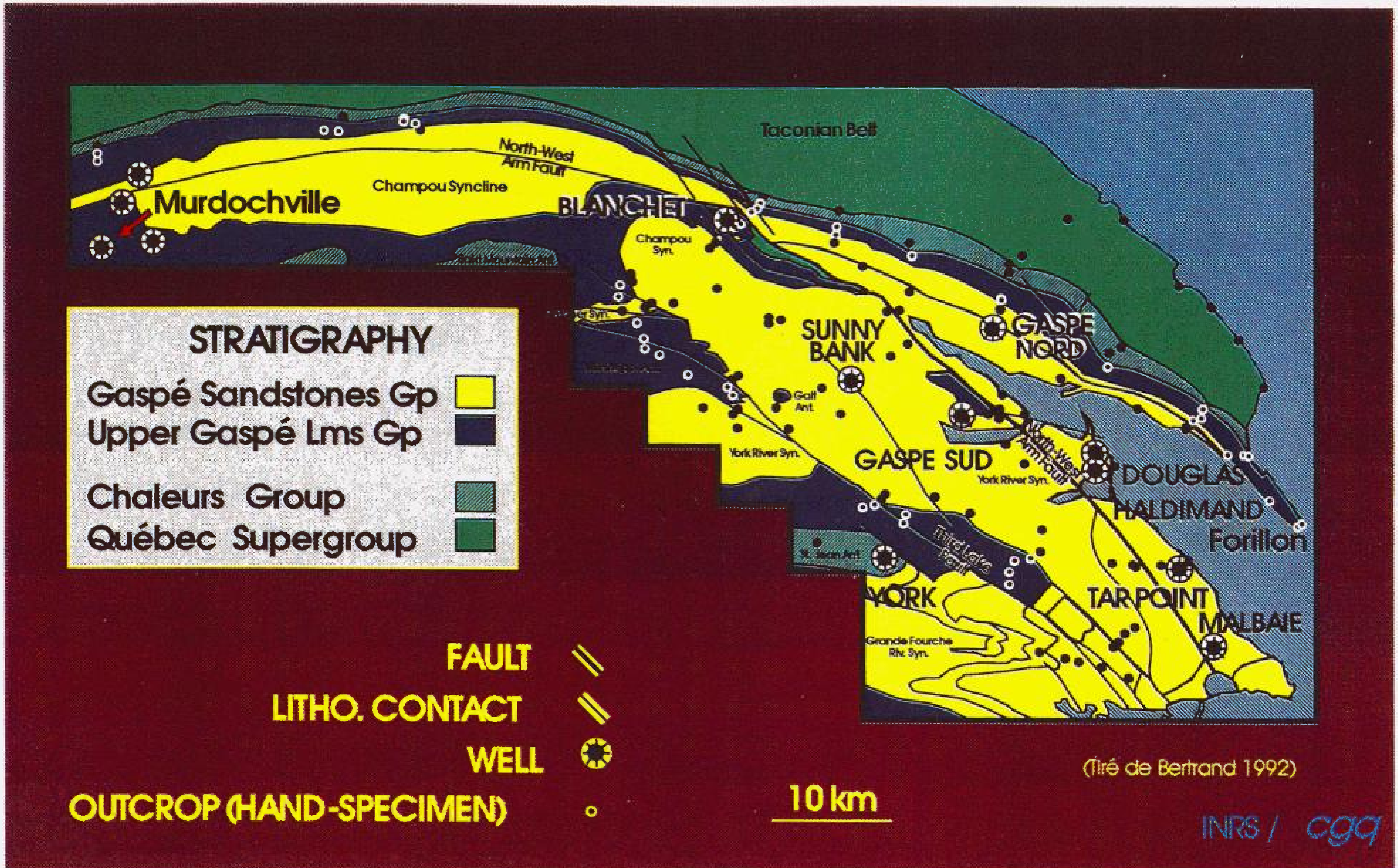
Taconian Belt
North-West Arm Fault
Champou Syncline
Murdochville
BLANCHET
Champou Syn.
SUNNY BANK
GASPE NORD
Galt Ant.
York River Syn.
GASPE SUD
York River Syn.
North-West Arm Fault
DOUGLAS
HALDIMAND
Forillon
Third Lake Fault
YORK
TAR POINT
MALBAIE
Grande Fourche Riv. Syn.
STRATIGRAPHY
Gaspé Sandstones Gp
Upper Gaspé Lms Gp
Chaleurs Group
Québec Supergroup
FAULT
LITHO. CONTACT
WELL
OUTCROP (HAND-SPECIMEN)
10 km
(Tiré de Bertrand 1992)
INRS / cgq

Figure 4.1

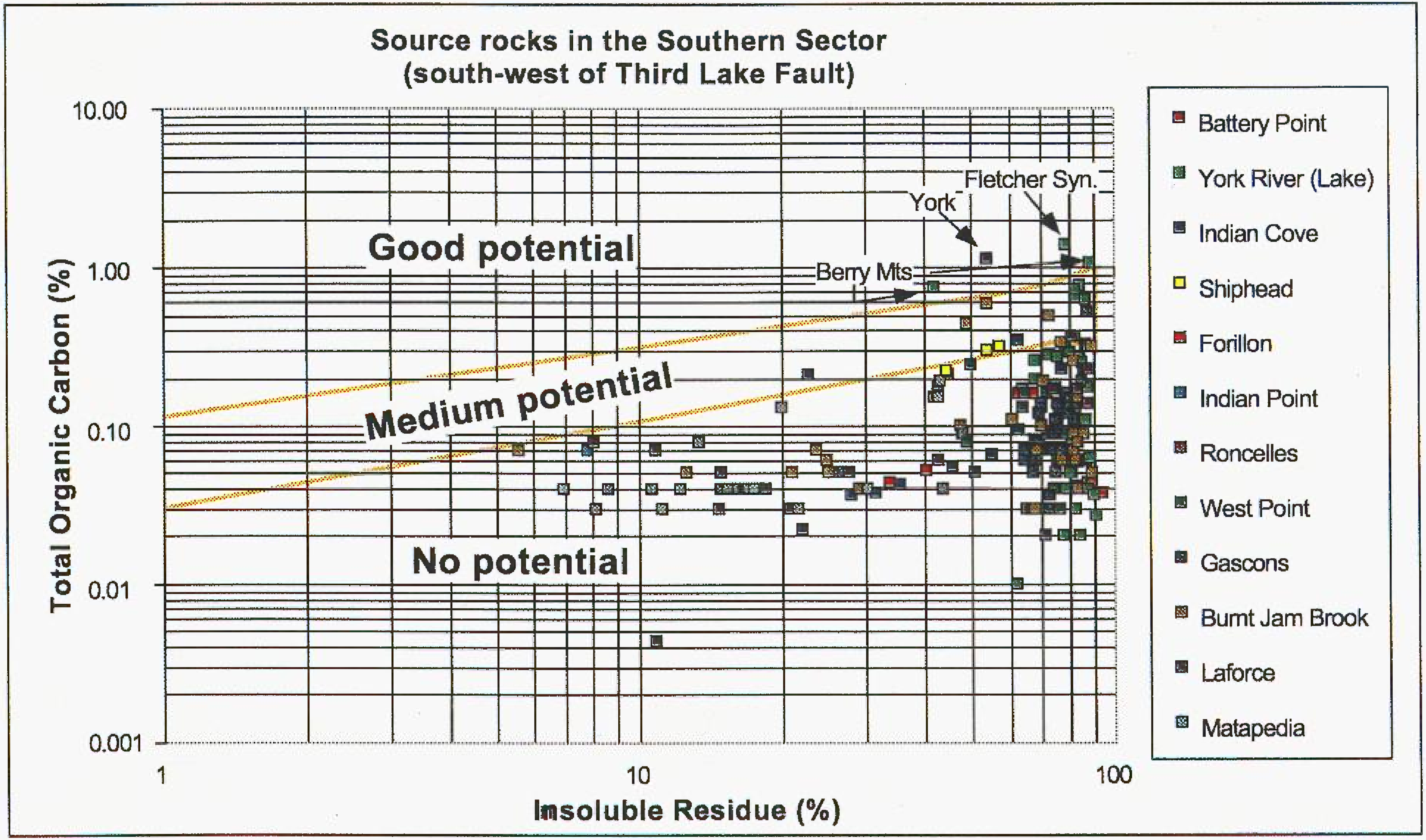
Source rocks in the Southern Sector
(south-west of Third Lake Fault)
Total Organic Carbon (%)
10.00
1.00
0.10
0.01
0.001
1
10
100
Insoluble Residue (%)
Good potential
Medium potential
No potential
York
Fletcher Syn.
Berry Mts
Battery Point
York River (Lake)
Indian Cove
Shiphead
Forillon
Indian Point
Roncelles
West Point
Gascons
Burnt Jam Brook
Laforce
Matapedia

Figure 4.2

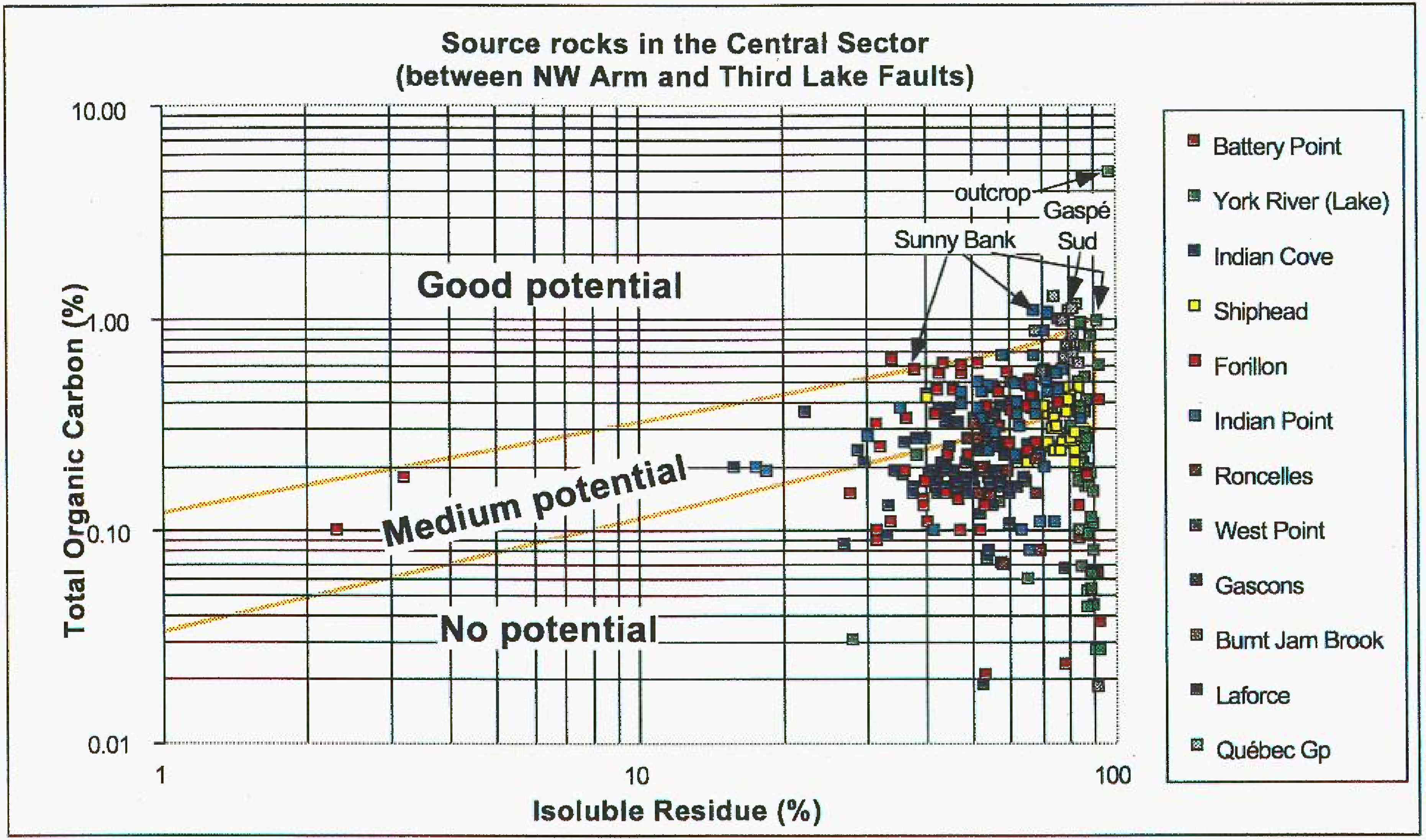
Source rocks in the Central Sector
(between NW Arm and Third Lake Faults)
10.00
1.00
0.10
0.01
Total Organic Carbon (%)
1
10
100
Isoluble Residue (%)
Good potential
Medium potential
No potential
outcrop
Gaspé
Sunny Bank
Sud
Battery Point
York River (Lake)
Indian Cove
Shiphead
Forillon
Indian Point
Roncelles
West Point
Gascons
Burnt Jam Brook
Laforce
Québec Gp

Figure 4.3

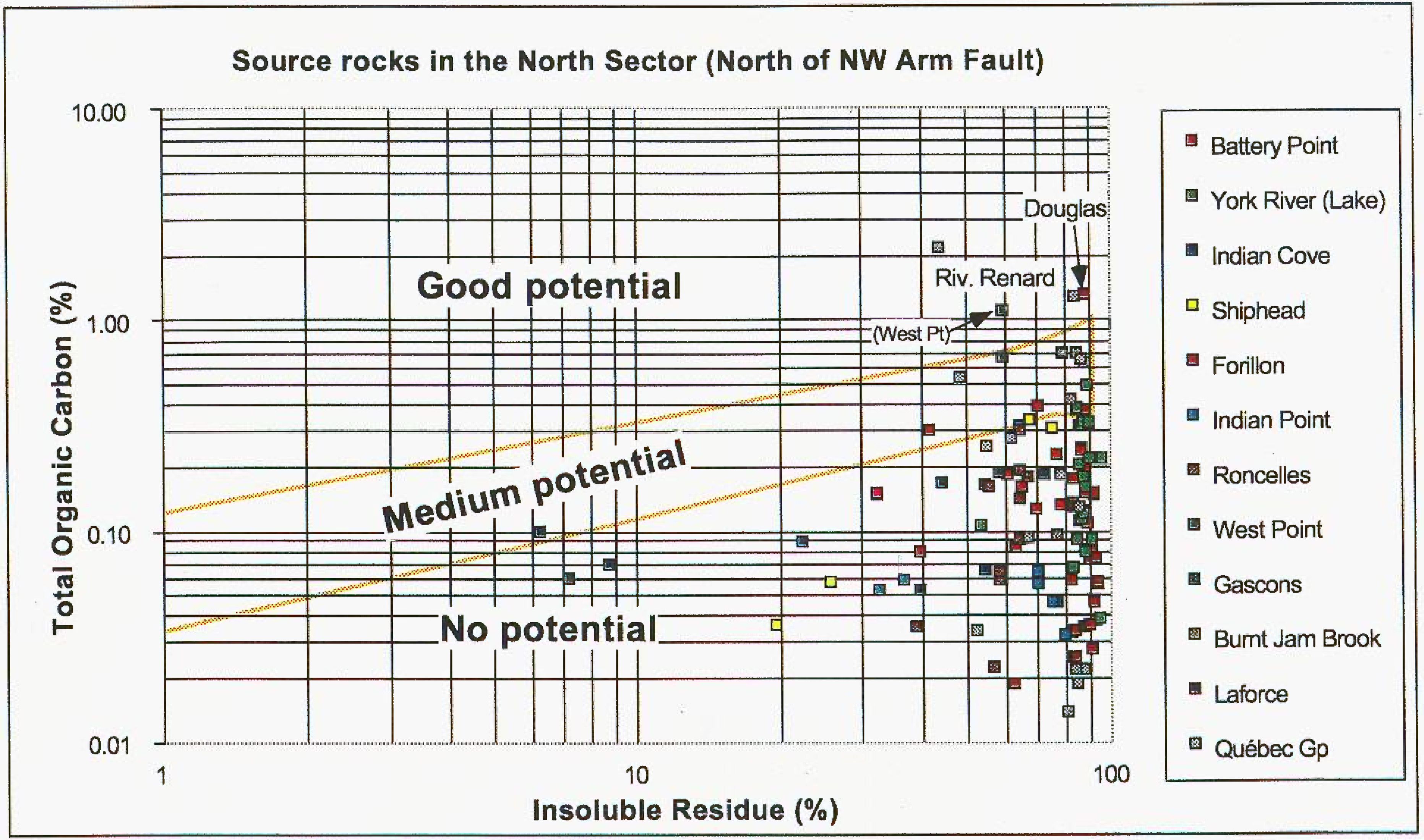
Source rocks in the North Sector (North of NW Arm Fault)
Total Organic Carbon (%)
10.00
1.00
0.10
0.01
1
10
100
Insoluble Residue (%)
Good potential
Medium potential
No potential
Douglas
Riv. Renard
(West Pt)
Battery Point
York River (Lake)
Indian Cove
Shiphead
Forillon
Indian Point
Roncelles
West Point
Gascons
Burnt Jam Brook
Laforce
Québec Gp

Figure 4.4

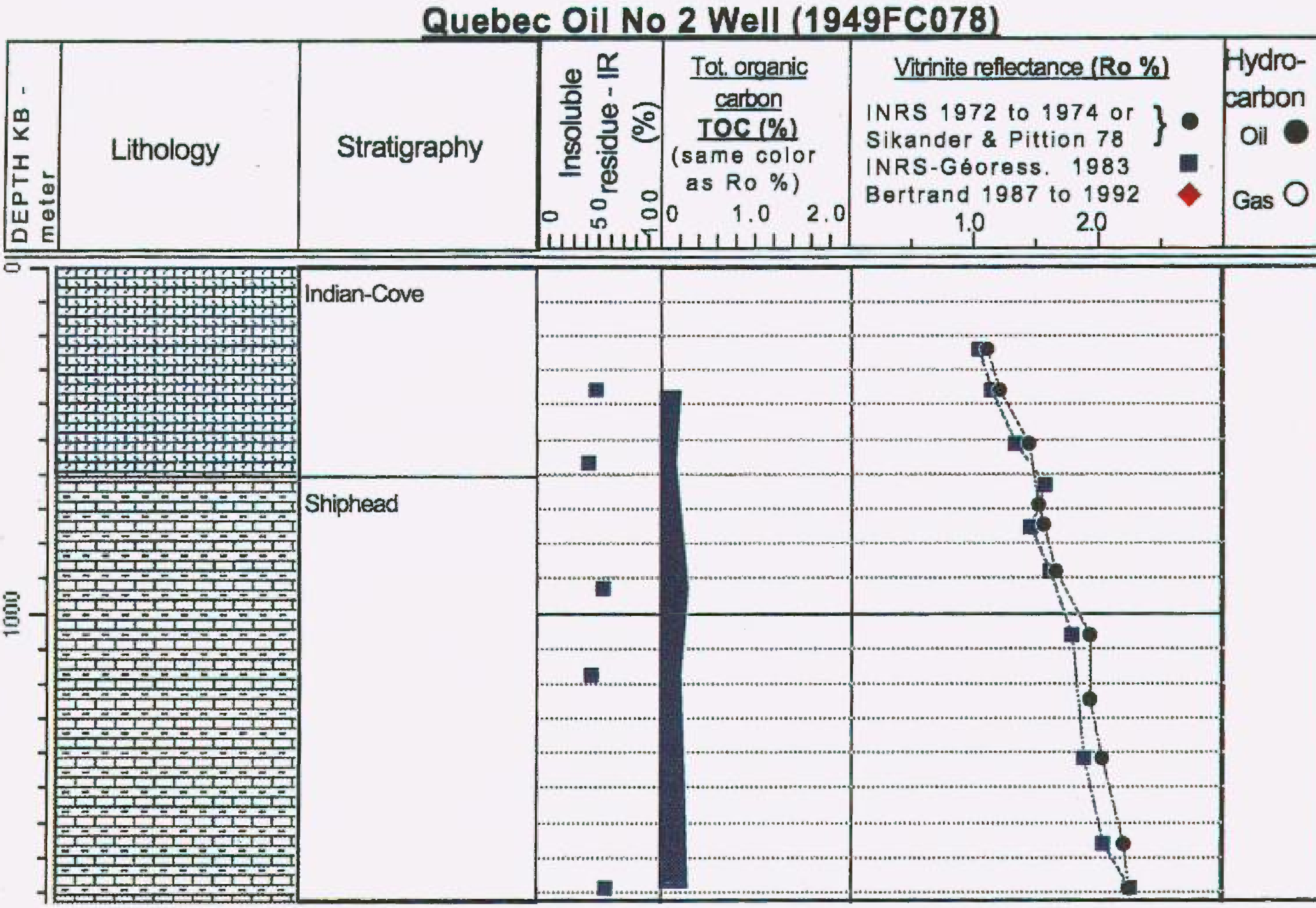

Figure 4.5A

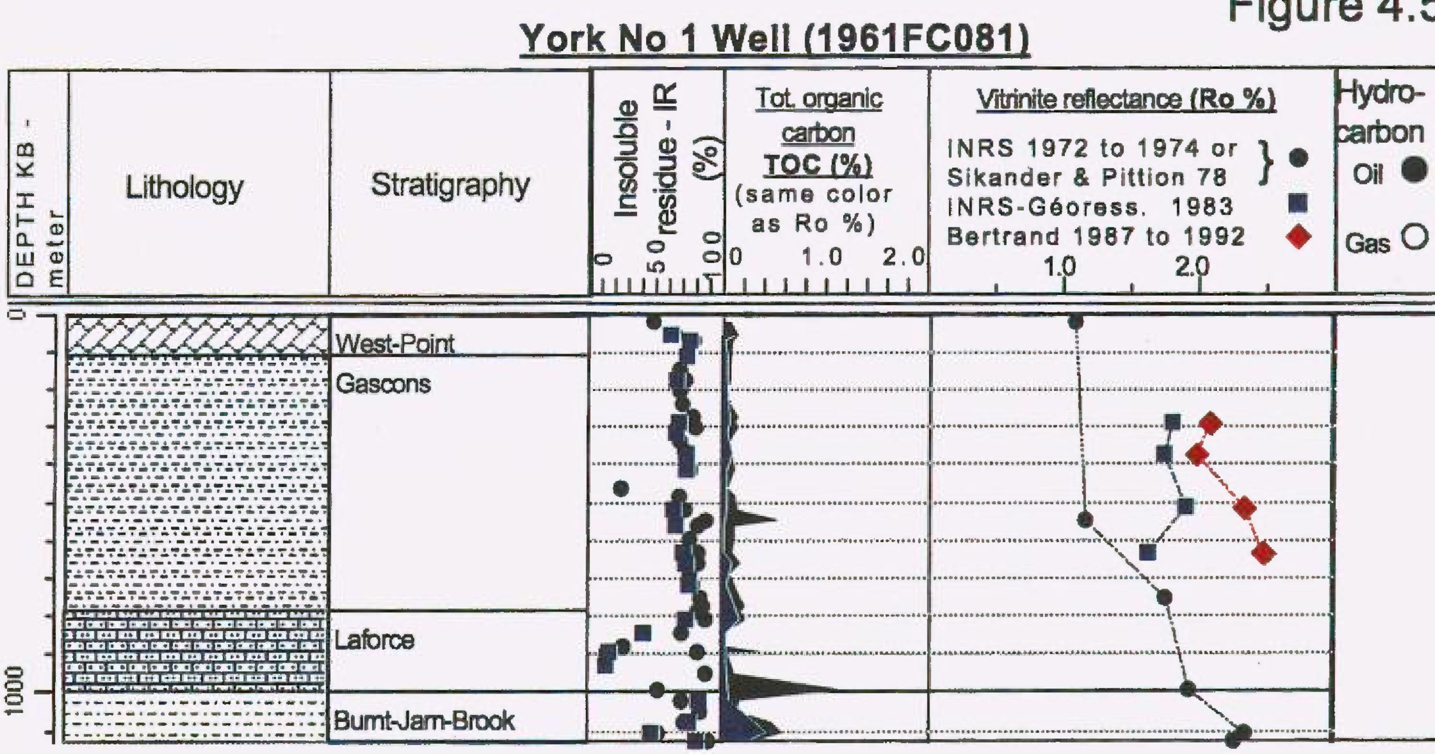

Figure 4.5B

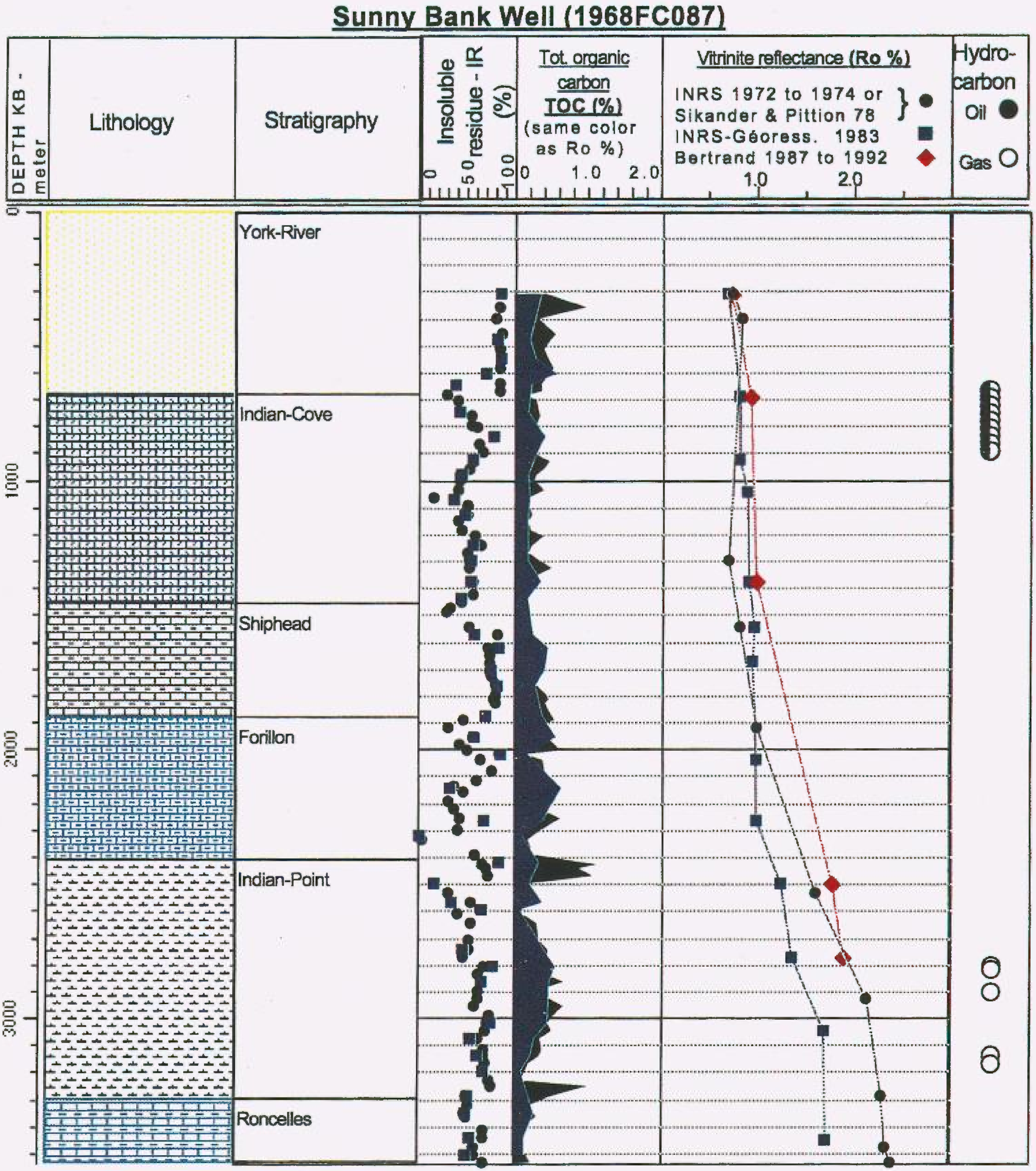

Sunny Bank Well (1968FC087)
DEPTH KB - meter
Lithology
Stratigraphy
Insoluble residue - IR (%)
0 50 100
Tot. organic carbon TOC (%) (same color as Ro %)
0 1.0 2.0
Vitrinite reflectance (Ro %)
INRS 1972 to 1974 or Sikander & Pittion 78
INRS-Géoress. 1983
Bertrand 1987 to 1992
1.0 2.0
Hydro-carbon
Oil
Gas
0
1000
2000
3000
York-River
Indian-Cove
Shiphead
Forillon
Indian-Point
Roncelles

Figure 4.6

Gaspé Sud Well (1979FC093)

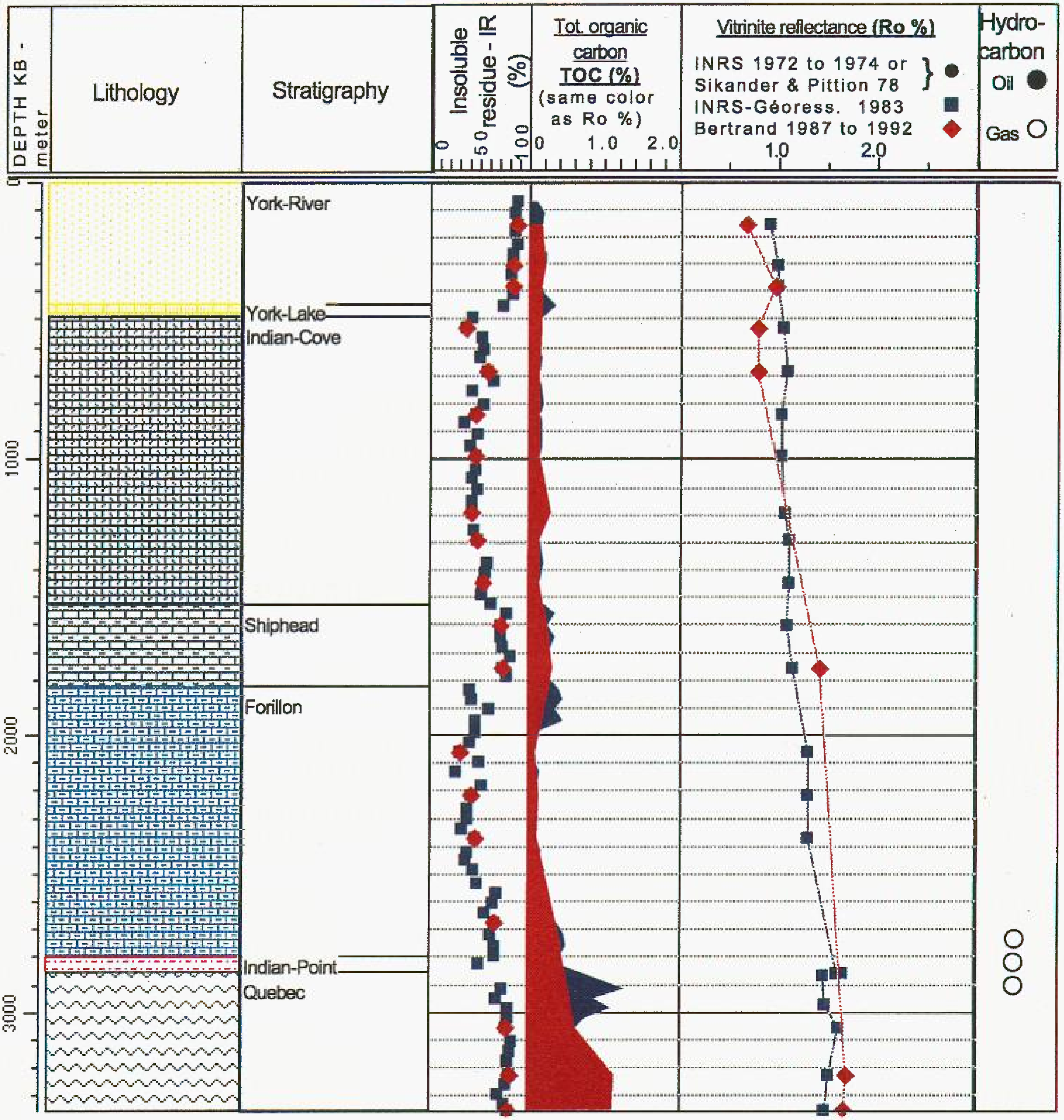

Figure 4.7

Gaspé Nord Well (1981FC099)

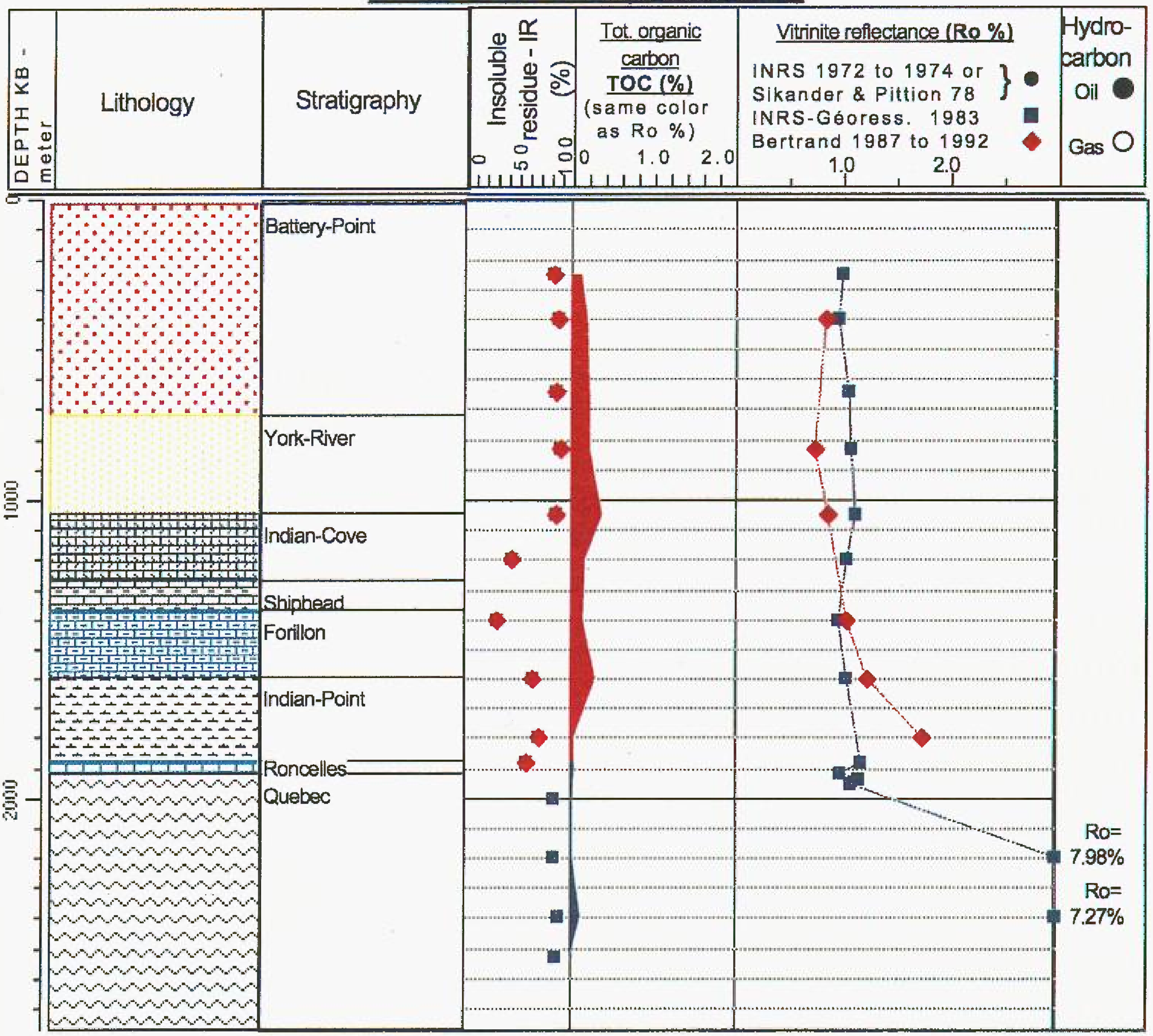

Figure 4.8B

Blanchet Well (1979FC096)

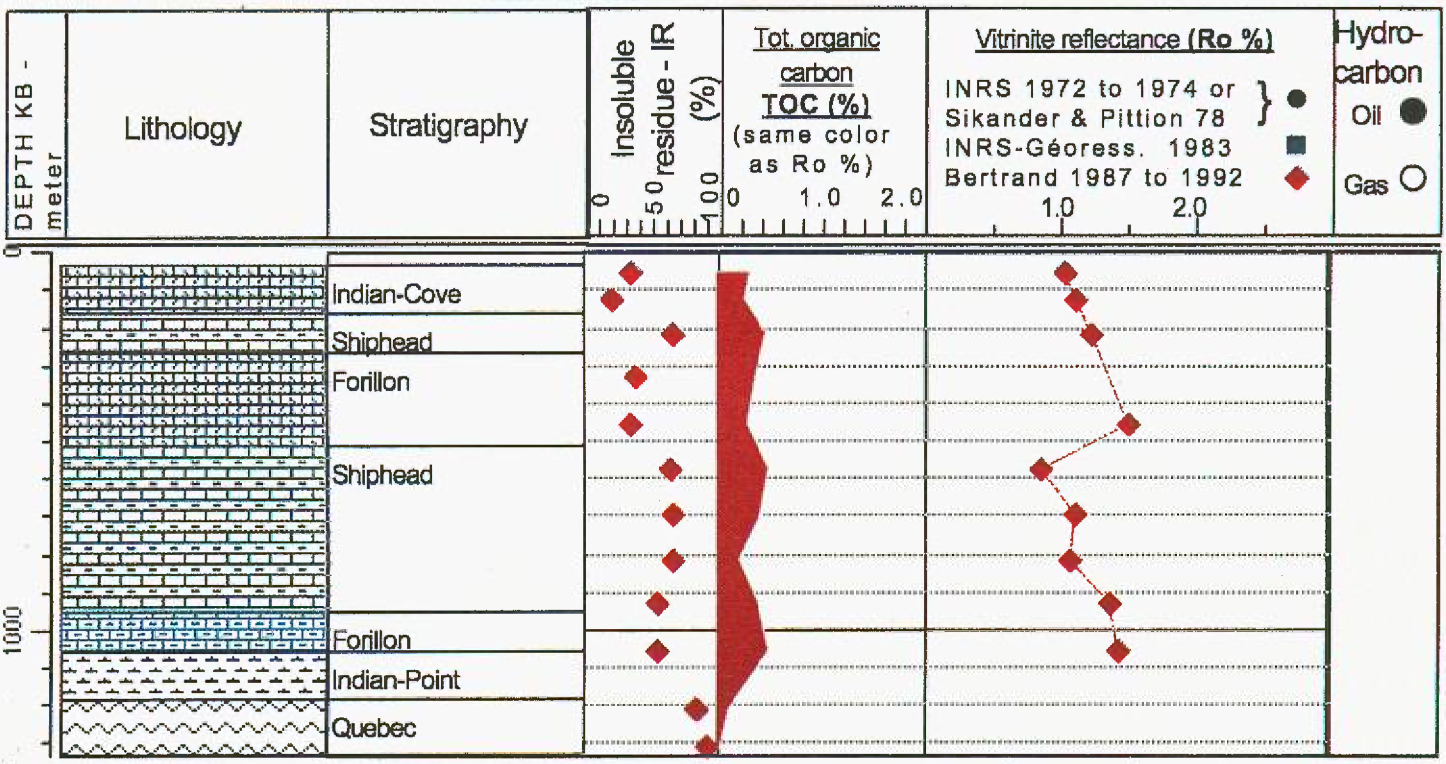

Figure 4.8A

Douglas Well (1979FC097)

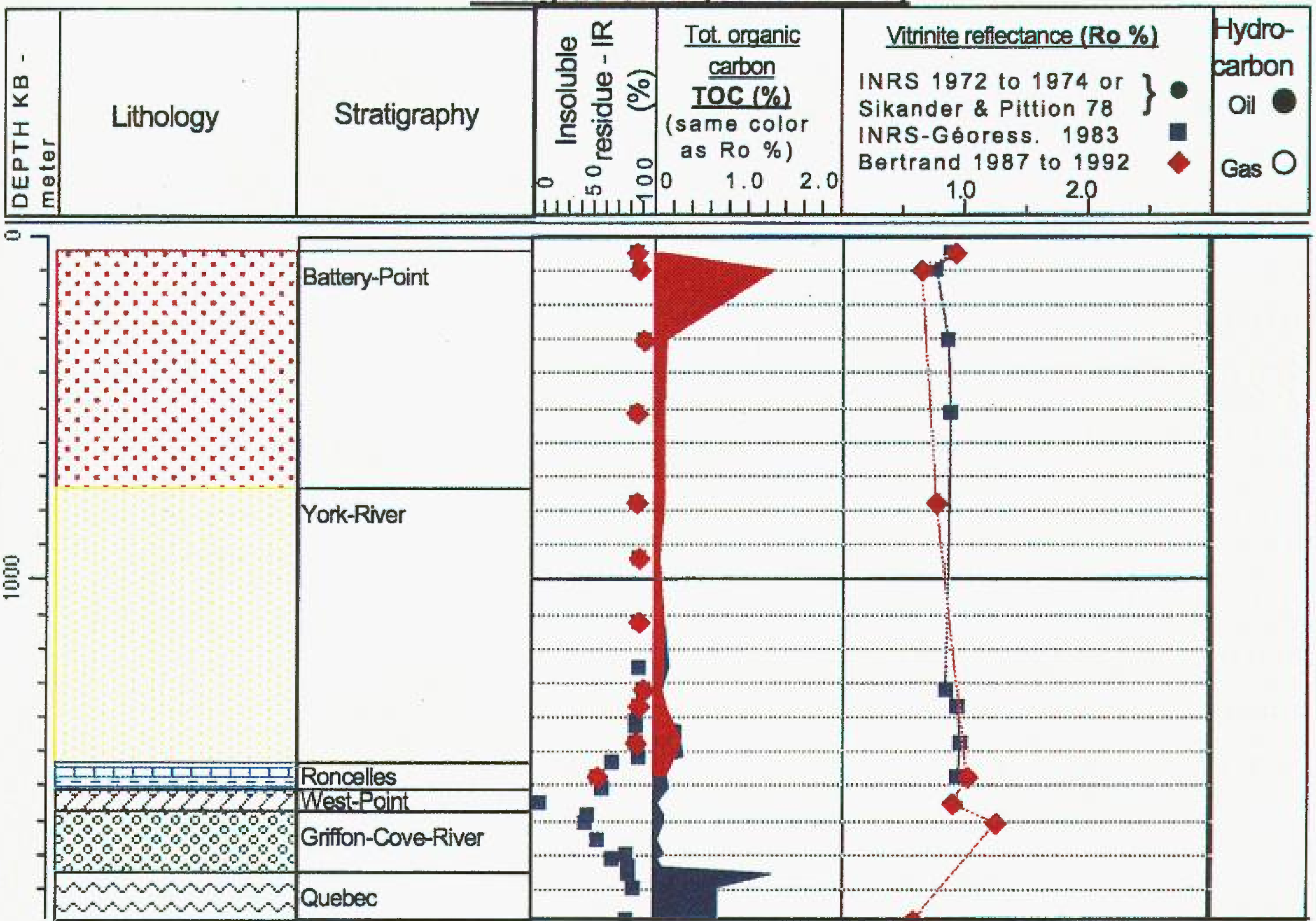

Figure 4.9B

Malbaie Well (1979FC094)

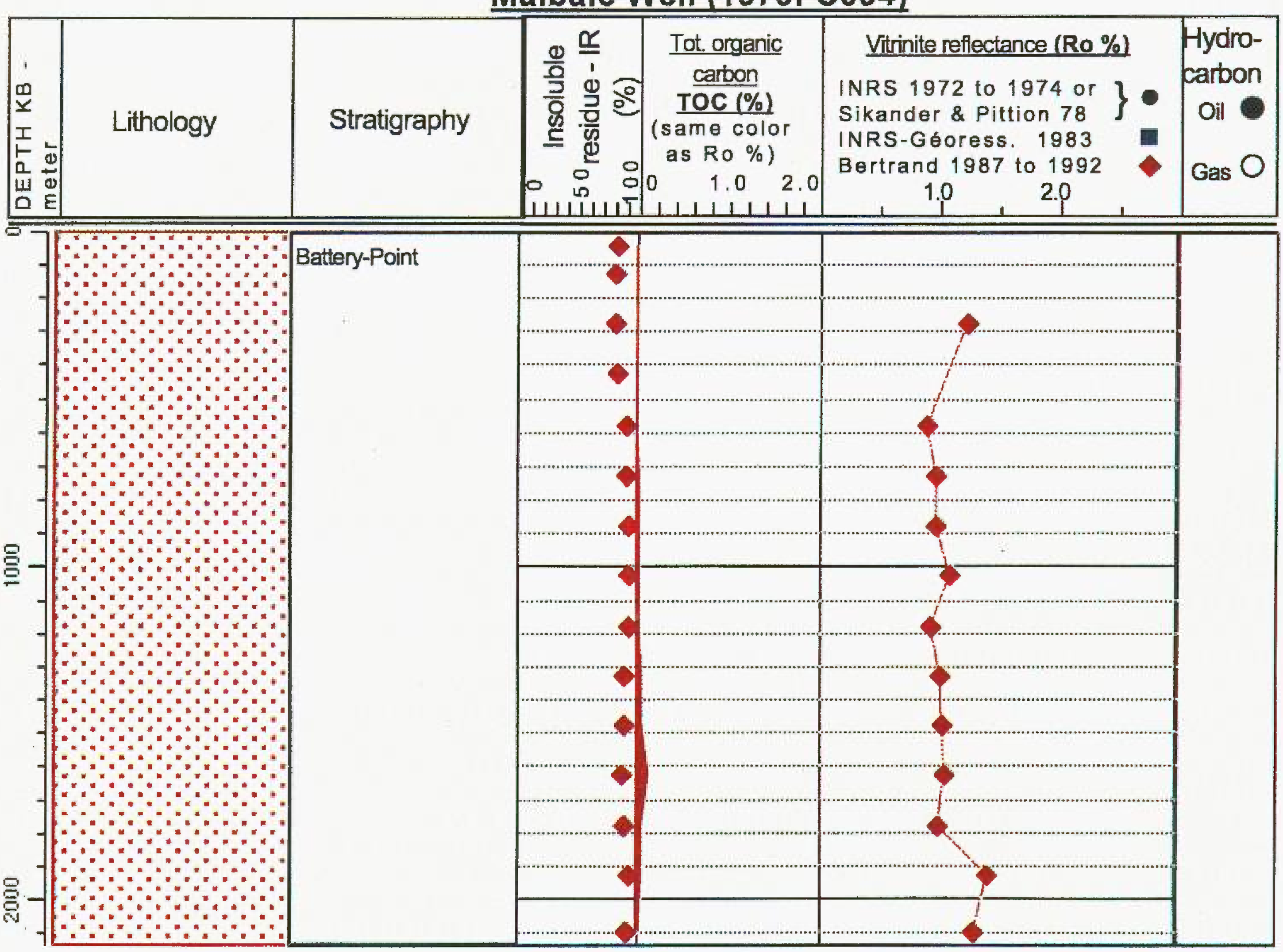

Figure 4.9A

Tar Point Well (1950FC079)

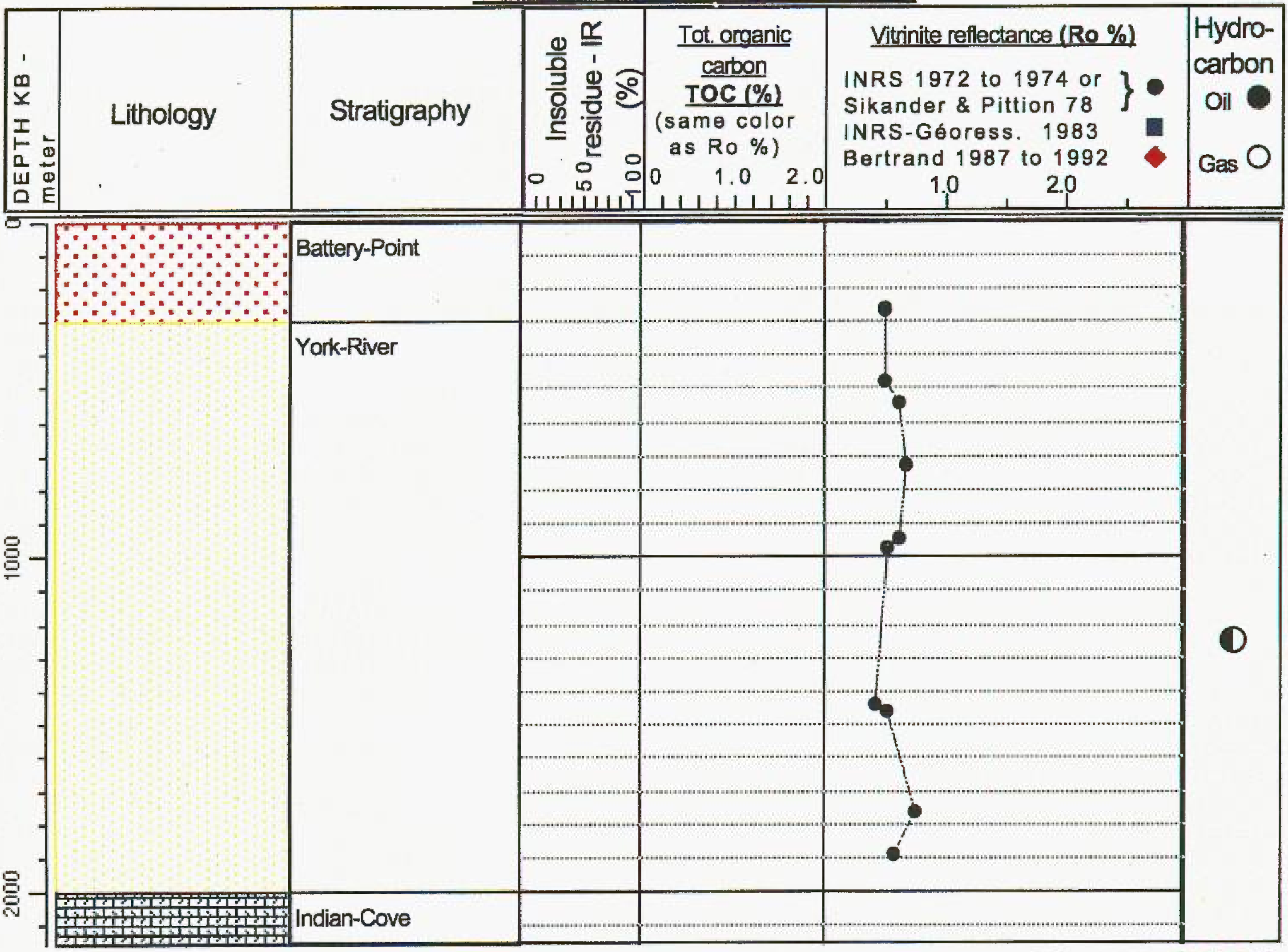

Figure 4.10B

Haldimand Well (1941FC016)

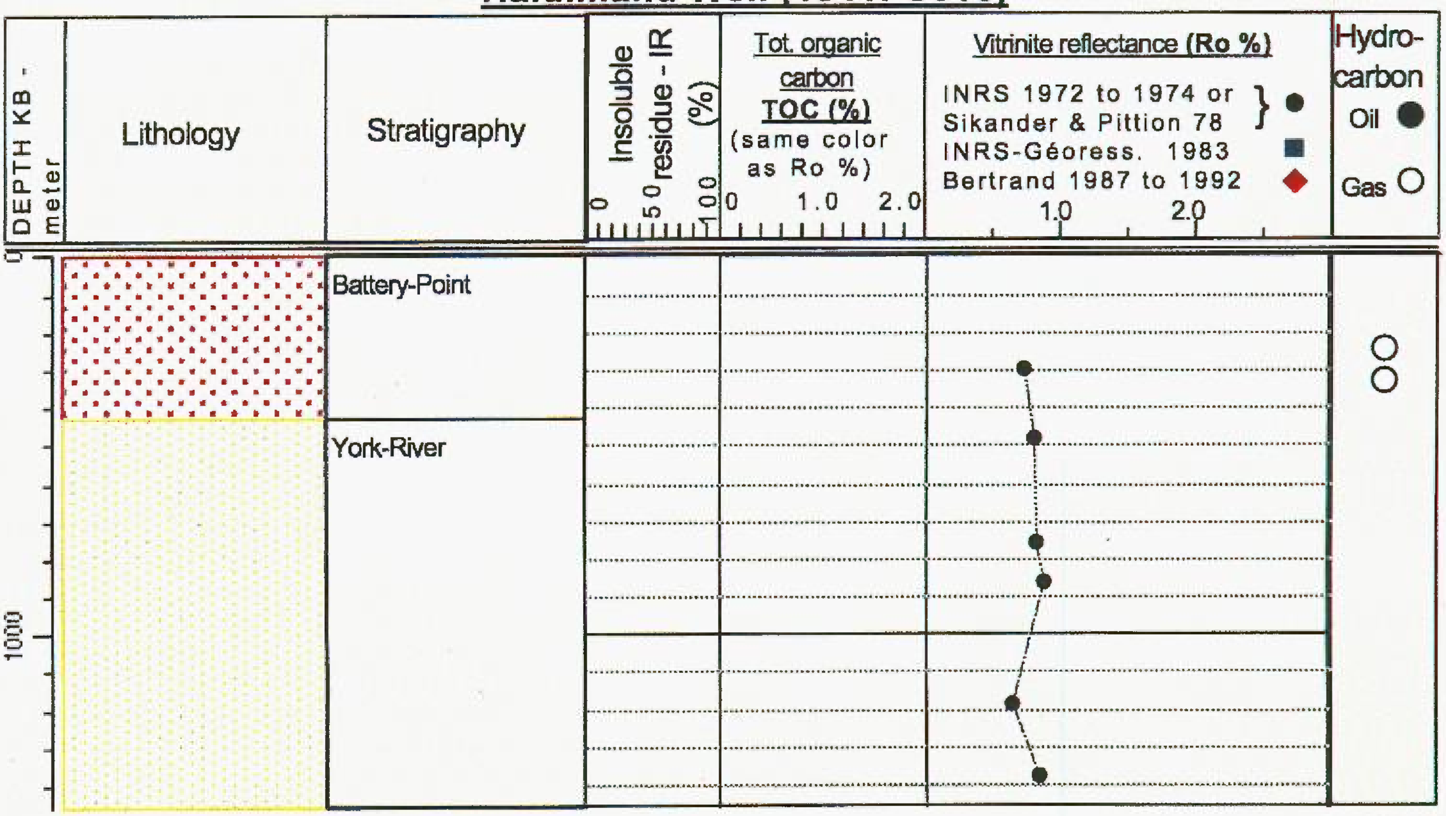

Figure 4.10A

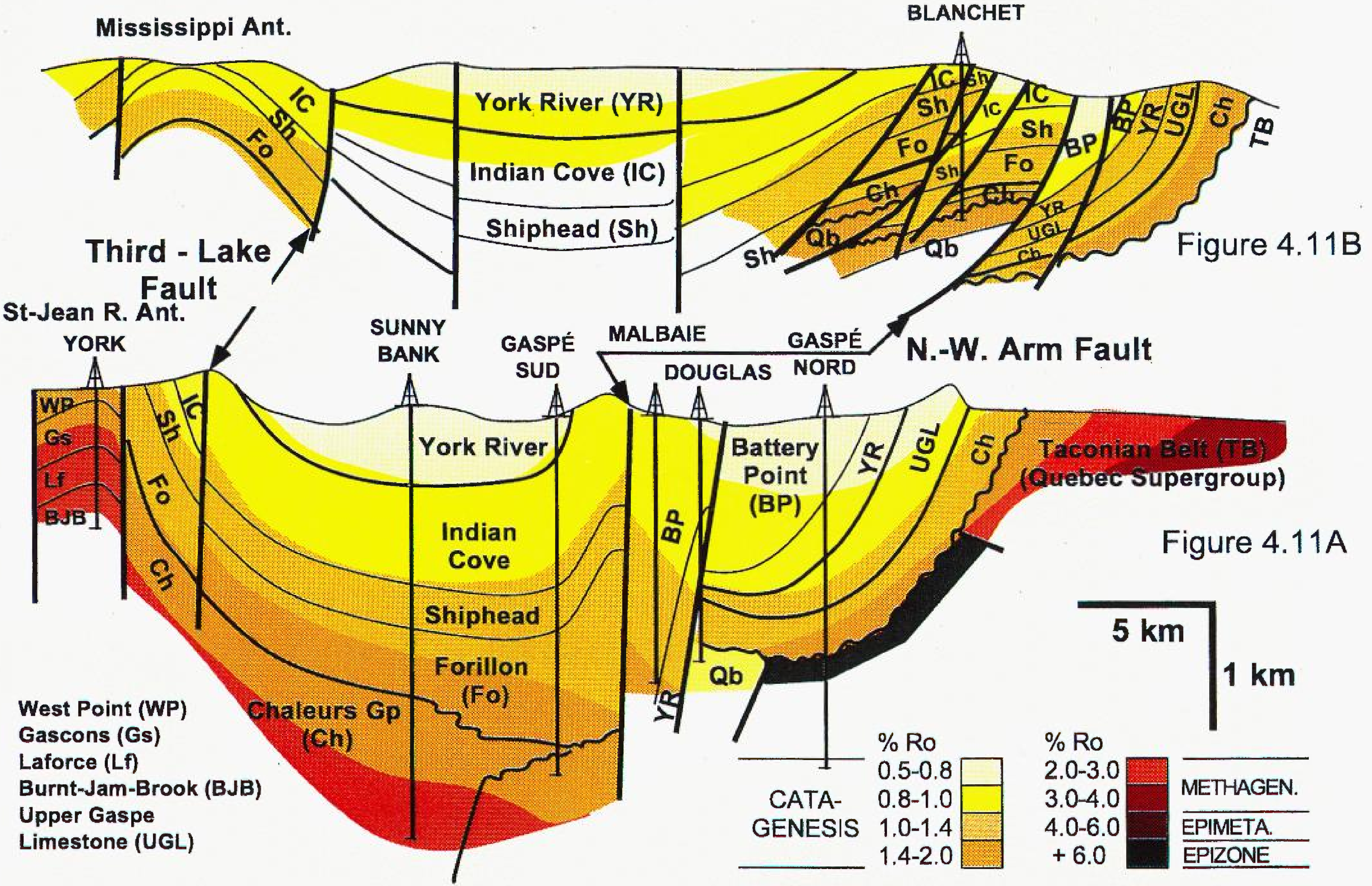

Mississippi Ant.
BLANCHET
York River (YR)
Indian Cove (IC)
Shiphead (Sh)
IC
Sh
Fo
Ch
Qb
BP
YR
UGL
TB
Third - Lake Fault
Figure 4.11B
St-Jean R. Ant.
YORK
SUNNY BANK
GASPÉ SUD
MALBAIE
DOUGLAS
GASPÉ NORD
N.-W. Arm Fault
WP
Gs
Lf
BJB
York River
Indian Cove
Shiphead
Forillon (Fo)
Chaleurs Gp (Ch)
Battery Point (BP)
Taconian Belt (TB) (Quebec Supergroup)
Figure 4.11A
5 km
1 km
West Point (WP)
Gascons (Gs)
Laforce (Lf)
Burnt-Jam-Brook (BJB)
Upper Gaspe Limestone (UGL)
% Ro
CATA-GENESIS
0.5-0.8
0.8-1.0
1.0-1.4
1.4-2.0
% Ro
2.0-3.0
3.0-4.0
4.0-6.0
+ 6.0
METHAGEN.
EPIMETA.
EPIZONE

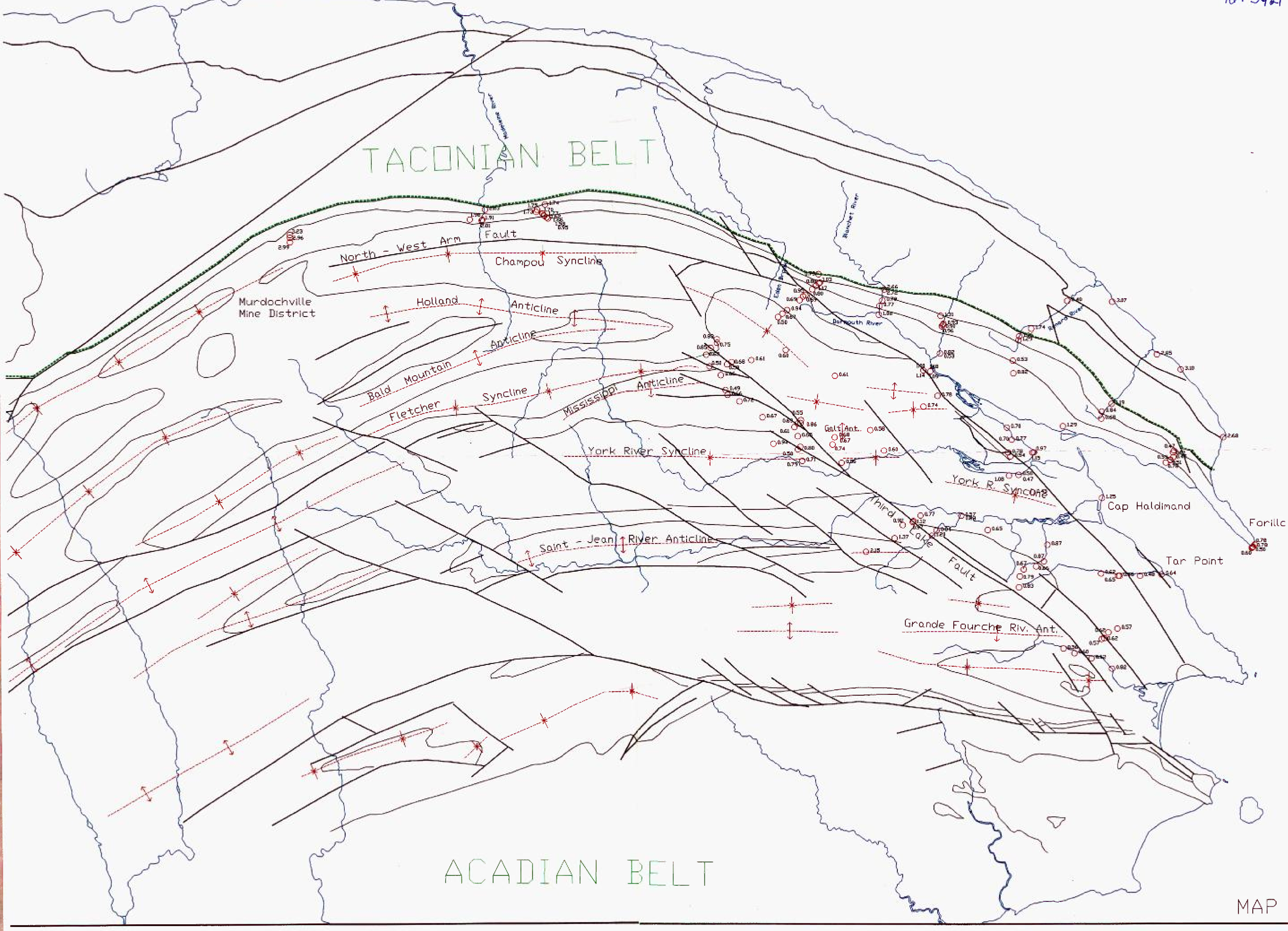

TACONIAN BELT
North - West Arm Fault
Champou Syncline
Murdochville
Mine District
Holland Anticline
Bald Mountain Anticline
Fletcher Syncline
Mississippi Anticline
York River Syncline
Galt Ant.
York R. Syncline
Cap Haldimand
Third Lake Fault
Saint - Jean River Anticline
Tar Point
Grande Fourche Riv. Ant.
ACADIAN BELT
MAP

96TS921

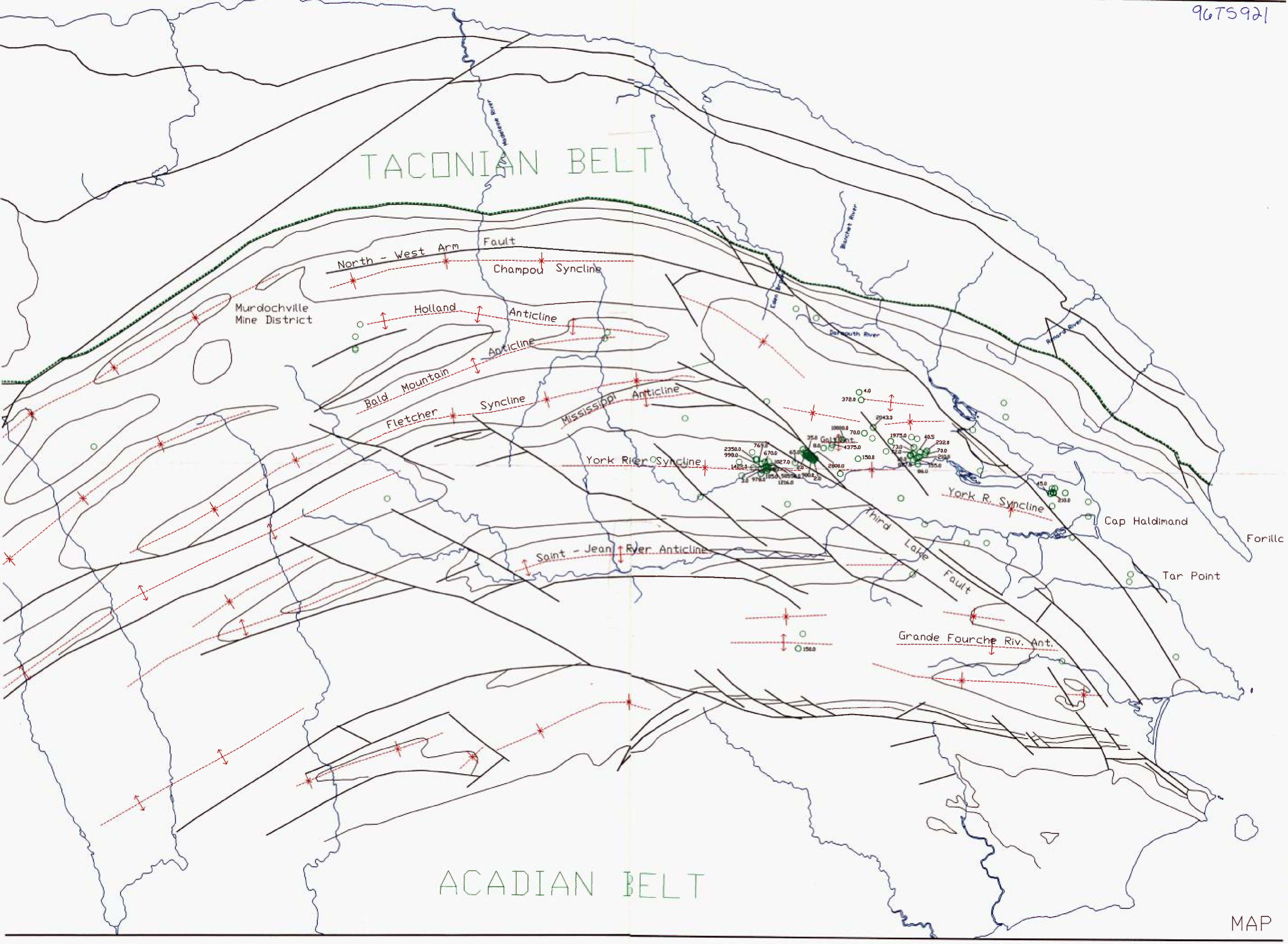
TACONIAN BELT
North - West Arm Fault
Champou Syncline
Murdochville
Mine District
Holland Anticline
Bald Mountain Anticline
Fletcher Syncline
Mississippi Anticline
York Rier Syncline
York R. Syncline
Third Lake Fault
Saint - Jean River Anticline
Grande Fourche Riv. Ant.
Cap Haldimand
Forillc
Tar Point
ACADIAN BELT
MAP

FICHE DESCRIPTIVE DE DOSSIER

UT x.x.x- Imprimer une fiche — P_IM_FIC.PRG

Numéro du dossier	:	**1996TS921**	Code gouvernemental:	0027 **(93-02-04-01)**
Nom du dossier	:	**RAPPORT DES TRAVAUX / 1995PG921**		
Informations supp.	:			
Grande-catégorie	:	PERM	Permis	
Catégorie	:	TS	Rapport statutaire	
Sous-catégorie	:	TF	Rapport de forage	
Intervenant	:			Actif (O/N) : O
Archivé ou Indexé[1]	:		Numéro de GM[2]:	
Date d'indexation[3]	:	/ /		Classeur : 0
Date pré-archivage[3]	:	/ /		Tiroir : 0
No pré-archivage	:	0		Boîte : 0

Groupe Exploration — 07/10/97

Légende:

1 A: Archivé; I: Indexé.
2 Le numéro de GM correspond au numéro tel que spécifié par le Secteur des mines.
3 Format de la date: AA/MM/JJ.

THE SILURIAN - DEVONIAN SUCCESSION IN NORTHEASTERN GASPÉ BASIN: RESERVOIR POTENTIAL-HYDROCARBON CHARGE AND TECTONIC HISTORY - PHASE 1

DENIS LAVOIE (GSC - Editor)

Rudolf Bertrand (INRS)
Pierre-André Bourque (Université Laval)
André Chagnon (INRS)
Guoxiang Chi (GSC)
Pauline Dansereau (Université Laval)
Michel Malo (INRS)
Michel Rocheleau (Université Laval)
Martine Savard (GSC)

TABLE OF CONTENTS

INTRODUCTION

This document reports the results of phase 1 of the research undertaken by GSC-Québec - INRS-Géoressources and Laval University addressing the reservoir potential, the hydrocarbon charge and the tectonic history of the eastern part of the Gaspé Peninsula. Following a precise working plan suggested by Shell Canada, review of available material and synthesis of our current state of knowledge was carried out. In particular, reservoir potential of Silurian - Devonian carbonates and Devonian sandstones, maturation and source rock potential of the entire succession and tectonic history of the area. Moreover, in the following document, the various chapters are all concluded by specific recommendations to Shell Canada in order to address the hydrocarbon potential of eastern Gaspé.

ORGANIZATION OF THE REPORT

This document consists of five chapters each addressing one of Shell Canada interests in the eastern Gaspé. Each chapter consists of a descriptive or synthesis text with various photographic, table or graph supports.

Chapter 1 by Bourque and Malo presents a detailed overview of the stratigraphic setting of the Silurian-Devonian succession in eastern Gaspé with much emphasis on the significance of the Salinian Disturbance and the locally resulting Salinian Unconformity for reef settlement, secondary porosity generation and fluid circulation in the Gaspé Basin.

Chapter 2 by Bourque, Lavoie, Savard, Malo, Dansereau and Chi comprises four sections each summarizing our research effort on available material within Laval, GSC and INRS collections for various carbonate units in eastern Gaspé. They are presented in "stratigraphic order", that is: 1) the latest Ordovician - earliest Silurian White Head Formation, 2) the Early Silurian Sayabec - Laforce formations, 3) the latest Silurian - earliest Devonian West Point Formation and 4) the Early Devonian Upper Gaspé Limestones. All these reports focus on primary and secondary porosity evolution, and the direct or indirect effects of the Salinian Disturbance on the reservoir potential of these various carbonate units.

Chapter 3 by Chagnon and Rocheleau summarizes our current state of knowledge on facies distribution, paleocurrent information and source areas for the Early - Middle Devonian Gaspé Sandstones in eastern and central Gaspé Peninsula. All the information available on porosity and permeability for these locally porous sandstones are presented and discussed.

Chapter 4 by Bertrand offers a detailed synthesis of all the available information on maturation studies, potential for source rocks and nature of seeping oils in eastern Gaspé.

Denis Lavoie (GSC)

Chapter 5 by Malo summarizes the current state of knowledge on the tectonic evolution of the Quebec Appalachians with an emphasis on the Gaspé Peninsula. The palinspastic reconstruction of the Gaspé Basin is presented and, possibly, interested readers should start first by reading this section because it bears important information for the comprehension of some fine details presented in the first chapters.

SIGNIFICANT POINTS

Each chapter clearly presents its own pertinent conclusions for the definition of a hydrocarbon play in eastern Gaspé. From this document reporting on research on available (and sometimes poorly suited) material or presenting synthesis, the following important conclusions could be viewed as critical elements upon which the proposition for phase 2 of the project was built and presented to Shell Canada.

A) The Salinian Disturbance and resulting Unconformity (Chapter 1) seemed to have played a critical role in the evolution of the Gaspé Basin, not only for reef development and depositional facies control (Chapter 2.3) but also for the possible generation of secondary porosity of either dissolution (Chapter 2.1 and 2.2) or fracture origin (Chapter 2.1 and 2.2) in both the White Head and Sayabec/Laforce formations. The fact that Devonian West Point pinnacles in northern Gaspé were built on highs left over by the Salinian Unconformity might also suggest that the Silurian West Point reefs (if present) could have been subjected to early meteoric diagenesis (Chapter 1 and 2.3). It is significant that a large number of hydrocarbon-charged fluid inclusions have been recognized in almost all carbonate units, either in fracture- or pore-filling calcites.

B) A younger sub-aerial event (possibly Pragian) is recognized within the cement succession present in the Devonian West Point pinnacles in northern Gaspé (Chapter 2.3). This sub-aerial event occurred possibly after the pinnacles were buried under 2 km of strata. A Pragian tectonic event has not formally been recognized in the Gaspé Basin, although, it is also suggested independently by the presence of reworked Upper Ordovician chitinozoans in the well-constrained Pragian-aged succession of the Upper Gaspé Limestones (Achab et al., in press, 1996; Chapter 2.4).

C) Hydrocarbon storage and some production (well or seeps) is known from the Upper Gaspé Limestones (Chapter 2.4) and Gaspé Sandstones (Chapter 3). The Upper Gaspé Limestones are typified by either secondary fracture-porosity or intraparticular primary pore space locally enhanced by dissolution. No evidence for meteoric effects has been observed so far; the various dissolution events are seemingly of burial origin. The nature of porosity within the Gaspé Sandstones has not been dealt with because the study was concerned with facies distribution. Available facies information on the Gaspé Sandstones is rather lean, the general sedimentology and paleoenvironmental setting are relatively well known, in particular for eastern Gaspé, although fine details are lacking and distribution of favourable reservoir facies is unknown.

D) Maturation studies indicate that the area where hydrocarbon seeps and minor production is concentrated (in east-central Gaspé, between the Bassin Nord-Ouest and Troisième Lac faults) is characterized by the low maturation (oil window) and a significant higher proportion of potential source rocks. Silurian - Devonian rocks in areas to the north and south are locally in the oil window but are more favourable for gas preservation; however, few possible local source rocks are known. However, these results are from autochthonous organic matter and do not rule out the possibility of late hydrocarbon charge of open pore space (as suggested also by the presence of low maturity migrated bitumen in the overmature Cambrian - Ordovician rocks in the Taconian Nappes Domain). Seeping oil and oil collected in ancient producing wells are typified by various API and color. No precise or definitive origin(s?) can yet be proposed.

E) The palinspastic reconstruction of the Gaspé Depositional Basin allows to better understand the facies distribution for Silurian - Devonian rocks. The proposed tectonic scenario with its along strike variations related to the inherited morphology of the Quebec Reentrant and St. Lawrence Promontory should be of great help in trying to understand old and possibly new seismic profiles crossing the area.

RECOMMENDATIONS

Recommendations for future works pertinent to various aspects covered by this initial study are presented at the end of each chapter/sections. There is no need to repeat these here, although it is significant to remember that the material studied (e.g. Chapter 2) was, at that time, not collected for a detailed diagenetic study. Results of phase 1 of the study helped to constrain areas and facies that should be looked in more details for the purpose of proposing a hydrocarbon play in eastern Gaspé.

The presence of possible siliciclastic reservoirs in the Silurian - Devonian succession of eastern Gaspé would gain from the study of the extensive quartzite sheet of the Val-Brillant Sandstone.

Maturation studies of new material and fingerprinting of oil for possible source rocks should provide key information about the thermal history of the area as well as on the recognition of more favourable areas for oil/gas storage.

Finally, a clear understanding of the physical expression (e.g. fractures) of the Salinian Disturbance and its distinction from the Taconian and Acadian fracture sets is critical in order to recognize areas that were possibly under (or near) sub-aerial conditions with fresh water recharge and associated karst development. All of this could led, depending on the age of the unit, in the formation of an early or late karstic porous system ready to be filled by hydrocarbon.

Details on individuals proposals for phase 2 of the research are presented in the various chapters of this report.

CHAPTER 1

THE SALINIAN DISTURBANCE AND UNCONFORMITY, AND THE OIL PLAY IN NORTHEASTERN GASPÉ

1 THE SALINIAN DISTURBANCE AND UNCONFORMITY, AND THE OIL PLAY IN NORTHEASTERN GASPÉ

1.1 INTRODUCTION

The Salinian Disturbance is a tectonic event that occurred in the Appalachian Orogen during late Silurian time, heralding the mid-Devonian Acadian Orogeny. In the Gaspé Basin, the disturbance is responsible for extensional faulting that strongly influenced facies development and distribution, particularly the reef bodies. Its understanding is therefore an essential key to develop strategies for oil exploration in northeastern Gaspé.

This part of the report focuses on this tectonic event and its influence on the sedimentary and diagenetic history of the Silurian and lowermost Devonian facies, and discusses the oil play in northeastern Gaspé with respect to the Salinian Disturbance. It provides a synthesis of the current status of our understanding of the disturbance and its effects. It is divided as follows:

- geological setting
- stratigraphy and facies
- structural features related to the Salinian Disturbance
- depositional history of northeastern Gaspé
- paleogeography of the Gaspé-Témiscouata Basin
- controls on reef settlement and development
- oil play in NE Gaspé with respect to Salinian Disturbance
- recommendations: rationale to proceed to field work, and detailed petrographic and geochemical work.

1.2 GEOLOGICAL SETTING

The Appalachian mountain belt has been shaped by two major orogenies: the Taconian which recorded the closure of the Iapetus Ocean and the arc collision with Laurentia margin in Late Ordovician, and the Acadian which culminated with the continental collision between the western margin of Gondwana and the Laurentia margin including the newly Taconian accreted terrane in Middle Devonian (see Chapter 5 of this report). Following the Taconian orogeny, a successor basin was born south of the allochthon belt that forms the Appalachian structural front at the Québec Reentrant and St. Laurence Promontory.

Sedimentary and volcanic facies deposited in this successor basin form the Gaspé Belt (Bourque et al., 1995) which preserves the most complete stratigraphic sequence of Upper Ordovician to Middle Devonian rocks that were deposited during a period of so-called quiescence which separates the Taconian and Acadian Orogenies. However, more and more data are being gathered which document deformation, magmatism, and/or metamorphism during the Silurian time, in Maine, New Brunswick, Nova Scotia and Newfoundland (Van Staal and De Roo, 1996;

Hibbard, 1994; Dunning et al., 1990), as well as in the Québec Appalachians (Malo and Bourque, 1993; Bourque et al., 1995; Bourque, Malo and Kirkwood, submitted, 1996), that invalidate the classical idea of a tectono-stratigraphic evolution separated into two distinct orogenic phases. In the Gaspé Peninsula, the Silurian tectonic activities are recorded as extensional faulting, minor folding, and a resulting unconformity dated as Late Silurian. Intraplate volcanism also occurred within the Gaspé Belt during the Late Silurian-Early Devonian time interval.

The Gaspé Belt in Gaspé Peninsula is divided into three major structural zones: the Connecticut Valley-Gaspé synclinorium, the Aroostook-Percé anticlinorium and the Chaleurs Bay synclinorium (Fig. 1.1). The Shell acreage in northeastern Gaspé Peninsula is part of the Connecticut Valley-Gaspé synclinorium. Structural style of the synclinorium (Fig. 1.2) is traditionally attributed to the Acadian deformation, although recent work demonstrates that part is inherited from the Salinian Disturbance (Malo and Bourque, 1993; Bourque et al., 1995; Bourque, Malo and Kirkwood, submitted 1996).

1.3 STRATIGRAPHY AND FACIES

Detailed stratigraphic nomenclature and correlations for northeastern Gaspé are given on chart of Figure 1.3. This part of the report is mostly concerned with three lithostratigraphic groups, the Honorat, Matapédia and Chaleurs groups, since they are the main units that were affected by the Salinian Disturbance.

1.3.1 HONORAT AND MATAPÉDIA GROUPS

The Honorat occurs only in the southeasternmost part of the Shell acreage (Fig. 3, column 8; see Chapter 5 of this report for relationships of the Honorat with the underlying Dunnage Zone).

The Honorat Group and the two formations that make up the Matapédia Group, the Pabos and White Head formations, are three conformably superposed units (Malo, 1979, 1986; Vennat, 1979; Skidmore and Lespérance, 1981; Lespérance et al., 1987). The Honorat is a terrigenous unit of claystone, mudstone, siltstone, quartz and lithic wackes, conglomerate, and silty limestone. The sandstones commonly exhibit turbidite-related structures.

The overlying Matapédia Group is carbonate dominated. The lower Pabos Formation consists of calcareous mudstone at the base, overlain by a sequence of calcareous mudstone, argillaceous limestone, calcareous siltstone, silty limestone, calcareous sandstone, calcareous conglomerate, and sandy calcarenite and calcilutite. The upper White Head Formation is a regularly thin-bedded calcilutite unit, with mudshale partings and a few thin beds and lenses of calcarenite, dark green calcareous mudstones, and thinly bedded silty and argillaceous limestone.

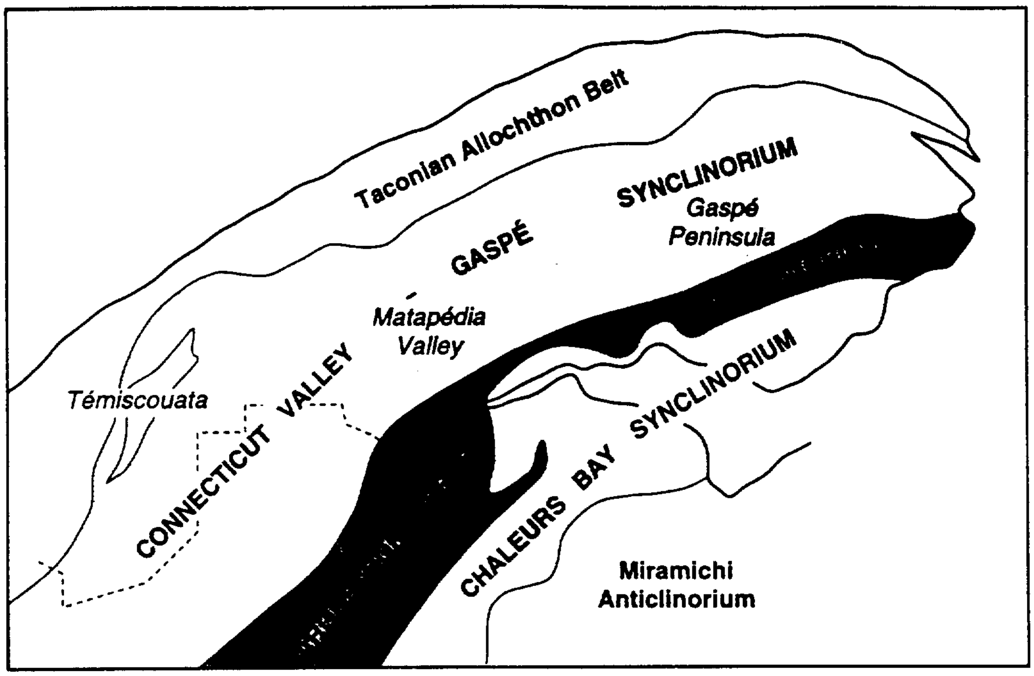

Figure 1.1 - The three main Acadian structural units of the Gaspé-Témiscouata segment of the Québec Appalachians.

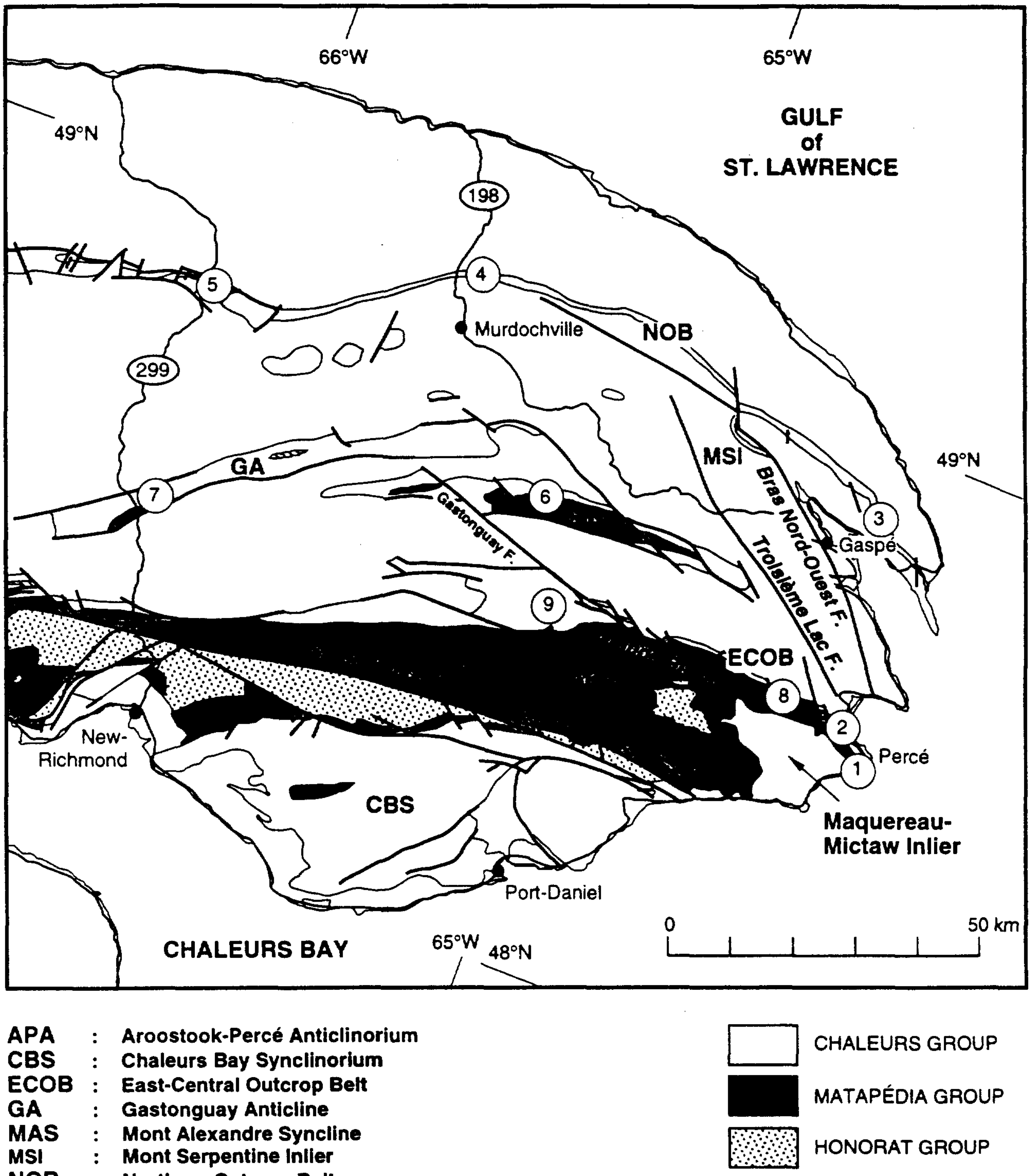

APA : **Aroostook-Percé Anticlinorium**
CBS : **Chaleurs Bay Synclinorium**
ECOB : **East-Central Outcrop Belt**
GA : **Gastonguay Anticline**
MAS : **Mont Alexandre Syncline**
MSI : **Mont Serpentine Inlier**
NOB : **Northern Outcrop Belt**
SJA : **Saint-Jean River Anticline**

Figure 1.2 - Simplified geological map of eastern Gaspé to show main structural features, and distribution of Upper Ordovician to lowermost Devonian rocks. Circled numbers refer to summary stratigraphical columns of Figure 1.3.

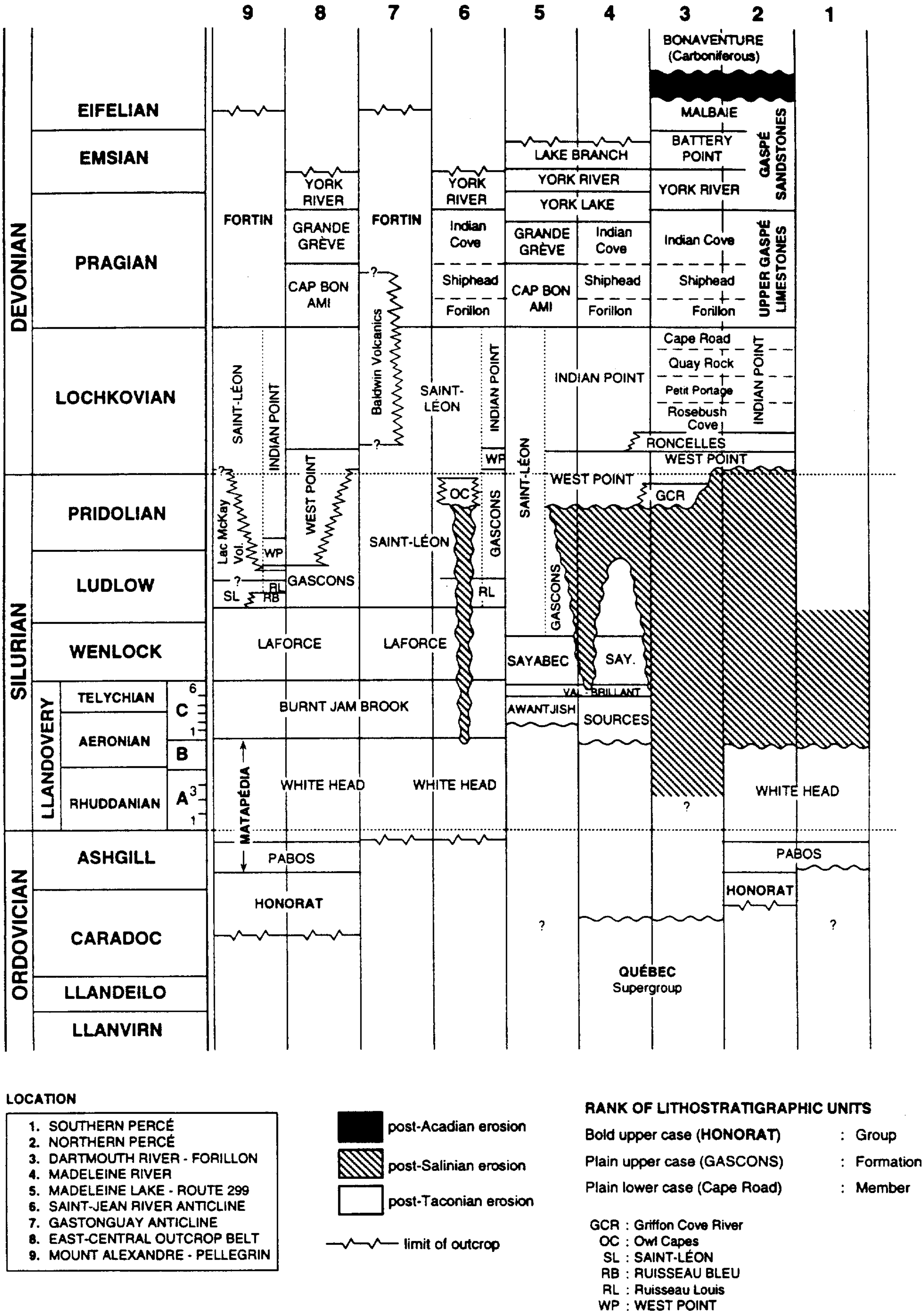

Figure 1.3 - *Correlation chart. Each column is representative of a given area and regroups data of one or more measured sections (dots of Figure 1.4). Position of columns indicated on Figure 1.2. Modified from Bourque et al. (1995).*

1.3.2 CHALEURS GROUP

Compared to the underlying groups, the Chaleurs Group is by far the most diversified group in terms of sedimentary facies. Detailed description of each lithostratigraphic units can be found in Bourque et al. (1993) and Globensky et al. (1993). In northeastern Gaspé, the group conformably overlies the Matapédia Group. The Chaleurs Group succession is better understood when described according to three broad superposed assemblages (Bourque et al., 1993): a lower terrigenous assemblage, a middle carbonate assemblage, and an upper terrigenous assemblage with local reef and volcanic bodies. Figures 1.5-1.7 show distribution and thickness variations of the Chaleurs Group lithostratigraphic units along three profiles (Fig. 1.4).

Lower terrigenous assemblage
The terrigenous sedimentation began in Llandoverian C time in the East-Central Outcrop Belt area (columns 8, 9, Fig. 1.3), and Saint-Jean River and Gastonguay anticlines (columns 7, 8, Fig. 1.3; Burnt Jam Brook Formations). In the Northern Outcrop Belt, the first deposits on the Cambrian-Ordovician folded rocks are terrigenous and occurred at beginning of Llandoverian time (columns 4, 5, Fig. 1.3; Awantjish and Sources formations).

Along the East-Central Outcrop Belt and Mont Alexandre syncline (Escuminac-Percé segment, Fig. 1.7) and the Saint-Jean River anticline (Route 299-Ascah Lake segment, Fig. 1.6), the lower terrigenous assemblage is represented by a single distinctive unit, the Burnt Jam Brook Formation. It is a claystone unit which contains a middle silty and sandy member. Obvious changes in the thickness of the Burnt Jam Brook Formation occur in the Escuminac-Percé segment. The formation is only a few tens of meter-thick east of the Grande Rivière fault, but thickens to 700 m west of it. Similarly, but to a lesser extent, there is a thickening of the Burnt Jam Brook Formation west of the Gastonguay fault in the Saint-Jean River anticline. This situation suggests accelerated subsidence and higher rate of sedimentation west of the Grande Rivière and Gastonguay faults.

In the Northern Outcrop Belt segment (Fig. 1.5), the lower terrigenous assemblage is composed mainly of two superposed formations, the Awantjish claystone, very similar to that of the Burnt Jam Brook Formation, and the overlying Val-Brillant clean, cross-bedded and parallel-laminated, quartz sandstone. Locally, a thinly-bedded fine-grained limestone unit, the Sources Formation, is interlayered with or replace the Awantjish claystone. East of the Madeleine River buildup, the lower terrigenous assemblage is absent because of late Silurian erosion.

Middle limestone assemblage
The Sayabec and Laforce formations form a distinctive limestone horizon of the Silurian succession. The Sayabec is a platformal limestone unit constituting a good chronological marker (Llandoverian C6-early Wenlockian). It is composed of peritidal, reefal and various subtidal facies. Facies identity of the Sayabec with those of the La Vieille Formation of the Chaleurs Bay

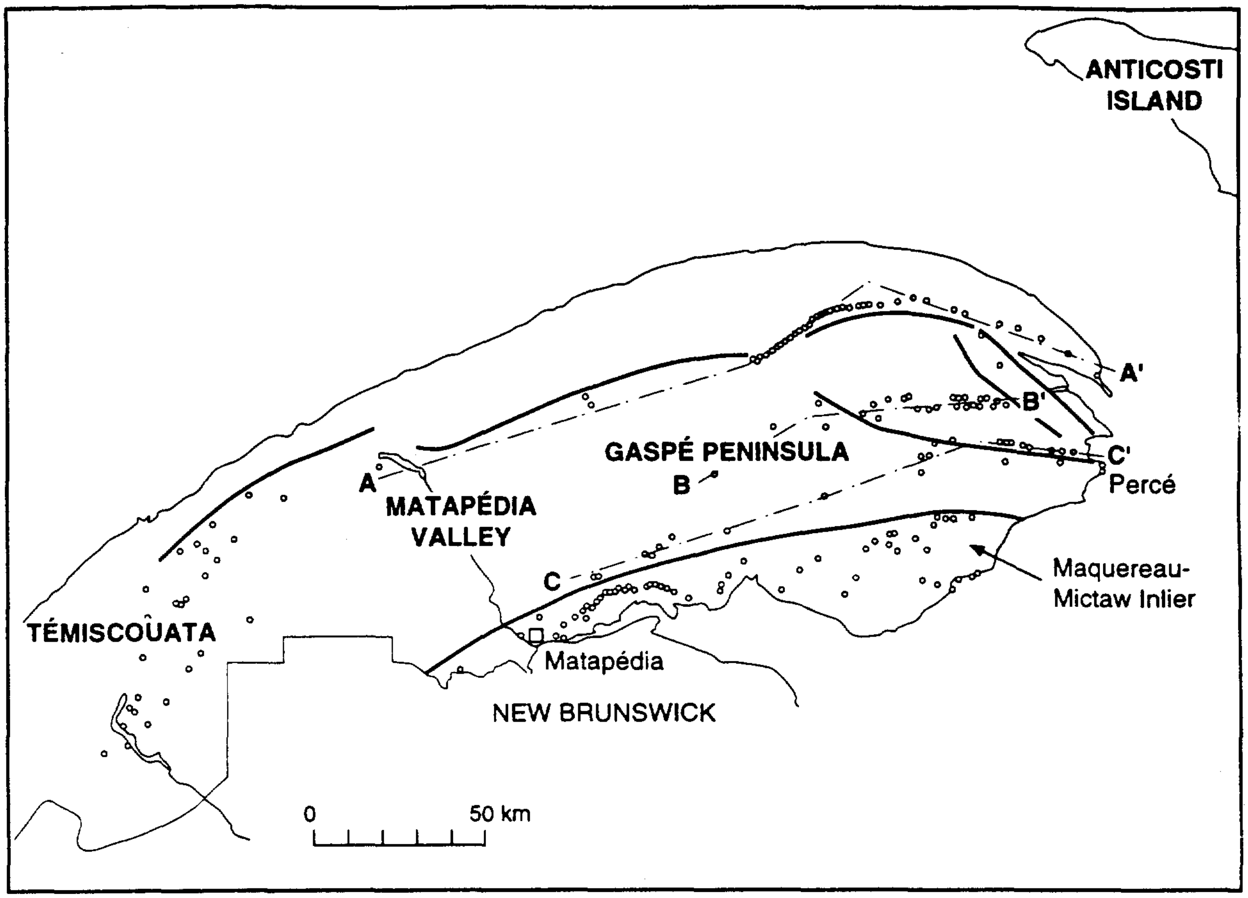

Figure 1.4 - *Present-day distribution of Silurian-lowermost Devonian measured section in Gaspé Peninsula-Témiscouata segment of the Québec Appalachians, and position of lithostratigraphic profiles of Figures 1.5-1.7. From Bourque, Malo and Kirkwood (submitted, 1996).*

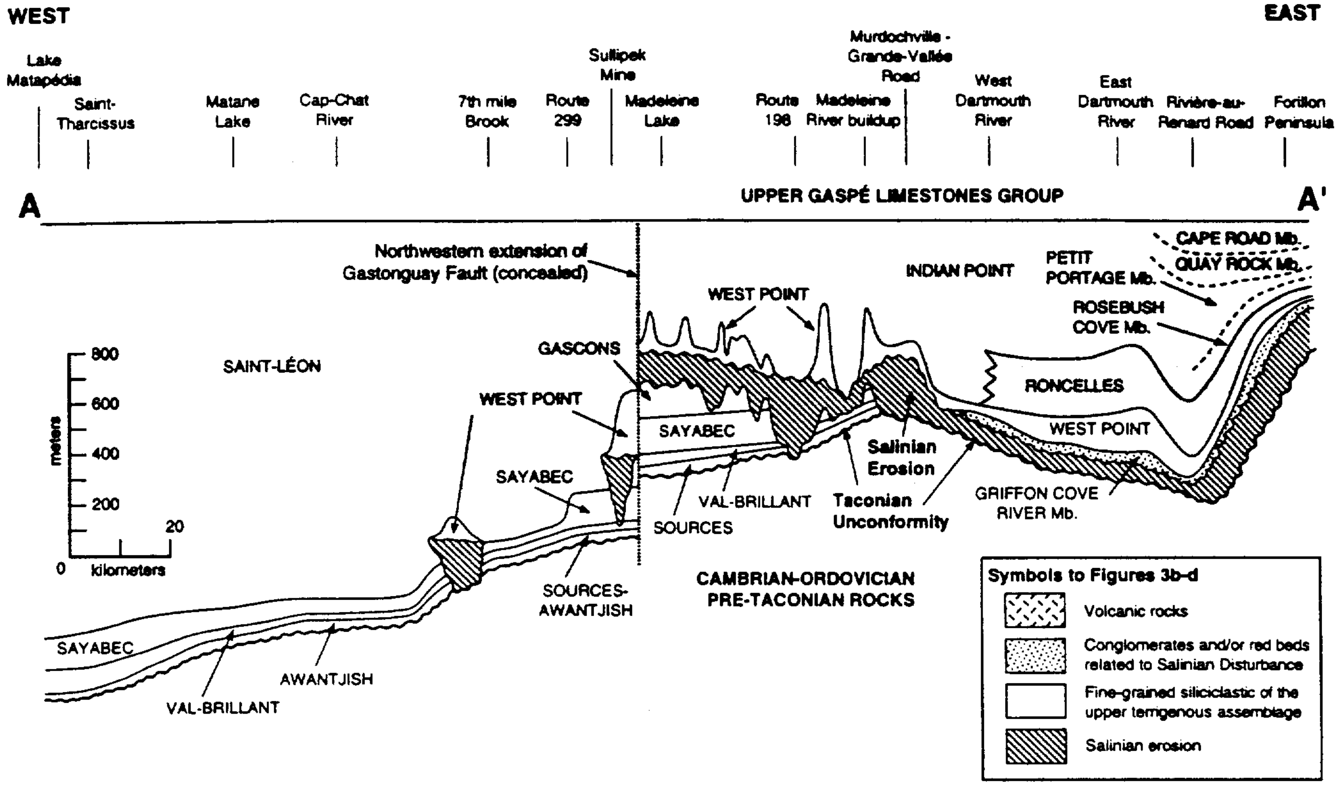

Figure 1.5 - *Lithostratigraphic profiles along the Northern Outcrop Belt segment of the Gaspé Belt. From Bourque, Malo and Kirkwood (submitted, 1996).*

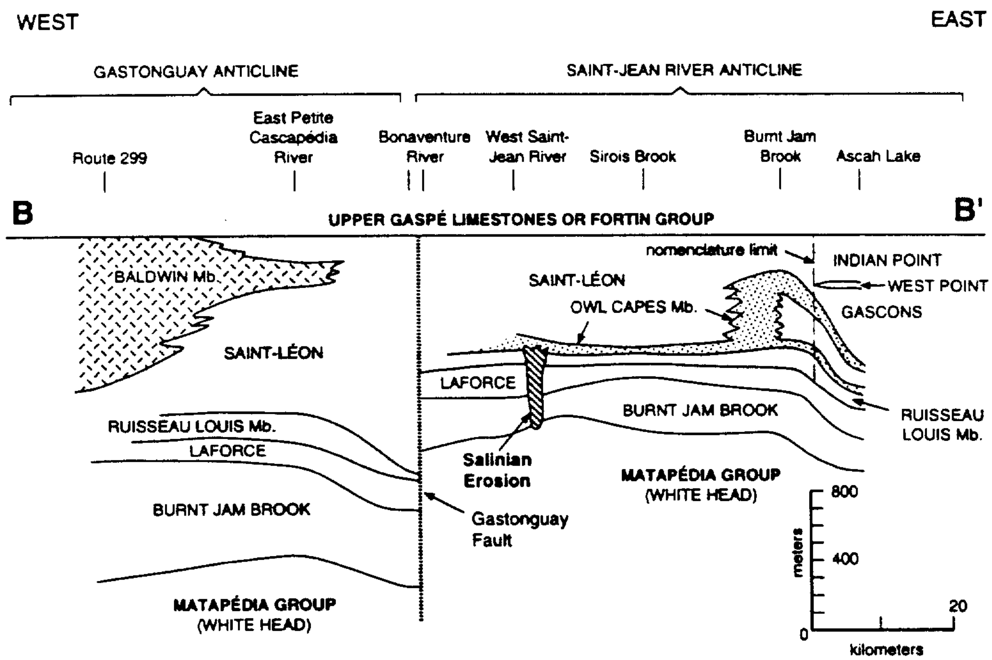

Figure 1.6 - *Lithostratigraphic profiles along the Route 199-Ascah Lake segment of the Gaspé Belt, including Saint-Jean River anticline. Symbols on Figure 5. From Bourque, Malo and Kirkwood (submitted, 1996).*

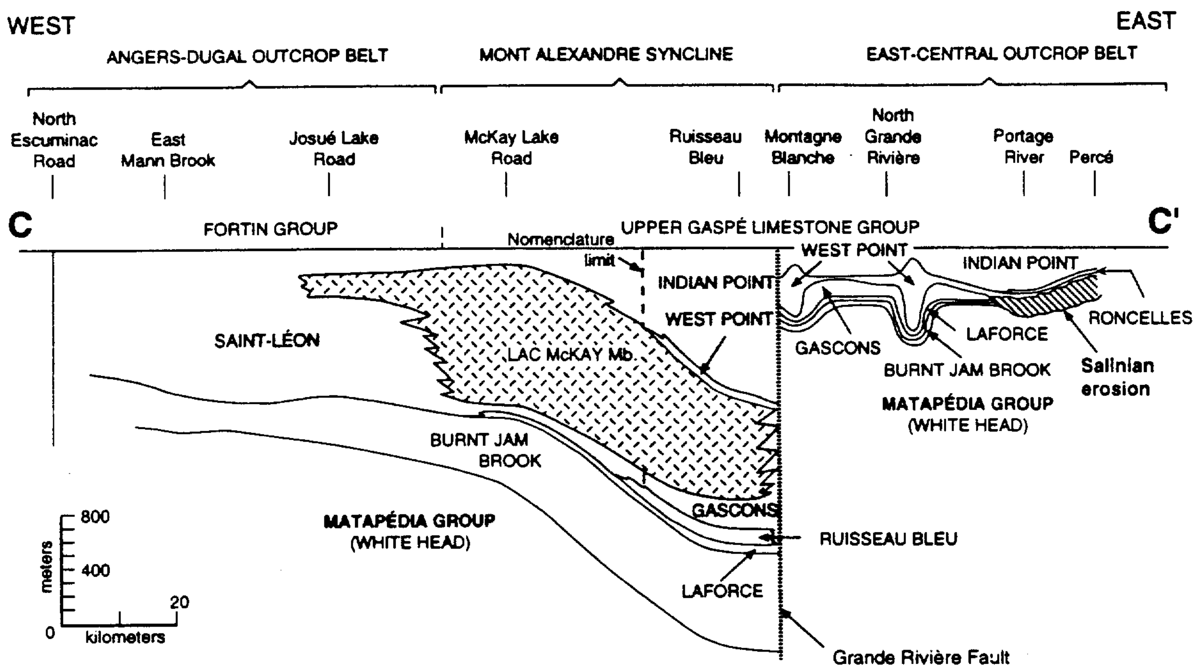

Figure 1.7 - Lithostratigraphic profiles along the Escuminac-Percé segment of the Gaspé Belt, including East-Central Outcrop Belt. Symbols on Figure 1.5. From Bourque, Malo and Kirkwood (submitted, 1996).

synclinorium is well established (Bourque et al., 1986; Lavoie et al., 1992). The Laforce Formation is composed of deeper water sandy lithoclastic calcarenites and calcirudites. The base of the formation is slightly younger than that of the Sayabec-La Vieille (earliest Wenlockian), as well as its top (early Ludlovian). Together with the lithoclastic nature of the limestone where a variety of a carbonate platform clasts are recognized, this age relationship would suggest derivation of the Laforce material from at least part of the Sayabec-La Vieille platform. Alternative possibility is derivation from the coeval nearby Anticosti shelf (see further).

Upper terrigenous assemblage
The upper terrigenous assemblage is dominated by the fine-grained siliciclastic facies of the Saint-Léon Formation and its lateral equivalent Gascons and Indian Point formations. The fine-grained siliciclastics contain three distinctive lithologies: conglomerate, volcanic rock and reef limestone bodies. Facies of the Saint-Léon, Gascons and Indian Point are very similar among themselves, and it is only a matter of nomenclature if they bear different names: the fine-grained siliciclastics are called Saint-Léon where the sequence does not comprise important reef limestone bodies (West Point Formation) and they are called Gascons and Indian Point where they underlie and overlie a West Point reef limestone horizon, respectively (Bourque, 1975; e.g., columns 5, 6, 9, Fig. 1.3 herein).

A striking feature within the upper terrigenous assemblage of the Chaleurs Group is the occurrence of an erosion unconformity related to the Salinian Disturbance (= Salinic Disturbance of Boucot, 1962; Malo and Bourque, 1993) now recognized throughout the northern Appalachians (Rast and Skeehan, 1993). This disturbance acted only locally in the Gaspé Peninsula and has left traces of erosion in eastern part of the Northern Outcrop Belt (Fig. 1.5), in easternmost part of the East-Central Outcrop Belt (Fig. 1.7), and in a small area of the Saint-Jean River anticline (Fig. 1.6). No rocks younger than Ludlovian have never been found below the unconformity, and beds above the unconformity are dated as Pridolian, therefore constraining the age of the peak of this tectonic event as Ludlovian-Pridolian (Fig. 1.8).

The Salinian unconformity has been carefully mapped in the Northern Outcrop Belt by Lachambre (1987) who showed the clear distinction between the Taconian and the Salinian unconformities (Fig. 1.5). The Salinian erosion has cut unequally into the Silurian sequence, reaching in places the underlying Cambrian-Ordovician rocks of the Québec Supergroup, thus cutting across the Taconian unconformity. This is the case in the eastern part of the Northern Outcrop Belt where the Pridolian facies overlie the Québec Supergroup with angular unconformity. Paleotopography left by the Salinian erosion has subsequently controlled development of Pridolian and Lochkovian facies, as exemplified by the close correspondence between location of West Point pinnacle reefs and that of paleotopographic highs (Fig. 1.5; see further).

The **conglomerate bodies** of the upper terrigenous assemblage are clearly associated with the Salinian unconformity. In the Northern Outcrop Belt, east of the Murdochville-Grande Vallée

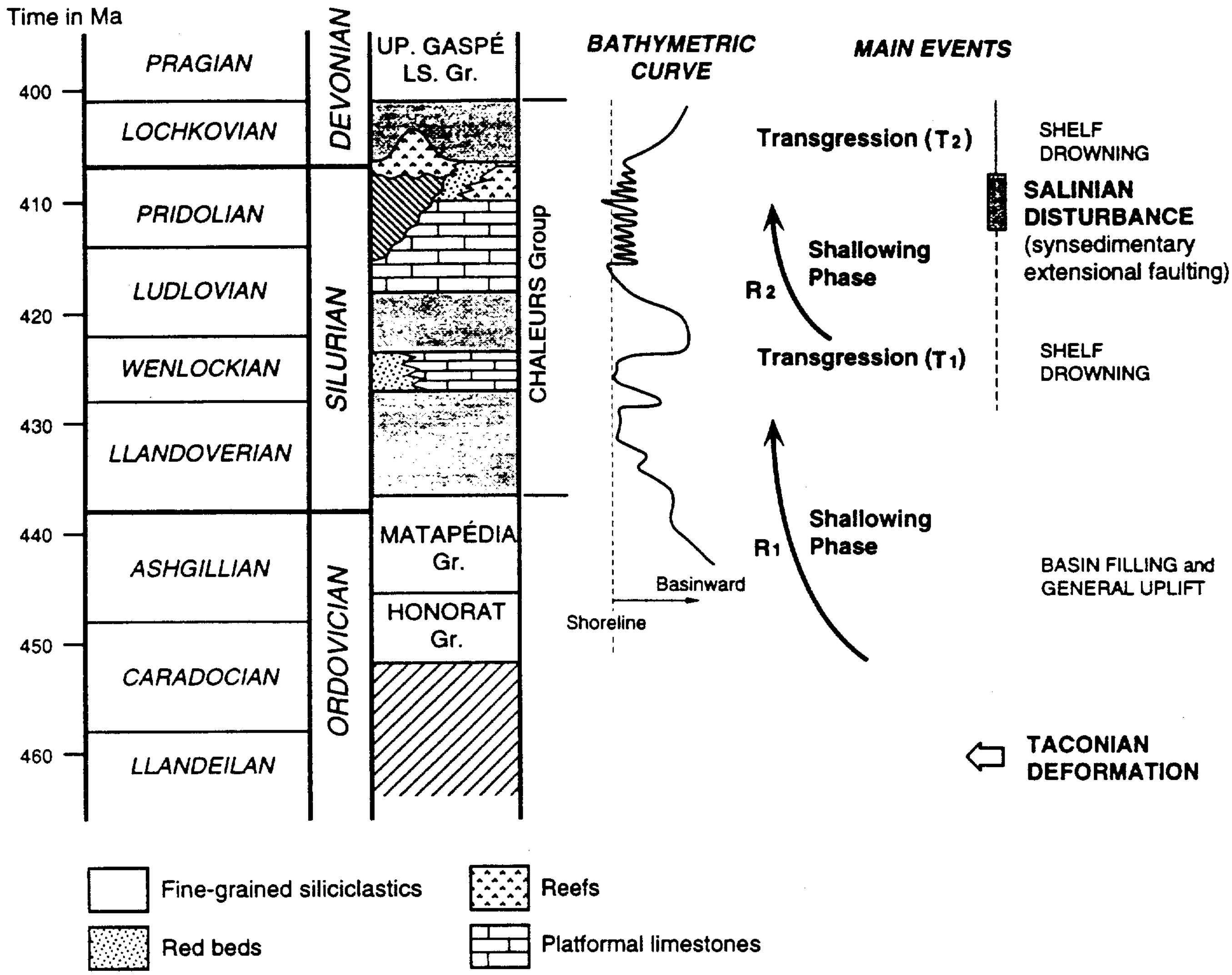

Figure 1.8 - *Summary of the main tectono-sedimentary events and bathymetric curve for the uppermost Ordovician-lowermost Devonian succession of the Gaspé-Témiscouata segment of the Québec Appalachians. From Bourque, Malo and Kirkwood (submitted, 1996).*

road, the Griffon Cove River conglomerate is the result of the Salinian erosion. It is composed of pebbles and cobbles of quartz, chert, mafic and felsic volcanic rocks, various sedimentary rocks and, in places, stromatoporoid clasts. In the Saint-Jean River anticline, the Owl Capes conglomerate is likely to be related to Salinian erosion since it has the same age as the Griffon Cove River conglomerate. It is made up of quartz pebbles and fragments of various limestones, corals, stromatoporoids, feldspathic wacke and mafic volcanic rocks in an abundant argillaceous matrix.

The **volcanic rock bodies** of the upper terrigenous assemblage form two members: the Silurian Lac McKay Member (column 9, Fig. 1.3; Fig. 1.7), and the uppermost Silurian-lower Devonian Baldwin Member (column 7, Fig. 1.3; Fig. 1.6). Although both members are predominantly mafic, there are differences. The Lac McKay Member is basaltic lava flows and volcaniclastics, with only a few felsic lavas. Basalts are of the transitional alkalic-tholeiitic type. The Baldwin Member includes a significant proportion of intermediate rocks and minor rhyolites, pyroclastites and hyaloclastites in addition to the tholeiitic basalts. These volcanic bodies are related to intraplate volcanism in an extensional and/or transpressional tectonic regime (Doyon and Dalpé, 1993; Dostal et al., 1993).

The **reef limestone bodies** of the upper terrigenous assemblage belong to the West Point Formation. The West Point is best developed in its type-area, the Chaleurs Bay synclinorium, where it reaches thicknesses of nearly 800 m (Bourque et al., 1986). It is composed of three superposed complexes (Fig. 1.9): a lower sponge mound and microbial reef complex, a middle crinoidal bank complex and an upper stromatoporoid reef complex. The landward part of the upper complex is made up of distinctive stromatoporoid rubbles, microbial laminites and mudcracked red beds. The West Point facies are amazingly similar for localities distant one another. For instances, the stromatoporoid rubble, microbial laminite and red bed assemblage found above the Griffon Cove River conglomerate in easternmost part of the Northern Outcrop Belt is identical to the same assemblage found in the upper complex in the Port-Daniel area, some 100 km to the southwest. Microbial reefs of the lower complex are found identical at western end of the East-Central Outcrop Belt. Clasts of the microbial reef lithology were identified in the Owl Cape conglomerate of the Saint-Jean River anticline. Limestone facies identical to those of the lower and upper complexes constitutes the clasts of the Neigette breccia (Fig. 1.4) in northern Témiscouata-Matapédia Valley area (Dansereau, 1989), indicating there were reef complexes north of the Neigette fault. The West Point reef construction ended during Late Pridolian time in the Chaleurs Bay synclinorium, but persisted into the Lochkovian time in the East-Central and Northern Outcrop Belts. In the latter, stromatoporoid pinnacle reefs reaching thicknesses up to 300 m developed on paleotopographic highs left by the Salinian erosion (Fig. 1.10). See further for discussion on controls on reef settlement and development.

1.4 STRUCTURAL FEATURES RELATED TO THE SALINIAN DISTURBANCE

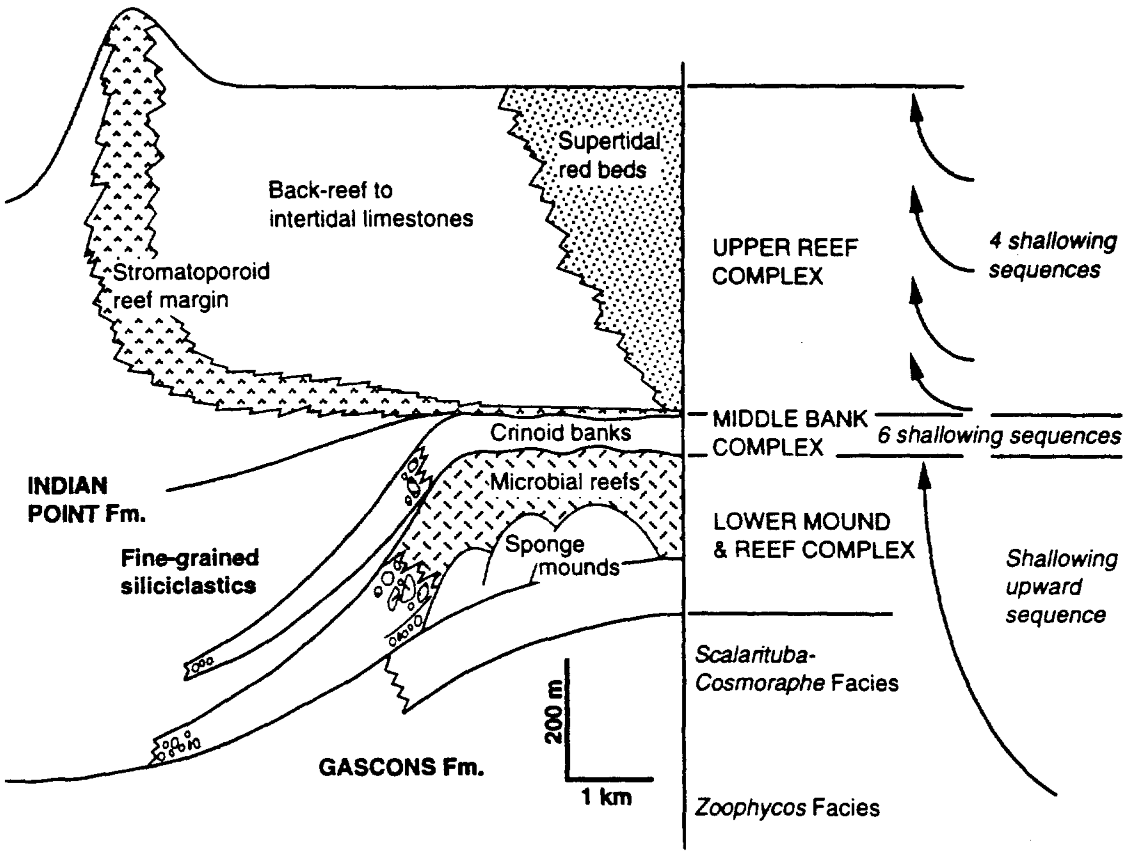

Figure 1.9 - *Upper Silurian West Point carbonate buildup in Chaleurs Bay synclinorium. The uppermost Gascons and the West Point formations have registered at least eleven shallowing upward sequences. From Bourque et al. (1986), and Bourque, Malo and Kirkwood (submitted, 1996).*

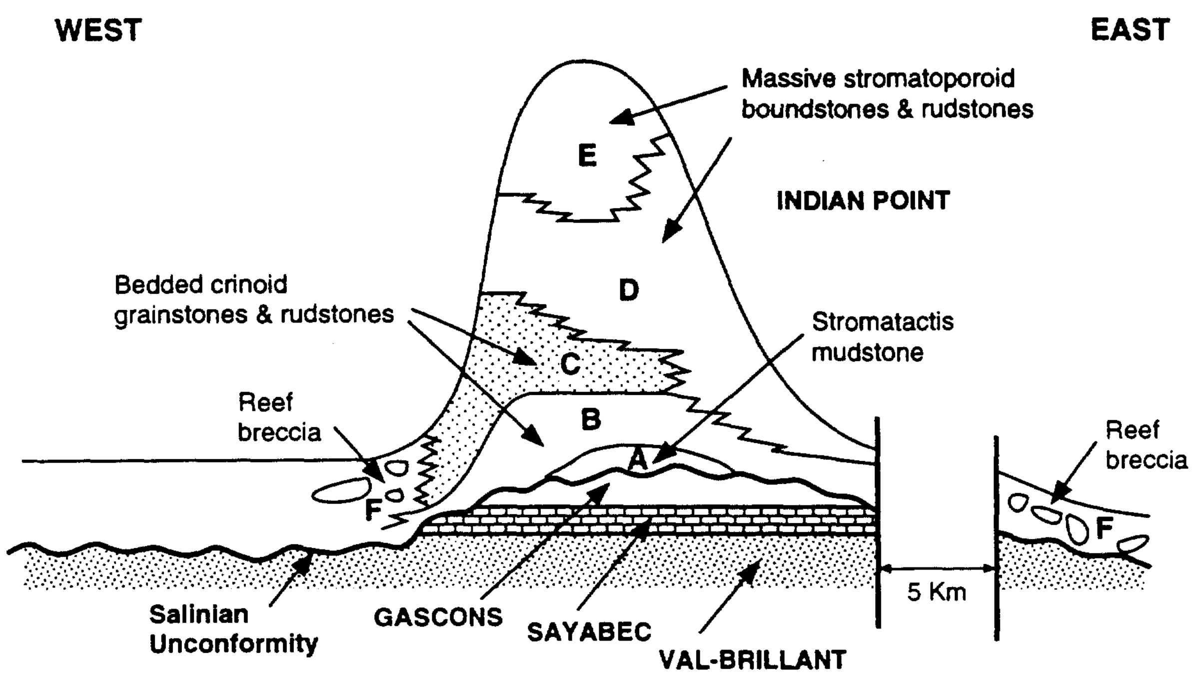

Figure 1.10 *- Geometry and facies relationships in the Madeleine River buildup of the Devonian West Point Formation. From Bourque (1977) and Bourque et al. (1986).*

As stated above, structural style of the Connecticut Valley-Gaspé synclinorium (Fig. 1.2) is traditionally attributed to the Acadian deformation, and separating structural features related to the Salinian deformation from those related to the Acadian deformation is not readily done.

The dominant trend of major faults, as well as the trend of regional folds, make the northeastern part of the Gaspé Belt structurally different from the rest of the belt. Indeed, the major Acadian structural trend of the Gaspé Belt rocks is oriented NE, but in the eastern part of the Connecticut Valley Gaspé synclinorium the regional fold trend varies from NE to nearly E (Fig. 5.19, Chapter 5 of this report). The faults in northeastern Gaspé are NW-trending, as compared to a NE trend in the western and central parts of the Connecticut Valley-Gaspé synclinorium, the western part of the Aroostook-Percé anticlinorium and the Ristigouche syncline, and an E trend in the eastern part of the Aroostook-Percé anticlinorium and the Chaleurs Bay synclinorium.

Those structural features in the northeastern part of the Gaspé Belt that do not fit the more classical style of deformation recognized elsewhere should be reevaluated in the light of our recognition of an episode of extensional faulting in Late Silurian-Early Devonian time, that is the Salinian Disturbance. The main geological feature related to the Salinian Disturbance is the Late Silurian Salinian Unconformity recognized within the Chaleurs Group in several localities of the Gaspé Belt. The unconformity is either an angular unconformity (e.g., Ristigouche syncline of the Chaleurs Bay synclinorium) or an erosional surface that cuts deeply into the underlying older Silurian and even Cambro-Ordovician rocks (see above under description of the *Upper terrigenous assemblage* of the Chaleurs Group, and below under Depositional History of Northeastern Gaspé).

1.4.1 FOLDS

Acadian NE-trending regional folds are generally open and upright, doubly plunging towards the NE and the SW in the Aroostook-Percé anticlinorium and have subhorizontal hinge lines in the Connecticut Valley Gaspé synclinorium and the Chaleurs Bay synclinorium. In the Connecticut Valley Gaspé synclinorium west of the Gastonguay fault, the regional folds are NE-trending (e.g., Gastonguay anticline, Fig. 1.2). From the Gastonguay fault to the east, regional folds tends to become more easterly oriented (e.g., Saint-Jean River anticline), and gets NW-trending close to the Bras Nord-Ouest fault. For example, the Champou syncline is E-trending south of the E-trending segment of the Bras Nord-Ouest fault and becomes NW-trending between the Troisième Lac and Bras Nord-Ouest faults (Fig. 5.19, Chapter 5 of this report). There is a close spatial relationship between NW-trending folds and faults, and it is likely that there is a genetic link between the development of both types of structures.

An earlier NW-trending folding, with no penetrative cleavage, precedes the regional NE-trending folding in the Aroostook-Percé anticlinorium and in the Ristigouche syncline (Malo and Béland, 1989). Malo and Kirkwood (1996) believed that the earlier NW-trending folds in the southern Gaspé Belt have a common origin with those of the northeastern part of the Gaspé Belt. Like those of the eastern Connecticut Valley Gaspé synclinorium, the early NW-trending folds are sometimes spatially associated to NW-trending faults (e.g. Percé and Carleton areas in the Aroostook-Percé anticlinorium). On the pre-Devonian palinspastic map (see Malo and Kirkwood, 1996; and Chapter 5 of this report), the early NW-trending folds are located mainly in the eastern part of the Gaspé Belt basin along the St. Lawrence promontory. They are interpreted as extensional forced folds which formed over faulted blocks delineated by the Late Silurian-Early Devonian Salinian extensional faults.

1.4.2 Faults

The northeastern part of the Gaspé Belt is characterized by the NW-trending faults (Fig. 1.11). The most important ones are the Bassin Nord-Ouest, the Troisième Lac, and the Gastonguay faults. The E-trending Grande Rivière fault, representing the limit between the Connecticut Valley Gaspé synclinorium and the Aroostook-Percé anticlinorium, is also a major fault in that part of the Gaspé Belt. These four faults have been used to delimit tectonic blocks (Roksandic and Granger, 1981; Héroux et al., 1983; Amyot, 1984; Bertrand, 1987; St-Julien and Bourque, 1990; Lavoie, 1992b; Berger and Ramsay, 1993): a NE block north of the Bassin Nord-Ouest fault, a central block between the Bassin Nord-Ouest and the Troisième Lac faults, and a SW block south of the Troisième Lac fault and north of the Grande Rivière fault. This latter SW block is limited to the west by the Gastonguay fault.

The E-trending Grande Rivière fault is part of the Acadian dextral strike-slip fault system of the southern Gaspé Belt (Malo and Béland, 1989). The Bassin Nord-Ouest, Troisième Lac and Gastonguay faults are part of a NW-trending fault system well developed only in the northeastern part of the Gaspé Belt. Structural analysis at the outcrop level along the Bassin Nord-Ouest and Troisième Lac faults (Béland, 1980; Berger and Ramsay, 1993) shows that the faults are Acadian dextral strike-slip faults with a vertical component of movement. The dextral strike-slip movement probably corresponds to the last Acadian movement in northeastern Gaspé Belt. For instance, in the Percé area, it has been shown that the southern extension of the Troisième Lac fault crosscuts E-trending faults associated to the Grande Rivière fault (Kirkwood, 1989) which is one of the major Acadian fault (Malo and Béland, 1989).

However, these NW-trending faults are probably older than late Acadian, and are thought to have been active during sedimentation of the Silurian and Lower Devonian facies of the Gaspé Belt. Indeed, sedimentological analysis of the Gaspé Sandstones (Rust, 1981; Amyot, 1984), the Upper Gaspé Limestones (Amyot, 1984; Lavoie, 1992b), and of the Chaleurs Group (Bourque et al., 1993, 1995, Bourque, Malo and Kirkwood, submitted 1996), thermal maturation studies of the northeastern Gaspé Peninsula (Héroux et al., 1983; Bertrand, 1987), and seismic reflection data (Roksandic and Granger, 1981) suggest synsedimentary movements along the faults (see further

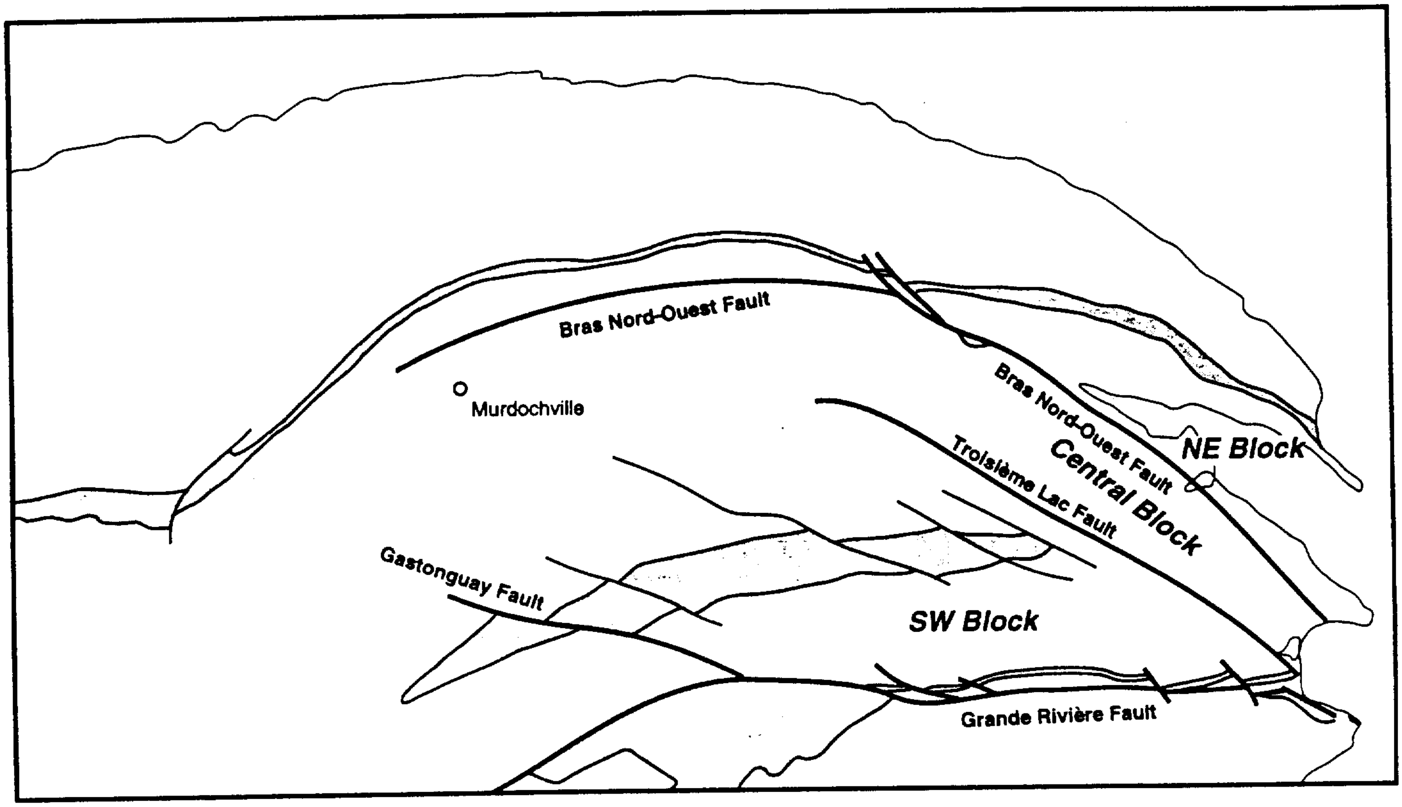

Figure 1.11 *- Faults that are postulated to have been active as normal faults during the Salinian Disturbance.*

under Model for Reef Settlement and Development). These movements started in Llandoverian time and continue until the Pragian. The Gastonguay and Grande Rivière faults started their activity during the sedimentation of the Burnt Jam Brook (Fig. 1.6), whereas the Bassin Nord-Ouest fault was still active during deposition of the Gaspé Sandstones (Rust, 1981; Amyot, 1984).

For one, the Bassin Nord-Ouest fault has a long and complex structural history. There is evidence for a pre-Silurian motion, before the normal motion during sedimentation of the Silurian-Devonian rocks (Béland, 1980; Berger and Ramsay, 1993). Subhorizontal mineral lineations in the Cambro-Ordovician rocks of the Mont Serpentine inlier (Fig. 1.2), along the Bassin Nord-Ouest fault, indicate a pre-Silurian ductile strike-slip motion that can be attributed to the Taconian orogeny (Malo and Kirkwood, 1996). Continued motion, as normal faulting during the Silurian-Devonian sedimentation was inverted in Late Devonian time by the Acadian transpression (strike-slip with high-angle reverse motion, hence the vertical movement in fault plane noted above).

1.5 DEPOSITIONAL HISTORY OF NORTHEASTERN GASPÉ

The Upper Ordovician - Lower Devonian Gaspé Belt succession has recorded two regressive phases (R_1 and R_2) and two transgressive phases (T_1 and T_2) (Bourque, Malo and Kirkwood, submitted, 1996; Fig. 1.8 herein).

East of Madeleine River, in the Dartmouth River-Forillon area at eastern end of the Northern Outcrop Belt, the Salinian erosion has striped the entire Silurian succession, so that phases R1, T1 and R2 cannot be observed, except for the Griffon Cove River conglomerate and the associated red beds that mark the culmination of regressive phase R2. The transgressive phase T2 is well documented in this area (Bourque et al., 1986; Bourque, 1989). The West Point above the Griffon Cove River is composed of a supertidal/intertidal mudcracked red bed, microbial limestone and stromatoporoid rubble assemblage that correlates with the upper complex of the West Point Formation of the Port-Daniel area in Chaleurs Bay synclinorium (Figs. 1.9, 1.12). As in the Port-Daniel area, four shallowing upward sequences were recognized in this intertidal/supertidal succession (Bourque, 1989; Fig. 1.12 herein). From there, the facies succession progressively evolved upsection to deep water lime mudstones of the Upper Gaspé Limestones Group (Lavoie, 1992a, 1992b), with thick-bedded structureless argillaceous and silty lime muds of the Roncelles Formation and turbiditic fine-grained siliciclastic sediments of the Indian Point Formation as intermediate facies.

In the Madeleine River area, the succession has recorded the two sedimentary cycles (R1-T1 and R2-T2). Its base lies unconformably on the Taconian deformed Cambrian-Ordovician rocks. Unlike the succession to the east, the Salinian Disturbance has caused erosion of only part of the Silurian succession. The transition from deep water clays and carbonate muds of the Awantjish-Sources Formation to coastal clean quartz sands of the Val-Brillant Formation (Lajoie, 1968)

STRATIGRAPHY				
DEVONIAN	*PRAGIAN*	UPPER GASPÉ LIMESTONE Gr.	531 m.	Calcareous mudstone, very fossiliferous in places. Tempestites.
DEVONIAN	*LOCHKOVIAN*	INDIAN POINT Fm.: Cape Road Mb., Quay Rock Mb., Petit Portage Mb., Rosebush Cove Mb.	470 m.	Thick-bedded fine-grained siliciclastites, local turbidite units
DEVONIAN	*LOCHKOVIAN*	RONCELLES Fm.	220 m.	Fossiliferous calcareous mudstone
SILURIAN	*PRIDOLI*	WEST POINT Fm.	61 m.	Assemblage of mud-cracked red beds, microbial laminites and stromatoporoid rubbles. Nodular calcarenite in upper part.
SILURIAN	*PRIDOLI*	GRIFFON COVE RIVER Mb.	5 m.	subaerial basal conglomerate
Salinian unconformity				
CAMBRIAN-ORDOVICIAN				

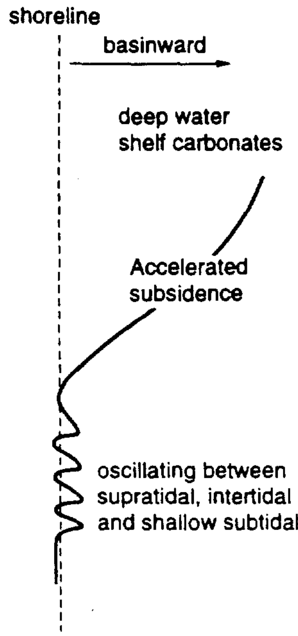

Figure 1.12 - *Pridoli-Lochkovian succession in easternmost part of the Northern Outcrop Belt. The four minor cycles recognized in the West Point Formation are correlated with the four ones recognized in the upper reef complex of the West Point in the Chaleurs Bay synclinorium (see Figure 9). From Bourque (1989), and Bourque, Malo and Kirkwood (submitted, 1996).*

constitutes the regressive phase R1, together with the overlying shallow water Sayabec Formation (Bourque et al., 1986; Lavoie et al., 1992). The transgressive phase T1 started in Wenlockian time with deposition of the nodular limestones of the upper part of the Sayabec and culminated with deposition of the offshore-type fine-grained siliciclastic sediments of the Gascons Formation. Second regressive phase R2 culminated with Salinian uplifting that caused partial erosion of Silurian deposits. Pinnacle reefs of the West Point Formation settled on topographic highs left by the erosion (Fig. 1.5) during early stages of the transgressive phase T2 and were buried under fine-grained siliciclastics of the Indian Point Formation when they could not keep pace to sea-level rise.

The succession of the Gastonguay anticline, the Saint-Jean River anticline, and the Mont Alexandre syncline is essentially composed of basinal facies: lime turbidites of the White Head, nearly azoic claystone of the Burnt Jam Brook, turbidites and debris flows of the Laforce (Lavoie, 1988), massive fine-grained siliciclastics with local graptolites of the Saint-Léon, and turbidites of the Fortin (Dalton, 1987; Hesse and Dalton, 1989). These deep water facies did not record the sedimentary cycles detected in the shelf successions.

1.6 PALEOGEOGRAPHY OF THE GASPÉ-TÉMISCOUATA BASIN

The following discussion on paleogeography embraces the entire Gaspé-Témiscouata basin for the Silurian-lowermost Devonian time interval, giving the frame into which the paleogeography of northeastern Gaspé Peninsula evolved. Paleogeographic maps (Fig. 1.13) are those of Bourque et al. (1995), revised and updated by Bourque, Malo and Kirkwood (submitted, 1996). They are constructed for five time slices, based on the 200 sections measured and described in the Témiscouata-Gaspé segment (Bourque et al., 1993), and palinspastically redistributed along the Gaspé Belt (Kirkwood, 1993; Fig. 1.13A herein).

1.6.1 Mid-Llandoverian (Early Aeronian)

During mid-Llandoverian time (Fig. 1.13B), the Gaspé Taconian Allochthon belt at northwestern margin of the basin was emerged, as well as the Maquereau-Mictaw massif to the south. The occurrence of nearshore sands and gravels (Weir and Anse Cascon formations) west of the Maquereau-Mictaw massif testifies to erosion of the latter. In the Témiscouata area, shallow water volcanic conglomerates with a few associated lava flows (Pointe-aux-Trembles Formation) indicate erosion of an active volcanic area (David and Gariépy, 1986). In between the two land areas, lime mud turbidites of the Matapédia Group (and Carys Mills Formation in New Brunswick) contributed to the basin filling. These muds were more likely derived from the Anticosti platform. This interpretation is supported by similarity between the conodont fauna of the Percé sequence and that of the coeval Anticosti sequence (Nowlan, 1981), the northeast-southwest lateral facies zonation from proximal to distal in the Matapédia Group, and

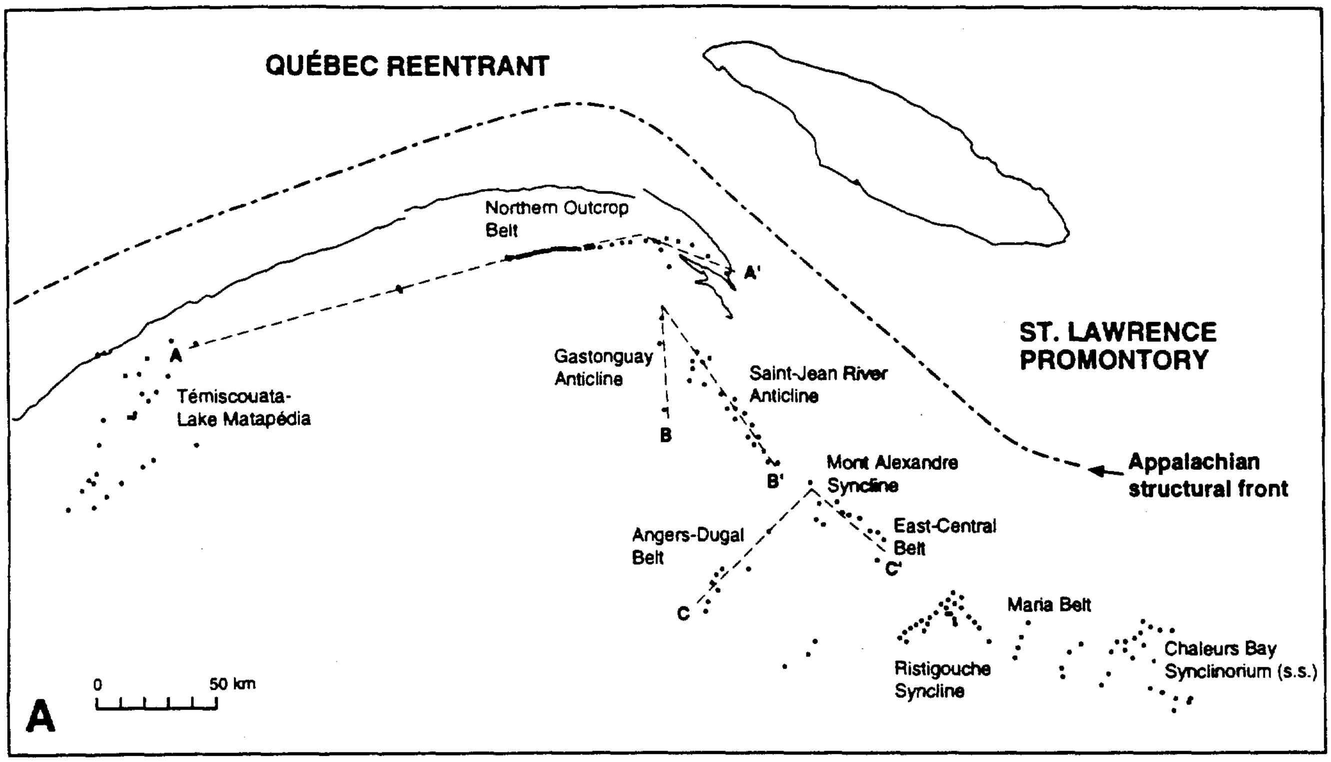
QUÉBEC REENTRANT
Northern Outcrop Belt
A'
A
Témiscouata-Lake Matapédia
Gastonguay Anticline
B
Saint-Jean River Anticline
B'
ST. LAWRENCE PROMONTORY
Appalachian structural front
Mont Alexandre Syncline
Angers-Dugal Belt
East-Central Belt
C
C'
Maria Belt
Ristigouche Syncline
Chaleurs Bay Synclinorium (s.s.)
0
50 km
A

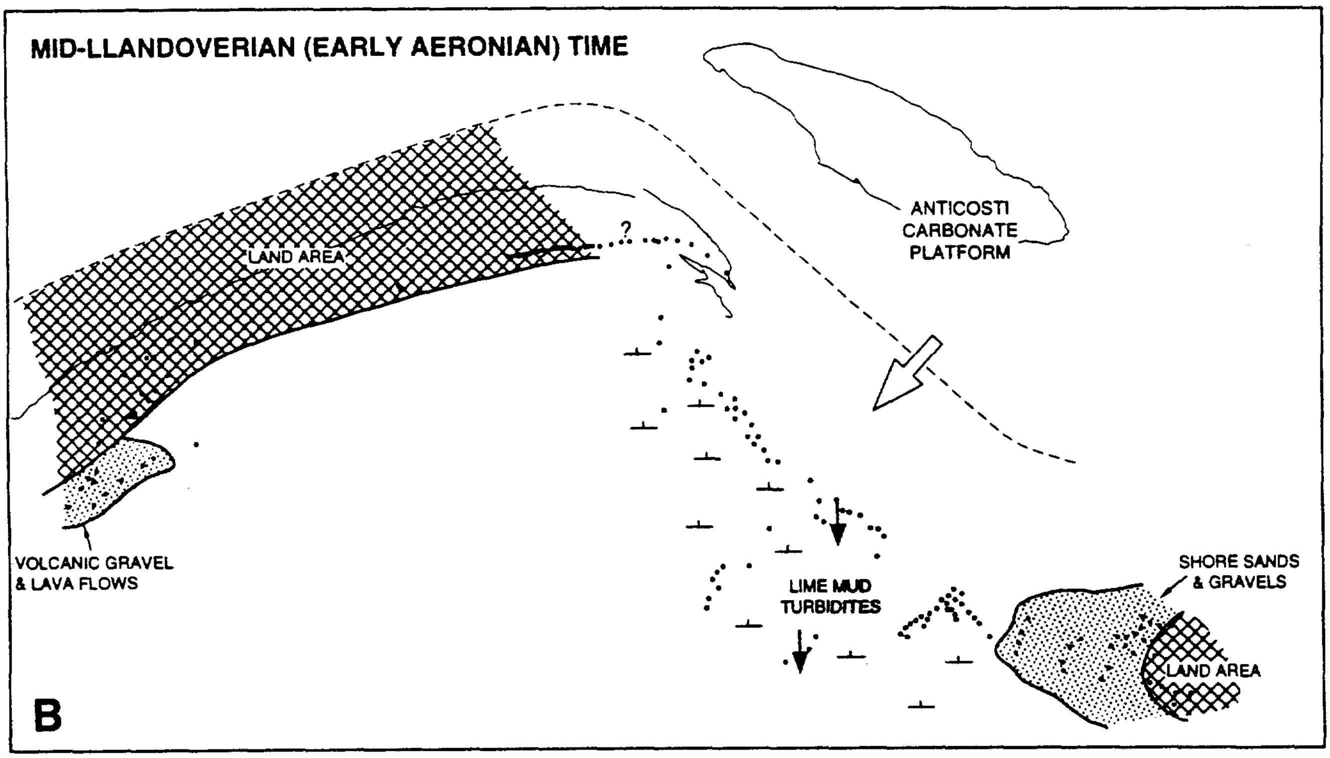
MID-LLANDOVERIAN (EARLY AERONIAN) TIME
?
LAND AREA
ANTICOSTI CARBONATE PLATFORM
VOLCANIC GRAVEL & LAVA FLOWS
LIME MUD TURBIDITES
SHORE SANDS & GRAVELS
LAND AREA
B

Figure 1.13 ...

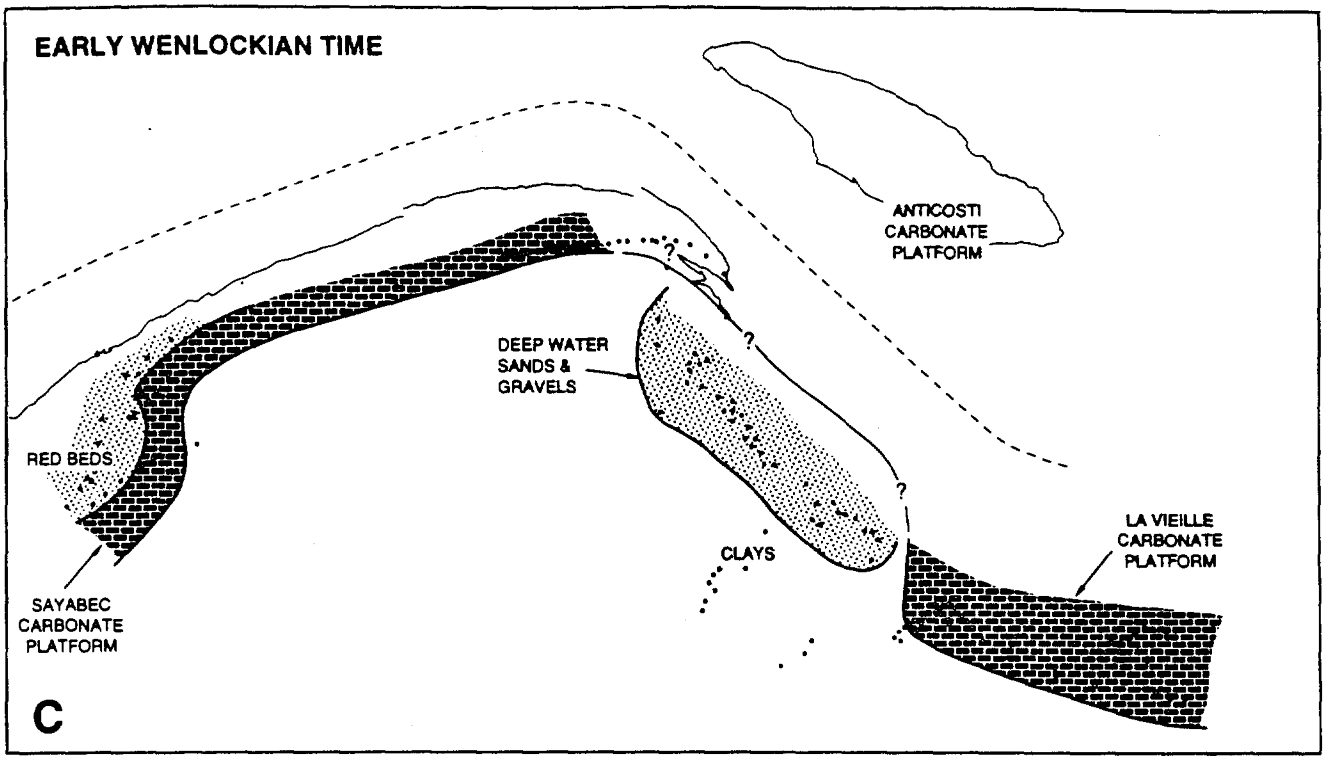
EARLY WENLOCKIAN TIME
ANTICOSTI
CARBONATE
PLATFORM
DEEP WATER
SANDS &
GRAVELS
RED BEDS
CLAYS
LA VIEILLE
CARBONATE
PLATFORM
SAYABEC
CARBONATE
PLATFORM
C

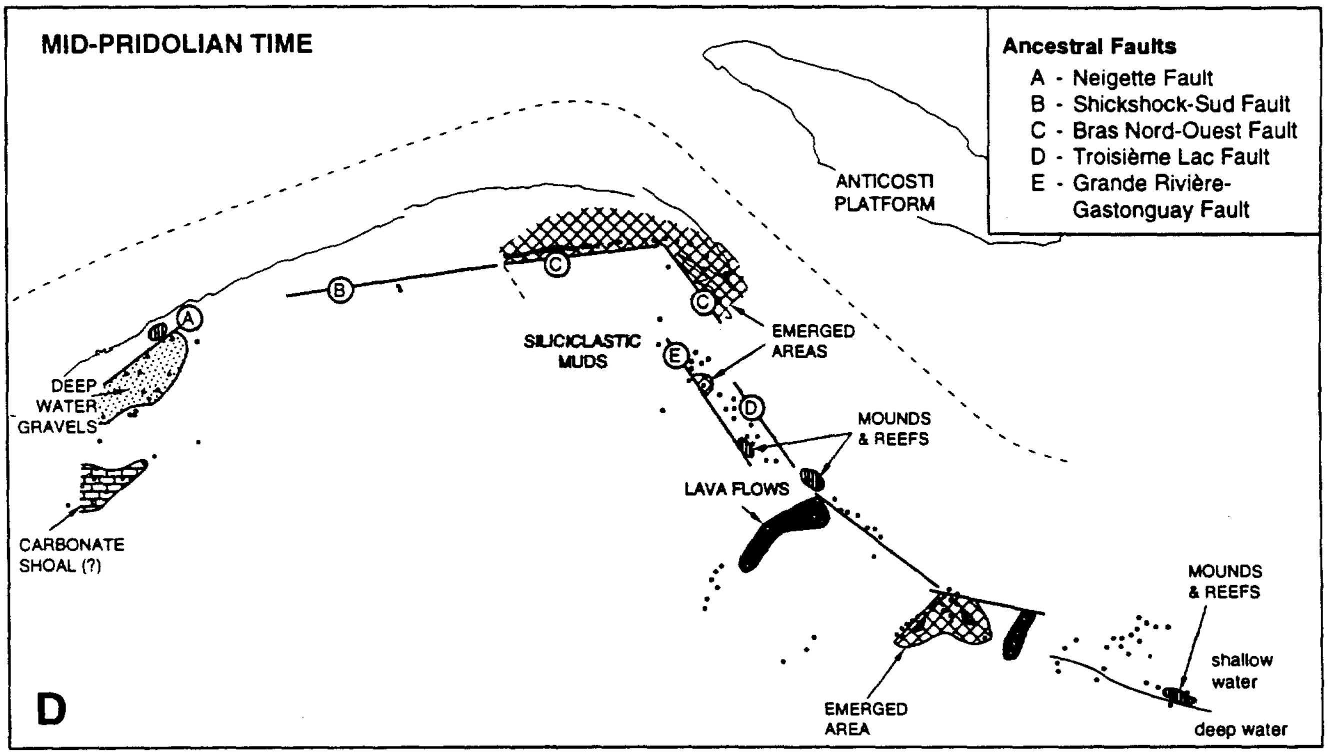
MID-PRIDOLIAN TIME
Ancestral Faults
A - Neigette Fault
B - Shickshock-Sud Fault
C - Bras Nord-Ouest Fault
D - Troisième Lac Fault
E - Grande Rivière-
Gastonguay Fault
ANTICOSTI
PLATFORM
SILICICLASTIC
MUDS
EMERGED
AREAS
DEEP
WATER
GRAVELS
MOUNDS
& REEFS
LAVA FLOWS
CARBONATE
SHOAL (?)
MOUNDS
& REEFS
shallow
water
deep water
EMERGED
AREA
D

Figure 1.13 ...

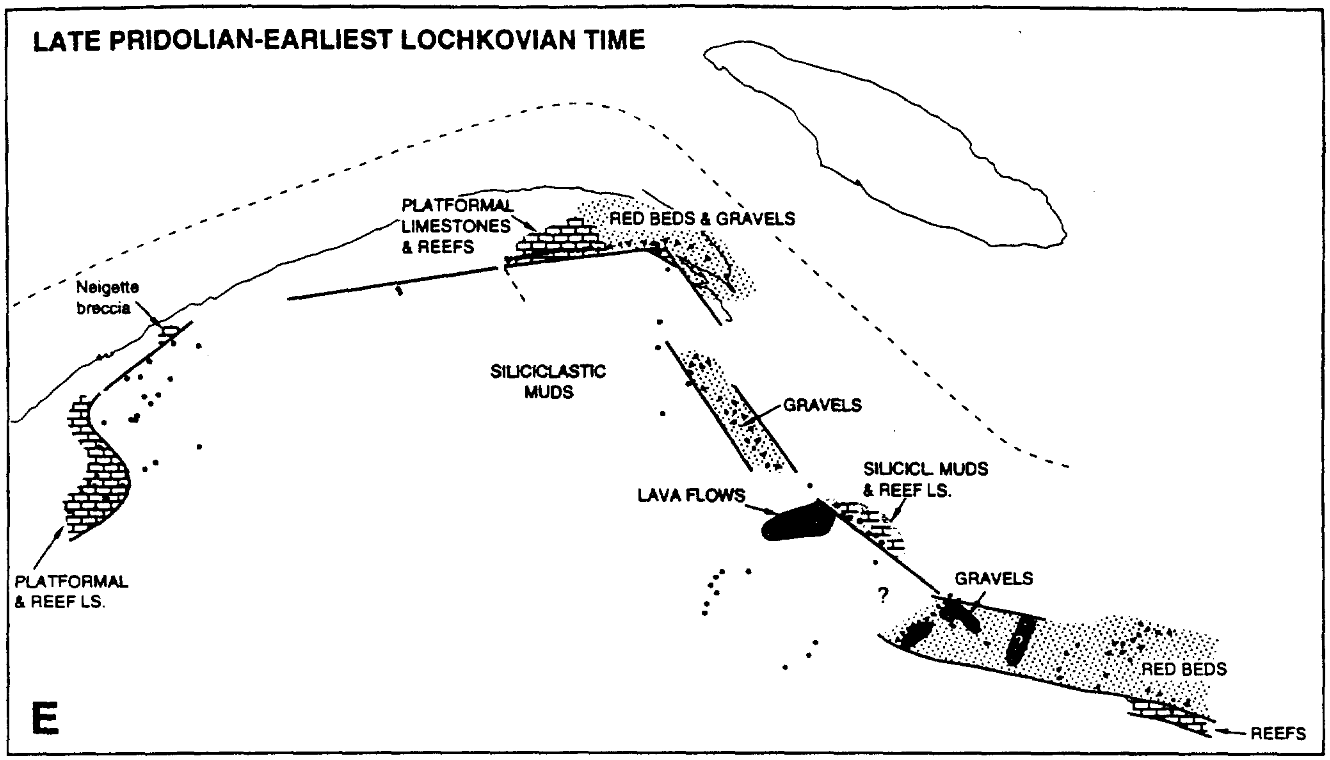

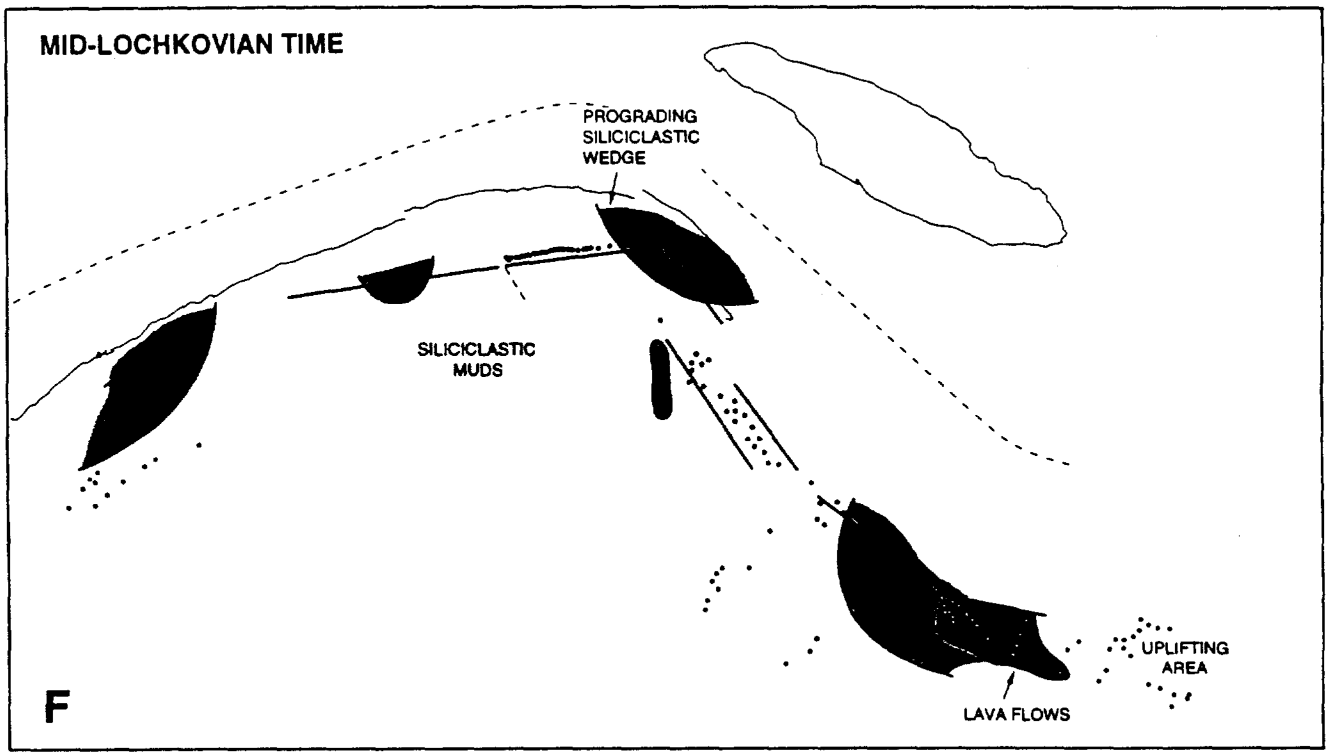

Figure 1.13 - *Paleogeography of the Gaspé Belt during the Late Ordovician-Early Devonian time interval. (A) Palinspastic base map of the Gaspé Belt basin showing distribution of the measured sections (see Fig. 1.4) at time of deposition of the Late Ordovician to Earliest Devonian facies. Dashed lines indicate approximate position of lithostratigraphic profiles of Figures 1.5-1.7. (B-F) Five selected time slices to illustrate paleogeography. Black arrows are sediment transport direction. From Bourque, Malo and Kirkwood (submitted, 1996).*

paleocurrent direction measurements in southern Matapédia Valley and central Gaspé Peninsula indicating a source area to the north (Ducharme, 1979; Malo, 1988). This implies that these regions were closer than they are now to Anticosti platform during time of deposition.

1.6.2 Early Wenlockian

During early Wenlockian time (Fig. 1.13C), limestone deposition dominated shallow water areas of the Gaspé Belt, on the Sayabec platform in the west and the northwest, and the La Vieille platform in the southeast. It is not clear whether these two very similar platforms (Lavoie et al. 1992) were connected or not, nor if the Sayabec platform extended into the northeasternmost part of the Northern Outcrop Belt. Grain composition of the carbonate sand and gravel body (Laforce Formation) in the clay basin (Burnt Jam Brook Formation) that succeeded to the lime turbidites of the Matapédia Group points to dismemberment of shallow water carbonates. This material was derived either from erosion of the Anticosti platform, thus indicating connection between the Anticosti platform and the Gaspé Belt basin, or from erosion of the coeval Sayabec-La Vieille platform, in which case the Sayabec-La Vieille was forming a single continuous carbonate belt. In the northwest, the Sayabec platform was bordering a terrestrial red bed area, whereas the land facies north of the La Vieille platform is unknown.

1.6.3 Mid-Pridolian

Mid-Pridolian time was marked by two major events: the climax of the sea-level lowstand of the R2 regressive phase (Fig. 1.8) and the Salinian Disturbance. Both contributed to caused local subaerial erosion. Significant thickening of the Saint-Léon Formation southwest of the Grande Rivière-Gastonguay fault (Figs. 1.5-1.7) testifies to accelerated subsidence and sedimentation in the basin related to occurrence of an active synsedimentary fault ancestral to the Grande Rivière-Gastonguay fault (Fig. 1.13D). Initiation of this ancestral fault shows to be diachronous from southeast to northeast. Indeed sediment thickening first occurred within the Burnt Jam Brook Formation (Upper Llandovery) in the Escuminac-Percé (Fig. 1.5) and the Route 299-Ascah Lake (Fig. 1.6) segments, whereas it occurred first within the Saint-Léon Formation (Pridoli) in the Northern Outcrop Belt (Fig. 1.5). Erosion of several hundreds of meters of strata (up to 1500 m in the Ristigouche syncline, 500 m in the Saint-Jean River anticline, and 400 m in the Northern Outcrop Belt, not taking into account compaction and subsidence) cannot be explained by sea-level fall only, and is more likely related to local fault-controlled block uplifting. Present-day main strike-slip faults such as the Neigette, Shickshock, Bassin-Nord-Ouest, Troisième Lac, Gastonguay, and Grande Rivière faults (see geological map of Gaspé Peninsula for location) probably had synsedimentary ancestors that started to act during Pridolian time (Salinian Disturbance), and possibly earlier for some (e.g. Grande Rivière and Gastonguay faults). Seismic sections in northeastern Gaspé Peninsula (Roksandic and Granger, 1981; SOQUIP, unpublished data) support the block faulting hypothesis. To the west, the Neigette fault of the Témiscouata-Lake Matapédia area (Fig. 1.13D) has been shown to have acted as normal synsedimentary fault during late Pridolian time (Dansereau and Bourque, 1988; Dansereau, 1989). It is likely that the thick deep water gravel facies (Lac des Baies Member) recorded in this area was related to active faulting during mid-Pridolian time.

Deep water mounds followed by shallow water microbial-algal reefs established on top or at margin of uplifted blocks in southern and central parts of the Gaspé Belt, and made the foundation of the West Point reef tract (Bourque et al., 1989). In western part of the belt (Témiscouata region), mound and reef facies of similar composition were recognized as large clasts in calcidebrites related to dismemberment of mounds and reefs north of the Neigette ancestral fault (Dansereau, 1989). Further west, the age of the Lac Croche carbonates is poorly constrained, and it is not certain if carbonate shoal developed at that time or later.

In southeastern part of the basin, thick transitional alkalic-tholeiitic basalts accumulated, possibly related to faulting (Dostal et al., 1994).

1.6.4 LATE PRIDOLIAN-EARLIEST LOCKHOVIAN

Late Pridolian time (Fig. 1.13E) is characterized by terrestrial red beds and a distinctive reef tract. The reef tract is formed by the West Point Formation in the east and the center of the Gaspé Belt, and the Lac Croche Formation in the west. It is made up either of barrier reefs, or cluster of individual reefs, or isolated patch and pinnacle reefs (Bourque et al., 1986). Although occurring patchily due to lack of outcrop continuity, it can be followed all along the Gaspé Belt between the Chaleurs Bay synclinorium and the Témiscouata region, for a distance of *circa* 700 km, and further southwest in Eastern Townships of Québec (Hughson and Stearn, 1989; Lavoie and Bourque, 1992), giving the reef tract a possible total extension of about 1000 km. The West Point reef tract developed at margin of a wide siliciclastic red bed land area. It seems likely that during that time, the Anticosti Platform was totally covered by red beds. Furthermore, red beds of the same age, the Clam Bank Group, also occur in western Newfoundland, on the southeast side of the St. Lawrence Promontory. Marine carbonates, like microbial laminites and stromatoporoid rubbles, and shallow water marine gravels, associated locally with the red beds, testify to sporadic marine invasion. South of the reef tract, fine-grained siliciclastic facies were deposited in outer shelf to basin environment. Consequently, the reef tract developed in a siliciclastic-dominated setting.

During earliest Lochkovian time, at beginning of transgression T2, the reefs were buried under fine-grained siliciclastics in southeastern part of the Gaspé Belt (Chaleurs Bay synclinorium), while pinnacle reefs grew up to 300 m on the carbonate platform of the Northern Outcrop Belt and the East-Central Outcrop Belt.

1.6.5 Mid-Lochkovian

In Early Devonian time (mid-Lochkovian), subsidence of the shelf and progradation of siliciclastic sediment wedges has buried the reefs and carbonate platforms (Fig. 1.13F). Burial depth indicators suggest that no Devonian deposits occurred in Québec part of the Chaleurs Bay synclinorium (Nowlan and Barnes, 1987; Savard and Bourque, 1989; Lavoie and Bourque, 1993; Y. Héroux, pers. comm. to P.-A. Bourque), suggesting that the area was uplifting in response to the diachronous building up of the Acadian orogeny, early in the Devonian. Submarine intraplate tholeiitic basalts and intermediate lava flows occurred in the northwest-southeast-oriented segment of the shelf (Dalhousie and Black-Cape volcanics) associated with shallow water sediments, and in the adjacent basin (Baldwin volcanics).

1.7 Controls on reef settlement and development

1.7.1 Reefs of the Sayabec platform

The model proposed for the La Vieille carbonate platform in the Chaleurs Bay synclinorium (Fig. 1.14) is applicable for the Sayabec platform in northern Gaspé Belt (Bourque et al., 1986; Lavoie et al., 1992). The reefs on this platform are low algal-coral-bryozoan knobs that developed at margin of extensive peritidal flat belt, in very shallow low energy environment. These reefs had limited primary porosity because the metazoan frame is thoroughly encrusted by stromatolitic material and infiltrated by lime mud. However, a belt of clean carbonate sands with higher primary porosity lies seaward of the reef belt.

In northeastern part of the Northern Outcrop Belt, the easternmost outcrops of the Sayabec Formation occur in the Madeleine River area (Figs. 1.5, 1.13C; Lachambre, 1987; Lavoie et al., 1992). No reefs occur there, but rather the peritidal facies, implying that the reef belt and the well-sorted clean carbonate sand belt lie south of the outcrop belt in subsurface.

1.7.2 The West Point reef platform and pinnacle reefs

As stated above, the West Point Formation is divisible into two reefal limestone packages: the Upper Silurian reef and bank complexes (Fig. 1.8), better developed in the Chaleurs Bay area, but also occurring in northeastern Gaspé; and the Lower Devonian pinnacle reefs (Fig. 1.10) mainly known in the Northern Outcrop Belt and the East-Central Outcrop Belt. For sake of practicability, we refer here to the Silurian West Point, and the Devonian West Point, respectively.

Silurian West Point

Of the three complexes of the Silurian West Point, the upper reef complex is the best developed, presenting a well laterally zoned reefal platform with facies from supertidal plain to reef margin (Fig. 1.9). For one, the landward part of this complex is made up of distinctive stromatoporoid

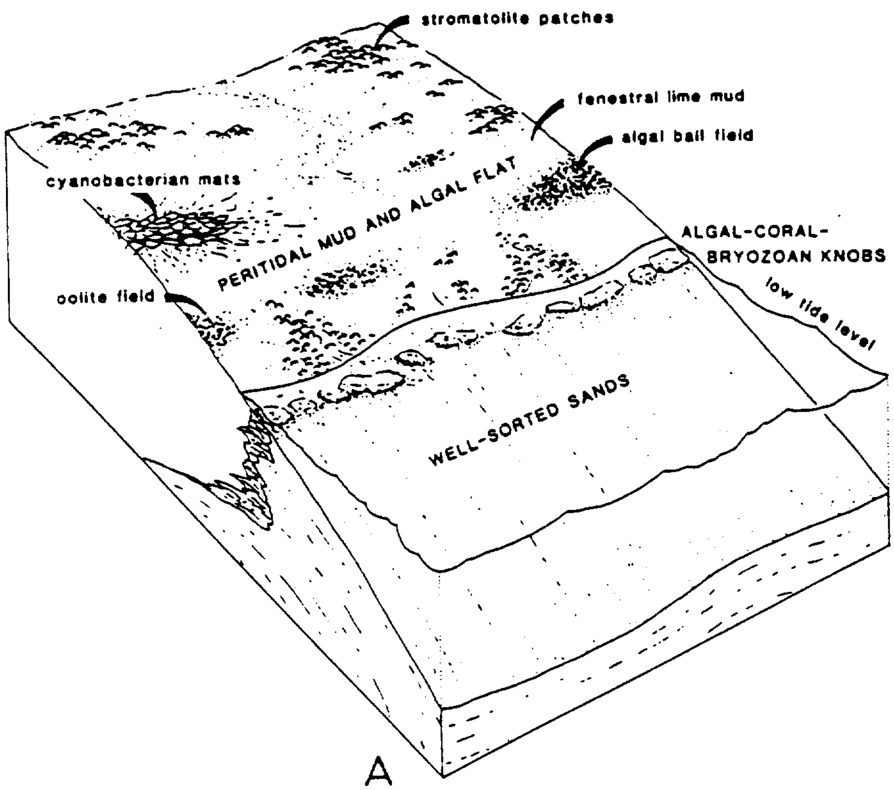

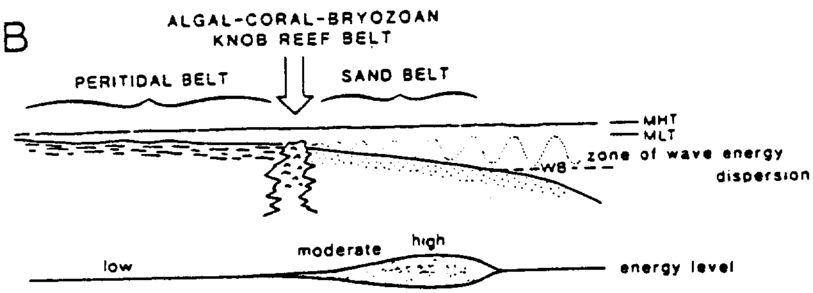

Figure 1.14 - *Model of the La Vieille carbonate platform (Chaleurs Bay synclinorium) in Early Wenlockian time. (A) Block diagram illustrating main features of platform. (B) Profile of platform and energy level. MHT: mean high tide; WB: wave base. From Bourque et al. (1986).*

rubbles, microbial laminites and mudcracked red beds, an assemblage also found above the Griffon Cove River conglomerate in easternmost part of the Northern Outcrop Belt (best exposure at Rivière-au-Renard Road section). Moreover, this Silurian West Point in the Northern Outcrop Belt has recorded the same four sedimentary cycles recorded in the Chaleurs Bay sections (Figs. 1.9, 1.12). Presence of the stromatoporoid rubble, interpreted in the Chaleurs Bay area as being derived from the reef margin during hurricanes (Bourque et al., 1986), suggests occurrence of a reef margin south of the Northern Outcrop Belt. Occurrence of all facies of the three Silurian West Point complexes in large clasts of a fault-controlled breccia (Neigette breccia, Fig. 1.13E) south of Rimouski in Matapédia Valley area also supports the idea that the Silurian West Point developed along the northern margin of the Gaspé Basin (Dansereau and Bourque, 1988; Dansereau, 1989).

Devonian West Point

The Devonian West Point differs from the Silurian one. It is made up of two main facies: a shallow water well-bedded crinoidal limestone, and massive stromatoporoid pinnacle reefs. The bedded crinoidal limestone is a thin sheet (a few 10's of meters thick maximum) traced all along the Northern and East-Central Outcrop Belts. A number of pinnacle reefs reaching thicknesses of 300 m are known along the Northern Outcrop Belt, between the Madeleine River and the road 299 (mapping by Lachambre, 1987; Fig. 1.15 herein). One of these pinnacle, the Madeleine River buildup, was the object of a detailed study (Bourque, 1972, 1977; Fig. 1.10 herein) and serves as model.

The reefs show a vertical zonation, from bedded crinoid-dominated grainstones-packstones and rudstones (facies B and C, Fig. 1.10) to massive stromatoporoid boundstones and rudstones (facies D and E). Facies C contains a significant proportion of well-rounded quartz grains similar to those of the underlying Val-Brillant Formation, suggesting that erosion of the latter was taking place during that part of reef growth. Interestingly, basal facies A is a stromatactis mudstone (a facies not recognized by Bourque at time of study in 1968-70), a facies similar to the Gros Morbe member of the Silurian West Point in Chaleurs Bay. However, no actual dating is available for that particular facies. The Devonian age given to the base of the Madeleine River buildup (Bourque, 1977) is based on brachiopod collections from facies B above the unconformity. The possibility that Silurian West Point occurs at base of pinnacle reefs is therefore left open. Reef breccias with cm- to m-sized clasts (facies F) occur at foot of the Madeleine River buildup. Two types of breccia occur: breccia with limestone matrix and breccia with fine-grained siliciclastic matrix. Clasts are often composed of stromatoporoid limestone, suggesting that breccia is syn- or post facies D and E deposition. Detailed sedimentological and diagenetic study should provide clue information as to the timing of breccia deposition and reef cementation history.

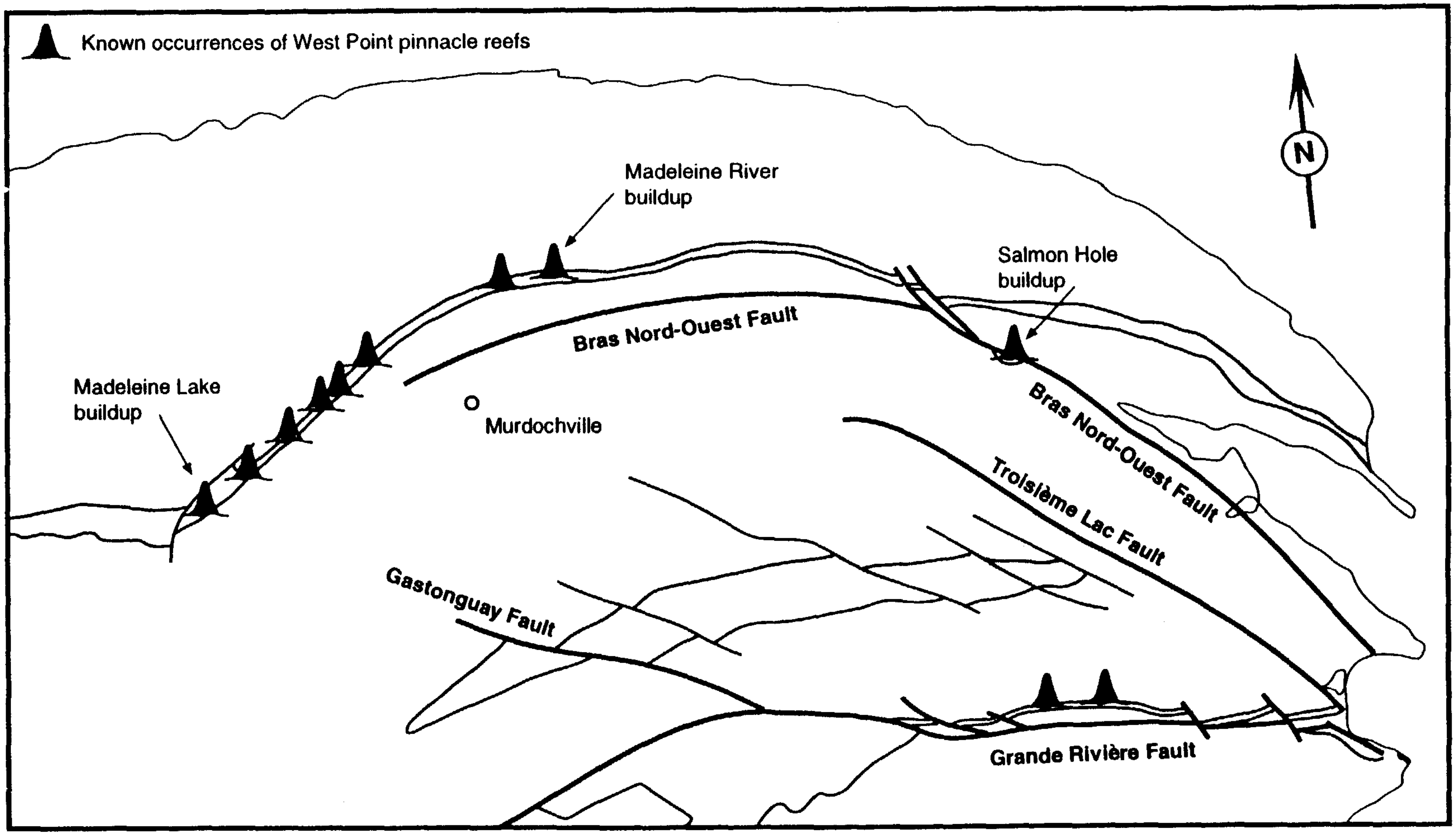

Figure 1.15 - *Distribution of known surface occurrences of Devonian West Point pinnacle reefs.*

1.7.3 MODEL FOR REEF SETTLEMENT AND DEVELOPMENT

We have shown above that the Salinian Disturbance produced extensional tectonic regime and block faulting in northeastern Gaspé Peninsula. Some of the SOQUIP seismic profiles indicate moreover tilting of the faulted blocks during the Salinian tectonics. For instance, a cross-section built from profiles P-19, P-20 and P-31 (Fig. 1.16) shows that thickening of the Chaleurs Group and Upper Gaspé Limestones from the south-west to the north-east occurs in both the central and the northeast blocks. Roksandic and Granger (1981) illustrated this trend very well in the northeast block.

The following model is proposed to illustrate the tectono-sedimentary evolution of the northeastern Gaspé Peninsula during Silurian-Early Devonian time, that is between the Taconian and Acadian orogenies (Fig. 1.17).

Stage 1. Sedimentation of the Matapédia - Burnt Jam Brook - Laforce - base of the Saint-Léon and Gascons units in a post-Taconian successor basin. Birth of the Grande Rivière-Gastonguay break during sedimentation of the Burnt Jam Brook. This major break forms a hinge line that separates the shelf part of the basin to the northeast (northeastern Gaspé Peninsula) from the basinal part to the southwest. Progressive burial of the Matapédia and the Burnt Jam Brook.

Stage 2. Generalized marine regression (Bourque, 1989) and block-faulting of the shelf by nascent ancestral Bassin Nord-Ouest and Troisième Lac faults delimiting three blocks: the SW, central and NE blocks. Culmination of the Salinian Disturbance. Important erosion on the NE block where all of the Silurian succession is removed, producing extensive Salinian unconformity. Erosion of emerged parts of the central and SW blocks producing local Salinian unconformities. Establishment of Silurian West Point in the form of reef complexes at margin of faulted blocks. Four T-R cycles recognized in the reef and peri-reef facies. The wedged infilling of the Chaleurs Group sediments indicates block tilting along normal listric faults.

Stage 3. Beginning of the T2 transgression. Settlement of the Devonian West Point pinnacle reefs on shoals provided by former Silurian reefs and/or paleotopographic highs left by the Salinian erosion (Figure 1.5 shows a close correspondence between highs left by Salinian erosion and location of pinnacle reefs).

Stage 4. Later phase of T2 transgression. Burial of the reefs by fine-grained siliciclastic sediments. Continuation of tilting and block-faulting expressed by the wedged sedimentation in the upper part of the Chaleurs Group and the Upper Gaspé Limestones. Following stage 4, marine regression (not illustrated) related to beginning of the Acadian Orogeny lead to sedimentation of the Gaspé Sandstones in a coastal and terrestrial environment.

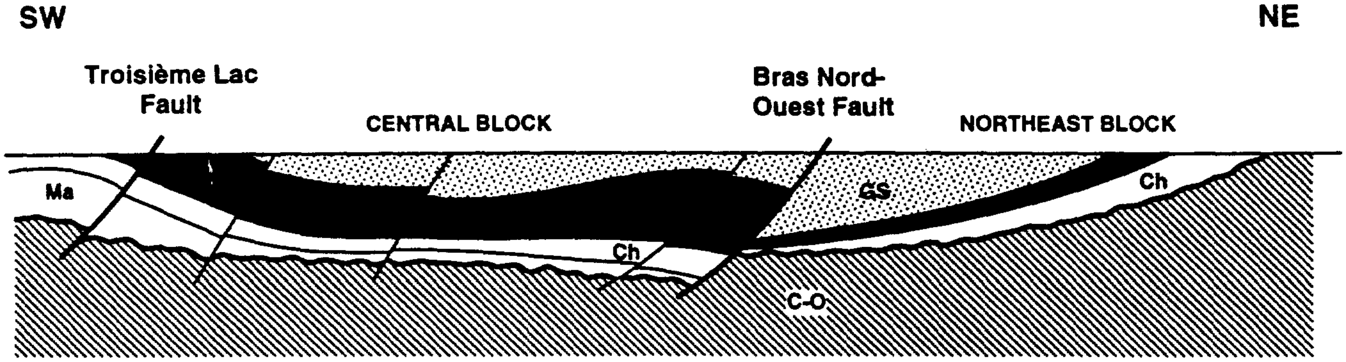

Figure 1.16 - *Geological cross-section inferred from* SOQUIP *seismic profiles P-19, P-10, and P-31. C-O: Taconian-deformed Cambrian-Ordovician rocks; Ma: Matapédia Group; Ch: Chaleurs Group; UGL: Upper Gaspé Limestones; GS: Gaspé Sandstones.*

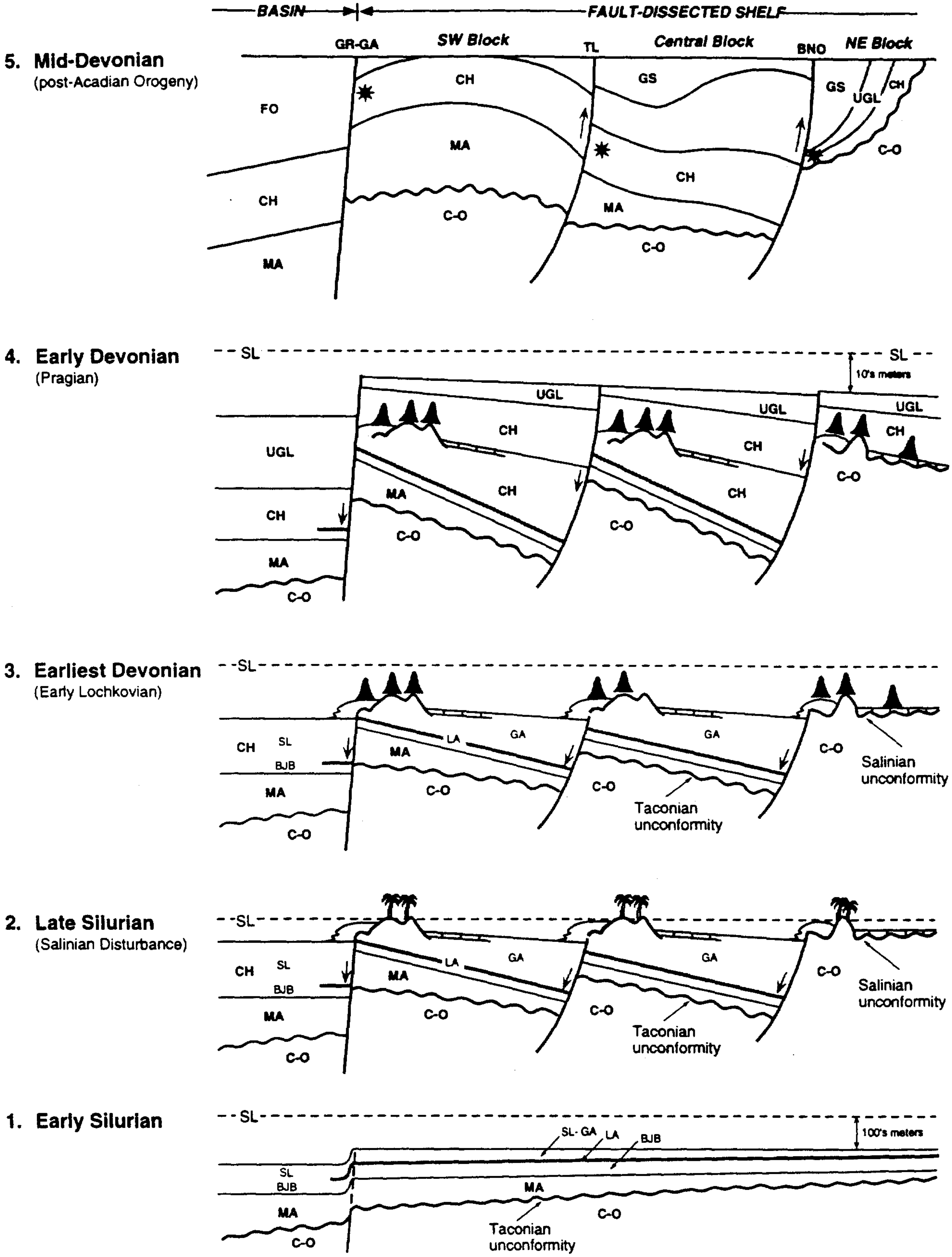

Figure 1.17 - *Tectono-sedimentary evolution of the northeastern part of the Gaspé Basin during the Early Silurian-Early Devonian time interval. C-O: Taconian-deformed Cambrian-Ordovician rocks; Ma: Matapédia Group; Ch: Chaleurs Group; UGL: Upper Gaspé Limestones; GS: Gaspé Sandstones; BJB: Burnt Jam Brook Formation; LA: Laforce Formation; SL: Saint-Léon Formation; GA: Gascons Formation. GR-GA: Grande Rivière-Gastongay fault; TL: troisième Lac fault; BNO: Bras Nord-Ouest fault. SL on dashed line: sea level.*

Stage 5. Acadian orogeny brings about a reversal of the movement along the major faults (from normal to strike-slip with a reverse component) which produces the present distribution of the Siluro-Devonian strata.
Probability of finding reefs in subsurface is therefore greater in the vicinity of the faults (stars on Fig. 1.17).

1.8 OIL PLAY IN NORTHEASTERN GASPÉ PENINSULA

Key points for evaluating the oil potential in northeastern Gaspé with respect to the Salinian Disturbance and its effects are the following.

1. Extensional tectonic regime of the Salinian Disturbance may have provided suitable plumbing system for oil migration at various time during the mid-Silurian-early Devonian time interval, for instance, for oil that may have been generated in the underlying Cambro-Ordovician shales.
2. The basin fluid migration path is not a simple one of updip migration from center of the basin to margins, which is a northeastward direction, as it would be the case if the shelf was not dissected by synsedimentary faulting. Rather, the migration should have been updip southwestward on each faulted block (Fig. 1.18).
3. There is significant change in formation thickness due to block tilting. These thickness variations should be taken into account when evaluating thermal maturation.
4. The extensional Salinian tectonics may well have fractured buried limestone units such as the Matapédia, the Sayabec, and the Laforce, and created fracture porosity.
5. The Silurian West Point reef complexes probably developed at margin of faulted blocks (Fig. 1.17). If such is the case, and according to our model of reef settlement, they should be looked for in subsurface:
   (1) southeast and south of the Northern Outcrop Belt between the Madeleine Lake and Salmon Hole buildups, particularly in the vicinity of the E-W trending portion of the Bras Nord-Ouest fault;
   (2) northeast of both the Bassin Nord-Ouest and the Troisième Lac faults.
6. The Devonian West Point pinnacle reefs may also occur in subsurface southeast and south of the Northern Outcrop Belt, as well as northeast of the Bassin Nord-Ouest and the Troisième Lac faults.
7. The subsurface area north of the East-Central Outcrop Belt (Grande Rivière fault) looks, for the moment, less attractive since it represents a "back-reef" area, although it is the only reefoid limestones where significant dolomitization has been observed (see Chapter 2).
8. The Devonian West Point crinoidal limestone sheet has a significant extension. Indeed, besides its surface occurrence in the Northern and East-Central Outcrop Belts (Figs. 1.5 and 1.7), St-Julien and Bourque (1990) have traced on SOQUIP seismic profiles P-11, P-13, P-15, P-16, P-17 and P-32 a reflector within the Chaleurs Group in a position compatible with the

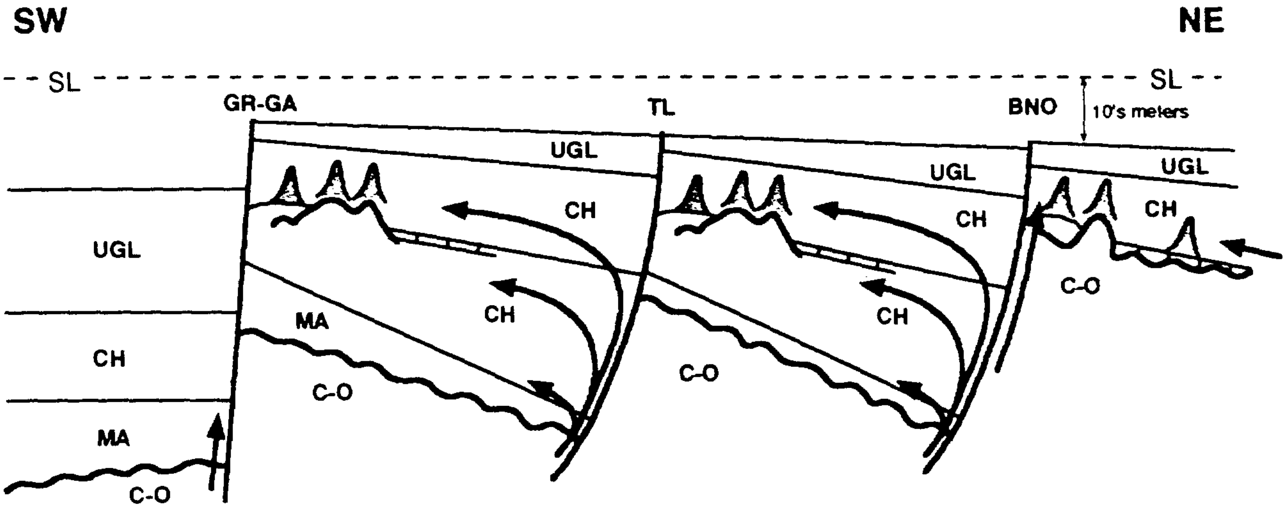

B. During Early Devonian time

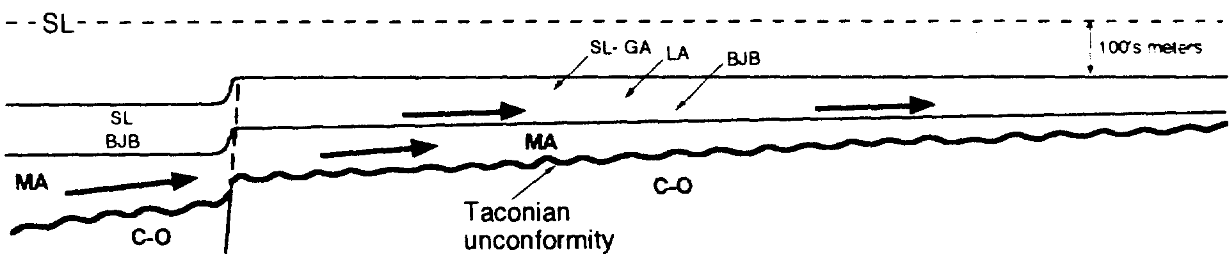

A. During Early Silurian time

Figure 1.18 *- Fluid migration path in northeastern part of the Gaspé Basin during (A) Early Silurian time and (B) Early Devonian time, according to model of Figure 1.17.*

stratigraphic position of this limestone sheet. The extent of the sheet seems to be particularly important within the NE and central blocks.

9. Key questions as to the reservoir potential of the Silurian-lower Devonian limestones, and the influence of the Salinian Disturbance are:
   - When did the high growth framework primary porosity of the reefs close?
   - Did extensional tectonic regime during and after the Salinian peak produce fracture porosity possibly enlarged by karstification?
   - Is there any evidence of secondary dolomitization or karst porosity in the carbonates units (Matapédia, Sayabec, West Point) related to subaerial exposure or fresh-water recharge related to the Salinian Unconformity?
   - Did the four sea-level lowstands at the end of Pridolian time create karst porosity in the platform-edge reefs of the Silurian West Point (Figs. 1.9, 1.12)?
   - Is there any vertical and/or lateral trends in reef limestone diagenesis that could predict high porosity sectors?

1.9 RECOMMENDATIONS

(1) New seismic work should explore the area south of the Northern Outcrop Belt between Madeleine Lake and Salmon Hole buildups, in order to decipher the effects of the E-W trending part of the Bassin Nord-Ouest fault on facies deposition and to detect possible reefs in subsurface.

(2) The older seismic lines that cross the Bassin Nord-Ouest and Troisième Lac faults should be re-examined to search for reefs on northeast side of the faults.

(3) A number of West Point buildups mapped by Bourque (1977) and Lachambre (1987) along the Northern Outcrop Belt should be revisited to check whether or not the Silurian West Point developed in that area (the Madeleine Lake buildup is to be checked particularly).

(4) A diagenetic study of the limestone horizons, particularly the reefal and the clean carbonate sand facies of the Sayabec and West Point Formations, should be carried out to decipher porosity history.

(5) A diagenetic study of the clean Val-Brillant Sandstone is worthy of being carried out in order to evaluate the reservoir potential of this unit.

(6) An integrated study of structural geology, cement stratigraphy and geochemistry in fractures, and fluid inclusion analysis of fracture cements should be carried out in order to check the timing of fractures, the extent to which they served as pipes during basin fluid migration, the nature of transported fluids, and the extent to which fracturation created porosity.

REFERENCES

Amyot, G., 1984. Lithostratigraphie de sous-surface de l'est de la Gaspésie. Ministère de l'Énergie et des Ressources du Québec, **ET 83-11**, 75 p.
Béland, J., 1980. Faille du Bassin Nord-Ouest et faille du Troisième Lac dans la partie est de la Gaspésie. Ministère de l'Énergie et des Ressources du Québec, rapport intérimaire **DP-740**, 20 p.
Berger, J., and Ramsay, E., 1993. Étude structurale et pétrologique de la région du mont de la Serpentine. Ministère de l'Énergie et des Ressources du Québec, Rapport final **MB 93-22**, 44 p.
Bertrand, R., 1987. Maturation thermique et potentiel pétroligène des séries post-taconiennes du nord-est de la Gaspésie et de l'Île d'Anticosti. Thèse de doctorat, Université de Neuchâtel, 550 p.
Boucot, A.J., 1962. Appalachian Siluro-Devonian. *In* Coe, K. (ed.) Some aspects of the Variscan fold belt. Manchester University Press, Manchester, England, 155-163.
Bourque, P.-A., 1972. Le complexe carbonaté de Lefrançois dans sa région type, Gaspé-Nord. Ministère des Richesses naturelles, Québec, **DP-46**, 26 p.
Bourque, P.-A., 1975. Lithostratigraphic framework and unified nomenclature for Silurian and basal Devonian rocks in eastern Gaspé Peninsula, Québec. Canadian Journal of Earth Sciences, **12**: 858-872.
Bourque, P.-A., 1977. Silurian and basal Devonian of northeastern Gaspé Peninsula: Québec, Department of Natural Resources, Special Paper **ES-29**, 323 p.
Bourque, P.-A., 1989. The Late Silurian-Early Devonian transgression of eastern Gaspé Peninsula. *In* Bourque, P.-A., Hesse, R., and Rust, B., 1989: Sedimentology, Paleoenvironments and Paleogeography of the Taconian to Acadian Rock Sequence of Gaspé Peninsula. Geological Association of Canada, Annual Meeting, Montréal, Guidebook to fieldtrip **B8**, 159-165.
Bourque, P.-A., Amyot, G., Desrochers, A., Gignac, H., Gosselin, C., Lachambre, G., and Laliberté, J.-Y., 1986. Silurian and Lower Devonian reef and carbonate complexes of the Gaspé Basin, Québec - A summary. Bulletin of Canadian Petroleum Geology, **34**, 452-489.
Bourque, P.-A., Brisebois, D., and Malo, M., 1995. Gaspé Belt. *In* H. Williams (ed.), Chapter 4 of Geology of the Appalachian-Caledonian Orogen in Canada and Greenland. Geological Society of America, The Geology of North America, **F-1**, 316-351.
Bourque, P.-A., Gosselin, C., Kirkwood, D., Malo, M., and St-Julien, P., 1993. Le Silurien du segment appalachien Gaspésie-Matapédia-Témiscouata: stratigraphie, géologie structurale et paléogéographie. Ministère de l'Énergie et des Ressources du Québec, **MB 93-25**, 115 p. + 23 maps.
Bourque, P.-A., Hesse, R., and Rust, B., 1989. Sedimentology, paleoenvironments and paleogeography of the Taconian to Acadian rock sequence of Gaspé Peninsula. Geological Association of Canada, Annual Meeting, Montréal, Guidebook to fieldtrip **B8**, 245 p.

Dalton, E, 1987. Sedimentary facies and diagenesis of the Lower Devonian Temiscouata and Fortin Formations, Northern Appalachians, Québec and New Brunswick. McGill University, Montréal, Unpublished M.Sc. thesis, 228 p.

Dansereau, P., 1989. Sédimentologie et diagenèse de la brèche calcaire de Neigette, Silurien supérieur du bassin de Gaspésie. Laval University, Québec City, Unpublished M.Sc. Thesis.

Dansereau, P., and Bourque, P.-A., 1988. A peculiar limestone breccia related to Late Silurian synsedimentary faulting in the Gaspé Basin, Québec Appalachians. Geological Association of Canada, Annual Meeting, St. John's, Newfoundland, Program with Abstracts, **13**, A28.

David, J., and Gariépy, C., 1986. Geochemistry of the Lower Pointe aux Trembles and Lac Raymond Formations, central Québec Appalachians: a preliminary report. *In* Current Research, Part B, Geological Survey of Canada, Paper **86-1B**, 131-140.

Dostal, J., Laurent, R., and Keppie, J.D., 1993. Late Silurian-Early Devonian rifting during dextral transpression in the southern Gaspé Peninsula (Québec): petrogenesis of volcanic rocks. Canadian Journal of Earth Sciences, **30**, 2283-2294.

Doyon, M., and Dalpé, C., 1993. Roches magmatiques siluro-dévoniennes de la Gaspésie. Ministère de l'Énergie et des Ressources du Québec, **MB 93-16**, 128 p.

Ducharme, D., 1979. Pétrographie du flysch de l'Ordovicien supérieur et du Silurien inférieur - Anticlinorium d'Aroostook-Percé, Gaspésie, Québec. University of Montréal, Montréal, Unpublished M.Sc. Memoir.

Dunning, G.R., O'Brien, S.J., Colman-Sadd, S.P., Blackwood, R.F., Dickson, W.L., O'Neil, P.P., and Krogh, T.E., 1990. Silurian Orogeny in the Newfoundland Appalachians. Journal of Geology, **98**, 895-914.

Globensky, Y. (coord.), 1993. Région des Appalaches, des Basses-Terres du Saint-Laurent et des Iles de la Madeleine. *In* Lexique stratigraphique canadien, Québec, Ministère de l'Énergie et des Ressources du Québec, **DV 91-23**, 327 p.

Héroux, Y., Bertrand, R., Achab, A., and Chagnon, A., 1983. Évolution thermique de l'extrémité orientale de la péninsule de Gaspé, en relation avec les déformations tectoniques. Ministère de l'Énergie et des Ressources du Québec, **DP 83-03**, 85 p.

Hesse, R., and Dalton, 1989. The Devonian Fortin Formation. *In* Bourque, P.-A., Hesse, R., and Rust, B. (eds.), 1989, Sedimentology, paleoenvironments and paleogeography of the Taconian to Acadian rock sequence of Gaspé Peninsula. Geological Association of Canada, Annual Meeting, Montréal, Guidebook to fieldtrip **B8**, 57-70.

Hibbard, J., 1994. Kinematics of Acadian deformation in the northern and Newfoundland Appalachians. Journal of Geology, **102**, 215-228.

Hughson, R.C., and Stearn, C.W., 1989. Upper Silurian reefal facies of the Memphremagog-Dudswell area, Eastern Townships, Québec Appalachians. *In* Geldsetzer, H.H., James, N.P., and Tebbut, G. (eds.), Reefs: Canada and adjacent areas. Canadian Society of Petroleum Geologists, Memoir **13**, 306-315.

Kirkwood, D., 1989. Géologie structurale de la région de Percé. Ministère de l'Énergie et des Ressources du Québec, Étude **ET 87-17**, 42 p.

Kirkwood, D., 1993. Étude qualitative et quantitative de la déformation acadienne du bassin siluro-dévonien de la péninsule gaspésienne, Appalaches du Nord. Laval University, Québec City, Unpublished M.Sc. Thesis.

Lachambre, G., 1987. Le Silurien et le Dévonien basal du Nord de la Gaspésie. Ministère de l'Énergie et des Ressources du Québec, **ET 84-06**, 83 p.

Lajoie, J., 1968. Dispersal and petrology of the Silurian Val-Brillant and Robitaille sandstones, Appalachians, Québec. Journal of Sedimentary Petrology, **38**, 643-647.

Lavoie, D., 1988. Stratigraphie, sédimentologie et diagenèse du Wenlockien (Silurien) du Bassin de Gaspésie-Matapédia. Laval University, Québec, Unpublished Ph.D. thesis.

Lavoie, D., 1992a. Lower Devonian facies in Forillon Peninsula, eastern Gaspé, Québec Appalachians; a storm-influenced, carbonate outer shelf. Bulletin of the Canadian Petroleum Geology, **40**, 303-320.

Lavoie, D., 1992b. Carbonate sedimentation in an extensional tectonic regime; the Lower Devonian Upper Gaspé Limestones, Québec Appalachians. Canadian Journal of Earth Sciences, **29**, 118-128.

Lavoie, D., and Bourque, P.-A., 1992. Stratigraphy, paleoenvironmental evolution and regional significance of the Silurian Lake Aylmer-Lake Saint-François belt, Eastern Townships, Québec. Atlantic Geology, **28**, 243-255.

Lavoie, D. and Bourque, P.-A. 1993. Marine, burial and meteoric diagenesis of Early Silurian carbonate ramps, Québec Appalachians, Canada. Journal of Sedimentary Petrology, **63**, 233-247.

Lavoie, D., Bourque, P.-A., and Héroux, Y., 1992. Early Silurian carbonate platform in the Appalachian orogenic belt: the Sayabec-La Vieille Formation of the Gaspé-Matapédia Basin, Québec. Canadian Journal of Earth Sciences, **29**, 704-719.

Lespérance, P.J., Malo, M., Sheehan, P.M., and Skidmore, W.B., 1987. A stratigraphical and faunal revision of the Ordovician-Silurian strata of the Percé area, Québec. Canadian Journal of Earth Sciences, **24**, 117-134.

Malo, M., 1979. L'axe Aroostook-Matapédia au nord de Chandler, Gaspésie, Québec. Laval University, Québec City, Unpublished M.Sc. Thesis.

Malo, M., 1986. Stratigraphie et structure de l'anticlinorium d'Aroostook-Percé en Gaspésie, Québec. University of Montréal, Montréal, Unpublished Ph.D. Thesis.

Malo, M., 1988. Stratigraphy of the Aroostook-Percé anticlinorium in the Gaspé Peninsula, Québec. Canadian Journal of Earth Sciences, **25**, 893-908.

Malo, M., and Béland, J., 1989. Acadian strike-slip tectonics in the Gaspé Region, Québec Appalachians. Canadian Journal of Earth Sciences, **26**, 1764-1777.

Malo. M., and Bourque, P.-A., 1993. Timing of the deformation events from Late Ordovician to Mid-Devonian in the Gaspé Peninsula. *In* D.C. Roy and J.W. Skehan (eds.), The Acadian Orogeny: Recent Studies in New England, Maritime Canada and the Autochtonous Foreland. Geological Society of America, Spec. Paper **275**, 101-122.

Malo. M., and Kirkwood, D., 1996. Faulting and progressive strain history of the Gaspé Peninsula in post-Taconian time: A review. *In* Hibbard, J.P., van Staal, C.R., Cawood, P. A.

(eds.), Current Perspectives in the Appalachian-Caledonian Orogen. Geological Association of Canada Special Paper **41** (in press).

Nowlan, G.S., 1981. Late Ordovician-Early Silurian conodont biostratigraphy of the Gaspé Peninsula - a preliminary report. *In* Lespérance P.J. (ed.), Field Meeting Anticosti-Gaspé, Québec. Subcommission on Silurian Stratigraphy, Ordovician-Silurian Boundary Working Group, **2**, Stratigraphy and Paleontology, 257-291.

Nowlan, G.S., and Barnes, C.R., 1987. Thermal maturation of Paleozoic strata in eastern Canada from conodont colour alteration index (CAI) data with implication for burial history, tectonic evolution, hotspot tracks and mineral and hydrocarbon exploration. Geological Survey of Canada, Bulletin **367**, 47 p.

Rast, N., and Skeehan, J.W., 1993. Mid-Paleozoic orogenies in the Nort Atlantic: the Acadian Orogeny. Geological Society of America, Special Paper **275**, 1-26.

Roksandic, M.M., and Granger, B., 1981. Structural style of Anticosti Island, Gaspé Passage, and eastern Gaspé peninsula inferred from reflection seismic data. *In* Lespérance P.J. (ed.), Field Meeting Anticosti-Gaspé, Québec. Subcommission on Silurian Stratigraphy, Ordovician-Silurian Boundary Working Group, **2**: Stratigraphy and Paleontology, 211-221.

Rust, B.R., 1981. Alluvial deposits and tectonic style: Devonian and Carboniferous successions in Eastern Gaspé. *In* Miall, A.D. (ed.), Sedimentology and Tectonics in Aluvial Bsins. Geological Association of Canada, Special Paper **23**, 49-76.

Savard, M., and Bourque, P.-A., 1989. iagenetic evolution of a Late Silurian reef platform, Gaspé Basin, Québec, based on cathodoluminescence petrography. Canadian Journal of Earth Sciences, **26**, 791-806.

Skidmore, W.B., and Lespérance, P.J., 1981. ercé area, The White Head Formation. *In* Lespérance P.J. (ed.), Field Meeting Anticosti-Gaspé, Québec: Subcommission on Silurian Stratigraphy, Ordovician-Silurian Boundary Working Group, vol. **2**: Stratigraphy and Paleontology, 31-40.

St-Julien, P., and Bourque, P.-A., 1990. Report on a geological and geophysical evaluation of the Malbaie-Fortin-York area, Gaspé Peninsula (Permits 842, 843 and 844). Unpublished report to Pétro-Québec Inc.

Van Staal, C.R., and De Roo, J.A., 1996. Mid-Paleozoic tectonic evolution of the Appalachian central mobile belt in northern New Brunswick, Canada: collision, extensional collapse, and dextral transpression. Geological Association of Canada Special Paper **41** (in press).

Vennat, G., 1979. Structure et stratigraphie de l'anticlinorium d'Aroostook-Percé dans la région de Saint-Omer Carleton, Gaspésie, Appalaches du Québec. University of Montréal, Montréal, Unpublished M.Sc. Memoir.

CHAPTER 2

RESERVOIR POTENTIAL OF THE SILURIAN-DEVONIAN CARBONATE UNITS IN NORTHEASTERN GASPÉ PENINSULA - A PRELIMINARY EVALUATION

2 RESERVOIR POTENTIAL OF THE SILURIAN-DEVONIAN CARBONATE UNITS IN NORTHEASTERN GASPÉ PENINSULA - A PRELIMINARY EVALUATION

INTRODUCTION

This chapter presents results of phase 1 of our ongoing study on porosity evolution and reservoir potential of the carbonate units in the Silurian-Devonian succession of northeastern Gaspé Peninsula, that is the White Head lime turbidites, the Sayabec-Laforce platformal limestones, the West Point reefs and reef complexes, and the Upper Gaspé Limestones outer ramp facies. It is based on study of material in Laval University, INRS and GSC collections. This phase of the study is intended to serve as reference and guide for activities of phase 2.

QUESTIONS TO BE ADDRESSED

To evaluate reservoir potential of these carbonates, a number of questions should be addressed (see also Chapter 1 of this report, under Oil Play in Northeastern Gaspé), such as:

- When did the interparticulate and/or growth framework primary porosity of the limestones close?
- Did extensional tectonic regime during and after the Salinian peak produce fracture porosity possibly enlarged by karstification?
- Is there any evidence of secondary dolomitization or karst porosity in the carbonates units, for instance, related to subaerial exposure or fresh-water recharge during the Salinian unconformity?
- Any porosity related to subsurface diagenesis, for instance by dissolution?
- Can we detect any vertical and/or lateral trends in limestone diagenesis that could predict high porosity sectors?

METHODS

The fact that present day porosity is tight in outcrops does not imply that it was tight at time of hydrocarbon migration, and a diagenetic analysis of the limestone units is necessary to track porosity history and to answer these questions. Our ongoing diagenetic analysis is using tools such as conventional and cathodoluminescence (CL) petrography, C and O stable isotope geochemistry and fluid inclusion microthermometry.

P.-A. Bourque (Laval), D. Lavoie (GSC), M. Savard (GSC), M. Malo (INRS), P. Dansereau (Laval), and G. Chi (GSC)

Conventional petrography on stained (Dickson's method) thin-sections: assessment of nature and amount of primary porosity; search for karst features, dolomitization, enlarged fracture porosity; identification of main diagenetic events; selection of best samples for CL study.

CL petrography on polished thin-sections: cement stratigraphy; preliminary appraisal of diagenetic and porosity evolution; selection of samples suitable for microsampling for isotope analyses.

C and O isotope geochemistry on cements phases identified in CL: characterization of parent waters for each cement phase; interpretation of diagenetic environment and evolution of porosity.

Fluid inclusion microthermometry on cement phases selected after their isotopic trends: evaluation of precipitation temperatures and salinity of parent waters, to elaborate time-porosity curves.

PREVIOUS WORK

Although there has been some work on petrography of the White Head lime turbidite Formation (Bourque, 1977; Malo, 1986), its diagenetic evolution and porosity history is unknown. The diagenetic evolution of the Sayabec platformal limestones is known (Lavoie, 1988, Lavoie and Bourque, 1993), but needs to be revisited to evaluate porosity history. Diagenesis of the Laforce limestones is poorly constrained but exotic clasts show an internal cement succession distinct from the interparticulate one (Lavoie, 1988). Depositional facies and microfacies of the West Point in NE Gaspé is fairly well known (Bourque et al., 1986), but the diagenetic trends and porosity evolution in these limestones are virtually unknown. A more detailed account on previous diagenetic work for each units is found under respective headings.

This report is divided into four sections:
1. White Head Formation
2. Sayabec-Laforce formations
3. West Point Formation
4. Upper Gaspé Limestones

WHITE HEAD FORMATION

2.0.1 STRATIGRAPHY

The White Head is the upper formation of the Matapédia Group (Malo, 1988). It crops out mainly in the Aroostook-Percé anticlinorium, but also in the Gastonguay and Rivière Saint-Jean anticlines of the Connecticut Valley-Gaspé synclinorium. In the Percé area, the White Head Formation consists of four members: Burmingham, Côte de la Surprise, L'Irlande and Des Jean (Lespérance et al., 1987). The type section of the formation is located at Cap Blanc (White Head), whereas the four members have their own type section in the Percé area (Fig. 2.1). The first two members are Ordovician, whereas the other two are Silurian. The Côte de la Surprise Member contains an Hirnantian fauna (Lespérance and Sheehan, 1976) and the first limestone strata of the overlying L'Irlande Member is considered to be the base of the Silurian.

The descriptions below are from Lespérance et al. (1987). The Burmingham Member consists of thin-bedded, grey to brown calcilutite with thinner interbeds of brown, calcareous mudshale, sometimes finely sandy; bioclastic and sandy calcarenite is also present. The most abundant rock type of the Côte de la Surprise Member is a dark green, calcareous mudstone sometimes reddish brown to yellow in alteration. A well-sorted, light grey, fine-grained, calcareous, thin- to medium bedded quartzose arenite is found near the top of the member. The L'Irlande Member is composed of grey-brown calcilutite in regular 7-15 cm beds with 2-5 cm calcareous mudshale interbeds, and rare bioclastic thin-bedded calcarenite. In the middle part of the member, a brown to green clayshale, with rare thin-bedded calcilutite and calcarenite, is found. The basal part of the Des Jean Member is constituted of limestone conglomerate, calcarenite, calcilutite, and sandy limestone in thin to very thick beds. The upper part of the member consists of thin-bedded silty and argillaceous limestone, calcareous shale, and calcarenite lenses. Silty limestones and calcarenites of the White Head Formation commonly possess internal sedimentary structures typical of turbidites (Malo, 1988). A general lack of shelly faunas, except for the Percé area, the presence of graptolites, deep water trace fossil assemblages and the turbidite facies indicate that the White Head occupies a relatively deep-water marine basin.

Thermal maturation studies of the White Head Formation have been done in the Aroostook-Percé anticlinorium (Duba and Williams-Jones 1983; Nowlan and Barnes, 1987; Chagnon, 1988; Malo et al., 1993). Duba and Williams-Jones (1983) used illite crystallinity and organic matter reflectance to study burial metamorphism in the western end of the Aroostook-Percé anticlinorium, in the Matapédia area. Nowlan and Barnes (1983) used conodont color alteration index (CAI) to study the thermal maturation of Paleozoic strata in Eastern Canada; they entirely covered the Aroostook-Percé anticlinorium area (their Matapédia basin). Chagnon (1988) used illite crystallinity to study burial metamorphism and hydrothermal alteration related to minerals occurrences in the Carleton and New Richmond areas of the Aroostook-Percé anticlinorium. The same technique was used by Malo et al. (1993) to study hydrothermal alteration related to copper-skarn mineralizations along the Grand Pabos fault. The study of Nowlan and Barnes (1987) covers the area under investigation in our present study and they present data in the Percé

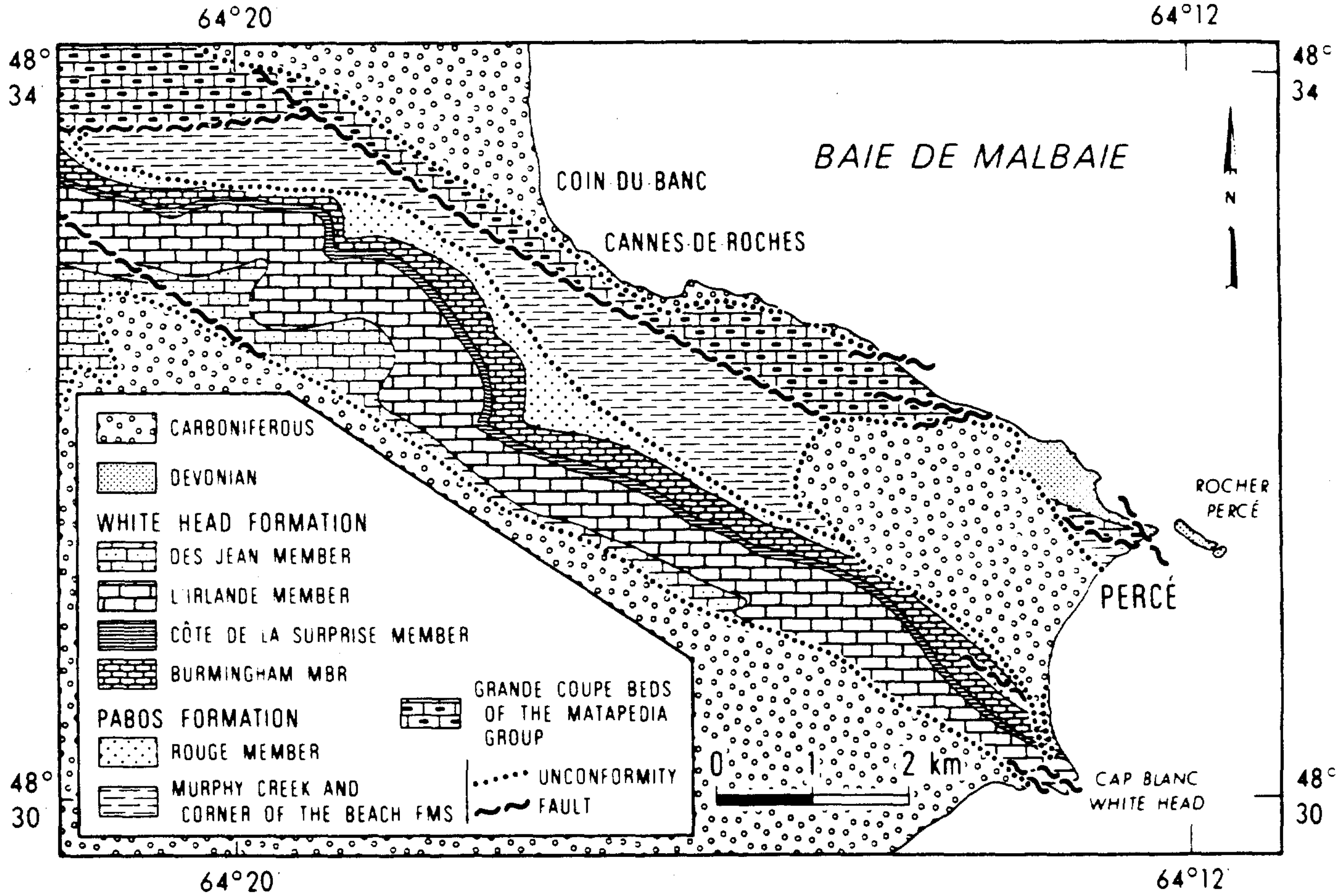

Figure 2.1. Geological map of the Percé area showing the distribution of the new members of the White Head and Pabos formations and the Grande Coupe beds. From Lespérance et al. (1987).

area and along the East-Central outcrop belt, near the Grande Rivière fault. From the Percé area to the west, the CAI vary from 1-1.5 to 3-3.5. This trend is the same for data coming either from the Ordovician part of the White Head Formation (Burmingham Member) or from the Silurian part of the formation (L'Irlande and Des Jean Member).

Our samples of the western part of the East-Central outcrop belt come from different locations along the Grande Rivière fault, west of location 8 on figure 1.2. Samples from the eastern part of the East-Central outcrop belt are from location 1 (69L-15-3A, 69L-15-4J), from location 2 (81-MM-28) and between the last two locations (81-MM-95) (see figure 1.2).

2.0.2 DIAGENESIS AND POROSITY EVOLUTION

This preliminary investigation of porosity evolution for the White Head Formation is based on 9 selected samples from eastern and western locations of the east-central outcrop belt (Ecob, Fig.1.2). Because the White Head is mostly comprised of fine limestones, the study was aimed at identifying development of secondary porosity and signs of hydrocarbon migration.

2.0.2.1 CHRONOLOGY OF DIAGENETIC FEATURES (FIG. 2.2)

Eastern Locations
The striking post-depositional feature in the wackestone and mudstone facies (sample 69L-15-4-J) consists of a microfracture network (Fig. 2.2A). Three generations of fractures (f1 to f3) postdate lithification of the fine limestone. Fractures f1 (av. width = 1 mm) are filled with inclusion-rich fibrous to equant calcite (dull in CL) (Fig. 2.2A, 2.2B) and are pre-stylolites; fractures f2 (0.1 < width < 0.4 mm) are occluded by equant inclusion-free calcite (dull to very dull in CL) and are post-f1 (Fig. 2.2A, 2.2B); and fractures f3, very fine (width ≤ 0.02 mm), are filled with xenomorphic inclusion-free calcite (bright in CL), are post-f2 (Fig. 2.2A) and syn-stylolites. The marine sediments (mud/microspar) are uniformly light dull in CL (like cements filling f1).

Crinoid and arthropod grainstones from the eastern locations show two diagenetic successions. Succession 1 observed on samples M95 and 69L-15-3A includes: i) replacive leutecite (fibrous silica), minor abundance; ii) xenomorphic calcite, dull in CL; iii) microfractures filled with xenomorphic calcite, very dull in CL; and iv) rhombohedric dolomite with non luminescent (NL) core and bright borders in CL.

Succession 2 (sample M28) includes: i) dissolution features (Fig. 2.2C, arrows); ii) xenomorphic calcite comprised of dull to very dull zones in CL, and luminescent (Lum) to dull zones, both with possibly pendent fabric (? thin sections not oriented; Fig. 2.2D, along arrows); iii) micro-fractures (??); iv) xenomorphic to poikilotopic calcite, NL (composite) followed by a dull uniform band in CL (pore centers on Fig. 2.2D).

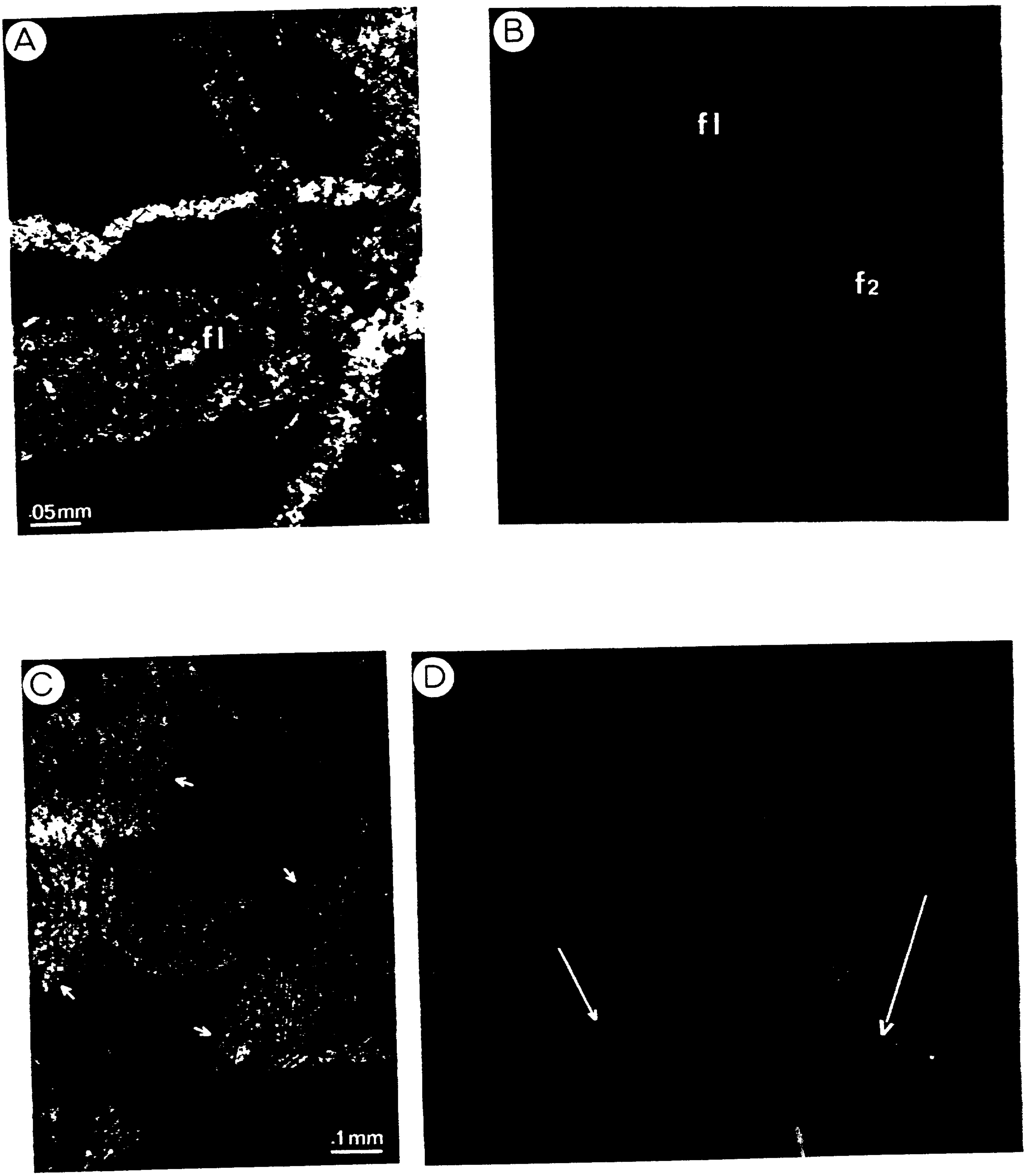

Fig. 2.2

Western Locations
Post-depositional features in the wackestone facies are similar to those of the eastern locations.

Crinoid and arthropod grainstones from the western locations show a standard succession of diagenetic features including: i) inclusion-rich, syntaxial cement, bladed to poikilotopic on crinoids or bladed on arthropods, and NL in CL; ii) xenomorphic calcite, luminescent in CL; iii) stylolites, microdolomite (zoned NL to Lum in CL) and microfractures; iv) inclusion-free, xenomorphic calcite fracture-filling, dull in CL.

2.0.2.2 ISOTOPE GEOCHEMISTRY (FIG. 2.3)

It was impossible to separate cements filling primary pores from the sediment matrix, so that except for fracture-filling cements, all microsamples are whole rock (Fig. 2.3A).

Eastern Locations
Numerous whole rock grainstone microsamples yielded $\delta^{18}O_{VPDB}$ and $\delta^{13}C$ values within the marine calcite range. A sample of fracture (f1)-filling, inclusion-rich, fibrous calcite from the mudstone facies also shows marine affinities. On the same hand sample (4-J on Fig. 2.3B), this cement is followed by f2-filling cement which has lower $\delta^{18}O_{VPDB}$. This overall time trend suggests marine diagenesis succeeded by burial.

Three microsamples from sample M28 (Ruisseau Blanc) possibly showing pendents (stippled line on Fig. 2.3A) yield a trend that has been likely produced in burial, as other samples of the White Head Formation which do not show meteoric petrographic features (western locations). Moreover, meteoric effect is unexpected as the White Head Formation was deposited in a deep water setting. Field observations, petrography on oriented thin sections and microsampling of pendent (?) cements are required to verify if meteoric diagenesis affected the Ruisseau Blanc section (location 8).

Western Locations
One grainstone result falls in the marine calcite field. Low $\delta^{18}O_{VPDB}$ between -7.4 and -6.1‰ and $\delta^{13}C$ at around 0.0‰ for grainstones and cement filling f2 fractures can be attributed to burial diagenesis. The overall isotopic profile suggests early marine diagenesis followed by progressive burial diagenesis (Fig. 2.3A).

> ***The preliminary study of White Head isotope geochemistry suggests that both eastern and western studied locations were lithified during marine and burial diagenesis. Lenticular grainstone beds from the Ruisseau Blanc might have been affected by meteoric diagenesis (? vadose ?).***

2.0.2.3 FEASIBILITY OF FLUID INCLUSION MICROTHERMOMETRY

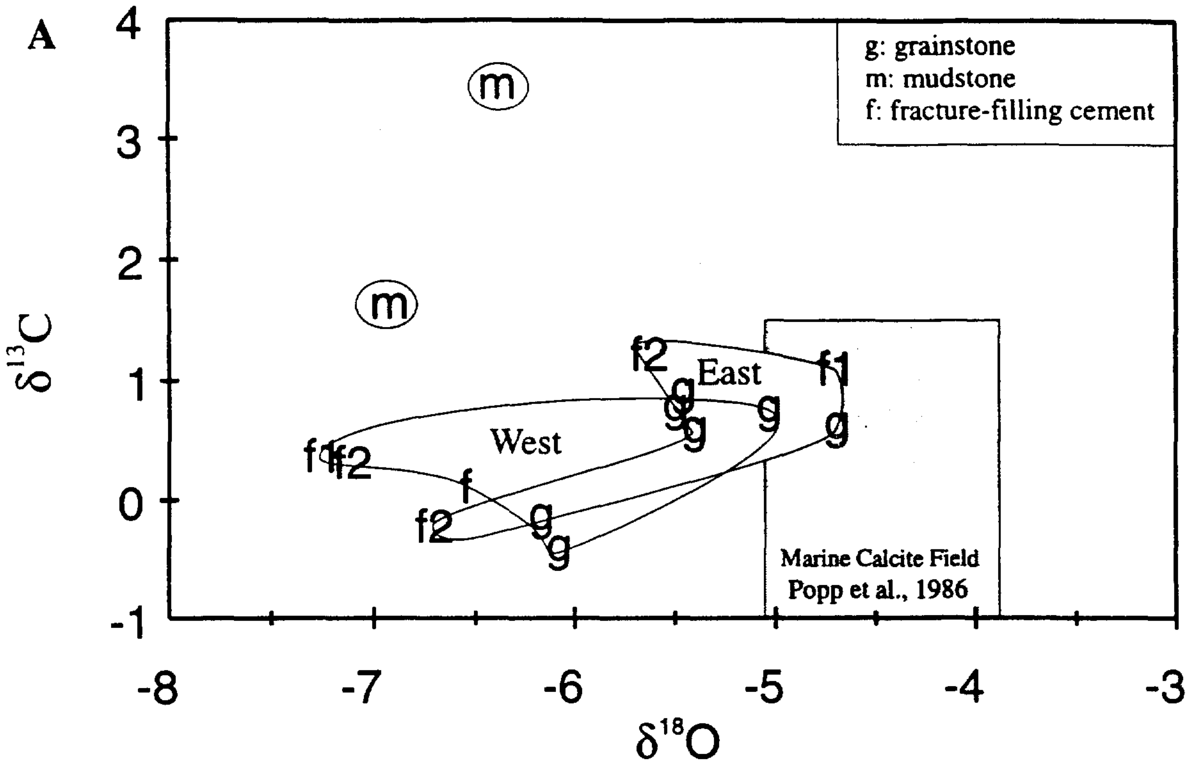

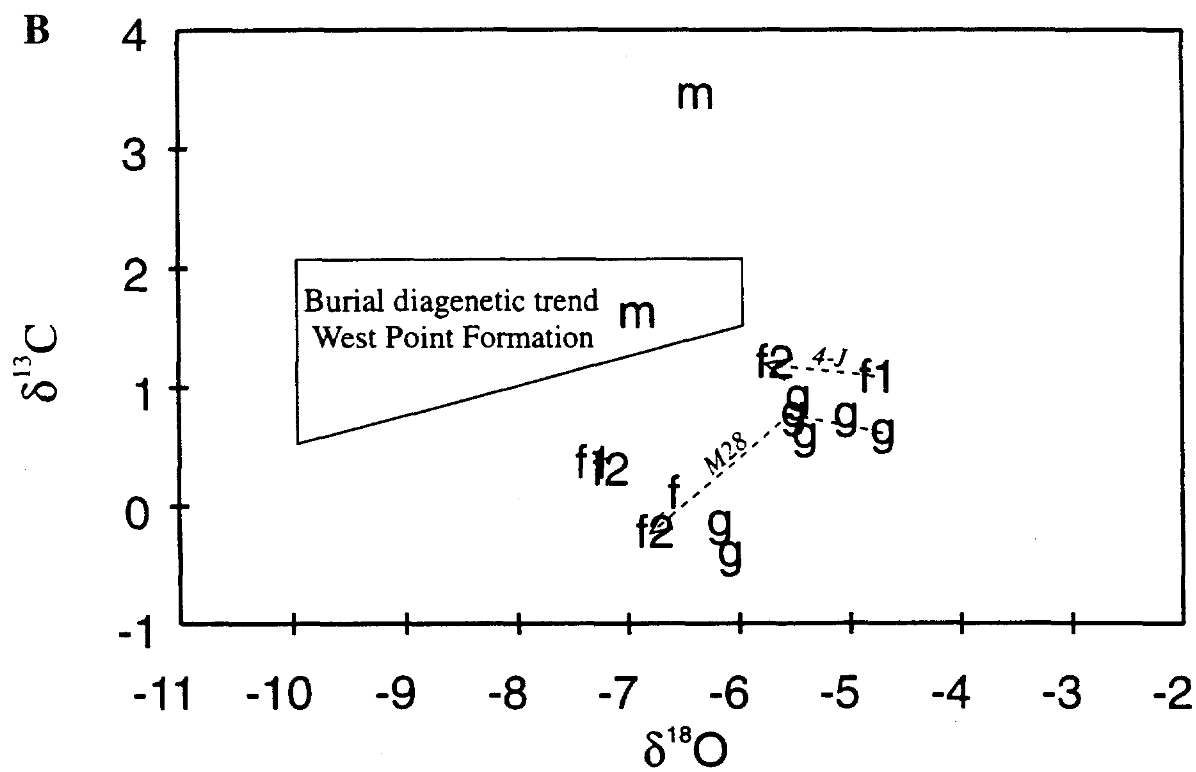

Figure 2-3. Stable Isotope Results - White Head Formation.
A) Results for western and eastern locations.
B) Comparison with burial trend for the West Point Formation.

All samples contain workable fluid inclusions except 82MM-376 and 389.

The inclusions are typically randomly distributed in pore-cements and many can be described as primary. Some are probably petroleum inclusions. Inclusions in fracture-filling cements are present but not as easy to study as these in pore-filling cements.

2.0.2.4 POROSITY EVOLUTION

Mudstone and wackestone make up more than 98 % of the White Head Formation, lenticular and bedded grainstones being minor lithofacies (<2%). Primary porosity was not significant for this formation. Lithification seems to have been rapid for the White Head, as cements filling fractures do not show very low $\delta^{18}O$ values. For comparison, the lightest values for the White Head Formation are 2.5‰ higher than those for burial cements of the West Point Formation (Savard and Bourque, 1989; and section 3.2.2, this report). Assuming similar parent waters, this suggests lower temperature (shallower burial depth) for the White Head than for West Point Formation, during late cement precipitation.

There is no evidence of secondary pore development other than: 1) at Ruisseau Blanc, possible vadose meteoric (?) dissolution of grainstone (very minor portion of the formation); and 2) microfractures which have been totally filled with marine to burial cements at an early stage.

2.0.2.5 IMPLICATIONS FOR HC PLAYS

After its lithification and mineralogical stabilization, the White Head Formation has possibly been affected by the Salinian Unconformity. Salinian meteoric waters have possibly used fractures to develop late karsts. Note: Karstification is more efficient in stabilized limestones than in metastable sediment terrane.

2.0.3 RECOMMENDATIONS

The microfracture network could be studied to verify: (1) if it has been enhanced by meteoric diagenesis (karsting) during the development of the Salinian unconformity and (2) if hydrocarbons migrated through it, if yes at which tectonic stage.

Method proposed: field work on fractures and on karst features in areas where the Salinian unconformity has been recognized, petrography, isotope geochemistry, fluid inclusion microthermometry.

2.1 THE EARLY SILURIAN SAYABEC - LAFORCE FORMATIONS

2.1.1 INTRODUCTION

The Paleozoic sequence in the Acadian Gaspé belt (*sensu* Bourque et al., 1995) of the Northern Appalachian orogen (Fig. 1.1) contains few shallow water carbonates, one of these are reef and carbonate complexes that developed during the Late Llandoverian - Wenlockian (Sayabec - La Vieille formations and the deeper marine Laforce Formation). The Early Silurian Sayabec - La Vieille formations mark the first occurrence of shallow water limestones in the Paleozoic sequence of the northern segment of the orogen. Conversely, the latest Early Silurian Laforce Formation records below wave base carbonate deposition. Various aspects of the sedimentology, biological communities, paleogeography of Sayabec/La Vieille and Laforce formations have been published (Bourque et al., 1986; Lavoie, 1988; Desrochers and Bourque 1989; Lavoie et al., 1992), although diagenetic history is only partly known for the Sayabec - La Vieille formations (Lavoie, 1988; Lavoie and Bourque, 1993).

In the Gaspé Belt, the Sayabec and La Vieille carbonate platforms developed at the margin of the Québec Reentrant and St. Lawrence Promontory, with the Laforce occurring in a more distal, basinward setting (Fig. 1.13C). The deposition of the Sayabec - La Vieille shallow water limestones corresponds to the peak of the first shallowing phase that marked the tectono-sedimentary history of the Gaspé Belt after the Taconian orogeny (late Middle Ordovician). Both platforms were gently south-dipping ramps and exhibited the same lateral facies zonation (Lavoie et al., 1992). Four parallel depositional belts are recognized (Fig. 1.14), from nearshore to offshore, (1) a wide peritidal mud flat dominated by microbial communities; (2) a knob reef rim built by a consortium of skeletal metazoans, skeletal calcareous algae and microbial communities; (3) a well-sorted lime sand belt and; (4) a deeper water nodular mud belt supporting a diverse biota. The ramps were buried by influx of deeper-water siliciclastics during a Late Wenlockian transgression (Lavoie et al., 1992). However, and very significantly for porosity evolution, parts of the ramps were tectonically exhumed in Ludlovian - Pridolian time during the Salinian Disturbance (Lavoie and Bourque, 1993; Bourque et al., 1995; Bourque and Malo, this report). This sub-aerial exposure led, in the case of the La Vieille Formation, to meteoric dissolution in limestones facies (Lavoie and Bourque, 1993). Although the Salinian event also affected the Sayabec Formation in easternmost Gaspé (Lavoie et al., 1992; Bourque et al., 1995; Bourque and Malo, this report), sub-aerial dissolution was not noted in Lavoie (1988) study more concerned with facies zonation.

The Laforce Formation has not been the subject of a detailed analysis. This unit is dominated by coarse-grained impure carbonates interlayered with various siliciclastics (Lavoie, 1988). Regional lithofacies distribution and paleocurrent indicators in the Laforce suggest that the source of sediments was located eastward to northeastward of actual exposures of the formation. The Laforce carbonate lithologies are predominantly lithoclastic-rich with an exotic source of sediments, the exact source of them being still problematic (Lavoie et al., 1992). However, all lithofacies recognized in the Laforce lithoclasts are known in the Sayabec Formation (Lavoie, 1988), some diagenetic elements found in clasts also suggest a Sayabec source (Lavoie, 1988) although a source located on the Anticosti carbonate platform could not be unequivocally rejected. It is also noteworthy that the Laforce has also been subaerially exposed, even though very locally, during the Salinian Disturbance (Bourque and Malo, this report).

No hydrocarbon production or seeps are known from either the shallow water (Sayabec - La Vieille) or the deeper marine (Laforce) facies. However, the significance for porosity evolution of the Salinian Disturbance for the Sayabec - Laforce formations and the diagenetic evolution of the entire Laforce Formation are definitively poorly known. A preliminary evaluation of the diagenetic evolution of the Laforce and the possible effects of sub-aerial exposure on Sayabec carbonate facies are the subject of this study concerned with available material for the area where Shell holds permit in eastern Gaspé.

2.1.2 METHODS

The Sayabec - Laforce material was collected during Lavoie Ph.D. study completed in 1988. Moreover, new Laforce material from the Imperial Lowlands Associated York hole #1 in eastern Gaspé has been examined.

More than 100 conventional stained thin sections for the Sayabec and Laforce formations from the study area have been reexamined. Thirty polished thin sections for cathodoluminescence petrography for the Sayabec Formation in easternmost Gaspé have been reexamined. Fifteen old and 10 new polished thin sections for the Laforce Formation have been studied under cathodoluminescence. These observations led to the recognition of various cement phases that have been micro-sampled for their stable isotope signatures. Six calcite samples from the Laforce Formation were analysed for their stable isotopes at the Delta-Lab at the CGQ following usual analytical procedures.

2.1.3 GEOLOGICAL AND STRATIGRAPHIC SETTINGS

Silurian - lowermost Devonian rocks crop out in a number of structural units in the Gaspé depositional belt (Fig. 1.2). This report is concerned with the eastern segment of the Gaspé Belt.

The Sayabec Formation can be assigned a Late Llandoverian to Middle/Late Wenlockian age on the basis of its brachiopods and graptolites (Bourque 1977; Lavoie et al., 1992; Bourque et al. 1995). On the basis of graptolites, the Laforce Formation is assigned a Middle Wenlockian to Early Ludlovian age (Lavoie, 1988).

2.1.3.1 SAYABEC FORMATION

The Sayabec Formation crops out in the northern segment of the Gaspé - Matapédia Basin (Northern outcrop belt and Lake Matapédia syncline; Fig. 1.2). The Sayabec Formation is divided into four informal members (labelled A to D; Lavoie, 1988; Lavoie et al., 1992). These four members are present in eastern Gaspé, they are: (A) a lower sandy limestone member; (B) a nodular limestone member; (C) a diversified shallow marine limestone member; and (D) a second nodular limestone member (Fig. 2.4a).

2.1.3.2 LAFORCE FORMATION

The Laforce Formation crops out in the St. Jean River Anticline, the Gastongay Anticline and the Mount Alexandre Syncline (Fig. 1.2). The Laforce is informally divided into two laterally equivalent members (labelled E and F; Lavoie, 1988). These two members are: (E) a coarse-grained, impure limestone unit and (F) an impure limestone / siliciclastic unit with more than 10% of fine-grained siliciclastic interbeds (Fig. 2.4b). The thicker member E is developed in the eastern part of the St. Jean River Anticline whereas the thinner member F occurs in the western segment of the St. Jean River Anticline and in the Gastongay Anticline and Mount Alexandre Syncline.

2.1.4 FACIES AND DEPOSITIONAL SETTING

2.1.4.1 SAYABEC FORMATION

Five facies comprising various lithologies have been recognized in the Sayabec Formation. They were grouped on the basis of similar origin or paleoenvironments of deposition. These facies are: (1) peritidal, (2) shallow subtidal, (3) biohermal / biostromal, (4) offshore muds and (5) nearshore sands. Details on these can be found in Lavoie et al. (1992). These facies were developed on a south-facing, gently sloping carbonate ramp typified by a fairly wide peritidal flat bordered by a small rim of algal-metazoan bioconstructions passing seaward to well sorted carbonate sands (Lavoie et al., 1992; and Bourque and Malo, this report fig. 1.14).

2.1.4.2 LAFORCE FORMATION

The Laforce carbonate lithologies are characterized by a significant amount of embedded quartz and other lithic fragments. Two major facies have been proposed: (1) below wave base calcarenite, calcirudite and sandstone and (2) deep marine mudstone and shale (Lavoie, 1988). The coarse-grained facies show sedimentary structures suggestive of turbidity currents. It is noteworthy that the abundant intraclasts in the calcarenites offer a complete spectrum of lithologies that could be found on a shallow marine carbonate setting.

2.1.5 DEPOSITIONAL HISTORY

2.1.5.1 SAYABEC FORMATION

Bourque et al (1986) and Lavoie et al. (1992) concluded that the Sayabec Formation of the Northern Outcrop Belt was the result of two superimposed transgression - regression cycles. These are expressed by the transition from one to the other major members. Within each member, smaller scale relative sea level fluctuations are recorded in the subtle transitions from one facies to

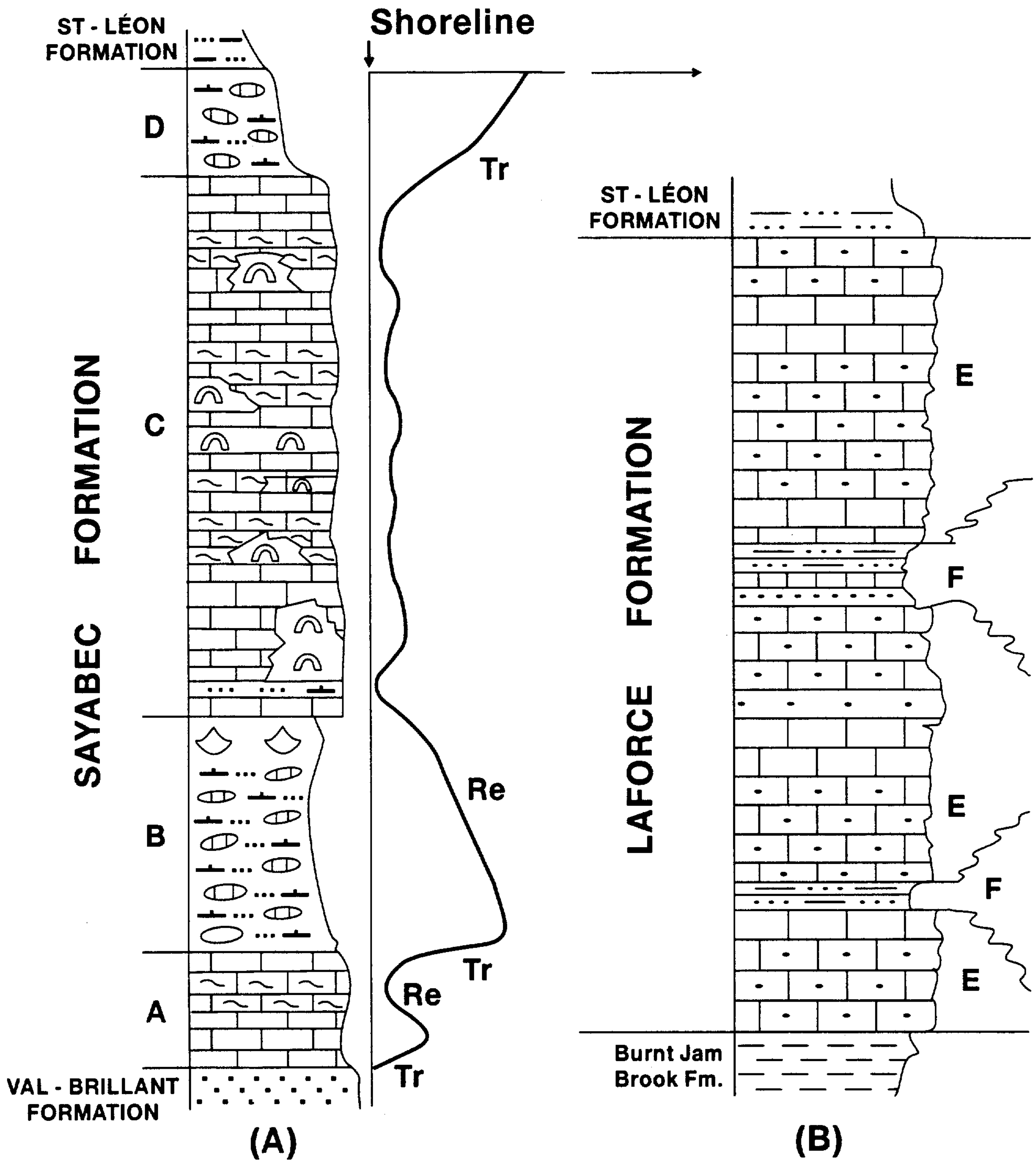

Fig. 2.4 : (A) Schematic section of the Sayabec Formation illustrating the four members and assumed relative sea-level fluctuations. (B) Schematic section of the Laforce Formation illustrating a tropical succession in the St. Jean River Anticline

the other (Lavoie, 1988; Lavoie et al., 1992), although no serious attempt has been made to assign these various relative sea level fluctuations to specific mechanism (s?).

2.1.5.2 LAFORCE FORMATION

From the assumed relative deep marine setting of the Laforce Formation, no attempt has been made to recognize sea level fluctuations in that unit. Lavoie (1988) focussed on possible source for the abundant carbonate intraclasts present in the Laforce. He proposed that the coeval to very slightly older Sayabec ramp could be the likely candidate for shedding these particles during sea level lowstands. This interpretation is also supported by the cement succession present in voids within intraclasts (see further). However, it should be reminded that those carbonate clasts could also have been derived from the Anticosti carbonate platform.

2.1.6 PETROGRAPHY OF CEMENTS

2.1.6.1 SAYABEC FORMATION

Reexamination under conventional microscope and cathodoluminoscope of Sayabec's thin sections for the area covered by Lavoie (1988) in the Northern Outcrop Belt, did not reveal any evidence for sub-aerial dissolution / cementation that could be related to the Salinian Disturbance. However, it should be pointed out that the easternmost section sampled by Lavoie (section #16 (Lac Madeleine), Lavoie, 1988 and Lavoie et al., 1992) is located at about 35 km eastward of the Rivière Madeleine area (see Bourque and Malo, this report) where the Salinian Unconformity deeply cuts through the Sayabec succession (e.g., same area where West Point reefs are currently being studied by Bourque, Savard and Dansereau, this report). For the purpose of this report, a brief summary of cement petrography for the Sayabec Formation in the Northern Outcrop Belt is presented. A preliminary study of fluid inclusions in calcite cements found in pores and fractures has shown that abundant workable fluid inclusions are present in both material, hydrocarbons fluid inclusions are likely present in two of the six thin sections that were surveyed (G. Chi, pers. comm).

Calcite cements are found in all major facies of the Sayabec with the exception of the outer shelf nodular mud facies. No outcrop of biohermal facies are known outside the Lake Matapédia Syncline, therefore, marine cements (LF1) of Lavoie and Bourque (1993) are not present although it should be kept in mind that those bioherms could be present in the subsurface. In order to keep the links between this report and the more detailed description found in Lavoie and Bourque (1993), cement nomenclature follows the one proposed by the latter. Therefore, cement description will start with LF2 (luminescence facies 2).

Luminescence facies LF2 was observed in more than 95% of the pores where it constitutes the first cement in the void space. Under CL, the LF2 cements (Fig. 2.5a) are represented by equant to bladed-prismatic, non-luminescent spar with bright laminae (less than 1 mm across), that grew orthogonally from pore walls and forms more or less continuous fringes. In plane-polarized light,

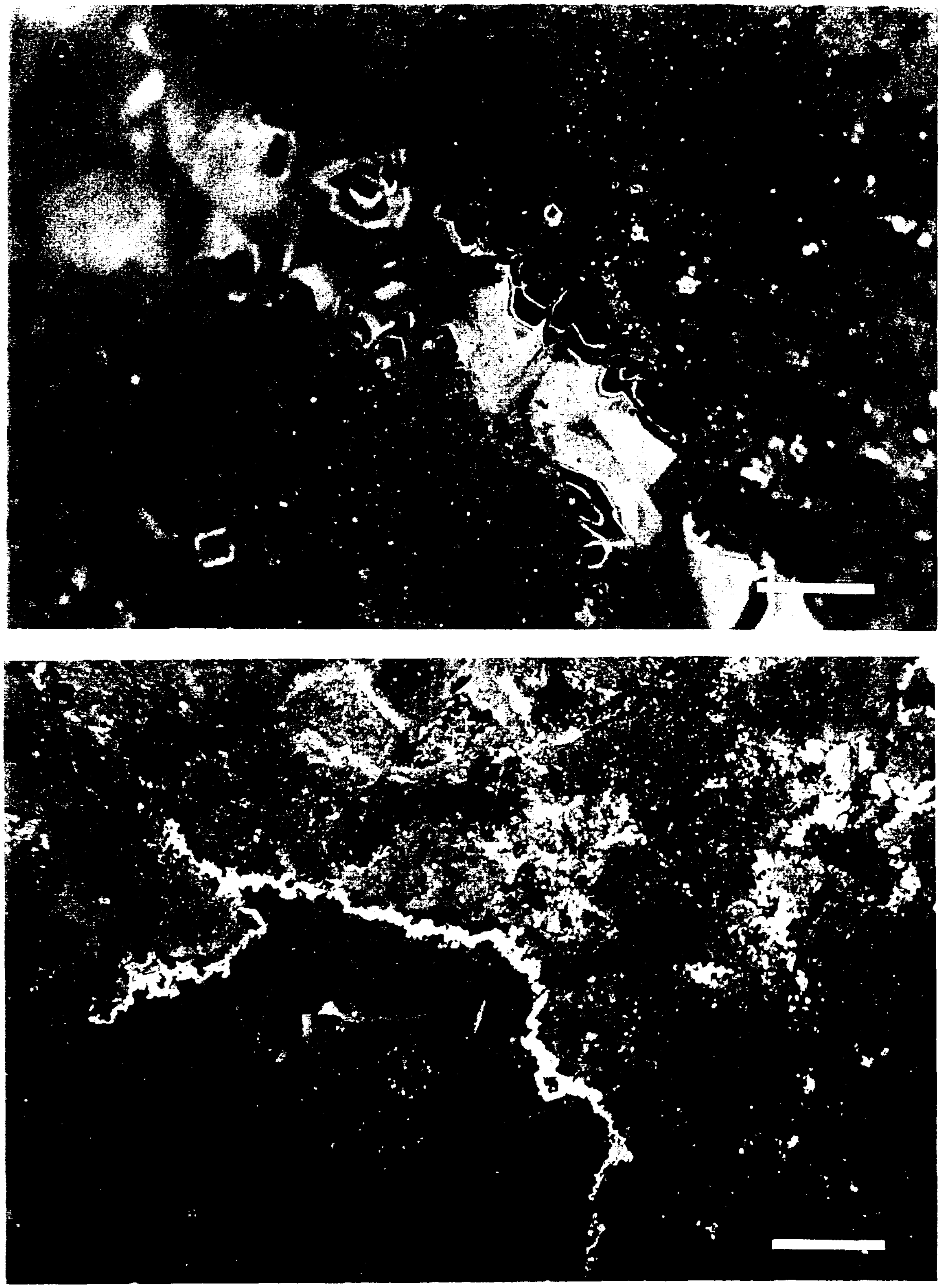

Figure 2.5: A) CL view of a fenestrae in peritidal facies of the Sayabec showing the non-luminescent LF2 cements followed by the bright luminescent crystals of LF3 and capped by the dull luminescent cements of LF4. B) CL view of a meteoric dissolution vug in the La Vieille with gravitational finely zoned bright luminescent cements of LF5 followed by the dull luminescent LF6 cement. Scale bars are 1 mm.

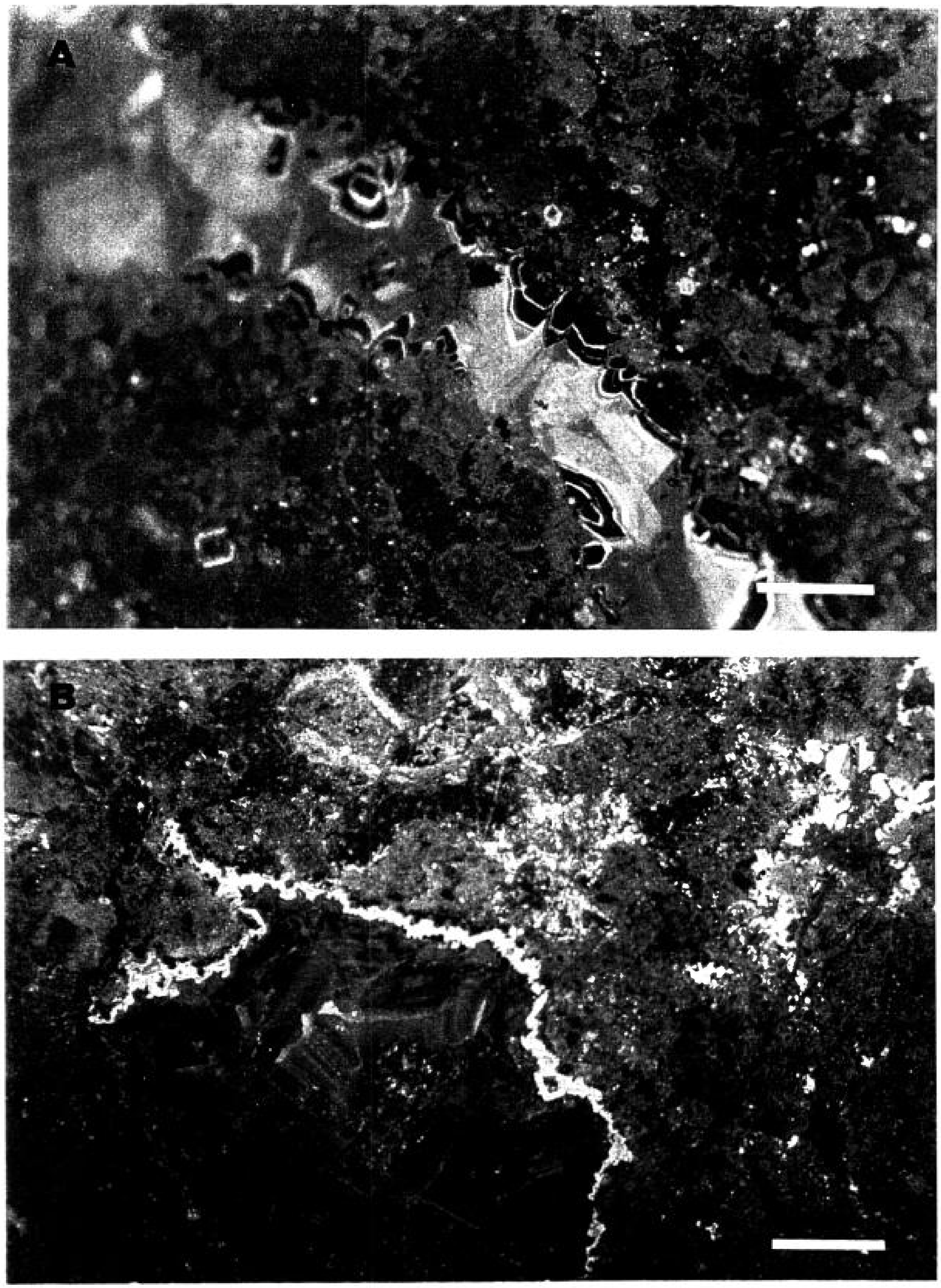

Figure 2.5: A) CL view of a fenestrae in peritidal facies of the Sayabec showing the non-luminescent LF2 cements followed by the bright luminescent crystals of LF3 and capped by the dull luminescent cements of LF4. B) CL view of a meteoric dissolution vug in the La Vieille with gravitational finely zoned bright luminescent cements of LF5 followed by the dull luminescent LF6 cement. Scale bars are 1 mm.

LF2 cement corresponds either to non-ferroan syntaxial overgrowths on echinoderm plates, or to non-ferroan equant calcite coating walls of primary pores.

Luminescence facies LF3 consists of scalenohedral (from 0.08 to 1 mm), zoned orange to brightly orange zoned spar. In all occurrences, it conformably overlies LF2 and mimics the latter shapes (Fig. 2.5a). In plane-polarized light, LF3 has the same petrographic attributes as LF2 and the two cannot be differentiated.

Luminescence facies LF4 consists of coarsely crystalline (up to 5 mm), irregularly zoned, brown to orange-dull luminescent equant spar (Fig. 2.5a). In some pores of the peritidal and shallow subtidal facies, LF4 gradationally overlies LF3 as evidenced by a progressive decrease of luminescence intensity. In plane-polarized light, LF4 cement corresponds to mm-sized, ferroan and non-ferroan, clear spar crystals.

Luminescence facies LF5 and LF6 were only observed, so far, in the western part of the La Vieille ramp; however, they are significant because they have been related to meteoric calcite cementation following subaerial exposure of the La Vieille ramp during the Salinian Disturbance. LF5 and LF6 occur in solution vugs that cut across bioclasts, mud matrix, diagenetic elements such as LF2 to LF4 cements and stylolites. Under CL, LF5 cement consists of equant to pyramidal spar crystals of variable sizes (from 0.1 to 0.5 mm in height and 0.05 to 0.2 mm in width). The spar is typified by alternating growth bands with, from wall to centre of pore: a patchy non-luminescent discontinuous zone, followed by a thin continuous brightly luminescent zone, and a last zone of thinly-banded bright, dull and non-luminescent sub-zones (Fig. 2.5b). LF5 is gravitational in large cavities where the cement occurs as thin crusts confined to the roof and is also observed in veins that cut across the limestone. In plane-polarized light, LF5 cements correspond to ferroan and non-ferroan zoned calcite.

LF6 cements conformably overly LF5 and consist of mm-sized xenomorphic crystals with a crudely zoned dull luminescence (Fig. 2.5b). Plane-polarized light shows that LF6 is ferroan calcite.

Finally, fracturing with minor cementation, stylolitization, minor dolomitization and sulfatization were observed in the Sayabec lithologies. They show complex relative timing relationships, they postdate LF4 cements and most of them predate LF5 cements. CL reveals the presence of three fracturing events: F1, filled with dull luminescent small equant spar; F2, filled with brightly luminescent equant spar; and F3 cemented by reddish luminescent fibrous spar. Fracturing and pressure-solution also show complex time relationships. Calcite spar mimicking sulfate crystal shapes is observed cutting across LF4 cements, but its relationship to post-LF4 diagenetic events is unknown. Stylolites (including sutured and non-sutured seams) are ubiquitous in every lithofacies.

Associated with the stylolites are small rhombs of dolomite with zoned luminescence. Interestingly, massive hydrothermal-related dolomitization is reported in the Sayabec at some localities near the Shickshock Sud Fault (Lachambre, 1987). At places, the rock is highly porous and base-metal mineralized. The timing of that dolomitization event with respect to the diagenetic evolution of the formation and possible hydrocarbon migration is currently unknown and worth some consideration. Saddle dolomite is present and post-dates all other diagenetic features.

2.1.6.2 Laforce Formation

Lavoie (1988) study of calcite cements present within the Laforce Formation could be termed as a preliminary regional survey. Limited number of CL thin sections were examined and no isotopic analysis were made. For this report, the principal conclusions will be repeated (with an emphasis on the cement history present in Laforce carbonate clasts). Moreover, new material from the Imperial Lowlands Associated York #1 hole has been studied both petrographically and isotopically. Six thin sections have been preliminary examined for fluid inclusions; workable fluid inclusions are present within pore- and fracture-filling calcites and many of them seemingly contain hydrocarbons (G. Chi, pers. comm.).

Interparticular pore-filling calcites are only present in the coarse-grained carbonate facies. Interestingly, calcite cements between clasts are ferroan with minor (and commonly absent) non-ferroan growth bands (Fig. 2.6a). Interparticular non-ferroan calcite cements are only significant in crinoidal-rich grainstones (Fig. 2.6b). Conversely, calcite present within clast pores are frequently non-ferroan suggesting that a significant part of these clasts were shed as cemented particles in the Laforce basin. Some of these clasts have pores cut at clast margins and show non-ferroan calcite "unconformably" overlain by ferroan calcite.

Under CL, three luminescence facies are found in the interparticular pores (labelled LF7 to LF9 in Lavoie, 1988). The first one is only developed in the crinoidal-rich grainstone facies. New material from the Imperial Lowlands Associated York #1 core also shows the presence of LF8 and LF9.

Luminescence facies LF7 consists of an initial irregular and commonly fractured rind of non-luminescent calcite overlain by dull luminescent calcite xenomorphic crystals (Fig. 2.7a). These fractured cements are healed by the following bright luminescence facies of LF8. In plane-polarized light, it corresponds to irregularly distributed syntaxial non-ferroan and ferroan calcites surrounding crinoidal plates (Fig. 2.6b).

Luminescence facies LF8 is frequently the only one seen in interparticular pore space of the Laforce Formation. It consists of large (up to a mm) xenomorphic bright yellow crystals (Fig. 2.7b). In plane-polarized light, it corresponds to ferroan and locally, to few non-ferroan calcite crystals.

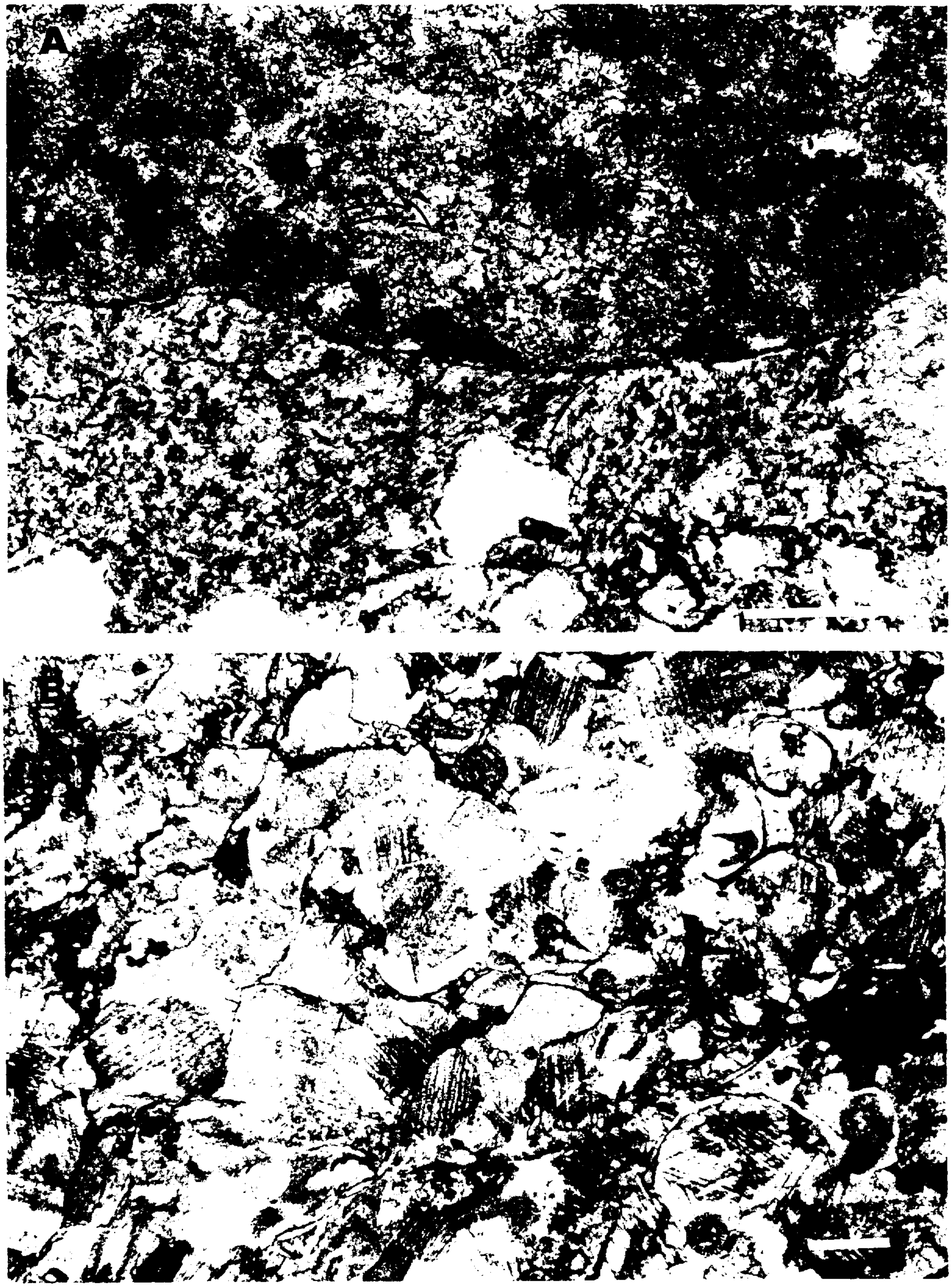

Figure 2.6: A) Plane-polarized photomicrograph showing a pelsparite clast with internal non-ferroan calcite cement (curved arrow), the clast is embedded in ferroan sparite. B) Plane-polarized photomicrograph of crinoidal grainstone with broken syntaxial non-ferroan calcite coatings on crinoids. Scale bars are 1 mm.

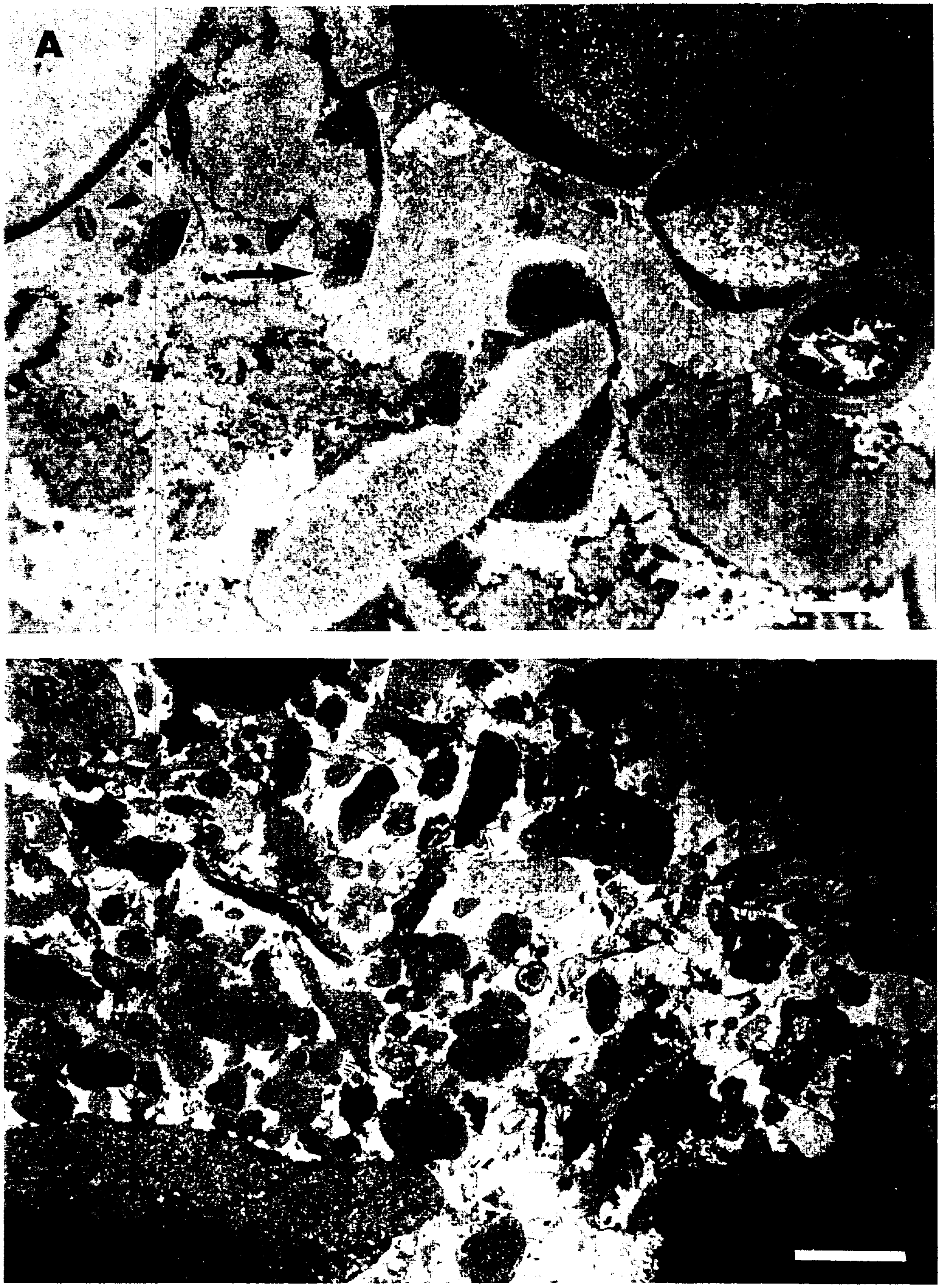

Figure 2.7: A) CL view of crinoidal grainstone showing broken crust of syntaxial calcite cements (arrow) of very dull luminescent (LF7 or LF2) cements followed by bright luminescent calcite (LF8 or LF3). Dull luminescent LF9 cements fill remaining void space. B) CL view of typical Laforce void filling cement mostly composed of bright luminescent LF8 xenomorphic spar. Scale bars are 1 mm. (Continued following page..)

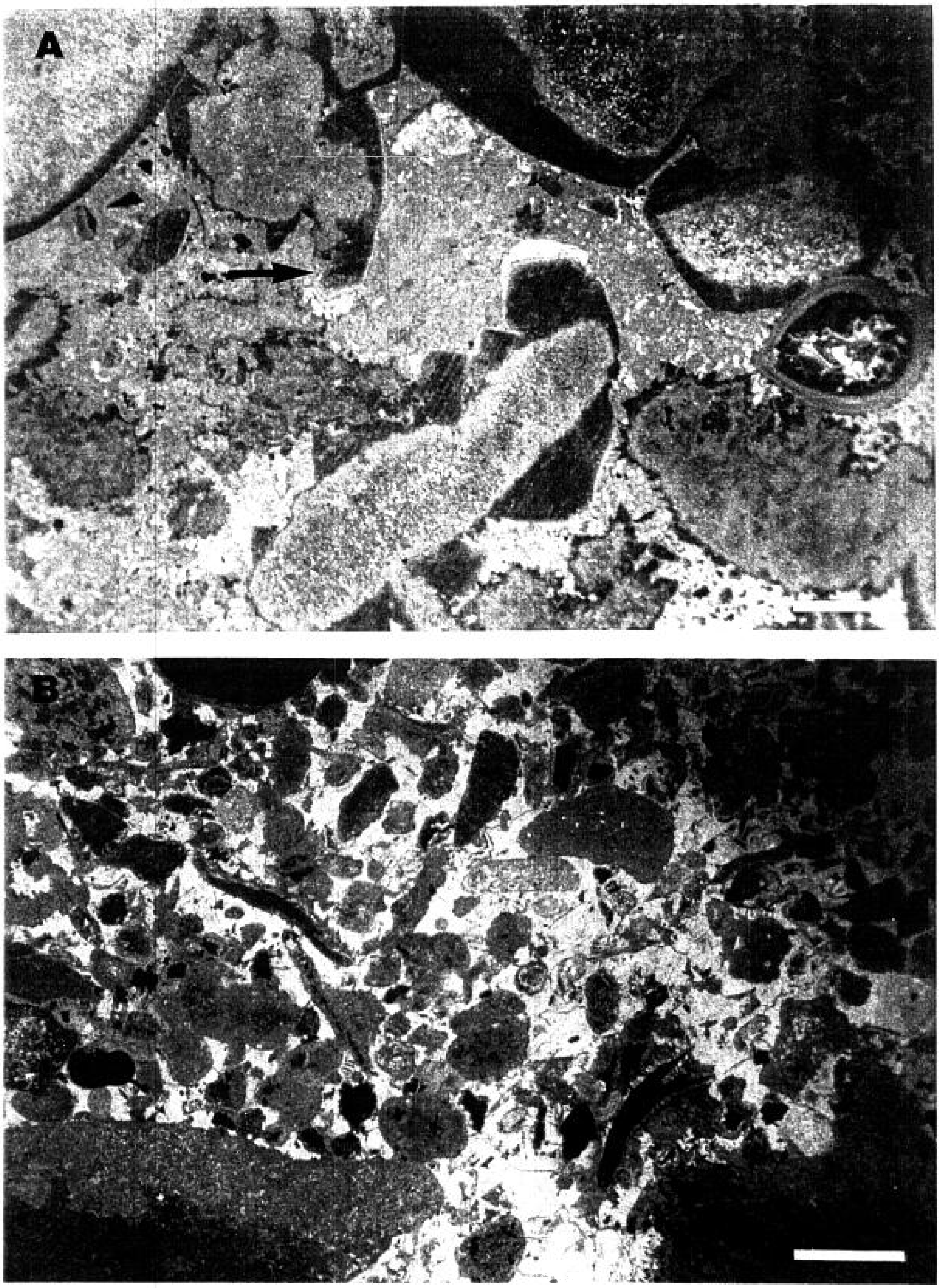

Figure 2.7: A) CL view of crinoidal grainstone showing broken crust of syntaxial calcite cements (arrow) of very dull luminescent (LF7 or LF2) cements followed by bright luminescent calcite (LF8 or LF3). Dull luminescent LF9 cements fill remaining void space. B) CL view of typical Laforce void filling cement mostly composed of bright luminescent LF8 xenomorphic spar. Scale bars are 1 mm. (Continued following page..)

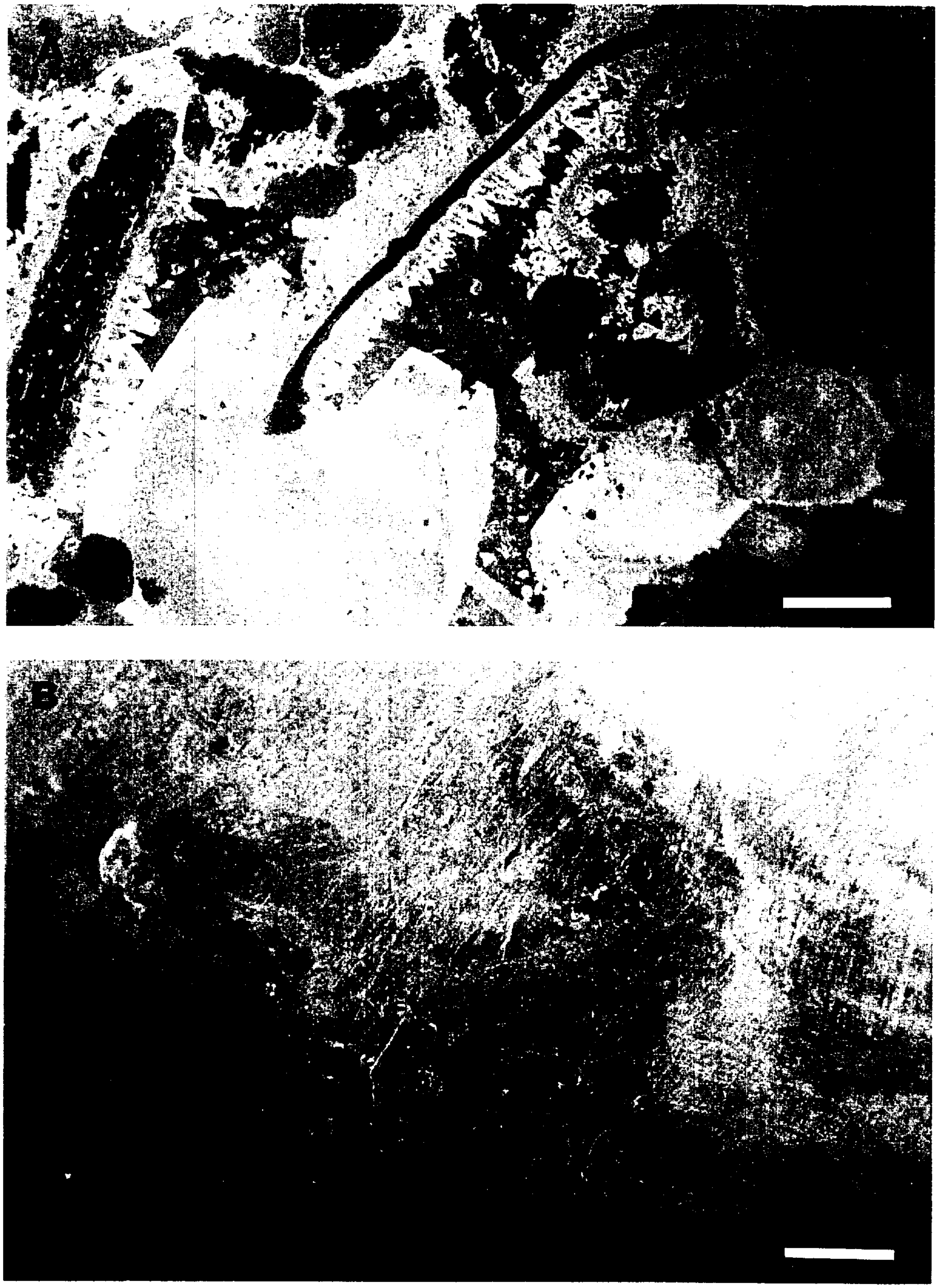

...... Figure 2.7: C) CL view of bioclastic grainstone showing syntaxial bright calcite cement of LF8 on crinoid. LF8 is also developed as thin crust of scalenohedral crystals on a trilobite fragment. The remaining void space is filled by dull luminescent xenomorphic spar of LF9. D) CL view of fracture-fill calcite. The xenomorphic spar shows an irregular composite dull-bright luminescence. Scale bars are 1 mm.

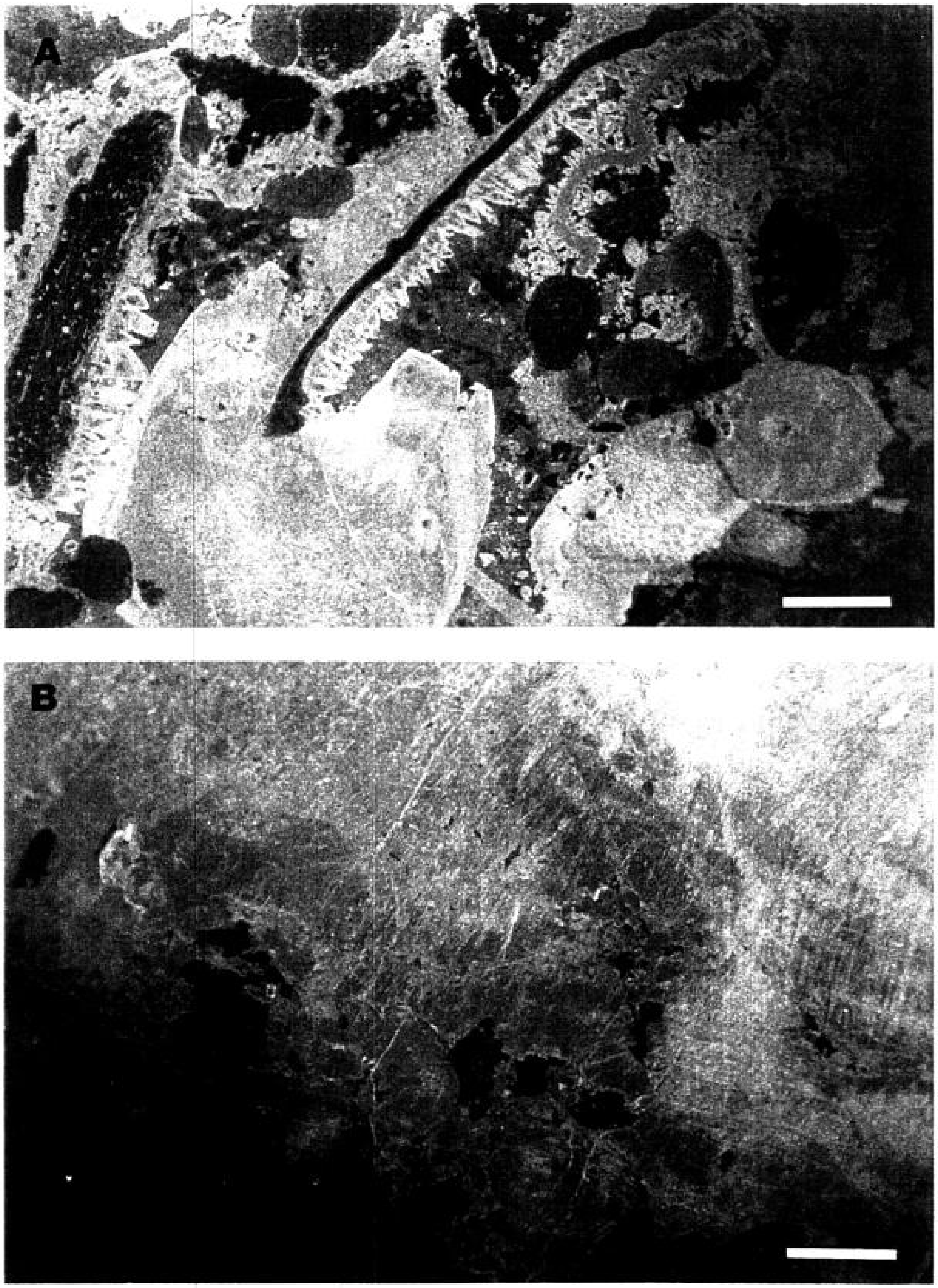

...... Figure 2.7: C) CL view of bioclastic grainstone showing syntaxial bright calcite cement of LF8 on crinoid. LF8 is also developed as thin crust of scalenohedral crystals on a trilobite fragment. The remaining void space is filled by dull luminescent xenomorphic spar of LF9. D) CL view of fracture-fill calcite. The xenomorphic spar shows an irregular composite dull-bright luminescence. Scale bars are 1 mm.

Luminescence facies LF9 consists of dull luminescent xenomorphic calcite crystals (Fig. 2.7c) either conformably or unconformably overlying LF8 crystals. In plane-polarized light, it corresponds to ferroan calcite crystals.

Interestingly, the cement succession present in pores of numerous clasts is strikingly different from the one observed in the interparticular porosity of the Laforce. In fact, pores are commonly filled by the LF2-LF3 cement succession (see above and Lavoie, 1988) recognized in the Sayabec facies and interpreted to be of shallow burial origin (Lavoie, 1988; Lavoie and Bourque, 1993). Obviously, such cement succession (non-luminescent crystals with bright hair-like laminae overlain by scalenohedral bright calcite crystals) is not restricted to the Sayabec Formation. However, it could be used as a supporting argument (with microfacies of the clasts and time relationships of both units) to suggest that the Sayabec was indeed the likely source of clasts in the Laforce basin during sea-level lowstands on the Sayabec ramp.

It is also significant that for almost all crinoidal plates (with many of them heavily broken and corroded) in the grainstone facies, the succession of cements visible under CL, almost invariably shows an initial cement phase (labelled LF7) commonly corroded and broken. Lavoie (1988) suggested that this cement phase could represent an initial stage of cementation on the shallow marine setting (or even very early burial) and that the crinoids and part of their syntaxial overgrowths were eroded from the ramp margin and shed in the Laforce Basin. This could again suggest relative small-scale sea-level fluctuation at the source area of the clasts. Obviously, this interpretation, which suggest repetitive exposures of marine carbonates to subaerial diagenesis, need to be better substantiated with new petrographic and isotopic data.

Fractured zones were avoided in the original material sampled by Lavoie (1988) for sedimentology purposes, although some were present in the material from Imperial Lowlands Associated York #1 core. Fracture-fill calcite consists of large xenomorphic zoned bright-dull luminescent crystals (Fig. 2.7d). In plane-polarized light, it corresponds to granular ferroan calcites. Finally, locally small non-luminescent dolomite rhombs and silica occurs as replacement after LF8 and LF9.

2.1.7 STABLE ISOTOPES RATIOS

2.1.7.1 SEAWATER COMPOSITION

The study of brachiopods and marine cements of Lavoie (1988) and Lavoie and Bourque (1993) provided ocean paleogeochemistry for the Early Silurian (Latest Llandoverian - Wenlockian). The values will serve as baseline to interpret the stable isotope signatures of Sayabec and Laforce calcite cements (Figs. 2.8, 2.9).

The $\delta^{13}C$ ratios for 5 non-luminescent brachiopods (NLB) range from −0.3 to +2.8‰ (mean +0.9‰) whereas 3 analysis of marine cements gave a range of +0.8 to +3.8‰ (mean +2.4‰). Conversely, the $\delta^{18}O_{PDB}$ ratios for NLB cluster at −6.5‰ whereas, presumably altered marine

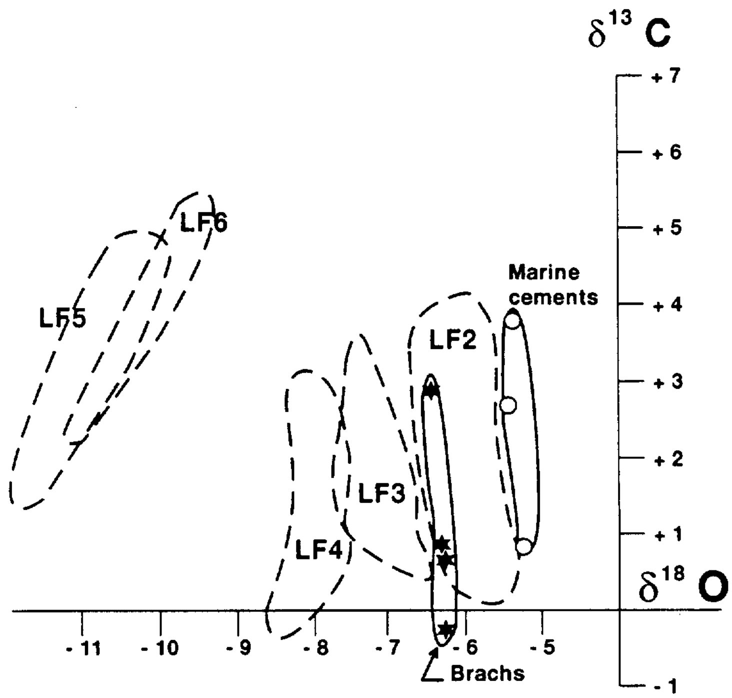

Fig. 2.8 : δ^{18} O vs δ^{13} C graph for Sayabec LF2 to LF4 cements and La Vieille LF5 / LF6 meteoric cements. Modified from Lavoie and Bourque (1993).

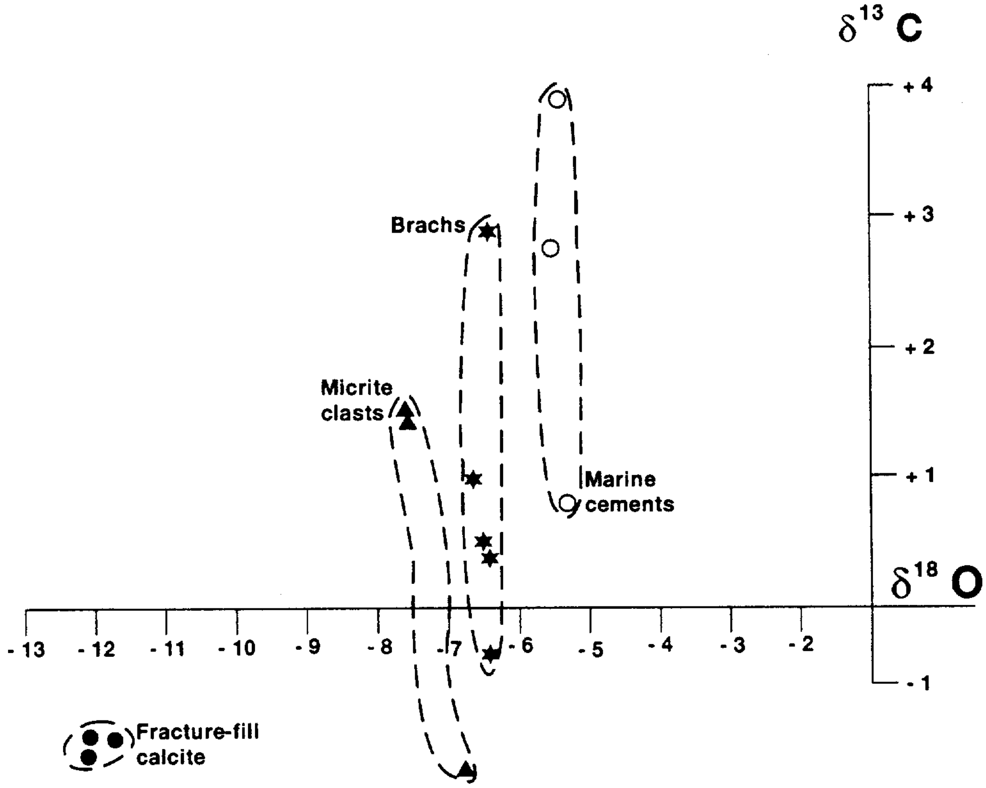

Fig. 2.9 : δ^{18} O vs δ^{13} C graph for Laforce fracture-fill calcite and micrite clasts. Brachiopod and marine cement fields are from Lavoie (1988)

cements gave a narrow range centered at −5.4‰. Indeed, the marine cements $\delta^{18}O$ ratios occur at the depleted end of ranges outlined by brachiopods for various eastern North America basins (Anticosti: −3.5 to −5‰; New York: −3 to −4‰; Intracratonic U.S.A.: −3 to −5‰; e.g., Lavoie and Bourque, 1993, their fig. 10). It is likely that both the NLB and marine cements carry a diagenetic signal. Therefore, even if alteration is recorded in the blotchy luminescent marine cements, its heaviest $\delta^{18}O_{PDB}$ ratio (−5.3‰) is taken as our best estimate for Early Silurian seawater composition for the Gaspé Basin.

2.1.7.2 SAYABEC FORMATION

The following isotopic values (Fig. 2.8) are from Lavoie (1988) and Lavoie and Bourque (1993), no effort has been put into resampling cements that were extensively analysed.

The $\delta^{18}O_{PDB}$ mean value for LF2 cements is −6.2‰ (13 samples; σ=0.3) whereas its $\delta^{13}C$ mean value is +1.9‰ (σ=1.4).

The $\delta^{18}O_{PDB}$ mean value for LF3 cements is −7.1‰ (5 samples; σ=0.5) whereas its $\delta^{13}C$ mean value is +2.0‰ (σ=1.4).

The $\delta^{18}O_{PDB}$ mean value for LF4 cements is −8.1‰ (9 samples; σ=0.3) whereas its $\delta^{13}C$ mean value is +1.6‰ (σ=1.2).

Restricted to the La Vieille Formation, the $\delta^{18}O_{PDB}$ mean value for LF5 cements is −10.7‰ (5 samples; σ=0.8) whereas its $\delta^{13}C$ mean value is +3.7‰ (σ=1.4). Conversely, the $\delta^{18}O_{PDB}$ mean value for LF6 cements is −10.1‰ (5 samples; σ=0.7) and its $\delta^{13}C$ mean value is +4.4‰ (σ=1.3).

A restricted number of 5 analysis were made for the various fracture-filling calcite cements, the low total number is explained by the nature of Lavoie's (1988) study. Therefore, the values are certainly statistically insignificant. The F1 event yielded mean $\delta^{18}O_{PDB}$ of −8.5‰ and $\delta^{13}C$ of +1.7‰, the later F2 event yielded mean $\delta^{18}O_{PDB}$ of −8.5‰ and $\delta^{13}C$ of +2.6‰, finally one analysis of the latest F3 event gave a $\delta^{18}O_{PDB}$ ratio of −10.9‰ and a $\delta^{13}C$ ratio of +1.6‰.

Interpretation
The interpretation put forward by Lavoie and Bourque (1993) for the various LF2 to LF6 cements seems still coherent. Therefore, the LF2 to LF4 succession is interpreted to record progressive $\delta^{18}O$ depletion through isotopic fractionation of the oxygen reservoir and increasing temperature through burial. Conversely, the $\delta^{13}C$ ratios are suggestive of normal marine carbon source and the very slight depletion through the cement succession does not seem statistically significant. The progressive burial interpretation is coherent with the petrographic characteristics of the cements.

The interpretation of meteoric cements for La Vieille LF5 and LF6 cements (based on field relationships, petrographic and isotopic data) is a solid case. Obviously, no such cements have been observed in the Sayabec Formation although analysis of samples from the area where the Salinic Unconformity deeply cuts through the Sayabec might have resulted in a similar scenario. Interestingly, the only one analysis (sample from the Northern Outcrop Belt) from calcite filling the F3 fracture event yielded a depleted $\delta^{18}O$ ratio (-10.9‰) that is only matched by meteoric cements of the La Vieille Formation, although an hydrothermal event could not be rejected unequivocally.

2.1.7.3 LAFORCE FORMATION

Lavoie (1988) did not analyse any pore- or fracture-fill calcites. In the course of this study, 2 samples of the LF8 cement were taken for analysis. However, not enough gaz was generated from the small volume of calcite powder (small sample in order to avoid contamination from other calcite phases) and no analysis could be done. Similarly, not enough material was available to analyse LF9.

Three samples from the zoned bright-dull luminescent calcite crystals found in veins of the Laforce Formation were analysed. $\delta^{18}O_{PDB}$ ratios (Fig. 2.9) are constant (-11.8, -12.1 and -12.1‰) as are also $\delta^{13}C$ ratios (-0.9, -1.0, -0.9‰).

Three samples from clasts of extrabasinal micrite were also taken in order to verify if any meteoric signature could be found in these resedimented fragments eroded from a shallow marine carbonate settings. The $\delta^{18}O_{PDB}$ ratios (Fig. 2.9) are fairly constant (-7.6, -7.6 and -6.8‰) whereas some variations are noted for $\delta^{13}C$ ratios (1.4, 1.5, -1.1‰).

Interpretation
Lavoie (1988) suggested on petrographic grounds that LF8 and LF9 cements represent burial calcites precipitated in Laforce interparticular pore space. The relative well preserved grain contacts might suggest that precipitation started fairly rapidly after initiation of burial. However, we currently lack the critical isotopic and fluid inclusion data to better constrained this interpretation.

The isotopic ratios of the zoned calcite found in fractures of the Laforce are intriguing. They have very depleted $\delta^{18}O_{PDB}$ ratios and negative $\delta^{13}C$ ratios. It could be tempting to relate these values to meteoric cementation as the $\delta^{18}O$ ratios are only slightly more depleted compared to meteoric cements of the La Vieille Formation (-9.4 to -11.8‰), moreover, the slightly negative $\delta^{13}C$ ratios could also be related to meteoric cementation. However, these ratios could also be explained by calcite precipitation at relatively high temperature with a significant input of $\delta^{13}C$-depleted organic CO_2. The petrographic observations are rather inconclusive so far, no textural properties commonly associated with meteoric cements could be found, although, we worked on a very limited number of samples not necessarily well suited for a precise diagenetic study.

The isotopic signature of the extrabasinal micrites did yield possible evidence for meteoric influence at the source of the clasts. One analysis of the micrite yielded a depleted $\delta^{13}C$ value (Fig. 2.9) which could suggest a meteoric effect. However, this limited study is certainly statistically insignificant. However, it is a well known fact that an already mineralogically stabilized carbonate sediment (which as to be the case for an eroded micrite clast) might easily escape isotopic resetting from short-lived sub-aerial exposure.

2.1.8 Dolomitization

Dolomite is uncommon within facies of the Sayabec Formation. Peritidal facies which are for many Lower Paleozoic carbonate successions the site of intense early dolomitization, are particularly poor in dolomite in the Sayabec. In fact, a small amount of dolomite is seen associated with stylolites and, therefore, is a late diagenetic product with no porosity associated. However, as previously discussed, massive hydrothermal dolomitization affecting all carbonate facies of the Sayabec succession (Lachambre, 1987) is present at some localities near the Shickshock Sud Fault (e.g., Isabelle Creek). Some of the dolomite facies of the Sayabec show significant volume of open vuggy pores. This late dolomitization was not addressed by Lavoie (1988) and therefore, nothing is known pertinent to its timing with respect to diagenesis of the unit or with possible hydrocarbon migration.

2.1.9 Conclusions

The Early Silurian Sayabec - Laforce formations of the Gaspé depositional belt mark the first significant shallow water carbonate deposits in the post-Taconian Gaspé Basin. The Sayabec Formation, in northern Gaspé, consists of various facies deposited on a shallow-water, south-dipping carbonate ramp. Conversely, the Laforce Formation, in central Gaspé, consists of coarse-grained carbonates and fine-grained siliciclastics deposited on a below wave base setting. The source of the ubiquitous limestone clasts in the Laforce is either the slightly older to coeval Sayabec Formation or an unknown unit on the Anticosti carbonate platform. The diagenetic history of the Sayabec Formation is definitively better known than that of the Laforce.

Reexamination of Sayabec's material did not reveal anything new that was not already described and isotopically characterized although the material collected at that time was mostly concerned with facies analysis. Suggestions for study of new material in the light of Shell's interests in the area are presented below.

The study of old and new Laforce material allows to propose preliminary interpretations on its diagenetic evolution. However, as for the Sayabec, material available was not collected for a specific diagenetic study and, therefore, information is rather lean. Three cement events are present in Laforce interparticular porosities, not enough material was available for isotopic analysis. Fractures were studied in the Imperial Lowlands Associated York #1 hole, the isotopic ratios could be interpreted either as resulting from meteoric cementation or from high-temperature deep burial cementation. CL petrography documented that some of the limestone clasts shed in the Laforce basin were already cemented and possible isotopic evidence for meteoric imprints were detected in one micrite clast.

2.1.10 IMPLICATIONS FOR HC PLAYS

2.1.10.1 SAYABEC FORMATION

The Sayabec Formation contains facies with relatively high initial depositional (carbonate sand) or growth (reef) porosity. The fact that facies outcropping along the Northern Outcrop Belt are mostly dominated by peritidal lithologies suggest that these favourable facies are likely present in the sub-surface south of the actual outcrop belt.

The cementation history of the unit is dominated by burial events, however, the effect of the Salinian Unconformity and of the hydrothermal dolomitization on porosity history are unknown.

2.1.10.2 LAFORCE FORMATION

Relatively coarse-grained facies with a significant amount of initial depositional porosity are present in the eastern part of the Rivière St. Jean Anticline. However, the cementation history of the unit is unknown. Restricted data on fractures cutting through the unit show that either high-temperature fluids loaded with biogenic CO_2 or meteoric waters circulated in this network. Whatever the case, abundant HC-rich fluid inclusions are present within fracture-filling calcites.

Finally, at places the Salinian Unconformity cuts through the Laforce Formation. Its effects on porosity history (karstification) for the Laforce are unknown.

2.1.11 RECOMMENDATIONS

The phase 1 study on the Sayabec - Laforce units has been limited by the small volume of material pertinent for a diagenetic study (both in location of the material and in its nature). However, preliminary study of fluid inclusions showed that for both units, a non-negligible part of them seem to carry hydrocarbons and that in pore- and fracture-fill calcites.

In order to evaluate the possible effects of the Salinian Disturbance on the Sayabec diagenetic evolution, it is proposed that new material (cement-rich facies and fractures) be collected in the area where the presence of the Salinian Unconformity is documented, that is in the Rivière Madeleine area. This precise locality was not covered by Lavoie (1988) Ph.D. study, moreover, this area is also the site of meteoric dissolution in the overlying West Point reefs (see Bourque et al., this report). Moreover, some samples of porous dolomite facies of the Sayabec will be collected at the best locality, the Isabelle Creek section.

The diagenetic evolution of the Laforce Formation needs to be seriously addressed by collecting material pertinent for such study (cement-rich facies and fractures). It is proposed that new material be collected at various sections (tip of the St.Jean River Anticline, Laforce Creek, Lachambre Creek). Moreover, possible effects (fractures - cements) of the Salinian Unconformity on the Laforce Formation could be recorded in sections present along the old Chandler - Murdochville road in the western part of the St. Jean River Anticline.

Sayabec and Laforce material will be examined petrographically (conventional and cathodoluminescence) as well for detailed microthermometry and composition of fluid inclusions. Cement phases will be analysed isotopically. The new results will enhance the actual lean data base and will allow for more comprehensive interpretations on the diagenetic evolution of both units in particular, in the light of possible effects of sub-aerial exposure on porosity evolution. The results of this phase 2 of the Sayabec-Laforce should be submitted to Shell Canada for December 1996.

2.2 WEST POINT FORMATION

The West Point Formation is divided into two reefal limestone packages: the Upper Silurian reef and bank complexes (Fig. 1.9, Chapter 1 of this report), better developed in the Chaleurs Bay area, but also occurring in northeastern Gaspé; and the Lower Devonian pinnacle reefs (Fig. 1.10, Chapter 1 of this report) mainly known in the Northern Outcrop Belt. As stated in Chapter 1 of this report, and for sake of practicability, we refer here to the Silurian West Point, and the Devonian West Point, respectively. In the East-Central Outcrop Belt, the West Point is dated as Uppermost Silurian to lowermost Devonian. Our discussion of the West Point Formation is presented below under three headings:

3.1 - Silurian West Point
3.2 - Devonian West Point of Northern Outcrop Belt
3.3 - Silurian-Devonian West Point of East-Central Outcrop Belt.

2.2.1 SILURIAN WEST POINT

The Silurian West Point has been extensively studied by the Laval University team (P.-A. Bourque, coordinator) and has been the subject of a number of M.Sc. theses (Gignac, 1980; Amyot, 1980; Gosselin, 1980; Laliberté, 1982; Savard, 1986; Raymond, 1986; Morin, 1987; Laforest, 1987; Dansereau, 1989; Alaoui, 1991; Blais, 1992). Although research focussed on sedimentology, petrography, facies relationships, paleoenvironments and facies controls (e.g. Bourque et al., 1986), some studies dealt with diagenesis (Savard, 1986; Raymond, 1986; Morin, 1987; Dansereau, 1989; Savard and Bourque, 1989; Alaoui, 1991; Bourque and Raymond, 1994).

The study by Savard (1986) and Savard and Bourque (1989) on the diagenesis of the upper reef complex in Chaleurs Bay (see Fig. 1.9, Chapter 1 of this report) dealt particularly with porosity history. This study concluded that, from a primary porosity of 30% in reef margin facies and 18% in back-reef facies, the porosity in both facies decreased to 18% in shallow burial environment (pre-chemical compaction), and to 8% in deeper burial environment (post-chemical compaction). All porosity was occluded at about 1 km for the base of the complex and a few hundred meters for the top, prior to attainment of the maximum burial depth of the reef complex for this region as based on chitinozoans alteration colour and organic matter maturation. No karst or secondary dolomitization porosity was detected. Obviously, these conclusions apply to the Port-Daniel area (Chaleurs Bay) where the syn-sedimentary tectonic history is different from that of northeastern Gaspé. It is therefore not possible to say whether or not the conclusions reached for the Port-Daniel area can be extended to the Silurian West Point of northeastern Gaspé until a diagenetic study is carried out there.

> *We did not carry out such study in phase 1 of our project because no material was available. Such a study is therefore planned for phase 2 of the project. Field work is necessary to get material* (see Recommendations).

2.2.2 DEVONIAN WEST POINT OF NORTHERN OUTCROP BELT

The Devonian West Point is made up of two main facies: a shallow water well-bedded crinoidal limestone, and massive stromatoporoid pinnacle reefs (see Chapter 1 of this report). The bedded crinoidal limestone is a thin sheet (a few 10's of meters thick at maximum) traced all along the Northern and East-Central Outcrop Belts (Figs. 1.5, and 1.7, chapter 1 of this report). A number of pinnacle reefs reaching thicknesses up to 300 m are known along the Northern Outcrop Belt, between the Madeleine River and Road 299 (Fig. 1.15, Chapter 1 of this report). Facies and facies architecture of two of these pinnacles were the object of detailed studies (Bourque, 1972, 1977; Lachambre, 1987): the well-known **Madeleine River buildup** (Lefrançois Member of Lespérance and Bourque, 1970; Figs. 1.10 and 1.15, Chapter 1 of this report; see also Lespérance and Bourque, 1970, fig. 5 for an aerial view of the buildup); and a pinnacle, here called the **Lac Brûlé buildup**, 8 km west of the Madeleine River buildup, and situated in the Northern Outcrop Belt, 1,5 km south of the Lac Brûlé.

2.2.2.1 FACIES AND FACIES ARCHITECTURE

The Madeleine River buildup is a pinnacle reef that shows a vertical zonation (Fig. 2.10), from bedded crinoid-dominated grainstones-packstones and rudstones (facies B and C), to massive stromatoporoid boundstones and rudstones (facies D and E). Facies C is similar to facies B, except it contains a significant proportion of well-rounded quartz grains. Stromatoporoids of facies D are smaller and of the tabular-type, as compare to those of facies E which are big (up to a few tens of cm) and of the massive-, hemispherical- and globular-types. As mentioned in Chapter 1 of this report, basal facies A is a stromatactis mudstone (a facies not recognized by Bourque at time of study in 1968-70), a facies similar to the Gros Morbe Member of the Silurian West Point in Chaleurs Bay, and the possibility that Silurian West Point occurs at base of the Madeleine River buildup is left open. Reef breccia (facies F) occurs at foot of the buildup. Clasts of the breccia are often composed of stromatoporoid limestone, suggesting that breccia is syn- or post facies D and E deposition.

> *Detailed sedimentological and diagenetic study of the breccias should provide key information as to the timing of breccia deposition and reef cementation history* (such a study should be considered in an eventual phase 3).

The Lac Brûlé buildup is in fact two limestone bodies separated by fine-grained siliciclastics similar to the surrounding Indian Point Formation siliciclastics. It is not clear if it is truly two distinct bodies in three-dimensions, or if we are looking at margin of a single body interfingering with the surrounding siliciclastics. The Lac Brûlé buildup comprises most of the Madeleine River buildup facies (facies B, C, D, E, F and possibly A). In addition, facies G makes up an important volume of the buildup. The latter is like facies B, but with a significant proportion of corals.

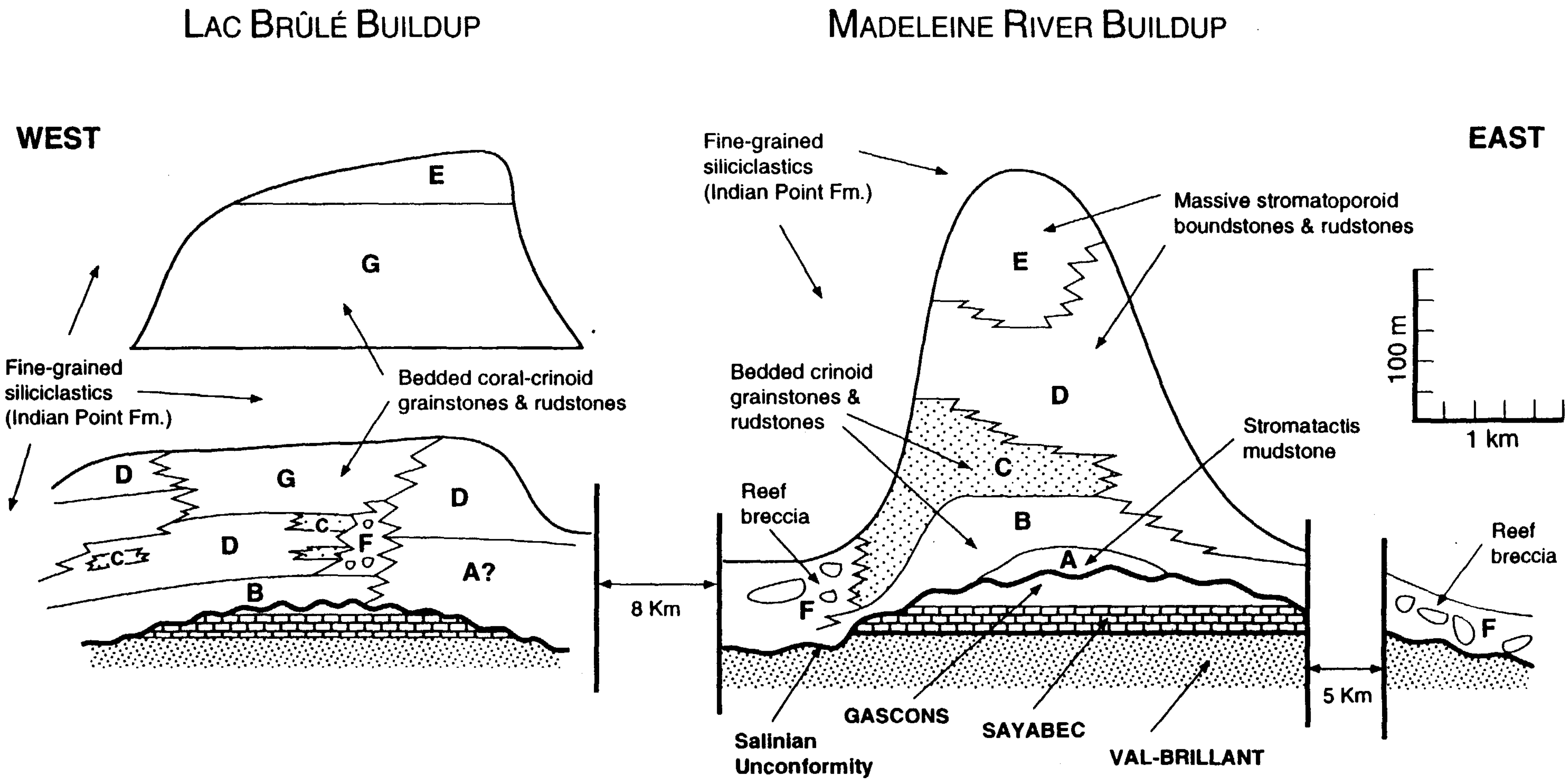

***Figure 2.10** - Facies architecture of the Lac Brûlé and Madeleine River buildups. From Bourque (1972, 1977), Bourque et al. (1986), and Lachambre (1987).*

2.2.2.2 CEMENT STRATIGRAPHY AND CHRONOLOGY OF DIAGENETIC EVENTS

In order to decipher porosity history of these limestone bodies, and to make a preliminary evaluation of their potential as reservoir rocks, we studied material in the Laval University collections from both buildups. This material was collected in the early 70's for microfacies and sedimentology study purposes. Sampling is therefore not necessarily suitable for a sound diagenetic study. Our conclusions should be evaluated in the light of this limitation. Nearly 350 thin-sections (unstained) from hand specimens and drill cores from the two pinnacles were examined to recognize the main diagenetic features. Out of these, 58 polished thin-sections were made up and studied under CL to establish cement stratigraphy. Thereafter, 30 polished blocks served to sample cements for C and O stable isotope analyses (50 analyses).

Cement phases are more abundant in the Lac Brûlé buildup than in the Madeleine River buildup. Seven phases of calcite cements (numbered C1 to C7) were recognized. Figure 2.11 summarizes cement succession, whereas Figure 2.12 presents chronology of the main diagenetic events for the Lac Brûlé buildup, including processes such as cementation, pore infilling by internal sediments, fracturation-dissolution, cement corrosion, brecciation and stylolitization.

Two episodes of fracturation, often accompanied with dissolution, are represented by calcite veins. A first episode of fracturation-dissolution (FS5 veins; Fig. 2.13) post-dates cement C4, cutting across C1 to C4. Open space is cemented by bright (in CL) C5 cement. A second episode post-dates dull C6 and is cemented by last dark dull C7 cement (FS7 veins; Fig. 2.14). Dissolution is obvious in the form of swarms of narrow seams (Fig. 2.15). Corrosion of cements C2 and C3 took place prior to C4 cementation (Figs. 2.16, 2.17).

Internal sediment infilling occurred during three discrete diagenetic episodes: during early marine cementation C1-C2 (SI1), during C3 cementation SI3), and during and post-C6 - pre-C7 cementations (SI6). A brecciation episode took place during and after C6 cementation. All cement phases and veins pre-dates stylolites, except in one sample where we observed a vein of C7 cutting across stylolite.

The Madeleine River buildup has a similar cement stratigraphy, but lacks the C4 and C5 cements (Fig. 2.18). Veins of bright-luminescent cement are uncommon, whereas these with C7 cement (FS7) are much less common than in the Lac Brûlé buildup.

2.2.2.3 ISOTOPE GEOCHEMISTRY

Trends in the two buildups (Fig. 2.19).

All stable isotope analysis results for the Lac Brûlé buildup and the Madeleine River buildup are shown on Figure 2.19. The micro-sampled early cements C1 and C2 show narrow ranges of values ($\delta^{18}O_{VPDB}$ = -5.9 to -4.8‰; $\delta^{13}C$ = +1.6 to +2.3‰) that are all included in the field of

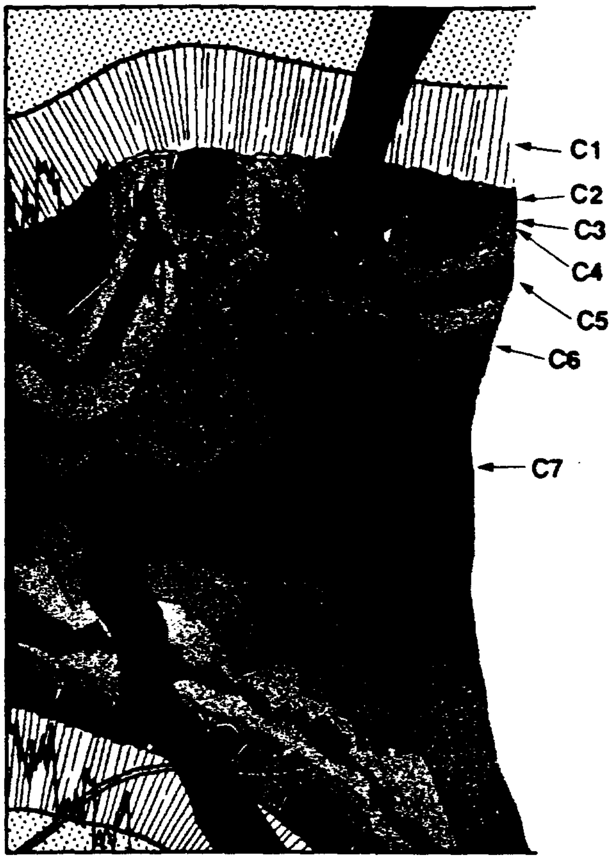

Cements	Habit	Luminescence
C1	Isopachous, fibrous-like, or syntaxial (on crinoids)	Non-luminescent to composite (due to probable alteration) Non-luminescent, with local luminescent banding
C2	Bladed, pinacoid, or granular crystals	Non-luminescent
C3	Thin crust, syntaxial on C2	Bright
C4	Syntaxial on C3	Light dull
C5	More or less syntaxial on C4	Zoned, bright/light dull
C6	Large xenomorphic crystals	Light dull, with local banding
	Large xenomorphic crystals	Darker dull

***Figure 2.11** - Cement types and succession in the Lac Brûlé buildup.*

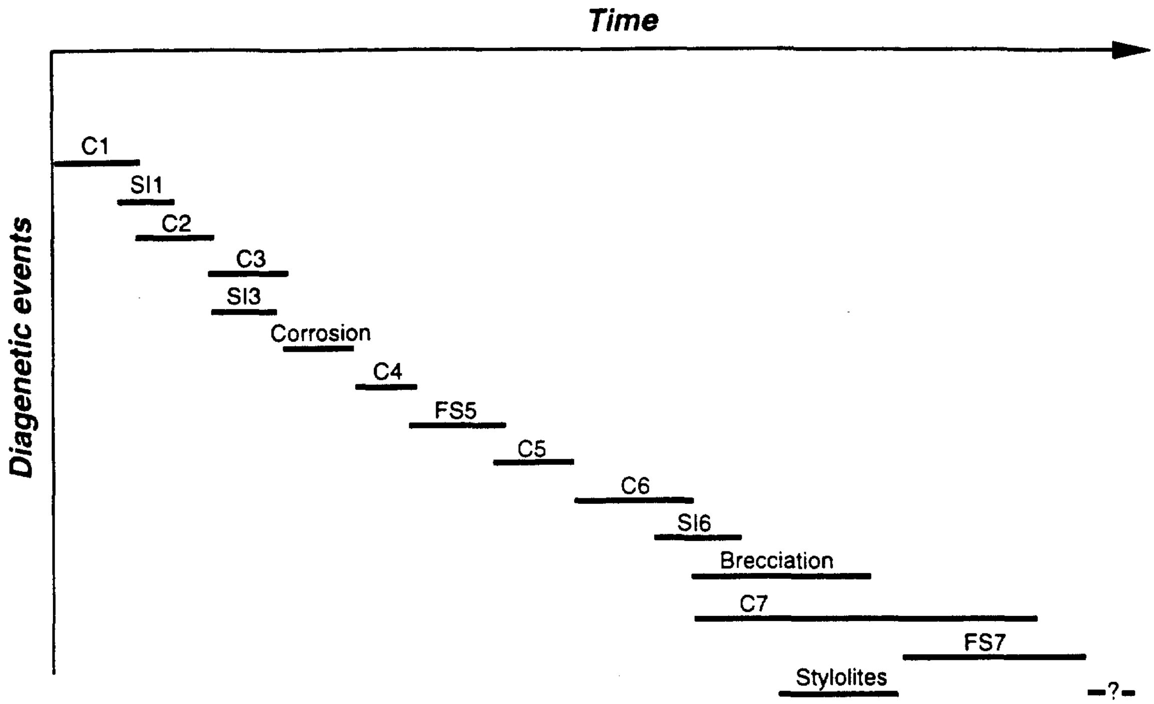

Figure 2.12 - Diagenetic events through time in the Lac Brûlé buildup. See Figure 2.22 for involved diagenetic environments.

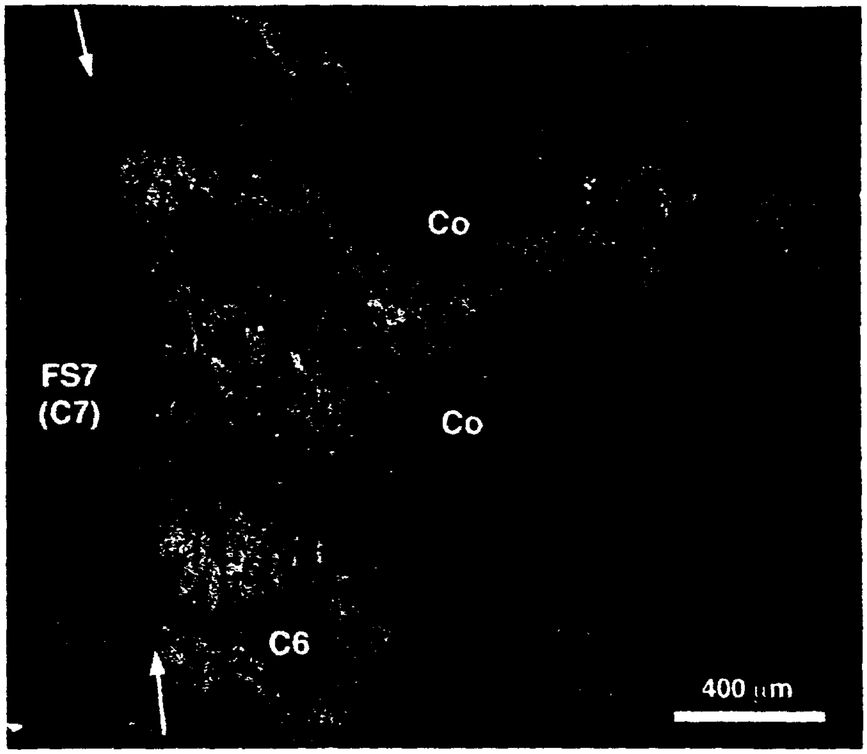

Figure 2.13 - *Cathodoluminescence photomicrograph to illustrate first (FS5) and second (FS7) phases of fracturation-dissolution. Note dissolution cutting across coral wall (Co) and cements C2 to C4 (black arrow). Note also vein of C7 cement (FS7) cutting across cements C2 to C6 (white arrows). Sample DY4-45.5, facies D, Lac Brûlé buildup.*

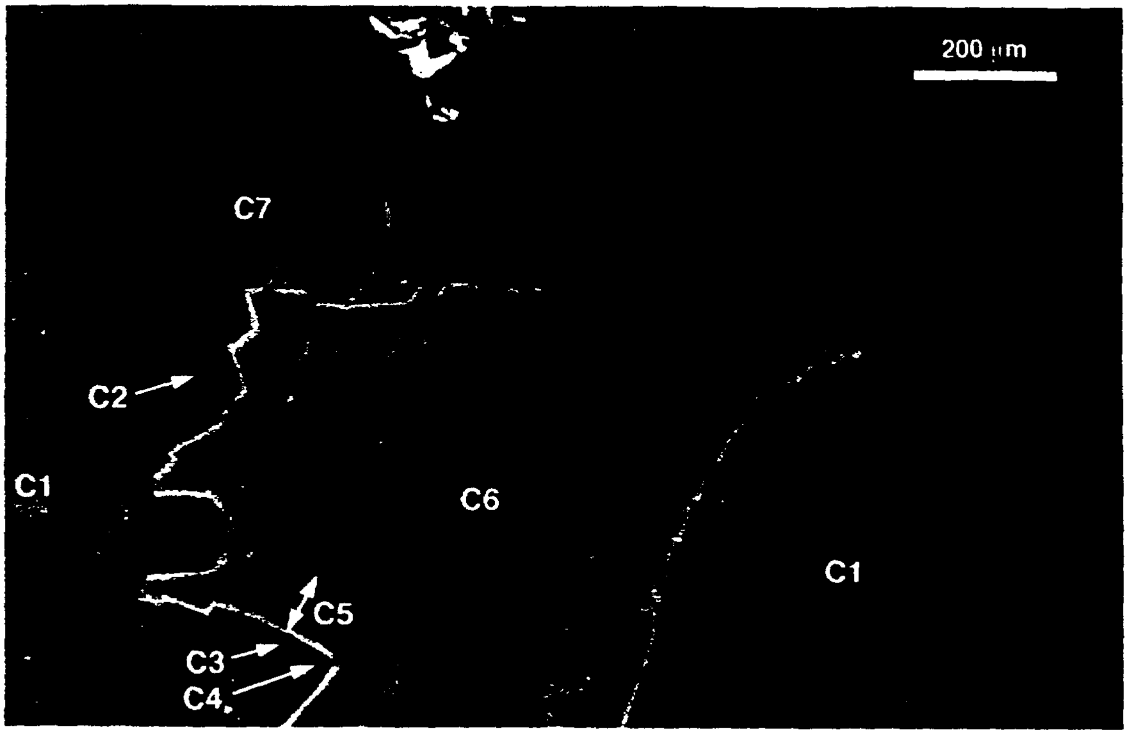

Figure 2.14 - Cathodoluminescence photomicrograph to illustrate phase FS7 of fracturation-dissolution. Vein of cement C7 clearly cuts cements C1 to C6. Sample DY1-98.7, facies E, Lac Brûlé buildup.

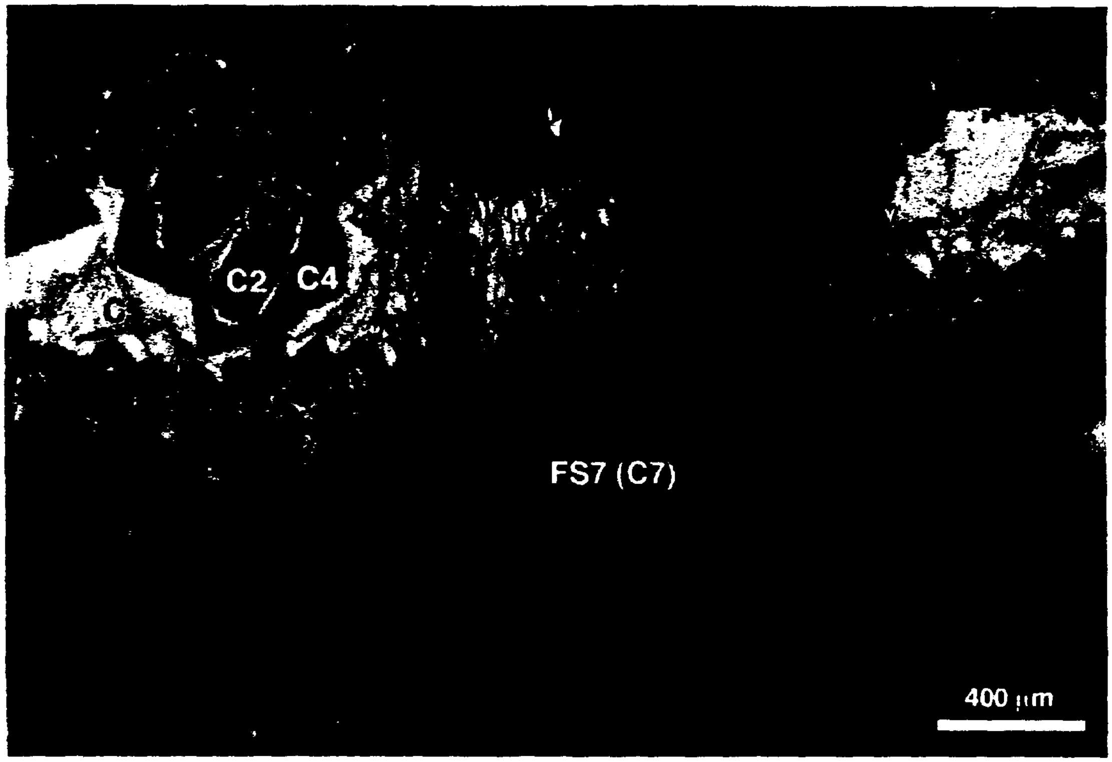

Figure 2.15 *- Cathodoluminescence photomicrograph showing a solution pipe (FS7) cutting across cements C1 to C5. Note swarms of narrow solution seams in cement C5. Sample DY4-45.5, facies D, Lac Brûlé buildup.*

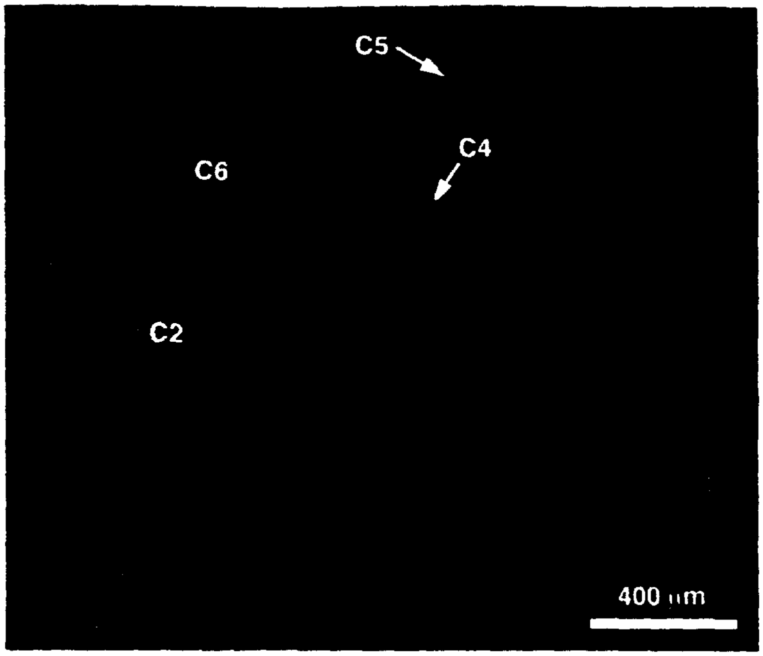

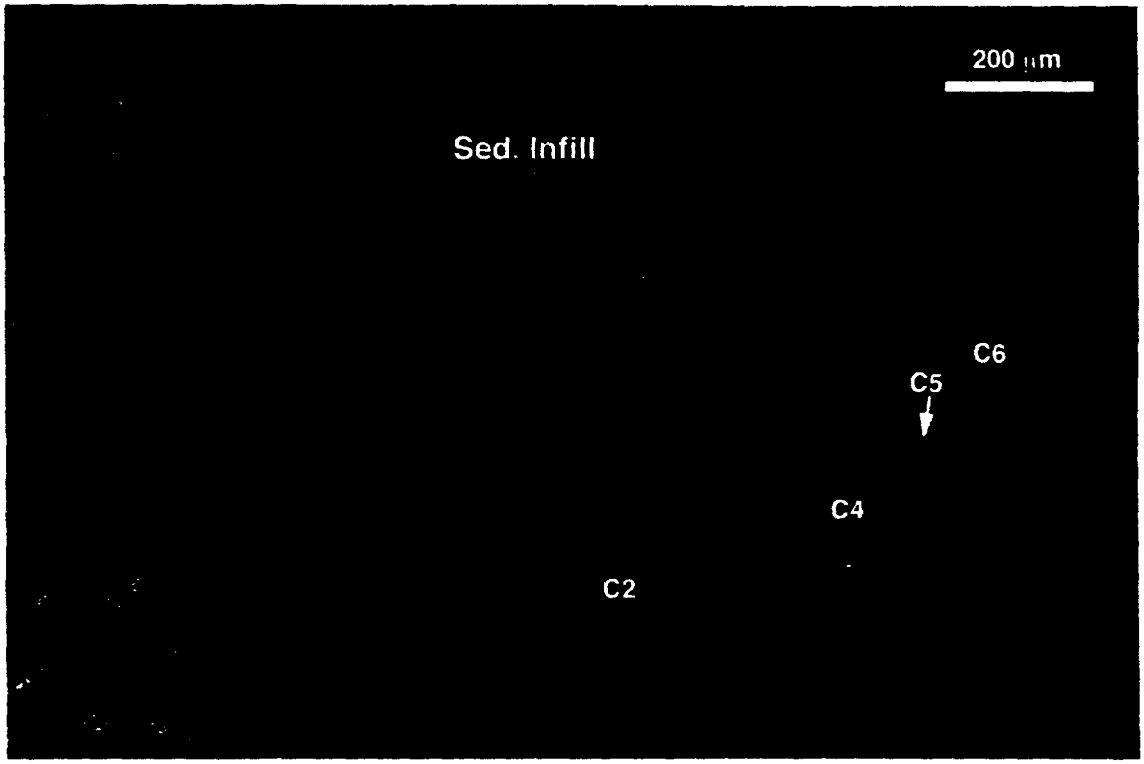

Figure 2.16 - *Cathodoluminescence photomicrograph showing corrosion of cements C2 prior to cementation by C4. Sample DY6-86.5, facies G, Lac Brûlé buildup.*

Figure 2.17 - *Close-up showing same corrosion phenomenon as in Figure 2.16. Sample DY6-86.5, facies G, Lac Brûlé buildup.*

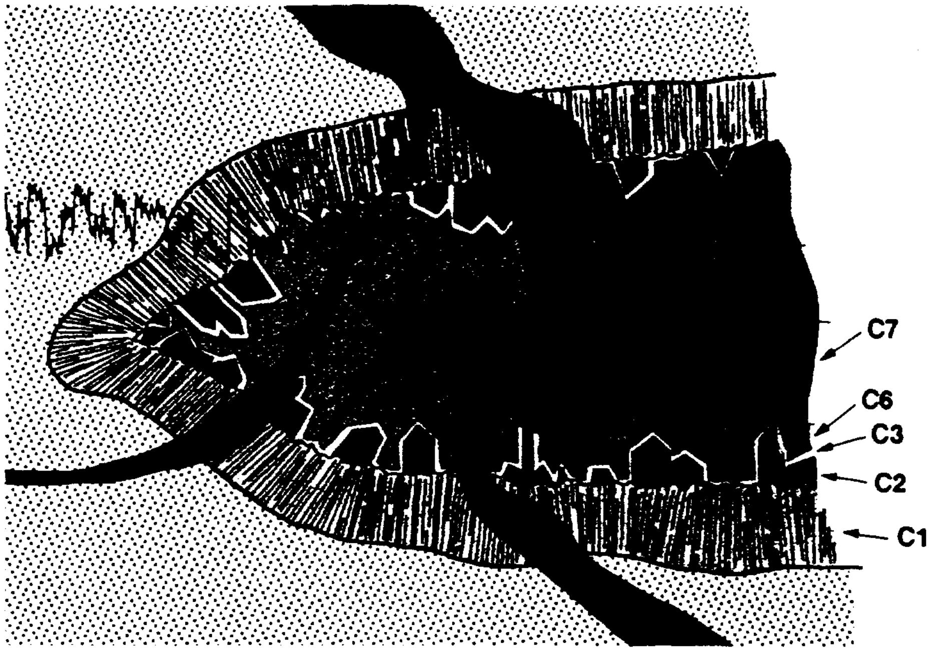

Cements	Habit	Luminescence
C1	Isopachous, fibrous-like, or syntaxial (on crinoids)	Non-luminescent to composite (due to probable alteration) Non-luminescent, with local luminescent banding
C2	Bladed, pinacoid, or granular crystals	Non-luminescent
C3	Thin crust, syntaxial on C2	Bright
	Large xenomorphic crystals	Light dull, with local banding
	Large xenomorphic crystals	Darker dull

***Figure 2.18** - Cement types and succession in the Madeleine River buildup.*

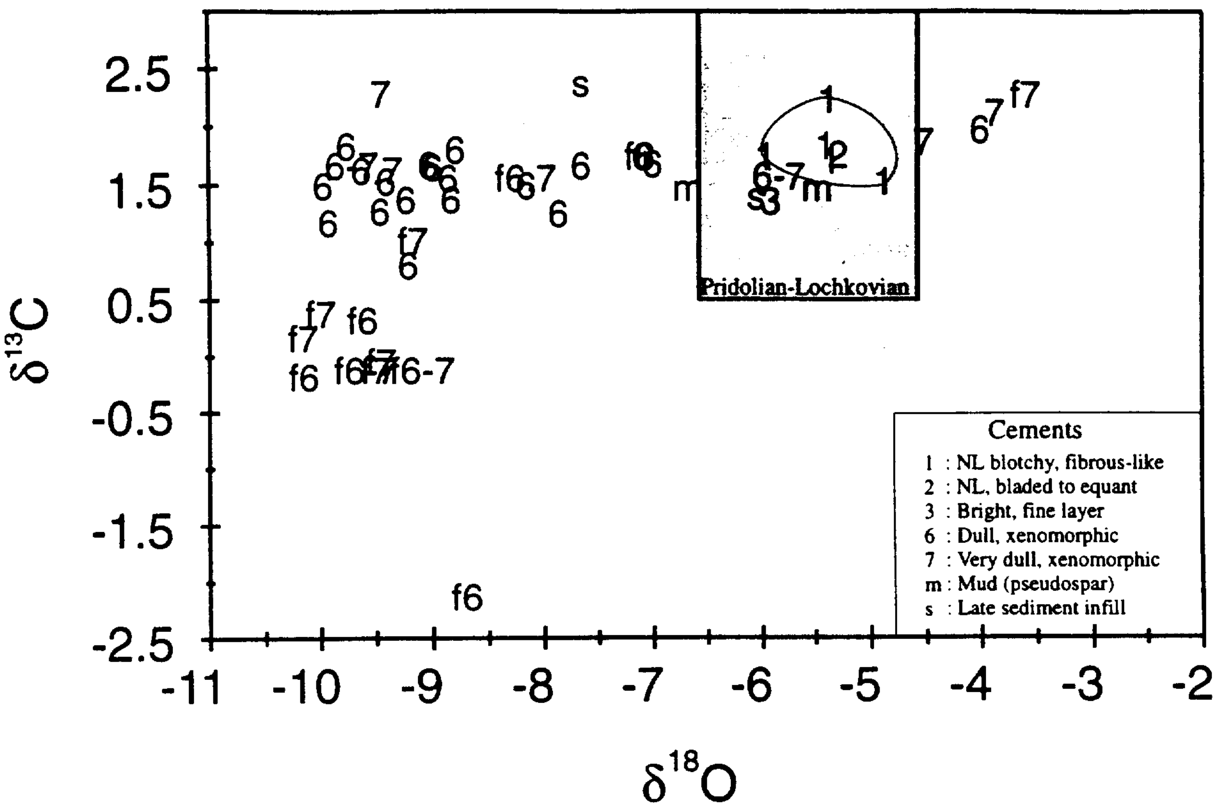

Figure 2.19 - Devonian West Point Buildups - Stable Isotope Geochemistry
All results. Grey box: Pridolian-Lochkovian marine calcite field from literature (see text). Grey circle: marine cements of this study. "f" preceeding a number indicates fracture-filling cements.

Pridolian-Lochkovian marine calcites (box on Fig. 2.19; e.g. Veizer et al., 1986; Savard and Bourque, 1989; Lohmann and Walker, 1989; Bourque and Raymond, 1994). Mud samples are either in or near the marine box.

These results clearly indicate that marine diagenesis affected the two buildups after their deposition.

The two late cements C6 and C7 filling primary pores are commonly postdated by stylolites, but the nature and orientation of the latter are unknown. These cements (C6 and C7) have identical isotopic ranges: a narrow $\delta^{13}C$ range (+0.8 to +2.3‰) for a wide spread range of $\delta^{18}O_{VPDB}$ values (-9.9 to -3.9‰). The heavy end-member of the range is higher than the marine field.

The $\delta^{18}O$ values indicate that extreme variations of conditions occurred during precipitation of the two cements, the carbon budget being mostly buffered by marine bicarbonate.

The low end-member of the $\delta^{18}O$ trend could be compatible with burial diagenesis, but standard burial diagenesis alone cannot explain the very broad $\delta^{18}O$ range, particularly the heavy end-member.

The fractures/solution conduits and fracture-filling cements C7 (noted thereafter as f7; see Fig. 2.19) clearly postdate C6 present in numerous pores, and stylolites in one sample. It is assumed that the fractures and dissolution features are of the same nature at the Madeleine River and Lac Brûlé buildups. Cements f7 and f6-7 (= cements C6 and/or C7 filling secondary pores which are fractures and cracks enhanced by dissolution) show a broad range of $\delta^{18}O_{VPDB}$ and $\delta^{13}C$ values: -10.1 to -3.5‰, and -2.1 to +2.3‰ , respectively.

Extreme variation of conditions existed during precipitation of f7 which fills tectonic fractures and cracks that were enhanced by dissolution. The f7 isotopic trend can hardly be explained entirely by burial diagenesis (see further).

A better understanding of the late cement origin can be reached by looking at isotopic results for each location, and at their isotopic variation in time.

Madeleine River buildup (Fig. 2.20).

The primary pore-filling and fracture filling cements again show extreme variations in $\delta^{18}O_{VPDB}$ (-9.9 to -3.9‰). Fracture-filling cements also show a broader $\delta^{13}C$ range than the cements filling primary pores (-0.1 to +2.3‰ vs +1.2 to 2.3‰).

At a smaller scale, microsamples from the same hand samples can indicate isotopic time trend of the diagenetic system that affected the buildup (i.e. water-rock (w/r) variations). Microsamples of

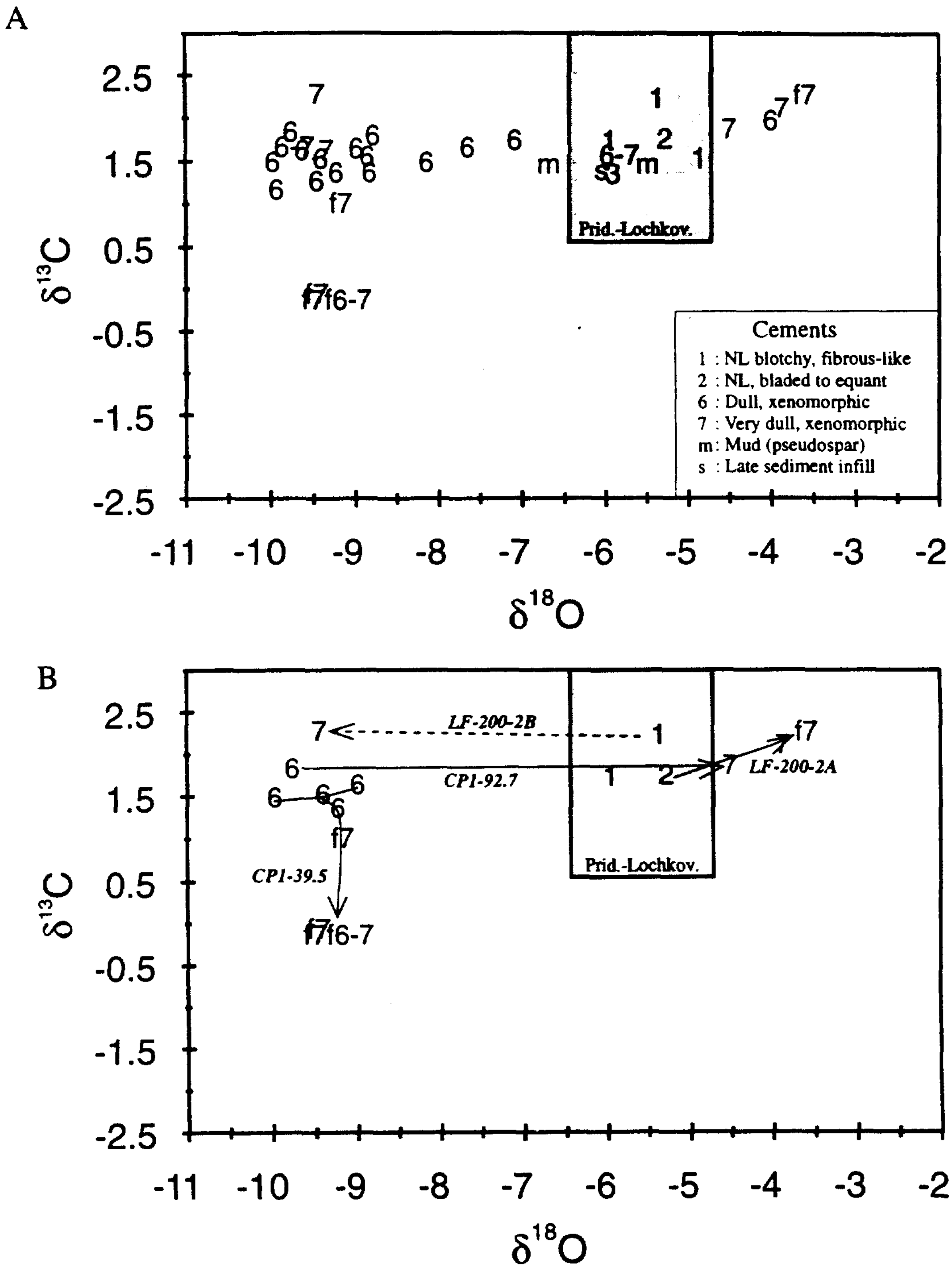

Figure 2.20 - Madeleine River Buildup - Stable Isotope Geochemistry
A). All results. B) Results from individual samples (italic numbers) showing isotopic trend in time (arrows). "f" preceeding a number indicates fracture-filling cements.

cements C1 and C7 from sample LF-200-2B show a $\delta^{18}O$ range (Fig. 2.20) compatible with progressive burial diagenesis after marine cementation as outlined in Savard and Bourque (1989). Microsamples of succeeding cements C6 and C7 from sample CP1-92.7 show a very broad $\delta^{18}O$ range, which in time evolves from -9.7 (C6) to -4.5 (C7) (Fig. 2.20). Within this sample, the low $\delta^{18}O$ end-member (C6) is compatible with burial diagenesis, but the heavy one (C7) suggests either influence of exotic waters such as metamorphic or organic waters (Sheppard, 1986; Sheppard and Charef, 1986) during burial diagenesis, or evaporative effects during surficial (meteoric/marine) diagenesis (Lohmann, 1988).

Four microsamples of C6 and four of f7 from sample CP1-39.5, show a narrow range of $\delta^{18}O_{VPDB}$ (mean -9.2‰) for a $\delta^{13}C$ time trend going from +1.5 (C6) to -0.1‰ (C7). Again suggesting burial diagenesis for the C6 end-member. The f7 end-member suggests incorporation of light carbon, a process that can be achieved either in burial due to organic matter decarboxylation (Tissot and Welte, 1984), or at surface by meteoric diagenesis (Lohmann, 1988). By contrast, sample LF-200-2A shows for f7 a $\delta^{18}O_{VPDB}$ value 1.8‰ heavier than the value for marine cement C2. The diagenetic model explaining the evolution of the Madeleine River buildup should reconcile the facts that cement f7 from samples CP1-39.5 and LF-200-2A showing extremely different isotopic signals, precipitated at the same time (after fracturing) and possibly from a unique water system (petrographic attributes). Influence of metamorphic waters to explain the heavy $\delta^{18}O$ end-member is rejected because there is no evidence of contemporaneous metamorphism in the area. Incorporation of mixed organic and formation waters is possible although the water dominated end-member (light $\delta^{18}O$) should show lower $\delta^{13}C$ values than those found in the present study (Sheppard, 1986). The most likely process was precipitation from meteoric waters (either pure meteoric), with evaporation increasing water $\delta^{18}O$ above the marine signal before calcite precipitation.

The possible meteoric line at -9.2‰ is compatible with the $\delta^{18}O$ expected for meteoric waters precipitating at latitudes known for Gaspé Peninsula during Devono-Carboniferous time (15 to 20°S), and originating from marine waters at around -5.0‰ (SMOW). Thereby, suggesting a near surface meteoric system.

> *Isotopic variation at the Madeleine River buildup, and isotopic variation at fine scale in time collectively suggest succession of three diagenetic systems: marine, burial and surficial dominated by meteoric waters. Broad $\delta^{18}O$ variations for the late cements C6 and C7 are explained by the passage from burial to surficial conditions, whereas broad $\delta^{18}O$ and $\delta^{13}C$ variations for f7 are explained by w/r effect on meteoric water signal, and by evaporation.*

Lac Brûlé buildup (Fig. 2.21).

Isotopic variation in time as shown by C1 and C6 from sample DY6-86.5 suggests marine to burial diagenesis. Cements C6 and f7 with low $\delta^{18}O$ values but with both heavy and light carbon,

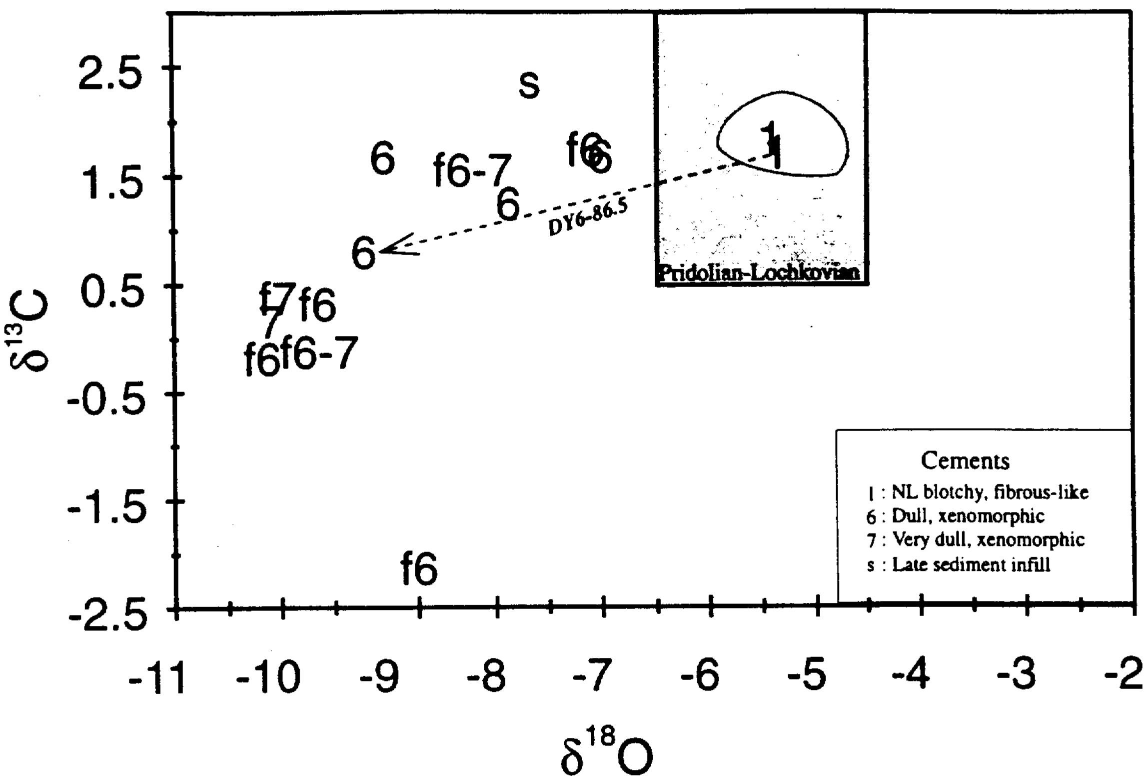

Figure 2.21 - Lac Brûlé Buildup - Stable Isotope Geochemistry
All results. Grey box: Pridolian-Lochkovian marine calcite field from literature (see text). Grey circle: marine cements of Madeleine River Buildup. Stippled line and italic number indicate microsamples from the same hand sample. "f" indicates fracture-filling cements.

respectively, sediment infill, and micro-fracturing/dissolution at a late stage all suggest similarity of the Madeleine River and Lac Brûlé buildups late diagenetic evolution (Fig. 2.22). Lower $\delta^{13}C$ values for fracture-filling cements (-2.1ä) and absence of heavy $\delta^{18}O$ values for Lac Brûlé buildup (max.: -7.2‰) suggest a paleogeographic location closer to a meteoric recharge. This suggestion is compatible with higher degree of dissolution at this location as based on petrographic observations.

The Lac Brûlé buildup trend is compatible with marine to progressive burial followed by surficial meteoric diagenesis.

At this stage, our working hypothesis is that the Madeleine River and the Lac Brûlé buildups both show evidence of marine, burial and surficial meteoric diagenesis in succession (summary in Fig. 2.22). The surficial meteoric trend at the two locations represents broad w/r variations in phreatic zones. The late surficial diagenesis at Madeleine River buildup is possibly marked by evaporation effects. The Lac Brûlé buildup is possibly closer to a recharge area.

Minimum Burial Depth and Stratigraphic Setting prior to Surficial Dissolution
Assuming that parent water with $\delta^{18}O_{SMOW}$ between -5 and -2‰ precipitated burial cement C6 prior to meteoric diagenesis and dissolution (Fig. 2.22), the range of temperature required to yield the most depleted C6 $\delta^{18}O_{VPDB}$ value (-9.9‰) would be 40-60 ¡C (O'Neil et al., 1969). Such temperature existed at an approximate burial range of 0.8 to 2 km if a geothermal gradient of 30°C/km and a surficial temperature of 15 ¡C are assumed.

As formation waters are generally saline, i.e., generally have $\delta^{18}O_{VPDB}$ heavier than marine waters, we suggest that the minimum burial depth is closer to 2 km. Deeper burial would be required if parent waters were heavier than -2‰ (SMOW), and/or if geothermal gradient was lower than 30°C/km.

The minimum burial depth to achieve C6 cementation in burial put constraints on the possible tectonic event responsible for the fracturing/dissolution of the buildups. Stratigraphy indicates that thicknesses of 1 km or more existed above the buildups during Pragian or after. Field investigations might help to pinpoint Salinian or Acadian deformation as the event responsible for microfracturing/dissolution.

Burial cementation operated down to an approximate minimum burial depth of 2 km. The structural event responsible for fracturing and bringing back surficial conditions occurred during or after Pragian.

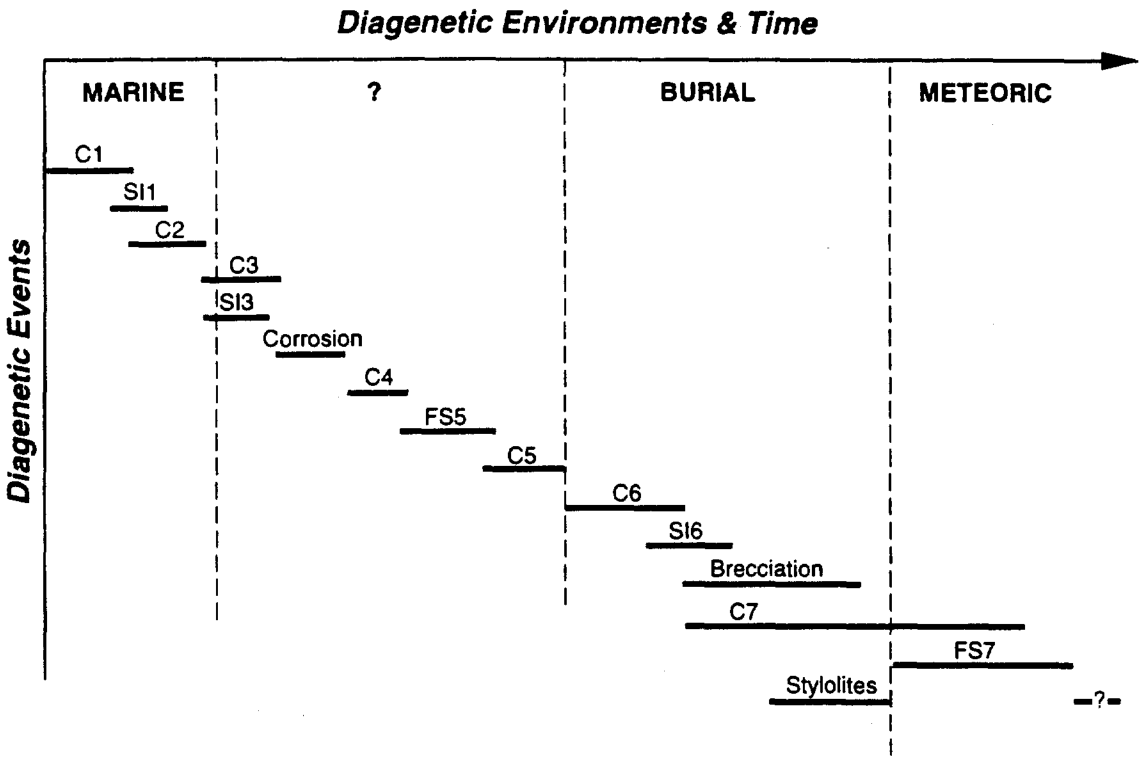

Figure 2.22 - *Relationships of diagenetic events and environments through time for the Lac Brûlé buildup, Northern Outcrop Belt.*

Porosity Evolution (Figs. 2.23, 2.24).

Porosity with respect to facies for both buildups was visually evaluated on thin-sections. From primary growth framework and intra- and interparticulate porosity that averages 26 and 30% for the Madeleine River and the Lac Brûlé buildups respectively, residual primary porosity significantly diminished after marine diagenesis (Early Cem. %). Remaining porosity averaging 6% for the Madeleine River buildup, and 10% for the Lac Brûlé buildup was practically occluded in burial, at an approximate burial depth of 2 km (Late Cem. %). Gain of porosity (av. 8 %) due to fracturing-dissolution (column F-S Po) is significant in the Lac Brûlé buildup where FS7 veins are ubiquitous. These were observed in almost all studied polished thin-sections (21). The veins are up to 10 mm-wide, commonly 0,2 to 4,0 mm, and are often accompanied with swarms of narrow seams (Fig. 2.15). In the Madeleine River buildup the gain of porosity due to fracturing-dissolution is insignificant (< 1%).

Implications for HC plays

- Possibility of early charge of HC for buildups in subsurface; HC could have migrated prior to total occlusion of primary pores (before Pragian).

- Possibility of late charge of HC for buildups in subsurface; after burial cementation was completed, in areas closer to meteoric recharge, HC could have migrated in well developed karsts of Pragian or younger age.

2.2.2.4 FLUID INCLUSION MICROTHERMOMETRY - STUDY OF FEASIBILITY

Numerous regular polished thin sections have been used to evaluate if late cements contained workable fluid inclusions. All samples contain workable fluid inclusions in C6 and C7. The inclusions are typically randomly distributed. Fluid inclusions in C7 occur in clusters or are isolated. Aqueous inclusions are mainly biphase (i.e. liquid+vapor). Some liquid-only and vapor-only inclusions are also observed; the latter probably contain methane.

Orange to brown inclusions are frequently observed mainly in C6. These inclusion are probably petroleum inclusions although, in many cases, they cannot be positively identified as such because the vapor bubble were not clearly seen. Exceptions are CP1-5T and LF-25-1, for which HC identification is clear. These have not been studied for isotope geochemistry so that the link between light $\delta^{13}C$ and presence of HC cannot be made.

2.2.3 SILURIAN-DEVONIAN WEST POINT OF EAST-CENTRAL OUTCROP BELT

Pridolian-Lochkovian reefoid limestones surrounded and interlayered with fine-grained siliciclastics of the upper terrigenous unit of the Chaleurs Group (see Chapter 1 of this report) were assigned to the West Point Formation by Bourque (1977). They are not as well exposed as

	Facies	Primary Po (%)		Early Cem. (%)		Late Cem. (%)		F-S Po (%)	N
MADELEINE RIVER BUILDUP	A	15-30	**23**	9-21	**15**	4-11	**7**		3
	B		**35**		**23**		**12**		1
	C	30-35	**32**	23-35	**28**	3-12	**4**		5
	D	5-40	**25**	1-40	**19**	0-21	**6**		19
	E		**30**		**29**		**1**		1
	Wt. Average		**26**		**20**		**6**	< 1	29
LAC BRÛLÉ BUILDUP	D	20-40	**33**	6-30	**23**	5-16	**10**	**7**	5
	E	10-30	**21**	1-20	**14**	3-12	**7**	**8**	5
	G	15-40	**33**	9-36	**21**	3-21	**12**	**9**	11
	Wt. Average		**30**		**20**		**10**	**8**	21

Figure 2.23 - *Porosity evolution in facies of the Madeleine River and Lac Brûllé buildups, Northern Outcrop Belt. Porosity is visualy evaluated in thin sections.*

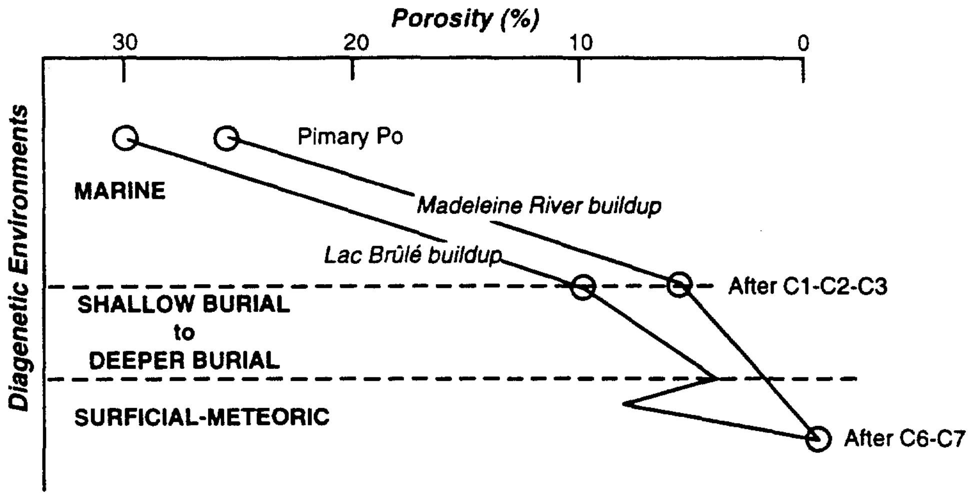

Figure 2.24 - *Porosity evolution vs diagenetic environments for the Madeleine River and Lac Brûlé buildups, Northern Outcrop Belt. Gain of porosity in the surficial-meteoric environment corresponds to fracturation-solution event FS7.*

those in the Northern Outcrop Belt, so that it is not clear whether or not they form actual reefs. Nevertheless, these bodies are crinoid and stromatoporoid limestones having facies similar to the West Point reefs.

Within the time-frame allowed for this phase of the project, we proceeded to a preliminary study of limited material available in Laval University collection. This material was collected originally (1970) for microfacies study, therefore avoiding veins and dolomite. Forty-five (45) thin-sections stained for carbonate mineralogy were studied. The samples come from three sections in the vicinity of the Grande Rivière (sections 80, 82, and 83 of Bourque et al., 1993).

Main conclusions of this study are:

- Fracturation accompanied with dissolution is ubiquitous. Two vein systems are recognized: non-Fe-calcite veins related to early fracturation-dissolution, and Fe-calcite veins related to later fracturation-dissolution. The last is more abundant.

- Out of the 45 studied samples, 15 show partial to total dolomitization. Dolomitization seems relatively early since it pre-dates Fe-calcite veins and stylolites. Four samples (section 80) are brecciated dolomite with dolomite and calcite veins.

Although Bourque and Malo (Chapter 1 of this report) consider that the subsurface area north of the East-Central Outcrop Belt (Grande Rivière fault) looks less attractive in terms of reef occurrences because it represents a "back-reef" area, *we think that the reefoid limestones of the belt are worth of investigations, because they are closely related to the Grande Rivière fault system, and that as such they can teach us something about diagenesis and a possible gain of secondary porosity (dolomitization ?) related to nature of fluids that circulated in the fault system, such conclusions that may eventually be extended to other fault systems (e.g. the Bassin Nord-Ouest Fault). Field work is necessary to get material* (see Recommendations).

2.2.4 RECOMMENDATIONS FOR PHASE 2

GENERAL

Diagenesis and porosity history initiated in phase 1 should be pursued and extended to other localities in order to obtain a regional view and to serve as framework in formulating exploration strategies. In phase 2, classical petrography, cathodoluminoscopy and isotope geochemistry should be complemented by fluid inclusion analyses and structural analysis of fracturation.

SPECIFIC

West Point Limestones

1. Completion of the diagenetic study of the Madeleine River and Lac Brûlé buildups.

The suggested model of diagenetic evolution for the RMB and LBB should be tested on the *field*, with more detailed *petrography and geochemistry*, and with *fluid inclusion microthermometry* (salinity and temperature). Particularly, nature of fractures, fracture relationship to stylolites and cement f7, and link of light carbon and presence of hydrocarbons should be clarified.

If, as proposed in the model, meteoric diagenesis follows burial, fluid inclusion studies could possibly document low salinities and support the model. A more detailed isotopic study could possibly predict locations of well developed karsts.

Field work for selective sampling to get complementary material; same steps as in phase 1 for laboratory work, but with the addition of fluid inclusion analyses. Try to see if there are differences between the basal bedded crinoidal limestones and the overlying massive stromatoporoid limestones.

2. Diagenetic studies of other sites in Northern Outcrop Belt.

In order to get data on porosity history of the West Point limestones all along the belt, and to seek for differences between the Silurian West Point (syn-Salinian unconformity, lowstand system tract) and the Devonian West Point (post-Salinian unconformity, transgressive system tract) it is proposed to study the following localities:

- The Silurian and the Devonian West Point in eastern part of the belt.

Field work and sampling of the well-dated Rivière-au-Renard Road, and Sydenham River sections; same steps in laboratory as for phase 1. Compare the bedded Devonian crinoidal limestone with basal crinoidal limestone (facies B and C) of Madeleine River and Lac Brûlé buildups.

- The Lac Madeleine buildup (westernmost pinnacle).

Facies recognition in the field to decipher between Silurian and Devonian West Point; sampling for same type of laboratory work done for the Madeleine River and Lac Brûlé buildups.

3. Diagenetic study of the reefoid limestones in the East-Central Outcrop Belt.

The reefoid limestones of this belt are closely related to the Grande Rivière fault system. Because of that, they can teach us something about diagenesis and a possible gain of secondary porosity, in particular dolomitization, related to nature of fluids that circulated in the fault system. Such conclusions may eventually be extended to other fault systems (e.g. the Bassin Nord-Ouest Fault).

Field work for facies identification and sampling at three sections (sections 80, 82, and 83 of Bourque et al., 1993), with particular attention to dolomitization.

2.3 THE UPPER GASPE LIMESTONES

2.3.1 INTRODUCTION

The Lower Devonian Upper Gaspé Limestones (Lespérance, 1980a) are one of the few carbonate intervals in the otherwise siliciclastic-dominated succession that accumulated during the post-Taconian basin history of the Gaspé depositional Belt (Bourque et al., 1995).

Recent studies of the Upper Gaspé Limestones have focused mainly on their lithostratigraphy, biostratigraphy, paleontology and sedimentology (Mason, 1971; Lespérance and Sheehan, 1975, 1988; Lespérance, 1980a and b; Rouillard, 1986; Lavoie et al., 1990, 1991, Lavoie, 1992a and b; Bourque et al., 1995; Achab et al., 1996, submitted). On the other hand, organic and to some extent clay diagenesis have been the subject of recent comprehensive studies (Bertrand, 1987). However, even if this unit has a proven potential for hydrocarbon reservoirs (seeps and Jaltin's producing well), less attention has been given to the carbonate diagenesis of this unit (Lavoie, 1993, 1995).

At Shell's request, available material of the Upper Gaspé Limestones in the area where they hold permit, has been studied to unravel part of its diagenetic history in the scope of evaluating the reservoir potential of this unit.

2.3.2 METHODS

The Upper Gaspé Limestones have recently been extensively sampled for their lithostratigraphy, biostratigraphy, sedimentology and to some extent for their geochemical significance. As a result, a collection of more than 600 conventional thin sections and 50 polished thin sections for cathodoluminescence petrography are readily available for study. Moreover, some stable and radiogenic isotopes are available from Lavoie's (1993, 1995) studies.

Previous works have documented that the porosities in the Upper Gaspé Limestones are of two types. The first one is secondary porosity in calcite-filled fractures present in the Forillon and Indian Cove formations, hydrocarbon storage is known in these fractures. The second one is preserved and locally enhanced, primary porosity in calcarenites in the upper part of the Indian Cove Formation in the northeastern segment of the Gaspé Peninsula, these voids are primary found in the abundant coquina beds of the "platy facies" of Lespérance (1980a).

Study of these two types of porosity has been made with the material available. In particular, calcite-filled fractures (not readily sample in the previous field campaigns) were studied from 10 Sunny Bank drill core samples already in our collection and from few field samples in eastern Gaspé. The primary porosity present in coquina has been studied from 15 samples.

Study under conventional and cathodoluminescence petrography of 50 old and new polished thin sections led to the recognition of various carbonate cement phases that were micro-sampled for their stable isotope (oxygen and carbon) ratios. The 22 analysis were made at the Delta-Lab of the CGQ and followed usual analytical procedures (see Lavoie, 1995). Moreover, observations on 6 conventional thin sections (e.g., not double polished) were made in order to verify if workable fluid inclusions are present and to obtain a preliminary estimate on the presence or not of hydrocarbons in some of the inclusions.

2.3.3 GEOLOGICAL SETTING

The Upper Gaspé Limestones crop out in the Silurian-Devonian Connecticut Valley - Gaspé Synclinorium (CVGS) of the Gaspé depositional Belt (Bourque et al., 1995). The CVGS lies between the Cambrian-Ordovician Taconian allochthons to the north, and the Middle Ordovician-earliest Silurian Aroostook - Percé Anticlinorium to the south (Fig. 1.1). The CVGS is an Acadian (Middle Devonian) structure (Malo and Béland, 1989) dissected by a number of faults (Fig. 1.2). In eastern Gaspé peninsula, the Bassin Nord-Ouest (BNO) and Troisième Lac (TL) faults are strike-slip structures with dextral displacements between 7 and 8 km (Brisebois, 1981; Kirkwood, 1986). These structures are reactivated normal listric faults that were active in Early Devonian time (Roksandic and Granger, 1981; Bourque, 1990; Lavoie, 1992a; Malo and Bourque, 1993; see also Chapter 5 by Malo in this report).

The Upper Gaspé Limestones (UGL) conformably overlie the Chaleurs Group of Early Silurian - earliest Devonian age. The Upper Gaspé Limestones are conformably overlain by the Gaspé Sandstones of latest Early Devonian - early Middle Devonian age (Fig. 1.3). In central Gaspé, the UGL are laterally equivalent to the siliciclastic Fortin Group (Lavoie, 1992a and Fig. 1.3 of this report).

Forillon Peninsula at the eastern end of Gaspé Peninsula is the type area of the UGL where a threefold division into Forillon, Shiphead and Indian Cove formations was proposed by Lespérance (1980a). These lithostratigraphic units can be recognized over the entire eastern Gaspé. However, south of the Acadian Bassin Nord-Ouest Fault (Fig. 1.2), the succession is considerably thicker and represented almost exclusively by a monotonous succession of lime mudstones and wackestones. South of the Troisième Lac Fault (Fig. 1.2), the UGL consist of a thick succession of impure limestones with abundant rotational and translational slide structures that interfinger with the coarse- to fine-grained siliciclastics of the Fortin Group (Rouillard, 1986; Lavoie, 1990a, 1992b; Lavoie et al., 1990). Based on sedimentologic analysis, one can define three different paleoenvironmental domains delineated by the BNO and TL faults, from north to south: 1) a northern proximal outer shelf, 2) a central, gently sloping distal outer shelf and 3) a southern slope / toe of slope. It has been suggested that the active faulting played a key role in controlling Early Devonian deposition in the eastern part of the Gaspé Belt (Amyot, 1984; Lavoie, 1992a; Malo and Bourque, 1993; Achab et al., 1996, submitted).

2.3.4 STRATIGRAPHY

2.3.4.1 FORILLON FORMATION (Fig. 2.25)

In the area north of the Bassin Nord-Ouest Fault, the Forillon Formation consists of two members: the Mont Saint-Alban and the Cap Gaspé members (Lavoie et al., 1990).

The Mont Saint-Alban Member consists of siliciclastic mudstone in 3 to 50 cm-thick beds. Rare shaly lime mudstone and wackestone beds are interlayered with the siliciclastics. These siliciclastic mudstones are poorly fossiliferous with the exception of few trilobites and brachiopods indicative of a Lochkovian age (Lespérance, 1980a; Bourque et al., 1995).

The Cap Gaspé Member consists of wavy-bedded lime mudstone and wackestone in 5 to 50 cm-thick beds. These carbonates are silicified, either slightly (diffuse silica) or pervasively, as shown by the formation of chert nodules of variable sizes and shapes. The wackestone displays well preserved macrofaunas with particularly abundant trilobites and brachiopods of the *Rennselaeria* (Lower Devonian) zone (Lespérance and Sheehan, 1975; Lespérance, 1980a). Scattered packstone beds that are less than 50 cm thick, also occur.

South of the Bassin Nord-Ouest Fault, the formation consists of a thick succession of argillaceous lime mudstone (5 to 15 cm-thick beds) interbedded with thin shale partings.

2.3.4.2 SHIPHEAD FORMATION (FIG. 2.25)

North of the Bassin Nord-Ouest Fault, the Shiphead Formation is a heterogeneous unit of interbedded impure carbonates (85%), fine- to coarse-grained siliciclastics (10%) and bentonitic clays (5%). Carbonates occur in beds of a few centimetres to 50 cm thick. They comprise silty lime mudstone and wackestone. Macrofaunas are similar to those of the Cap Gaspé Member. Beds of sandy packstone and grainstone interfinger with the lime mudstone and wackestone in the upper metres of the unit. Siliciclastics are mostly represented by grey mudstone with carbonate concretions. Bentonite occurs in heavily weathered, centimetre-thick layers.

South of the Bassin Nord-Ouest fault, the formation consists of a succession similar to the one of the Forillon Formation although significantly more argillaceous and silty.

2.3.4.3 INDIAN COVE FORMATION (Fig. 2.25)

In the northern domain, the Indian Cove Formation comprises siliceous to cherty lime mudstone and wackestone in wavy beds of 10 to 35 cm thick. The silicified carbonates are interbedded with less than 20% of cm-thick layers of shaly mudstone that are commonly silicified. The wackestone contains an abundant fauna dominated by trilobites and brachiopods with species of the *Etymothyris* (Emsian) zone in the uppermost part of the formation (Lespérance, 1980a).

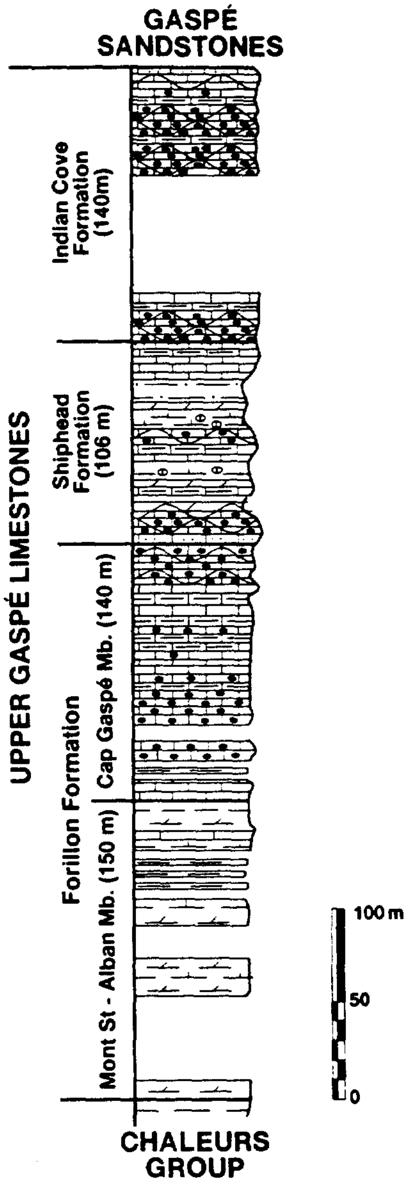

Fig. 2.25 : Composite stratigraphic section for the Upper Gaspé Limestones, Nothern Domain. Modified from Lavoie (1992a).

Significant amount (20% of the unit) of cement- and allochem-rich, packstone, grainstone and coquina beds (15 to 45 cm-thick) are found in the upper half of the unit.

South of the Bassin Nord-Ouest Fault, the formation consists of a well bedded succession of locally siliceous lime mudstone and wackestone (5 to 20 cm-thick) with thin shale partings.

The UGL in the area north of the Bassin Nord-Ouest Fault are suggestive of proximal outer shelf deposits (Lavoie 1992b), with fine-grained sediment representing background sedimentation and coarser-grained limestones interpreted as storm beds. They record the shallowest depositional environment on Gaspé Peninsula in Early Devonian time (Lavoie, 1992a). Conversely, the succession south of the Bassin Nord-Ouest Fault represents sedimentation on a distal, gently sloping outer shelf.

2.3.5 Petrography of Cements

2.3.5.1 Calcite cements in fractures

Calcite-filled fractures have been recognized in the three units of the UGL from outcrops and drill cores and that over the entire area held by Shell. The width of these fractures range from about a millimetre up to 5 centimetres. Some of these fractures in the Sunny Bank drill cores have mm- to cm-sized secondary dissolution vugs cutting through the calcite cement. The walls of the secondary voids are locally (seen in one sample from the Sunny Bank drill core) lined by scalenohedral dark calcite crystals. However, it should be noted that it was impossible to have a thin section made from the latter material although isotopic analysis were made.

Under light microscope, the cement consists of predominantly ferroan blocky calcite with crystals ranging from 0.1 to 2 mm in size. Two different calcite events are suggested from the presence or lack of dense clouds of inclusions. Inclusion-rich calcite usually coats walls of fractures with the later calcite being inclusion-poor (Fig. 2.26a). Calcite crystals are locally broken and corroded between cement events or after the latest calcite cement; the open pore network is definitively dissolution-related (Fig. 2.26b). Locally, corroded early calcite cements in the fractures are coated by bitumen (Fig. 2.26a) suggesting that hydrocarbon migrated repeatedly during cementation/dissolution history of the fractures. Preliminary observations on 3 thin sections has shown that workable fluid inclusions are present in calcite cements and some of them contain hydrocarbons.

Petrographic examination under cathodoluminescence (CL) has revealed that these calcite cements consist of two cement events. The first one is equant-shaped moderately bright luminescent calcite overlain by equant-shaped dull to very dull luminescent calcite (Fig. 2.26c). At places, dissolution events are clearly visible between the two cement types and even within any given phase (Fig. 2.26d). Therefore, within a single fracture, numerous dissolution/cementation events are present, only the last dissolution event remained partly opened.

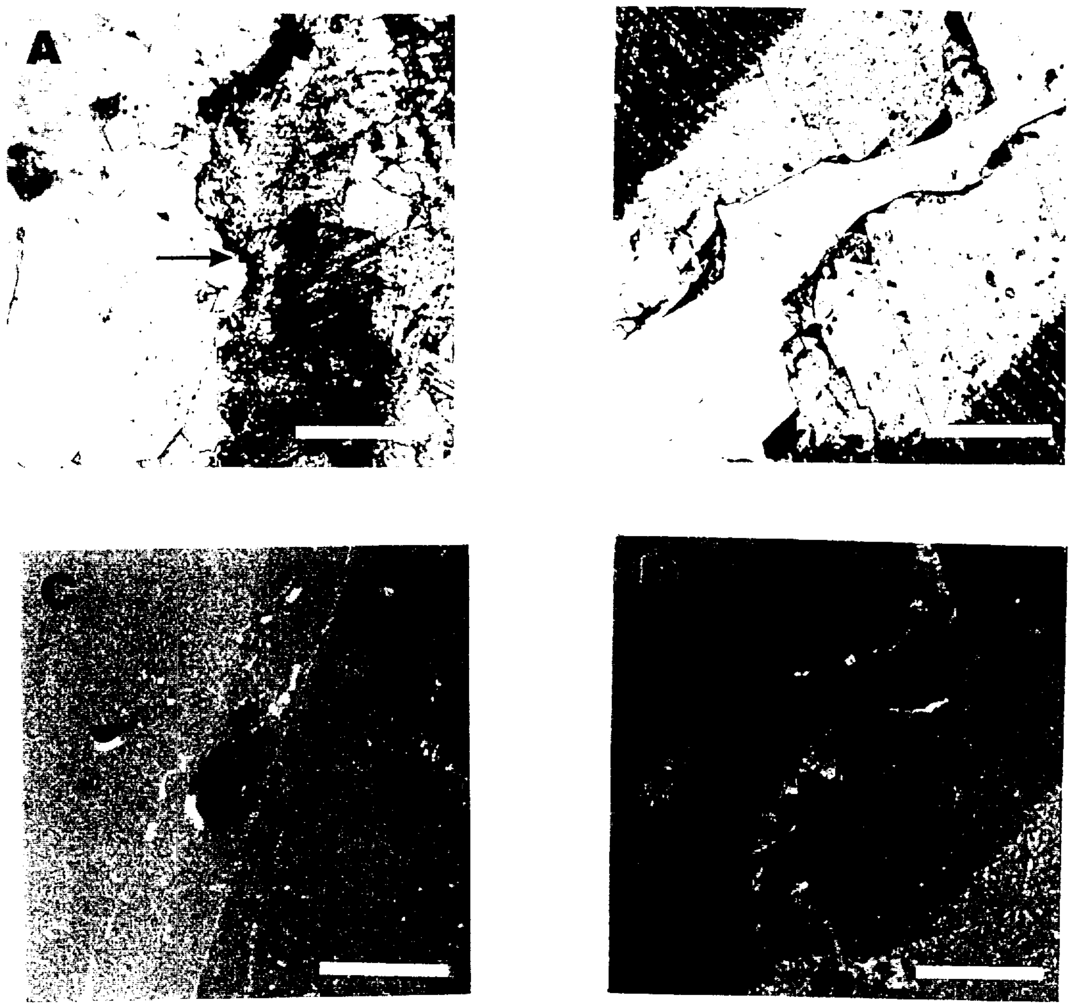

Fig. 2.26: A) Plane-polarized view of fracture-filling calcite showing an early phase of inclusion-rich calcite overlain by later inclusion-poor calcite. The first cement is corroded and coated with bitumen (arrow). B) Plane-polarized view of dissolved calcite in fracture, both early (bottom of photo) and late calcite were affected by the dissolution event. C) CL view of the bright luminescent (inclusion-rich) and dull luminescent (inclusion-poor) calcites. Note the dissolution vug at the contact between the two cement types. D) CL view of B) showing the dissolution event affecting both the late dull luminescent and early bright luminescent calcite cements. All scale bars are 1 mm.

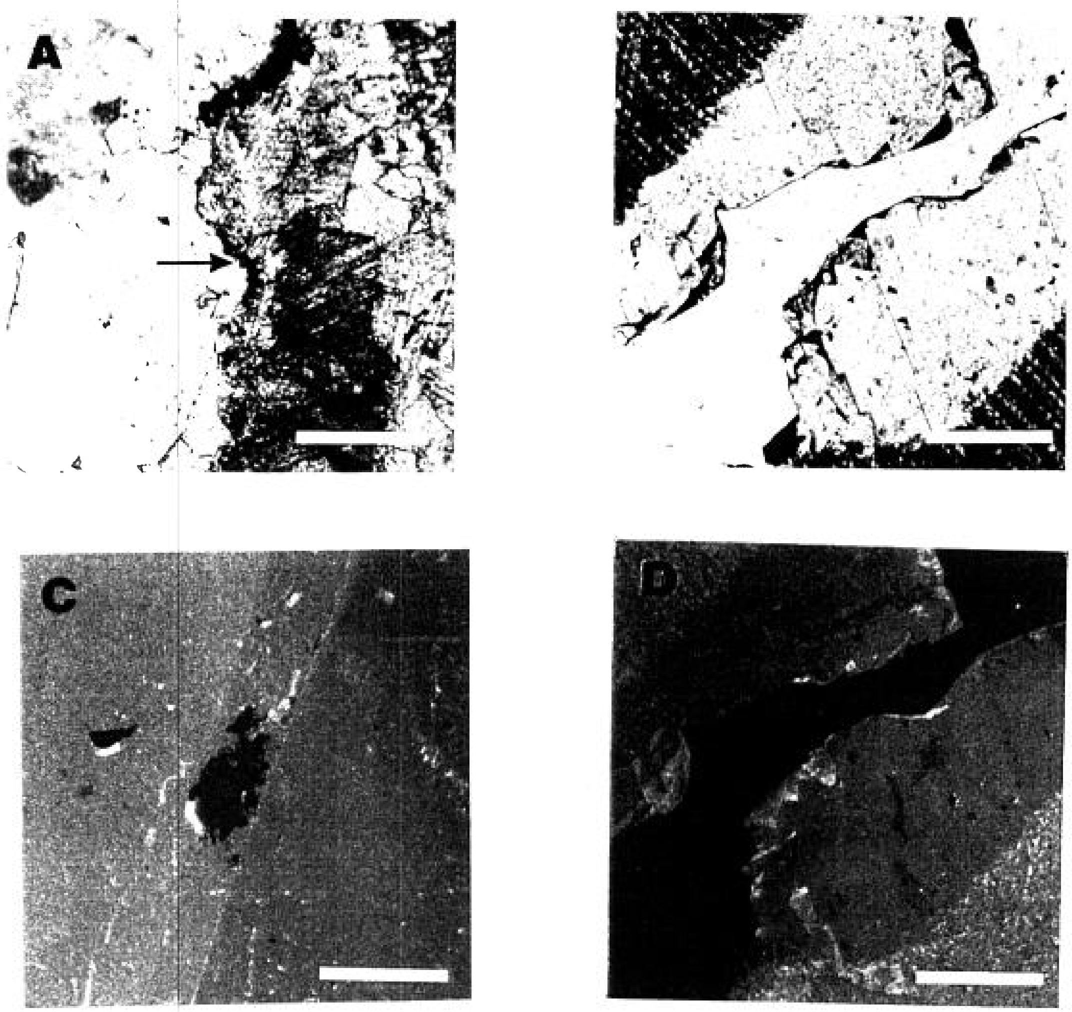

Fig. 2.26: A) Plane-polarized view of fracture-filling calcite showing an early phase of inclusion-rich calcite overlain by later inclusion-poor calcite. The first cement is corroded and coated with bitumen (arrow). B) Plane-polarized view of dissolved calcite in fracture, both early (bottom of photo) and late calcite were affected by the dissolution event. C) CL view of the bright luminescent (inclusion-rich) and dull luminescent (inclusion-poor) calcites. Note the dissolution vug at the contact between the two cement types. D) CL view of B) showing the dissolution event affecting both the late dull luminescent and early bright luminescent calcite cements. All scale bars are 1 mm.

2.3.5.2 CALCITE CEMENTS IN GRAINSTONES AND COQUINA

The UGL are dominated by fine-grained carbonate facies with little primary pore space. However, primary depositional porosity was higher in some coarse-grained facies found in the upper part of the Indian Cove Formation but only in the northern domain. This porosity is preserved and locally dissolution-enhanced as voids in center of brachiopod internal space.

The intergranular and intraparticular (brachiopods) cements consist of non-ferroan calcite crystals with, in the case of the larger pores, some later ferroan calcites. This cement succession is sometimes capped by a later euhedral-shaped silica cement. The calcite cements occur in 0.1 to 1 mm blocky crystals that coarsen towards the center of pore space (Fig. 2.27a). Where open pore space is preserved, local evidence for cement dissolution is visible although well preserved crystal tips pointing towards the center of open vugs are also seen. Preliminary observations on 3 thin sections from this material has shown that workable fluid inclusions are present with some of them being hydrocarbon-rich.

CL petrography reveals that the non-ferroan calcite cement consists of an initial relatively thin, more-or-less isopachous band of non-luminescent to blotchy-luminescent calcite coating the internal and external walls of brachiopod shells (Fig. 2.27b). This cement is conformably overlain by dull-bright calcite with growth zones either brighter or more dull in luminescence (Fig. 2.27c). The later ferroan calcite is very dull luminescent. The last two cements are rhombic-shaped and well preserved crystal tips pointing towards the center of voids are locally seen and argue for the preservation of primary pore space. However, at many places, corrosion of crystal ends is visible suggesting some dissolution enhancement of pore space (Fig. 2.27d).

2.3.6 STABLE ISOTOPES RATIOS

2.3.6.1 SEAWATER COMPOSITION

The study of brachiopods from the UGL (Lavoie, 1993, 1994) provided ocean paleogeochemistry for the Early Devonian (Siegenian-earliest Emsian). The values will serve as a baseline for interpreting the stable isotope signatures of the various cements sampled for this study.

The $\delta^{13}C$ for non-luminescent brachiopods (NLB) closely cluster around +1.5‰, which is assumed to be a realistic indication of $\delta^{13}C$ in Early Devonian seawater.

The heaviest (presumably unaltered) $\delta^{18}O_{VPDB}$ value for NLB is −3.3‰ for the Forillon Formation (Siegenian), and −2.7‰ for the Indian Cove Formation (earliest Emsian). The $\delta^{18}O$ values of these Early Devonian NLB relative to $\delta^{18}O$ values of other Emsian brachiopods is probably controlled by the paleodepth of the sedimentary environment. When corrected for such an environmental effect, the $\delta^{18}O$ value for Early Devonian seawater of the Gaspé Depositional Belt (Figs. 2.28 and 2.29) is somewhere between −4.5 to −5.1‰ (Lavoie, 1993, 1994).

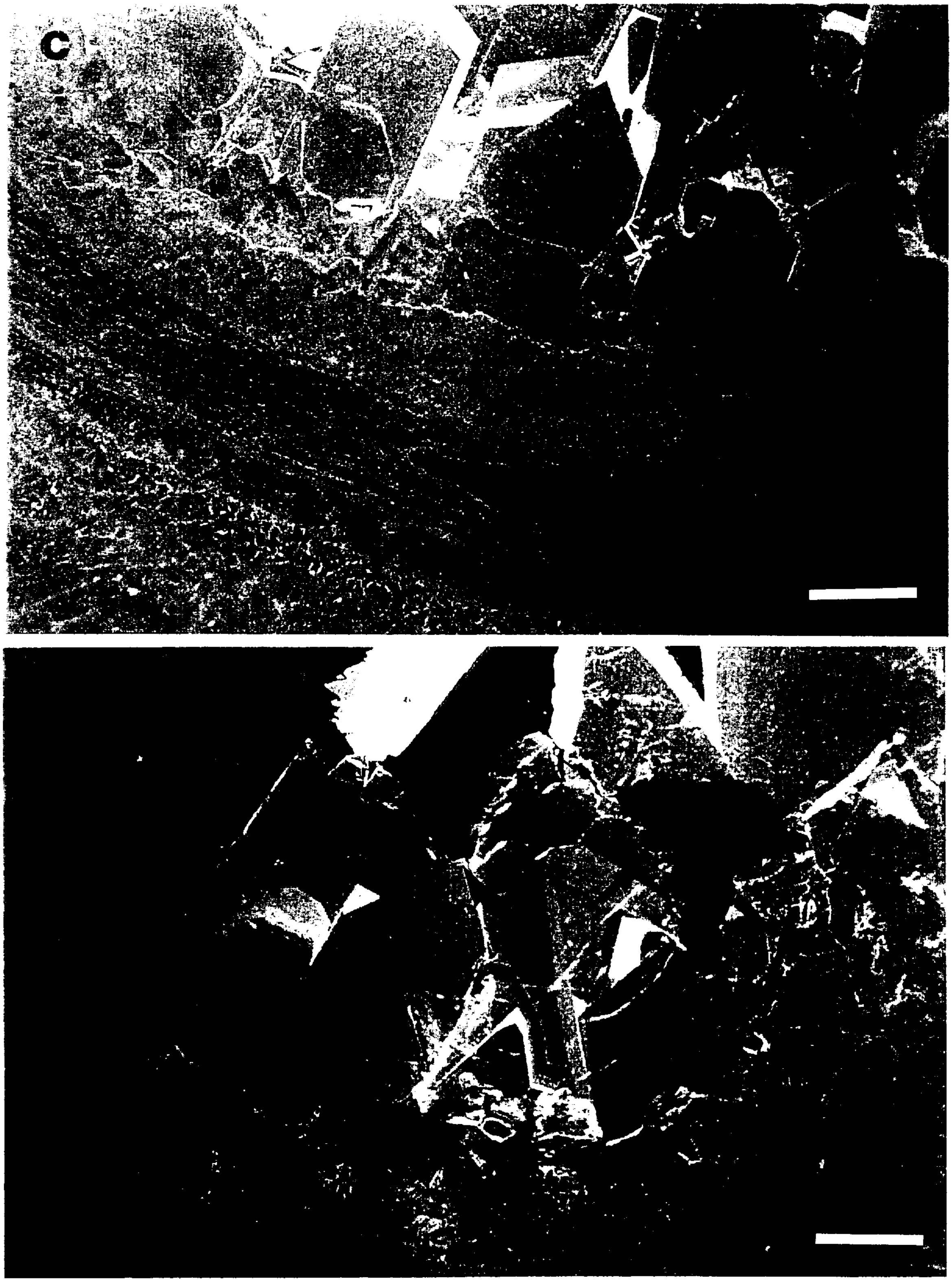

....Fig. 2.27: C) CL view of intrabrachiopod pore space showing the blotchy luminescence of the inclusion-rich early calcite followed well zoned dull-bright calcite cement with very dull calcite cement capping the succession. Note the increase in crystal size towards the center of pore space. Open pore space is locally lined by well preserved calcite crystals (arrow). D) CL view of intrabrachiopod pore space showing the complete cement succession previously described; note heavily corroded crystal tips and edges (arrows) suggesting enhanced dissolution of pore space. All scale bars are 1 mm

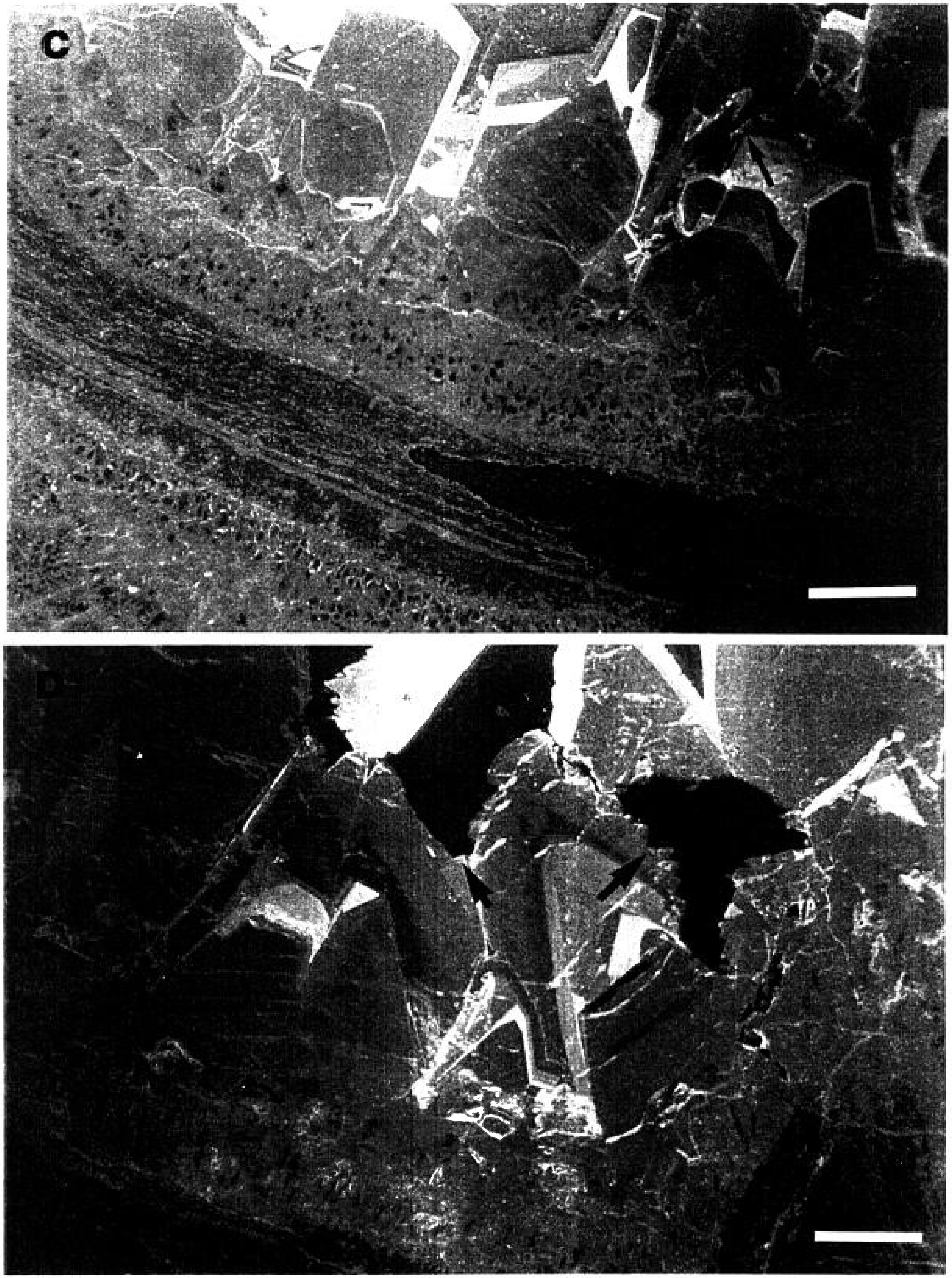

....Fig. 2.27: C) CL view of intrabrachiopod pore space showing the blotchy luminescence of the inclusion-rich early calcite followed well zoned dull-bright calcite cement with very dull calcite cement capping the succession. Note the increase in crystal size towards the center of pore space. Open pore space is locally lined by well preserved calcite crystals (arrow). D) CL view of intrabrachiopod pore space showing the complete cement succession previously described; note heavily corroded crystal tips and edges (arrows) suggesting enhanced dissolution of pore space. All scale bars are 1 mm

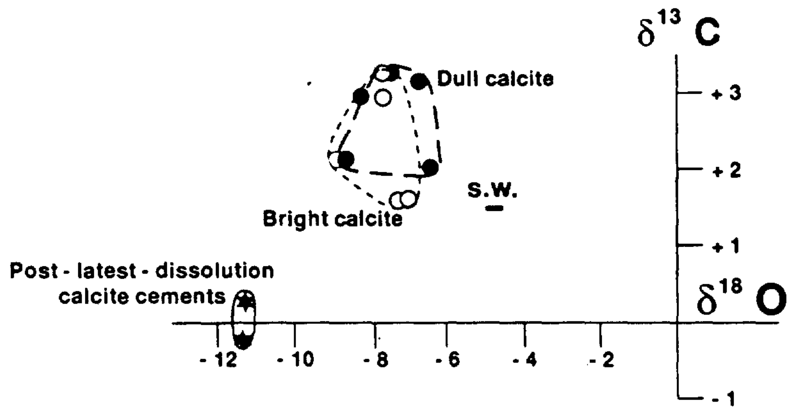

Fig. 2.28: δ^{18} O vs δ^{13} C graph for the fracture-fill calcite cements of the Upper Gaspé Limestones. Samples are from the Sunny Bank drill core, Indian Cove Formation.
Seawater (s.w.) is from Lavoie (1993).

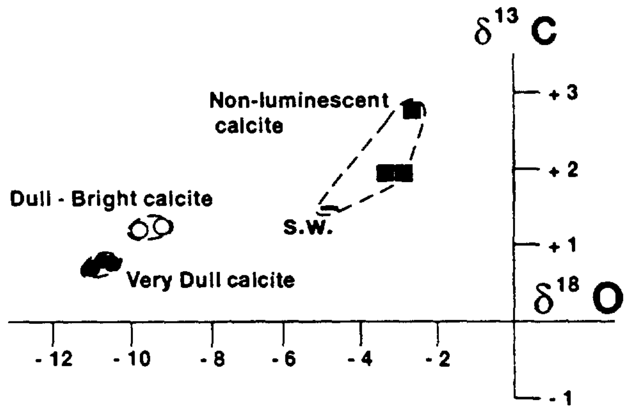

Fig. 2.29 : $\delta^{18}O$ vs $\delta^{13}C$ graph for the calcite cements found in the brachiopod coquina beds in the upper part of the Indian Cove Formation.
Seawater (s.w.) is from Lavoie (1993).

2.3.7 Calcite cements in fractures (Fig. 2.28)

5 analysis of the bright (mean $\delta^{18}O_{VPDB}$: −7.6‰; mean $\delta^{13}C$: +2.3‰) and as much of the dull luminescent calcite (mean $\delta^{18}O_{VPDB}$: −7.5‰; mean $\delta^{13}C$: +2.7‰) cements present in the fractures have been made. Moreover, 2 analysis of the dark calcite crystals coating the walls of the vuggy porosity have been made ($\delta^{18}O_{VPDB}$: −11.2 and −11.3‰; δ13C: 0.3 and −0.2‰). The results indicate that all cements are significantly $\delta^{18}O$-depleted compared to coeval seawater (S.W. on figure 2.28). Conversely, a fairly wide range of $\delta^{13}C$ values is noted. Figure 2.28 also shows that a very significant overlap of the data fields for both the bright and dull cement types. It is also noteworthy that the two analysis from the dark calcite crystals are significantly different in both isotopes compared to the other cements.

Interpretation

The bright and dull luminescent calcites are interpreted to represent calcite cements precipitated in open fractures in the burial realm. This interpretation is based on (1) the relative high concentration of Fe in the calcite, (2) the shape of the crystals as seen under CL suggesting relatively slow growth, (3) the depleted $\delta^{18}O$ ratios for cements suggesting precipitation at moderately high temperature, (4) the relatively normal marine carbon isotopic signature and (5) the lack of regional evidence for meteoric cementation in the Upper Gaspé Limestones (Lavoie, 1993; 1995). By simplistically assuming that a seawater-derived fluid was responsible for the precipitation of these cements, temperature of precipitation would be around 31°C. This, however, represent only a rough estimate because isotopic compositions of the fluid responsible for the precipitation of these cements can not be unequivocally ascertained; temperatures of precipitation can better be obtained from detailed study of fluid inclusions. Nonetheless, the overall evidence point to a burial-seated cementation event.

The isotopic ratios of the small post-last-dissolution dark calcite crystals are very significant. This cement coats walls of the latest dissolution cavities and therefore, record the geochemical setting after this event. This cement is highly-depleted in $\delta^{18}O$ (−11.2‰ and −11.3‰) and also offers the most-depleted $\delta^{13}C$ ratios of all these analysis (+0.3‰ and −0.2‰). From these values, this cement could be regarded either as a meteoric or a high-temperature burial cement with significant input of organic-derived CO_2. Right now, the burial scenario is preferred for the following reason: if precipitation of this cement is related to meteoric waters, paleolatitude of the basin would have to be high in order to accommodate the $\delta^{18}O$ data, this is not the case (the Gaspé Basin was at about 15°S, Lavoie, 1993). The burial interpretation would require precipitation at relatively high temperature with a significant input in the fluid of ^{13}C-depleted carbon of most likely organic origin (Tissot and Welte, 1984). The presence of hydrocarbons is suggested from the preliminary survey of fluid inclusions, it is also known that hydrocarbons are locally stored in the vuggy porosity.

2.3.7.1 Calcite cement in grainstones and coquina (Fig. 2.29)

Four analyses of the non-luminescent/blotchy (mean $\delta^{18}O$: -3.4‰; mean $\delta^{13}C$: +2.1‰), 2 of the dull-bright (mean $\delta^{18}O$: -9.5‰; mean $\delta^{13}C$: +1.3‰) and 5 of the dull luminescent (mean $\delta^{18}O$: -10.8‰; mean $\delta^{13}C$: +0.8‰) calcite cements present in intra-brachiopod space have been made. The non-luminescent/blotchy cement has both $\delta^{18}O$ and $\delta^{13}C$ ratios near the Emsian seawater composition (S.W. on figure 2.29: around -4.5‰ and +1.5‰, respectively). The following dull-bright and very dull luminescent calcites are considerably depleted in $\delta^{18}O$ compared to the assumed ratio of coeval seawater, conversely, $\delta^{13}C$ ratios are more depleted than that of Emsian seawater. The isotopic field for these last two cements do not overlap, although the number of analysis is rather minimal.

Interpretation

The early non-luminescent/blotchy calcite cement is interpreted to represent an early marine cement phase. This interpretation is based on (1) its position in the cement succession, (2) its non-ferroan nature (3) its isopachous fabric similar to most modern and ancient examples of marine cements and (4) its relatively heavy oxygen and carbon isotopic ratios (close to the coeval marine signal deduced from non-luminescent brachiopod shells, Lavoie, 1993). These marine cements have been already described by Lavoie (1992c).

The following succession of dull-bright and very dull luminescent calcite cements is petrographically fairly similar to the succession recognized in the fractures of the Upper Gaspé Limestones (see above). However, no physical/temporal link between pore- and fracture-filling calcite was found during this phase of the study possibly because the material available was not, at that time, collected for such purpose. It is noteworthy however, that the isotopic composition of the pore-filling calcites is significantly more depleted in $\delta^{18}O$ (close to 3‰) compared to petrographically similar cements in fractures. Again in a simplistic manner, the precipitation of these two cements (if from a marine-derived diagenetic fluid) would have occurred at temperature ranging between 41°C and 50°C which would translate to significant burial depths. As in the case for the fracture-filled calcite cements, detailed analysis of fluid inclusions would help in constraining temperature of precipitation and composition of diagenetic fluids. The carbon isotopic ratios are also significant, they are definitively more depleted than that of coeval seawater and are also more depleted for the latest dull luminescent cement. This information coupled with the preliminary observation of hydrocarbon-rich fluid inclusions in the late calcites suggest that decarboxylation of organic matter was possibly the source of ^{13}C-depleted carbon that mixed with isotopic normal or close to normal marine carbon in the diagenetic fluid reservoir. Bearing in mind that local dissolution has locally been observed in the diagenetic succession of the coquina beds, it seems that pore space was preserved long enough to allow for some hydrocarbon migration during and after deep burial calcite cementation.

2.3.8 CONCLUSIONS

The Lower Devonian Upper Gaspé Limestones consist in ascending order, of the Forillon, Shiphead and Indian Cove formations. The three formations are present everywhere in eastern

Gaspé with however, some changes in lithofacies occurring near the major Acadian dextral strike-slip faults in NE Gaspé. These faults were active during sedimentation and delineate major depositional belts in the Early Devonian Gaspé Basin with the shallower setting (proximal outer shelf) in the northern segment of the actual outcrop belt. Before this study, the carbonate diagenesis of this unit was poorly to completely unknown even if significantly, hydrocarbon seeps and well production are known.

Conventional and CL petrography has documented that the fracture-filling calcite consists of two cement phases, an early moderately bright phase (mean $\delta^{18}O$: -7.6‰; mean $\delta^{13}C$: +2.3‰) and a later dull luminescent one (mean $\delta^{18}O$: -7.5‰; mean $\delta^{13}C$: +2.7‰). Dissolution events occurred repeatedly during cementation history with a last event with preserved vug space locally lined with small dark calcite crystal (mean $\delta^{18}O$: -11.3‰; mean $\delta^{13}C$: 0‰). Preliminary observation of fluid inclusion has documented the presence of workable ones with some of them having hydrocarbons. The pre-last-dissolution calcites are interpreted to represent burial-calcite cements precipitated from moderately high-temperature fluids. Conversely, the post-last-dissolution calcite represents a high-temperature event with a significant amount of ^{13}C-depleted of likely organic origin in the diagenetic fluid reservoir. Hydrocarbon storage is known in these vuggy fractures.

Intrabrachiopod pore space in the upper part of the Indian Cove Formation is locally the site of preserved and locally dissolution-enhanced primary voids. Petrographic examination has shown that the cement succession within the brachiopods consist of an initial rind of non-luminescent to blotchy luminescent calcite (mean $\delta^{18}O$: -3.4‰; mean $\delta^{13}C$: +2.1‰), followed by dull-bright (mean $\delta^{18}O$: -9.5‰; mean $\delta^{13}C$: +1.3‰) and very dull luminescent cement (mean $\delta^{18}O$: -10.8‰; mean $\delta^{13}C$: +0.8‰). Locally, some silica cement is found. The last calcite cement in the void space shows either well preserved rhombic tip or dissolved crystal ends suggesting that at least locally a late dissolution event increased the volume of pore space. The cement succession is interpreted to represent an initial minor marine event that allowed preservation of pore space for a significant time - depth interval followed by precipitation of relatively high-temperatures burial calcite with evidence for ^{13}C-depleted carbon of likely organic origin in the diagenetic fluids. It is significant that hydrocarbon-rich fluid inclusions have been preliminary noted in the late calcites.

2.3.9 Implications for HC Plays

The UGL are the only carbonate unit in the Gaspé Basin with proven open pore space and HC storage. This preliminary study has documented the presence of numerous burial-seated dissolution events possibly related to CO_2 migration heralding HC migration (Feazel and Schatzinger, 1985). Primary pore space is locally preserved and even enhanced by some dissolution.

2.3.10 Recommendations

The preliminary results on fracture-filling and primary pore-filling calcites are based on a modest total of samples localized in specific areas (e.g., Sunny Bank drill core for the fracture study and Forillon Peninsula for the coquina study). However, results suggest that vugs either primary or secondary in origin are present and hydrocarbon migration in this porosity network is suggested from carbon isotopic ratio of late calcite phases and from preliminary fluid inclusions study.

It is recommended to Shell that new material being collected in other areas not covered by this report. Specifically, material for primary pore space in the Indian Cove Formation could be collected at roads 132 and 197 as well as at the Dartmouth River section (see locations in Lavoie, 1992a). Material for the fracture study will also be collected at these localities (e.g., relationships between pore and fracture cements) as well as at the Mississippi Anticline and Oatcake Creek areas (see locations in Lavoie, 1992a). Material will be examined petrographically (conventional and CL) as well as for detailed microthermometric and composition of fluid inclusions. Cement phases will be analysed isotopically with new results enhancing the actually thin data base. The results of this phase 2 of the Upper Gaspé Limestones should be submitted to Shell Canada for December 1996.

2.4 HIGHLIGHTS - CARBONATES

2.4.1 White Head Formation

Primary porosity: totally occluded at shallow burial for the studied locations.

Secondary porosity: possibly developed by early meteoric dissolution (?) in grainstone of Ruisseau Blanc, and developed after lithification by fracturing at all locations, and occluded by burial cementation.

Implications for HC plays
After its lithification and mineralogical stabilization, the White Head Formation has possibly been affected by the Salinian Unconformity and related late karsting.

2.4.2 Sayabec - Laforce Formations

Primary porosity: Sayabec: totally occluded under relatively shallow burial, *Laforce:* possibly occluded under moderate burial.

Secondary porosity: Sayabec: possibly locally developed (fracturing and dissolution) where the Salinian Unconformity cuts through the formation, *Laforce*: fracturing of tectonic and/or sub-aerial origin.

Implications for HC plays
Possible development of karsts in both formations related to the Salinian event.

2.4.3 West Point Formation

Primary porosity: Open down to an approximate burial depth of 2 km.

Secondary porosity: Developed by fracturing and dissolution during meteoric diagenesis, due to a structural event that occurred during or after Pragian.

Implications for HC plays
- Possibility of early charge of HC for buildups in subsurface, prior to total occlusion of primary pores (before Pragian).

- Late charge of HC for subsurface buildups, in possible karsts of Pragian or younger age.

2.4.4 Upper Gaspé Limestones

Primary porosity: Only significant in coquina beds at the top of the group. Preserved and dissolution-enhanced pore space is present.

Secondary porosity: Fracturing and dissolution in the deep burial realm. Open pore space is present.

Implications for HC plays
The Upper Gaspé Limestones offer both open primary and secondary pore space. HC storage and production is known in the secondary porosity.

REFERENCES

Achab, A., Asselin, E., Lavoie, D., and Mussard, J.M., submitted. Chitinozoan assemblages from the third-order transgressive-regressive cycles of the Upper Gaspé Limestones (Lower Devonian) of eastern Canada. Review of Palaeobotany and Palynology.

Alaoui, J., 1991. Diagenèse de bancs à crinoïdes, Membres de l'Anse McInnis et du Cap de l'Enfer, Formation de West Point (Silurien supérieur), Gaspésie. M.Sc. thesis, Université Laval, Québec.

Amyot, G., 1980. Analyse paléo-environnementale d'un complexe récif-lagon-estran de la Formation de West Point (Silurien) en Gaspésie. M.Sc. thesis, Université Laval, Québec, 45 p. + 10 pl.

Amyot, G., 1984. Lithostratigraphie de sous-surface de l'est de la Gaspésie. Ministère de l'Énergie et des Ressources du Québec, **ET 83-11**, 75 p.

Bertrand, R., 1987. Maturation thermique et potentiel pétroligène des séries post-taconiennes du Nord-Est de la Gaspésie et de l'Ile d'Anticosti. D.Sc. thesis, Neufchatel, Switzerland, 647p.

Blais, N., 1992. Sédimentologie de la Formation de Gascons, secteur de Port-Daniel/Gascons, Baie des Chaleurs. M.Sc. thesis, Université Laval, Québec.

Bourque, P.-A., 1972. Le complexe carbonaté de Lefrançois dans sa région type, Gaspé-Nord. Ministère des Richesses naturelles, Québec, **DP-46**, 26 p.

Bourque, P.A., 1977. Silurian and basal Devonian of northeastern Gaspé Peninsula: Québec. Department of Natural Resources, Special Paper **ES-29**, 323 p.

Bourque, P.-A., 1990. La pulsation salinienne en Gaspésie-Témiscouata; nature de la déformation et contrôle de la distribution des récifs de la fin Silurien - début Dévonien. *In* Malo, M., Lavoie, D., and Kirkwood, D. (eds.), Québec - Maine - New Brunswick Appalachian Workshop, Program with abstracts. Geological Survey of Canada, Open File **2235**, 25-26.

Bourque, P.-A., Amyot, G., Desrochers, A., Gignac, H., Gosselin, C., Lachambre, G., and Laliberté, J.-Y. 1986. Silurian and Lower Devonian reefs and carbonate complexes of the Gaspé basin, Québec - A summary. Bulletin of Canadian Petroleum Geology, **34**, 452-489.

Bourque, P.-A., and Raymond, L., 1994. Diagenetic alteration of early marine cements of Upper Silurian stromatactis. Sedimentology, **41**, 255-269.

Bourque, P.-A., Brisebois, D., and Malo, M., 1995. Gaspé Belt. *In* H. Williams (ed.), Chapter 4 of Geology of the Appalachian/Caledonian Orogen in Canada and Greenland. Geological Society of America, The Geology of North America, v. **F-1**, 316-351.

Bourque, P.-A., Brisebois, D., and Malo, M., 1995. Middle Paleozoic rocks of Québec and adjacent New-Brunswick. *In* H. Williams (ed.), Geology of the Appalachian/Caledonian Orogen in Canada and Greenland. Geological Survey of Canada, Geology of Canada, **6**, 316-351.

Brisebois, D., 1981. Géologie de la région de Gaspé. Ministère de l'Énergie et des Ressources du Québec, **DPV-824**, 19 p.

Chagnon, A., 1988. Géologie des argiles: diagenèse et altération hydrothermale dans l'anticlinorium d'Aroostook-Percé, Québec (Canada). D.Sc. thesis, Université de Neufchâtel, Switzerland, 367 p.

Dansereau, P., 1989. Sédimentologie et diagenèse de la brèche calcaire de Neigette, Silurien supérieur du bassin de Gaspésie. M.Sc. thesis, Université Laval, Québec.

Desrochers, A., and Bourque, P.-A., 1989. Lower Silurian biostromes and bioherms of southern Gaspé, Québec Appalachians. *In* H.H.J. Geldsetzer, N.P. James, and G.E. Tebbutt (eds.), Reefs, Canada and adjacent areas. Canadian Society of Petroleum Geologists, Memoir **13**, 299-303.

Duba, D., and Williams-Jones, A.E., 1983. Studies of burial metamorphism in the post-Taconic stage of the Appalachian orogen southwestern Gaspé. Canadian Journal of Earth Sciences, **20**, 1152-1158.

Feazel, C.T., and Schatzinger, R.A., 1985. Prevention of carbonate cementation in petroleum reservoirs. *In* N. Schneiderman and P.M. Harris (eds.), Carbonate Cements. Society of Economic Paleontologists and Mineralogists, Special Publication No. **36**, 97-106.

Gignac, H. 1980. Étude du faciès de Gros Morbe du complexe récifal inférieur de West Point, région de Port-Daniel, Gaspésie. M.Sc. thesis, Université Laval, 41 p. + 12 pl.

Gosselin, C., 1980. Étude paléo-environnementale d'un faciès à crinoïdes silurien, Formation de West Point, Port-Daniel, Gaspésie, Québec. M.Sc. thesis, Université Laval, Québec, 46 p. + 6 pl.

Kirkwood, D., 1986. Géologie structurale de la région de Percé, Gaspésie, Québec. Unpublished M.Sc. Memoir, University of Montréal, Montréal.

Lachambre, G., 1987. Le Silurien et le Dévonien basal du nord de la Gaspésie. Ministère de l'Énergie et des Ressources du Québec, **ET 84-06**, 83 p.

Laforest, A., 1987. Le West Point à la marge septentrionale du Synclinorium de la Baie des Chaleurs: stratigraphie et analyse paléo-environnementale. M.Sc. thesis, Université Laval, Québec.

Laliberté, J.-Y., 1982. Étude des faciès de Bouleaux et d'Anse à la Barbe de la Formation de West Point à la pointe au Bouleau, Baie des Chaleurs, Gaspésie, Québec. M.Sc. thesis, Université Laval, Québec, 53 p. + 10 pl.

Lavoie, D., 1988. Stratigraphie, sédimentologie et diagenèse du Wenlockien (Silurien) du Bassin de Gaspésie - Matapédia. Unpublished Ph.D. thesis, Université Laval, Québec.

Lavoie, D., 1990a. Les faciès du Dévonien inférieur (Praguien) dans l'est de la Gaspésie: de la plate-forme externe à la pente profonde. *In* Malo, M., Lavoie, D., and Kirkwood, D. (eds.), Québec - Maine - New Brunswick Appalachian Workshop, Program with abstracts. Geological Survey of Canada, Open File **2235**, 14-16.

Lavoie, D., 1990b. An unexposed lower Devonian shallow water carbonate platform, Québec Appalachians: Facies recognition using clasts of outer shelf storm layers. Thirteen International Sedimentological Congress, Nottingham, Abstracts of papers volume, 298.

Lavoie, D., 1992a. Carbonate sedimentation in extensional tectonic regime: The Lower Devonian Upper Gaspé Limestones, Québec Appalachians. Canadian Journal of Earth Sciences, **29**, 118-128.

Lavoie, D., 1992b. Contrasting styles of Lower Devonian sedimentation: The Upper Gaspé Limestones of the southeastern (Percé area) and western (lac Matapédia area) segments of Gaspé Peninsula. Geological Survey of Canada, Current Research, Part D, Paper **92-1D**, 235-245.

Lavoie, D., 1992c. A major Early Devonian $\delta^{18}O$ positive shift for marine calcites: Brachiopods and marine cements from the Upper Gaspé Limestones, Gaspé Peninsula, Canada. Geological Society of America, annual meeting, program with abstracts, **24**, no. 7, A37.

Lavoie, D., 1993. Early Devonian marine isotopic signatures: Brachiopods from the Upper Gaspé Limestones, Gaspé Peninsula, Québec, Canada. Journal of Sedimentary Petrology, **63**, 620-627.

Lavoie, D., 1994. Early Devonian marine isotopic signatures: Brachiopods from the Upper Gaspé Limestones, Gaspé Peninsula, Québec, Canada - Reply. Journal of Sedimentary Research, **A64**, 408-411.

Lavoie, D., 1995. Carbonate botryoids in Lower Devonian amygdaloidal basalts: Evidence for precipitation of high-magnesium calcite from heated and volcanic CO_2-buffered marine waters. Journal of Sedimentary Research, **A65**, 541-546.

Lavoie, D., Tassé, N., and Asselin, E., 1990. Lithostratigraphic framework of the Upper Gaspé Limestones (Early Devonian) in eastern Gaspé basin, Québec. Current Research, Part B, Geological Survey of Canada, Paper **90-1B**, 17-27.

Lavoie, D., Tassé, N., and Asselin, E., 1991. Lithostratigraphy of the Upper Gaspé Limestones Group (Early Devonian) west of Murdochville, Gaspé Peninsula. Current Research, part D Geological Survey of Canada, Paper **91-1D**, 25-35.

Lavoie, D., Bourque, P.-A., and Héroux, Y., 1992. Early Silurian carbonate platform in the Appalachian Orogenic Belt: The Sayabec - La Vieille formations of the Gaspé - Matapédia basin, Québec. Canadian Journal of Earth Sciences, **29**, 704-719.

Lavoie. D., and Bourque, P.-A., 1993. Marine, burial, and meteoric diagenesis of Early Silurian carbonate ramps, Québec Appalachians, Canada. Journal of Sedimentary Petrology, **63**, 233-247.

Lespérance, P.J., 1980a. Calcaires Supérieurs de Gaspé. Les aires-types et le prolongement vers l'ouest. Québec. Ministère de l'Énergie et des Ressources du Québec, **DPV-595**, 92 p.

Lespérance, P.J., 1980b. Les Calcaires Supérieurs de Gaspé (Dévonien Inférieur) dans le nord-est de la Gaspésie. Ministère de l'Énergie et des Ressources du Québec, **DPV-751**, 35 p.

Lespérance, P.J., and Bourque, P.-A., 1970. Silurian and basal Devonian stratigraphy of Northeastern Gaspé Peninsula, Québec. American Association of Petroleum Geologists Bulletin, **54**, 1868-1886.

Lespérance, P.J., and Sheehan, P.M., 1975. Middle Gaspé Limestones communities on the Forillon peninsula, Québec, Canada (Siegenian Lower Devonian). Palaeogeography, Palaeoclimatology, Palaeoecology, **17**, 309-326.

Lespérance, P.J., and Sheehan. P.M., 1976. Brachiopods from the Hirnantian stage (Ordovician-Silurian) at Percé, Québec. Paleontology, **19**, 719-731.

Lespérance, P.J., Malo, M., Sheehan, P.M., and Skidmore, W.B., 1987. A stratigraphical and faunal revision of the Ordovician-Silurian strata of the Percé area, Québec. Canadian Journal of Earth Sciences, **24**, 117-134.

Lespérance, P.J. and Sheehan, P.M., 1988. Faunal assemblages of the Upper Gaspé Limestones, Early Devonian of eastern Gaspé, Québec. Canadian Journal of Earth Sciences, **25**, 1432-1449.

Lohmann, K.C., 1988. Geochemical patterns of meteoric diagenetic systems. In James, N.P. and Choquette, P.W. (eds.), Paleokarst, Springer-Verlag, 58-80.

Lohmann, K.C., and Walker, J.C.G., 1989. The ^{18}O record of Phanerozoic abiotic marine calcite cements. Geophysical Research Letters, **16**, 319-322.

Malo, M., 1988. Stratigraphy of the Aroostook-Percé anticlinorium in the Gaspé Peninsula, Québec. Canadian Journal of Earth Sciences, **25**, 893-908.

Malo, M., and Béland, J., 1989. Acadian strike-slip tectonics in the Gaspé région, Québec Appalachians. Canadian Journal of Earth Sciences, **26**, 1764-1777.

Malo, M., and Bourque, P.-A., 1993. Timing of the deformation events from Late Ordovician to Mid-Devonian in the Gaspé Peninsula. *In* Roy, D., and Skehan, S.J. (eds.), The Acadian Orogeny - Recent Studies in New England, Maritime Canada and the Authochthonous Foreland. Geological Society of America, Special Paper **275**, 101-122.

Malo, M., Moritz, R., Chagnon, A., and Roy., F., 1993. Géologie et métallogénie du segment oriental de la faille du Grand Pabos, Gaspésie. Ministère de l'Énergie et des Ressources du Québec, **MB 93-55**, 123 p.

Mason, G.D., 1971. A stratigraphic and paleoenvironmental study of the upper Gaspé Limestone and lower Gaspé Sandstone groups (Lower Devonian) of eastern Gaspé Peninsula, Québec. Unpublished Ph.D. thesis, Carleton University, Ottawa, Ontario, 194 p.

Morin, C., 1987. Anatomie d'un complexe péritidal silurien supérieur en climat aride: le faciès de Place Woodmans du complexe de West Point, Gaspésie. M.Sc. thesis, Université Laval, Québec.

Nowlan, G.S., and Barnes, C.R., 1987. Thermal maturation of paleozoic strata in eastern Canada from conodont colour alteratio index (CAI) data with implications for burial history, tectonic evolution, hotspot tracks and mineral and hydrocarbon exploration. Geological Survey of Canada, Bulletin **367**, 47 p.

O'Neil, J.R., Clayton, R.N., and Mayeda, T.K., 1969. Oxygen isotope fractionation in divalent metal carbonates. Journal of Chemical Physics, **12**, 5547-5558.

Popp, B.N., Anderson, T.F., and Sandberg, P.A., 1986. Brachiopods as indicators of original isotopic composition is some Paleozoic limestones. Geological Society of America Bulletin, **97**, 1262-1269.

Raymond, L., 1986. Sédimentologie d'un talus récifal, complexe récifal inférieur du West Point, Gaspésie: M.Sc. thesis, Université Laval, Québec.

Roksandic, M.M., and Granger, B., 1981. Structural styles of Anticosti Island, Gaspé Passage and eastern Gaspé Peninsula inferred from reflection seismic data. *In* Lespérance, P.J. (ed.), Subcommission on Silurian stratigraphy, Ordovician-Silurian boundary working group. Field meeting, Anticosti-Gaspé, 1981, Volume II, Stratigraphy and Paleontology. Université de Montréal, Montréal, Québec, 211-221.

Rouillard, M., 1986. Les Calcaires Supérieurs de Gaspé (Dévonien inférieur), Gaspésie. Ministère de l'Énergie et des Ressources du Québec, **MB 86-15**, 94 p.

Savard, M., 1986. Pétrographie en cathodoluminescence et évolution diagénétique des faciès d'une plate-forme récifale silurienne, complexe de West Point, Gaspésie. M.Sc. thesis, Université Laval, Québec.

Savard, M., and Bourque, P.-A., 1989. Diagenetic evolution of a Late Silurian reef platform, Gaspé Basin, Québec, based on cathodoluminescence petrography: Canadian Journal of Earth Sciences, **26**, 791-806.

Sheppard, S.M.F., 1986. Characterization and isotopic variations in natural waters. *In* Stable Isotopes in High Temperature Geological Processes, reviews in Mineralogy, **16**, Mineralogical Society of America, 165-182.

Sheppard, S.M.F., and Charef, A., 1986. Eau organique: caractérisation isotopique et évidence de son rôle dans le gisement Pb-Zn de Fedj-el Adoum, Tunisie. Comptes Rendus de l'Académie des Sciences de Paris, tome **302**, série II, No. 19, 1189-1192.

Tissot, B.P., and Welte, D.H., 1984. Petroleum formation and occurrence. Springer-Verlag, Berlin, Heidelberg, New York, Tokyo, 699 p.

Veizer, J., Fritz, P., and Jones, B., 1986. Geochemistry of brachiopods: oxygen and carbon isotopic records of Paleozoic oceans. Geochimica et Cosmochimica Acta, **50**, 1679-1696.

CHAPTER 3

FACIES DISTRIBUTION AND RESERVOIR QUALITY IN THE GASPE SANDSTONES

3 FACIES DISTRIBUTION AND RESERVOIR QUALITY IN THE GASPE SANDSTONES

3.1 INTRODUCTION

3.1.1 GENERAL REMARKS

The term Gaspé Sandstones was coined by Logan (1863) to designate the Devonian terrigenous rock sequence overlying the Gaspé Limestones also defined by the same author in the Forillon Peninsula near Gaspé. These upper Lower to Middle Devonian (Emsian to possibly Eifelian) sandstones occur on top of the Acadian stratigraphic sequence in the Connecticut Valley-Gaspé Synclinorium of the Gaspé belt in Gaspé Peninsula (Brisebois et al., 1991; Bourque et al., 1995).

The Gaspé Sandstones consist of a clastic wedge formed in direct (tectonic) and indirect (climatic) response to early Acadian deformation. Subsequent works formalized the Gaspé Sandstones and divided it into four formations: in ascending order, the York Lake (Jones, 1935), York River (Williams, 1910; McGerrigle, 1950), Battery Point (McGerrigle, 1950), and Malbaie (Alcock, 1935). In the Big Berry Mountains Syncline in central Gaspé area, the Gaspé Sandstones show roughly the same stratigraphic sequence as in northeastern Gaspé, except for the occurrence of the Lake Branch Formation (Carbonneau, 1959) between the York River and Battery Point formations, and for the absence of the Malbaie Formation on top of the sequence. South of the Rivière Saint-Jean Anticline, the Fortin Group (McGerrigle, 1950; Skidmore, 1965; Brisebois, 1981; Simard, 1988a, 1988b) represents a lithostratigraphic unit, partly equivalent to the Upper Gaspé Limestones and to the Gaspé Sandstones.

Observations that support the presence of an hydrocarbon potential in the Gaspé Sandstones can be summarized as follow:

1) Presence of oil seeps and oil showings in some drill holes in the Gaspé Sandstones,
2) Presence of potential source-rocks for hydrocarbons within and below the sandstone sequence,
3) Favourable organic matter maturation,
4) Presence of favourable facies for the development of reservoirs and stratigraphic traps,
5) Paleoenvironment analogous to rich producing fields.

Despite the presence of numerous seeps and oil showings in Gaspé area (see Bertrand, chapter 4), no commercial accumulation of oil or gas has been found to date and no specific facies has been recognized as a reservoir, or as a potential one, in this geological unit.

3.1.2 QUESTIONS TO BE ADDRESSED AND OBJECTIVES

The purpose of this project on the Gaspé Sandstones is to review the literature in order to evaluate the reservoir potential of these sandstones. The main questions to be addressed are:

1) The architecture of the Gaspé Sandstones body is an important factor controlling the geometry and the thickness of the lithofacies forming the sandstone sequences.

What is the geometry of the clastic wedge deposit? What is the paleoenvironmental relationships between the laterally equivalent fine clastic Fortin Group and the deltaic York River and Battery Point formations? Can we localize, vertically and laterally in the sedimentary sequence, distributary channels, secondary channels, mudflats, prodeltaic environments, etc.?

2) The reservoir quality is essentially related to the porosity and the permeability of the clastic framework of the rock.

Porosity and permeability result from two main factors:

- the original texture of the lithofacies (grain size, grain sorting, grain shape, grain packing and intergranular matrix),

- the evolution of pore filling during diagenesis (grain alteration and dissolution, cementation, authigenic clays).

Can we, from the literature, localize the more favourable lithofacies in the stratigraphic sequence or can we modelize their location and evolution?

3.1.3 METHODS

1) Review of the literature on the Gaspé Sandstones from two bibliographical data base: Georef and Examine.

2) Twenty-two (22) drill holes and nine (9) field sections were compiled from the literature in eastern Gaspé (Fig. 3.1; Table 3.1) and seven (7) road and river sections from central Gaspé (Table 3.1).

3) Construction of isopach and lithofacies maps in order to modelize the architecture and the geometry of the deposit.

4) Selection of the best sections and exploration wells for study of the most favourable lithofacies during a possible phase 2 of the project.

3.1.4 AREA OF INVESTIGATION

For the purpose of this study, the literature on the Gaspé Sandstones from northeastern Gaspé was first investigated for facies distribution and reservoir quality. A brief evaluation of the Devonian siliciclastic sequence in the Big Berry Mountains Syncline in central Gaspé and of the

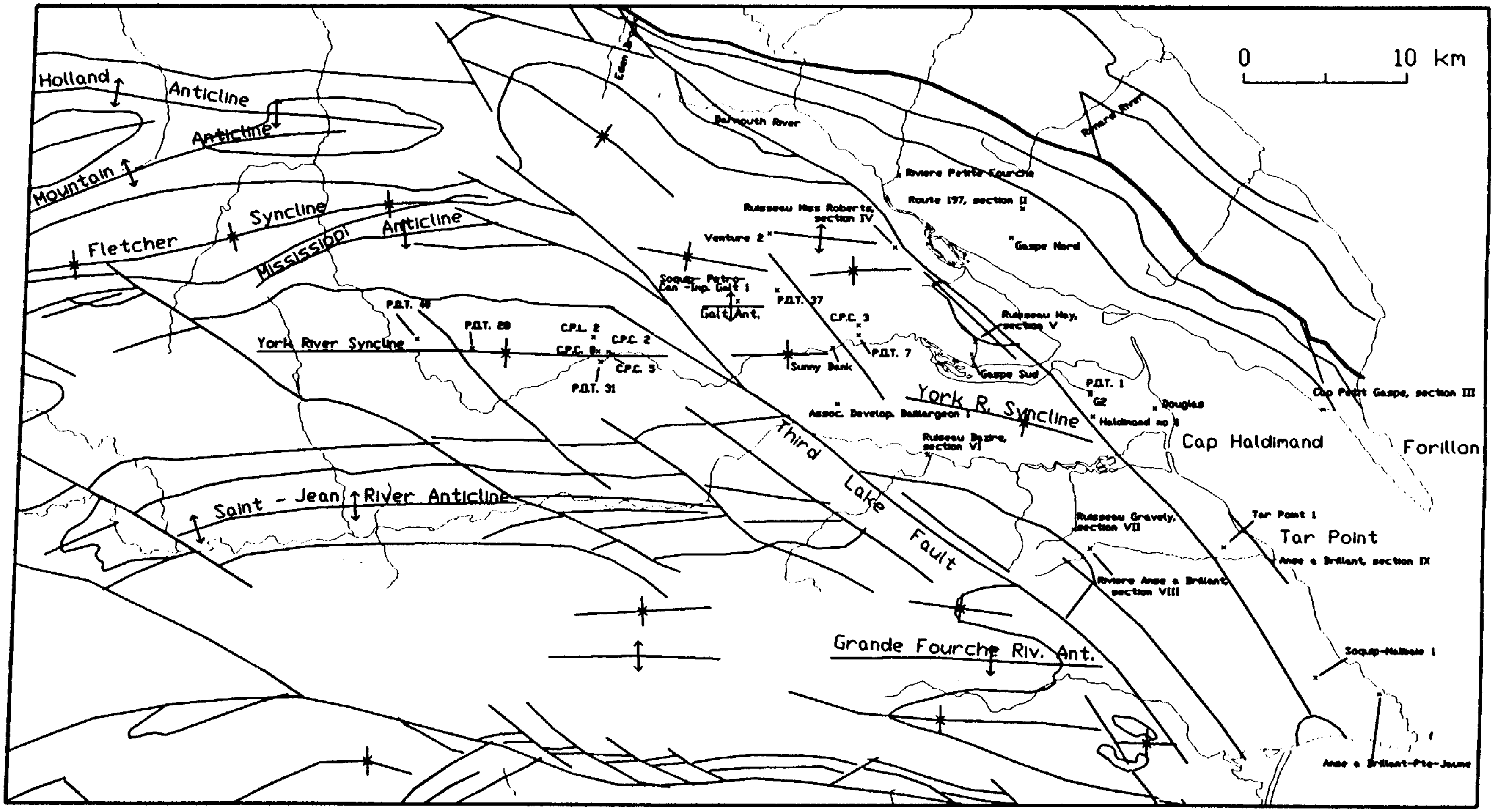

Figure 3.1: Geological map of Eastern Gaspe and location of field sections and drill holes

TABLE 3.1 Summary of the stratigraphic intersections, thickness of the stratigraphic units and sandstone/mudstone ratios compiled from field sections and drill holes in Gaspé Sandstones.

WELL/SECTION	UTM COOR.		YORK LAKE FORMATION			YORK RIVER FORMATION			BATTERY POINT FORMATION			Y.R. thick	B.P. thick	Y.L. thick.	L.B.thick.
	Lat. N.	Long E	BASE	TOP	SS/SH	BASE	TOP	SS/SH	BASE	TOP	SS/SH				
Well, Gaspé area															
Gaspé Nord	5416859	388795				1150	720	85	720	0	75	430	720		
Gaspé Sud	5409650	386327	485	455		455	0	25				455	0	30	
Sunny Bank	5410049	377688				675	0	45				675	0		
Douglas	5406435	397667				1545	742	51	742	0	75	803	742		
Haldimand no 1	5405949	393883				1471	431	63	431	0	28	1040	431		
Tar Point 1	5397925	401987				2000	300	50	300	0	80	1700	300		
Soquip-Malbaie 1	5390015	407689							2115	0	85	0	2115		
Soquip- Petro-Can -Imp. Galt 1	5412836	371858	583	495		495	5,5					489,5		88	
Assoc. Develop. Baillargeon 1	5406644	378001				795	17					778			
C.P.C. 2	5409751	363852				485	11					474			
C.P.C. 3	5411404	379288				655	0					655			
C.P.C. 5	5409591	364093				655	0					655			
C.P.C. 8	5409767	363220				713	0					713			
C.P.L. 2	5410639	362915				720	9					711			
Venture 2	5417055	373808				591	4					587			
G 2	5407250	393725				276	183		183	4		93	179		
P.O.T. 40	5410516	352000				703	0					703			
P.O.T. 37	5413523	374258				792	22					770			
P.O.T. 31	5409115	363327				762	14					748			
P.O.T. 28	5409933	355391				1074	0					1074			
P.O.T. 7	5410817	379316				727	8					719			
P.O.T. 1	5407373	393727				741	183		183	0		558	183		

TABLE 3.1 Summary of the stratigraphic intersections, thickness of the stratigraphic units and sandstone/mudstone ratios compiled from field sections and drill holes in Gaspé Sandstones.

WELL/SECTION	UTM COOR.		YORK LAKE FORMATION			YORK RIVER FORMATION			BATTERY POINT FORMATION			Y.R. thick	B.P. thick	Y.L. thick	L.B.thick.
	Lat. N.	Long. E	BASE	TOP	SS/SH	BASE	TOP	SS/SH	BASE	TOP	SS/SH				
Section, Gaspé area															
Rivière Petite Fourche, section I, S.D.91	5420711	381789						80				890			
Route 197, section II, S,D,91	5418637	389482						80				440			
Cap Petit Gaspé, section III, S.D.91	5409075	405567						80				312			
Ruisseau Miss Roberts, section IV, S.D.9	5416206	381551						60							
Ruisseau Hay, section V, S.D. 91	5410159	388682						15							
Ruiseau Bazire, section VI, S.D.91	5418532	387017						80				1200			
Ruisseau Gravely, section VII, S.D. 91	5397989	391791						80				890			
Rivière Anse à Brillant, section VIII, S.D.9	5395801	389950						75							
Anse à Brillant, section IX, S.D.91	5397070	405017						50				1834			
Anse à Brillant-Pte-Jaune, D.L. 86	5389025	411614											2300		
Section, Berry Mountain area															
Cascapédia Branche du Lac O. A.S 75	5375693	677868										1220	817		122
Cascapédia Bras aux Saumons. A.S 75	5405726	697921										610		380	
Ruisseau Brandy. A.S. 75	5412552	707149										533		305	396
Rivière Nouvelle sud. A.S. 75	5370825	680283										1370	548		335
Ruisseau Marcil O. A.S. 75	5384148	716366										1158			
Ruiseau Caron. A.S. 75	5387426	721162										1585			

Fortin Group, south of the Saint-Jean River Anticline was added to our investigation. Figure 3.1 shows the location of drill holes and sections pertinent to the study.

3.2 NORTHEASTERN GASPÉ PENINSULA

3.2.1 GENERAL GEOLOGY AND STRATIGRAPHY

In northeastern Gaspé, the Gaspé Sandstones occur at the top of the stratigraphic sequence at the eastern limit of the Connecticut Valley-Gaspé Synclinorium. In the studied area, this synclinorium is characterized by several broad and flat synclines of Devonian rocks trending east-west and northeasterly, and relatively narrow and steep-flanked anticlines of Silurian-lowermost Devonian rocks (Fig. 3.1). That area is also dissected into three blocks limited by two dextral strike-slip northwesterly trending faults: the Bassin Nord-Ouest and Troisième Lac faults (Fig. 3.1).

As stated above, the Devonian Gaspé Sandstones are made up of four formations: in ascending order, the York Lake, York River, Battery Point and Malbaie formations. These strata rest conformably on the Upper Gaspé Limestones, a predominantly limestone succession of marine platform origin. More westerly, there is a transitional unit between the Upper Gaspé Limestones and the York River, known as the York Lake Formation and, south of the Saint-Jean River Anticline, the Fortin Group consists of interbedded carbonates and fine basinal clastics.

For each stratigraphic unit part of the Gaspé Sandstones, geometry, facies distribution, petrography, paleoenvironment and reservoir potential will be discussed.

3.2.2 THE YORK LAKE FORMATION

The York Lake Formation (Jones, 1935) only occurs in the northwestern part of the studied area, and is considered by some authors as a basal facies of the York River Formation.

The York Lake strata represent a transition between the Indian Cove Formation of the Upper Gaspé Limestones and the York River Formation. It consists of alternating siliceous calcilutites with minor quartz arenites and wackes similar to the underlying Indian Cove Formation, and greenish grey medium-grained feldspathic wackes similar to those of the overlying York River Formation (Bourque et al., 1995).

The geometry of this unit is not well understood. The thickness of the sandstones and limestones forming the York Lake is commonly measured in metres or in tens of metres. This unit outcrops in the Grande Fourche River, and in some of its tributaries, where it exhibits a thickness of 98 m (Lespérance 1980). The York Lake strata were also identified into two exploration wells: Soquip Gaspé Sud with a thickness of 30 m (Amyot, 1984), and Soquip-Petrocan-Imp. Galt 1 with a thickness of 88 m (Fig. 3.1, Table 3.1). The formation maximum thickness occurs at its type-section on the hillside, west of Lake York, near Murdochville where it reaches 500 m (Bourque et al., 1995). The succession thins progressively to zero eastward and southward. But as the definition of the limits between the York Lake Formation and the under- and overlying formations may change between different authors, it is near impossible to modelize the geometry of the York Lake.

We did not find any detailed studies on this formation. Nothing is known about lithofacies subdivision of this formation, paleoenvironmental interpretation, petrography and reservoir potential. The only conclusion is that the York Lake Formation represents a transitional environment between the rapidly shallowing outer shelf of the Upper Gaspé Limestones (Lavoie, 1992a) and the shallow marine to terrestrial facies of the Gaspé Sandstones (Rust, 1981; Lawrence, 1986; Lawrence and Williams, 1987; Desbiens, 1991).

3.2.3 THE YORK RIVER FORMATION

The most recent and comprehensive reports on the York River Formation are the synthesis of Brisebois (1981), Amyot (1984, 1990) and Desbiens (1991). The sandstones of the York River Formation are mostly lithic and feldspathic wackes; few arenites and lithic conglomerates are reported (Amyot, 1984; Desbiens, 1991). The formation contains a marine fauna, including brachiopods, and also shows evidence of shallow-water to intertidal deposition in the form of ripples and mudcracks. The York River Formation coarsens upwards from a lower mudstone-siltstone-sandstone assemblage with a few calcarenites to an upper sandstone assemblage with minor mudstone. Locally, the upper assemblage is distinctive enough to be recognized as the Anse à Brillant Member (Brisebois, 1981; Amyot, 1984). The lower limit of the formation is put at the disappearance of calcilutite beds and this contact is easily recognized (Desbiens, 1991). The upper limit definition is more problematic; McGerrigle (1950) suggests that the contact York River - Battery Point corresponds to the appearance of pink feldspars in the sandstones, but his own map does not respect this criteria. Desbiens (1991) used three criteria to define the top of the York River Formation: 1) disappearance of thick mudstone beds, 2) presence of red beds in the Battery Point and 3) presence of quartz and granite pebble conglomerate when this last criteria is consistent with the first two ones. Two isobath maps illustrate the topography of the lower (Fig. 3.2) and upper limits (Fig. 3.3) of the formation as interpreted from the data found in the literature.

The thickness of the formation ranges from 312 m at Petit Gaspé in the northern part of the area (Desbiens, 1991) to 1700 m in the Tar Point exploration well to the southeast (Amyot, 1984). Desbiens (1991) proposed an interpretative isopach map of the York River Formation on a palinspastic reconstitution (Fig. 3.4). It shows a clastic wedge thickening from north to southwest, suggesting more rapid basin subsidence in the southwest related to synsedimentary movements along the northwesterly faults. Our interpretation of the data (Figs. 3.5, 3.6 and 3.7) suggests that Desbiens might be wrong. Most of Desbiens' data are incomplete, because, for many localities, the bottom and/or the top of the formation is not present, giving only minimum

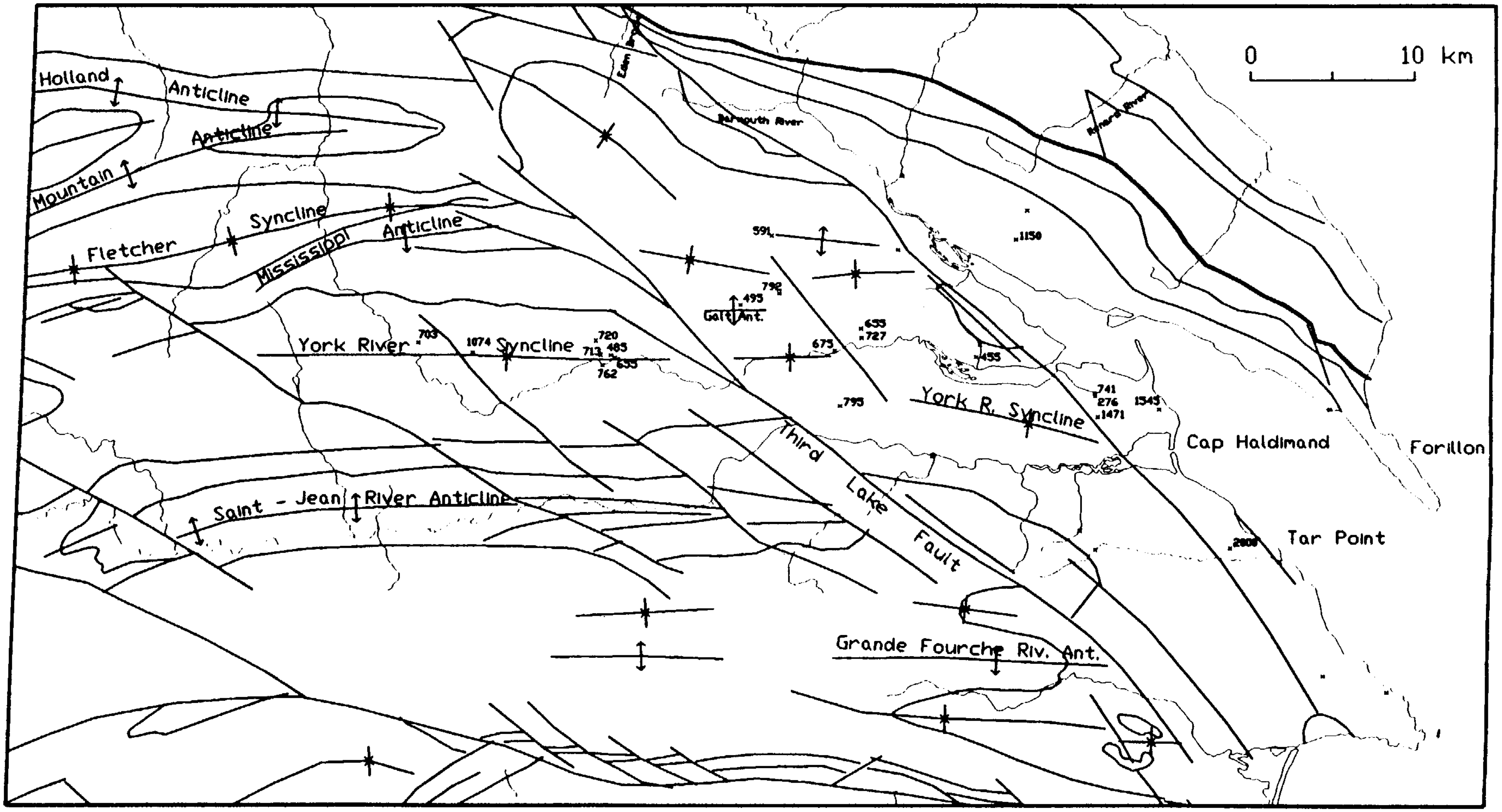

Figure 3.2: Isobath map of the bottom contact of the York River Formation, Eastern gaspe

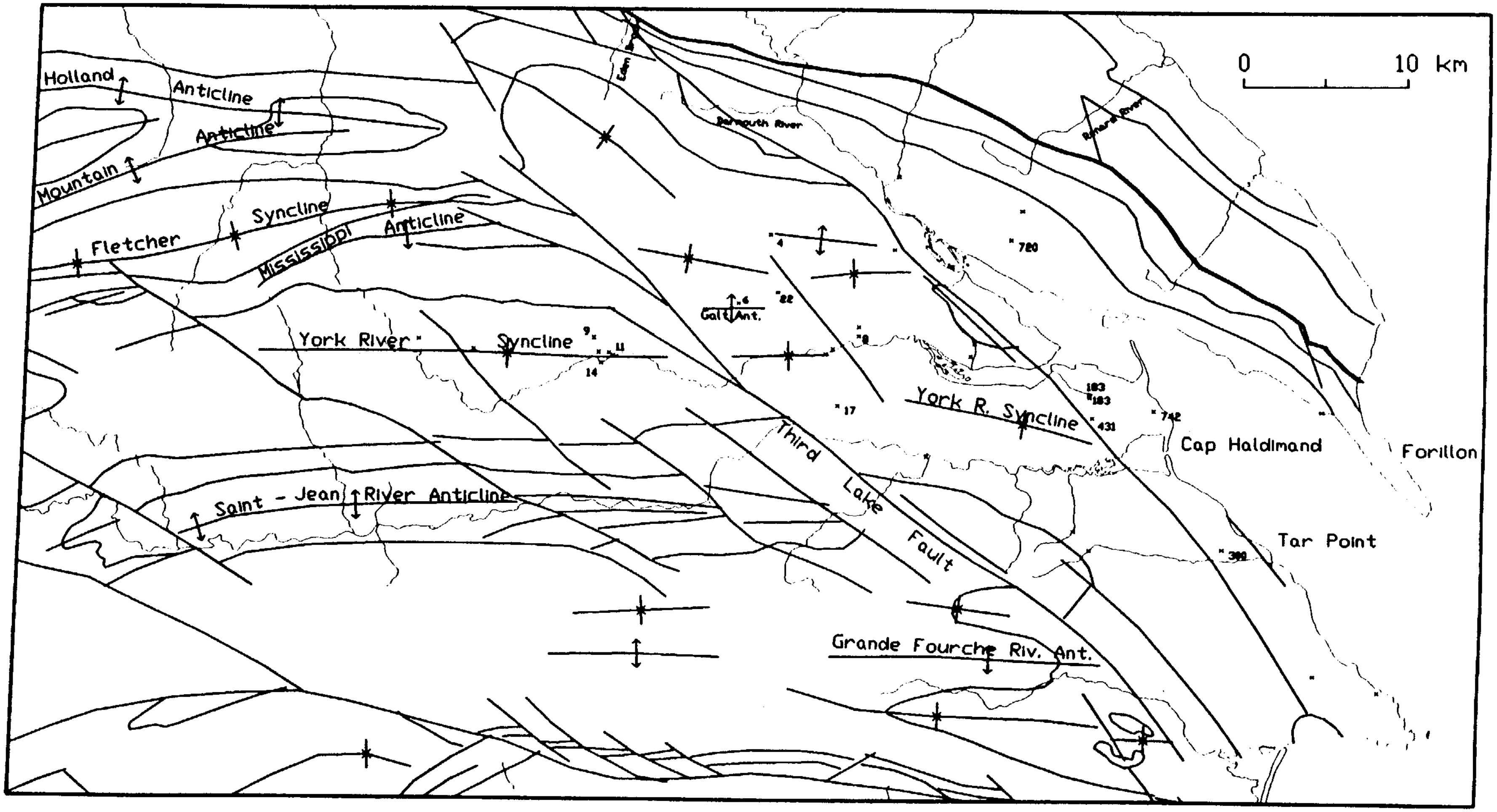

Figure 3.3: Isobath map of the top contact of the York River Formation, Eastern Gaspe

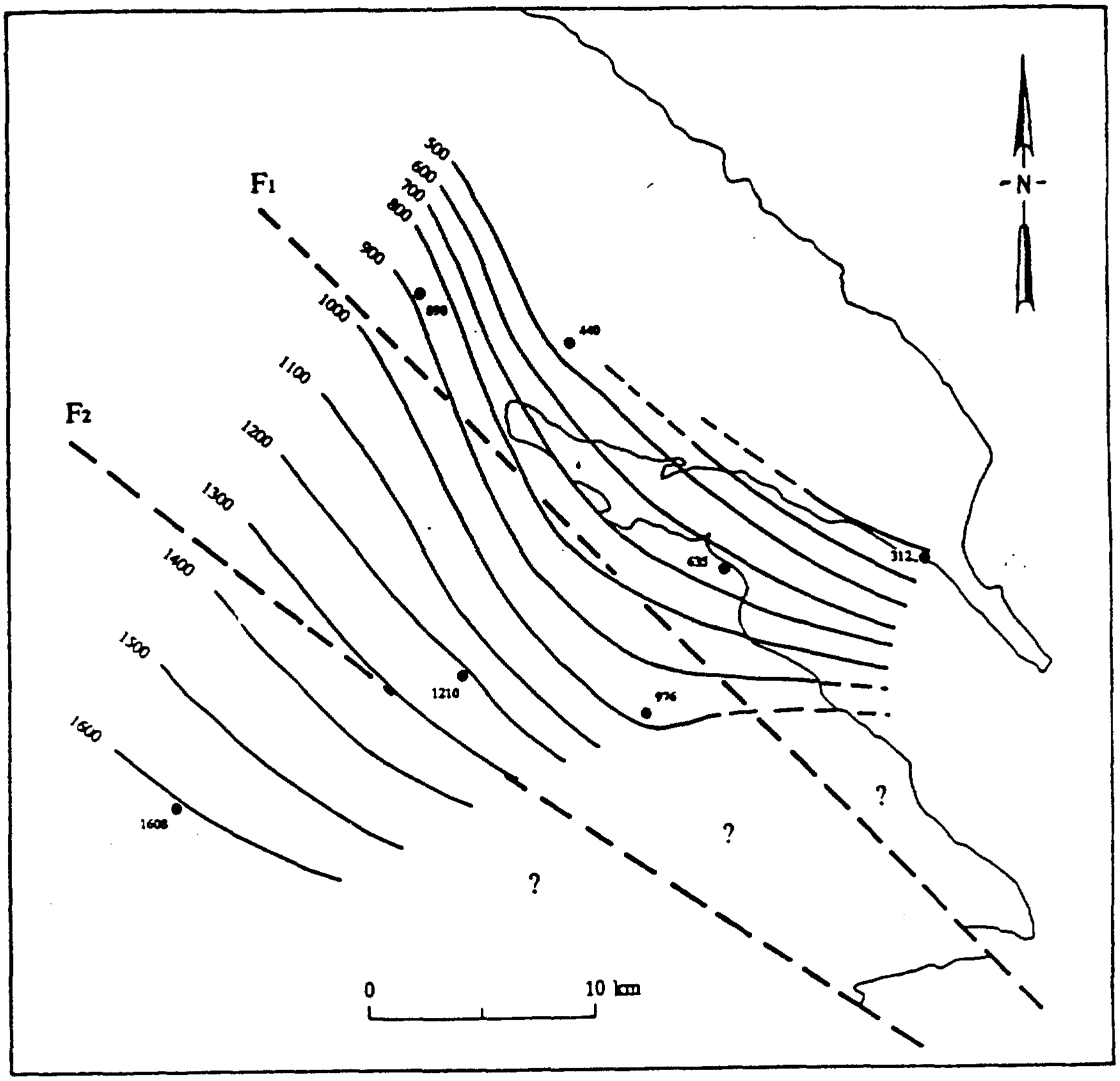

FIGURE 3.4 Isopach map of the York River Formation on a palynspastic reconstitution, Eastern Gaspésie. Senester displacement of 2 km along Bras Nord-Ouest Fault (F1) and 14 km along Troisième Lac Fault (F2). From Desbiens (1991, figure 12)

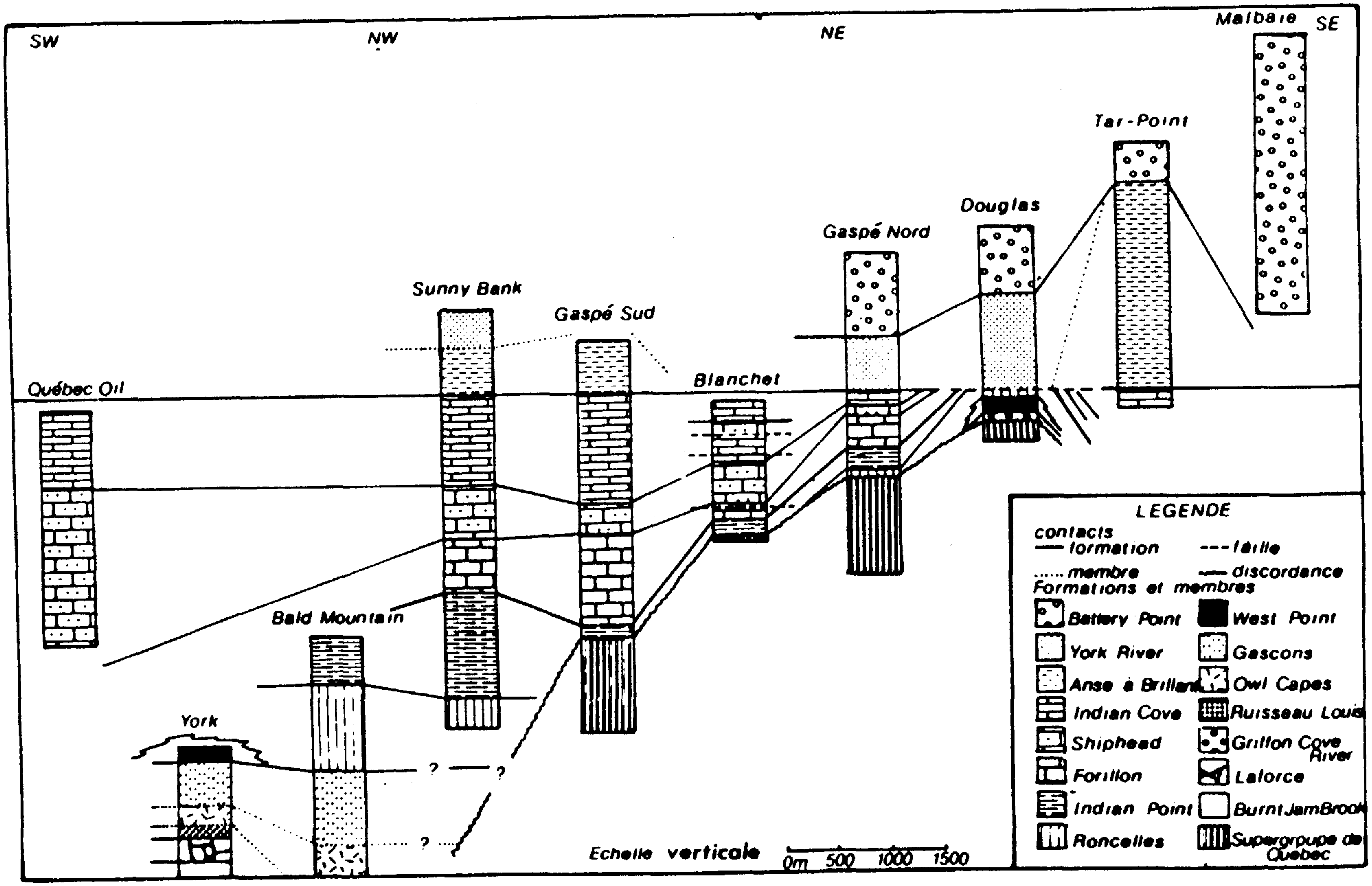

FIGURE 3.5 Lithostratigraphic correlations between few exploration wells, Eastern Gaspésie. From Amyot (1984, figure 4)

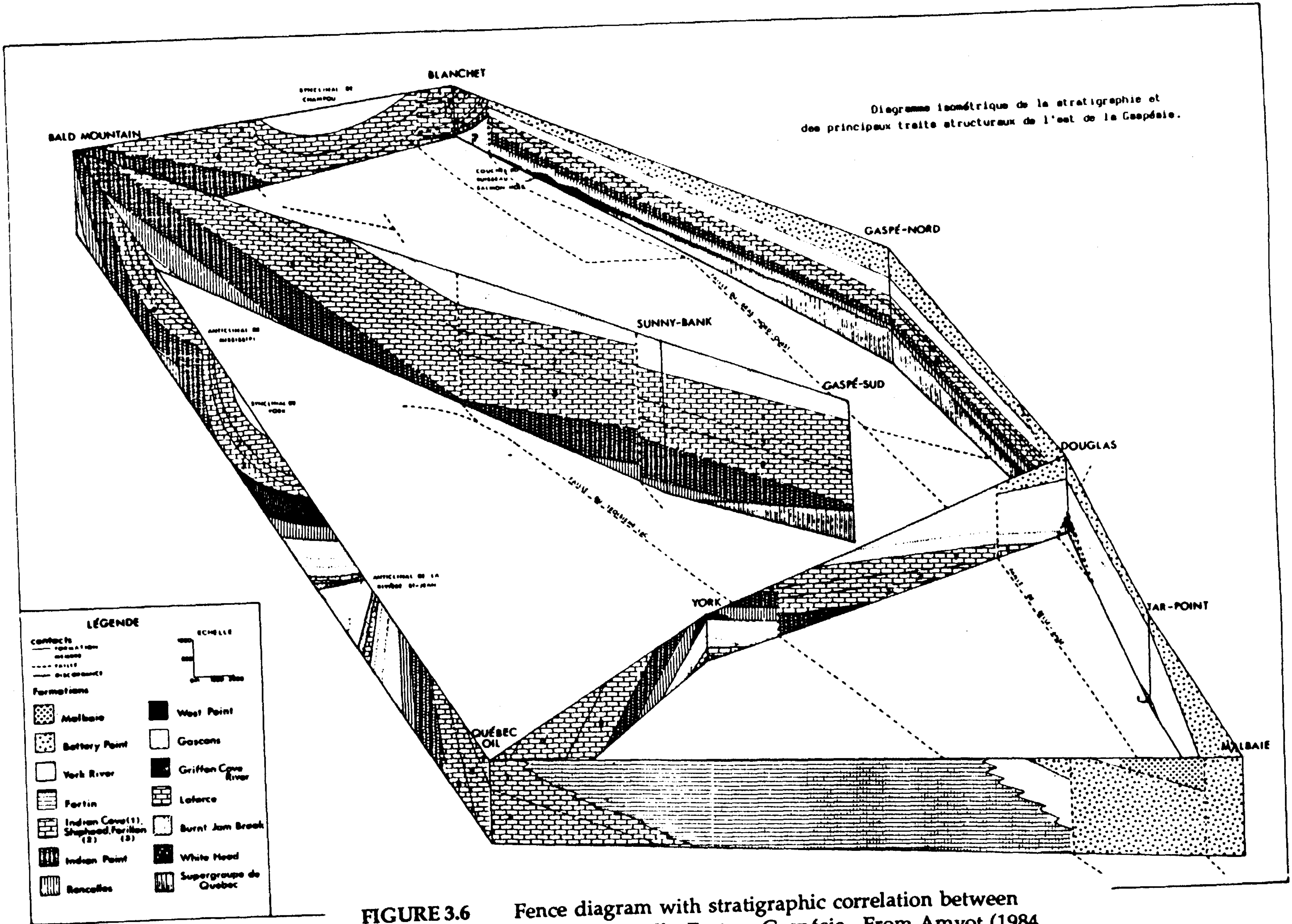

FIGURE 3.6 Fence diagram with stratigraphic correlation between exploration wells, Eastern Gaspésie. From Amyot (1984, figure 6)

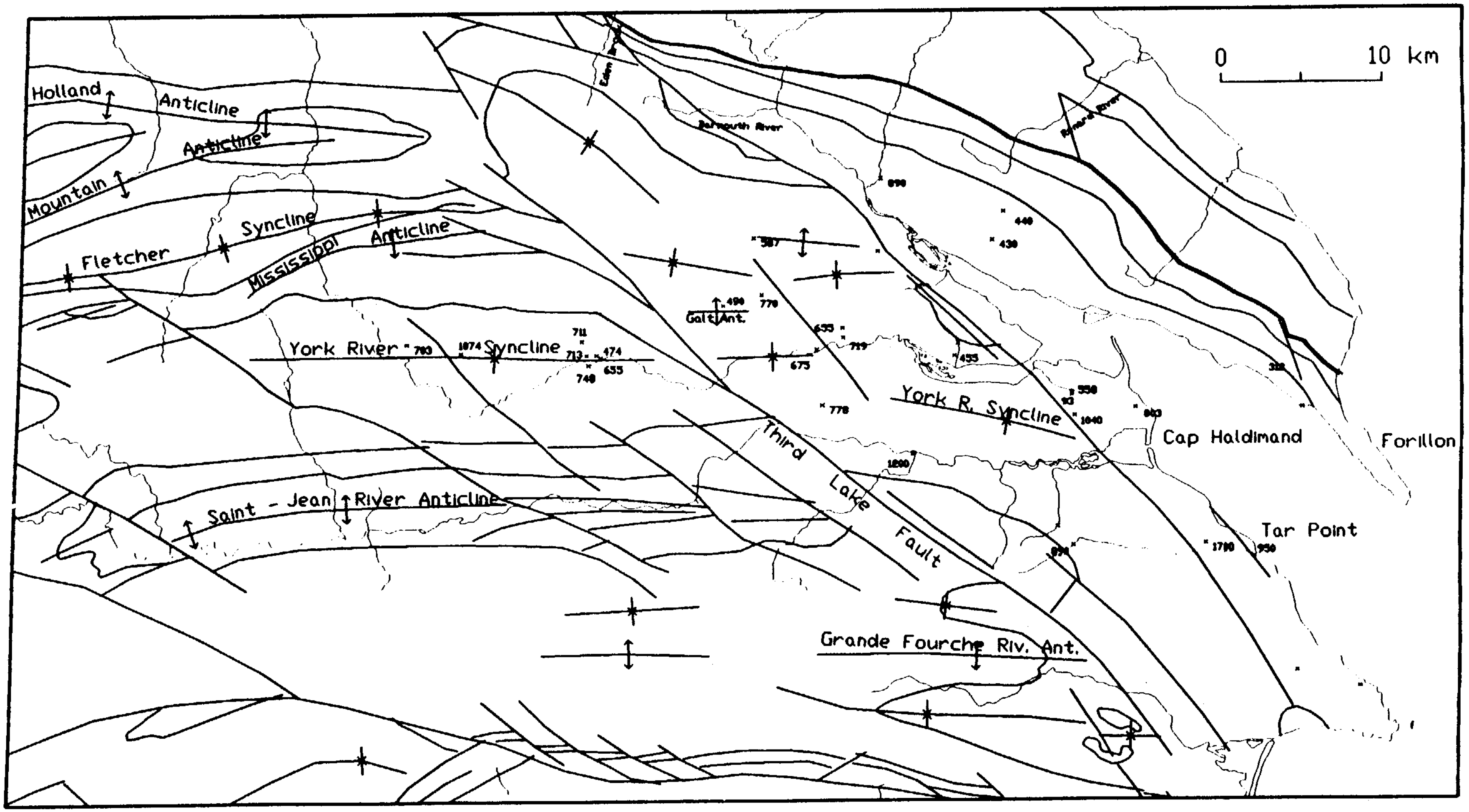

Figure 3.7: Compilation map illustrating measured thicknesses of the York River Formation, Eastern Gaspe

thickness for the formation. Our interpretation of the data indicate a thickening of the formation from the northwest to the southeast along the Gaspé Bay.

Based on grain size and sedimentary structures, Desbiens (1991) recognized twelve (12) lithofacies: six (6) sandy lithofacies, one (1) conglomeratic lithofacies, three (3) muddy or silty lithofacies and two (2) different types of coal beds. Sequence analysis was preformed in order to recognize cyclicity and to support paleoenvironmental interpretation. But, as illustrated in Desbiens (1991), it is difficult to correlate the sedimentary sequences between the different measured sections (Fig. 3.8). A facies map showing mudstone / sandstone ratios and paleocurrent directions (Fig. 3.9) suggests southern and northern source areas and a westerly main paleoflow of the fine material (Desbiens, 1991). Data from other workers are consistent with this interpretation (Fig. 3.10). A petrographic interpretation made from Dickinson and Suczek (1979) diagrams suggest a recycled orogen as source area (Fig. 3.11).

Fluvially-dominated deltas with muddy lagoons and interdistributary bays have been proposed by Mason (1971) and Desbiens (1991) as the general paleoenvironmental setting for the York River Formation.

There are very few data on porosity and permeability of the York River Sandstones. Héroux and Tassé (1985) made some measurements on three (3) sandstone samples (Table 3.2). Porosity ranges from 6,8% to 9% and permeability from 0,4 md to 14,5 md. However, this limited data set does not allow to establish a relationship between a given lithofacies and porosity or permeability. The nature and evolution of the porosity is mostly unknown as no detailed diagenetic study has been done on the York River Formation. Thin sections of the York River sandstones (Plates 1 and 2) show diagenetic clay and cement alteration of primary pore space. Some porosity and permeability should exist in the formation because some oil is seeping from it (see Bertrand, this report).

3.2.4 THE BATTERY POINT FORMATION

Our main references on the Battery Point Formation are the synthesis of Cant and Walker (1976), Brisebois (1981), Rust (1981), Amyot (1984), Lawrence (1986) and Lawrence and Williams (1987). A good summary is found in Bourque et al. (1995). The Battery Point Formation represents a coarsening-upward sequence and can be divided into four informal assemblages. The lower assemblage consists of superposed fining-upward sequences of conglomeratic sandstone, medium- to coarse-grained sandstone, and minor siltstone and mudstone (Cant and Walker, 1976). It is overlain by another assemblage of fining upward sequences into which red mudstone and siltstone are abundant (Walker and Cant, 1979; Rust, 1981). The third assemblage is similar to the first, but with coarser facies and less clearly defined fining-upward sequences. The upper assemblage is a redbed unit of sandstone, siltstone and mudstone restricted to the southeastern part of the area.

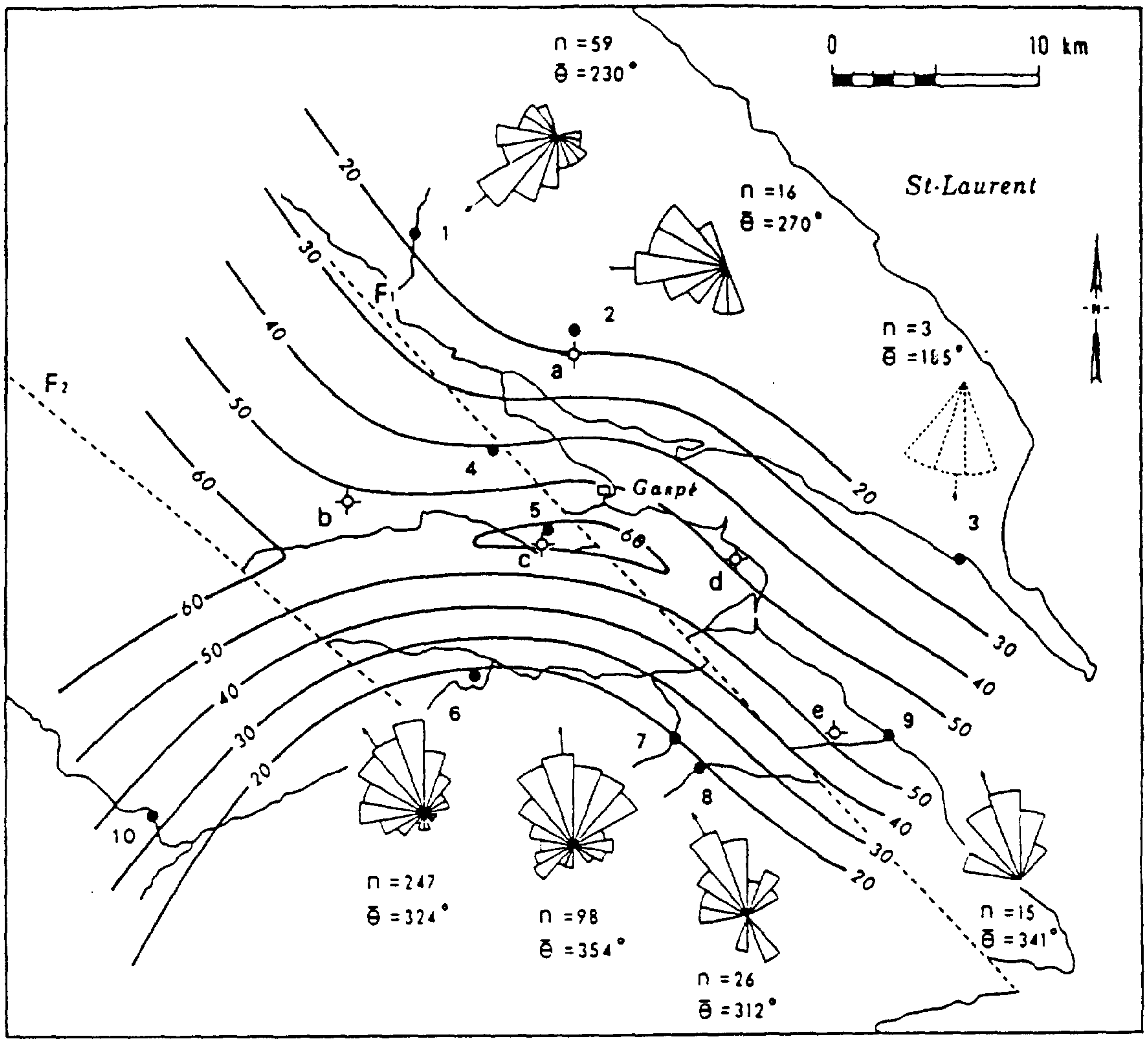

FIGURE 3.9 Facies map (mudstone/sandstone ratio) and paleocurrent directions for the York River Formation, Eastern Gaspésie. From Desbiens (1991, figure 10)

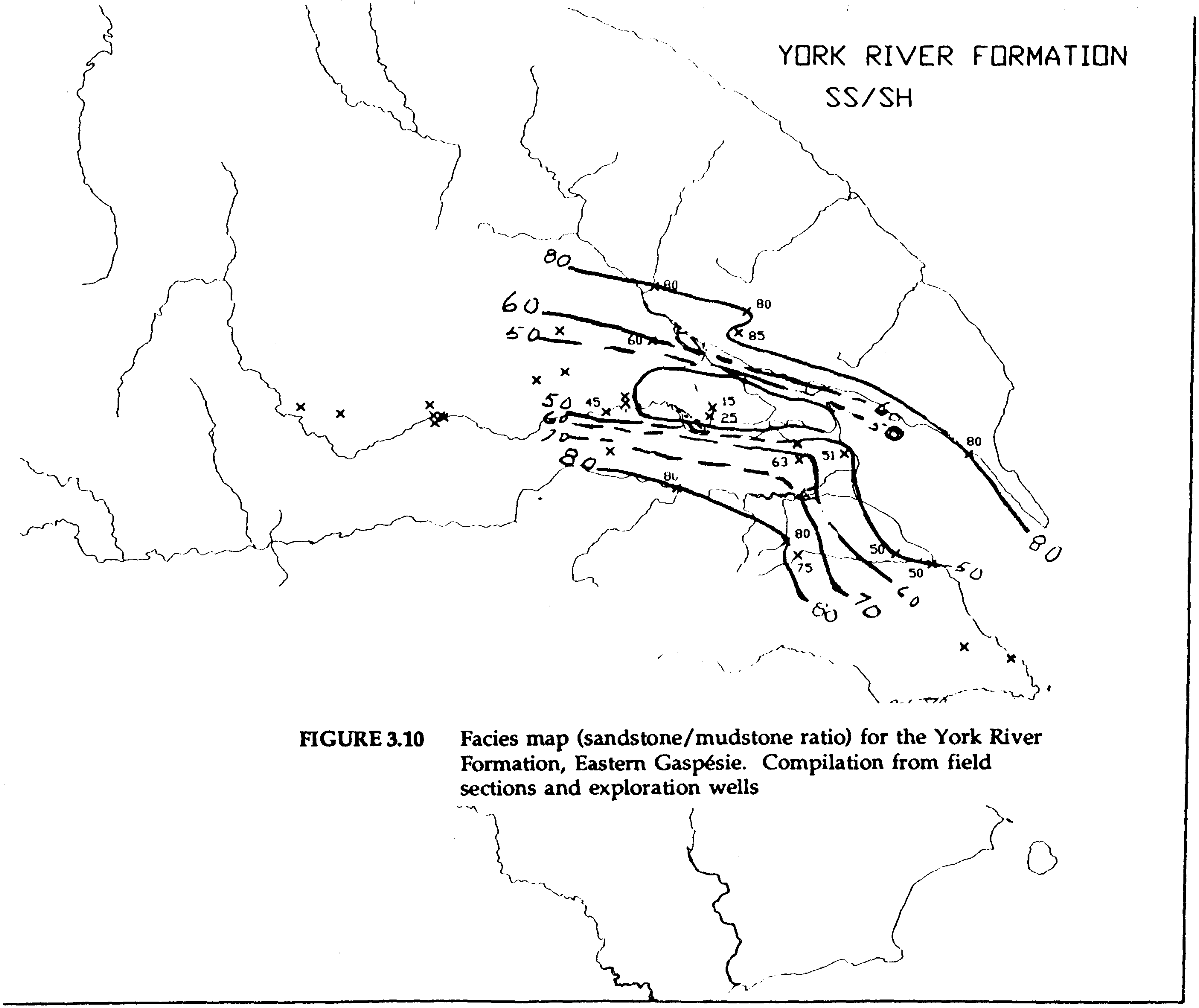

FIGURE 3.10 Facies map (sandstone/mudstone ratio) for the York River Formation, Eastern Gaspésie. Compilation from field sections and exploration wells

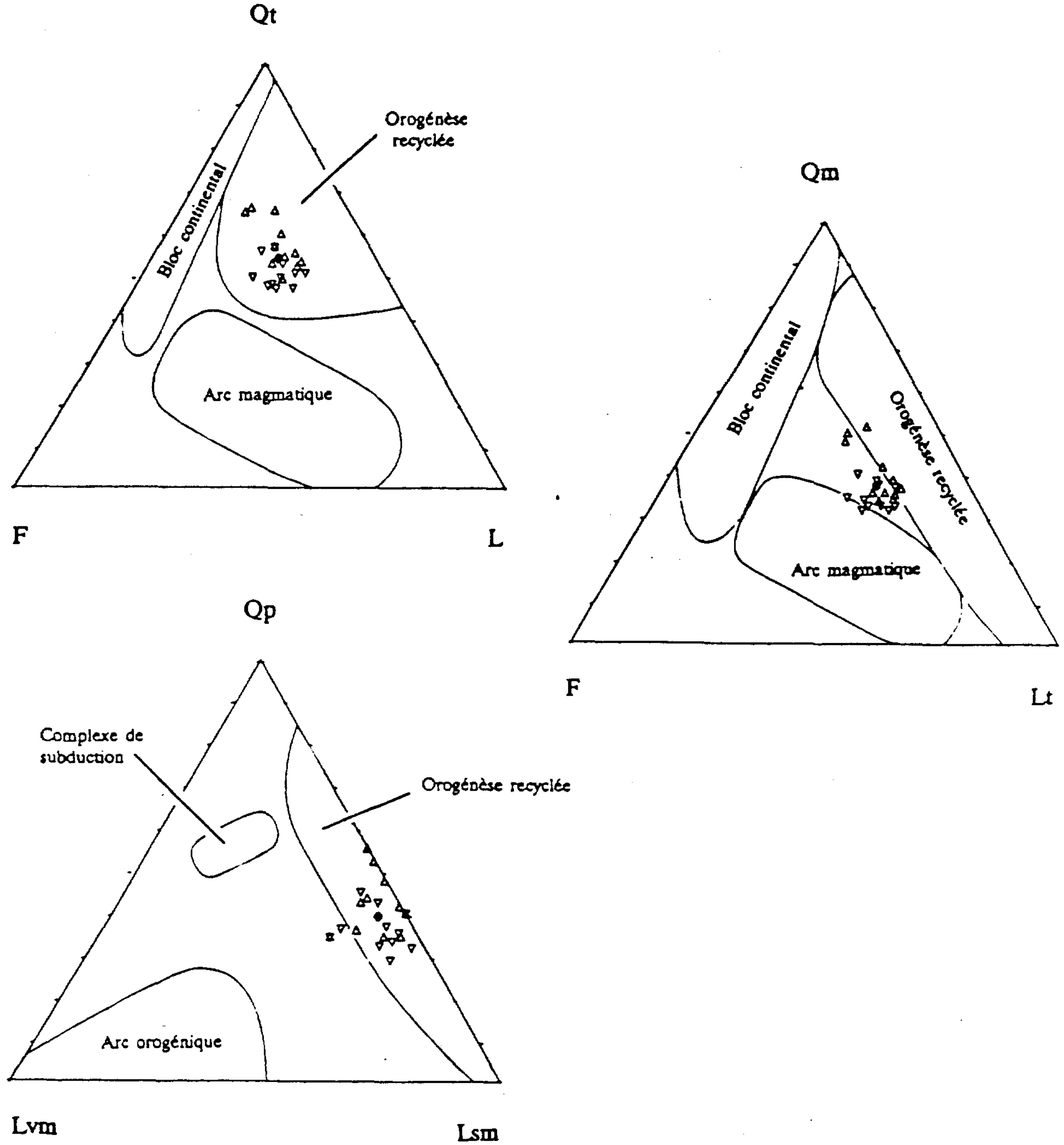

FIGURE 3.11 Dickinson and Suczek (1979) diagrams for the York River Formation. From Desbiens (1991, figure 3)

TABLE 3.2. Porosity and permeability data as reported in the literature

EASTERN GASPÉ(Héroux et Tassé, 1985)

YORK RIVER FORMATION

DRILL HOLE	SAMPLE	POROSITY %	PERMEABILITY, md
GALT NO 2	84-13-176	9	0,5
GALT NO 2	84-13-180	9	14,5
GALT NO 2	84-13-182	6,8	0,4

CENTRAL GASPÉ (INRS-Pétrole, 1975)

YORK RIVER FORMATION

SECTION	SAMPLE	POROSITY %	PERMEABILITY, md
WEST SQUARE FORKS	6-19-57D	2,69	12,12
WEST SQUARE FORKS	6-19-59C	0,18	11.66
CASCAPEDIA LAKE BRANCH	7-8-60A4	9,58	13,39
CASCAPEDIA LAKE BRANCH	7-8-62-6	3,38	9,72
CASCAPEDIA LAKE BRANCH	7-8-62-8	2,78	12,96
CASCAPEDIA LAKE BRANCH	7-8-62-14	2,03	11.23
CASCAPEDIA LAKE BRANCH	7-8-62-21	9,07	11.23

BATTERY POINT FORMATION

SECTION	SAMPLE	POROSITY %	PERMEABILITY, md
CASCAPEDIA LAKE BRANCH	6-19-52	3,19	11,23
WEST SQUARE FORKS	6-19-55	3,95	12,96

The top of the formation is rarely exposed so that true thicknesses are few. Lawrence (1986) measured 1060 m along the north shore of Gaspé Bay and 2290 m along its south shore. The Soquip-Malbaie 1 drill hole (Fig. 3.1) gives a minimum thickness of 2115 m for the Battery Point Formation (Amyot, 1984), but the upper limit of the formation is unknown. The geometry of this formation is not well established; but it might be thickening southeasterly.

The most detailed lithofacies and sequence analysis are from Cant and Walker (1976), Rust (1981), Lawrence (1986) and Lawrence and Williams (1987). The lithofacies coarsen towards the south for the upper part of the section. Various facies assemblages were recognized and related to paleoenvironmental interpretation but the internal architecture of the deposit and its evolution in time and space are still to be determined.

A summary of the paleoenvironment interpretation is given by Rust (1989). The lower assemblage on the north shore of Gaspé Bay is interpreted as the deposit of a distal sandy braided river. Paleocurrents indicate westward flow on the north shore of Gaspé Bay, and northward flow on the south shore. Lawrence and Williams (1987) interpreted this situation as indicating a north-facing main paleoslope draining into a westward-flowing axial system (Fig. 3.12). The lower part of the overlying assemblage on the north shore is attributed to deposition on a north-flowing meandering river system, whereas a distal braidplain (also north flowing) was maintained on the south shore, similar to that of the underlying assemblage. Higher up in this second assemblage, marine influence in the form of brackish marine fauna and tidal channels on a mud-dominated coastal plain is suggested. North-sloping fluvial environments were also maintained, with both braidplain and meander-belt deposition represented. Higher in the formation, paleoenvironment is characterized by channel deposition in vegetated coastal plain; a notable change was the development of eastward axial drainage as opposed to the westward axial flow of the lower Battery Point Formation (Fig. 3.12).

We did not find any detailed petrographic work on the different lithofacies and apparently nothing is known about the mineral diagenesis and on the nature and evolution of the porosity and permeability. The Battery Point Formation represents a sedimentary environment, like the one of the York River Formation, characterized by important lateral facies variations favourable for development of stratigraphic traps. But, and as discussed for the other units of the Gaspé Sandstones, the most favourable facies for reservoir development are still to be determined. However, unlike in the York River Formation, no oil seeps or showings are reported in the Battery Point Formation.

3.2.5 The Malbaie Formation

The Malbaie Formation is only recognized in a faulted block area located in the southeastern part of the Gaspé Bay, north of the village of Percé. This formation is a conglomerate red bed unit, conformably overlying the Battery Point Formation (Rust, 1976, 1981, 1984). The trend of coarsening-upward and changing paleocurrents in the upper part of the Battery Point Formation

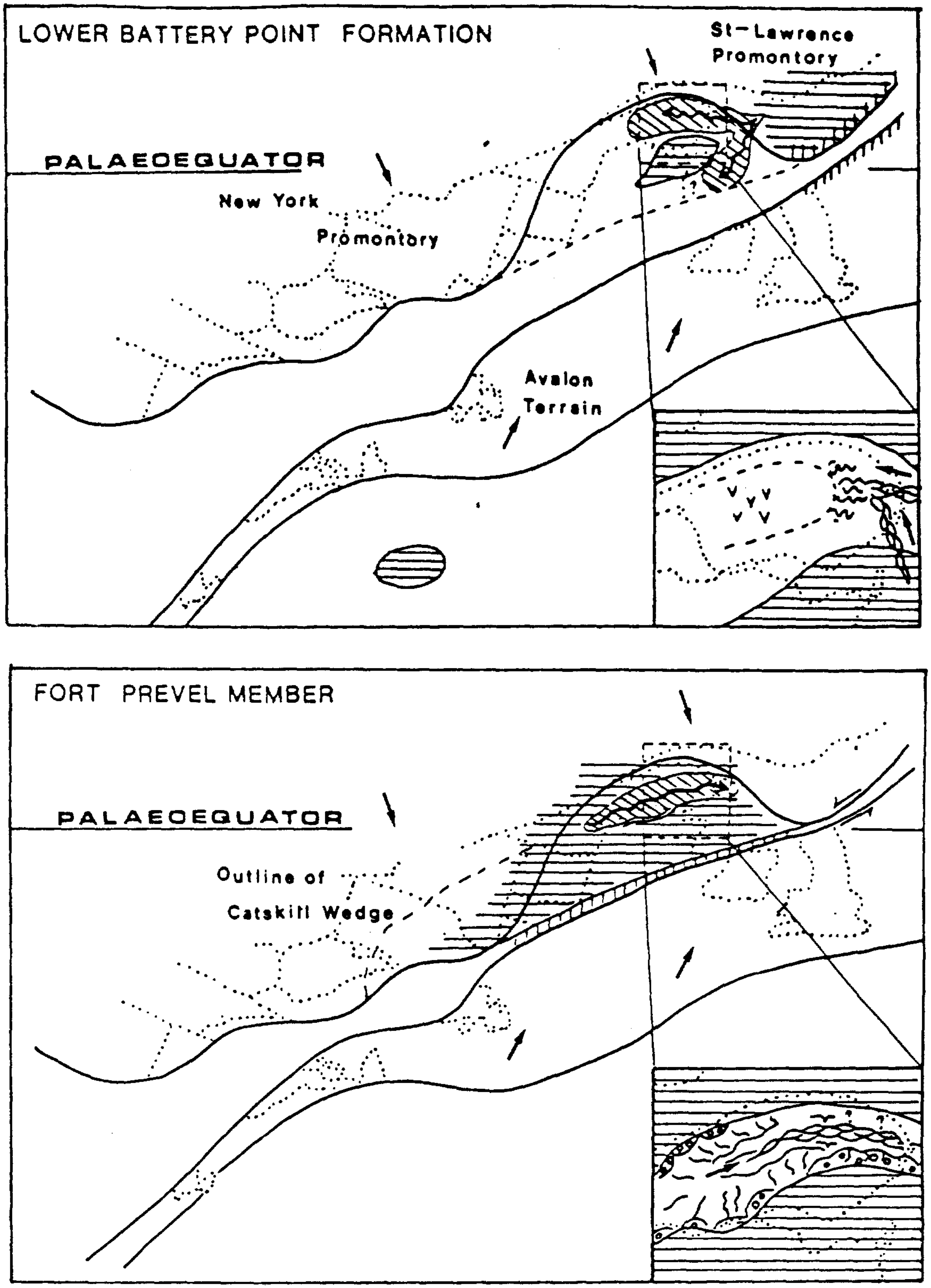

FIGURE 3.12 Summary diagram of the tectonic evolution of the Gaspé Basin during deposition of the Battery Point Formation, with inset schematic diagram of evolving drainage systems. Arrows refer to directions of convergence of opposing plates. From Lawrence and Williams (1987, figure 13)

still persists in the Malbaie Formation. The conglomerate is thickly-bedded and composed of pebbles and cobles of limestone, siliciclastic and volcanic fragments derived from the older Matapédia and Chaleurs groups. The conglomerate is interbedded with medium- to coarse-grained red sandstone. Maximum measured thickness of the Malbaie is 1300 m (Bourque et al., 1995). This formation is unconformably overlain by Carboniferous rocks. The geometry of this conglomerate body has yet to be determined.

The petrography of sandstones and conglomerate matrix was estimated by point counting on thin-sections, which were compared with outcrop point counting of conglomerate megaclasts (Rust, 1984). Six (6) representative conglomerate outcrops, six (6) thin sections of the sandstones and six (6) thin sections of conglomerate matrix were studied. The sandstone and conglomerate matrix are lithic wackes and arenites and the conglomerates are polymict lithic conglomerates. Rust (1984) suggested that the sandstones and the conglomerates were derived from the same source, probably the older Paleozoic rocks, which were actively uplifting in mountains to the south. The nature and evolution of the porosity is unknown and no diagenetic study has been done on this formation.

The best lithofacies analysis and paleoenvironment interpretation were done by Rust (1984): two conglomerate facies and two sandstone facies were recognized. The main conglomerate facies is horizontally stratified, with well-developed imbrication, characteristic of deposition on a high-energy, proximal braidplain. Minor cross-stratified conglomerate shows well-defined size sorting, attributed to avalanching down foresets and sorting within minor bedforms on bar tops. The sandstone units containing erosion surfaces are overlain by mudstone intraclasts, alternating with lineated low-angle to horizontally stratified sandstones or through cross-stratified sandstones. The sandstone units were deposited on a proximal braidplain with highly variable discharge, but the absence of calcrete indicates that dry periods were not prolonged.

The paleocurrents measured in the sandstone units are consistently eastward (Fig. 3.13). This situation is attributed to eastward flow on a sandy axial braidplain, while gravel was transported northward down a proximal gravelly braidplain (Rust, 1984). The paleogeography of the upper part of the Battery Point Formation was maintained, except that the alluvial surfaces were steepened considerably (Fig. 3.14).

3.2.6 THE FORTIN GROUP

The most recent mapping of the Fortin Group is the work of Brisebois (1981) and Simard (1988a, 1988b) in eastern Gaspé and by Dalton (1987) and Kirkwood and St-Julien (1987) in Matapédia River Valley. In its type-area (Fortin township), the Fortin Group overlies the Upper Gaspé Limestones and is overlain by the York River Formation. The Fortin probably occurs at the same stratigraphic position as the York Lake Formation of the Murdochville area and is a lateral equivalent of the lower part of the Gaspé Sandstones. However, as suggested by the work of Skidmore (1965) and Lavoie (1992b), parts of the Fortin Group is also equivalent to parts of the

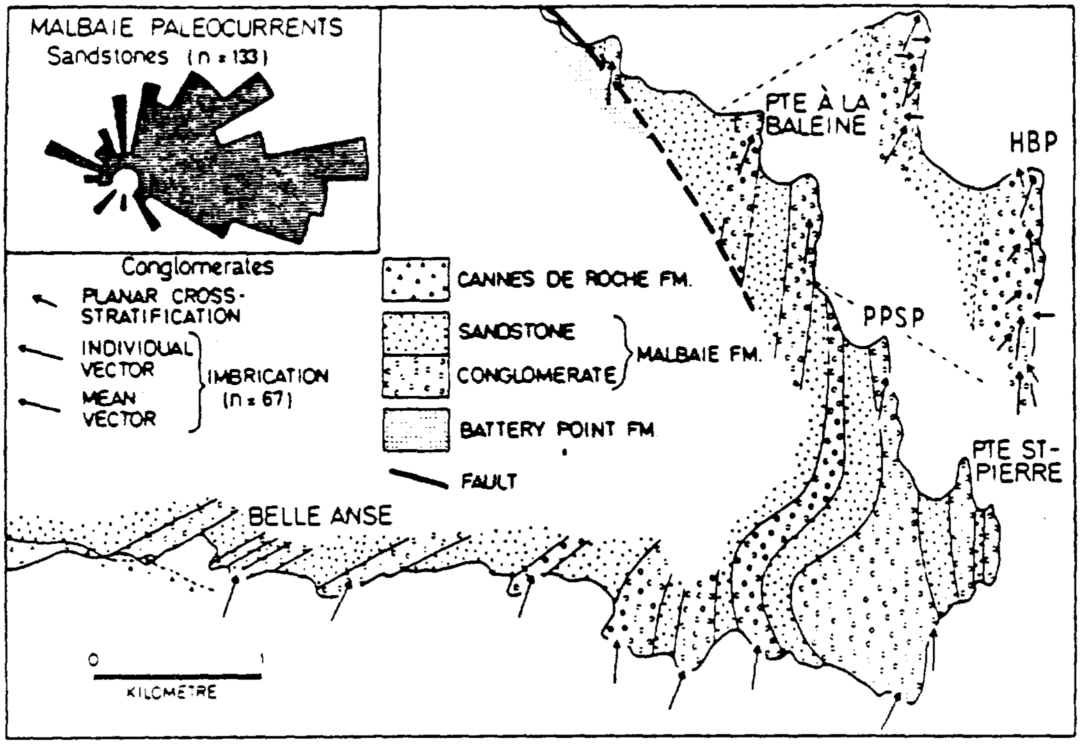

FIGURE 3.13 Geological map and paleocurrent data for the Malbaie Formation, Eastern Gaspésie. From Rust (1984, figure 5)

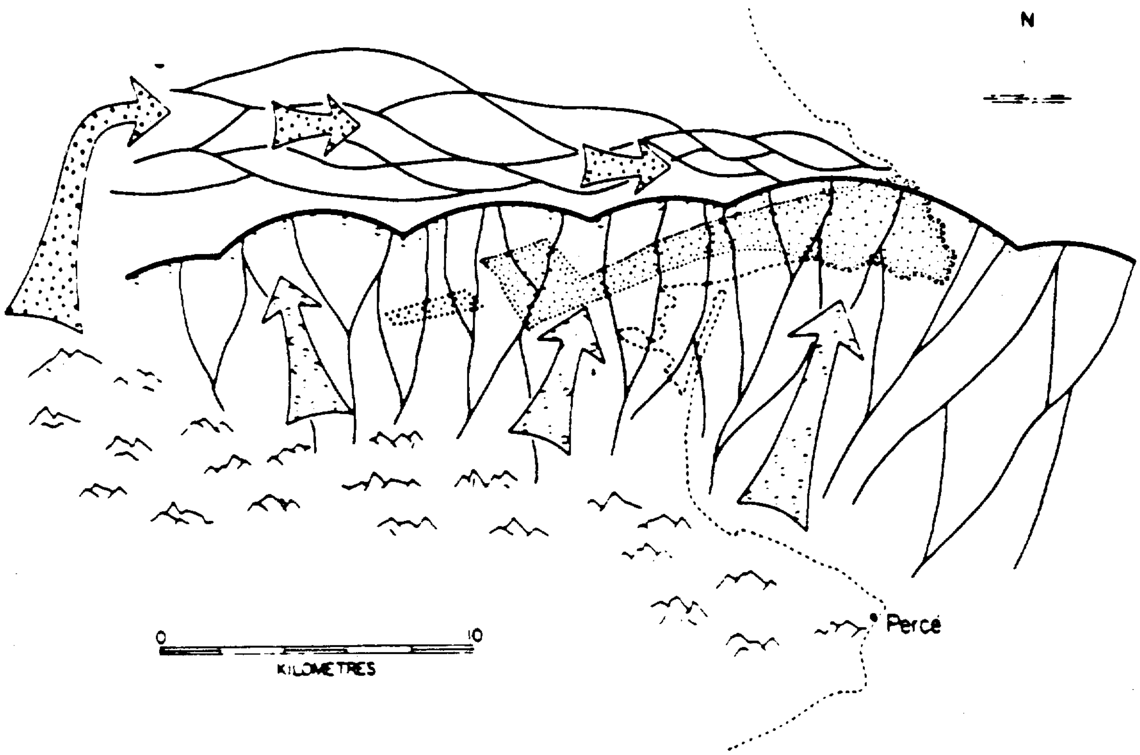

FIGURE 3.14 Depositional model for the Malbaie Formation, Eastern Gaspésie. From Rust (1984, figure 17)

Upper Gaspé Limestones. In Matapédia and Témiscouata areas, the age of the Fortin and its equivalent Temiscouata Formation has been determined with brachiopods and ranges from Lochkovian to Emsian (St-Peter and Boucot, 1981), matching the ranges of the Upper Gaspé Limestones and Gaspé Sandstones.

The strata are strongly folded and present a well developed cleavage. Simard (1988a) recognized two units:
- a lower unit characterized by calcareous mudstone and siltstone, sandstone and conglomerate;
- an upper unit mostly composed of calcareous mudstone and siltstone. There is no other detailed lithofacies analysis on this formation in eastern Gaspé.

The true thickness of the formation is difficult to estimate because of tectonic deformation and lack of stratigraphic markers. McGerrigle (1950) measured a thickness of 1500 m for this unit along the Grande Rivière Nord. This thickness is greater in the Matapédia Valley, where a minimum thickness of 2650 m has been evaluated by Kirkwood and St-Julien (1987).

The environment of deposition for the Fortin Group is roughly interpreted as a deep marine, intermediate between the deep marine platform of the Upper Gaspé Limestones and the clastic deltaic complex developed in the lower part of the Gaspé Sandstones (Simard, 1988a). The source of the clastic material is likely from the east.

More mapping with stratigraphic and sedimentological studies are necessary to get a more coherent understanding of the relationships between this group and the Gaspé Sandstones in Eastern Gaspé. Mineral diagenesis and evolution of the porosity are unknown in this stratigraphic unit and reservoir potential has yet to be evaluated. Some thermal maturation evaluation are available from Bertrand (this report).

3.3 BIG BERRY MOUNTAINS SYNCLINE - CENTRAL GASPÉ

The most recent work on the stratigraphy and reservoir potential of the Gaspé Sandstones in the Big Berry Mountains Syncline area is the synthesis of Sikander (1975). A good summary of the stratigraphy is presented in Bourque et al (1995). In the Big Berry Mountains Syncline area, the Gaspé Sandstones offer roughly the same stratigraphic succession as in northeastern Gaspé, except for the occurrence of the Lake Branch Formation between the York River and Battery Point formations, and for the absence of the Malbaie Formation at the top of the sequence. Figure 3.15 presents a geological map of the Big Berry Mountains Syncline area reproduced from Sikander (1975).

The ***York Lake Formation*** is the same as in northeastern Gaspé. However, the limestones are muddier and the sandstones are finer-grained and more argillaceous; the upper part of the

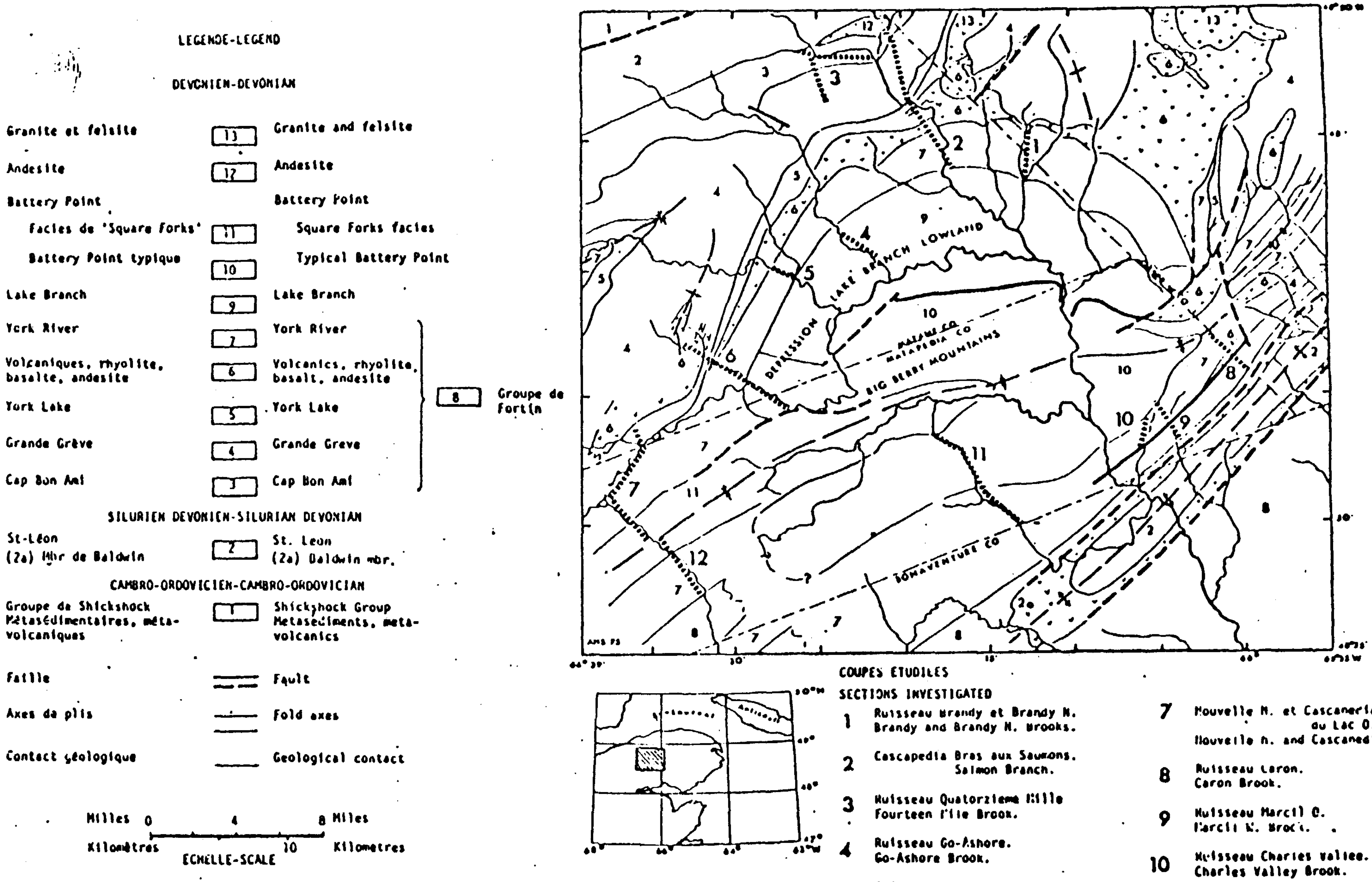

COUPES ETUDILES
SECTIONS INVESTIGATED

1 Ruisseau Brandy et Brandy N. Brandy and Brandy N. Brooks.
2 Cascapedia Bras aux Saumons. Salmon Branch.
3 Ruisseau Quatorzieme Mille Fourteen Mile Brook.
4 Ruisseau Go-Ashore. Go-Ashore Brook.
5 Ruisseau Miner Miner Brook
6 Cascapedia Branche du Lac. Lake Branch.
7 Nouvelle N. et Cascapedia Branch du Lac O. Nouvelle N. and Cascapedia Lake
8 Ruisseau Caron. Caron Brook.
9 Ruisseau Marcil O. Marcil W. Brook.
10 Ruisseau Charles Vallee. Charles Valley Brook.
11 Route Square Forks, et les Lacs Square Forks Road, and Josue La
12 Rivière Nouvelle S. Nouvelle River S.

FIGURE 3.15 Geological map of the Big Berry Mountains Syncline, Central Gaspésie. From Sikander (1975, figure 10) formation contains mafic lava flows and pyroclastic rocks (Sikander, 1975). Its thickness ranges from 300 m to the north to 600 m to the east, and thins to zero to the south.

The overlying ***York River Formation*** consists of cross-bedded, fine- to medium-grained, grey feldspathic sandstone interbedded with grey mudstone and siltstone (Sikander, 1975). The grey rocks contain intercalations of red or brown siltstone, mudstone and sandstone with mudcracks and ripple marks. Both red and grey facies are fossiliferous (brachiopods and bivalves). The York River Formation contains thick bimodal volcanic sequences (Doyon and Valiquette, 1986; Doyon 1988). A complete volcanic sequence consists of initial basaltic flows and mafic pyroclastic rocks, followed by rhyolitic flows and felsic pyroclastic rocks, and capped by rhyolitic flows. In the northeastern part of the Big Berry Mountains Syncline, mafic volcanic rocks occur at the top of the unit. Thickness of the York River is about 600 m to the north and up to 3000 m to the south (Carbonneau, 1959). Figure 3.16 illustrates an isopach map of the York River Formation compiled by Sikander (1975) from measured road and river sections.

The ***Lake Branch Formation*** above the York River is limited to the north limb of the Big Berry Mountains Syncline and is poorly exposed (Carbonneau, 1959). It is a 1500 m thick unit of red to brownish red shale with siltstone and fine-grained sandstone. Mudcracks and ripple-marks are sparse; fossils are absent.

The overlying ***Battery Point Formation*** constitutes the core of the Big Berry Mountains Syncline. Sikander (1975) subdivided the formation into two informal units:
- a 2500 m lower "typical Battery Point" unit of crossbedded, fine- to medium-grained, light grey feldspathic sandstone with minor grey or reddish shale, siltstone and granule conglomerate;
- a 500 m upper redbed unit of fine- to medium-grained silty sandstone and minor shale with common ripple-marks, rain-prints and mudcracks. Except for palynomorphs, fossils are absent in both units. Thickness estimates and paleocurrent directions for the Battery Point Formation were compiled by Sikander (1975) and are shown in figure 3.17.

There is no detailed sedimentological and/or petrographical work on the Gaspé Sandstones in this area. Tentative paleoenvironmental interpretation proposed by Sikander (1975) suggests that the York Lake and York River formations represent mostly shoreface to nearshore bar and tidal environments. The sedimentation of the Lake Branch Formation corresponds to the development of a delta fringe and/or a lower deltaic plain environment with an upward evolution in alluvial braided channel environment for the Battery Point Formation (Sikander, 1975). Westerly and southwesterly prograding fluvial systems are proposed.

The hydrocarbon potential of the Big Berry Mountains Syncline is discussed by Sikander (1975). From the lack of organic matter, the York River is consider to have a poor source-rock potential. Maturation studies (vitrinite reflectance and organic matter carbonisation) suggest that the York River and the Lake Branch formations are characterized by favourable levels of organic diagenesis for oil and gas generation with the western part of the area having a greater potential for oil

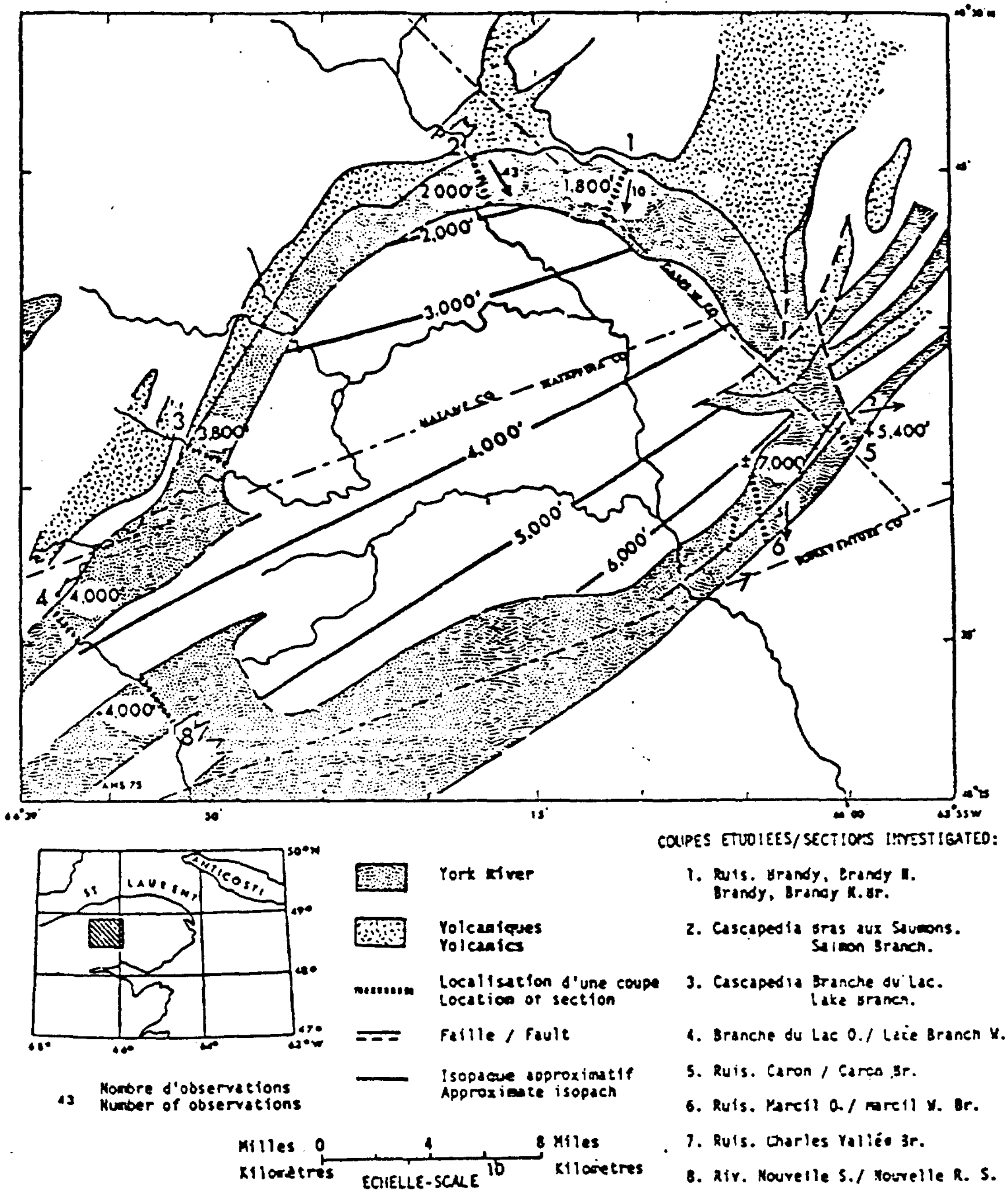

FIGURE 3.16 Isopach map, paleocurrent directions, York River Formation, Big Berry Mountains Syncline, Central Gaspésie. From Sikander (1975, figure 15)

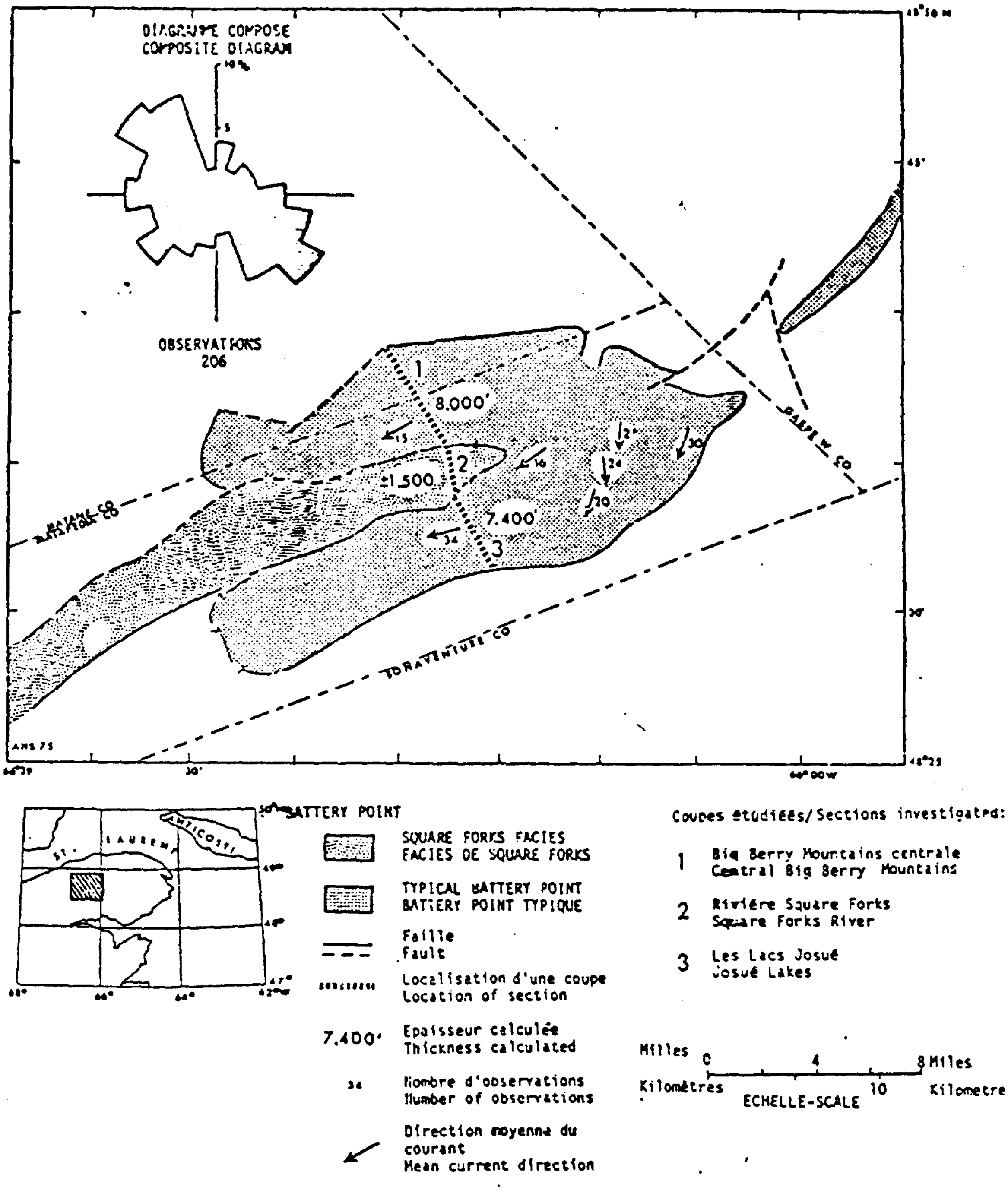

FIGURE 3.17 Thickness estimates, paleocurrent directions, Battery Point Formation, Big Berry Mountains Syncline, Central Gaspésie. From Sikander (1975, figure 16)

(Sikander, 1975). The metamorphic effects at volcanic and sedimentary rock contacts are of an very local extent (Sikander, 1975).

The field work did not reveal the presence of sandstones with interesting reservoir possibilities (Sikander, 1975). Porosity and permeability studies were done by INRS-Pétrole (1975) on the most promising samples and reported in Sikander (1975). Seven (7) sandstones samples from the York River Formation and two (2) from the Battery Point Formation were evaluated (Table 3.2). Porosity ranges from 0,18% to 9,58% and permeability from 9,72 md to 13,39 md. No relationship between given lithofacies and porosity or permeability could be recognized.

The low porosity in the Gaspé Sandstones is attributed to the presence of illite, chlorite, rare kaolinite, altered feldspars, and occasional calcite and silica cement (Sikander, 1975). The effect of surface weathering and the formation of authigenic illite and chlorite on the potential reservoir sand is not clear (Sikander, 1975). But the exact nature and evolution of the porosity is unknown and more detailed diagenetic studies are needed on the Gaspé Sandstones in the Big Berry Mountains.

Sikander (1975) considers that from the poor rock exposure and from the lack of well data, judgement on source and reservoir can not be made.

3.4 SUMMARY AND CONCLUSIONS

3.4.1 GENERAL GEOLOGY AND STRATIGRAPHY

The Gaspé Sandstones are relatively well known in terms of sedimentology and paleoenvironments; they are better known in eastern than in central Gaspé. Many published articles and technical reports are devoted to the subject.

The Lower to Mid-Devonian Gaspé Sandstones consist of four clastic formations, conformably overlying the Upper Gaspé Limestones. These formations form a progradational sequence from shallow marine and deltaic sandstone and mudstone deposits of the York Lake and the York River formations to sandy braidplain and meandering fluvial systems of the Battery Point Formation. This sequence coarsens upward into proximal braidplain conglomeratic deposits of the Malbaie Formation. The sequence may be very thick: 312 m in the northeast reaching 1700 m in the southeast and more westward for the York River Formation, 2300 m thick and more westward for the Battery Point Formation and 1300 m thick for the Malbaie Formation.

In southwestern part of the area, the Fortin Group is a transitional to laterally equivalent unit of the Upper Gaspé Limestones and the Gaspé Sandstones. This unit is essentially a fine deep marine clastic deposit with interbeds of silty and sandy limestones. The stratigraphic and paleogeographic relationships between the Fortin Group, south of the Saint-Jean River Anticline, and the Gaspé Sandstones, to the northeast, are not well understood.

In the Big Berry Mountains Syncline area, the Gaspé Sandstones have roughly the same stratigraphic sequence as in northeastern Gaspé, except for the occurrence of the deltaic Lake Branch Formation between the York River and Battery Point formations, and for the absence of the Malbaie Formation on top of the sequence.

The Gaspé Sandstones represent the shallowing upward phase III of Bourque et al. (1995) developed in Emsian time (Fig. 3.18). This third shallowing phase culminated with Acadian Orogeny. Figure 3.19 illustrates the paleogeography of the Gaspé-Témiscouata depositional basin on a palinspastic base map (Bourque et al., 1995).

3.4.2 DIAGENESIS, POROSITY AND PERMEABILITY

Few data and information about mineral diagenetic evolution, porosity and permeability of the sandstones are available. From one report (Héroux and Tassé, 1985) we know that the sandstones were submitted, in some areas, to relatively complex mineral diagenesis including clay, quartz and feldspar authigenic formation. Porosity and permeability measurements are very few and vary between 0,18% and 9,58%, and 0,4 md to 14,5 md, respectively (Table 3.2). These values are not correlated, so far, to specific facies of the sandstones. Petrographic descriptions were not performed on impregnated thin-sections; thus, there is no description dealing with porosity and everything besides the coarser fraction of the rock is considered as matrix or cement.

3.4.3 CONCLUSIONS

The purpose of this project on the Gaspé Sandstones was to review the literature in order to determine to what extent it was possible to evaluate the reservoir potential of these sandstones. As presented in the introduction, the questions are:

> *1) The architecture of the Gaspé Sandstones body is an important factor controlling the geometry and the thickness of the lithofacies forming the sandstone sequences.*

What is the geometry of the clastic wedge deposit? What is the paleoenvironmental relationships between the transitional fine clastic Fortin Group and the deltaic York River and Battery Point formations? Can we localize, vertically and laterally in the sedimentary sequence, distributary channels, secondary channels, mudflats, prodeltaic environments, etc?

> *2) The reservoir quality is essentially related to the porosity and the permeability of the clastic framework of the rock.*

Porosity and permeability result from two main factors:
- the original texture of the lithofacies (grain size, grain sorting, grain shape, grain packing and intergranular matrix),

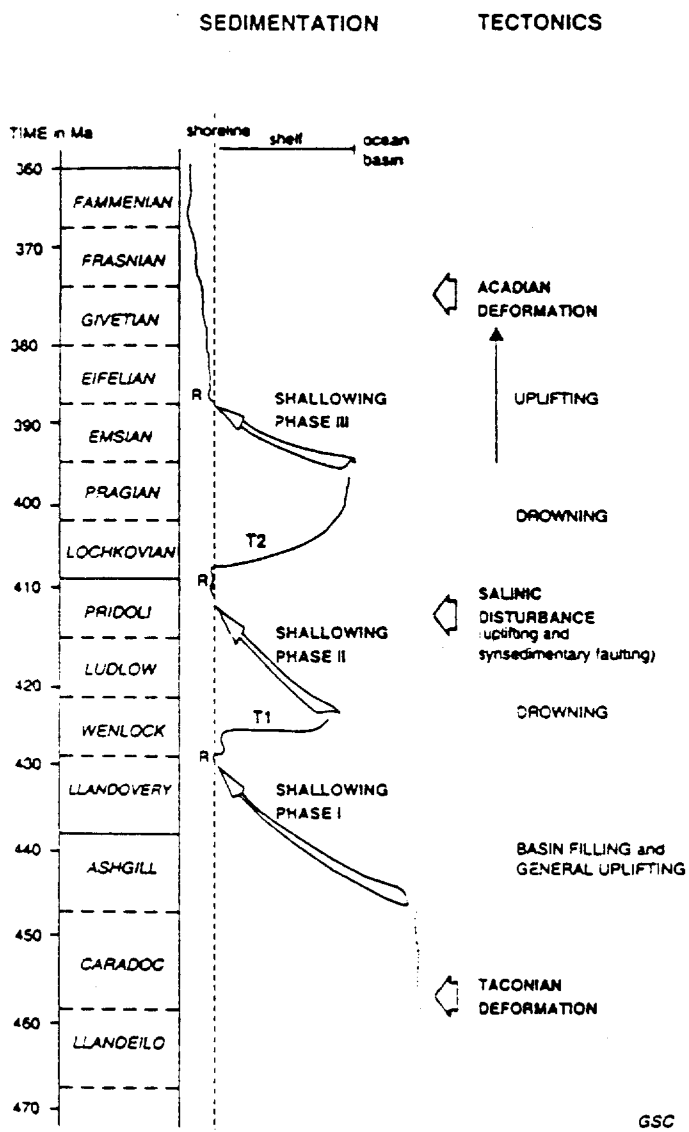

FIGURE 3.18 Summary of sedimentary and tectonic evolution of the upper Middle Ordovician to Upper Devonian sequence of the Gaspé Belt. T1 and T2 are transgressive episodes. R, denotes redbeds. From Bourque *et al.* (1995)

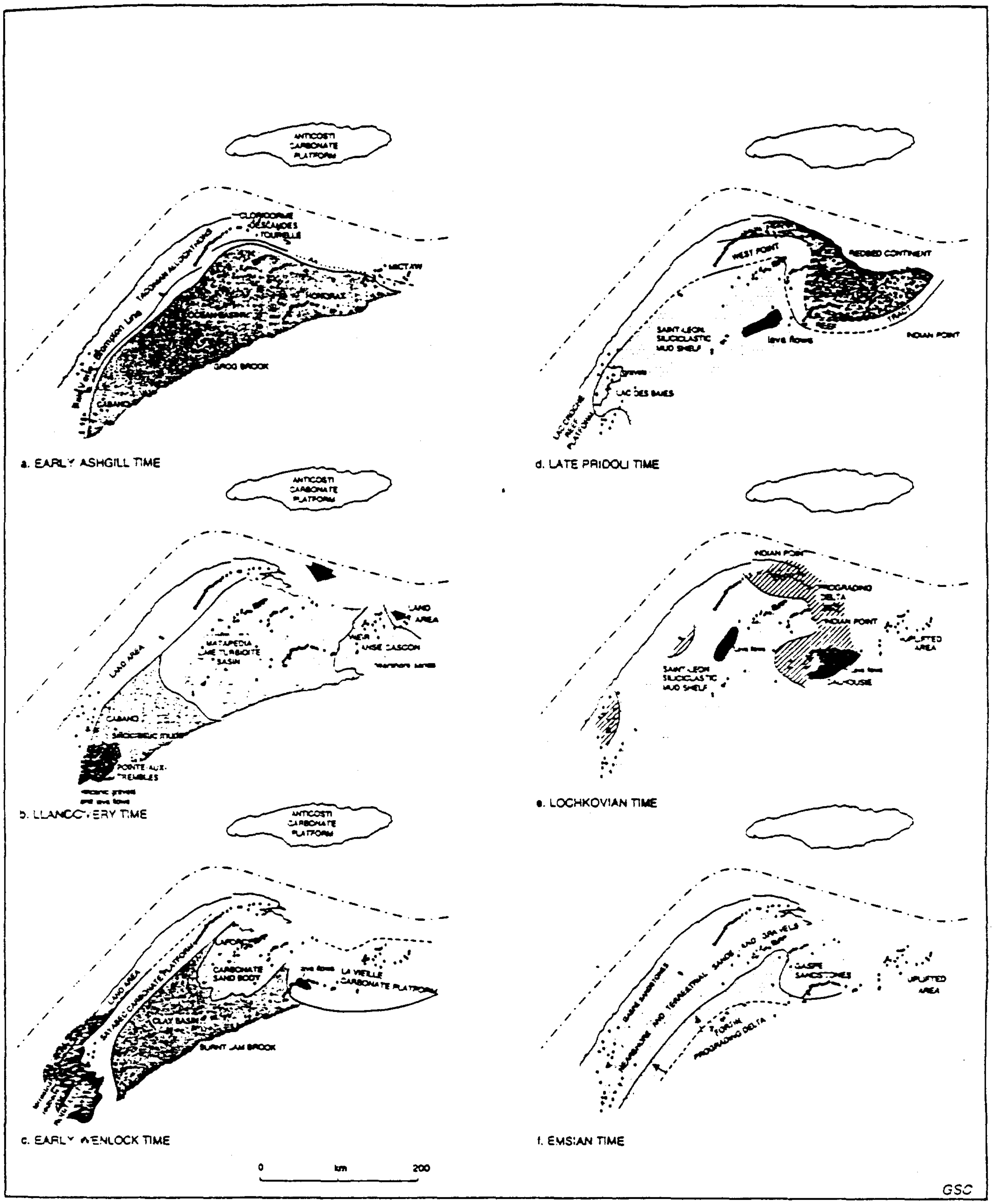

FIGURE 3.19 Paleogeography of the Gaspé-Témiscouata segment of the Gaspé Belt, from post-Taconic Orogeny trough Acadian Orogeny. Facies were plotted on palinspastic base map. Arrows indicate direction of sedimentary transport. From Bourque *et al.* (1995)

- the evolution of pore filling during diagenesis (grain alteration and dissolution, cementation, authigenic clays).

Can we, from the literature, localize the more favourable lithofacies in the stratigraphic sequence or can we modelized their location and evolution?

Only parts of these questions can be answered from available data and information. The sedimentology and general paleoenvironments are relatively well defined, but the various lithofacies, representing different sub-environments (distributary channels, levees, shoreface, etc.) are not well recognized, and more significantly, their lateral extension is unknown.

As far as porosity and permeability are concerned, there is almost no available data. The mineral diagenesis, which is a critical factor controlling the porosity in sandstones, has yet to be studied.

> *Therefore, it is actually impossible from the available information found to define and map the most favourable lithofacies for reservoir. However, the overall sedimentology and paleoenvironmental interpretations of the Gaspé Sandstones indicate interesting similarities with rich producing oil fields.*

3.5 RECOMMENDATIONS

From the above conclusions, it is obvious that more works are needed in order to define and map potential reservoirs. The overall facies architecture of these sandstones has to be precisely defined which requires significant field works. The mineral diagenesis also has to be established in order to monitor the porosity evolution with respect to oil generation and migration.

In most oil fields producing from fluviodeltaic depositional paleoenvironments, the main reservoirs are fluvial channel-fill sandstones and conglomerates, delta-front/mouth-bar sandstones and point-bar sandstones (Barwis et al.,1990). These types of facies most likely occurs in the Gaspé Sandstones but they are not always interpreted or defined as such. Moreover, their lateral extensions are unknown. Some months of field work are needed to precise these hypothesis and to define those relationships.

Mineral diagenesis and porosity/permeability evolution studies are based on laboratory works: X-ray diffraction, scanning electron microscopy, impregnated thin-sections microscopic studies, organic matter petrography and geochemistry.

These works could be done as Ph.D. or M.Sc. research projects in a longer term perspective.

REFERENCES

Alcock, F.J., 1935. Geology of Chaleurs Bay region. Geological Survey of Canada, Memoir **183**, 146 p.

Amyot, G., 1984. Lithostratigraphie de sous-surface de l'est de la Gaspésie. Ministère de l'Énergie et des Ressources du Québec, **ET 83-11**, 83 p.

Amyot, G., 1990. Petrography of the York River, ruisseau Bazire (Gaspésie). Ministère de l'Énergie et des Ressources du Québec, **MB 90-06**, 83 p.

Barwis, J.H., McPherson, J.G., and Studlick, R.J., 1990. Sandstone petroleum reservoir. Springer-Verlag, New York, 583 p.

Bourque, P.-A., Brisebois, D., and Malo, M., 1995. Ceinture de Gaspé. *In* Williams, H. (ed.), Géologie de l'Orogène Appalachien-Calédonien au Canada et au Groenland, chap. 4, Commission géologique du Canada, Géologie du Canada, **6**, 348-387.

Brisebois, D., 1981. Géologie de la région de Gaspé. Ministère de l'Énergie et des Ressources du Québec, Rapport intérimaire, **DPV-824**, 19 p., 1 carte.

Brisebois, D., Lachambre, G., and Piché, G., 1991. Carte géologique Péninsule de la Gaspésie 22A, 22B, 22G, 22H et 21O, 3e édition. Ministère de l'Énergie et des Ressources du Québec, Carte 2146 - **DV 91-21**.

Cant, D.J., and Walker, R.G., 1976. Development of a braided-fluvial facies model for the Devonian Battery Point Sandstone, Québec. Canadian Journal of Earth Sciences **13**, 102-119.

Carbonneau, C., 1959. Région de Richard-Gravier, péninsule de Gaspé, Québec. Ministère des Mines du Québec, **RG 90**, 75 p.

Dalton, E., 1987. Sedimentary facies and diagenesis of the Lower Devonian Temiscouata and Fortin formations, Northern Appalachians, Québec and New Brunswick. M.Sc. thesis, McGill University, Montréal, 228 p.

Desbiens, S., 1991. Le complexe deltaïque de la Formation de York River (Dévonien inférieur) de la région de Gaspé: paléoécologie et biostratigraphie. Ph.D. thesis, Université de Montréal.

Dickinson, W.R., and Suczek, C.A., 1979. Plate tectonics and sandstone composition. American Association of Petroleum Geologists Bulletin, **63**, 2164-2182.

Doyon, M., 1988. Synthèse géologique des roches volcaniques du Centre Nord de la Gaspésie. M.Sc. thesis, École polytechnique, Montréal, (Québec), 244 p.

Doyon, M., and Valiquette, G., 1986. Synthèse géologique des volcanites du Centre Nord de la Gaspésie, Québec. Ministère de l'Énergie et des Ressources du Québec, **MB 86-48**.

Héroux, Y., and Tassé, N., 1985. Pétrographie des grès de la Formation de York River du canton de Galt. Rapport au ministère de l'Énergie et des Ressources du Québec, ref. 33030500, 29p.

INRS-PÉTROLE, 1975. Analytical investigation , mineralogy, geochemistry, palynology, and reflectometry of the Gaspé Sandstone Series of Central Gaspé, Québec. Direction de l'Énergie, Ministère des Richesses naturelles du Québec, Open file report, 80 p.

Jones, I.W., 1935. Upper York River map area, Gaspé Peninsula, Québec. Department of Mines, Annual Reports, part D, 1934-1936, 3-28.

Kirkwood, D., and St-Julien, P., 1987. Analyse structurale du Siluro-Dévonien dans la Vallée de la Matapédia. Ministère de l'Energie et des Ressources du Québec, **MB 87-33**, 17 p.

Lavoie, D., 1992a. Lower Devonian facies in Forillon peninsula, eastern Gaspé, Québec Appalachians: a storm-influenced carbonate outer shelf. Bulletin of Canadian Petroleum Geology, **40**, 303-320.

Lavoie, D., 1992b. Carbonate sedimentation in an extensional tectonic regime: the lower Devonian Upper Gaspé Limestones, Québec Appalachians. Canadian Journal of Earth Sciences, **29**, 118-128.

Lawrence, D.A., 1986. Sedimentology of the Lower Devonian Battery Point Formation, Eastern Gaspé Peninsula, Québec, Canada. Ph.D. thesis, University of Bristol, England.

Lawrence, D.A., and Williams, B.P.J., 1987. Evolution of drainage systems in response to Acadian deformation: The Devonian Battery Point Formation, Eastern Canada. *In* Ethridge, F.G., Flores, R.M., Harvey, M.D. (eds.), Recent Developments in Fluvial Sedimentology, Society of Economic Paleontologists and Mineralogists, Special Publication **39**, 287-300.

Lespérance, P.J., 1980. Calcaires Supérieurs de Gaspé: les aires-types et le prolongement ouest. Ministère de l'Énergie et des Ressources du Québec, **DPV 595**.

Logan, W.E., 1863. Report on the geology of Canada. Dawson Brothers, Montréal, 983 p.

Mason, G.D., 1971. A stratigraphical and paleoenvironmental study of the Upper Gaspé Limestone and Lower Gaspé Sandstone Groups (Lower Devonian) of Eastern Gaspé peninsula, Québec. Ph.D. thesis, Carleton University, Ottawa.

McGerrigle, H.W., 1950. The geology of eastern Gaspé. Ministère des Mines du Québec, Geological Report **35**, 168 p.

Rust, B., 1976. Stratigraphic relationships of the Malbaie Formation (Devonian), Gaspé, Québec. Canadian Journal of Earth Sciences, **13**, 1556-1559.

Rust, B., 1981. Alluvial deposits and tectonic style: Devonian and Carboniferous successions in Eastern Gaspé. *In* Miall, A.D. (ed.), Sedimentation and Tectonics in Alluvial Basins, Geological Association of Canada, Special Paper **23**, 49-76.

Rust, B., 1984. Proximal braidplain deposits in the Middle Devonian Malbaie Formation of eastern Gaspé, Québec, Canada. Sedimentology, **1**, 675-695.

Rust, B., 1989. The Devonian clastic wedge in Eastern Gaspé peninsula. *In* P.-A. Bourque, R. Hesse, B., Rust (eds.), Field Trip B8: Sedimentology, Paleoenvironments and Paleogeography of the Taconian to Acadian Rock Sequence of Gaspé Peninsula. Guidebook GAC-MAC, Annual meeting, Montréal 1989, 165-180.

Sikander, A.H., 1975. Geology for hydrocarbon potential of the Berry Mountain Syncline, central Gaspé (Matane, Matapédia, Gaspé W and Bonaventure counties). Ministère des Richesses naturelles du Québec, **DP-376**, 119 p.

Simard, M., 1988a. Géologie de la région de Joncas-Power (Gaspésie). Ministère de l'Énergie et des Ressources du Québec, **ET 86-10**, 34 p.

Simard, M., 1988b. Géologie de la région de Dufour (Gaspésie). Ministère de l'Énergie et des Ressources du Québec, **ET 86-12**, 20 p.

Skidmore, W.B., 1965. Région de Castonguay - Mourier, comtés de Gaspé-nord, Gaspé-sud et Bonaventure. Ministère des Richesses naturelles du Québec, **RG-105**, 88 p.

St. Peter, C., and Boucot, A.J., 1981. Age and regional significance of brachiopods from the Temiscouata Formation of Madawaska County, New Brunswick. Maritime Sediments and Atlantic Geology, **17**, 88-95.

Walker, R.G., and Cant, D.J., 1979. Facies model 3: Sandy fluvial system, *In* Walker, R.G. (ed.), Facies Models, Geoscience Canada, Reprint Series **1**, 23-31.

Williams, H.S., 1910. Age of the Gaspé Sandstones. Geological Society of America Bulletin, **20**, 688-698.

PLATE 1

A. Photomicrograph of a York River Sandstones sample showing the occlusion of the primary porosity by quartz overgrowths on detrital quartz grains.

B. Feldspar overgrowth around a plagioclase slightly altered in sericite.

C. Quartz grain partly coated with clay minerals. The clays are most probably authigenic. A silica cement covers the clay minerals indicating a late precipitation of this mineral.

D. Quartz grain totally coated with authigenic clay minerals (probably chlorite). The a-b plane of the clay is perpendicular to the quartz grain surface.

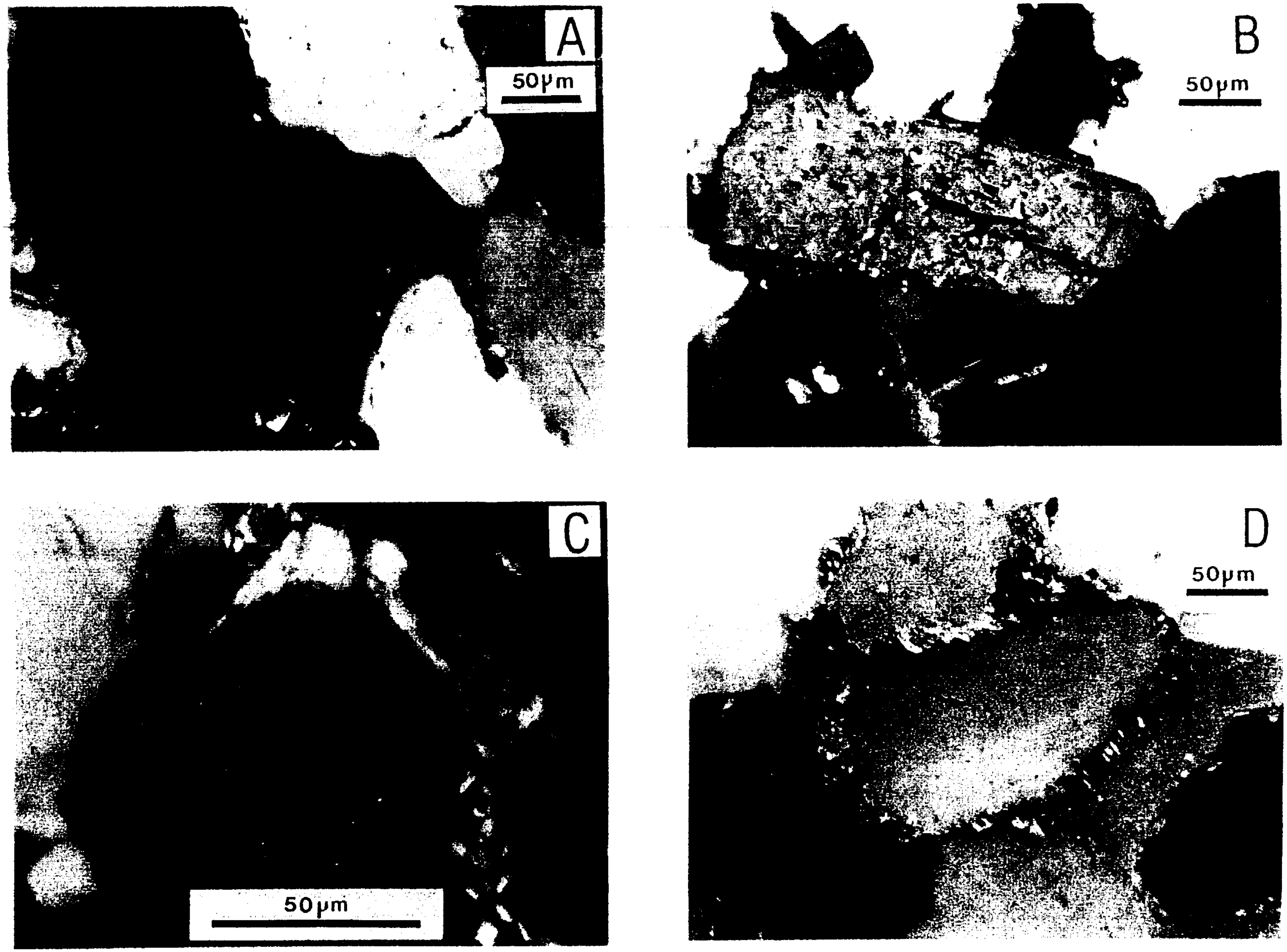

Pl. I

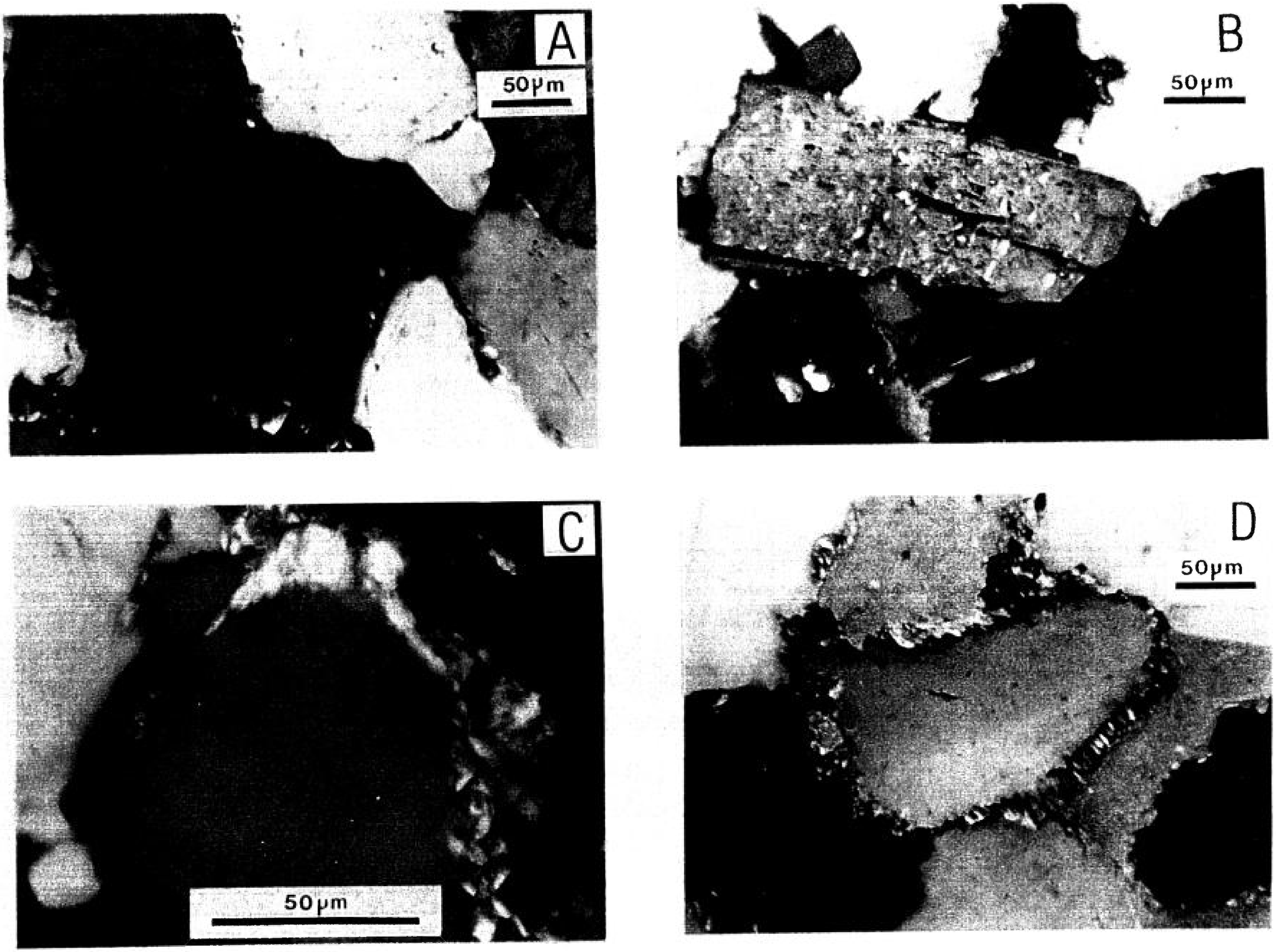

Pl. I

PLATE 2

A. Authigenic pyrite in a chlorite matrix and at the interface of quartz grains

B. Euhedral pyrite on the surface of altered quartz and feldspar grains underlying the contours of a primary pore. This pore is filled by authigenic chlorite.

C-D. Pore filled with authigenic chlorite. No pyrite is observed. Some porosity is left in the center of the chlorite fill.

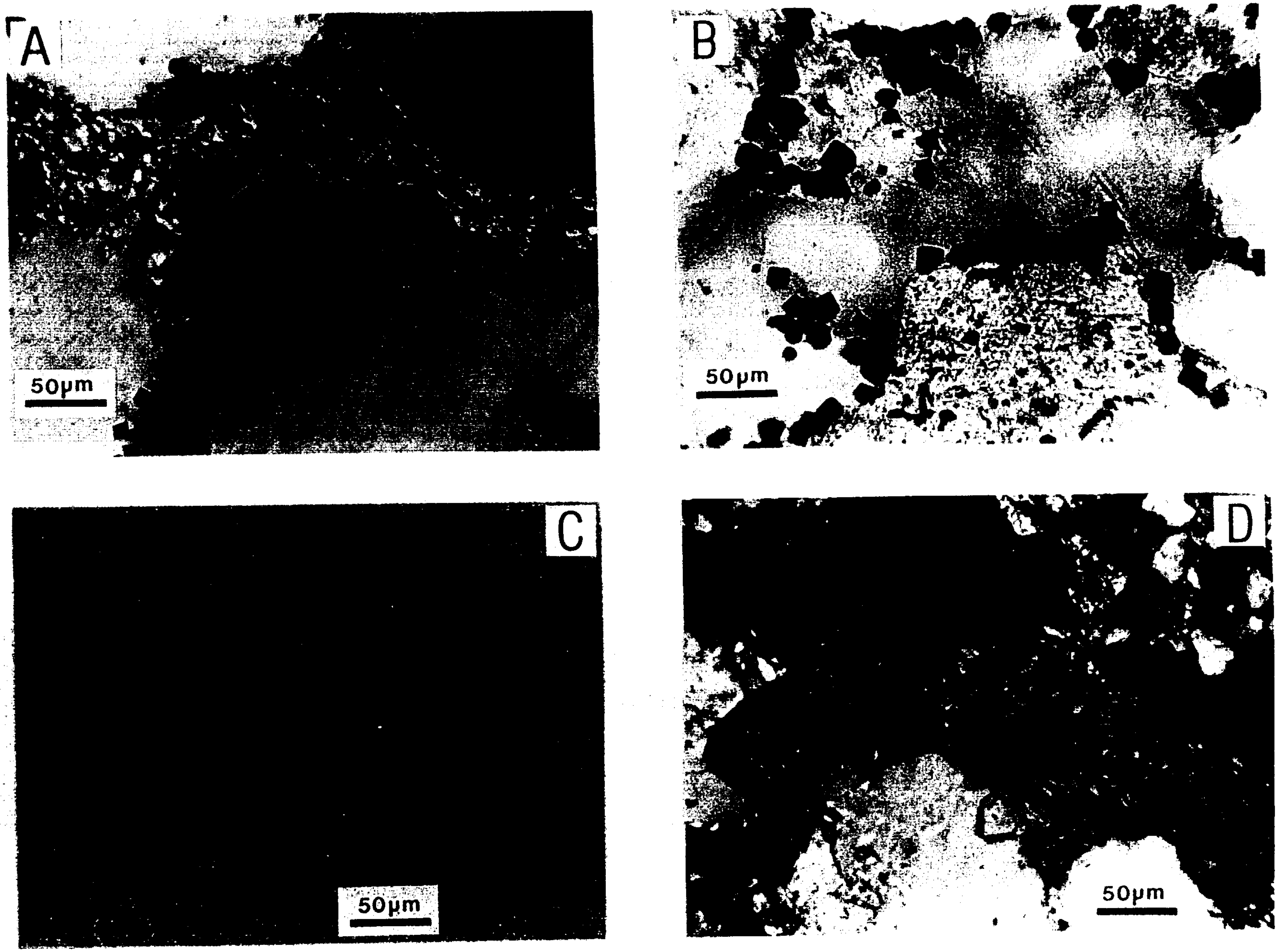

Pl.2

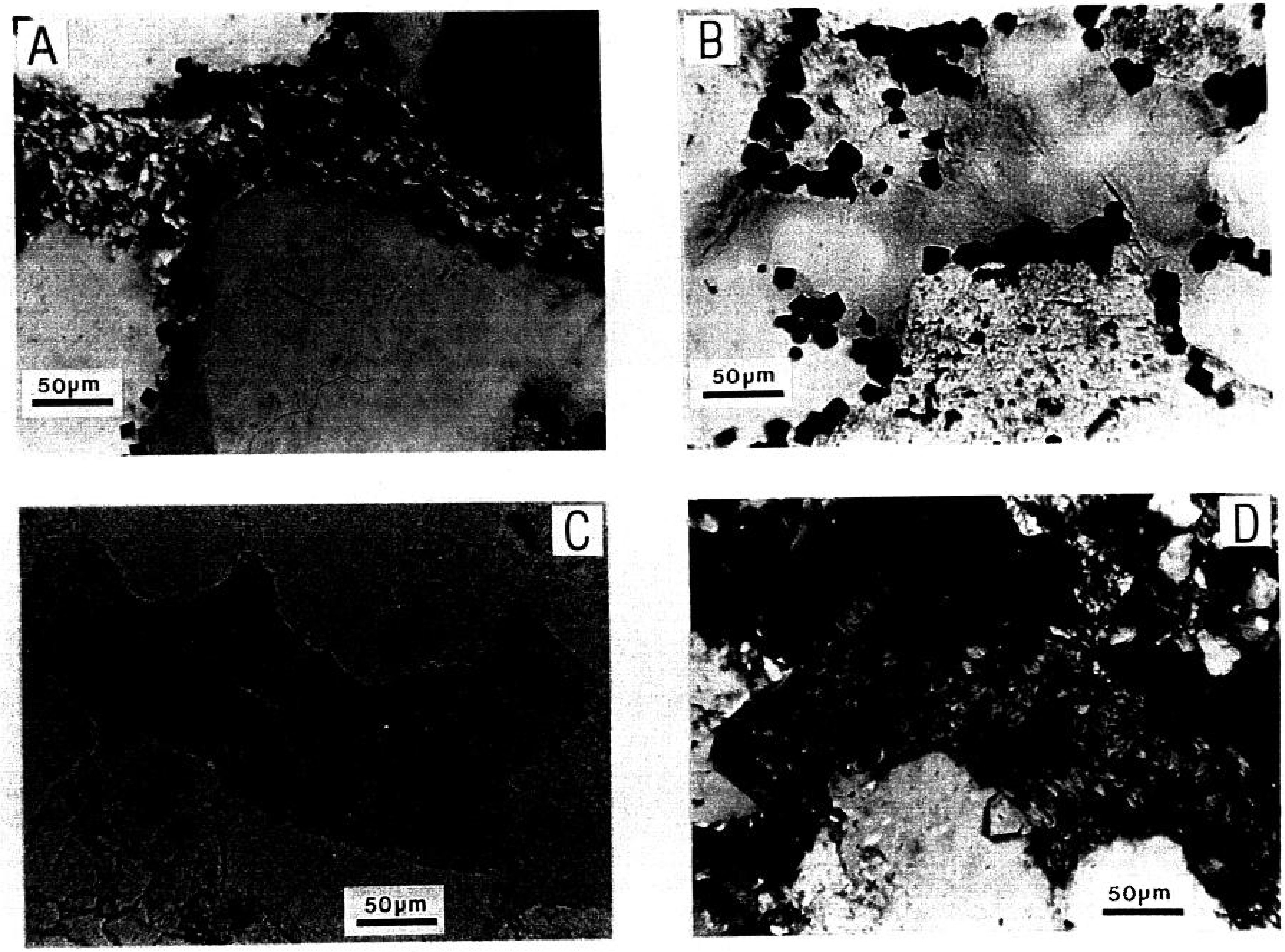

Pl. 2

CHAPTER 4

OIL SEEPS, SOURCE ROCK INVENTORY AND THERMAL MATURATION IN EASTERN GASPÉ PENINSULA

4 OIL SEEPS, SOURCE ROCK INVENTORY AND THERMAL MATURATION IN EASTERN GASPÉ PENINSULA

4.1 OBJECTIVE

The objective of this study is to present an inventory of all maturity, source rock and oil seep data from the Gaspé Peninsula and to locate oil seeps or shows that can still be sampled for geochemical analyses.

4.2 METHODS

The compilation is based on published literature, thesis and government reports. The later were submitted for the most part by the INRS-Pétrole and Géoressources in the last 20 years or so. Moreover, unpublished INRS files are added in this compilation.

Well data files published by the Ministère de l'Énergie et des Ressources of Quebec are used to locate wells and to gather various characteristics on oil and gas shows. Source rock and thermal maturation data are compiled on Excel spreadsheet and illustrated in tables. Data on wells are compiled on a MS-Word file and illustrated in a table. The most pertinent data are illustrated in XY diagrams, well logs, and maps.

4.3 REGIONAL GEOLOGY

The deep and shallow marine sequences of Gaspé Peninsula were involved in both Taconian and Acadian orogenies. The Taconian Belt is located on the northern segment of Gaspé Peninsula (Fig. 4.1) and is composed of highly deformed thrust slices of the Québec Supergroup. The Acadian belt (Fig. 4.1: Chaleurs Group.; Upper Gaspé Limestones and Gaspé Sandstones), is composed of slightly folded strata dissected by two major faults: the Bassin Nord-Ouest (North-West Arm) and Troisième Lac (Third Lake) faults which are used to divide the area into three sectors: the North Sector, which is located on the north side of the Bassin Nord-Ouest fault, the South Sector, located south of the Troisième Lac fault, and the Central Sector, located between the two faults.

The Gaspé succession includes Cambrian to Mississippian strata. The Cambrian - Ordovician Québec Supergroup (Fig. 4.1) consists of deep marine clastic rocks overlying shallow marine carbonates. The Post-Taconian successions consist of various mixed clastic and carbonate strata (Fig. 4.1: Chaleurs Group and Upper Gaspé Limestones), overlain by thick regressive and continental clastic sequences (Fig. 4.1: Gaspé Sandstones). Stratigraphic contacts between formations and groups in wells are from Amyot (1984).

4.4 SOURCE ROCKS

Total organic carbon content data are mostly from Bertrand (1987), INRS-Géoressources (1983), Lefèvre (1982), and INRS-Pétrole (1972, 1975). Data are compiled in Annex 1 and plotted in XY diagrams (Figs. 4.2 to 4.4) and logs (Figs. 4.5 to 4.10).

INRS-Géoressources (1983) and Bertrand (1987) both include Rock Eval and total organic carbon (TOC) data, mostly from well and outcrop samples, respectively. Owing to the lack of accuracy of the INRS (1983) data, related to problems solved in Bertrand (1987), both Rock Eval results are not illustrated on logs and only data coming from Bertrand (1987) are presented in Annex 1. The INRS-Pétrole (1975) report includes outcrop data form the Berry Mountain area, which is outside the Shell's Gaspé permit.

Our analysis of source rock potential of the study area is therefore mostly based on TOC and insoluble residue (IR) data. The diagram of Sourisse and Gauthier (1969) is used to define the oil potential of a source rock based on its TOC and IR content (Figs. 4.2 to 4.4). Combination of these two data produces a diagram divided in no potential, medium potential or good potential fields into which any given sample will plot. In order to determine the source rock potential of a study area, the data are plotted according to the three tectonic sectors described above. TOC values are also illustrated in log profiles (Figs. 4.5 to 4.10).

4.4.1 SOUTH SECTOR

In the South Sector (Fig. 4.2), the majority of data-points indicate that those rock have no potential for being HC source rock. Only three outcrop sandstones of the York River Formation and a shale from the Burnt Jam Brook Formation seem to have some good source potential. One of the sandstone is from the Fletcher Syncline (Fig. 4.1), located between the Mississippi and the Bald Mountain anticlines well within Shell's permit area. The other two are from the Big Berry Mountain Syncline, outside the permit area (Map 1b). The organic-rich shale of the Burnt Jam Brook Formation is from the York well (Fig. 4.5B), located at the top of the Saint-Jean Anticline (Fig. 4.1).

4.4.2 NORTH SECTOR

The North Sector is as organic-poor as the south one (Fig 4.4). The vast majority of data-points fall in the "No-potential" zone of the Sourisse and Gauthier (1969) diagram. Four data-points only spot in the "Good potential" zone of the diagram. Two of these are from outcrops in the Quebec Supergroup along the Renard River (Map 1a). Another one is from a 30 cm thick shale bed underlying West Point limestone in the same field section. The last favourable analysis is from a cutting sample of the Battery Point Formation in the Douglas well (Fig. 4.9B).

4.4.3 Central Sector

The Central Sector is significantly more favourable than the two previous sectors (Fig. 4.3). Between one third and half of the analysed samples plot in the medium and good potential fields of Sourisse and Gauthier (1969) diagram. From their TOC content, samples plotting in the "Medium potential" field can be considered as having a gas potential instead of an oil one. A significant number of Upper Gaspé Limestones samples (mostly from the Forillon Formation but also some from the Shiphead and Indian Cove formations), and others from the Chaleurs Group (Indian Point Formation) and the Gaspé Sandstones (York River Formation) share this characteristic. Samples with a good source rock potential are found in the Indian Point, Forillon and York River formations and, as in the North Sector, in the Quebec Supergroup. However, good source rock indications for the Indian Point, Forillon and York River formations are mostly from the Sunny Bank well (Fig. 4.6). Other TOC-rich samples come from an outcrop of the York River Formation, located near the tip of the Bald Mountain Anticline, and from Quebec Supergroup shales, found at the bottom of the Gaspé Sud well (Fig. 4.7).

4.5 THERMAL MATURATION

Thermal maturation data include reflectance on vitrinite, liptinite, inertinite, zooclasts (chitinozoans, scolecodonts and hydroids) and solid bitumen (Bertrand, 1987; Bertrand et al., 1992). Measurements of reflectance on inertinite, vitrinite, liptinite and solid bitumen are reported in INRS-Géoressources (1983). Reflectance measurements used in Sikander et Pittion (1978), and INRS-Pétrole (1972; 1974a, b, c; 1975) are reported to be done on vitrinite. Measurements made by Islam (1981) and Islam et al. (1982) were done on undifferentiated solid bitumen and some zooclasts. All data are compiled in Annex 2 and illustrated in logs (Figs. 4.5 to 4.10) and Maps 1A and B.

Islam (1981) and Islam et al. (1982) data come exclusively from outcrop samples in the Taconian Belt, outside the permit area. The precise location of these samples is poorly known. In addition to the previously mentioned INRS-Pétrole (1972, 1975) reports which contain both TOC and reflectance data from wells and outcrops respectively, more data from three others wells are reported by INRS-Pétrole (1974a, b, c) (Fig. 4.10A-B and Appendix 2).

As for the previously presented source rock section, results are discussed according to the three tectonic sectors of the area.

4.5.1 North Sector

The Taconian Belt offers reflectance values higher than those of Acadian Belt (Map 1A). In the Gaspé Sandstones, the reflectance seems to increase from the Tar Point well both easterly and westerly. Easterly, towards the Malbaie well (Fig. 4.1), this increase seems to be controlled by increasing burial (Figs. 4.9A, 4.10A). Lowest reflectance values in all units are observed in the Forillon area (Map 1A). In the Chaleurs Group, reflectance reaches a maximum in the Gaspé Nord well area, then it decreases towards the Blanchet well area. The entire Acadian sequence (Silurian to Devonian) in the eastern part of the North Sector (east of Blanchet well) belongs to the oil window, and the threshold of the condensate zone (Ro = 1.35%) is reach between Blanchet well and 25 km west it (Map 1A). Minimum Ro values in the Chaleurs Group are observed in the Douglas well (Fig 4.9B) and from outcrops nearby the Blanchet well; there the Roncelles and the West Point formations are still in the oil window (Ro < 1.0%). According to few data, the reflectance increases westerly from this point towards the Murdochville mine district (Map 1A).

Reflectance gradients with depth in wells located in this sector are very low (Figs. 4.9 and 4.10), in particular in the Gaspé Sandstones. The Gaspé Nord well is an exception because the reflectance increases very rapidly below the Forillon Formation to reach values of nearly 8% in the Quebec Supergroup (Fig. 4.8B). The presence of highly conductive metamorphic rocks or magmatism is the likely cause of this phenomena. Abnormal low reflectance value of solid bitumen in the Quebec Supergroup in the Douglas well is likely due to secondary hydrocarbon migration (Fig. 4.9B).

4.5.2 Central Sector

If the reflectance data from the Sunny Bank (Fig. 4.6) and Gaspé Sud wells (Fig. 4.7) are compared and plotted on a composite cross-section (Fig. 4.11), the central part of the York River Syncline is shown to be less mature than its border. The reflectance in the Central Sector follows the structural contours (Fig. 4.11). The abnormal zonation of reflectance in the Blanchet well results from thrust faulting (Fig. 4.8A). Stratigraphically, the Shiphead and overlying units are in the oil window (Ro < 1.35%); the Forillon and Indian Point formations are in the condensate zone

(1.35 < Ro < 2.0%), and the remaining part of the Chaleurs Group and underlying units are in the dry gas zone (Ro > 2%).

Reflectance gradients are variable in the Central Sector (Fig. 4.11). This gradient is very low in the Gaspé Sud well (Fig. 4.7), located near the Bassin Nord-Ouest fault, the gradient is intermediate in the Sunny Bank well (Fig. 4.6), and very high in the Blanchet well (Fig. 4.8BA), located above ultramafic rocks.

4.5.3 SOUTH SECTOR

Similarly to the Central Sector, the reflectance in the South Sector seems to follow the structural contours of the area although few data are available (Fig. 4.11 and Map 1A). Thermal maturation of stratigraphic units overlying the Shiphead Formation is similar to those in the Central Sector. Moreover, the thermal maturation of the Chaleurs Group in the York well (Fig. 4.5) , nearly in stratigraphic continuity with the Sunny Bank succession (Fig. 4.6), is slightly less matured than expected.

Significant variations occur when approaching the Murdochville mining district in a westerly direction from the Blanchet well area. The few data suggest a progressive increase of reflectance towards the mine; there the reflectance can reach values higher than 8% (Map 1A and Annex 2). These values are similar to those found at the base of Gaspé North well (Fig. 4.8B).

The reflectance gradient of the Québec Oil well is one of the highest of the Gaspé area (Fig. 4.5A), it could easily be compared with the gradient measured in the Blanchet well (Fig. 4.8A) and with the one characterizing the base of the Gaspé Nord well (Fig. 4.8B). Similar causes can be invoked to explain the high reflectance gradient of Québec Oil well, but evidence has yet to be found.

4.6 OIL SEEPS AND OIL SHOWS

Oil seeps and show locations, and oil analyses are from Sikander (1975), INRS-Pétrole (1972), McGerrigle (1950). Conventional analyses of oil samples were compiled from McGerrigle (1950) and Sikander (1974, 1975) (Tab. 1). Geochemical analyses (i.e. chromatography of extract and crude oil, GC-mass spectrometry of saturates) are from INRS-Pétrole (1972) and Sikander (1975). Geographic and stratigraphic locations of oil seeps and oil and gas producing wells are compiled from McGerrigle (1950), Roliff (1952), Sikander (1975), MRN (1974), and Laliberté (personal communication). The data are compiled in Table 1, Annex 3 and illustrated in Map 3.

Well number	Sample (4)	Formation	Colour	Gravity		Sulphur	Viscosity	Pour Point °F.	B.T.U.	Residuum	Petroleum base
				Sp. Gr.	*A.P.I.	% by wt.	Saybolt U. 100°F		per lb.	% by wt.	
*	I.O.C. seep	York River	Br.-black	0.937	19.6	0.29	1,705 sec.	0	19,094	56.62	Intermediate
FC006	C.P.C. 3	Y. R. / I. Cove.	Br.-black	0.863	32.4	0.09	55 sec.	below 25	19,570	24.31	Intermediate
FC012	P.O.T. 9		Grn.-black	0.861	32.8	0.11	53	below 0	19,620	22.8	Intermediate
FC021	C.P.L. 1st after acid	Indian Cove	Amber	0.803	44.8	0.05	36 sec.	20		26.9	
FC022	C.P.L. 2 1,925 ft.	York River	Amber.	0.796	46.3	0.04	35 sec.	30		11.3	
FC022	C.P.L. 2 2,046 ft.	York River	Amber	0.816	41.9	0.05	39 sec.	45		14.9	
FC022	C.P.L. 2 2,338 ft.	York River	Amber	0.791	47.4	0.05	34 sec.	10		9.4	
FC027	Conant	York River	Br.-black	0.843	36.4	0.09	52 sec.	below 25		26.9	
FC027	Conant	York River	Br.-green	0.875	30.2	0.15	145	below 0	19,720	39.0	Intermediate
FC039	P.O.T. 5	York River	Dark	0.855		0.22	53 sec.		18,700		
FC041	P.O.T. 7	York River	Br.-black	0.853	34.3	0.07	47 sec.	15	19,588	20.78	Intermediate
FC045	P.O.T. 11	Indian Cove	Br.-black	0.863	32.5	0.08	32 sec.		19.490		
FC049	P.O.T. 15	Y. R. / I. Cove.	Br.-black	0.840	36.9	0.09	40 sec.	below 25	19.625	17.37	Intermediate
FC054	P.O.T. 20	Y. R. / I. Cove.	Amber.	0.800	45.5	0.06	36 sec.	30	19,852	12.04	Paraffin
FC054	P.O.T. 20	York River	Light red	0.800	45.4	0.07	35	30	19,550	12.0	Paraffin
FC054	P.O.T. 20	York River	Claret-red	0.811	43.0	0.13	38	45	19,500	14.0	Paraffin
FC065	P.O.T. 31	York River	Amber.	0.803	45.9	0.05	36 sec.	35	19,879	13.06	Paraffin
FC066	P.O.T. 32	Y. R. / I. Cove.	Light red.	0.798	45.9	0.05	35 sec.	25	19,863	12.02	Paraffin
FC068	P.O.T. 34	York River	Claret-red	0.793	46.9	0.09	35	30		12.4	Paraffin
FC076	P.O.T. 42		Br.-black	0.890	27.4	0.22	119 sec.	below 25	19,363	33.28	Intermediate

Table 1: Conventional analyses of Gaspé oils.

Sources:
Energy Branch, Department of Natural Ressources, Governement of Quebec Files; McGerrigle (1950); Parks (1929); Roseware et al. (1936); Sikander (1975).
P.O.T. - Petroleum Oil Trust; C.P.C. - Canada Petroleum Co.; Conant = Gaspé Oil co.; C.P.L. = Continental Petroleums Ltd.; I.O.C. = International Oil Co.
Well number in heavy caracters indicates that a oil sample was collected.

Identification No INRS	Depth Upper limit	Lower	Meter (m) feet (ft)		SECTION OR WELL NAME	UTM Zone	UTM COORDINATES		Formation
							UTM East	UTM North	
28700	6256,0	6256,5	ft		Sunny Bank	20	376931	5412722	Forillon
28701	6265,0	6265,5	ft		Sunny Bank	20	376931	5412722	Forillon
28702	6275,0	6275,5	ft		Sunny Bank	20	376931	5412722	Forillon
28703	6280,0	6280,5	ft		Sunny Bank	20	376931	5412722	Forillon
28704	6337,9	6338,2	ft		Sunny Bank	20	376931	5412722	Forillon
28705	6340,0	6340,8	ft		Sunny Bank	20	376931	5412722	Forillon
28706	6459,3	6459,5	ft		Sunny Bank	20	376931	5412722	Forillon
28707	6462,1	6462,3	ft		Sunny Bank	20	376931	5412722	Forillon
28708	6546,8	6547,2	ft		Sunny Bank	20	376931	5412722	Forillon
28709	6549,0	6549,0	ft		Sunny Bank	20	376931	5412722	Forillon
28710	6559,0	6559,0	ft		Sunny Bank	20	376931	5412722	Forillon
28711	6564,0	6564,0	ft		Sunny Bank	20	376931	5412722	Forillon
28712	6590,2	6590,7	ft		Sunny Bank	20	376931	5412722	Forillon
28713	6618,5	6618,0	ft		Sunny Bank	20	376931	5412722	Forillon
28714	6621,5	6621,8	ft		Sunny Bank	20	376931	5412722	Forillon
28715	6686,3	6686,8	ft		Sunny Bank	20	376931	5412722	Forillon
28716	6692,0	6692,5	ft		Sunny Bank	20	376931	5412722	Forillon
28717	6699,5	6700,0	ft		Sunny Bank	20	376931	5412722	Forillon
28718	6701,0	6701,5	ft		Sunny Bank	20	376931	5412722	Forillon
28719	6706,8	6707,3	ft		Sunny Bank	20	376931	5412722	Forillon
28720	6726,5	6726,8	ft		Sunny Bank	20	376931	5412722	Forillon
28721	6739,5	6739,8	ft		Sunny Bank	20	376931	5412722	Forillon
28722	6744,5	6745,0	ft		Sunny Bank	20	376931	5412722	Forillon
28723	6754,5	6754,8	ft		Sunny Bank	20	376931	5412722	Forillon
28724	6952,0	6952,5	ft		Sunny Bank	20	376931	5412722	Forillon
28725	6958,1	6958,5	ft		Sunny Bank	20	376931	5412722	Forillon
28726	7246,5	7247,0	ft		Sunny Bank	20	376931	5412722	Forillon
28727	7250,5	7251,0	ft		Sunny Bank	20	376931	5412722	Forillon

4.6.1 OIL SEEPS

The 80 seeps in Gaspé Peninsula reported by Park (1929) are grouped into seven main occurrences (McGerrigle 1950, Sikander 1974, 1975). They are mostly concentrated in the Indian Cove and York River formations near faulted contacts and/or in tightly folded successions. Oil occurrences in the Battery Point Formation and dike of diabase in the Tar Point anticline are exceptions. According to Sikander (1975), the oil colors from seeps varies from amber and green to black.

4.6.2 OIL SHOWS

Oil shows were found in many old wells in Gaspé Peninsula. Conventional analyses were performed on many of these oils (McGerrigle 1950), but chromatographic and mass spectrometry analysis of crude oil has been done on one sample only (Sikander 1975) (Annex 3: Baillargeon No 1, 1959FC001). Other geochemical analyses, including 8 GC on saturates and 2 GC-mass spectrometry were made on source rock extracts from the Sunny Bank well only (INRS-Pétrole 1972: 853, 1151, 1703, 1711, 2331 and 2900 m; Sikander 1975: 915 and 2008 m).

Table 1, modified from McGerrigle (1950), shows that a seep near the Troisième Lac fault contains heavy oil (API = 19.6). Conversely, the well shows are typified by lighter oil, having API ranging between 27 - 39 (black oil) to 43 - 47 (amber to red oil) (Table 1).

As reported by Sikander (1975), there is no relationship between the oil type and the lithology of occurrences. Secondary migration along faults, which are usually present close to these wells, is likely responsible for this lack of relationship.

The oil test production values are reported in Annex 3 and plotted on Map 2. Higher values are mostly concentrated along an east-west corridor in the York River Syncline and Galt Anticline, the former including both the Baillargeon and Sunny Bank wells. Highest values of oil test production, ranging from 2500 to 50000 gallons, are restricted to the western part of this corridor. This area is located on both sides of the Troisième Lac fault (Map 2).

Despite obvious differences in the global composition, the oil being richer in alkanes than the extracts, geochemical analyses of source rock extracts from Sunny Bank well and the geochemical analysis of oils from the Baillargeon well indicate a similitude in composition. Oil in the York River formation from the Baillargeon well resembles the Indian Cove extract of the Sunny Bank well, and both extracts from the Indian Cove and Forillon formations of the Sunny Bank wells show similarities. However, no positive correlation can be made between source rock extracts and York River formation oil. According to geochemical data and estimated maturation of both oil and source rocks, Sikander (1975) suggested that the oil in the York River Formation originated from the deeper marine and more mature kerogen of the underlying Indian Cove and Forillon formations.

Correlations between the composition of source rock extracts reported by INRS-Pétrole (1972) and Sikander (1975) are uneasy. At a similar depth, the amount of saturates is significantly lower in the older study. However, as in Sikander (1975), chromatographic analyses of the Indian Cove to Indian Point formations of the Sunny Bank well suggest that the organic matter is essentially of marine origin, the maturity increases significantly from the top of the Indian Cove to the middle of the Indian Point Formation and hydrocarbons migrated upwards.

4.7 SOURCE ROCKS, OIL SEEPS AND OIL SHOWS SAMPLING

In order to prepare further investigations on the origin of oil occurring in Gaspé Peninsula, source rocks and oil shows and seeps have been sampled.

Examination of well logs of the Sunny Bank, Gaspé Sud, Galt and Gaspé Nord (Amyot, 1984), suggest that the upper part of the Forillon Formation could be a source rock. In order to verify this hypothesis, also suggested by figures 4.3 and 4.6, some intervals of the Forillon Formation from the Sunny Bank and the Gaspé Nord wells were sampled. These two wells span the entire known range of thermal maturation for this formation. The list of intervals sampled is presented in Table 2.

The only seep sampled belongs to the first group of occurrences of Sikander (1975) (Plate 4.2.4). It is located in the York River Formation, near its contact with the Indian Cove Formation, along the Troisième Lac fault, south of the Mississippi Anticline. The sample collected is a black, heavy tar oil, which fills a small 1.5X4 m wide pond.

The oils from 8 wells have been sampled (Plates 4.1 and 4.2). From these, only one oil listed in McGerrigle (1950) was sampled (Table 1: FC054 - POT 20; Plate 4.1.4). The other oil samples (Table 3; Plates 4.1.1 to 4.1.3 and 4.2.1 to 4.2.3) have not been previously studied by McGerrigle (1950) or any other known authors for that matter. The oils sampled from old wells are shown by heavy contours in Annex 3. This Annex 3 summarises all known data from Gaspé Peninsula wells. Sampled oils are found in all representative areas along the York Syncline. These oils show all the color range described in McGerrigle (1950) and Sikander (1975).

Nearby rock were also sampled in order to determine if the oils have a local origin or were derived from migration.

Identification No INRS	Depth Upper limit	Lower	Meter (m) feet (ft)		SECTION OR WELL NAME	UTM Zone	UTM COORDINATES		Formation
							UTM East	UTM North	
28728	1250	1250	m		Gaspé Nord	20	388787	5416881	Forillon
28729	1255	1255	m		Gaspé Nord	20	388787	5416881	Forillon
28730	1260	1260	m		Gaspé Nord	20	388787	5416881	Forillon
28731	1265	1265	m		Gaspé Nord	20	388787	5416881	Forillon
28732	1270	1270	m		Gaspé Nord	20	388787	5416881	Forillon
28733	1275	1275	m		Gaspé Nord	20	388787	5416881	Forillon
28734	1280	1280	m		Gaspé Nord	20	388787	5416881	Forillon
28735	1285	1285	m		Gaspé Nord	20	388787	5416881	Forillon
28736	1290	1290	m		Gaspé Nord	20	388787	5416881	Forillon
28737	1295	1295	m		Gaspé Nord	20	388787	5416881	Forillon
28738	1300	1300	m		Gaspé Nord	20	388787	5416881	Forillon
28739	1305	1305	m		Gaspé Nord	20	388787	5416881	Forillon
28740	1310	1310	m		Gaspé Nord	20	388787	5416881	Forillon
28741	1315	1315	m		Gaspé Nord	20	388787	5416881	Forillon
28742	1320	1320	m		Gaspé Nord	20	388787	5416881	Forillon
28743	1325	1325	m		Gaspé Nord	20	388787	5416881	Forillon
28744	1330	1330	m		Gaspé Nord	20	388787	5416881	Forillon
28745	1335	1335	m		Gaspé Nord	20	388787	5416881	Forillon
28746	1340	1340	m		Gaspé Nord	20	388787	5416881	Forillon
28747	1345	1345	m		Gaspé Nord	20	388787	5416881	Forillon
28748	1350	1350	m		Gaspé Nord	20	388787	5416881	Forillon
28749	1355	1355	m		Gaspé Nord	20	388787	5416881	Forillon
28750	1365	1365	m		Gaspé Nord	20	388787	5416881	Forillon

Table 2: List of depths sampled for source rock analyses in Sunny Bank and Gaspé Nord wells.

WELL NAME (1)	WELL NUMBER	LATITUDE DMS north	LONGITUDE DMS west	CONDITION McGerrigle (1950) **ACTUAL CONDITION**	UPPER GASPE LMS & LOWER(2)	INDIAN COVE - Y. RIVER LIMIT (2)	YORK RIVER (2)	BATTERY POINT (2)	TOTAL DEPTH meter
P.O.T. No 2	1890FC036	48 48 59,00	64 26 28,80	Square wooden conductor; casing. Fresh water from around casing. Green oil to 1 m. Where hole blocked. Bubbles of gas. **Suspended - oil and gas seepage**			787	152 294	787
P.O.T. No 4	1890FC038	48 44 08,30	64 19 52,40	Wooden conductor. Casing; plugged 8 cm water with dark scum or oil. **Suspended - oil and water seepage**			675		905
P.O.T. No 16	1894FC050	48 50 22,30	64 43 25,90	Wooden conductor. Water with bubbles, gas and light bluish oil. Yellow scum around well. **Unknown- oil seepage**		866	812		892
P.O.T. No 20	1896FC054	48 50 08,50	64 52 10,30	Stand-pipe 61 cm above ground; blocked 3 m from top. Occasional overflow oil; ground soaked. **Suspended/ - oil seepage**			627		662
Pétro Gaspé, Galt No. 3	1984FC109	48 50 21,40	64 47 16,70	**Suspended/ oil**			Oil: 69 - 71 m		85
Gaspésie, Galt No. 1	1985FC113	48 50 21,90	64 47 38,20	**Suspended - presurized gas , oil and water in well**		Oil: 101 m			100
Pétro Gaspé, Galt No. 5	1987FC115	48 50 27,00	64 47 58,00	**Suspended/ gas and oil indice.**	Oil and gas: 281 m				701
Suint. - 1		48 50 18,00	64 47 05,00	**Tar pond, 1.5/5 m wide. 150 m from P. G. Galt No 3**					0

Table 3. List of oil seepage and oils shows sampled for geochemical analyses an source rock correlations..

Compiled from McGerrigle (1950), MRN (1974) and upgrade to 1988, J.-Y. Laliberté (personnel communication) from MRN Quebec files.

4.8 DISCUSSION AND CONCLUSIONS

The compiled data suggest that significant amount of potential source rocks are mostly restricted to the area between the Bassin Nord-Ouest and Troisième Lac faults designated as the Central Sector. However, the paucity of data and the stratigraphic bias of sampling in the South Sector (south of the Troisième Lac fault), do not allow to reject the possible presence of major source rocks in the South Sector.

Excluding the York well, reflectance results from various studies are quite similar. For a given stratigraphic interval, maturation increases southerly but exceptions, related to the tectonic setting, are ubiquitous (Blanchet, Gaspé Sud and York wells). In the North Sector, all stratigraphic units are still in the oil window. However, only the Shiphead Formation and overlying units, are suitable for oil preservation in the South and Central sectors. Nevertheless, the actual thermal maturity data for the area indicate that the entire Silurian - Devonian succession in eastern Gaspé is still prospective for gas.

A small area in the North Sector seems to be overcooked due either to abnormal thermal events or to tectonic setting. Moreover, the easternmost part of this sector is less suitable for oil preservation because of the great thickness of Gaspé Sandstones

The Ordovician successions, outcropping in the Taconian Belt of the North Sector and penetrated by drill holes in the North and Central Sectors, seem always to be overmatured (dry gas zone). However, due to secondary syn- or post maximal burial migrations, these successions locally contain solid bitumen with thermal maturation between the threshold of the oil window and the condensate zone (Douglas and Gaspé Sud wells). These solid bitumens were probably derived from the alteration of oil pools migrated most likely from Silurian or Devonian source rocks.

Wells have produced a significant amount of oil, and seeps are abundant in the area. The P.O.T. 20 (1896FC 054), P.O.T. 27 (1896FC 061), and Soquip et al. Galt No 1 (1981FC100) have produced approximately 70, 1440 and 290 barrels of oil during tests, respectively. These well are grouped in an area located on both sides of the Troisième Lac fault where it cross-cuts the York River Syncline and Galt Anticline. Numerous seeps are observed in the same area. Based from these data and observations, a tentative correlation can be proposed between the organic-matter rich - low maturity Central Sector, abundance of seeps and significant values of oil production during well tests.

According to their subsurface reservoir rock and outcropping lithologies at well sites, no obvious relationship explains the color and the visual physical properties of the sampled oil shows.

However, a relationship seems to exist between the color of the oil and the tectonic settling around oil shows. In the area of oil seeps, the Troisième Lac fault is divided into two branches, which dissect the York River Syncline. On one hand, oils sampled far from the fault zone, on both north-east and south-west sides of it, show light yellow to red colored oils (POT No 16 and 18 wells, and previously sampled Soquip et al. Galt No 1). On the other hand, oil coming from wells located between those branches are as black as the tar sampled in a seepage. Many similar seepages are reported in this faulted area. This relationship suggests the hypothesis that an oil field, located beneath the area of seepages, spills its oil into the overlying strata. This originally mature and light yellow to red oil should be altered to black oil by biodegradation, due to meteoric water circulating along fractures in the fault zone.

The last sampled shows (POT No 2) is a blackish oil, presumably of moderate high API. It can be distinguished from the previous black oils by its greater transparency and green iridescence under daylight. This oil is found at the top of the Gaspé Sandstone succession, isolated from Cambro-Ordovician strata by a thin nonconformable Chaleurs Group succession. The pores of those Cambro-Ordovician strata are saturated by marginally mature solid bitumen (Douglas well). Being located in the eastern part of York River Syncline, our hypothesis about the origin of the light yellow to red oils, coming from the western part of the same syncline, could be further extended to propose that oil shows in Devonian rocks could be derived from the Cambro-Ordovician organic-rich rocks. Nevertheless, only oil to oil geochemical comparisons could confirm or infirm this hypothesis. The yellowish colors of POT 16 and 20 oils should be explained by the deasphalting of a POT No 2 oil type, percolating through a thick fractured Upper Gaspé Limestones succession as it is observed in the Troisième Lac fault area.

4.9 RECOMMENDATIONS

In order to improve our knowledge of the most favourable areas to find oil or gas in eastern Gaspé, which is in our opinion, only half covered by the previous maturation studies and nearly unknown from a source rock point of view (amount and nature of kerogen), some recommendations are made.

We suggest thermal maturation (reflectance) and source rock analyses (Rock Eval and petrography) of cutting samples taken in wells and outcrops located near seeps, mainly on the west side of the Troisième Lac fault (Shampou to the Grande Rivière synclines). Biomarkers analyses (GC-MS and/or GC-IRMS) of oil seeps, oils from old wells, and hydrocarbon extracts from rocks are also suggested. Improvements can be made in other areas in the Central and North sectors but our knowledge of the South Sector has to be improved significantly.

Burial basin modelling, hydrocarbon generation histories and migration pathways have to be determined in order to locate the most favourable areas for oil or gas pools. These types of studies have been initiated by a few previous workers. Preliminary results strongly suggest that this type of analysis is a major key for exploration. This type of analysis will permit to determine if a formation have the potential for oil or gas, the timing of generation and the timing of hydrocarbon migration, according to the stratigraphic position of the source rock.

REFERENCES

Amyot, G., 1984. Lithostratigraphie de sous-surface de l'est de la Gaspésie. Ministère de l'Énergie et des Ressources du Québec, **ET 83-11**, 75 p., 1 annex out of text.

Bertrand, R., 1987. Maturation thermique et potentiel pétroligène des séries post-taconiennes du nord-est de la Gaspésie et de l'île d'Anticosti. Ph.D. thesis, Neuchâtel University, Switzerland, 647 p.

Bertrand, R., Héroux, H., and Goodarzi, F., 1992a. Regional maturity and hydrocarbon potential in Paleozoic rocks of the northeastern Gaspé Peninsula. GAC/MAC Annual Meeting, Acadian University, Wolfville, Nova Scotia, Program with Abstracts, **17**, A8.

Bertrand, R., Lavoie, D., and Goodarzi, F., 1992b. Évolution de la maturation thermique dans les Calcaires Supérieurs de Gaspé entre la péninsule de Forillon et Murdochville, Québec. Geological Survey of Canada, Current Research Forum, Ottawa Congress Center, Program with Abstracts, p. 9.

Espitalié, J., Laporte, J.-L., Madec, M., Marquis, F., Leplat, P., Poulet, J. et Boutefeu, A., 1977. Méthode rapide de caractéristique des roches mères, de leur potentiel pétrolier et de leur degré d'évolution. Revue de l'Institut français du Pétrole, **32**, 23-42.

Espitalié, J., Madec, M., and Tissot, B., 1980. Role of mineral matrix in kerogen pyrolysis: Influence on petroleum generation and migration. American Association of Petroleum Geologists Bulletin, **64**, 59-66.

INRS-Géoressources, 1983. Évolution thermique de l'extrémité orientale de la péninsule de Gaspé en relation avec les déformations tectoniques. Ministère de l'Énergie et des Ressources du Québec, **DP 83-03**, 96 p.

INRS-Pétrole, 1972. Étude géochimique de la série siluro-dévonienne des sondages Gulf Sunny-Bank et Imperial Lowlands Associated York #1, péninsule de Gaspé. Ministère de l'Énergie et des Ressources du Québec, **GM-27748**.

INRS-Pétrole, 1974a. Québec Oil No 2 (M.R.N. 78). Log lithostratigraphique, diagenèse organique et minérale. Rapport Soquip.

INRS-Pétrole 1974b. Haldimand No 1 (M.R.N. 16). Log lithostratigraphique, diagenèse organique et minérale. Rapport Soquip.

INRS-Pétrole 1974c. Tar Point No 1 (M.R.N. 79). Log lithostratigraphique, diagenèse organique et minérale. Rapport Soquip.

INRS-Pétrole, 1975. Analyse minéralogique, géochimique, palynologique et réflectométrique de la série des "Grès de Gaspé", Gaspésie centrale, Québec. Ministère de l'Énergie et des Ressources du Québec, **DP-0319**, 82 p., 12 photographic plates, 13 plates out of text.

Islam, S., 1981. Thermal maturation patterns in Cambro-Ordovician flysch sediments of the Taconic Belt, Gaspé Peninsula. Ph.D. thesis, McGill University, 191 p.

Islam, S., Hesse, R., and Chagnon, A., 1982. Zonation of diagenesis and low-grade metamorphism in Cambro-Ordovician flysch of Gaspé Peninsula Québec Appalachians. Canadian Mineralogist, **20**, 155-167.

Lefèvre, Y., 1982. Le carbone organique dans les séquences sédimentaires du Llandovérien de la Gaspésie et du nord-est du Nouveau-Brunswick. M.Sc. thesis, Laval University, 34 p.

McGerrigle, H.W., 1950. La géologie de l'Est de Gaspé. Ministère des Mines du Québec, **RG-35**, 174 p.

Ministère des Richesses Naturelles, 1974. Data on wells drilled for petroleum and gas in the Gaspé and Gulf of St. Lawrence area (Anticosti and Magdalen Islands). Ministère des Richesses naturelles du Québec, wells FC001 to FC091, Addendum 1988: wells FC92 to 117.

Park, W.A., 1929. Report on the oil and gas resources of the Province of Québec. Québec Bureau of Mines, Annual Report, Pt B, 7-56.

Roliff, W.A., 1952. Oil occurrences of East Central Gaspé. Transactions of Royal Society of Canada, **46**, Serie 3, 53-67.

Rosewarne, P.V., Chantler, H.McD., and Swinnerton, A.A., 1936. Analysis of Canadian crude oil, naphtas, shale oil, and bitumen. Mines Branch, Department of Mines, Ottawa, Pub. No. 765.

Sikander, A.H., 1974. Occurrence of oil in the Devonian rocks of eastern Gaspé, Québec. Ministère des Richesses naturelles du Québec, **DP-295**, 24 p.

Sikander, A.H., 1975. Occurrence of oil in the Devonian rocks of eastern Gaspé, Québec. Bulletin of Canadian Petroleum Geology, **23**, 278-294.

Sikander, A.H., 1976. Lithological observation on Grande Grève, York River and Battery Point Formations, and hydrocarbon possibilities in Eastern Gaspé, Québec. Direction générale de l'Énergie, Ministère des Richesses naturelles du Québec, **GM-33690**, 59 p., 16 figs out of text.

Sikander, A.H., and Pittion, J.-L., 1978. Reflectance studies on organic matter in Lower Paleozoic sediments of Québec. Bulletin of Canadian Petroleum Geology, **26**, 132-151.

Sourisse, C., and Gauthier, J., 1969. Contribution à la géochimie du carbone organique des roches sédimentaires. Centre de Recherche de Pau - Société nationale des Pétroles d'Aquitaine (SNPA), Unpublished report.

Plate 4.1

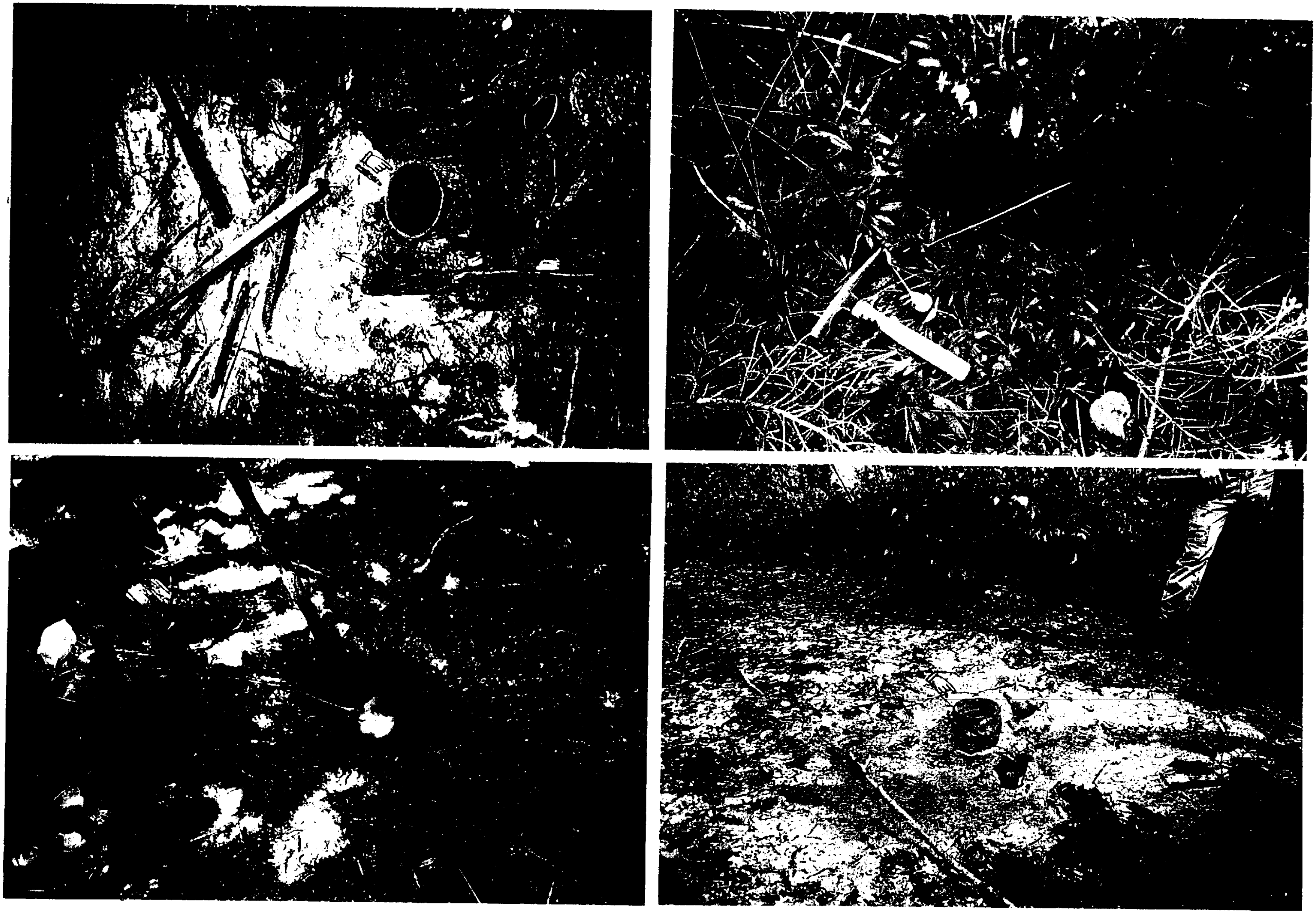

Plate 4.1

Annex 4.1: Source rock data; Rock Eval and total organic carbon (TOC) analyses

IR% = insoluble residue in %

Tmax = temperature of maximum pyrolysis (Espitalié et al. 1977)

PI = production index (S1/(S1+S2) of Espitalié et al. 1977)

GP = genetic potential (total of S1 and S2 of Espitalié et al. 1977)

IH = hydrogen index (S2/TOC)

IO = oxygen index (S3/TOC)

CHI = correct HI for matrix effect (Espitalié et al. 1980)

18 pages

Plate 4.2

Plate 4.2

INRS	Outcrop location		Strati. location m	Formation	IR %	TOC %	Tmax °C	PI	GP mg/g	HI mg/g	CHI mg/g	OI mg/g
	UTM east	UTM north										
13262	401133	5405320		Battery Pt	88,93	0,37	555	0,15	0,45	91	151	20
13279	394700	5413040		Battery Pt	84,47	0,03	555	0,41	0,24	459	592	35
13261	405143	5408370		Battery Pt	88,6	0,04		0,47	0,2	298	350	78
13102	389300	5411603		Battery Pt	91,13	0,06	438	0,36	0,34	299	348	29
13108	389200	5410500		Battery Pt	91,98	0,41	435	0,24	4,19	702	702	28
13117	380750	5418850		Battery Pt	90,22	0,04		0,53	0,2	238	359	28
13123	381770	5420750		Battery Pt	89,87	0,11	522	0,57	0,21	75	84	6
13153	398750	5405300		Battery Pt	87,45	0,03		0,69	0,18	136	140	28
13155	398750	5405300		Battery Pt	88,28	0,04		0,53	0,25	294	309	11
13160	402730	5397000		Battery Pt	62,57	0,02		0,41	0,18	406	465	13
13280	391470	5410200		Battery Pt	83,46	0,18	522	0,2	0,48	181	250	3
13281	391625	5410226		Battery Pt	83,11	0,06	555	0,35	0,4	396	479	22
13294	394600	5389350		Battery Pt	89,84	0,04	555	0,39	0,33	435	489	33
13296	395750	5388850		Battery Pt	94,13	0,04	522	0,46	0,27	380	435	41
13297	397550	5388300		Battery Pt	87,63	0,04	522	0,41	0,36	394	445	34
13302	398650	5390350		Battery Pt	86,26	0,18	455	0,33	0,36	111	127	84
13305	399700	5387200		Battery Pt	53,06	0,02		0,72	0,1	71	86	20
13306	400550	5397000		Battery Pt	92,7	0,04	555	0,52	0,21	265	272	35
13308	400420	5397000		Battery Pt	83,31	0,09	547	0,43	0,28	142	182	62
13309	398600	5397250		Battery Pt	77,92	0,02	505	0,61	0,23	349	377	12
13105	389150	5409770		York River	89,91	0,11	442	0,48	0,48	214	214	39
13111	381500	5416250		York River	88,25	0,19	457	0,27	0,49	160	169	3
13114	380000	5415100		York River	84,91	0,07	497	0,36	0,31	257	297	26
13119	380000	5418950		York River	87,7	0,32	438	0,31	2,29	422	422	19
13120	380000	5418950		York River	90,75	0,32	447	0,39	2,43	418	418	14
13151	389500	5418650		York River	89,17	0,49	447	0,11	0,55	89	128	8
13161	389972	5407784		York River	89,74	0,06	438	0,54	0,17	112	121	31
13163	389972	5407784		York River	89,79	0,08	438	0,51	0,31	172	173	47
13167	367050	5413650		York River	88,78	0,12	447	0,36	0,54	271	284	13
13173	375800	5410430		York River	86,02	0,25	447	0,24	0,48	124	144	53
13175	374365	5412610		York River	89,59	0,15	447	0,14	0,61	304	315	46
13176	366959	5410823		York River	83,42	0,04		0,36	0,32	374	407	11
13188	371323	5409079		York River	88,48	0,06	442	0,35	0,34	317	330	11
13189	370371	5411073		York River	88,59	0,06	505	0,37	0,28	266	298	5
13199	365488	5421103		York River	89,11	0,19	447	0,15	0,73	289	289	48
13213	365125	5424970		York River	96,77	4,88	447	0,02	32,58	630	630	19
13215	364674	5424607		York River	91,88	0,61	447	0,06	1,99	283	283	38
13218	370673	5418357		York River	86,03	0,74	440	0,09	2,35	250	250	59
13219	358216	5422248		York River	87,17	0,04	538	0,4	0,39	465	510	24
13221	358232	5421877		York River	87,03	0,10	547	0,42	0,33	172	201	23
13228	361865	5420023		York River	91,14	0,98	442	0,05	5,39	479	621	17
13229	359772	5419812		York River	87,82	0,19	522	0,31	0,43	136	170	28
13245	379596	5403440		York River	86,79	0,05	530	0,36	0,25	285	300	5
13251	383905	5403426		York River	83,56	0,28	447	0,19	0,74	182	204	2
13252	383905	5403426		York River	88,79	0,83	447	0,05	5,13	526	526	14
13259	405532	5409100		York River	85,79	0,21	447	0,21	0,47	156	172	2

INRS	Outcrop location		Strati. location	Formation	IR	TOC	Tmax	PI	GP	HI	CHI	OI
	UTM east	UTM north	m		%	%	°C		mg/g	mg/g	mg/g	mg/g
13289	392950	5400300		York River	89,8	0,04	555	0,31	0,34	501	522	39
13293	392400	5389550		York River	91,1	0,03	555	0,43	0,28	510	565	67
13126	375320	5424850		York River (A.B.)	95,07	0,04		0,76	0,22	136	136	15
13157	405000	5397150		York River (A.B.)	89,97	0,32	438	0,17	0,6	136	174	5
13158	405000	5397150		York River (A.B.)	83,59	0,07	505	0,41	0,21	143	197	22
13179	366713	5410549		York River (A.B.)	87,69	0,18	447	0,2	0,49	194	205	4
13182	367165	5409275		York River (A.B.)	86,78	0,33	452	0,17	0,63	138	147	3
13186	367165	5409275		York River (A.B.)	87,4	0,31	452	0,18	0,73	166	172	2
13226	357454	5419358		York River (A.B.)	88,57	1,05	442	0,06	4,33	340	340	64
13237	364122	5411150		York River (A.B.)	83,56	0,06	530	0,27	0,32	351	394	13
13244	378861	5402833		York River (A.B.)	90,69	0,04	488	0,18	0,44	945	1269	4
13255	386680	5401890		York River (A.B.)	87,1	0,27	447	0,19	0,83	216	229	7
13288	392600	5398520		York River (A.B.)	88,85	0,05	505	0,21	0,35	483	530	23
13298	399350	5391050		York River (A.B.)	92,26	0,03	538	0,27	0,38	863	911	39
13301	398920	5390450		York River (A.B.)	90,5	0,03	497	0,25	0,34	899	1023	17
13290	391450	5405900		York River (A.B.)	88,78	0,05	555	0,33	0,32	340	358	26
13299	400300	5391450		York River (A.B.)	65,31	0,06	505	0,5	0,31	164	187	8
13129	375400	5425820		York Lake	53,49	0,11	443	0,25	0,58	217	242	7
13192	370602	5411841		York Lake	28,14	0,03	447	0,23	0,39	285	306	5
13208	368298	5427571		York Lake	87,28	0,11	447	0,2	0,65	387	412	20
13287	391770	5398000		York Lake	57	0,14	447	0,13	0,91	332	390	9
13240	376859	5401008		Forillon	67,31	0,16	447	0,33	0,63	172	209	6
13145	389450	5420000		Indian Cove	39,75	0,05	447	0,19	0,65	415	480	12
13164	367000	5413350		Indian Cove	78,24	0,45	442	0,39	3,5	371	413	8
13165	366700	5413300		Indian Cove	40,3	0,08	435	0,25	1,16	428	449	5
13169	366350	5412920		Indian Cove	45,84	0,06	447	0,29	0,61	353	401	11
13170	366700	5411950		Indian Cove	35,47	0,04	447	0,23	0,54	342	362	5
13211	366967	5426421		Indian Cove	37,84	0,09	442	0,2	0,51	166	274	8
13212	365636	5425363		Indian Cove	33,26	0,07	443	0,16	0,91	377	410	7
13222	357557	5421333		Indian Cove	62,41	0,35	438	0,41	4,83	504	538	5
13224	357102	5420600		Indian Cove	27,96	0,04	442	0,27	0,58	328	355	6
13231	358641	5418411		Indian Cove	77,29	0,23	442	0,42	2,17	419	439	14
13234	359349	5416329		Indian Cove	44,89	0,21	450	0,14	1,7	318	335	3
13236	362996	5413949		Indian Cove	22,08	0,02	440	0,19	0,47	391	512	5
13242	377724	5402418		Indian Cove	62,89	0,09	447	0,18	0,53	296	324	3
13243	378779	5402741		Indian Cove	31,43	0,04	447	0,16	0,47	327	348	2
13246	380806	5401280		Indian Cove	55,19	0,07	447	0,34	0,48	266	315	2
13248	381298	5401829		Indian Cove	59,64	0,07	448	0,21	0,55	362	451	2
13282	389950	5395800		Indian Cove	52,89	0,07	448	0,26	0,64	332	332	14
13283	390050	5396950		Indian Cove	26,85	0,02	447	0,23	0,25	288	354	9
13284	390450	5397700		Indian Cove	57,27	0,09	447	0,16	0,61	349	396	7
13291	388894	5410212		Indian Cove	54,24	0,11	442	0,16	0,78	321	411	5
13292	388782	5412898		Indian Cove	54,64	0,07	448	0,17	0,56	382	416	5
13206	368667	5427936		Shiphead	19,73	0,04	438	0,15	0,65	312	418	9
13210	367336	5426816		Shiphead	25,68	0,06	447	0,15	0,78	303	325	10
13235	360579	5415628		Forillon	33,7	0,04	443	0,2	0,59	368	394	5
13132	375700	5426400		Shiphead	67,68	0,33	443	0,16	2,1	360	360	9

INRS	Outcrop location		Strati. location m	Formation	IR %	TOC %	Tmax °C	PI	GP mg/g	HI mg/g	CHI mg/g	OI mg/g
	UTM east	UTM north										
13204	369120	5428280		Forillon	69,72	0,13	438	0,2	0,46	202	251	8
13205	369015	5428207		Forillon	54,79	0,16	447	0,12	1,37	400	559	5
13209	367581	5426935		Forillon	70,89	0,39	438	0,16	1,82	276	302	2
13232	359131	5416858		Forillon	40,24	0,05	447	0,23	0,62	367	428	6
13271	398750	5413850		Forillon	64,99	0,16	440	0,15	1,04	352	468	7
13268	398800	5414600		Indian Pt	32,63	0,05	438	0,23	0,39	189	268	7
13140	381850	5424750		Indian Pt	77,02	0,05		0,42	0,25	261	386	20
13147	390050	5422170		Indian Pt	36,83	0,06	438	0,22	0,5	239	380	22
13148	390050	5422170		Indian Pt	36,83	0,06	437	0,22	0,54	261	406	12
13142	381850	5424750		Indian Pt	75,8	0,05		0,52	0,21	163	247	68
13203	369245	5428821		Roncelles	56,76	0,02		0,32	0,29	491	578	7
13267	399857	5415400		Roncelles	39,02	0,04	447	0,28	0,23	190	287	15
13201	368970	5429166		West Point	6,03	0,00	430	0,33	0,17	220	336	20
13238	373817	5399554		Laforce	10,79	0,00	448	0,29	0,13	237	237	11
13135	375900	5427550		Quebec Gp	78,53	0,09	530	0,38	0,27	143	156	3
13136	375900	5427550		Quebec Gp	76,85	0,09	535	0,33	0,36	200	228	9
13272	391400	5423400		Quebec Gp	48,42	0,03	488	0,28	0,3	333	437	14
13273	395214	5426350		Quebec Gp	87,1	0,18	505	0,24	0,45	159	199	10
13274	399950	5426250		Quebec Gp	52,28	0,65	492	0,23	1,33	82	85	1
13275	404650	5420650		Quebec Gp	62,37	0.53	485	0.16	0,77	76	96	0
13276	409350	5415850		Quebec Gp	55,34	0.42	497	0.19	0,68	72	104	3
13277	407150	5419050		Quebec Gp	82.55	0.27	497	0.19	0,34	82	100	8
13278	411600	5411850		Quebec Gp	84,43	0.25	502	0,28	0.45	109	150	17
14539	390118	5423275	1850	West Point	59,5	1.11	500	0.17	0,52	39	39	119
14539	390118	5423275	1850	West Point	59.5	0.66	500	0.17	0,52	39	39	119
14544	390165	5423212	1800	Roncelles	64,77	0.14	478	0,34	0,34	123	164	9
14544	390165	5423212	1800	Roncelles	64.77	0.09	478	0.34	0,34	123	164	9
14547	390116	5423088	1740	Roncelles	64.39	0.30	487	0.28	0.64	114	152	6
14547	390116	5423088	1740	Roncelles	64,39	0.19	487	0.28	0,64	114	152	6
14553	390161	5422869	1570	Indian Pt	77,35	0,05		0,43	0,12	82	127	21
14568	389996	5421216	940	Forillon	41,89	0.30	447	0,22	1,26	294	330	17
14569	410320	5408450	2010	Quebec Gp	89.04	2.20	470	0.22	3.05	108	108	1
14571	410250	5408350	2012	Quebec Gp	81,26	0.62	448	0.23	1,05	114	130	5
14572	407110	5410590	2013	Quebec Gp	43,89	0,02		0.28	0,03	81	102	13
14573	407140	5410540	1080	Indian Pt	80,38	0.03		0.52	0,09	91	141	14
14576	406490	5410700	990	Forillon	78,51	0.13	442	0.19	0,5	255	318	32
14579	406460	5410490	860	Forillon	60,85	0.18	442	0.14	0,66	259	323	13
14582	406380	5410430	795	Forillon	77,25	0.23	442	0,13	1,43	427	533	20
14586	406330	5410270	655	Forillon	63,33	0.08	442	0.17	0,4	319	398	19
14587	406280	5410210	625	Forillon	39,76	0.08	458	0,15	0.36	319	398	24
14589	406320	5409690	390	Shiphead	75,8	0.30	433	0,11	1,29	319	389	30
14596	406320	5409510	300	Indian Cove	72.85	0.18	442	0,19	1,12	454	517	45
14600	406270	5409390	210	Indian Cove	22,4	0.09	437	0.23	0,4	320	364	24
14601	406160	5409360	180	Indian Cove	8,77	0.07	442	0.3	0,34	313	334	25
14605	405990	5409360	140	Indian Cove	6.25	0.10	445	0,15	0,35	306	306	13
14606	405990	5409390	55	York River	95.82	0.22	442	0.13	0.62	246	246	75

Well name	INRS	Depth		Formation	IR %	TOC %	Tmax °C	PI	GP mg/g	HI mg/g	CHI mg/g	OI mg/g
		sup.	inf.									
Blanchet	13310	35	80	Indian Cove	36,14	0,32	442	0,28	1,06	227	242	12
	13311	105	150	Indian Cove	22,33	0,26	442	0,26	0,66	186	186	2
	13312	195	240	Shiphead	66,86	0,46	442	0,27	1,43	205	227	3
	13313	305	350	Indian Cove	40,14	0,36	442	0,27	1,33	239	268	2
	13314	435	480	Indian Cove	35,83	0,27	447	0,23	1,02	262	294	13
	13315	550	600	Shiphead	65,28	0,48	447	0,29	1,64	192	244	2
	13316	675	720	Shiphead	67,54	0,42	447	0,25	1,47	205	261	2
	13317	795	840	Shiphead	65,71	0,21	442	0,28	0,95	209	323	16
	13318	915	940	Forillon	53,95	0,39	442	0,43	1,45	184	215	1
	13319	1035	1080	Indian Pt	54,12	0,48	447	0,43	1,93	196	229	1
	13320	1190	1235	Quebec Gp	83,76	0,10	450	0,29	0,55	294	379	12
	13321	1285	1330	Quebec Gp	91,73	0,02		0,3	0,23	568	732	1
Malbaie	13322	20	65	Battery Pt	83,34	0,03	485	0,28	0,43	921	921	23
	13323	105	150	Battery Pt	82,38	0,03	485	0,2	0,42	919	919	2
	13324	250	300	Battery Pt	83,25	0,03		0,45	0,11	208	208	27
	13325	405	450	Battery Pt	84,27	0,03		0,61	0,16	202	202	2
	13326	555	600	Battery Pt	91,23	0,03		0,6	0,2	307	307	3
	13327	705	750	Battery Pt	92,08	0,05	505	0,55	0,15	142	142	0
	13328	855	900	Battery Pt	93,43	0,04		0,7	0,24	169	169	40
	13329	1005	1050	Battery Pt	93,97	0,06		0,64	0,45	264	264	9
	13330	1155	1200	Battery Pt	94,09	0,06		0,71	0,27	141	141	6
	13331	1305	1350	Battery Pt	90,05	0,08		0,55	0,21	115	115	8
	13332	1455	1500	Battery Pt	90,98	0,08		0,58	0,16	79	79	4
	13333	1605	1650	Battery Pt	88,41	0,15	455	0,48	0,45	153	153	1
	13334	1755	1800	Battery Pt	90,52	0,07	452	0,51	0,27	199	199	1
	13335	1905	1950	Battery Pt	93,24	0,07		0,64	0,25	134	134	12
	13336	2075	2125	Battery Pt	92	0,05		0,71	0,31	177	177	3
Sunny Bank	13077	308	309	York River	86,09	0,36	453	0,17	0,81	186	186	7
	13089	607	610	York River	70,58	0,57	457	0,1	1,38	219	219	7
	13093	688	693	Indian Cove	38,49	0,24	432	0,5	1,04	205	219	8
	14001	846	853	Indian Cove	78,39	0,40	448	0,53	2,55	282	301	10
	14006	919	925	Indian Cove	55,97	0,25	442	0,49	1,48	266	303	12
	14022	1148	1151	Indian Cove	48,84	0,18	442	0,44	0,88	244	278	12
	14037	1376	1377	Indian Cove	55,27	0,35	442	0,33	0,94	169	180	7
	14047	1544	1547	Shiphead	59,38	0,26	442	0,55	0,67	98	119	9
	14049	1604	1607	Shiphead	83,35	0,47	445	0,47	1,05	107	118	18
	14053	1672	1675	Shiphead	76,35	0,41	443	0,49	1,1	124	137	5
	14072	1933	1936	Forillon	59,2	0,56	448	0,46	0,89	76	85	6
	14079	2041	2045	Forillon	86,73	0,18	447	0,53	0,3	62	77	2
	14086	2143	2146	Forillon	34,11	0,64	442	0,45	0,55	47	47	7
	14094	2258	2280	Forillon	68,35	0,38	430	0,6	0,88	82	92	3

Well name	INRS	Depth sup.	Depth inf.	Formation	IR %	TOC %	Tmax °C	PI	GP mg/g	HI mg/g	CHI mg/g	OI mg/g
	14099	2340	2373	Forillon	2,32	0,10	428	0,41	0,23	134	134	11
	14121	2771	2775	Indian Pt	47,54	0,40	432	0,55	0,33	29	36	2
	14128	2989	2993	Indian Pt	75,97	0,46		1	0,08	0	0	2
	14130	3047	3049	Indian Pt	55,65	0,29		1	0,05	0	0	1
	14133	3138	3141	Indian Pt	61,93	0,23		0,76	0,17	11	17	3
	14141	3367	3370	Roncelles	51,72	0,27		1	0,02	0	0	2
	14143	3446	3449	Roncelles	54,87	0,15		1	0,04	0	0	0
York	14169	521	523	Gascons	64,67	0,07	520	0,15	0,16	214	214	7
	14176		637	Gascons	72,81	0,04		0,33	0,1	192	192	0
Douglas	14202		55	Battery Pt	86,07	0,11	442	0,35	0,17	96	96	6
	14203		100	Battery Pt	88,44	1,32	423	0,06	3,49	248	248	16
	14204		305	Battery Pt	92,12	0,15	437	0,5	0,87	294	294	10
	14205		520	Battery Pt	85,85	0,13	437	0,54	0,62	223	223	7
	14206		780	York River	85,45	0,13	442	0,4	0,13	61	61	2
	14207		940	York River	88,61	0,08		0,44	0,11	77	77	1
	14208		1125	York River	87,98	0,12		0,45	0,16	72	72	2
	14210		1320	York River	91,35	0,09	428	0,56	0,51	244	244	10
	14211		1370	York River	88,69	0,16	453	0,52	0,37	109	109	5
	14214		1475	York River	86,64	0,31	447	0,31	0,85	188	188	9
	14217		1575	Roncelles	55,67	0,16	440	0,47	0,46	114	152	11
Gaspe Sud	14231	150	160	York River	87,32	0,18	450	0,51	0,75	199	199	10
	14235	300	310	York River	84,66	0,22	445	0,69	0,16	22	22	1
	14237	380	390	York River	83,96	0,19	447	0,66	0,13	23	23	1
	14241	530	540	Indian Cove	37,67	0,18	442	0,45	0,63	167	190	9
	14245	680	690	Indian Cove	59.7	0,16	447	0,5	0,7	197	224	15
	14249	835	845	Indian Cove	46,32	0,15	440	0,51	0,62	178	202	11
	14253	990	995	Indian Cove	46,72	0,16	445	0,39	0,76	259	295	9
	14258	1190	1205	Indian Cove	42,25	0,32	412	0,29	1,07	224	239	12
	14260	1290	1300	Indian Cove	48.9	0,16	447	0,5	0,62	171	194	8
	14263	1445	1450	Indian Cove	54,76	0,16	447	0,56	0,62	146	166	8
	14267	1600	1610	Shiphead	72,55	0,25	447	0,34	0,62	137	167	4
	14271	1755	1765	Shiphead	74,19	0,34	445	0,55	1,12	121	147	3
	14279	2060	2070	Forillon	31.66	0,10	437	0,65	0,38	109	136	34
	14283	2215	2225	Forillon	43,95	0,15	437	0,43	0,56	171	213	6
	14287	2370	2380	Forillon	46,99	0,14	442	0,59	0,59	137	171	5
	14295	2670	2680	Forillon	66,95	0,38	447	0,49	0,83	97	109	2
	14304	3055	3065	Quebec Gp	78	0,65	487	0,46	0,86	63	72	3
	14308	3225	3235	Quebec Gp	82,61	1,16	457	0,31	1,31	77	77	2
	14312	3350	3354	Quebec Gp	81.12	1.12	457	0.19	0,83	60	60	3

Well name	INRS	Depth sup.	Depth inf.	Formation	IR %	TOC %	Tmax °C	PI	GP mg/g	HI mg/g	CHI mg/g	OI mg/g
Gaspe Nord	14347		255	Battery Pt	83,64	0,13	457	0,12	0,13	82	82	10
	14348		400	Battery Pt	88,69	0,20	442	0,21	0,1	40	40	10
	14349		640	Battery Pt	86,71	0,24	457	0,18	0,17	56	56	3
	14350		830	York River	90,62	0,22	453	0,09	0,26	107	107	6
	14351		1050	York River	85,59	0,38	445	0,25	0,46	91	91	7
	14352		1200	Indian Cove	44,41	0,17	445	0,22	0,58	232	264	5
	14353		1400	Forillon	32,28	0,15	447	0,29	0,41	160	200	6
	14354		1600	Indian Pt	64,72	0,31	437	0,25	0,96	150	232	5
	14355		1800	Indian Pt	70,52	0,06	445	0,22	0,2	171	265	10
	14356		1885	Roncelles	58,47	0,06	553	0,45	0,21	140	187	7

Well name	INRS	Depth sup. m	Depth inf. m	Formation	Insoluble Residue %	Total Organic Carbon %
York	14148		57	West Point	63,7	0,13
York	14149		76	West Point	76,1	0,03
York	14150		112	West Point	74,3	0,04
York	14153		182	Gascons	67,2	0,05
York	14156		291	Gascons	67,9	0,08
York	14158		319	Gascons	66,5	0,06
York	14162		377	Gascons	73,9	0,09
York	14164		418	Gascons	75,0	0,05
York	14169		522	Gascons	64,7	0,06
York	14172		566	Gascons	66,5	0,03
York	14176		637	Gascons	72,8	0,03
York	14177		666	Gascons	74,8	0,11
York	14179		722	Gascons	75,6	0,06
York	14184		810	Laforce	74,1	0,17
York	14187		851	Laforce	42,8	0,06
York	14191		901	Laforce	18,5	0,04
York	14193		935	Laforce	15,9	0,04
York	14197		1022	Burnt Jam Brook	83,5	0,08
York	14199		1080	Burnt Jam Brook	77,4	0,34
York	14200		1109	Burnt Jam Brook	49,2	0,44
York	14201		1129	Burnt Jam Brook	81,7	0,26
Quebec Oil	2468	358	361	Indian Cove	49,9	0,24
Quebec Oil	2471	569	578	Indian Cove	42,7	0,18
Quebec Oil	2477	935	938	Shiphead	54,2	0,30
Quebec Oil	2481	1181	1184	Shiphead	44,3	0,22
Quebec Oil	2491	1794	1797	Shiphead	57,6	0,32
Sunny Bank	13077	308	309	York River	86,1	0,36
Sunny Bank	13085	480	486	York River	81,7	0,20
Sunny Bank	13087	549	558	York River	86,3	0,29
Sunny Bank	13089	607	610	York River	70,6	0,57
Sunny Bank	13091	0	652	York River	38,5	0,23
Sunny Bank	13095	0	747	Indian Cove	44,0	0,18
Sunny Bank	14000	835	844	Indian Cove	78,4	0,40
Sunny Bank	14006	919	925	Indian Cove	56,0	0,25
Sunny Bank	14010	977	981	Indian Cove	45,2	0,19
Sunny Bank	14017	1072	1075	Indian Cove	36,4	0,20
Sunny Bank	14021	1132	1133	Indian Cove	48,8	0,18
Sunny Bank	14029	1238	1241	Indian Cove	56,6	0,18
Sunny Bank	14033	1295	1297	Indian Cove	55,2	0,19
Sunny Bank	14037	1376	1377	Indian Cove	55,3	0,35
Sunny Bank	14042	1436	1439	Indian Cove	45,7	0,17
Sunny Bank	14048	1576	1579	Shiphead	59,4	0,26
Sunny Bank	14050	1623	1625	Shiphead	83,4	0,47
Sunny Bank	14056	1708	1711	Shiphead	76,4	0,40
Sunny Bank	14060	1765	1768	Shiphead	82,1	0,29
Sunny Bank	14068	1877	1878	Shiphead	70,7	0,39

Well name	INRS	Depth		Formation	Insoluble Residue	Total Organic Carbon
		sup. m	inf. m		%	%
Sunny Bank	14073	1951	1954	Forillon	59,2	0,56
Sunny Bank	14078	2019	2022	Forillon	86,7	0,18
Sunny Bank	14085	2136	2156	Forillon	34,1	0,64
Sunny Bank	14094	2258	2280	Forillon	68,4	0,38
Sunny Bank	14098	2319	2322	Forillon	2,3	0,10
Sunny Bank	14105	2417	2419	Indian Point	84,8	0,34
Sunny Bank	14110	2498	2501	Indian Point	17,7	0,20
Sunny Bank	14115	2566	2571	Indian Point	35,3	0,38
Sunny Bank	14116	2598	2600	Indian Point	66,1	0,08
Sunny Bank	14120	2744	2747	Indian Point	47,5	0,40
Sunny Bank	14122	2808	2809	Indian Point	77,6	0,57
Sunny Bank	14124	2865	2868	Indian Point	67,0	0,48
Sunny Bank	14129	3018	3020	Indian Point	76,0	0,46
Sunny Bank	14131	3076	3079	Indian Point	55,7	0,29
Sunny Bank	14133	3138	3141	Indian Point	61,9	0,23
Sunny Bank	14135	3198	3201	Indian Point	69,1	0,11
Sunny Bank	14138	3289	3293	Roncelles	52,0	0,20
Sunny Bank	14140	3355	3358	Roncelles	51,7	0,27
Sunny Bank	14143	3446	3449	Roncelles	54,9	0,15
Sunny Bank	14145	3506	3509	Roncelles	51,5	0,15
Gaspé Nord	14347		255	Battery Pt	83,6	0,13
Gaspé Nord	14348		400	Battery Pt	88,7	0,20
Gaspé Nord	14349		640	Battery Pt	86,7	0,24
Gaspé Nord	14350		830	York River	90,6	0,22
Gaspé Nord	14351		1050	York River	85,6	0,38
Gaspé Nord	14352		1200	Indian Cove	44,4	0,17
Gaspé Nord	14353		1400	Forillon	32,3	0,15
Gaspé Nord	14354		1600	Indian Point	64,7	0,31
Gaspé Nord	14355		1800	Indian Point	70,5	0,06
Gaspé Nord	14356		1885	Roncelles	58,5	0,06
Gaspé Nord	14381		2000	Quebec Gp	85,2	0,02
Gaspé Nord	14382		2200	Quebec Gp	84,8	0,02
Gaspé Nord	14383		2400	Quebec Gp	87,6	0,13
Gaspé Nord	14384		2530	Quebec Gp	85,8	0,01

Well name	INRS	Depth sup. m	Depth inf. m	Formation	Insoluble Residue %	Total Organic Carbon %
Gaspé Sud	14229		75	York River	87,4	0,10
Gaspé Sud	14230		115	York River	85,7	0,21
Gaspé Sud	14231	150	160	York River	87,3	0,18
Gaspé Sud	14232		180	York River	86,4	0,16
Gaspé Sud	14233		230	York River	87,7	0,16
Gaspé Sud	14234		265	York River	84,6	0,22
Gaspé Sud	14235	300	310	York River	84,7	0,22
Gaspé Sud	14236		340	York River	83,3	0,17
Gaspé Sud	14237		390	York River	84,0	0,19
Gaspé Sud	14238		415	York River	84,2	0,21
Gaspé Sud	14239		455	York River	73,6	0,35
Gaspé Sud	14240		500	Indian Cove	42,4	0,19
Gaspé Sud	14241	530	540	Indian Cove	37,7	0,18
Gaspé Sud	14242		570	Indian Cove	52,2	0,15
Gaspé Sud	14243		610	Indian Cove	54,4	0,12
Gaspé Sud	14244		640	Indian Cove	50,6	0,18
Gaspé Sud	14245	680	690	Indian Cove	59,7	0,16
Gaspé Sud	14246		725	Indian Cove	64,9	0,16
Gaspé Sud	14247		760	Indian Cove	43,2	0,17
Gaspé Sud	14248		805	Indian Cove	54,8	0,21
Gaspé Sud	14249	835	845	Indian Cove	46,3	0,15
Gaspé Sud	14250		870	Indian Cove	34,6	0,17
Gaspé Sud	14251		915	Indian Cove	50,0	0,19
Gaspé Sud	14252		955	Indian Cove	42,0	0,18
Gaspé Sud	14253	990	995	Indian Cove	46,7	0,16
Gaspé Sud	14254		1040	Indian Cove	46,9	0,17
Gaspé Sud	14255		1070	Indian Cove	42,4	0,17
Gaspé Sud	14256		1110	Indian Cove	49,1	0,15
Gaspé Sud	14257		1150	Indian Cove	44,1	0,15
Gaspé Sud	14258	1190	1205	Indian Cove	42,3	0,32
Gaspé Sud	14259		1260	Indian Cove	44,2	0,18
Gaspé Sud	14260	1290	1300	Indian Cove	48,9	0,16
Gaspé Sud	14261		1375	Indian Cove	59,3	0,21
Gaspé Sud	14262		1415	Indian Cove	56,8	0,19
Gaspé Sud	14263	1445	1455	Indian Cove	54,8	0,16
Gaspé Sud	14264		1490	Indian Cove	53,1	0,16
Gaspé Sud	14265		1525	Indian Cove	62,0	0,20
Gaspé Sud	14266		1560	Shiphead	78,8	0,36
Gaspé Sud	14267	1600	1610	Shiphead	72,6	0,25
Gaspé Sud	14268		1645	Shiphead	72,4	0,35
Gaspé Sud	14269		1680	Shiphead	73,7	0,30
Gaspé Sud	14270		1715	Shiphead	82,4	0,24
Gaspé Sud	14271	1755	1765	Shiphead	74,2	0,34
Gaspé Sud	14272		1790	Shiphead	77,6	0,26
Gaspé Sud	14273		1835	Shiphead	40,4	0,42
Gaspé Sud	14274		1870	Forillon	42,3	0,46

Well name	INRS	Depth sup. m	Depth inf. m	Formation	Insoluble Residue %	Total Organic Carbon %
Gaspé Sud	14275	1905	1915	Forillon	60,2	0,37
Gaspé Sud	14276		1950	Forillon	46,1	0,46
Gaspé Sud	14277		1990	Forillon	47,3	0,10
Gaspé Sud	14278		2030	Forillon	40,5	0,11
Gaspé Sud	14279	2060	2070	Forillon	31,7	0,09
Gaspé Sud	14280		2100	Forillon	51,9	0,10
Gaspé Sud	14281		2135	Forillon	27,8	0,15
Gaspé Sud	14282		2180	Forillon	53,1	0,13
Gaspé Sud	14283	2215	2225	Forillon	44,0	0,15
Gaspé Sud	14284		2270	Forillon	39,7	0,14
Gaspé Sud	14285		2305	Forillon	39,6	0,13
Gaspé Sud	14286		2335	Forillon	33,7	0,11
Gaspé Sud	14287	2370	2380	Forillon	47,0	0,14
Gaspé Sud	14288		2420	Forillon	40,0	0,17
Gaspé Sud	14289		2450	Forillon	36,3	0,19
Gaspé Sud	14290		2485	Forillon	44,7	0,23
Gaspé Sud	14291	2530	2540	Forillon	48,9	0,23
Gaspé Sud	14292		2570	Forillon	67,8	0,26
Gaspé Sud	14293	2600	2610	Forillon	65,2	0,24
Gaspé Sud	14294		2640	Forillon	57,1	0,31
Gaspé Sud	14295	2670	2680	Forillon	67,0	0,38
Gaspé Sud	14296		2720	Forillon	63,3	0,49
Gaspé Sud	14297	2755	2765	Forillon	66,0	0,51
Gaspé Sud	14298		2795	Forillon	67,0	0,44
Gaspé Sud	14299		2825	Indian Point	51,8	0,38
Gaspé Sud	**14300**		**2915**	**Quebec Gp**	**74,3**	**1,28**
Gaspé Sud	14301		2950	Quebec Gp	67,9	0,87
Gaspé Sud	**14302**		**2990**	**Quebec Gp**	**79,6**	**1,10**
Gaspé Sud	14303		3025	Quebec Gp	80,5	0,77
Gaspé Sud	14304	3055	3065	Quebec Gp	78,0	0,65
Gaspé Sud	14305		3110	Quebec Gp	83,4	0,61
Gaspé Sud	14306		3145	Quebec Gp	81,6	0,69
Gaspé Sud	14307		3180	Quebec Gp	81,1	0,83
Gaspé Sud	**14308**	**3225**	**3235**	**Quebec Gp**	**82,6**	**1,16**
Gaspé Sud	14309		3260	Quebec Gp	79,2	0,75
Gaspé Sud	14310		3295	Quebec Gp	69,8	0,56
Gaspé Sud	14311		3335	Quebec Gp	77,1	0,97
Gaspé Sud	**14312**	**3350**	**3354**	**Quebec Gp**	**81,1**	**1,12**

Well name	INRS	Depth sup. m	Depth inf. m	Formation	Insoluble Residue %	Total Organic Carbon %
Douglas	14202		55	Battery Pt	86,1	0,11
Douglas	**14203**		**100**	**Battery Pt**	**88,4**	**1,32**
Douglas	14204		305	Battery Pt	92,1	0,15
Douglas	14205		520	Battery Pt	85,9	0,13
Douglas	14206		780	York River	85,5	0,13
Douglas	14207		940	York River	88,6	0,08
Douglas	14208		1125	York River	88,0	0,12
Douglas	14209		1260	York River	87,4	0,18
Douglas	14210		1320	York River	91,4	0,09
Douglas	14211		1370	York River	88,7	0,16
Douglas	14212		1410	York River	85,4	0,09
Douglas	14213		1425	York River	85,8	0,31
Douglas	14214		1475	York River	86,6	0,31
Douglas	14215		1520	York River	88,5	0,33
Douglas	14216		1535	Roncelles	67,3	0,18
Douglas	14217		1575	Roncelles	55,7	0,16
Douglas	14218		1610	West Point	58,4	0,19
Douglas	14219		1650	West Point	7,2	0,06
Douglas	14220		1690	Griffon Cove	47,6	0,13
Douglas	14221		1710	Griffon Cove	44,7	0,13
Douglas	14222		1760	Griffon Cove	54,2	0,04
Douglas	14223		1800	Griffon Cove	77,8	0,12
Douglas	14224		1815	Griffon Cove	67,3	0,05
Douglas	14225		1840	Griffon Cove	81,0	0,11
Douglas	**14226**		**1855**	**Quebec Gp**	**80,0**	**1,28**
Douglas	14227		1900	Quebec Gp	84,1	0,69
Douglas	14228		1990	Quebec Gp	79,4	0,70

INRS	Section name	Location - zone 19		Formation	Strati. depth	Insoluble Residue %	Total Organic carbon %
		UTM east	UTM north				
6701	Ruisseau Go A Shore	693120	5394960	Lake Branch	486	78	0,05
6703	Rivière Nouvelle Nord	677400	5374380	Battery Pt	0	82	0,06
6580	Rivière Nouvelle Sud	680500	5372310	York River	1416	88	0,04
6586	Rivière Nouvelle Sud	679950	5372420	York River	1566	80	0,05
	ROUTE SQUARE						
6563	Forks Ouest	686160	5381550	York River	843	70	0,14
6562	Forks Ouest	686160	5381550	York River	869	84	0,02
6561	Forks Ouest	686160	5381550	York River	879	81	0,05
6560	Forks Ouest	683140	5379660	York River	915	88	0,04
6558	Forks Ouest	683760	5361140	York River	984	83	0,03
6557	Forks Ouest	682570	5360330	York River	1095	79	0,12
6556	Forks Ouest	682570	5360330	York River	1107	81	0,08
6554	Forks Ouest	681320	5378090	York River	1263	86	0,04
6552	Forks Ouest	679950	5376690	York River	1323	79	1,4
	RIVIÈRE CASCAPEDIA						
	BRANCHE DU LAC						
6550	Branche du Lac	689040	5382440	York River	1046	79	0,04
6566	Branche du Lac	688650	5382440	York River	1338	83	0,03
6653	Branche du Lac	686840	5383340	York River	2352	42	0,75
6610	Branche du Lac	686300	5384490	York River	2688	70	0,03
6609	Branche du Lac	686300	5384490	York River	2736	78	0,02
6656	Branche du Lac	686300	5384490	York River	2740	65	0,03
6650	Branche du Lac	684360	5385540	York River	3336	84	0,27
6637	Detailled section	684660	5385240	York River	3430	73	0,28
6635	Detailled section	684510	5385350	York River	3497	76	0,27
6633	Detailled section	684460	5385390	York River	3521	79	0,32
6631	Detailled section	684420	5385430	York River	3543	84	0,76
6628	Detailled section	684360	5385470	York River	3567	80	0,29
6626	Detailled section	684340	5385490	York River	3576	87	0,11
6624	Detailled section	684330	5385500	York River	3585	85	0,25
6622	Detailled section	684280	5385540	York River	3605	68	0,2
6619	Detailled section	684230	5385580	York River	3632	75	0,18
6617	Detailled section	684210	5385590	York River	3637	80	0,13
6658	Branche du Lac	683330	5386370	York Lake	3744	62	0,01
6651	Branche du Lac	682970	5386640	York Lake	3786	42	0,15
6654	Branche du Lac	682070	5387970	Cap-Bon-Ami	4584	63	0,16
6664	Bras aux Saumons	699410	5401200	York River	132	68	0,07
6528	Route des Lacs Josué	704300	5383760	Battery Pt	1542	79	0,06
6529	Route des Lacs Josué	704130	5383780	Battery Pt	1548	79	0,06
6603	Ruisseau Marcil Ouest	716710	5387410	York River	366	64	0,17
6599	Ruisseau Marcil Ouest	716710	5387280	York River	606	87	0,06
6595	Ruisseau Marcil Ouest	717070	5385650	York River	1170	87	0,63
6593	Ruisseau Marcil Ouest	717000	5385220	York River	1224	83	0,73

INRS	Section name	Location - zone 19		Formation	Strati.	Insoluble Residue	Total Organic carbon
		UTM east	UTM north		depth	%	%
6708	Ruisseau Caron	719750	5389210	volcanic	150	71	0,04
6709	Ruisseau Caron	720000	5388770	York River	372	77	0,09
6712	Ruisseau Caron	720270	5388290	York River	612	83	0,65
6714	Ruisseau Caron	720800	5387660	York River	948	68	0,26
6716	Ruisseau Caron	721180	5387020	York River	1398	83	0,37

Lefèvre spl number	Section name	Location of the base of rock sections - zone 20		Formation	Stratigraphic position (m)	Insoluble Residue %	Total Org. Carbon %
		UTM east	UTM north				
79-314	No 3 - Lachambre Brook	36 27 50	54 00 500	Burnt Jam Brook	250	89,35	0,05
79-315	No 3 - Lachambre Brook	36 27 50	54 00 500	Burnt Jam Brook	249	85,81	0,09
79-316	No 3 - Lachambre Brook	36 27 50	54 00 500	Burnt Jam Brook	166	68,32	0,07
79-317	No 3 - Lachambre Brook	36 27 50	54 00 500	Burnt Jam Brook	159	81,61	0,09
79-318	No 3 - Lachambre Brook	36 27 50	54 00 500	Burnt Jam Brook	138	82,33	0,06
79-298	No 4 - Bleu Brook	40 97 50	53 73 750	Matapédia	6	13,32	0,08
79-299	No 4 - Bleu Brook	40 97 50	53 73 750	Matapédia	13	42,64	0,15
79-300	No 4 - Bleu Brook	40 97 50	53 73 750	Matapédia	20	19,99	0,13
79-301	No 4 - Bleu Brook	40 97 50	53 73 750	Matapédia	35	42,9	0,19
79-302	No 4 - Bleu Brook	40 97 50	53 73 750	Matapédia	48	43,49	0,04
79-303	No 4 - Bleu Brook	40 97 50	53 73 750	Burnt Jam Brook	823	83,37	0,04
79-304	No 4 - Bleu Brook	40 97 50	53 73 750	Burnt Jam Brook	841	81,98	0,07
79-305	No 4 - Bleu Brook	40 97 50	53 73 750	Burnt Jam Brook	844	68,05	0,03
79-306	No 4 - Bleu Brook	40 97 50	53 73 750	Burnt Jam Brook	855	77,38	0,06
79-307	No 4 - Bleu Brook	40 97 50	53 73 750	Burnt Jam Brook	880	25,15	0,05
79-308	No 4 - Bleu Brook	40 97 50	53 73 750	Laforce	953	14,73	0,03
79-309	No 4 - Bleu Brook	40 97 50	53 73 750	Laforce	969	20,86	0,03
79-310	No 4 - Bleu Brook	40 97 50	53 73 750	Laforce	970	51,07	0,05
79-134	No 5 - Flynn Road (Percé)	34 60 00	53 77 630	White Head	113	6,94	0,04
79-137	No 5 - Flynn Road (Percé)	34 60 00	53 77 630	White Head	127	10,62	0,04
79-139	No 5 - Flynn Road (Percé)	34 60 00	53 77 630	White Head	137	16,93	0,04
79-140	No 5 - Flynn Road (Percé)	34 60 00	53 77 630	White Head	142	30,08	0,04
79-141	No 5 - Flynn Road (Percé)	34 60 00	53 77 630	White Head	144	15,7	0,04
79-143	No 5 - Flynn Road (Percé)	34 60 00	53 77 630	White Head	151	11,11	0,03
79-145	No 5 - Flynn Road (Percé)	34 60 00	53 77 630	White Head	168	17,47	0,04
79-148	No 5 - Flynn Road (Percé)	34 60 00	53 77 630	White Head	200	14,91	0,04
79-150	No 5 - Flynn Road (Percé)	34 60 00	53 77 630	White Head	206	8,66	0,04
79-153	No 5 - Flynn Road (Percé)	34 60 00	53 77 630	White Head	212	21,58	0,03
79-155	No 5 - Flynn Road (Percé)	34 60 00	53 77 630	White Head	222	8,14	0,03
79-157	No 5 - Flynn Road (Percé)	34 60 00	53 77 630	White Head	233	15,33	0,04
79-160	No 5 - Flynn Road (Percé)	34 60 00	53 77 630	White Head	238	17,45	0,04
79-164	No 5 - Flynn Road (Percé)	34 60 00	53 77 630	White Head	247	12,15	0,04
79-231	No 5 - Flynn Road (Percé)	34 60 00	53 77 630	White Head	261	47,89	0,09

Lefèvre spl number	Section name	Location of the base of rock sections - zone 20		Formation	Stratigraphic position (m)	Insoluble Residue %	Total Org. Carbon %
		UTM east	UTM north				
79-234	No 5 - Flynn Road (Percé)	34 60 00	53 77 630	Burnt Jam Brook	267	47,39	0,10
79-235	No 5 - Flynn Road (Percé)	34 60 00	53 77 630	Burnt Jam Brook	269	24,73	0,06
79-236	No 5 - Flynn Road (Percé)	34 60 00	53 77 630	Burnt Jam Brook	275	60,9	0,11
79-237	No 5 - Flynn Road (Percé)	34 60 00	53 77 630	Burnt Jam Brook	279	23,59	0,07
79-238	No 5 - Flynn Road (Percé)	34 60 00	53 77 630	Burnt Jam Brook	280	21,05	0,05
79-239	No 5 - Flynn Road (Percé)	34 60 00	53 77 630	Burnt Jam Brook	282	70,04	0,10
79-240	No 5 - Flynn Road (Percé)	34 60 00	53 77 630	Burnt Jam Brook	285	28,93	0,04
79-241	No 5 - Flynn Road (Percé)	34 60 00	53 77 630	Burnt Jam Brook	286	5,59	0,07
79-242	No 5 - Flynn Road (Percé)	34 60 00	53 77 630	Burnt Jam Brook	288	12,54	0,05
79-245	No 5 - Flynn Road (Percé)	34 60 00	53 77 630	Laforce	290	8,06	0,08
79-246	No 5 - Flynn Road (Percé)	34 60 00	53 77 630	Laforce	292	22,69	0,21
79-247	No 5 - Flynn Road (Percé)	34 60 00	53 77 630	Laforce	295	10,87	0,07
79-248	No 5 - Flynn Road (Percé)	34 60 00	53 77 630	Saint-Léon	300	7,85	0,07
79-249	No 5 - Flynn Road (Percé)	34 60 00	53 77 630	Saint-Léon	306	7,83	0,07

Well name	Depth sup. m	Depth inf. m	Formation	Insoluble Residue %	Total Org. Carbon %	Organic extract %	Extract composition (%) Saturated	Aromatic	Resin	Asphalt.
Sunny Bank	308	309	York River	87.1	0,41					
Sunny Bank	363	366	York River	84.5	0,96					
Sunny Bank	400	403	York River	80,6	0,31					
Sunny Bank	456	459	York River	86,3	0,53					
Sunny Bank	513	516	York River	84,9	0,39					
Sunny Bank	583	585	York River	83,7	0,50					
Sunny Bank	646	644	York River	83,8	0,36					
Sunny Bank	670	673	York River	84,9	0,36					
Sunny Bank	688	689	Indian Cove	28,8	0,16	0,032	38	27	28	7
Sunny Bank	707	710	Indian Cove	40,9	0,27	0,056				
Sunny Bank	760	764	Indian Cove	55.5	0,33					
Sunny Bank	791	799	Indian Cove	55.6	0,27					
Sunny Bank	805	808	Indian Cove	60.7	0,28					
Sunny Bank	869	872	Indian Cove	62,3	0,27	0,033	28	19	39	14
Sunny Bank	895	900	Indian Cove	65,7	0,22	0,072				
Sunny Bank	928	934	Indian Cove	57,6	0,47					
Sunny Bank	957	960	Indian Cove	53,6	0,39					
Sunny Bank	977	981	Indian Cove	43.3	0,28	0,187				
Sunny Bank	1006	1007	Indian Cove	42.7	0,25					
Sunny Bank	1032	1038	Indian Cove	41.7	0,38	0,166				
Sunny Bank	1065	1067	Indian Cove	15.8	0,19					
Sunny Bank	1095	1098	Indian Cove	51.9	0,19					
Sunny Bank	1126	1129	Indian Cove	50.3	0.24					
Sunny Bank	1148	1151	Indian Cove	40.7	0,18	0,043	34	28	29	9
Sunny Bank	1181	1184	Indian Cove	44.9	0,21					
Sunny Bank	1209	1212	Indian Cove	58.7	0,38					
Sunny Bank	1238	1241	Indian Cove	63.9	0,23					
Sunny Bank	1267	1270	Indian Cove	50.6	0,19					
Sunny Bank	1295	1297	Indian Cove	53.2	0,34					
Sunny Bank	1329	1332	Indian Cove	53.0	0,48					
Sunny Bank	1376	1377	Indian Cove	56.0	0,13	0,023				
Sunny Bank	1427	1430	Indian Cove	57.6	0.13					
Sunny Bank	1455	1459	Indian Cove	44.3	0.19					
Sunny Bank	1472	1475	Indian Cove	33.5	0,20	0,033	40	24	24	12
Sunny Bank	1487	1489	Indian Cove	29.6	0,13					
Sunny Bank	1544	1547	Indian Cove	53.8	0,21					
Sunny Bank	1576	1579	Shiphead	81.9	0,21					
Sunny Bank	1623	1626	Shiphead	72.4	0,26					
Sunny Bank	1653	1654	Shiphead	75.4	0,24					
Sunny Bank	1676	1678	Shiphead	75.2	0,31	0,065				
Sunny Bank	1708	1711	Shiphead	74.3	0,24	0,046	37	18	36	9
Sunny Bank	1725	1728	Shiphead	76.4	0.24					
Sunny Bank	1757	1758	Shiphead	80.8	0.27					
Sunny Bank	1798	1801	Shiphead	80.2	0,43					
Sunny Bank	1816	1818	Shiphead	77.8	0,47	0.043				
Sunny Bank	1828	1831	Shiphead	79.8	0,41	0.034	39	21	27	13

Well name	Depth sup. m	Depth inf. m	Formation	Insoluble Residue %	Total Org. Carbon %	Organic extract %	Extract composition (%) Saturated	Aromatic	Resin	Asphalt.
Sunny Bank	1890	1893	Forillon	47,6	0,55	0,051				
Sunny Bank	1918	1921	Forillon	32,2	0,25					
Sunny Bank	1951	1954	Forillon	57,0	0,45					
Sunny Bank	1983	1986	Forillon	42,7	0,55					
Sunny Bank	2008		Forillon	51,4	0,62	0,048	42	20	31	7
Sunny Bank	2019	2022	Forillon	83,7	0,13					
Sunny Bank	2041	2045	Forillon	64,8	0,39					
Sunny Bank	2084	2087	Forillon	75,5	0,40	0,134				
Sunny Bank	2116	2119	Forillon	60,7	0,50					
Sunny Bank	2136	2137	Forillon	38,2	0,58					
Sunny Bank	2159	2161	Forillon	47,8	0,60					
Sunny Bank	2191	2195	Forillon	31,4	0,32					
Sunny Bank	2223	2227	Forillon	36,4	0,34	0,049	45	21	28	6
Sunny Bank	2258	2261	Forillon	43,6	0,62					
Sunny Bank	2297	2300	Forillon	41,9	0,35					
Sunny Bank	2338	2343	Forillon	3,2	0,18	0,042	52	23	24	1
Sunny Bank	2388	2391	Forillon	59,6	0,26					
Sunny Bank	2429	2432	Indian Pt	67,6	1,10					
Sunny Bank	2443	2445	Indian Pt	71,0	0,87					
Sunny Bank	2469	2474	Indian Pt	72,0	1,06					
Sunny Bank	2498	2501	Indian Pt	18,6	0,19					
Sunny Bank	2530	2533	Indian Pt	30,4	0,28					
Sunny Bank	2566	2571	Indian Pt	54,2	0,24					
Sunny Bank	2598	2600	Indian Pt	63,8	0,10					
Sunny Bank	2613	2615	Indian Pt	41.6	0.10	0.023	48	14	36	2
Sunny Bank	2649	2652	Indian Pt	54.9	0,30					
Sunny Bank	2711	2715	Indian Pt	52,4	0.34	0.025	49	18	32	1
Sunny Bank	2744	2747	Indian Pt	52,7	0,45					
Sunny Bank	2771	2775	Indian Pt	47,5	0,45					
Sunny Bank	2808	2809	Indian Pt	69,2	0,23					
Sunny Bank	2836	2839	Indian Pt	62.1	0,40					
Sunny Bank	2865	2868	Indian Pt	67,5	0,67					
Sunny Bank	2898	2900	Indian Pt	62,7	0.31	0,031	44	22,6	33	0,4
Sunny Bank	2925	2929	Indian Pt	61,8	0,49					
Sunny Bank	2958	2960	Indian Pt	58,1	0,67					
Sunny Bank	2989	2993	Indian Pt	75.4	0,55	0,006				
Sunny Bank	3018	3020	Indian Pt	72,4	0,45					
Sunny Bank	3047	3050	Indian Pt	71,2	0,52					
Sunny Bank	3076	3079	Indian Pt	62.2	0,35					
Sunny Bank	3107	3138	Indian Pt	68,0	0.39					
Sunny Bank	3138	3141	Indian Pt	68,3	0,35					
Sunny Bank	3168	3171	Indian Pt	70,5	0,20					
Sunny Bank	3229	3232	Indian Pt	74,4	0,11					
Sunny Bank	3253	3256	Indian Pt	76,1	0,99	0,003				
Sunny Bank	3289	3293	Indian Pt	51,6	0,50					
Sunny Bank	3318	3324	Roncelles	52.5	0.20					

Well name	Depth sup. m	Depth inf. m	Formation	Insoluble Residue %	Total Org. Carbon %	Organic extract %	Extract composition (%) Saturated	Aromatic	Resin	Asphalt.
Sunny Bank	3355	3358	Roncelles	49,3	0.27					
Sunny Bank	3367	3370	Roncelles	50,6	0.32	0,010				
Sunny Bank	3413	3419	Roncelles	69,6	0.08					
Sunny Bank	3446	3449	Roncelles	67,7	0,15					
Sunny Bank	3475	3478	Roncelles	58,3	0,07					
Sunny Bank	3506	3509	Roncelles	59,0	0,19					
Sunny Bank	3533	3536	Roncelles	68,2	0,22					
York		26	West Point	49,2	0,08	0,002				
York		57	West Point	64,4	0,16					
York		76	West Point	78,8	0,09					
York		152	Gascons	68,6	0,07					
York		182	Gascons	73,3	0,07					
York		209	Gascons	68,4	0,06					
York		239	Gascons	70,1	0,07					
York		274	Gascons	78,6	0,16					
York		291	Gascons	69,7	0,13					
York		303	Gascons	80,1	0,15					
York		338	Gascons	69,0	0,08					
York		368	Gascons	71,9	0,09					
York	392	393	Gascons	75.3	0,10					
York	418	419	Gascons	76,4	0.13					
York	468	469	Gascons	26.4	0.05					
York	489	491	Gascons	69,1	0.12					
York	521	523	Gascons	71,9	0,16					
York	550	555	Gascons	87,4	0.53	0,045	35	27	38	
York	565	567	Gascons	83,0	0,13					
York	600	602	Gascons	75,9	0.14	0,004				
York	636	637	Gascons	81,9	0,11					
York		666	Gascons	83,2	0,17					
York	695	700	Gascons	76,9	0,07					
York		723	Gascons	79,4	0,12					
York		755	Gascons	84.8	0.19					
York		781	Gascons	85.8	0.23					
York		793	Laforce	83,2	0,17					
York	809	811	Laforce	87,9	0,23					
York	850	852	Laforce	71.4	0,02					
York	882	884	Laforce	27,7	0,05					
York	896	898	Laforce	81,4	0,37					
York	901	902	Laforce	14,9	0,05					
York	956	957	Laforce	88.0	0,14					
York		994	Laforce	53,9	1,12					
York	1021	1023	Burnt Jam Brook	70.4	0,19					
York		1052	Burnt Jam Brook	83.5	0.15					
York		1080	Burnt Jam Brook	72,9	0.49	0,011				
York		1109	Burnt Jam Brook	53,9	0,59					
York		1129	Burnt Jam Brook	89.3	0.32					

Annex 4.2: Thermal maturation of Gaspé Peninsula; reflectance data

STAT = statistical parameters: n : number of measurements, moy: mean value of reflectance, Sx : standard deviation of reflectance values

Inert. = mean reflectance (Ro) of inertinite in %; Tel = Ro of telinite; tcoll = Ro of collotellinite; Spore = Ro of sporinite; Exinite = Ro of undifferentiated exinite; Chit. = Ro of chitinozoans; Hydr. = Ro of hydroids; Scol. = Ro of scolecodonts; Protob. Ro of protobitumen; Pyrob. = Ro of undifferentiated asphaltic pyrobitumen; Coke = Ro of native coke.

Mean est. Ro = Estimated mean reflectance of standard vitrinite (collotelinite) according the reflectance of undifferentiated asphaltic pyrobitumen

Mean est. Ro telocol.. = Mean values of the estimated Ro of telocollinite (collotelinite) calculate according the mean values Ro of telinite (Tel.), collotelinite (Tcoll), sporinite (Spor.), hydroids (Hyd.) and scolecodonts (Scol).

26 pages

INRS	Location		Depth/ Stratigraphic position	Well number	Formation	STAT	Macerals					Zooclasts			Solid bitumen			Estimated Ro of telocollinite						Mean est Ro Pyro.	Mean est Ro telocol.
	UTM est	UTM west					Inert	Tel.	Tcoll	Spore	Exinite	Chit.	Hydr.	Scol.	Protob.	Pyrob.	Coke	Tel.	Tcoll	Spor.	Chit.	Hyd.	Scol.		
24370	229600	5427700	24,4	P. 30-815	Indian Cove	n	1	10				37				8									
						moy	7,03	5,11				7,93				5,93		5,11			5,60			5,45	5,49
						Sx	0,00	0,30				1,93				1,43									
24371	229600	5427700	61,0	P. 30-815	Indian Cove	n	37	11				3				3									
						moy	5,22	4,94				7,35				7,35		4,94			5,33			6,24	5,02
						Sx	0,64	0,89				2,31				1,04									
24372	229600	5427700	176,8	P. 30-815	Indian Cove	n	10	31	27							15									
						moy	5,56	6,83	7,27							6,29		6,83	7,27					5,65	7,03
						Sx	0,77	1,32	1,11							1,34									
24373	229600	5427700	219,5	P. 30-815	Indian Cove	n	6	45	9			1	5												
						moy	6,57	6,14	8,23			5,49	8,65					6,14	8,23		4,40	6,87			6,48
						Sx	1,29	1,25	1,11				0,69												
24428	232600	5424120	4,0	P. 30-841	Grande Grève	n	5	38	5			30				7	4								
						moy	3,92	5,07	5,48			8,75				5,03	5,20	5,07	5,48		5,96			4,91	5,46
						Sx	0,57	0,79	0,82			1,24				0,66	0,24								
24429	232600	5424120	45,7	P. 30-841	Grande Grève	n	16	5				34				20	8								
						moy	4,82	5,38				9,62				5,64	5,73	5,38			6,33			5,27	6,21
						Sx	0,62	0,65				1,42				1,04	0,71								
24431	232600	5424120	177,7	P. 30-841	Grande Grève	n	8	8	8			40	3			12	3								
						moy	3,20	4,00	4,00			8,14	7,97			5,23	4,77	4,00	4,00		5,69	6,41		5,03	5,27
						Sx	0,40	0,90	0,90			2,16	1,69			1,41	0,35								
24437	232600	5424120	381,0	P. 30-841	Cap-Bon-Ami	n		6				16				2									
						moy		6,15				7,65				3,68		6,15			5,47			3,96	5,66
						Sx		1,51				0,68				0,26									
24529	231610	5430280	4,6	P. 30-854	Grande Grève	n	14	66	7			10				5									
						moy	4,09	4,07	4,33			4,13				3,70		4,07	4,33		3,61			3,98	4,03
						Sx	0,55	0,53	0,35			0,53				0,69									
24532	231610	5430280	128,0	P. 30-854	Grande Grève	n	3	54	5	2		10				2	3								
						moy	3,83	3,59	4,00	3,30		4,02				3,12	6,02	3,59	4,00		3,54			3,50	3,51
						Sx	0,24	0,37	0,41	0,16		0,56				0,20	0,01								
24537	231610	5430280	472,4	P. 30-854	Grande Grève	n	19	25	11	10		14				20	2								
						moy	4,22	4,17	4,29	3,71		5,29				4,25	4,68	4,17	4,29		4,29			4,39	3,52
						Sx	0,36	0,37	0,26	0,51		0,56				0,48	0,68								
24539	231610	5430280	583,4	P. 30-854	Grande Grève	n	17	9		16		27													
						moy	4,81	4,50		3,86		5,36						4,50			4,33				3,03
						Sx	0,50	0,72		0,38		0,81													
24541	231610	5430280	702,6	P. 30-854	Grande Grève	n	2	15	9			31				18	3								
						moy	3,90	5,06	5,36			6,05				4,72	4,36	5,06	5,36		4,69			4,71	4,90
						Sx	0,15	0,71	0,77			0,58				0,99	0,08								
24544	231610	5430280	771,8	P. 30-854	Cap-Bon-Ami	n	4	61	5			21													
						moy	5,55	4,64	5,01			5,99	5,50					4,64	5,01		4,66	4,67			4,66
						Sx	0,24	0,68	0,35			0,55													
24549	231610	5430280	1145,1	P. 30-854	Cap-Bon-Ami	n		23	17				3			9									
						moy		5,47	5,27				4,33			5,10		5,47	5,27			3,80		4,95	5,28
						Sx		0,76	0,60				0,73			0,76									
24553	231610	5430280	1365,2	P. 30-854	St-Léon 7	n		7				5	3			2									
						moy		5,13				7,29	7,22			6,11		5,13			5,30	5,89		5,55	5,34
						Sx		0,58				0,82	0,21			0,15									

INRS	Location		Depth/ Stratigraphic position	Well number	Formation	STAT	Macerals					Zooclasts			Solid bitumen			*Estimated Ro of telocollinite*						*Mean est. Ro Pyro.*	*Mean est. Ro telocol.*
	UTM est	UTM west					Inert.	Tel.	Tcoll	Spore	Exinite	Chit.	Hydr.	Scol.	Protob.	Pyrob.	Coke	*Tel.*	*Tcoll*	*Spor.*	*Chit.*	*Hyd.*	*Scol.*		
24558	228450	5423160	3,0	P. 34-90-1	Indian Cove	n	17	9	13			8				34	2								
						moy	5,02	5,91	6,02			6,90				4,72	4,06	5,91	6,02		5,12			4,71	5,75
						Sx	0,96	1,02	0,93			0,80				0,71	0,14								
24559	228450	5423160	13,7	P. 34-90-1	Indian Cove	n	4			14	9	60													
						moy	7,26			4,56	4,52	7,11								4,56	5,22				5,09
						Sx	0,35			0,46	0,72	0,93													
24705	414800	5400300	0,5	1A-1001	Forillon	n		3	5			2	18	13	9										
						moy		1,05	1,28			0,83	0,75	0,55	0,45			0,92	1,28		0,65	0,68	0,71		0,78
						Sx		0,05	0,13			0,17	0,04	0,06	0,08										
24717	414622	5400092	107,0	1A-1026	Shiphead	n	3	18	3		13	16		12	30	6									
						moy	1,27	1,09	0,74		0,13	0,72		0,63	0,40	0,65		0,98	0,74		0,51		0,86	0,52	0,78
						Sx	0,08	0,05	0,02		0,03	0,03		0,12	0,06	0,03									
24721	414558	5400017	145,5	1A-1039	Shiphead	n		6				60	5												
						moy		0,79				0,70	0,61					0,61			0,49	0,53			0,50
						Sx		0,05				0,04	0,01												
24726	414500	5399950	180,5	1A-1046	Indian Cove	n	8	30	13			42	18												
						moy	1,75	0,73	0,76			0,76	0,75					0,55	0,76		0,56	0,68			0,60
						Sx	0,41	0,13	0,07			0,06	0,06												
24760	382140	5423900	29,0	5-1011	Forillon	n	16	16	3	3		48	3	3	6										
						moy	1,48	1,17	0,95	0,52		0,99	1,04	0,71	0,58			1,08	0,95	1,01	0,88	1,02	1,01		0,94
						Sx	0,72	0,09	0,04	0,01		0,07	0,03	0,01	0,02										
24763	382080	5423800	227,3	5-1017	Forillon	n	13	21	5			35		5	5	16									
						moy	1,37	0,97	1,29			1,01		0,59	0,52	0,84		0,82	1,29		0,91		0,79	0,82	0,90
						Sx	0,12	0,21	0,08			0,11		0,02	0,03	0,09									
24764	381970	[illegible]	271,5	5-1022	Shiphead	n	3	9	9		3	36				5									
						moy	1,69	1,23	1,23		0,12	0,97				0,92		1,16	1,23		0,85			0,96	0,96
						Sx	0,03	0,08	0,08		0,01	0,07				0,01									
24783	340200	5436600	33,0	9-1003	Saint-Léon	n	2	17	6	11	7	29	6		2	13									
						moy	2,37	1,91	1,43	1,03	0,95	1,77	1,78	1,40	1,18	1,21		1,91	1,43	1,44	1,82	1,78	1,95	1,46	1,74
						Sx	0,08	0,18	0,24	0,09	0,14	0,19	0,24		0,01	0,08									
24785	339350	5436050	220,0	9-1008	Forillon	n	16	48	5	1	8	20	5		3	3									
						moy	2,27	1,72	1,77	1,59	0,46	1,75	1,87		0,85	1,38		1,72	1,77	1,65	1,80	1,86		1,68	1,75
						Sx	0,20	0,15	0,11		0,27	0,10	0,06		0,03	0,02									
24786	339250	5435800	425,0	9-1010	Forillon	n	8	29	2		13	18			2	4									
						moy	1,96	1,65	1,41		0,73	1,85			0,87	1,29		1,65	1,41		1,90			1,57	1,73
						Sx	0,05	0,10	0,03		0,08	0,12			0,04	0,18									
24788	339900	5435650	511,0	9-1014	Shiphead	n	24	40				29			10	2									
						moy	2,28	1,68				1,69			0,62	1,58		1,68			1,75			1,92	1,71
						Sx	0,17	0,20				0,19			0,15	0,02									
24789	339926	5435611	571,0	9-1016	Shiphead	n	27	54	18			6			7	16	2								
						moy	2,29	1,74	1,65			1,90			0,60	1,47	3,46	1,74·	1,65		1,94			1,79	1,73
						Sx	0,18	0,21	0,13			0,12			0,15	0,34	0,18								
24791	340063	5435450	770,0	9-1022	Indian Cove	n	30	29			4	27				12	5								
						moy	2,44	1,63			0,67	1,55				1,30	2,02	1,63			1,61			1,58	1,62
						Sx	0,58	0,18			0,00	0,12				0,21	0,08								
24793	340134	5435393	805,0	9-1025	Indian Cove	n	15	28				55			4	6									
						moy	2,37	1,80				1,54			0,63	1,17		1,80			1,60			1,41	1,67
						Sx	0,26	0,08				0,21			0,13	0,33									

INRS	Location		Depth/ Stratigraphic position	Well number	Formation	STAT	Macerals					Zooclasts			Solid bitumen			*Estimated Ro of telocollinite*						*Mean est. Ro*	*Mean est. Ro*
	UTM est	UTM west					Inert.	Tel.	Tcoll	Spore	Exinite	Chit.	Hydr.	Scol.	Protob	Pyrob.	Coke	*Tel.*	*Tcoll*	*Spor.*	*Chit.*	*Hyd.*	*Scol.*	*Pyro.*	*telocol.*
24795	340352	5435218	912,0	9-1031	Indian Cove	n		8	8		11	27			6	39									
						moy		1,40	1,61		0,25	1,57			0,47	1,09		1,40	1,61		1,63			1,27	1,58
						Sx		0,11	0,08		0,06	0,21			0,15	0,26									
24797	340497	5435103	983,0	9-1034	York Lake	n	66		14			1			9	22									
						moy	1,61		0,95			1,06			0,76	1,15			0,95		0,98			1,38	0,95
						Sx	0,20		0,01						0,1	0,33									
24799	333860	5436050	-0,9	10-1004	Saint-Léon	n	6	3	5			2													
						moy	2,37	1,94	1,82			2,84						1,94	1,82		2,72				2,04
						Sx	0,79	0,07	0,11			0,72													
24802	333578	5434978	301,5	10-1010	Forillon	n	12	43	6	1		19	6			9	2								
						moy	3,28	1,92	2,07	1,25		1,83	1,95			1,76	4,87	1,92	2,07	1,54	1,88	1,92		2,13	1,92
						Sx	0,40	0,25	0,21			0,20	0,06			0,09	0,95								
24805	333500	5434900	334,5	10-1017	Forillon	n	5	39		3		43				12									
						moy	2,81	1,99		1,82		2,02				1,91		1,99		1,82	2,05			2,30	2,01
						Sx	0,29	0,20		0,04		0,28				0,21									
24806	332250	5435000	537,0	10-1018	Shiphead	n	23	18	21	4		13			4	11	3								
						moy	2,58	2,00	1,96	1,64		2,06			1,33	1,83	2,03	2,00	1,96	1,67	2,09			2,21	1,98
						Sx	0,18	0,14	0,12	0,43		0,24			0,09	0,26	0,13								
24807	313250	5432600	207,0	11-1002	Forillon	n	6		6	14		4				23	2								
						moy	3,49		2,95	2,98		3,35				3,24	2,76		2,95	2,98	3,09			3,61	2,99
						Sx	0,53		0,16	0,23		0,43				0,37	0,18								
24808	313250	5433100	167,0	11-1008	Forillon	n	58	15	4			8				1	1								
						moy	3,61	2,91	2,65			3,52				3,86	3,86	2,91	2,65		3,21			4,10	2,96
						Sx	0,27	0,11	0,31			0,67				0,00									
24810	313250	5433380	20,0	11-1012	Forillon	n		16		3		10				15									
						moy		3,22		3,78		3,33				3,36		3,22		3,78	3,08			3,70	3,23
						Sx		0,28		0,21		0,47				0,58									

INRS	Location		Formation	STAT	Macerals				Zooclasts				Solid bitumen			Estimated Ro of telocollinite						Mean est. Ro	Mean est. Ro
					Inert	Tel.	Tcoll	Exinite	Chit.	Grap.	Hydr.	Scol.	Protob.	Pyrob.	Coke								
	UTM est	UTM west														Tel.	Tcoll	Chit.	Grapt.	Hyd.	Scol.	Pyro.	telocol.
13192	370602	5411841	Cap-Bon-Ami	n				14	24		8		29	13									
13192				moy				0,49	0,85		0,74		0,34	0,75				0,68		0,67		0,69	0,68
13192				Sx				0,08	0,07		0,04		0,11	0,14									
13145	389450	5420000	Indian Cove	n	28	10			28			9	20	18									
13145				moy	1,23	0,85			0,70			0,44	0,35	0,85		0,68		0,49			0,51	0,84	0,54
13145				Sx	0,16	0,05			0,06			0,03	0,05	0,24									
13164	367000	5413350	Indian Cove	n				5	21				22	16									
13164				moy				0,11	0,98				0,27	1,08				0,86				1,21	0,86
13164				Sx				0,02	0,06				0,07	0,46									
13165	366700	5413300	Indian Cove	n	6	25			52			30	23	11									
13165				moy	1,27	0,95			0,88			0,50	0,39	0,74		0,73		0,72			0,62	0,68	0,70
13165				Sx	0,20	0,11			0,10			0,04	0,11	0,20									
13169	366350	5412920	Indian Cove	n	5				60				24	20									
13169				moy	1,25				0,80				0,36	0,67				0,61				0,58	0,61
13169				Sx	0,17				0,10				0,11	0,24									
13170	366700	5411950	Indian Cove	n		8		6	18			10	21	21									
13170				moy		1,02		0,11	0,77			0,53	0,37	0,72		0,79		0,57			0,68	0,65	0,65
13170				Sx		0,09		0,06	0,06			0,02	0,12	0,09									
13211	366967	5426421	Indian Cove	n	6	10		28					34	11									
13211				moy	1,12	0,86		0,12					0,51	1,20		0,69						1,42	0,69
13211				Sx	0,11	0,06		0,04					0,13	0,15									
13212	365636	5425363	Indian Cove	n	13	41		21	36			14	24	14									
13212				moy	1,50	1,07		0,22	1,05			0,65	0,53	0,90		0,95		0,96			0,90	0,93	0,95
13212				Sx	0,12	0,22		0,06	0,08			0,03	0,06	0,13									
13222	357557	5421333	Indian Cove	n	6		6	10	14				14	26									
13222				moy	1,73		1,05	0,16	0,91				0,32	1,12			1,05	0,76				1,33	0,85
13222				Sx	0,05		0,04	0,02	0,11				0,09	0,25									
13224	357102	5420600	Indian Cove	n				34	22			10	8										
13224				moy				0,12	0,80			0,54	0,43					0,61			0,69		0,64
13224				Sx				0,01	0,07			0,02	0,07										
13231	358641	5418411	Indian Cove	n		20			13				11	12									
13231				moy		0,85			0,82				0,35	0,82		0,68		0,64				0,79	0,66
13231				Sx		0,14			0,04				0,11	0,27									
13234	359349	5416329	Indian Cove	n				9	39				11	27									
13234				moy				0,10	0,84				0,45	0,56				0,67				0,41	0,67
13234				Sx				0,06	0,05				0,08	0,09									
13236	362996	5413949	Indian Cove	n	5			5	55		8		19										
13236				moy	1,26			0,47	0,84		0,78		0,28					0,67		0,72			0,67
13236				Sx	0,10			0,02	0,07		0,08		0,09										
13242	377724	5402418	Indian Cove	n				18	36			8	18	28									
13242				moy				0,17	1,03			0,63	0,44	0,82				0,94			0,86	0,79	0,92
13242				Sx				0,06	0,09			0,02	0,06	0,17									
13243	378779	5402741	Indian Cove	n				7	22				32	11									
13243				moy				0,09	1,06				0,49	0,86				0,98				0,85	0,98
13243				Sx				0,02	0,11				0,06	0,10									
13246	380806	5401280	Indian Cove	n				21	6														
13246				moy				0,14	1,21									1,20					1,20
13246				Sx				0,04	0,07														

INRS	Location		Formation	STAT	Macerals				Zooclasts				Solid bitumen			*Estimated Ro of telocollinite*						*Mean est. Ro*	*Mean est. Ro*
	UTM est	UTM west			Inert	Tel.	Tcoll	Exinite	Chit.	Grap.	Hydr.	Scol.	Protob.	Pyrob.	Coke	*Tel.*	*Tcoll*	*Chit.*	*Grapt.*	*Hyd.*	*Scol.*	*Pyro.*	*telocol.*
13248	381298	5401829	Indian Cove	n				10	16		8		6										
13248				moy				0,16	1,02		0,77		0,42					0,92		0,70			0,85
13248				Sx				0,09	0,09		0,05		0,10										
13282	389950	5395800	Indian Cove	n	21	20		19	33				24	17									
13282				moy	1,42	0,95		0,20	0,97				0,43	1,08		0,80		0,85				1,25	0,83
13282				Sx	0,17	0,18		0,02	0,07				0,14	0,33									
13283	390050	5396950	Indian Cove	n	8	27		19	38				19	15									
13283				moy	1,46	0,87		0,11	1,00				0,36	0,75		0,66		0,89				0,67	0,80
13283				Sx	0,24	0,20		0,00	0,09				0,11	0,05									
13284	390450	5397700	Indian Cove	n	27	40		21	43		11	24	12	7									
13284				moy	1,19	0,80		0,17	0,88		0,78	0,52	0,40	0,81		0,62		0,72		0,72	0,66	0,77	0,68
13284				Sx	0,15	0,15		0,02	0,06		0,06	0,02	0,11	0,20									
13291	388894	5410212	Indian Cove	n	20	22			58		10	33	22	9									
13291				moy	1,29	0,98			0,94		0,83	0,56	0,48	0,94		0,84		0,81		0,77	0,73	1,00	0,79
13291				Sx	0,10	0,17			0,08		0,04	0,04	0,09	0,35									
13292	388782	5412898	Indian Cove	n	21	36			48		8	9	22										
13292				moy	1,33	0,81			0,91		0,83	0,49	0,40			0,63		0,76		0,77	0,60		0,70
13292				Sx	0,13	0,07			0,07		0,13	0,02	0,12										
13206	368667	5427936	Shiphead	n				48					27	9									
13206				moy				0,09					0,33	1,04								1,18	
13206				Sx				0,02					0,11	0,25									
13210	367336	5426816	Shiphead	n				19	14				20	24									
13210				moy				0,27	0,86				0,45	0,59				0,70				0,44	0,70
13210				Sx				0,02	0,12				0,08	0,18									
13132	375700	5426400	Shiphead	n	39	6		17	47					10									
13132				moy	1,30	0,85		0,14	0,94					0,97		0,68		0,81				1,05	0,79
13132				Sx	0,17	0,02		0,02	0,07					0,30									
13204	369120	5428280	Forillon	n	6	46		7															
13204				moy	1,41	1,13		0,05								1,03							1,03
13204				Sx	0,11	0,08		0,05															
13205	369015	5428207	Forillon	n	11	22		5				6	16	20									
13205				moy	1,49	1,14		0,10				0,41	0,41	0,70		0,90					0,47	0,59	0,81
13205				Sx	0,12	0,10		0,03				0,01	0,07	0,06									
13209	367581	5426935	Forillon	n	18	41	7	12	15				26	12									
13209				moy	1,38	1,06	1,04	0,03	1,05				0,40	0,86		0,94	1,04	0,96				0,86	0,96
13209				Sx	0,09	0,08	0,07	0,02	0,08				0,15	0,18									
13232	359131	5416858	Forillon	n	9			17	37		12		26	15									
13232				moy	1,48			0,14	0,68		0,66		0,41	0,73				0,47		0,58		0,64	0,50
13232				Sx	0,44			0,00	0,05		0,02		0,08	0,34									
13235	360579	5415628	Forillon	n		11		12	39				31	12									
13235				moy		1,06		0,05	0,86				0,30	0,67		0,83		0,70				0,55	0,72
13235				Sx		0,07		0,01	0,05				0,12	0,05									
13240	376859	5401008	Forillon	n	81	20	6							87									
13240				moy	1,79	1,43	1,21							1,11	-	1,43	1,21					1,31	1,38
13240				Sx	0,24	0,19	0,05							0,22									
13271	398750	5413850	Forillon	n	13	16	13	23	57			11	13	20									
13271				moy	1,69	1,04	0,75	0,13	0,82			0,42	0,46	0,88		0,91	0,75	0,64			0,49	0,89	0,68
13271				Sx	0,53	0,06	0,09	0,03	0,07			0,02	0,05	0,23									

INRS	Location		Formation	STAT	Macerals				Zooclasts				Solid bitumen			Estimated Ro of telocollinite						Mean est. Ro	Mean est. Ro
	UTM est	UTM west			Inert	Tel.	Tcoll	Exinite	Chit.	Grap.	Hydr.	Scol.	Protob	Pyrob.	Coke	*Tel.*	*Tcoll*	*Chit.*	*Grapt.*	*Hyd.*	*Scol.*	*Pyro.*	*telocol.*
13140	381850	5424750	Indian Pt	n	12																		
13140				moy	1,69																		
13140				Sx	0,11																		
13142	381850	5424750	Indian Pt	n	33	6		30						7									
13142				moy	1,74	1,34		0,18						1,07		*1,32*						1,23	1,32
13142				Sx	0,33	0,23		0,03						0,05									
13148	390050	5422170	Indian Pt	n	21			28	31			37		12									
13148				moy	1,76			0,48	1,20			0,91		0,79				*1,19*			*1,38*	0,74	1,29
13148				Sx	0,21			0,03	0,10			0,07		0,12									
13268	398800	5414600	Indian Pt	n	33	15		13	35			17	24										
13268				moy	1,22	0,88		0,10	1,00			0,63	0,50			*0,72*		*0,89*			*0,86*		0,84
13268				Sx	0,08	0,10		0,06	0,09			0,05	0,09										
13203	369245	5428821	Roncelles	n				19															
13203				moy				0,17															
13203				Sx				0,03															
13267	399857	5415400	Roncelles	n				22			6	15		37									
13267				moy				0,24			1,04	0,85		0,81						*1,02*	*1,27*	0,77	1,20
13267				Sx				0,00			0,05	0,07		0,09									
13201	368970	5429166	West Point	n			6	48				8	12	8									
13201				moy			0,68	0,14				0,64	0,40	0,66			*0,68*				*0,88*	0,53	0,79
13201				Sx			0,04	0,01				0,03	0,14	0,18									
13238	373817	5399554	Laforce	n				5						73	7								
13238				moy				0,09						1,78	2,46							2,16	
13238				Sx				0,01						0,21	0,13								
13135	375900	5427550	Quebec Gp	n										34									
13135				moy										2,30								2,72	
13135				Sx										0,24									
13136	375900	5427550	Quebec Gp	n										41	5								
13136				moy										2,25	2,71							2,67	
13136				Sx										0,14	0,11								
13272	391400	5423400	Quebec Gp	n										6									
13272				moy										1,43								1,74	
13272				Sx										0,83									
13273	395214	5426350	Quebec Gp	n					12					33									
13273				moy					2,44					2,35				*2,41*				2,77	2,41
13273				Sx					0,11					0,17									
13274	[illegible]	5426250	Quebec Gp	n										43									
13274				moy										2,66								3,08	
13274				Sx										0,15									
13275	404650	5420650	Quebec Gp	n					20	10				52									
13275				moy					3,06	3,00				2,93				*2,89*	*2,80*			3,33	2,86
13275				Sx					0,24	0,18				0,25									
13276	407150	5419050	Quebec Gp	n										38									
13276				moy										2,69								3,11	
13276				Sx										0,21									
13278	411600	5411850	Quebec Gp	n						28				16									
13278				moy						2,83				2,44					*2,68*			2,86	2,68
13278				Sx						0,18				0,17									

INRS	Location		Formation	STAT	Macerals						Zooclasts		Solid bitumen			Estimated Ro of telocollinite					Mean est. Ro	Mean est. Ro
	UTM est	UTM west			Inert	Tel.	Tcoll	Coll	Spor.	other exinite	Chit.	Scol.	Protob.	Pyrob.	Coke	*Tel.*	*Tcoll*	*Spor.*	*Chit.*	*Scol.*	*Pyro.*	*telocol.*
13102	389300	5411603	Battery Pt	n						5				**26**								
13102			Battery Pt	moy						0,12				**0,85**							***0,77***	
13102			Battery Pt	Sx						0,03				**0,11**								
13102	389300	5411603	Battery Pt	n			**20**			22				**12**								
13102			Battery Pt	moy			**0,70**			0,12				**0,98**			*0,70*				***0,90***	**0.70**
13102			Battery Pt	Sx			**0,07**			0,03				**0,08**								
13117	380750	5418850	Battery Pt	n										**30**								
13117			Battery Pt	moy										**1,28**							***1,18***	
13117			Battery Pt	Sx										**0,09**								
13117	380750	5418850	Battery Pt	n										**60**								
13117			Battery Pt	moy										**1,19**							***1,10***	
13117			Battery Pt	Sx										**0,15**								
13123	381770	5420750	Battery Pt	n	10									**20**								
13123			Battery Pt	moy	1,63									**0,91**							***0,82***	
13123			Battery Pt	Sx	0,13									**0,11**								
13123	381770	5420750	Battery Pt	n	12					27			39	**43**								
13123			Battery Pt	moy	1,02					0,13			0,39	**0,60**							***0,54***	
13123			Battery Pt	Sx	0,09					0,03			0,13	**0,21**								
13155	398750	5405300	Battery Pt	n					**5**				8	**12**	**9**							
13155			Battery Pt	moy					**0,75**				0,47	**1,00**	**5,35**			*1,26*			***0,91***	**1.26**
13155			Battery Pt	Sx					**0,04**				0,12	**0,37**	**0,43**							
13160	402730	5397000	Battery Pt	n	6			6	**8**	6			31	**23**	**5**							
13160			Battery Pt	moy	1,19			1,04	**0,17**	0,19			0,36	**0,73**	**2,12**			*0,49*			***0,66***	**0.49**
13160			Battery Pt	Sx	0,11			0,04	**0,01**	0,01			0,06	**0,11**	**0,77**							
13261	405143	5408370	Battery Pt	n									7									
13261			Battery Pt	moy									0,42									
13261			Battery Pt	Sx									0,05									
13262	401133	5405320	Battery Pt	n	50	**28**																
13262			Battery Pt	moy	1,76	**1,17**										*1,08*						**1.08**
13262			Battery Pt	Sx	0,18	**0,15**																
13279	394700	5413040	Battery Pt	n						11			8	**29**								
13279			Battery Pt	moy						0,14			0,22	**1,40**							***1,30***	
13279			Battery Pt	Sx						0,03			0,05	**0,34**								
13280	391470	5410200	Battery Pt	n	39	**34**	**15**		**10**	9			7	**12**	**6**							
13280			Battery Pt	moy	1,46	**1,22**	**1,31**		**0,47**	0,25			0,64	**1,31**	**1,41**	*1,15*	*1,31*	*0,95*			***1,21***	**1.16**
13280			Battery Pt	Sx	0,15	**0,07**	**0,10**		**0,19**	0,04			0,47	**0,19**	**0,20**							
13281	391625	5410226	Battery Pt	n	60	**6**		51		6				**8**								
13281			Battery Pt	moy	1,52	**1,09**		0,86		0,24				**0,78**		*0,98*					***0,71***	**0.98**
13281			Battery Pt	Sx	0,20	**0,06**		0,14		0,02				**0,06**								
13295	394600	5389350	Battery Pt	n	32	**30**		7	**24**				11	**11**								
13295			Battery Pt	moy	1,29	**0,75**		0,74	**0,21**				0,43	**1,02**		*0,57*		*0,57*			***0,93***	**0.57**
13295			Battery Pt	Sx	0,27	**0,28**		0,16	**0,03**				0,33	**0,20**								
13296	395750	5388850	Battery Pt	n	40	**14**		7	**24**				19	**11**								
13296			Battery Pt	moy	1,23	**0,85**		0,74	**0,21**				0,39	**1,02**		*0,68*		*0,57*			***0,93***	**0.61**
13296			Battery Pt	Sx	0,24	**0,07**		0,16	**0,03**				0,26	**0,20**								

INRS	Location		Formation	STAT	Macerals						Zooclasts		Solid bitumen			Estimated Ro of telocollinite					Mean est. Ro	Mean est. Ro
	UTM est	UTM west			Inert	Tel.	Tcoll	Coll	Spor	other exinite	Chit.	Scol.	Protob.	Pyrob.	Coke	Tel.	Tcoll	Spor.	Chit.	Scol.	Pyro.	telocol.
13297	397550	5388300	Battery Pt	n	41	14		9		25				10								
13297			Battery Pt	moy	1,20	0,71		0,64		0,19				1,06		0,52					0,97	0,52
13297			Battery Pt	Sx	0,13	0,09		0,06		0,12				0,21								
13302	398650	5390350	Battery Pt	n	39	41	15	6		17				10								
13302			Battery Pt	moy	1,07	0,72	0,67	0,57		0,13				1,09		0,53	0,67				1,00	0,57
13302			Battery Pt	Sx	0,09	0,09	0,06	0,04		0,03				0,30								
13305	399700	5387200	Battery Pt	n	6		5							5								
13305			Battery Pt	moy	1,00		0,82							1,04			0,82				0,95	0,82
13305			Battery Pt	Sx	0,17		0,06							0,59								
13306	400550	5397000	Battery Pt	n	36	5				19			17	39								
13306			Battery Pt	moy	0,98	0,64				0,10			0,25	0,75		0,46					0,68	0,46
13306			Battery Pt	Sx	0,12	0,05				0,04			0,07	0,24								
13308	400420	5397000	Battery Pt	n	53	6		37		6			7	32								
13308			Battery Pt	moy	0,95	0,83		0,42		0,15			0,26	0,91		0,66					0,83	0,66
13308			Battery Pt	Sx	0,24	0,17		0,13		0,08			0,03	0,32								
13309	398600	5397250	Battery Pt	n	48		31	15		25			16	20	6							
13309			Battery Pt	moy	1,20		0,62	0,71		0,16			0,35	0,96	2,72		0,62				0,88	0,62
13309			Battery Pt	Sx	0,13		0,08	0,11		0,09			0,09	0,27	1,33							
13105	389150	5409770	York River	n	24		27			30			5	44								
13105			York River	moy	1,16		0,54			0,10			0,44	0,61			0,54				0,55	0,54
13105			York River	Sx	0,13		0,12			0,02			0,02	0,12								
13111	381500	5416250	York River	n	39		33	6		21				6								
13111			York River	moy	1,25		0,78	0,72		0,19				0,87			0,78				0,79	0,78
13111			York River	Sx	0,17		0,13	0,08		0,07				0,15								
13114	380000	5415100	York River	n						28				65								
13114			York River	moy						0,15				0,82							0,74	
13114			York River	Sx						0,05				0,38								
13119	380000	5418950	York River	n						16			5	70								
13119			York River	moy						0,16			0,42	1,24							1,14	
13119			York River	Sx						0,03			0,03	0,54								
13120	380000	5418950	York River	n	37									54								
13120			York River	moy	0,94									1,10							1,01	
13120			York River	Sx	0,10									0,17								
13151	389500	5418650	York River	n	56	32	14		7					10								
13151			York River	moy	1,37	0,96	0,88		0,35					0,92		0,81	0,88	0,80			0,84	0,83
13151			York River	Sx	0,16	0,15	0,09		0,07					0,20								
13161	389972	5407784	York River	n	10		20			28			16	15								
13161			York River	moy	0,78		0,47			0,11			0,25	0,45			0,47				0,42	0,47
13161			York River	Sx	0,09		0,12			0,04			0,04	0,09								
13163	389972	5407784	York River	n		9	11							21								
13163			York River	moy		0,65	0,54							0,89		0,46	0,54				0,81	0,50
13163			York River	Sx		0,03	0,08							0,15								
13167	367050	5413650	York River	n	24	22	18	6		17				18								
13167			York River	moy	1,07	0,72	0,58	0,62		0,14				1,29		0,53	0,58				1,19	0,56
13167			York River	Sx	0,11	0,04	0,10	0,15		0,02				0,64								

INRS	Location		Formation	STAT	Macerals						Zooclasts		Solid bitumen			Estimated Ro of telocollinite					Mean est. Ro	Mean est. Ro
	UTM est	UTM west			Inert.	Tel.	Tcoll	Coll	Spor.	other exinite	Chit.	Scol.	Protob.	Pyrob.	Coke	Tel.	Tcoll	Spor.	Chit.	Scol.	Pyro.	telocol.
13173	375800	5410430	York River	n	44	50	31							5								
13173			York River	moy	1,25	0,81	0,55							1,21		0,63	0,55				1,12	0.60
13173			York River	Sx	0,20	0,12	0,17							0,17								
13175	374365	5412610	York River	n	13	25	15	12		16				22								
13175			York River	moy	1,35	0,76	0,60	0,51		0,16				0,91		0,58	0,60				0,83	0.59
13175			York River	Sx	0,12	0,10	0,05	0,04		0,05				0,28								
13176	366959	5410823	York River	n										17	6							
13176			York River	moy										0,88	3,39						0,80	
13176			York River	Sx										0,40	1,60							
13188	371323	5409079	York River	n	38		25			12			18	17								
13188			York River	moy	0,97		0,56			0,09			0,35	0,98			0,56				0,89	0.56
13188			York River	Sx	0,17		0,08			0,02			0,06	0,43								
13189	370371	5411073	York River	n	7		35			15				7								
13189			York River	moy	0,94		0,74			0,10				1,11			0,74				1,02	0.74
13189			York River	Sx	0,03		0,08			0,02				0,59								
13199	365488	5421103	York River	n	20		51	8		8				8								
13199			York River	moy	0,92		0,60	0,48		0,17				0,63			0,60				0,56	0.60
13199			York River	Sx	0,21		0,09	0,02		0,01				0,27								
13213	365125	5424970	York River	n	29		52			8												
13213			York River	moy	1,35		0,67			0,12							0,67					0.67
13213			York River	Sx	0,09		0,08			0,04												
13215	364674	5424607	York River	n	40		25	10		14			8									
13215			York River	moy	1,48		0,50	0,38		0,16			0,36				0,50					0.50
13215			York River	Sx	0,18		0,09	0,03		0,03			0,03									
13218	370673	5418357	York River	n	56		35			7			5									
13218			York River	moy	1,48		0,61			0,10			0,25				0,61					0.61
13218			York River	Sx	0,23		0,14			0,02			0,02									
13219	358216	5422248	York River	n	19		20			5												
13219			York River	moy	1,31		0,88			0,11							0,88					0.88
13219			York River	Sx	0,09		0,14			0,02												
13221	358232	5421877	York River	n	32	11				7			9	43								
13221			York River	moy	1,31	0,91				0,12			0,29	0,82		0,75					0,74	0.75
13221			York River	Sx	0,14	0,10				0,02			0,05	0,29								
13228	361865	5420023	York River	n	27	29	48	8					9									
13228			York River	moy	1,19	0,76	0,63	0,56					0,40			0,58	0,63					0.61
13228			York River	Sx	0,09	0,05	0,06	0,05					0,03									
13229	359772	5419812	York River	n	32	43	17							13	5							
13229			York River	moy	1,28	0,90	0,67							0,73	1,70	0,68	0,67				0,66	0.68
13229			York River	Sx	0,07	0,10	0,13							0,30	0,15							
13245	379596	5403440	York River	n			6							14								
13245			York River	moy			0,77							0,97			0,77				0,89	0.77
13245			York River	Sx			0,04							0,27								
13251	383905	5403426	York River	n	27	36	23		14	8				9								
13251			York River	moy	1,43	0,84	0,61		0,26	0,24				0,65		0,63	0,61	0,66			0,58	0.63
13251			York River	Sx	0,24	0,10	0,07		0,05	0,02				0,03								

INRS	Location UTM est	Location UTM west	Formation	STAT	Macerals Inert	Macerals Tel.	Macerals Tcoll	Macerals Coll	Macerals Spor	Macerals other exinite	Zooclasts Chit.	Zooclasts Scol.	Solid bitumen Protob.	Solid bitumen Pyrob.	Solid bitumen Coke	Estimated Ro of telocollinite Tel.	Estimated Ro of telocollinite Tcoll	Estimated Ro of telocollinite Spor.	Estimated Ro of telocollinite Chit.	Estimated Ro of telocollinite Scol.	Mean est. Ro Pyro.	Mean est. Ro telocol.
13252	383905	5403426	York River	n	67	12	56						6									
13252			York River	moy	1,18	0,85	0,55						0,36			*0,68*	*0,55*					0,57
13252			York River	Sx	0,19	0,18	0,09						0,04									
13259	405532	5409100	York River	n	62	20	28	12						10								
13259			York River	moy	1,40	0,87	0,84	0,68						0,80		*0,70*	*0,84*				*0,72*	0,78
13259			York River	Sx	0,27	0,09	0,08	0,05						0,09								
13289	392950	5400300	York River	n	20	5	26	10		9			6	19	14							
13289			York River	moy	1,01	1,01	0,87	0,69		0,12			0,27	1,08	4,77	*0,87*	*0,87*				*0,99*	0,87
13289			York River	Sx	0,06	0,11	0,23	0,08		0,05			0,01	0,23	1,12							
13126	375320	5424850	York River (A B)	n	47	15					5			7								
13126			York River (A B)	moy	1,74	1,20					1,05			1,26		*1,12*			*0,96*		*1,16*	1,08
13126			York River (A B)	Sx	0,16	0,21					0,04			0,08								
13157	405000	5397150	York River (A B)	n	40	22	7		5	27			6	21								
13157			York River (A B.)	moy	1,30	0,84	0,68		0,26	0,10			0,25	0,60		*0,63*	*0,68*	*0,66*			*0,54*	0,65
13157			York River (A B)	Sx	0,11	0,08	0,03		0,05	0,02			0,02	0,06								
13179	366713	5410549	York River (A B.)	n	28	22	25			7			12	18								
13179			York River (A B)	moy	1,32	0,80	0,57			0,13			0,47	0,76		*0,60*	*0,57*				*0,69*	0,58
13179			York River (A B)	Sx	0,18	0,13	0,11			0,02			0,07	0,17								
13182	367165	5409275	York River (A B)	n	24	19	34	19		11				9								
13182			York River (A B)	moy	1,18	0,84	0,74	0,66		0,17				0,94		*0,67*	*0,74*				*0,86*	0,71
13182			York River (A B)	Sx	0,11	0,06	0,07	0,03		0,06				0,29								
13186	367165	5409275	York River (A B)	n	67	26	25			9				7								
13186			York River (A B)	moy	1,40	0,90	0,85			0,24				0,86		*0,74*	*0,85*				*0,78*	0,79
13186			York River (A B)	Sx	0,17	0,05	0,06			0,25				0,03								
13226	357454	5419358	York River (A B)	n	6		58			21			10	7								
13226			York River (A B)	moy	1,26		0,50			0,16			0,26	1,14			*0,50*				*1,05*	0,50
13226			York River (A B)	Sx	0,34		0,11			0,09			0,06	0,42								
13237	364122	5411150	York River (A B)	n	52	34	17			9				9								
13237			York River (A B)	moy	1,42	1,03	1,03			0,12				1,26		*0,90*	*1,03*				*1,16*	0,94
13237			York River (A.B)	Sx	0,24	0,22	0,19			0,01				0,11								
13244	378861	5402833	York River (A B)	n										15								
13244			York River (A.B)	moy										1,22							*1,12*	
13244			York River (A.B.)	Sx										0,57								
13255	386680	5401890	York River (A B)	n	26	27	10		13	15			19	25								
13255			York River (A.B.)	moy	1,40	0,84	0,65		0,30	0,17			0,28	0,64		*0,63*	*0,65*	*0,72*			*0,57*	0,66
13255			York River (A.B.)	Sx	0,16	0,14	0,05		0,09	0,03			0,13	0,22								
13288	392600	5398520	York River (A.B.)	n	24	6	27		14					31								
13288			York River (A B.)	moy	1,29	1,06	0,78		0,55				.	1,01		*0,94*	*0,78*	*1,05*			*0,92*	0,88
13288			York River (A B)	Sx	0,22	0,04	0,06		0,04					0,25								
13290	391450	5405900	York River (A B)	n	5		33			15			17	16								
13290			York River (A.B.)	moy	0,90		0,45			0,10			0,20	0,86			*0,45*				*0,78*	0,45
13290			York River (A.B)	Sx	0,07		0,10			0,01			0,05	0,29								
13298	399350	5391050	York River (A B.)	n	13		11			9				17	5							
13298			York River (A.B.)	moy	1,27		0,62			0,15				0,72	4,52		*0,62*				*0,65*	0,62
13298			York River (A.B)	Sx	0,17		0,08			0,05				0,20	1,17							

INRS	Location		Formation	STAT	Macerals						Zooclasts		Solid bitumen			Estimated Ro of telocollinite					Mean est. Ro	Mean est. Ro
	UTM est	UTM west			Inert	Tel.	Tcoll	Coll	Spor	other exinite	Chit.	Scol.	Protob	Pyrob.	Coke	*Tel.*	*Tcoll*	*Spor.*	*Chit.*	*Scol.*	*Pyro.*	*telocol.*
13299	400300	5391450	York River (A B)	n	28	**17**	**24**			11				**34**	**12**							
13299			York River (A B)	moy	1,39	**0,73**	**0,59**			0,12				**1,47**	**2,11**	*0,55*	*0,59*				*1,37*	**0.57**
13299			York River (A B)	Sx	0,21	**0,09**	**0,15**			0,04				**0,43**	**0,21**							
13301	398920	5390450	York River (A B)	n	29	**9**				7				**26**								
13301			York River (A B)	moy	1,24	**0,80**				0,34				**1,14**		*0,62*					*1,05*	**0.62**
13301			York River (A B)	Sx	0,20	**0,02**				0,03				**0,21**								
13129	375400	5425820	York Lake	n	65	**28**	**18**				**11**	**7**	9									
13129			York Lake	moy	1,35	**0,86**	**0,85**				**1,04**	**0,51**	0,44			*0,70*	*0,85*		*0,95*	*0,64*		**0.78**
13129			York Lake	Sx	0,17	**0,11**	**0,12**				**0,06**	**0,02**	0,03									
13192	370602	5411841	York Lake	n							**24**		43	13								
13192			York Lake	moy							**0,85**		0,39	0,75					*0,68*		*0,68*	**0.68**
13192			York Lake	Sx							**0,07**		0,1	0,14								
13208	368298	5427571	York Lake	n	42		11	15		18			10	27								
13208			York Lake	moy	0,98		0,8	0,71		0,14			0,35	1,2			*0,80*				*1,11*	**0.80**
13208			York Lake	Sx	0,09		0,07	0,19		0,03			0,21	0,34								
13230	359303	5419573	York Lake	n	36	**23**	30	6		11		**8**	8	10								
13230			York Lake	moy	1,51	**0,77**	0,57	0,62		0,20		**0,52**	0,18	0,63		0,57	*0,57*			*0,66*	*0,56*	**0.58**
13230			York Lake	Sx	0,22	**0,15**	0,16	0,05		0,10		**0,03**	0,03	0,14								
13287	391770	5398000	York Lake	n	27	**37**	12			26		**12**	16	20								
13287			York Lake	moy	1,26	**0,89**	0,54			0,13		**0,58**	0,31	0,71		0,68	*0,54*			*0,77*	*0,64*	**0.67**
13287			York Lake	Sx	0,10	**0,12**	0,1			0,03		**0,03**	0,16	0,17								

INRS	Well	Depth sup.	Depth inf.	FM	STAT	Macerals						Zooclasts			Solid bitumen			Estimated Ro of telocollinite						Mean est. Ro from pyro.	Mean est. Ro telocol.
						Inert.	Tel.	Tcoll	Coll	Spor	other exinite	Chit.	Hydr.	Scol.	Protob.	Pyrob.	Res.b.	Tel.	Tcoll	Spor.	Chit.	Hyd.	Scol.		
13310	Blanchet	35	80	Indian Cove	n	21	5				9			16	25	11									
13310	Blanchet	35	80	Indian Cove	moy	1,57	1,08				0,14			0,75	0,46	1,00		0,96					1,08	1,08	1,05
13310	Blanchet	35	80	Indian Cove	Sx	0,24	0,09				0,07			0,04	0,18	0,35									
13311	Blanchet	105	150	Indian Cove	n	22	27				11	8		14	9	15									
13311	Blanchet	105	150	Indian Cove	moy	1,48	1,20				0,10	1,16		0,76	0,43	1,10		1,12			1,13		1,10	1,25	1,12
13311	Blanchet	105	150	Indian Cove	Sx	0,16	0,13				0,02	0,07		0,04	0,10	0,36									
13312	Blanchet	195	240	Shiphead	n	25	7				7			11	21	15									
13312	Blanchet	195	240	Shiphead	moy	1,51	1,23				0,11			0,87	0,53	1,00		1,16					1,30	1,08	1,25
13312	Blanchet	195	240	Shiphead	Sx	0,13	0,08				0,02			0,04	0,14	0,22									
13313	Blanchet	305	350	Indian Cove	n						19				17	7									
13313	Blanchet	305	350	Indian Cove	moy						0,13				0,56	1,36								1,62	
13313	Blanchet	305	350	Indian Cove	Sx						0,04				0,13	0,19									
13314	Blanchet	435	480	Indian Cove	n						15	5			30	11									
13314	Blanchet	435	480	Indian Cove	moy						0,15	1,45			0,52	1,33					1,51			1,62	1,51
13314	Blanchet	435	480	Indian Cove	Sx						0,06	0,06			0,14	0,15									
13315	Blanchet	550	600	Shiphead	n	34	22					11		6	18	22									
13315	Blanchet	550	600	Shiphead	moy	1,46	1,13					1,09		0,85	0,54	0,99		1,03			1,02			1,09	0,87
13315	Blanchet	550	600	Shiphead	Sx	0,11	0,12					0,14		0,03	0,12	0,20									
13316	Blanchet	675	720	Shiphead	n	29	36				28	10			26	9									
13316	Blanchet	675	720	Shiphead	moy	1,47	1,21				0,14	1,11			0,38	0,98		1,13			1,05			1,07	1,12
13316	Blanchet	675	720	Shiphead	Sx	0,11	0,13				0,05	0,05			0,19	0,16									
13117	Blanchet	795	840	Shiphead	n	37	25		7						13	23									
13117	Blanchet	795	840	Shiphead	moy	1,66	1,18		1,00						0,55	1,08		1,09						1,25	1,09
13117	Blanchet	795	840	Shiphead	Sx	0,14	0,09		0,11						0,07	0,36									
13318	Blanchet	915	960	Forillon	n	18	30				22	25		7	5	19									
13318	Blanchet	915	960	Forillon	moy	1,66	1,34				0,23	1,33		1,18	0,55	1,13		1,32			1,38		1,71	1,34	1,39
13318	Blanchet	915	960	Forillon	Sx	0,21	0,16				0,09	0,13		0,08	0,08	0,13									
13319	Blanchet	1035	1080	Indian Pt	n	28	5					24				20									
13319	Blanchet	1035	1080	Indian Pt	moy	1,62	1,43					1,38				1,30		1,43			1,44			1,58	1,44
13319	Blanchet	1035	1080	Indian Pt	Sx	0,14	0,06					0,10				0,24									
13320	Blanchet	1190	1235	Quebec Gp	n											13	50								
13320	Blanchet	1190	1235	Quebec Gp	moy											1,21	1,17							1,46	
13320	Blanchet	1190	1235	Quebec Gp	Sx											0,15	0,12								
13322	Malbaie	20	65	Battery Pt	n										7	31	5								
13322	Malbaie	20	65	Battery Pt	moy										0,16	1,75	1,09							2,12	
13322	Malbaie	20	65	Battery Pt	Sx										0,03	0,22	0,05								
13323	Malbaie	105	150	Battery Pt	n	8										25									
13323	Malbaie	105	150	Battery Pt	moy	1,40										1,35								1,64	
13323	Malbaie	105	150	Battery Pt	Sx	0,05										0,19									
13324	Malbaie	250	300	Battery Pt	n	19	7			7						45									
13324	Malbaie	250	300	Battery Pt	moy	1,71	1,48			0,51						1,57		1,48		1,00				1,91	1,24
13324	Malbaie	250	300	Battery Pt	Sx	0,28	0,12			0,08						0,18									
13325	Malbaie	405	450	Battery Pt	n	8										10									
13325	Malbaie	405	450	Battery Pt	moy	1,42										1,44								1,75	
13325	Malbaie	405	450	Battery Pt	Sx	0,11										0,28									
13326	Malbaie	555	600	Battery Pt	n	53	17	7											7						
13326	Malbaie	555	600	Battery Pt	moy	1,38	0,99	1,06										0,85	1,06						0,91
13326	Malbaie	555	600	Battery Pt	Sx	0,16	0,08	0,06											0,06						

INRS	Well	Depth sup.	Depth inf.	FM	STAT	Macerals: Inert.	Tel.	Tcoll	Coll	Spor.	other exinite	Zooclasts: Chit.	Hydr.	Scol.	Solid bitumen: Protob.	Pyrob.	Res.b.	Estimated Ro of telocollinite: Tel.	Tcoll	Spor.	Chit.	Hyd.	Scol.	Mean est. Ro from pyro.	Mean est. Ro telocol.
13227	Malbaie	705	750	Battery Pt	n	42	28	26	37										26						
13227	Malbaie	705	750	Battery Pt	moy	1,37	1,05	1,05	0,78									0,92	1,05						0,98
13227	Malbaie	705	750	Battery Pt	Sx	0,13	0,14	0,11	0,13										0,11						
13328	Malbaie	855	900	Battery Pt	n	19	17	12	18		8								12						
13328	Malbaie	855	900	Battery Pt	moy	1,32	1,07	1,03	0,86		0,13							0,95	1,03						0,98
13328	Malbaie	855	900	Battery Pt	Sx	0,17	0,10	0,15	0,08		0,03								0,15						
13329	Malbaie	1005	1050	Battery Pt	n	50	9	26	7		7				17	7			26						
13329	Malbaie	1005	1050	Battery Pt	moy	1,63	1,14	1,14	0,92		0,08				0,47	1,08		1,04	1,14					1,25	1,11
13329	Malbaie	1005	1050	Battery Pt	Sx	0,21	0,11	0,12	0,09		0,01				0,42	0,10			0,12						
13330	Malbaie	1155	1200	Battery Pt	n	39	17	9	30		20				12	0			9						
13330	Malbaie	1155	1200	Battery Pt	moy	1,80	1,05	0,97	0,82		0,10				0,44			0,92	0,97						0,94
13330	Malbaie	1155	1200	Battery Pt	Sx	0,17	0,12	0,06	0,09		0,02				0,46				0,06						
13331	Malbaie	1305	1350	Battery Pt	n	60	14	40								9			40						
13331	Malbaie	1305	1350	Battery Pt	moy	1,82	1,21	0,99								1,35		1,13	0,99					1,64	1,03
13331	Malbaie	1305	1350	Battery Pt	Sx	0,15	0,12	0,10								0,37			0,10						
13332	Malbaie	1455	1500	Battery Pt	n	61	42	36	12										36						
13332	Malbaie	1455	1500	Battery Pt	moy	1,69	1,19	0,99	0,73									1,11	0,99						1,05
13332	Malbaie	1455	1500	Battery Pt	Sx	0,16	0,21	0,15	0,21										0,15						
13333	Malbaie	1605	1650	Battery Pt	n	52	20	38			22					18			38						
13333	Malbaie	1605	1650	Battery Pt	moy	1,75	1,19	1,05			0,18					0,84		1,11	1,05					0,82	1,07
13333	Malbaie	1605	1650	Battery Pt	Sx	0,21	0,11	0,11			0,10					0,30			0,11						
13334	Malbaie	1755	1800	Battery Pt	n	56	48	12			5				7	5			12						
13334	Malbaie	1755	1800	Battery Pt	moy	1,55	1,10	1,11			0,19				0,79	1,48		0,99	1,11					1,80	1,01
13334	Malbaie	1755	1800	Battery Pt	Sx	0,24	0,14	0,10			0,03				0,28	0,12			0,10						
13335	Malbaie	1905	1950	Battery Pt	n	44	24	28	9		24				12	11			28						
13335	Malbaie	1905	1950	Battery Pt	moy	1,83	1,60	1,29	1,28		0,32				0,70	1,51		1,60	1,29					1,84	1,43
13335	Malbaie	1905	1950	Battery Pt	Sx	0,17	0,09	0,14	0,07		0,05				0,31	0,08			0,14						
13336	Malbaie	2075	2125	Battery Pt	n	56	23	25	14		5				13				25						
13336	Malbaie	2075	2125	Battery Pt	moy	1,55	1,39	1,23	1,08		0,16				0,63			1,39	1,23						1,31
13336	Malbaie	2075	2125	Battery Pt	Sx	0,11	0,10	0,11	0,09		0,02				0,15				0,11						
13077	S. Bank	308	309	York River	n	24	32	25			10					19			25						
13077	S. Bank	308	309	York River	moy	1,23	0,93	0,68			0,13					0,79		0,78	0,68					0,74	0,73
13077	S. Bank	308	309	York River	Sx	0,15	0,07	0,09			0,02					0,07			0,09						
13093	S. Bank	686	693	Indian Cove	n	6	14		6			9		8	48	26									
13093	S. Bank	686	693	Indian Cove	moy	1,29	1,16		0,93			0,91		0,63	0,35	0,82		1,07			0,76		0,86	0,79	0,93
13093	S. Bank	686	693	Indian Cove	Sx	0,10	0,05		0,29			0,07		0,02	0,03	0,25									
14037	S. Bank	1376	1377	Indian Cove	n						10	21			30	21	7								
14037	S. Bank	1376	1377	Indian Cove	moy						0,12	1,07			0,48	0,95	0,57				0,99			1,02	0,99
14037	S. Bank	1376	1377	Indian Cove	Sx						0,04	0,10			0,12	0,20	0,04								
14079	S. Bank	2041	2045	Forillon	n											50	5								
14079	S. Bank	2041	2045	Forillon	moy											1,19	1,28							1,44	
14079	S. Bank	2041	2045	Forillon	Sx											0,18	0,04								
14110	S. Bank	2498	2501	Indian Pt	n	16	16				11	5				14	27								
14110	S. Bank	2498	2501	Indian Pt	moy	2,32	1,64				2,57	2,19				1,46	1,39	1,64			2,20			1,78	1,77
14110	S. Bank	2498	2501	Indian Pt	Sx	0,49	0,18				0,36	0,48				0,29	0,20								
14121	S. Bank	2771	2775	Indian Pt	n		8									58									
14121	S. Bank	2771	2775	Indian Pt	moy		1,89									1,86		1,89						2,25	1,89
14121	S. Bank	2771	2775	Indian Pt	Sx		0,22									0,28									

INRS	Well	Depth sup.	Depth inf.	FM	STAT	Macerals						Zooclasts			Solid bitumen			Estimated Ro of telocollinite						Mean est. Ro from pyro.	Mean est. Ro telocol.
						Inert	Tel.	Tcoll	Coll	Spor	other exinite	Chit.	Hydr.	Scol.	Protob.	Pyrob.	Res b.	*Tel.*	*Tcoll*	*Spor.*	*Chit.*	*Hyd.*	*Scol.*		
14143	S. Bank	3446	3449	Roncelles	n											20									
14143	S. Bank	3446	3449	Roncelles	moy											2,15								2,56	
14143	S. Bank	3446	3449	Roncelles	Sx											0,71									
14156	York		291	Saint-Léon	n			27				55				11			*27*						
14156	York		291	Saint-Léon	moy			1,98				2,14				1,85			*1,98*		*2,16*			2,24	2,10
14156	York		291	Saint-Léon	Sx			0,14				0,13				0,15			*0,14*						
14162	York		377	Saint-Léon	n			6				11				24			*6*						
14162	York		377	Saint-Léon	moy			1,98				1,97				1,80			*1,98*		*2,01*			2,18	2,00
14162	York		377	Saint-Léon	Sx			0,04				0,13				0,23			*0,04*						
14169	York	521	523	Saint-Léon	n	5										14									
14169	York	521	523	Saint-Léon	moy	2,48										1,95								2,35	
14169	York	521	523	Saint-Léon	Sx	0,13										0,25									
14176	York		637	Saint-Léon	n											22	7								
14176	York		637	Saint-Léon	moy											2,08	1,86							2,49	
14176	York		637	Saint-Léon	Sx											0,24	0,08								
14202	Douglas		55	Battery Pt	n	52	21	30			8								*30*						
14202	Douglas		55	Battery Pt	moy	1,52	1,05	0,91			0,14							*0,92*	*0,91*						0,92
14202	Douglas		55	Battery Pt	Sx	0,15	0,10	0,10			0,02								*0,10*						
14203	Douglas		100	Battery Pt	n	38	33	25			8				7	8			*25*						
14203	Douglas		100	Battery Pt	moy	1,46	0,80	0,72			0,08				0,18	0,63		*0,62*	*0,72*					0,49	0,66
14203	Douglas		100	Battery Pt	Sx	0,19	0,07	0,06			0,02				0,06	0,01			*0,06*						
14206	Douglas		780	York River	n	55	26	16											*16*						
14206	Douglas		780	York River	moy	1,32	0,93	0,77										*0,78*	*0,77*						0,77
14206	Douglas		780	York River	Sx	0,19	0,12	0,10											*0,10*						
14217	Douglas		1575	Roncelles	n	29	20		9			9		20		44									
14217	Douglas		1575	Roncelles	moy	1,51	0,95		0,84			1,12		0,82		0,85		*0,80*			*1,07*		*1,21*	0,84	1,02
14217	Douglas		1575	Roncelles	Sx	0,10	0,13		0,05			0,06		0,04		0,20									
14219	Douglas		1650	West Point	n	13	13	9						23	13	36			*9*						
14219	Douglas		1650	West Point	moy	1,66	0,94	0,65						0,74	0,34	0,82		*0,79*	*0,65*				*1,06*	0,79	0,90
14219	Douglas		1650	West Point	Sx	0,10	0,21	0,03						0,04	0,12	0,14			*0,03*						
14221	Douglas		1710	Griffon Cove	n			5			6			32	8	27			*5*						
14221	Douglas		1710	Griffon Cove	moy			1,19			0,08			0,85	0,65	0,91			*1,19*				*1,27*	0,94	1,26
14221	Douglas		1710	Griffon Cove	Sx			0,06			0,01			0,05	0,15	0,14			*0,06*						
13228	Douglas		1990	Quebec Gp	n											50									
13228	Douglas		1990	Quebec Gp	moy											0,70								0,59	
13228	Douglas		1990	Quebec Gp	Sx											0,17									
14231	Gaspe Sud	150	160	York River	n	33	35	36			20					15			*36*						
14231	Gaspe Sud	150	160	York River	moy	1,36	0,88	0,65			0,22					0,79		*0,72*	*0,65*					0,74	0,68
14231	Gaspe Sud	150	160	York River	Sx	0,13	0,14	0,06			0,04					0,12			*0,06*						
14237	Gaspe Sud	380	390	York River	n	48	14	7			9				15	27			*7*						
14237	Gaspe Sud	380	390	York River	moy	1,50	1,09	0,94			0,12				0,35	0,86		*0,98*	*0,94*					0,86	0,96
14237	Gaspe Sud	380	390	York River	Sx	0,23	0,09	0,16			0,01				0,12	0,19			*0,16*						
14241	Gaspe Sud	530	540	Indian Cove	n	14	7					14			13	42									
14241	Gaspe Sud	530	540	Indian Cove	moy	1,56	0,96					0,91			0,46	0,69		*0,81*			*0,76*			0,58	0,78
14241	Gaspe Sud	530	540	Indian Cove	Sx	0,18	0,13					0,07			0,07	0,19									
14245	Gaspe Sud	680	690	Indian Cove	n	15	7					20			13	28									
14245	Gaspe Sud	680	690	Indian Cove	moy	1,57	0,95					0,93			0,37	0,87		*0,80*			*0,79*			0,88	0,72
14245	Gaspe Sud	680	690	Indian Cove	Sx	0,17	0,16					0,06			0,06	0,38									

INRS	Well	Depth sup	Depth inf	FM	STAT	Macerals: Inert.	Tel.	Tcoll	Coll	Spor	other exinite	Zooclasts: Chit.	Hydr.	Scol.	Solid bitumen: Protob.	Pyrob.	Res.b.	Estimated Ro of telocollinite: Tel.	Tcoll	Spor.	Chit.	Hyd.	Scol.	Mean est. Ro from pyro.	Mean est. Ro telocol.
14271	Gaspe Sud	1755	1765	Shiphead	n	9						21				12									
14271	Gaspe Sud	1755	1765	Shiphead	moy	1,80						1,36				1,13					1,42			1,34	1,42
14271	Gaspe Sud	1755	1765	Shiphead	Sx	0,24						0,15				0,35									
14308	Gaspe Sud	3225	3235	Quebec Gp	n											26									
14308	Gaspe Sud	3225	3235	Quebec Gp	moy											1,40								1,70	
14308	Gaspe Sud	3225	3235	Quebec Gp	Sx											0,12									
14312	Gaspe Sud	3350	3354	Quebec Gp	n											12									
14312	Gaspe Sud	3350	3354	Quebec Gp	moy											1,38								1,68	
14312	Gaspe Sud	3350	3354	Quebec Gp	Sx											0,11									
14348	Gaspé Nord		400	Battery Pt	n	29	43				8				10	29									
14348	Gaspé Nord		400	Battery Pt	moy	1,64	0,98				0,31				0,45	0,93		0,84						0,98	0,84
14348	Gaspé Nord		400	Battery Pt	Sx	0,32	0,16				0,07				0,04	0,17									
14350	Gaspé Nord		830	York River	n	15	22			6	26					45									
14350	Gaspé Nord		830	York River	moy	1,47	0,90			0,36	0,21					0,80		0,74		0,81				0,76	0,75
14350	Gaspé Nord		830	York River	Sx	0,25	0,15			0,14	0,10					0,17									
14351	Gaspé Nord		1050	York River	n	30	39		7		24					32									
14351	Gaspé Nord		1050	York River	moy	1,77	1,01		0,53		0,22					0,87		0,87						0,88	0,87
14351	Gaspé Nord		1050	York River	Sx	0,35	0,20		0,07		0,09					0,13									
14353	Gaspé Nord		1400	Forillon	n	6	17				21	27				23									
14353	Gaspé Nord		1400	Forillon	moy	1,97	1,13				0,15	1,12				0,84		1,03			1,07			0,82	1,05
14353	Gaspé Nord		1400	Forillon	Sx	0,29	0,26				0,11	0,13				0,18									
14354	Gaspé Nord		1600	Forillon	n	15	7					29		11		23									
14354	Gaspé Nord		1600	Forillon	moy	1,94	1,42					1,23		0,82		0,80		1,42			1,23		1,21	0,76	1,25
14354	Gaspé Nord		1600	Forillon	Sx	0,25	0,08					0,12		0,05		0,13									
14355	Gaspé Nord		1800	Indian Pt	n	8	25			33		23													
14355	Gaspé Nord		1800	Indian Pt	moy	2,12	2,09			0,79		2,03						2,09		1,28	2,06				1,75
14355	Gaspé Nord		1800	Indian Pt	Sx	0,18	0,20			0,17		0,12													
14606	Forillon-		55	York River	n		10				57				30	21									
14606	Riv. Renard		55	York River	moy		0,74				0,21				0,31	0,77		0,56						0,71	0,56
14606	Forillon-		55	York River	Sx		0,26				0,07				0,06	0,25									
14605	Riv. Renard		150	Indian Cove	n	14	12		6	6	9	31			26	18									
14605	Forillon-		150	Indian Cove	moy	1,30	0,81		0,46	0,14	0,21	0,69			0,39	0,58		0,63		0,44	0,48			0,43	0,51
14605	Riv. Renard		150	Indian Cove	Sx	0,37	0,08		0,03	0,02	0,08	0,06			0,03	0,11									
14589	Forillon-		400	Shiphead	n		17			15	30	7		9	22	5									
14589	Riv. Renard		400	Shiphead	moy		0,74			0,11	0,14	0,56		0,39	0,36	0,61		0,56		0,38	0,35		0,44	0,47	0,45
14589	Forillon-		400	Shiphead	Sx		0,15			0,04	0,05	0,05		0,05	0,10	0,12									
14587	Riv. Renard		620	Forillon	n	34	15			10		28		6	21	9									
14587	Forillon-		620	Forillon	moy	1,54	0,65			0,12		0,78		0,43	0,39	0,72		0,47		0,40	0,59		0,50	0,62	0,52
14587	Riv. Renard		620	Forillon	Sx	0,59	0,10			0,05		0,05		0,03	0,12	0,07									
14582	Forillon-		795	Forillon	n		20			13		28			10	32									
14582	Riv. Renard		795	Forillon	moy		0,61			0,13		0,74			0,20	0,57		0,44		0,42	0,54			0,42	0,48
14582	Forillon-		795	Forillon	Sx		0,17			0,05		0,05			0,07	0,12									
14555	Riv. Renard		1235	Indian Pt	n	7					48	14													
14555	Forillon-		1235	Indian Pt	moy	1,84					0,35	1,32									1,37				1,37
14555	Riv. Renard		1235	Indian Pt	Sx	0,36					0,09	0,07													

INRS	Well	Depth sup	Depth inf	Formation	STAT	Macerals Pvitr. & semif./pyrb	Vitr., zoo. & pyrb.-vitr	pyb.-alg. coll./exin.	Estimated Ro
14231	Gaspé Sud	150	160	York River	n	18	39	50	
	Gaspé Sud				moy	1,40	0,91	0,62	**0.91**
	Gaspé Sud				Sx	0,18	0,13	0,09	
14235	Gaspé Sud	300	310	York River	n	50	50	50	
	Gaspé Sud				moy	1,44	0,98	0,52	**0.98**
	Gaspé Sud				Sx	0,14	0,1	0,12	
14237	Gaspé Sud	380	390	York River	n	23	40	50	
	Gaspé Sud				moy	1,45	0,99	0,57	**0.99**
	Gaspé Sud				Sx	0,23	0,11	0,16	
14241	Gaspé Sud	530	540	Indian Cove	n	18	23	50	
	Gaspé Sud				moy	1,55	1,04	0,53	**1.04**
	Gaspé Sud				Sx	0,21	0,13	0,07	
14245	Gaspé Sud	680	690	Indian Cove	n	23	27	50	
	Gaspé Sud				moy	1,67	1,09	0,56	**1.09**
	Gaspé Sud				Sx	0,25	0,17	0,15	
14249	Gaspé Sud	835	845	Indian Cove	n	11	38	50	
	Gaspé Sud				moy	1,67	1,03	0,62	**1.03**
	Gaspé Sud				Sx	0,27	0,14	0,12	
14253	Gaspé Sud	990	995	Indian Cove	n	13	50	50	
	Gaspé Sud				moy	1,71	1,03	0,64	**1.03**
	Gaspé Sud				Sx	0,24	0,1	0,1	
14258	Gaspé Sud	1190	1205	Indian Cove	n	13	50	50	
	Gaspé Sud				moy	1,71	1,07	0,59	**1.07**
	Gaspé Sud				Sx	0,25	0,12	0,18	
14260	Gaspé Sud	1290	1300	Indian Cove	n	10	14	35	
	Gaspé Sud				moy	1,95	1,11	0,69	**1.11**
	Gaspé Sud				Sx	0,3	0,15	0,15	
14263	Gaspé Sud	1445	1450	Indian Cove	n	9	37	44	
	Gaspé Sud				moy	2	1,11	0,7	**1.11**
	Gaspé Sud				Sx	0,29	0,2	0,13	
14267	Gaspé Sud	1600	1610	Shiphead	n		50	26	
	Gaspé Sud				moy		1,09	0,8	**1.09**
	Gaspé Sud				Sx		0,13	0,13	
14271	Gaspé Sud	1755	1765	Shiphead	n		30	5	
	Gaspé Sud				moy		1,14	0,78	**1.14**
	Gaspé Sud				Sx		0,15	0,17	
14275	Gaspé Sud	1905	1910	Forillon	n			21	
	Gaspé Sud				moy			0,83	
	Gaspé Sud				Sx			0,12	
14279	Gaspé Sud	2060	2070	Forillon	n		41	16	
	Gaspé Sud				moy		1,31	1,01	**1.31**
	Gaspé Sud				Sx		0,17	0,12	
14283	Gaspé Sud	2215	2225	Forillon	n		28	8	
	Gaspé Sud				moy		1,3	1,02	**1.3**
	Gaspé Sud				Sx		0,11	0,13	
14287	Gaspé Sud	2370	2380	Forillon	n		9		
	Gaspé Sud				moy		1,31		**1.31**
	Gaspé Sud				Sx		0,12		
12656	Gaspé Sud		2860	Quebec Gp	n		50		
	Gaspé Sud				moy		1,6		**1.6**
	Gaspé Sud				Sx		0,16		
12657	Gaspé Sud		2860	Quebec Gp	n		50		
	Gaspé Sud				moy		1,65		**1.65**
	Gaspé Sud				Sx		0,14		
12657	Gaspé Sud		2865	Quebec Gp	n		80		
	Gaspé Sud				moy		1,47		**1.47**
	Gaspé Sud				Sx		0,21		
12674	Gaspé Sud		2970	Quebec Gp	n		50		
	Gaspé Sud				moy		1,48		**1.48**
	Gaspé Sud				Sx		0,14		
14304	Gaspé Sud	3055	3065	Quebec Gp	n		50	50	
	Gaspé Sud				moy		1,62	1,62	**1.62**
	Gaspé Sud				Sx		0,13	0,13	
14308	Gaspé Sud	3225	3235	Quebec Gp	n		50	50	
	Gaspé Sud				moy		1,52	1,52	**1.52**
	Gaspé Sud				Sx		0,14	0,14	
14312	Gaspé Sud	3350	3354	Quebec Gp	n		50	50	

INRS	Well	Depth sup	Depth inf	Formation	STAT	Macerals: Pvitr. & semif.-pyrb	Macerals: Vitr., zoo & pyrb.-vitr	Macerals: pyb.-alg. coll. exin.	Estimated Ro
	Gaspé Sud				moy		1,48	1,48	**1,48**
	Gaspé Sud				Sx		0,17	0,17	
14347	Gaspé Nord		255	Battery Pt	n	41	27		
	Gaspé Nord				moy	1,59	1,01		**1,01**
	Gaspé Nord				Sx	0,15	0,13		
14348	Gaspé Nord		400	Battery Pt	n	31	23		
	Gaspé Nord				moy	1,57	0,97		**0,97**
	Gaspé Nord				Sx	0,19	0,11		
14349	Gaspé Nord		640	Battery Pt	n		30		
	Gaspé Nord				moy		1,06		**1,06**
	Gaspé Nord				Sx		0,11		
14350	Gaspé Nord		830	York River	n	50	50		
	Gaspé Nord				moy	1,62	1,08		**1,08**
	Gaspé Nord				Sx	0,17	0,15		
14351	Gaspé Nord		1050	York River	n	33	33		
	Gaspé Nord				moy	1,53	1,12		**1,12**
	Gaspé Nord				Sx	0,18	0,17		
14352	Gaspé Nord		1200	Indian Cove	n	15	46		
	Gaspé Nord				moy	1,66	1,05		**1,05**
	Gaspé Nord				Sx	0,22	0,11		
14353	Gaspé Nord		1400	Forillon	n	11	50		
	Gaspé Nord				moy	1,73	0,97		**0,97**
	Gaspé Nord				Sx	0,27	0,13		
14354	Gaspé Nord		1600	Indian Pt	n		50		
	Gaspé Nord				moy		1,05		**1,05**
	Gaspé Nord				Sx		0,09		
14356	Gaspé Nord		1885	Roncelles	n		6		
	Gaspé Nord				moy		1,18		**1,18**
	Gaspé Nord				Sx		0,16		
14395	Gaspé Nord		1920	Griffon Cove	n		37		
	Gaspé Nord				moy		0,98		**0,98**
	Gaspé Nord				Sx		0,08		
14396	Gaspé Nord		1935	Griffon Cove	n		47		
	Gaspé Nord				moy		1,17		**1,17**
	Gaspé Nord				Sx		0,19		
14397	Gaspé Nord		1955	Griffon Cove	n		50		
	Gaspé Nord				moy		1,09		**1,09**
	Gaspé Nord				Sx		0,18		
14382	Gaspé Nord		2200	Quebec Gp	n		21		
	Gaspé Nord				moy		7,98		**7,98**
	Gaspé Nord				Sx		0,91		
14383	Gaspé Nord		2400	Quebec Gp	n		8		
	Gaspé Nord				moy		7,27		**7,27**
	Gaspé Nord				Sx		0,39		
2466	Québec Oil	240	243	Indian Cove	n		50		
	Québec Oil				moy		1,04		**1,04**
	Québec Oil				Sx		0,17		
2468	Québec Oil	358	361	Indian Cove	n		50		
	Québec Oil				moy		1,15		**1,15**
	Québec Oil				Sx		0,17		
2470	Québec Oil	514	517	Indian Cove	n		38		
	Québec Oil				moy		1,34		**1,34**
	Québec Oil				Sx		0,19		
2472	Québec Oil	633	636	Shiphead	n		50		
	Québec Oil				moy		1,57		**1,57**
	Québec Oil				Sx		0,27		
2474	Québec Oil	752	755	Shiphead	n		44		
	Québec Oil				moy		1,47		**1,47**
	Québec Oil				Sx		0,34		
2476	Québec Oil	880	883	Shiphead	n		50		
	Québec Oil				moy		1,62		**1,62**
	Québec Oil				Sx		0,3		
2479	Québec Oil	1063	1066	Shiphead	n		50		
	Québec Oil				moy		1,79		**1,79**
	Québec Oil				Sx		0,29		
2485	Québec Oil	1419	1422	Shiphead	n		36		
	Québec Oil				moy		1,9		**1,9**

INRS	Well	Depth sup.	Depth inf	Formation	STAT	Macerals: Pvitr & semif pyrb	Macerals: Vitr, zoo & pyrb-vitr	Macerals: pyb.-alg. coll./exin.	Estimated Ro
	Quebec Oil				Sx		0,32		
2489	Quebec Oil	1666	1669	Shiphead	n		26		
	Québec Oil				moy		2,05		2.05
	Québec Oil				Sx		0,15		
2491	Québec Oil	1794	1797	Shiphead	n		50		
	Québec Oil				moy		2,27		2.27
	Québec Oil				Sx		0,25		
13077	Sunny Bank	308	309	York River	n	50	50	50	
	Sunny Bank				moy	1,38	0,7	0,22	0.7
	Sunny Bank				Sx	0,22	0,15	0,11	
13093	Sunny Bank	688	693	York River	n	31	18	50	
	Sunny Bank				moy	1,24	0,8	0,38	0.8
	Sunny Bank				Sx	0,13	0,08	0,05	
14006	Sunny Bank	919	925	Indian Cove	n	24	20	26	
	Sunny Bank				moy	1,48	0,81	0,51	0.81
	Sunny Bank				Sx	0,28	0,09	0,11	
14015	Sunny Bank	1046	1047	Indian Cove	n	9	28	30	
	Sunny Bank				moy	1,53	0,89	0,57	0.89
	Sunny Bank				Sx	0,19	0,09	0,11	
14037	Sunny Bank	1376	1377	Indian Cove	n	11	50	42	
	Sunny Bank				moy	1,41	0,91	0,56	0.91
	Sunny Bank				Sx	0,26	0,12	0,11	
14047	Sunny Bank	1544	1547	Shiphead	n	12	10	18	
	Sunny Bank				moy	1,56	0,96	0,57	0.96
	Sunny Bank				Sx	0,29	0,15	0,1	
14053	Sunny Bank	1672	1675	Shiphead	n	11	30	23	
	Sunny Bank				moy	1,55	0,95	0,64	0.95
	Sunny Bank				Sx	0,19	0,14	0,13	
14079	Sunny Bank	2041	2045	Forillon	n	7	50	31	
	Sunny Bank				moy	1,58	0,99	0,79	0.99
	Sunny Bank				Sx	0,34	0,11	0,07	
14095	Sunny Bank	2267	2270	Forillon	n	13	39	11	
	Sunny Bank				moy	1,77	0,99	0,76	0.99
	Sunny Bank				Sx	0,27	0,12	0,06	
14110	Sunny Bank	2498	2501	Indian Pt	n	21	36		
	Sunny Bank				moy	1,85	1,25		1.25
	Sunny Bank				Sx	0,23	0,19		
14121	Sunny Bank	2771	2775	Indian Pt	n	20	26		
	Sunny Bank				moy	1,97	1,37		1.37
	Sunny Bank				Sx	0,18	0,18		
14130	Sunny Bank	3047	3049	Indian Pt	n	15	30		
	Sunny Bank				moy	2,35	1,69		1.69
	Sunny Bank				Sx	0,21	0,16		
14143	Sunny Bank	3446	3449	Roncelles	n		10		
	Sunny Bank				moy		1,72		1.72
	Sunny Bank				Sx		0,23		
14202	Douglas		55	Battery Pt	n	50	19	27	
	Douglas				moy	1,4	0,89	0,34	0.89
	Douglas				Sx	0,22	0,09	0,13	
14203	Douglas		100	Battery Pt	n	27	31	29	
	Douglas				moy	1,36	0,76	0,25	0.76
	Douglas				Sx	0,21	0,07	0,13	
14204	Douglas		305	Battery Pt	n	22	31	33	
	Douglas				moy	1,36	0,86	0,27	0.86
	Douglas				Sx	0,21	0,1	0,1	
14205	Douglas		520	Battery Pt	n	36	40	10	
	Douglas				moy	1,27	0,89	0,31	0.89
	Douglas				Sx	0,19	0,11	0,19	
14206	Douglas		780	York River	n	36			
	Douglas				moy	1,47			
	Douglas				Sx	0,24			
14207	Douglas		940	York River	n	25			
	Douglas				moy	1,53			
	Douglas				Sx	0,15			
14208	Douglas		1125	York River	n	16			
	Douglas				moy	1,54			
	Douglas				Sx	0,19			

INRS	Well	Depth sup	Depth inf.	Formation	STAT	Macerals			Estimated
						Pvitr. & semif. pyrb	Vitr., zoo. & pyrb.-vitr	pyb.-alg. coll./exin.	Ro
14210	Douglas		1320	York River	n	33	50	33	
	Douglas				moy	1,43	0,85	0,49	**0.85**
	Douglas				Sx	0,25	0,11	0,2	
14211	Douglas		1370	York River	n	50	50	31	
	Douglas				moy	1,57	0,94	0,45	**0.94**
	Douglas				Sx	0,18	0,12	0,21	
14214	Douglas		1475	York River	n	50	41	50	
	Douglas				moy	1,51	0,96	0,55	**0.96**
	Douglas				Sx	0,17	0,18	0,12	
14217	Douglas		1575	Roncelles	n	22	50	50	
	Douglas				moy	1,56	0,94	0,65	**0.94**
	Douglas				Sx	0,18	0,13	0,13	
14219	Douglas		1650	West Point	n			50	
	Douglas				moy			0,61	
	Douglas				Sx			0,1	
14221	Douglas		1710	Griffon Cove	n			50	
	Douglas				moy			0,71	
	Douglas				Sx			0,15	
14225	Douglas		1840	Griffon Cove	n			50	
	Douglas				moy			0,75	
	Douglas				Sx			0,12	
14227	Douglas		1900	Quebec Gp	n			50	
	Douglas				moy			0,62	
	Douglas				Sx			0,13	
14228	Douglas		1990	Quebec Gp	n			50	
	Douglas				moy			0,62	
	Douglas				Sx			0,14	

Section name	Approximative location of section		Formation	STAT	Macerals Pyrobitumen	Mean estimated Ro of vitrinite if the lithology is a	
	UTM est	UTM west				**Shale (min.)**	**Limestone (max.)**
CR-1-2	407000	5413000	Cap-des-Rosiers	n	50		
				moy	2,52	**2,53**	**2,88**
				Sx	0,211		
DL-1-4	406000	5416000	Des Landes	n	58		
				moy	2,6	**2,59**	**2,97**
				Sx	0,95		
DL-1-5	406000	5416000	Des Landes	n	53		
				moy	2,7	**2,66**	**3,07**
				Sx	0,123		
DL-1-10	406000	5416000	Des Landes	n	9		
				moy	2,24	**2,33**	**2,59**
				Sx	0,493		
DL-2-21	397000	5428000	Des Landes	n	33		
				moy	2,66	**2,63**	**3,03**
				Sx	0,154		
DL-2-23	394000	5425000	Des Landes	n	39		
				moy	2,7	**2,66**	**3,07**
				Sx	0,158		
DL-2-25	394000	5425000	Des Landes	n	4		
				moy	2,1	**2,22**	**2,45**
				Sx	-		
CR-2-28	390000	5423000	Cap-des-Rosiers	n	6		
				moy	2,24	**2,33**	**2,59**
				Sx	0,24		
CL-3-35	389000	5435000	Cloridorme	n	50		
				moy	2,53	**2,54**	**2,89**
				Sx	0,174		
CL-3-36	389000	5435000	Cloridorme	n	49		
				moy	2,44	**2,47**	**2,80**
				Sx	0,466		
DL-3-37	389000	5435000	Des Landes	n	50		
				moy	2,41	**2,45**	**2,77**
				Sx	0,049		
DL-3-42	389000	5435000	Des Landes	n	50		
				moy	2,62	**2,60**	**2,99**
				Sx	0,144		
CR-3-44	389000	5435000	Cap-des-Rosiers	n	28		
				moy	2,21	**2,30**	**2,56**
				Sx	0,079		
DL-3-50	389000	5435000	Des Landes	n	53		
				moy	2,7	**2,66**	**3,07**
				Sx	1,23		
CL-4-51	376000	5442000	Cloridorme	n	44		
				moy	2,73	**2,68**	**3,10**
				Sx	0,238		
CL-4-54	376000	5442000	Cloridorme	n	23		
				moy	2,38	**2,43**	**2,74**
				Sx	0,18		
CL-4-55	376000	5442000	Des Landes	n	41		
				moy	2,4	**2,44**	**2,76**
				Sx	0,301		
DL-4-59	376000	5442000	Des Landes	n	47		
				moy	2,45	**2,48**	**2,81**
				Sx	0,234		
CR-4-62	376000	5442000	Cap-des-Rosiers	n	51		
				moy	2,24	**2,33**	**2,59**
				Sx	0,124		
CR-4-65	376000	5442000	Cap-des-Rosiers	n	50		
				moy	2,21	**2,30**	**2,56**
				Sx	0,107		
CL-5-66	363000	5450000	Cloridorme	n	50		
				moy	2,34	**2,40**	**2,70**
				Sx	0,353		
CL-5-67	363000	5450000	Cloridorme	n	52		
				moy	2,55	**2,55**	**2,91**
				Sx	0,282		
CL-5-70	363000	5450000	Cloridorme	n	20		
				moy	2,75	**2,69**	**3,12**
				Sx	0,123		

Section name	Appoximative location of section		Formation	STAT	Macerals Pyrobitumen	**Mean estimated Ro of vitrinite if the lithology is a**	
	UTM est	UTM west				**Shale (min.)**	**Limestone (max.)**
CL-5-71	363000	5450000	Clondorme	n	13		
				moy	2,86	**2,77**	**3,23**
				Sx	0,112		
CL-5-72	363000	5450000	Clondorme	n	6		
				moy	3,18	**2,99**	**3,56**
				Sx	0,454		
CL-5-73	363000	5450000	Clondorme	n	53		
				moy	2,98	**2,85**	**3,35**
				Sx	0,265		
CL-5-75	363000	5450000	Clondorme	n	50		
				moy	3,25	**3,04**	**3,63**
				Sx	0,181		
DL-5-80	363000	5450000	Des Landes	n	58		
				moy	2,64	**2,62**	**3,01**
				Sx	0,27		
CL-6-87	358000	5452000	Clondorme	n	19		
				moy	2,92	**2,81**	**3,29**
				Sx	0,449		
CL-6-88	358000	5452000	Clondorme	n	48		
				moy	2,57	**2,57**	**2,93**
				Sx	0,354		
CL-6-90	358000	5452000	Clondorme	n	49		
				moy	2,72	**2,67**	**3,09**
				Sx	0,234		
CL-6-92	358000	5452000	Clondorme	n	53		
				moy	3,1	**2,94**	**3,48**
				Sx	0,191		
CL-6-93	358000	5452000	Clondorme	n	48		
				moy	3,04	**2,90**	**3,42**
				Sx	0,116		
CL-6-95	358000	5452000	Clondorme	n	45		
				moy	3,19	**3,00**	**3,57**
				Sx	0,257		
CR-6-98	358000	5452000	Cap-des-Rosiers	n	7		
				moy	2,4	**2,44**	**2,76**
				Sx	0,06		
CL-7-101	342000	5455000	Clondorme	n	32		
				moy	3,68	**3,32**	**4,06**
				Sx	0,566		
CL-7-102	342000	5455000	Clondorme	n	50		
				moy	3,28	**3,06**	**3,66**
				Sx	0,475		
CL-7-104	342000	5455000	Clondorme	n	50		
				moy	3,85	**3,43**	**4,23**
				Sx	0,387		
DL-7-107	342000	5455000	Des Landes	n	50		
				moy	3,05	**2,90**	**3,43**
				Sx	0,158		
CR-7-112	342000	5455000	Cap-des-Rosiers	n	50		
				moy	2,68	**2,64**	**3,05**
				Sx	0,84		
CR-7-119	342000	5455000	Cap-des-Rosiers	n	50		
				moy	4,07	**3,57**	**4,45**
				Sx	0,194		
CL-7-124	342000	5455000	Clondorme	n	50		
				moy	3,39	**3,13**	**3,77**
				Sx	0,45		
CL-8-126	324000	5457000	Clondorme	n	12		
				moy	3,77	**3,38**	**4,15**
				Sx	0,529		
CL-8-129	324000	5457000	Clondorme	n	7		
				moy	3,33	**3,09**	**3,71**
				Sx	0,11		
CL-8-132	324000	5457000	Clondorme	n	49		
				moy	3,8	**3,40**	**4,18**
				Sx	3,03		
CL-8-134	324000	5457000	Clondorme	n	54		
				moy	3,95	**3,49**	**4,33**
				Sx	0,309		

Section name	Approximative location of section		Formation	STAT	Macerals Pyrobitumen	Mean estimated Ro of vitrinite if the lithology is a	
	UTM est	UTM west				Shale (min.)	Limestone (max.)
CL-8-135	324000	5457000	Clondorme	n	50		
				moy	4	3,53	4,38
				Sx	0,419		
CL-9-136	311000	5458000	Clondorme	n	53		
				moy	4,41	3,78	4,78
				Sx	0,558		
CL-9-138	311000	5458000	Clondorme	n	52		
				moy	5,58	4,48	5,92
				Sx	1,011		
CL-9-141	311000	5458000	Clondorme	n	9		
				moy	4,9	4,08	5,26
				Sx	0,81		
DL-9-144	311000	5458000	Des Landes	n	17		
				moy	3,68	3,32	4,06
				Sx	0,22		
CR-9-147	311000	5458000	Cap-des-Rosiers	n	49		
				moy	3,18	2,99	3,56
				Sx	0,685		
CR-9-149	311000	5458000	Cap-des-Rosiers	n	50		
				moy	2,73	2,68	3,10
				Sx	0,133		
CL10-151	300000	5457000	Cloridorme	n	54		
				moy	4,09	3,58	4,47
				Sx	0,361		
CL10-155	300000	5457000	Clondorme	n	48		
				moy	4,11	3,60	4,49
				Sx	0,411		
CL10-155	300000	5457000	Clondorme	n	15		
				moy	5,25	4,29	5,60
				Sx	0,529		
DL10-155	300000	5457000	Des Landes	n	52		
				moy	5,56	4,47	5,90
				Sx	0,644		
DL10-161	300000	5457000	Des Landes	n	35		
				moy	6,06	4,75	6,37
				Sx	0,807		
CL11-168	292000	5457000	Clondorme	n	38		
				moy	4,16	3,63	4,54
				Sx	0,172		
CL12-177	283000	5457000	Clondorme	n	51		
				moy	3,77	3,38	4,15
				Sx	0,833		
DL12-179	283000	5457000	Des Landes	n	45		
				moy	4,85	4,05	5,21
				Sx	0,404		
DL12-185	283000	5457000	Des Landes	n	58		
				moy	5,58	4,48	5,92
				Sx	0,882		
DL13-202	271000	5455000	Des Landes	n	50		
				moy	2,98	2,85	3,35
				Sx	0,182		
CM13-204	271000	5455000	Cap-Chat Mélange	n	50		
				moy	2,93	2,82	3,30
				Sx	0,193		
CL13-209	271000	5455000	Cloridorme	n	50		
				moy	4,01	3,53	4,39
				Sx	0,411		
DL13-215	271000	5455000	Des Landes	n	7		
				moy	4,68	3,95	5,05
				Sx	0,324		
DL13-217	271000	5455000	Des Landes	n	39		
				moy	5,1	4,20	5,45
				Sx	0,589		
DL13-221	271000	5455000	Des Landes	n	46		
				moy	5,38	4,36	5,72
				Sx	0,33		

INRS	Section name	Location - zone 19		Formation	Strat. depth	STAT	Macerals Vitrinite ind.	Mean est. Ro vitrinite
		UTM est	UTM west					
6702	Rivière Nouvelle Nord	677400	5374380	Battery Pt	0	n	44	
						moy	1.10	1.10
						Sx	.11	
6704	Rivière Nouvelle Nord	677250	5374410	York River	210	n	5	
						moy	1.14	1.14
						Sx	.22	
6706	Rivière Nouvelle Nord	677040	5374460	York River	390	n	30	
						moy	1.56	1.56
						Sx	.14	
6580	Rivière Nouvelle Sud	680500	5372310	York River	1416	n	50	
						moy	1.04	1.04
						Sx	.10	
6583	Rivière Nouvelle Sud	680300	5372340	York River	1494	n	31	
						moy	1.26	1.26
						Sx	.11	
6584	Rivière Nouvelle Sud	680110	5372390	York River	1524	n	35	
						moy	1.13	1.13
						Sx	.15	
	ROUTE SQUARE							
6563	Forks Ouest	686160	5381550	York River	843	n	30	
						moy	1.26	1.26
						Sx	.07	
6562	Forks Ouest	686160	5381550	York River	869	n	30	
						moy	1.35	1.35
						Sx		
6557	Forks Ouest	682570	5360330	York River	1095	n	30	
						moy	1.37	1.37
						Sx	.09	
6558	Forks Ouest	683760	5361140	York River	984	n	22	
						moy	1.06	1.06
						Sx	.13	
	RIVIÈRE CASCAPEDIA BRANCHE DU LAC							
6635	Detailed section	684510	5385350	York River	3497	n	31	
						moy	.84	.84
						Sx	.21	
6633	Detailed section	684460	5385390	York River	3521	n	50	
						moy	.68	.68
						Sx	.07	
6630	Detailed section	684390	5385450	York River	3555	n	29	
						moy	.88	.88
						Sx	.22	
6628	Detailed section	684360	5385470	York River	3567	n	36	
						moy	.70	.70
						Sx	.08	
6626	Detailed section	684340	5385490	York River	3576	n	30	
						moy	.66	.66
						Sx	.08	
6624	Detailed section	684330	5385500	York River	3585	n	36	
						moy	.81	.81
						Sx	.09	
6622	Detailed section	684280	5385540	York River	3605	n	50	
						moy	.74	.74
						Sx	.09	
6619	Detailed section	684230	5385580	York River	3632	n	25	
						moy	.68	.68
						Sx	.09	
6617	Detailed section	684210	5385590	York River	3637	n	25	
						moy	.69	.69
						Sx	.10	
6612	Detailed section	684180	5385630	York River	3656	n	13	
						moy	.74	.74
						Sx	.07	
6567	Branche du Lac	687910	5382970	York River	1146	n	40	
						moy	1.34	1.34
						Sx	.13	

INRS	Section name	Location - zone 19		Formation	Strati. depth	STAT	Macerals Vitrinite und.	Mean est. Ro vitrinite
		UTM est	UTM west					
6653	Branche du Lac	686840	5383340	York River	2352	n	50	
						moy	.90	.90
						Sx	.10	
6650	Branche du Lac	684360	5385540	York River	3336	n	50	
						moy	.78	.78
						Sx	.11	
6648	Branche du Lac	681180	5385600	York River	3474	n	25	
						moy	.78	.78
						Sx	.13	
6639	Branche du Lac	683330	5386370	York River	3660	n	30	
						moy	.61	.61
						Sx	.13	
6642	Branche du Lac	683330	5386370	York River	3726	n	25	
						moy	.73	.73
						Sx	.16	
6654	Branche du Lac	682070	5387970	York River	4584	n	20	
						moy	2.28	2.28
						Sx	.42	
6662	Bras aux Saumons	698980	5400750	York River	84	n	30	
						moy	1.37	1.37
						Sx	.11	
6664	Bras aux Saumons	699410	5401200	York River	132	n	40	
						moy	1.58	1.58
						Sx	.18	
6670	Bras aux Saumons	698340	5405370	York River	606	n	39	
						moy	1.05	1.05
						Sx	.14	
8071	Bras aux Saumons	697430	5405580	Grande Grève	894	n	21	
						moy	1.23	1.23
						Sx	.37	
6687	Ruisseau Brandy Nord	704750	5401550	York River	1584	n	30	
						moy	1.50	1.50
						Sx	.15	
6685	Ruisseau Brandy Nord	704750	5401550	York River	1770	n	15	
						moy	.66	.66
						Sx	.12	
6672	Ruisseau Brandy	706840	5403880	York River	300	n	50	
						moy	1.09	1.09
						Sx	.12	
6528	Route des Lacs Josué	704300	53833760	Battery Pt	1542	n	23	
						moy	1.08	1.08
						Sx	.11	
6529	Route des Lacs Josué	704130	5383780	Battery Pt	1548	n	30	
						moy	1.58	1.58
						Sx	.15	
6606	Ruisseau Marcil Ouest	716710	5387500	York River	210	n	40	
						moy	1.24	1.24
						Sx	.16	
6598	Ruisseau Marcil Ouest	716720	5387190	York River	786	n	39	
						moy	1.51	1.51
						Sx	.17	
6597	Ruisseau Marcil Ouest	716970	5386060	York River	912	n	30	
						moy	1.41	1.41
						Sx	.11	
6594	Ruisseau Marcil Ouest	717090	5385600	York River	1206	n	30	
						moy	1.51	1.51
						Sx	.12	
6593	Ruisseau Marcil Ouest	717000	5385220	York River	1224	n	25	
						moy	1.56	1.56
						Sx	.14	
6591	Ruisseau Marcil Ouest	716770	5384840	York River	1248	n	50	
						moy	1.53	1.53
						Sx	.14	
6709	Ruisseau Caron	720000	5388770	York River	372	n	10	
						moy	2.16	2.16
						Sx	.20	

INRS	Section name	Location - zone 19		Formation	Strati depth	STAT	Macerals Vitrinite und.	*Mean est. Ro vitrinite*
		UTM est	UTM west					
6712	Ruisseau Caron	720270	5388290	York River	612	n	**50**	
						moy	**2.35**	**2.35**
						Sx	**.21**	
6714	Ruisseau Caron	720800	5387660	York River	948	n	**22**	
						moy	**2.13**	**2.13**
						Sx	**.21**	
6716	Ruisseau Caron	721180	5387020	York River	1398	n	**50**	
						moy	**2.15**	**2.15**
						Sx	**.24**	

Well	INRS	Depth sup	Depth inf	Formation	STAT	Ro Vitr Hér. 83	Ro vitr. INRS 74	Well	INRS	Depth inf	Formation	STAT	Ro vitr. INRS 74	Well	INRS	Depth sup.	Depth inf.	Formation	STAT	Ro vitr. INRS 74
Quebec Oil No 2	2466	239,6	242,6	Indian Cove	n	50	50	Tar Point		263,7	Battery Pt	n	17	Haldimand		283,5	323,1	Battery Pt	n	50
					moy	1,04	**1.10**					moy	**0.51**						moy	**0.73**
					Sx	0,17	0,11					Sx	0,04						Sx	0,06
Quebec Oil No 2	2468	358,4	361,5	Indian Cove	n	50	50	Tar Point		272,8	Battery Pt	n	36	Haldimand		484,6	487,7	Battery Pt	n	50
					moy	1,15	**1.21**					moy	**0.52**						moy	**0.81**
					Sx	0,17	0,12					Sx	0,06						Sx	0,06
Quebec Oil No 2	2470	513,9	516,9	Indian Cove	n	38	50	Tar Point	2278	484,6	York River	n	20	Haldimand	2278	759	762	York River	n	29
					moy	1,34	**1.45**					moy	**0.51**						moy	**0.83**
					Sx	0,19	0,17					Sx	0,07						Sx	0,20
Quebec Oil No 2	2472	632,8	753,5	Shiphead	n	50	49	Tar Point	2279	548,6	York River	n	10	Haldimand	2279	859,5	862,6	York River	n	24
					moy	1,57	**1.51**					moy	**0.63**						moy	**0.89**
					Sx	0,27	0,20					Sx	0,09						Sx	0,90
Quebec Oil No 2	2474	751,6	754,7	Shiphead	n	44	35	Tar Point	2782	731,5	York River	n	13	Haldimand	2782	1190	1192	York River	n	52
					moy	1,47	**1.55**					moy	**0.69**						moy	**0.65**
					Sx	0,34	0,15					Sx	0,08						Sx	0,10
Quebec Oil No 2	2476	879,7	882,7	Shiphead	n	50	46	Tar Point		947,9	York River	n	33	Haldimand		1362	1402	York River	n	48
					moy	1,62	**1.65**					moy	**0.64**						moy	**0.85**
					Sx	0,30	0,17					Sx	0,04						Sx	0,10
Quebec Oil No 2	2479	1063	1066	Shiphead	n	50	40	Tar Point	2286	975,4	York River	n	19	Sunny Bank		308	309	York River	moy	**0.73**
					moy	1,79	**1.93**					moy	**0.53**	Sunny Bank		400	403	York River	moy	**0.82**
					Sx	0,29	0,19					Sx	0,06	Sunny Bank		1295	1297	Indian Cove	moy	**0.69**
Quebec Oil No 2	2482	1245	1248	Shiphead	n		50	Tar Point		1439	York River	n	15	Sunny Bank		1544	1547	Indian Cove	moy	**0.81**
					moy		**1.93**					moy	**0.43**	Sunny Bank		1918	1921	Forillon	moy	**0.99**
					Sx		0,18					Sx	0,04	Sunny Bank		2530	2533	Indian Pt	moy	**1.6**
Quebec Oil No 2	2485	1419	1422	Shiphead	n	36	30	Tar Point	2293	1466	York River	n	53	Sunny Bank		2925	2929	Indian Pt	moy	**2.14**
					moy	1,90	**2.03**					moy	**0.53**	Sunny Bank		3289	3293	Indian Pt	moy	**2.29**
					Sx	0,32	0,17					Sx	0,07	Sunny Bank		3475	3478	Roncelles	moy	**2.33**
Quebec Oil No 2	2489	1666	1669	Shiphead	n	26	30	Tar Point	2298	1768	York River	n	53	Sunny Bank		3533	3536	Roncelles	moy	**2.39**
					moy	2,05	**2.21**					moy	**0.77**	York			26	West Point	moy	**1.09**
					Sx	0,15	0,20					Sx	0,07	York		550	555	Gascons	moy	**1.17**
Quebec Oil No 2	2491	1794	1797	Shiphead	n	50	50	Tar Point	2300	1894	York River	n	48	York			755	Gascons	moy	**1.76**
					moy	2,27	**2.25**					moy	**0.60**	York			994	Laforce	moy	**1.94**
					Sx	0,25	0,14					Sx	0,06	York			1109	Burnt Jam Brook	moy	**2.35**
														York			1129	Burnt Jam Brook	moy	**2.26**

Annex 4.3 : Location, descriptions and origin and quantity of oil produced during tests in all Gaspé Peninsula wells

Data from McGerrigle (1950), MRN (1974 and upgrade 1988), Ministère of énergie and ressources of Québec files.

10 out of text pages

CHAPTER 5

TECTONOSTRATIGRAPHY AND TECTONIC EVOLUTION OF THE GASPÉ PENINSULA

5 TECTONOSTRATIGRAPHY AND TECTONIC EVOLUTION OF THE GASPÉ PENINSULA

PREAMBLE

This report is a synthesis of the current understanding of the tectonic and structural history of the Gaspé Peninsula from pre-Taconian to post-Alleghanian time. The first part gives an introduction to the zonation of the Canadian Appalachians, whereas the second part is a summary of the tectonostratigraphy of the Québec Appalachians. The main part of the report concerns the Appalachians of the Gaspé Peninsula. Most of the stratigraphic units of the Gaspé Peninsula, from the Cambrian to the Carboniferous, are described according to the tectonostratigraphic framework recognized in the Canadian Appalachians. The structural style of folding and faulting is discussed for each zones and the tectonic evolution of the Appalachians of the Gaspé Peninsula during Paleozoic time is presented. The stratigraphic nomenclature of the recent geological map of the peninsula is used in this report (Carte géologique, Péninsule de la Gaspésie, by Brisebois et al., 1991).

Synthesis papers that I have written with collaborators were consulted for this report. I would like to acknowledge Donna Kirkwood, Pierre-André Bourque and Alain Tremblay for numerous discussions while I was working on these papers with them.

5.1 INTRODUCTION TO THE CANADIAN APPALACHIANS

Extending from the Gulf of Mexico to Newfoundland along the eastern margin of North America, the Appalachian Orogen, is quite possibly the most familiar fold belt in the world. The Appalachians are part of the vast Appalachian-Caledonian orogen which, after being disrupted by the Mesozoic opening of the Atlantic Ocean, now spreads over several continents (Fig. 5.1). From the geosynclinal concepts of Hall (1859) and Kay (1951), the tectonic models of Wilson (1966) and Williams and Hatcher (1982), and the deep seismic studies of the 1980's (Keen et al., 1986; Marillier et al., 1989; Stockmal et al., 1990), the Appalachians have played an important role in the evolution of scientific concepts on orogens. The orogen documents the full spectrum of tectonostratigraphic processes within a latest Proterozoic-Paleozoic Wilson cycle, including ocean rifting and spreading, island arc collision and obduction, accretion of microcontinental terranes, and final continental collision. The orogen also shows fine examples of foreland and successor basins. The orogen is exposed at a range of structural levels, and has excellent chronologic control.

The Canadian segment of the Appalachians has recorded much of the geologic history of the orogen, from the opening of the Iapetus Ocean in Late Precambrian time, to closure in the Paleozoic, followed by the eventual opening of the Atlantic ocean in Mesozoic time. Although orogenic processes were active from Ordovician to Carboniferous time, three major pulses are

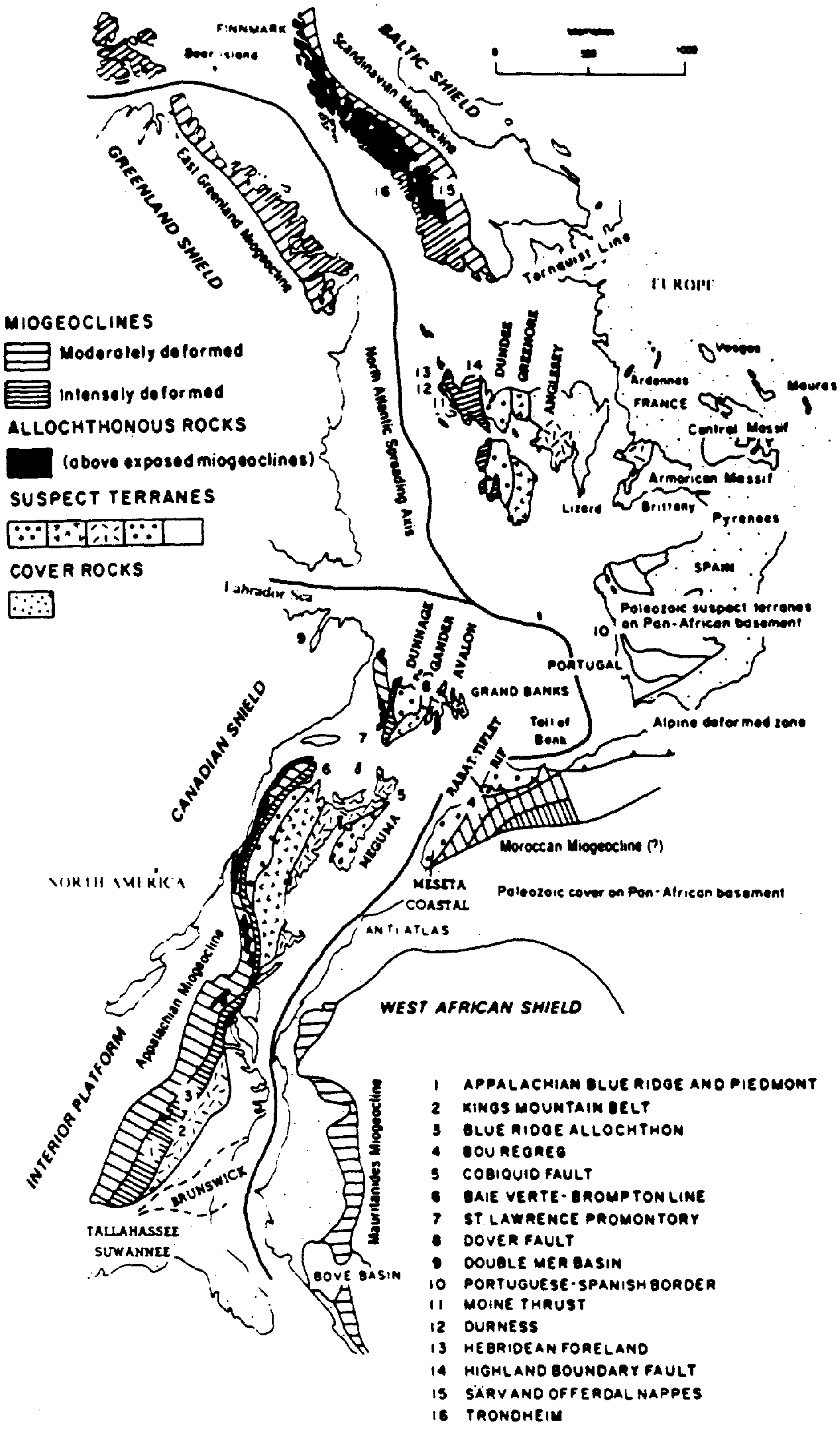

Figure 5.1. Tectonic elements of the North Atlantic region. From Williams (1984).

recognized: the middle Ordovician Taconian, the Siluro-Devonian Acadian and the Permo-Carboniferous Alleghanian orogenies (Williams, 1979). Although, some include all pre-Carboniferous deformation features in the Silurian and Devonian rocks within the Acadian orogeny (e.g. Williams, 1993), distinct Silurian and Devonian tectonic events are recognized in the northern Appalachians (Dunning et al., 1990; Hibbard, 1994; van Staal and de Roo, 1996). The term Salinian orogeny is now used for distinct Silurian deformation events in Newfoundland (Dunning et al., 1990). Paleozoic rocks of the Canadian Appalachians can be divided into four temporal assemblages: 1) Latest Precambrian to Late Ordovician rocks (referred to as the Cambro-Ordovician), 2) Late Ordovician to Middle Devonian rocks (referred to as the Siluro-Devonian), 3) Late Devonian and Carboniferous rocks and 4) Mesozoic rocks. The four rock assemblages are distinct and separated by important structural or depositional unconformities.

Cambro-Ordovician rocks of the Canadian Appalachians were divided into a number of tectono-stratigraphic zones by Williams (1979). These are, from northwest to southeast: the Humber, Dunnage, Gander, Avalon and Meguma zones (Fig. 5.2). The Humber Zone represents the ancient passive continental margin formed on Laurentia, situated on the western side of the Paleozoic Iapetus ocean. The other zones are viewed as suspect terranes outboard of the North American miogeocline that were accreted to Laurentia (Williams and Hatcher, 1983) during the orogenic pulses. The Dunnage Zone represents vestiges of the Iapetus Ocean and of island arc sequences and mélanges built upon it. The Gander Zone represents the destroyed eastern continental margin of Iapetus (Williams, 1979). The Avalon Zone was a stable platform in the early Paleozoic, whereas the Meguma Zone has been interpreted as a remnant of the continental embankment of ancient northwest Africa.

Siluro-Devonian sedimentary and volcanic rock assemblages represent successor basins which developed after the middle to late Ordovician Taconian orogeny. They have been subsequently deformed by the Salinian and Acadian orogenies in Silurian and/or Devonian times. Siluro-Devonian rocks are well exposed within the Maritime Appalachians, as opposed to Newfoundland where they are rare and poorly exposed. The Siluro-Devonian sequences have been divided into depositional belts (e.g. Gaspé Belt; Fig. 5.3) (Williams, 1995).

Upper Devonian to Carboniferous rocks include terrestrial sandstones and conglomerates, plus volcanic, carbonate and evaporite units which form the vast Maritimes Basin (Howie and Barss 1975) (Fig. 5.4). In some places in Nova Scotia, these rocks are deformed by the late Paleozoic Alleghanian orogeny.

Mesozoic rocks are uncommon in the Canadian Appalachians. However, Triassic sedimentary and volcanic rocks are abundant in the Minas rift-basin of the Bay of Fundy area where they unconformably overlie deformed Carboniferous rocks. Mafic dykes of Triassic to Cretaceous age occur in a few places.

5.2 <u>TECTONOSTRATIGRAPHY OF THE QUEBEC APPALACHIANS</u>

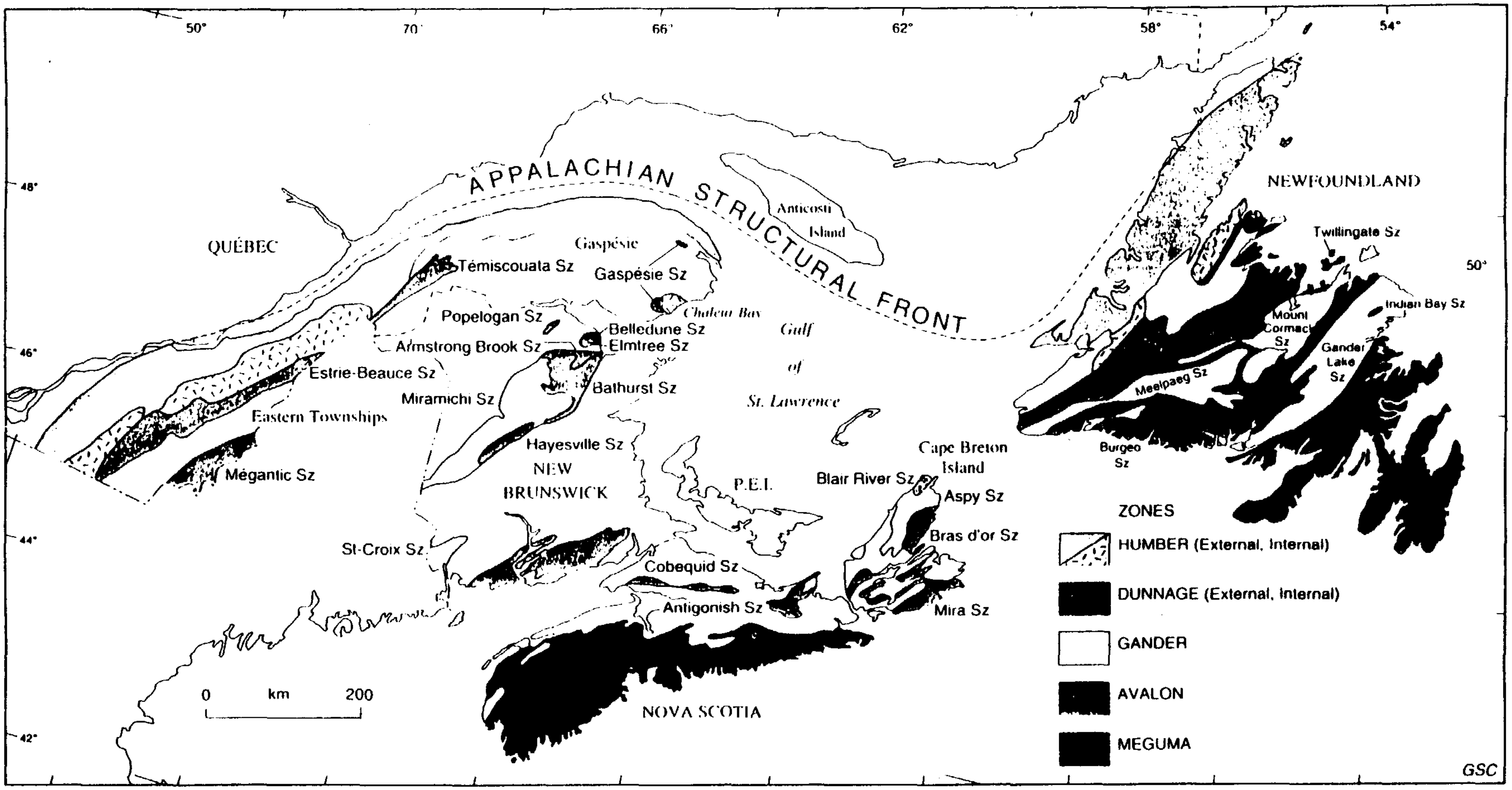

Figure 5.2. Outcrop areas of lower Paleozoic and older rocks that define zones and subzones of the Canadian Appalachians. From Williams (1995).

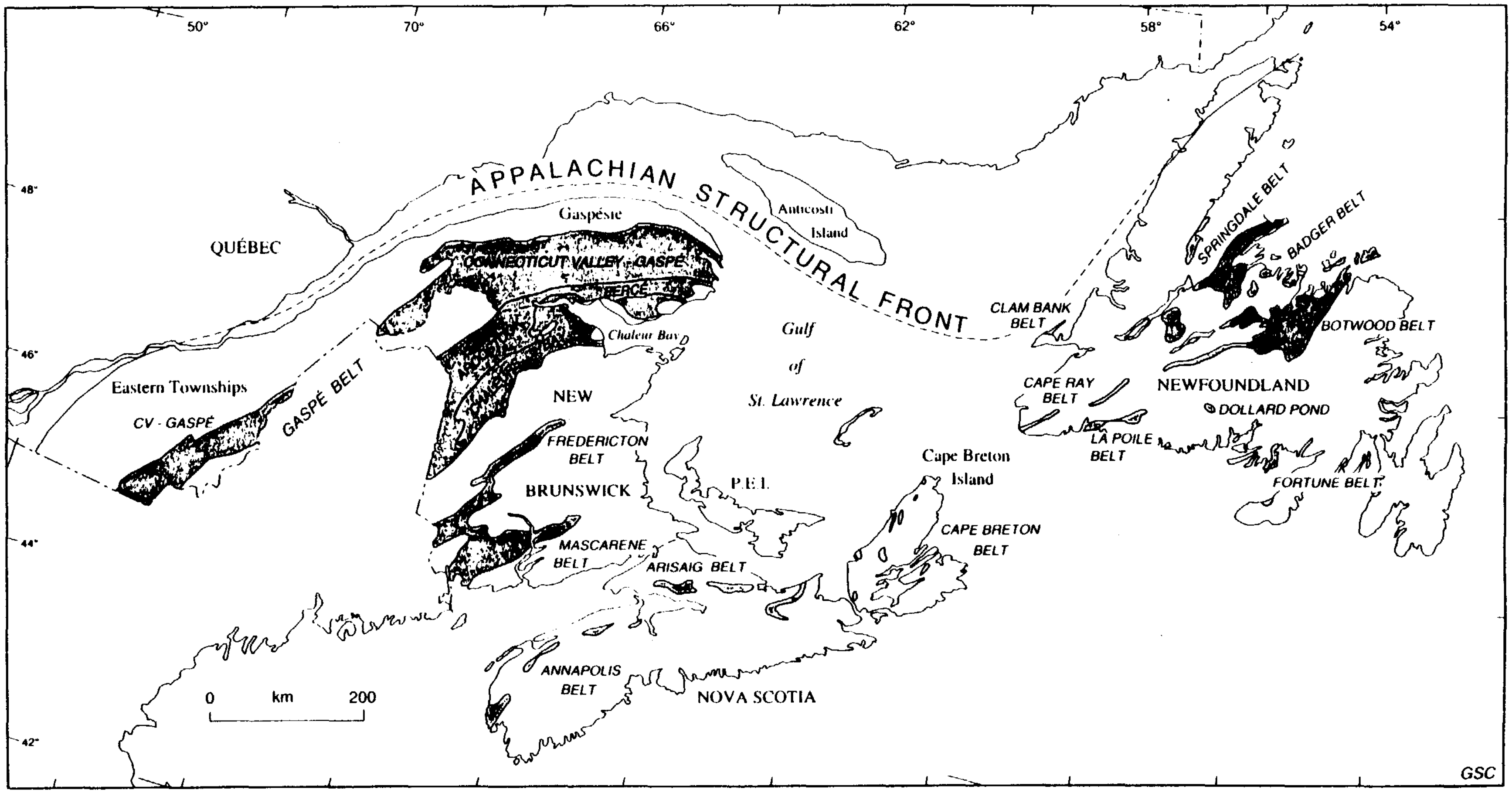

Figure 5.3. Outcrop areas of Middle Paleozoic rocks that define belts of the Canadian Appalachians. From Williams (1995).

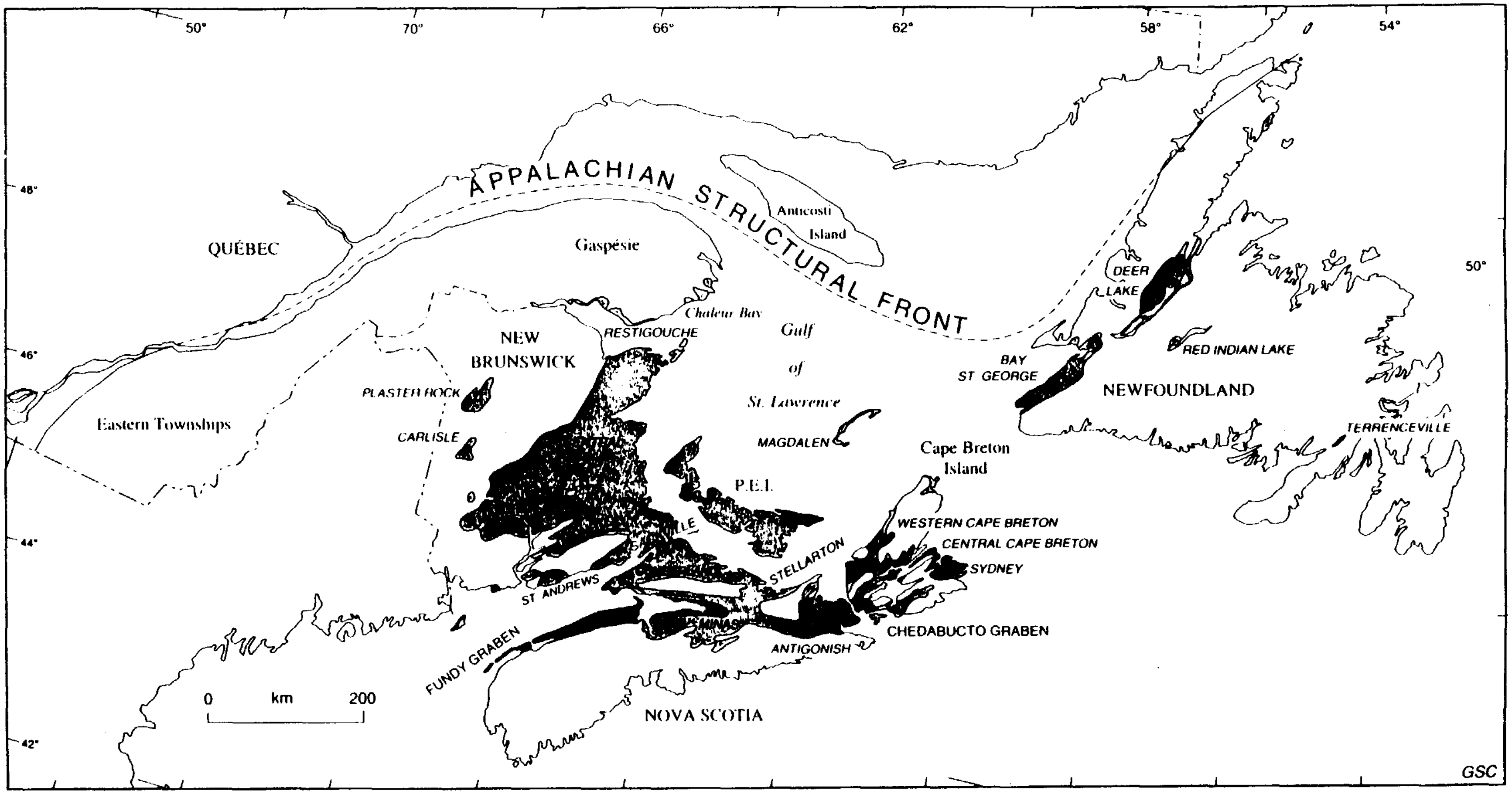

Figure 5.4. Outcrop areas of upper Paleozoic and Mesozoic rocks that define basins and graben, respectively, of the Canadian Appalachians.

The sinuous trace of the Appalachian Orogen is marked by a series of reentrants and promontories, defined by the configuration of the craton-orogen boundary. In the northern Appalachians, the Quebec Reentrant separates the St. Lawrence (Newfoundland) and the New York (New England) promontories. Within this reentrant lies the most complete paleontological and stratigraphic record for the orogen, the lowest grades of metamorphism and the least intensity of deformation. The Québec Appalachians occupy most of the Québec Reentrant and the Gaspé Peninsula is located at the northeastern end of this reentrant, close to the St. Lawrence Promontory.

In Québec, the Appalachian orogen is comprised of the first three rocks assemblages recognized in the Canadian Appalachians (Fig. 5.5): 1) Lower Cambrian (uppermost Precambrian ?) to Upper Ordovician rocks, (Cambro-Ordovician); 2) Upper Ordovician to Middle Devonian rocks (Siluro-Devonian); and 3) Upper Devonian to Carboniferous rocks. The first rock assemblage was involved in both the Taconian (Late Ordovician) and Acadian (Middle Devonian) orogenies (St-Julien and Hubert, 1975), whereas the second rock assemblage was mainly deformed by the Acadian orogeny and also record structural features related to the Salinian disturbance in the Gaspé Peninsula (Boucot, 1962). The effects of the Alleghanian (Late Carboniferous-Permian) orogeny were minimal on Carboniferous rocks which crop out only in Gaspé Peninsula. The Cretaceous plutons of the Monteregians Hills of southern Québec (near Montréal) are the youngest rocks to occur in the Québec Appalachians (not shown on Fig. 5.5).

In the Québec Appalachians, the Taconian orogeny was interpreted as the result of a collision between the Early Paleozoic passive continental margin of Laurentia and island arc terrane or a continental magmatic arc above an east-dipping subduction zone (St-Julien and Hubert, 1975; de Broucker, 1987). In southern Québec, Taconian tectonism is mainly related to the obduction of a large ophiolitic nappe (Pinet and Tremblay, 1995). The Acadian orogeny in the Québec Appalachians is interpreted in terms of a continental collision of Gondwana along the irregular margin of Laurentian and its Taconian accreted terranes (Malo et al., 1995). Continued convergence between the Taconian and Acadian orogenies and a polarity flip of the Taconian subduction zone may have cause the Salinian deformation on the Gander margin of the Appalachians (van Staal, 1994), while the Laurentian margin experienced an extensional regime of deformation between the two major orogenies (Malo and Kirkwood, 1996; Bourque et al., submitted, 1996).

5.2.1 CAMBRO-ORDOVICIAN ROCKS: HUMBER AND DUNNAGE ZONES

Pre- to syn-Taconian Cambro-Ordovician rocks are divided into two tectonostratigraphic zones, Humber and Dunnage zones (Williams, 1979) which are in tectonic contact along the Baie Verte - Brompton Line (BBL) (Williams and St-Julien, 1982) (Fig. 5.5). The BBL has been interpreted as the surface expression of the Taconian tectonic contact between early Paleozoic continental and oceanic domains of the Humber and Dunnage zones, respectively (Williams and St-Julien

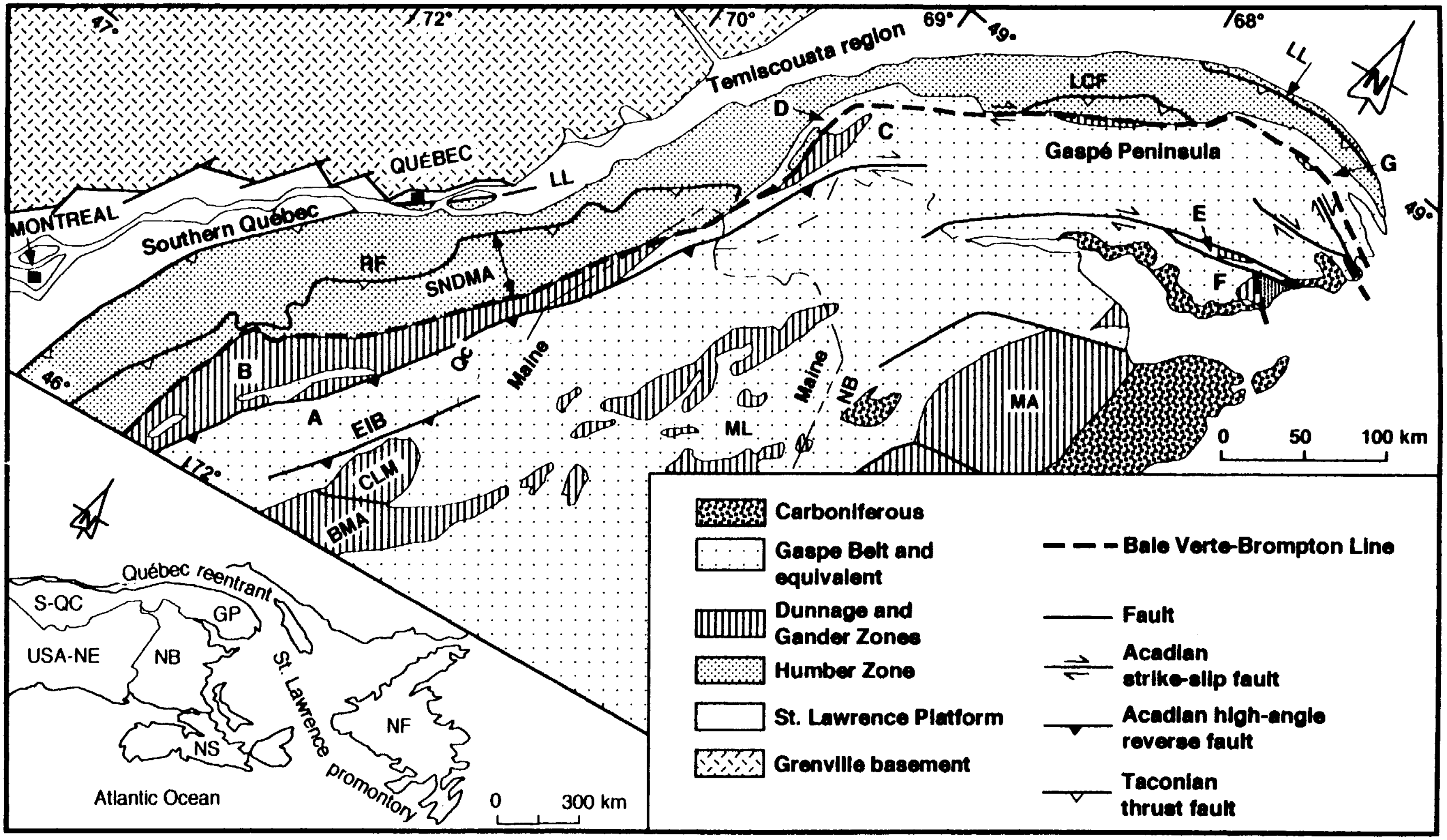

Figure 5.5. Geological map of the Québec Appalachians (modified from Williams, 1978). Locations of stratigraphic columns A to G of figure 5.8. BMA: Boundary Montain anticlinorium, CLM: Chain Lake Massif, LL: Logan's Line, LCF: Lac Cascapédia fault, MA: Miramichi anticlinorium, NB: New Brunswick, PMA: Pennington Mountain anticlinorium, Qc: Québec, RF: Richardson fault, SNDA: Sutton Notre-Dame anticlinorium, TI: Trinité inlier. The area covered by the Dunnage Zone in the Trinité inlier includes also rocks of the Lower Temiscouata sequence. Modified rom Malo et al. (1995).

1982). The BBL was reactivated and folded during both the Taconian and Acadian orogenies (Malo et al., 1992; Pinet and Tremblay, 1995). The Humber Zone is made up of Lower Paleozoic, platform sequence, slope and rise deposits of the Laurentian continental margin. The Humber Zone can be divided into four tectonic domains, from the northwest to the southeast: the autochthonous domain, the foreland thrust belt, the external and internal nappe domains (St-Julien et al., 1983). The autochthonous domain, or the St. Lawrence Lowlands platform (Fig. 5.5), is composed of a nearly undeformed Cambrian to Upper Ordovician platform sequence covered by synorogenic turbidites. The St. Lawrence Lowlands platform is bounded to the north by the Grenville basement and to the south by the first thrust faults of the foreland thrust belt. The foreland thrust belt and the two nappe domains are allochthonous on autochthonous cover rocks of the St. Lawrence Lowlands platform (Fig. 5.5). The foreland thrust belt, limited to the south by the Logan's Line (St-Julien and Hubert, 1975), is composed of rocks of the St. Lawrence Lowlands platform that are repeated many times and imbricated within thrust slices. The allochthonous rocks of the Québec Appalachians, external facies of the platform sequence with chronologically well dated slope and rise deposits, are found in northwest-verging thrust sheets of the external and internal nappe domains. The external nappe domain is limited to the north by Logan's Line and to the south by the Richardson fault, in southern Québec, and the Lac Cascapédia fault, in the Gaspé Peninsula (Figs. 5.5, 5.6). The southern limit of the internal nappe domains is the BBL. The regional deformation and metamorphism of the nappe domains of the Humber Zone rocks are mainly related to the Taconian orogeny (St-Julien and Hubert, 1975). Rocks of the external nappe domains attain the prehnite-pumpellyite facies of regional metamorphism (St-Julien et al., 1983), whereas rocks of the internal nappe domain are regionally metamorphosed to greenschist grade. Locally amphibolite grade is found just north of the Shickshock-Sud fault within the internal nappe domain of the Humber Zone (Camiré et al., 1993a) and also at the base of major ophiolitic sheets (e.g. Mont Albert nappe in Gaspé Peninsula, Thetford ophiolitic complex in southern Québec).

Rocks of the Dunnage Zone record the development of subduction-related terranes during the Ordovician and include ophiolite rocks, mélanges, arc volcanics and forearc basin deposits (Tremblay et al., 1995). We can divide the Dunnage Zone into three domains, from northwest to southeast: the mélange domain, the fore-arc basin and the arc volcanic domain (Tremblay et al., 1995). The northern limit of the Dunnage Zone is the BBL, whereas, to the south, the Dunnage Zone rocks are either unconformably overlain by the Gaspé Belt rocks or in fault contact with them. The mélange domain, located just south of the BBL throughout the Québec Appalachians, is composed of Lower to Middle Ordovician rocks with high stratigraphic and structural complexities resulting from both olistostromal and tectonic processes (Cousineau, 1990; Tremblay and St. Julien, 1990). The mélange is described as a graphitic pebbly mudstone (Slivitzky and St-Julien, 1987) with different lithofacies (Cousineau, 1990) including ophiolitic rocks, ophiolitic mélanges and volcanic rocks. The fore-arc basin, to the south of the mélange domain, is composed of a Middle Ordovician flysch-dominated sequence from southern Québec to the Gaspé Peninsula. The Ascot Complex (Tremblay and St-Julien, 1990) represents the arc volcanic domain of the Dunnage Zone. It is only recognized in southern Québec and is comprised mainly

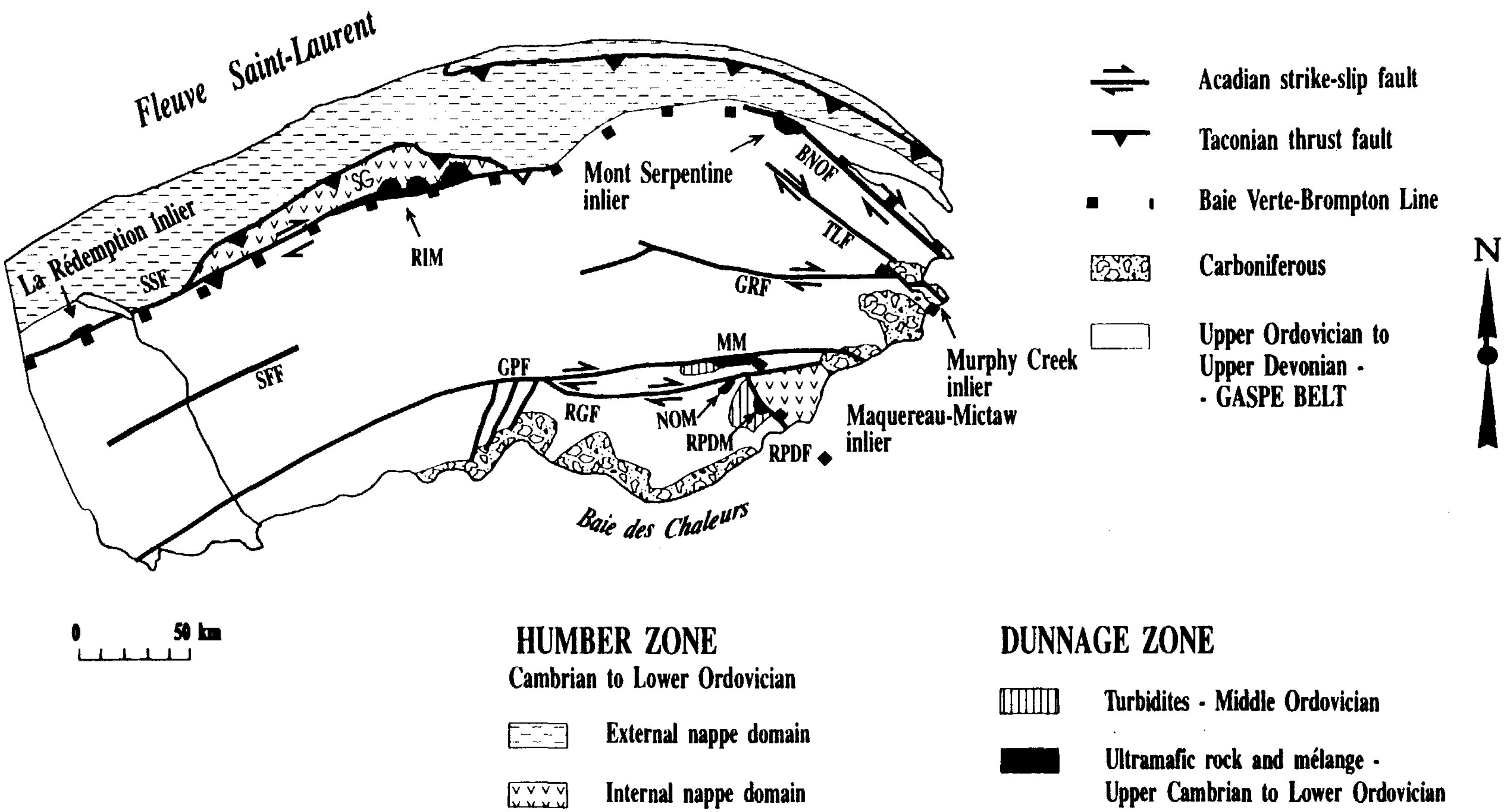

Figure 5.6. Geological map of the Gaspé Peninsula showing the BBL in relation to Cambro-Ordovician Humber and Dunnage Zones and the major Acadian faults (in capital bold lettters). BNOF: Bassin Nord-Ouest fault, GPF: Grand Pabos fault, GRF: Grande Rivière fault, MM: McCrea mélange, NOM: Nadeau ophiolitic Mélange, RGF: Rivière Garin fault, RIM: Ruisseau Isabelle mélange, RPDF: Rivière Port-Daniel fault, RPDM: Rivière Port-Daniel Mélange, SFF: Sainte-Florence fault, SG:Shickshock Gr., SSF: Shickshock-Sud fault, TLF: Troisième Lac fault. Modified from Malo et al. (1992).

of felsic and mafic volcanic rocks, some metamorphic schists and plutonic rocks (Tremblay, 1992). In the Québec Appalachians, the Dunnage Zone is allochthonous on the Humber Zone to the NW (St-Julien et al., 1983). Regional deformation and lower greenschist metamorphism of the Dunnage rocks in the Québec Appalachians are clearly associated with the Middle Devonian Acadian orogeny (Tremblay et al., 1995; Malo and Bourque, 1993), although some deformation in the mélange units may originate from Taconian-related accretionary processes (Cousineau and Tremblay, 1993; Tremblay et al., 1995).

5.2.2 SILURO-DEVONIAN ROCKS: THE GASPÉ BELT

Post-Taconian rocks of the Québec Appalachians form a single depositional belt, the Gaspé Belt (Malo and Bourque, 1993), which includes Upper Ordovician to Middle Devonian rocks located mainly to the south of the BBL and which overly rocks of the Dunnage Zone (Fig. 5.5). These rocks are divided into three major structural zones, from north to south: the Connecticut Valley-Gaspé synclinorium (CVGS), the Aroostook-Percé anticlinorium (APA) and the Chaleurs Bay synclinorium (CBS) (Fig. 1.1 of Bourque and Malo, part 1 of this report; and Fig. 5.7). The APA and the CBS are found only in the Gaspé Peninsula (Fig. 1.1 of Bourque and Malo, part 1 of this report; and Fig. 5.7). The Gaspé Belt comprises four broad temporal and lithological rock assemblages: 1) Upper Ordovician-lowermost Silurian deep water fine-grained siliciclastic and carbonate facies, 2) Silurian-lowermost Devonian shallow to deep water shelf facies, 3) Lower Devonian mixed siliciclastic and carbonate fine-grained deep shelf and basin facies, and 4) Lower to Middle Devonian nearshore to terrestrial coarse-grained facies. North of the BBL, in the Témiscouata region and the Gaspé Peninsula, rocks of the northern edge of the Gaspé Belt unconformably overlie rocks of the Humber Zone (Figs. 5.5; 5.8 - columns D-G). This angular unconformity has long been cited as evidence for the Taconian orogeny throughout the northern Appalachians (Pavlides et al., 1968). South of the BBL, rocks of the Gaspé Belt unconformably (Fig.5.8, column E) or disconformably (Fig. 5.8, columns A, B, E, and F) overly those of the Dunnage Zone. In the Témiscouata region, sedimentation is continuous from the upper Middle Ordovician to Middle Devonian (Fig. 5.8, column C) and comprises a unique depositional succession not recognized elsewhere in the Québec Appalachians, the Lower Témiscouata sequence (David, 1994). The upper Middle Ordovician to lowermost Silurian flysch of the Cabano Formation (LTS-F on Fig. 5.8) unconformably overlies mélange-type units assigned to the Dunnage Zone and is in turn conformably overlain by Lower Silurian volcanic rocks of the Pointe-aux-Trembles and Lac Raymond formations (LTS-V on Fig. 5.8). The Lower Témiscouata sequence is conformably overlain by rocks of the Gaspé Belt (rocks assemblage 2) (Fig. 5.8, column C).

In southern Québec, NW of the La Guadeloupe fault, Upper Silurian rocks (rock assemblage 2) of the Gaspé Belt disconformably overly syn- to late-Taconian turbidite deposits of the Dunnage Zone. Although the upper strata of the Dunnage Zone and the lower beds of the Gaspé Belt are unfossiliferous, available data suggest a hiatus comprising much of the Late Ordovician-early Late Silurian time interval (Lavoie and Bourque, 1992) (Fig. 5.8, column B). Upper Silurian to Lower

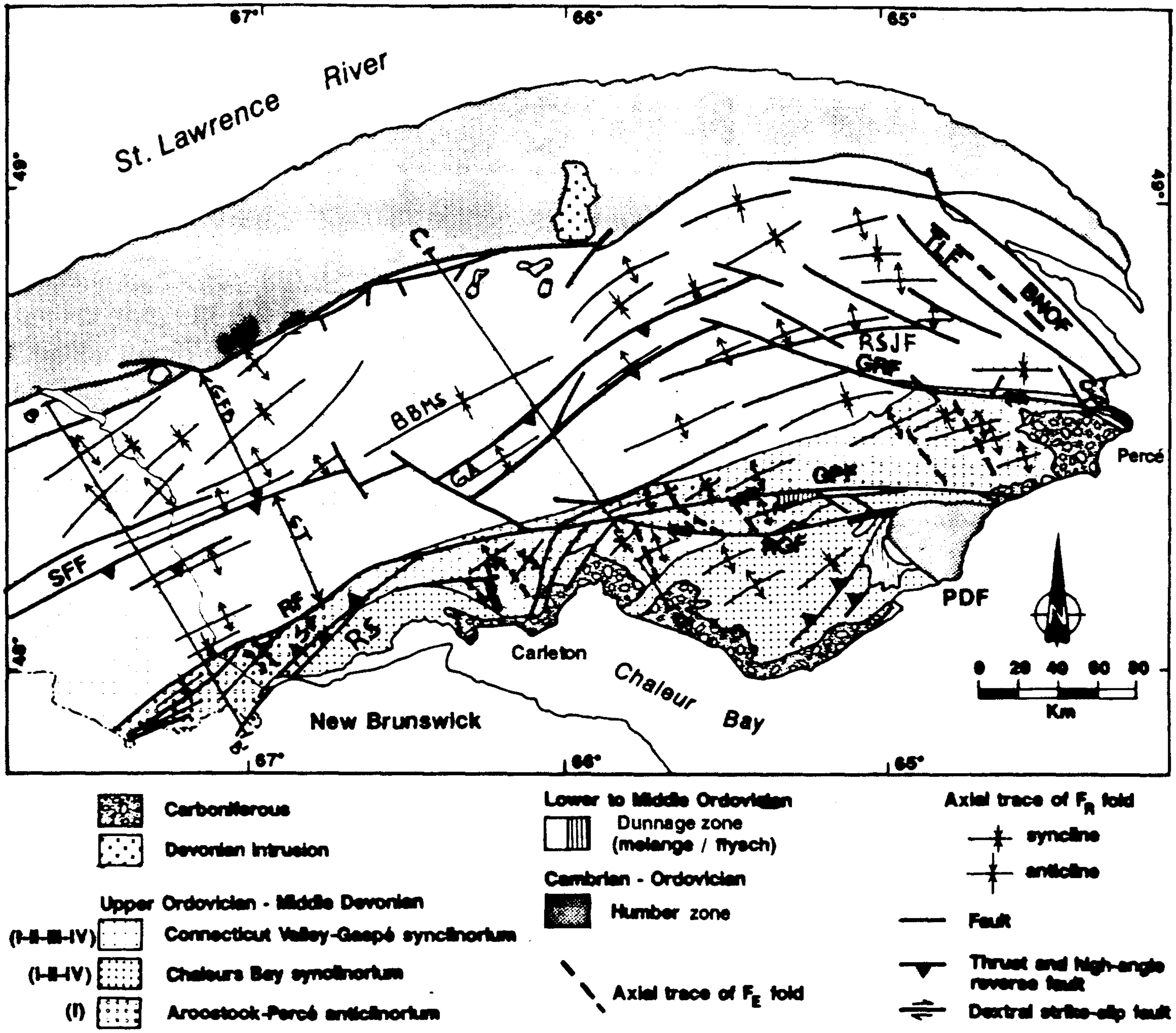

Figure 5.7. Geological map of the Gaspé Peninsula showing the three Acadian structural zones. BBMS: Big Berry Mountain syncline, BNOF: Bassin Nord-Ouest fault, GA: Gastonguay anticline, GFB: Gaspé Folded Belt, GPF: Grand Pabos fault, GRF: Grande Rivière fault, GT: Gaspé Trough, RF: Restigouche fault, RGF: Rivière Garin fault, RSJA: Rivière Saint-Jean anticline, SF: Sellarsville fault, SFF: Sainte-Florence fault, SSF: Shickshock-Sud fault, TLF: Troisième Lac fault. Modified from Malo et al. (1995).

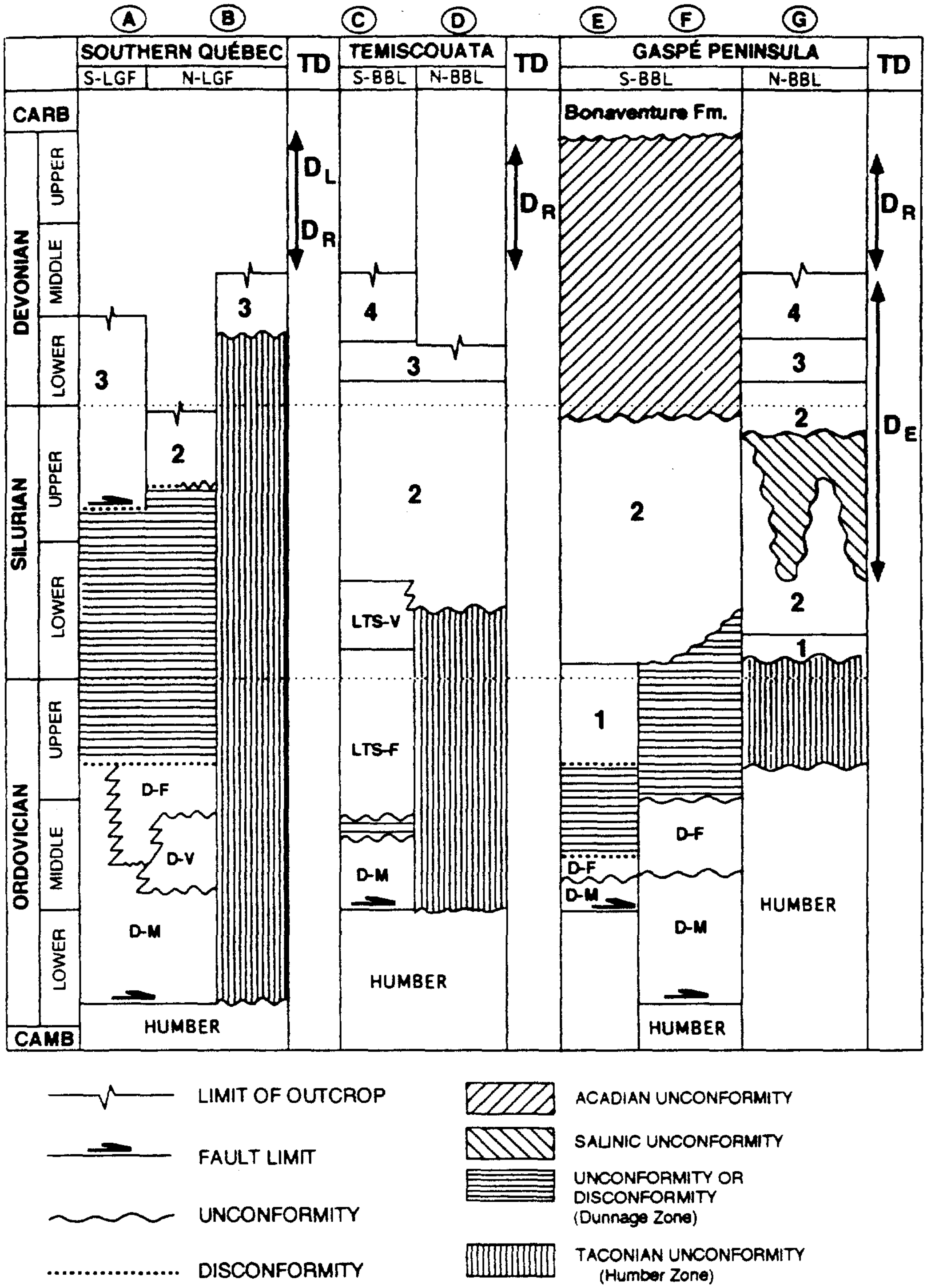

Figure 5.8 Correlation chart of Middle Paleozoic rocks of Gaspé Belt in the Québec Appalachians and stratigraphic range of unconformities. Summarized from Bourque et al. (1991). Letters at top of columns refer to figure 1. I, II, III, IV: Gaspé Belt rock assemblage, D-F: Dunnage flysch, D-M: Dunnage mélange, D-V: Dunnage volcanite, LTS-F: Lower Temiscouata sequence flysch, LTS-V: Lower Temiscouata volcanite. From Malo et al. (1995).

Devonian allochthonous rock units of rock assemblage 3 within the CVGS (Fig. 5.8, column A) are in tectonic contact along the La Guadeloupe fault with the Dunnage Zone rocks and overlying autochthonous Upper Silurian Gaspé Belt rocks north of the fault. Although the underlying rocks are not exposed, correlations from Gaspé and southern New England suggest that rocks of the Gaspé Belt were deposited on rocks of the Dunnage Zone (Pinet and Tremblay, 1995).

A late Ludlovian - early Pridolian unconformity corresponding to the Salinian disturbance (Boucot, 1962) is recorded in the Gaspé Belt sequence of the Gaspé Peninsula (Fig. 5.8, column G), the unconformity resulting from synsedimentary extensional faulting (Malo and Kirkwood, 1996). Except for the local occurrence of within-plate basalts in southern Québec (Desjardins et al., 1994), there is no indication of Siluro-Devonian extension elsewhere in the Québec Appalachians. In the Gaspé Peninsula, rocks of the Gaspé Belt are unconformably overlain by Carboniferous deposits (Bonaventure Formation) that are not affected by penetrative deformation (Figs. 5.5 and 5.8, columns E and F). The sub-Silurian and sub-Carboniferous angular unconformities are used to constrain the timing of the main deformation within the Gaspé Belt basin in the Gaspé Peninsula where Upper Ordovician to Middle Devonian rocks record folding and faulting that are clearly dated as Middle to Late Devonian (Kirkwood and Malo, 1993; Malo and Bourque, 1993).

In the Québec Appalachians, the Acadian metamorphism is of low grade and increases gradually from the Gaspé Peninsula to southern Québec. In the Gaspé Peninsula, the Gaspé Belt rocks were affected by regional anchi- to low-grade metamorphism (Hesse and Dalton, 1991). In southern Québec, Siluro-Devonian rocks were metamorphosed to the greenschist grade, varying from the chlorite zone in the Chaudière river area to the biotite zone near the Québec -Vermont international border (Fig. 5.5). From southern Québec to southern New England metamorphic grade increases significantly to amphibolite facies (Osberg et al., 1989; Armstrong et al., 1992). Acadian plutonism varies in intensity with increasing metamorphism and was much more extensive in New England than in adjacent Québec. In the Gaspé Peninsula, post-Taconian intrusions are restricted to the northern part of the peninsula (Fig. 5.7) where the 390 to 370 Ma Mont McGerrigle plutonic complex (Whalen, 1993) occurs within rocks of the Humber Zone, and several stocks and dykes intrude the CVGS rocks further south. In southern Québec, rock units of the CVGS were intruded by syn- to late-orogenic granitic plutons of Late to Middle Devonian age (384 Ma to 374 Ma; Simonetti and Doig, 1990).

The extent and nature of Acadian structures to the northwest are unclear. The BBL was considered as the northwestern limit of the Acadian deformation in southern Québec (St-Julien and Hubert, 1975), although it was argued that some large late structures of the Humber Zone are Acadian (Sikander and Fyson, 1969; Carrara and Fyson, 1973; Pinet and Tremblay, 1995; Slivitzky and St-Julien, 1987). Recent structural analysis show that late upright folds in the southeastern part the Humber Zone, within the internal nappe domain of the Humber Zone (Fig. 5.5), are Acadian (Cousineau, 1990; Tremblay and Pinet, 1994). Interpretative structural cross-sections across Anticosti Island and Gaspé Peninsula shows large open synclines and thrust faults that are believed to be Acadian (Roksandic and Granger, 1981). On the basis of different structural styles and metamorphic grade, the Acadian orogen is divided into a northwestern external zone and a southeastern internal zone. In southern Québec, the external-internal boundary corresponds approximately to the Rivière Victoria fault (Fig. 5.5; Tremblay and Pinet, 1994). The external zone is characterized by a single phase of folding, metamorphism and plutonism. The CVGS north of the Rivière Victoria fault, in southern Québec, the Témiscouata region and the Gaspé Peninsula all lie within the external zone of the Acadian orogen. The internal zone, located south of the Rivière Victoria fault is characterized by superposed folding and faulting. Further southeast in adjacent New England, the intensity of Acadian deformation and metamorphism increases strongly in the core of the Bronson Hill-Boundary Mountain anticlinorium (Fig. 5.5) (Osberg et al., 1989), the most internal part of the Acadian orogen. In northern Maine, two phases of folding are ascribed to the Late Silurian-Early Devonian time interval (Hibbard, 1994) whereas, three distinct deformation events are recorded from Late Silurian to Middle Devonian in northern New Brunswick (van Staal and de Roo, 1996). The external-internal boundary probably lies northwest of the Millimagassett Lake area and the Miramichi anticlinorium (Fig. 5.5).

Structural analysis of Upper Ordovician to Middle Devonian supracrustal rocks of the external zone of the Acadian orogen, the Gaspé Belt, shows two different deformational regimes in the Québec Appalachians: strike-slip tectonics in the Gaspé Peninsula and thrust or dip-slip tectonics in southern Québec (Malo et al., 1995).

5.3 THE GASPÉ PENINSULA

5.3.1 CAMBRO-ORDOVICIAN ROCKS

Cambro-Ordovician rocks of the Humber and Dunnage zones constitute the immediate basement on which the sedimentation of the Gaspé Belt evolved. In the Gaspé Peninsula, the Humber and Dunnage zones are both allochthonous over the Grenville basement (Marillier et al., 1989). Rocks of the Humber Zone occupy mainly the northern part of the Gaspé Peninsula and two inliers in the southern part (Maquereau-Mictaw and Murphy Creek inliers; Fig. 5.6) whereas, those of the Dunnage Zone are found in inliers close to the BBL in northern and southern Gaspé Peninsula (Fig. 5.6). As for the rest of the Québec Appalachians, the BBL marks the tectonic contact between the two Cambro-Ordovician zones. In Québec, the BBL is well defined in the Eastern Townships and in the Maquereau-Mictaw inlier of the southern Gaspé Peninsula (Williams and St-Julien, 1982). Between these two regions, its trace was interpretative for most of its length under the cover rocks of the Gaspé Belt (Williams, 1979). Based on the presence of ultramafic bodies and mélanges, as well as the reinterpretation of gravimetric and aeromagnetic data of the peninsula, the trace of the BBL is thought to follow the Shickshock-Sud and the Bassin Nord-Ouest faults, and then is dextrally offset by at least three faults, the Grande Rivière, the Grand Pabos and the Rivière Garin faults, and reappears in the Maquereau-Mictaw inlier (Fig. 5.6) (Malo et al., 1992).

In the Gaspé Peninsula, Precambrian rocks occur in three localities: 1) the Mont Serpentine inlier, 2) the Nadeau ophiolitic mélange, and 3) the Maquereau-Mictaw inlier (Fig. 5.7). In the northwestern part of the Maquereau-Mictaw inlier (Fig. 5.9), a block of orthogneiss and amphibolite has been mapped along the Port Daniel fault which border the Humber Zone (De Broucker, 1987). The petrography of this block, the geochemistry and the age of 998 Ma of the orthogneiss suggest that the orthogneiss-amphibolite assemblage represent a sliver of Grenville basement (De Broucker, 1987). A rock assemblage of tuffaceous metagreywacke with a cataclastic texture and foliated amphibolite within the Nadeau ophiolitic mélange is Precambrian. Zircon U/Pb age of the tuffaceous metagreywacke indicates that it was derived from source rocks with ages between 1395 to 1812 Ma (De Broucker, 1987). Metagreywackes and metaarkose exhibiting a cataclastic textures found in the Lady Step complex within the Mont Serpentine inlier (Fig. 5.10) are thought to be correlative with dated Precambrian rocks of the Nadeau ophiolitic mélange (Berger and Ramsay, 1993; De Broucker, 1987). The Nadeau ophiolitic and the Lady Step complex in the northeastern Gaspé are equated with the Rivière des Plantes mélange in the Eastern Townships (Cousineau, 1991; De Broucker, 1987). These three mélanges in the Québec Appalachians are correlated lithologically with the Chain Lake Massif in Maine (Fig 5.5) and the age of the tuffaceous metagreywackes in the Nadeau ophiolitic mélange is also compatible with the age of the Chain Lakes Massif (Naylor et al., 1973).

Tectonostratigraphy of the Humber Zone

In the northern Gaspé, from north to south, the Humber Zone comprises three tectonic domains, (Slivitzky et al., 1991; St-Julien and Hubert, 1975) (Fig. 5.11): (1) the parautochthon domain or the foreland thrust belt, (2) the external nappe domain and (3) the internal nappe domain. The last two domains constitute the allochthon, thrusted to the northwest during the Taconian orogeny (Fig. 5.11). Logan's Line separates the nappe domains from the thrust-imbricated structures of the foreland thrust belt. The external nappe domain is constituted of the Cap-Chat mélange, the Rivière Marsoui and Rivière Sainte-Anne nappes (Figs. 5.11, 5.12). The Méchins-Carcy fault separates the two external nappes. To the south, the internal nappe domain, which comprises the Mont Albert and Mont Logan nappes, is bounded to the north by the Lac Cascapédia fault and to the south by the Shickshock-Sud fault (Figs. 5.10, 5.13). In the southern Gaspé Peninsula, some other Taconian terranes are present in the Maquereau-Mictaw and the Murphy Creek inliers (Fig. 5.6). Rocks of the Murphy Creek inlier (Fig. 5.14) correlate with some of the Rivière Sainte-Anne nappe (Kirkwood, 1989), whereas the Maquereau Group in the Maquereau-Mictaw inlier (Fig. 5.9) correlates with the Shickshock Group of the internal nappe domain (De Broucker, 1987). The St. Lawrence Lowlands platform rocks, well exposed in southern Québec, are absent in the Gaspé Peninsula. The platform sequence is found northeast of the Gaspé Peninsula, on the other side of the Gulf of St. Lawrence, on the Anticosti Island (Fig. 5.1).

The Mont Albert nappe comprises three massifs of Upper Cambrian to Lower Ordovician ultramafic rocks (Mont Paul, Mont Sud and Mont Albert) which overthrust the southern part of the Mont Logan nappe (Fig. 5.13). The three massifs of ultramafic rocks form the Mont Albert complex which is underlain by the Amphibolite du Diable (Fig. 5.13). The Mont Albert complex

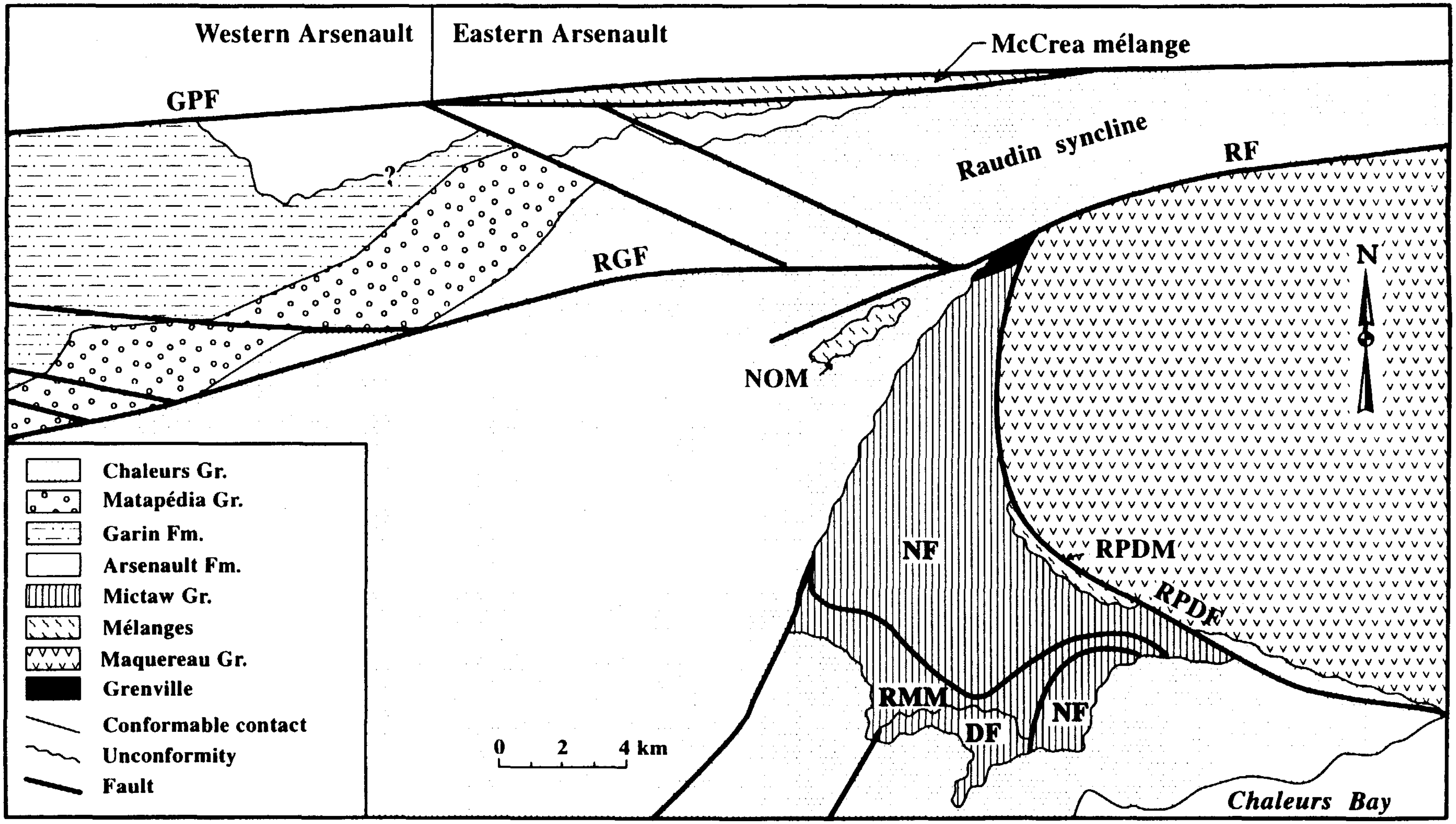

Figure 5.9. Localization of mélange rocks units, the Mictaw Gr., and the Arsenault Fm. in the southeastern Gaspé Peninsula. DF: Dubuc Fm., GPF: Grand Pabos fault, MRM: Rivière du Milieu mélange, NF: Neckwick Fm., NOM: Nadeau ophiolitic mélange, RG:Rivière Garin fault, RPDF: Rivière Port-Daniel fault, RPDM: Rivière Port-Daniel mélange. Modified from Malo and Bourque (1993).

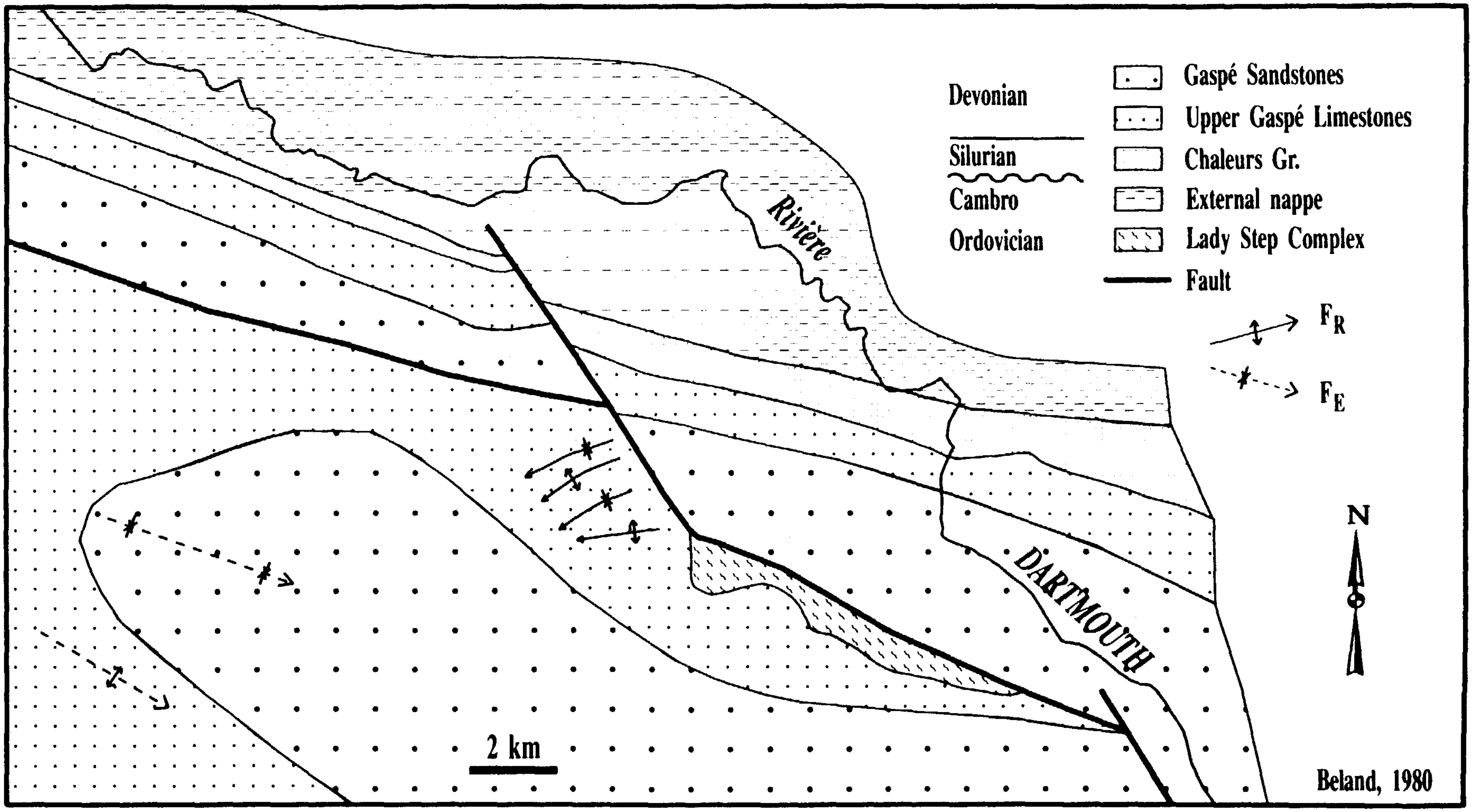

Figure 5.10. Geology of the Mont Serpentine inlier area in the northeastern Gaspé Peninsula. Modified from Béland (1980).

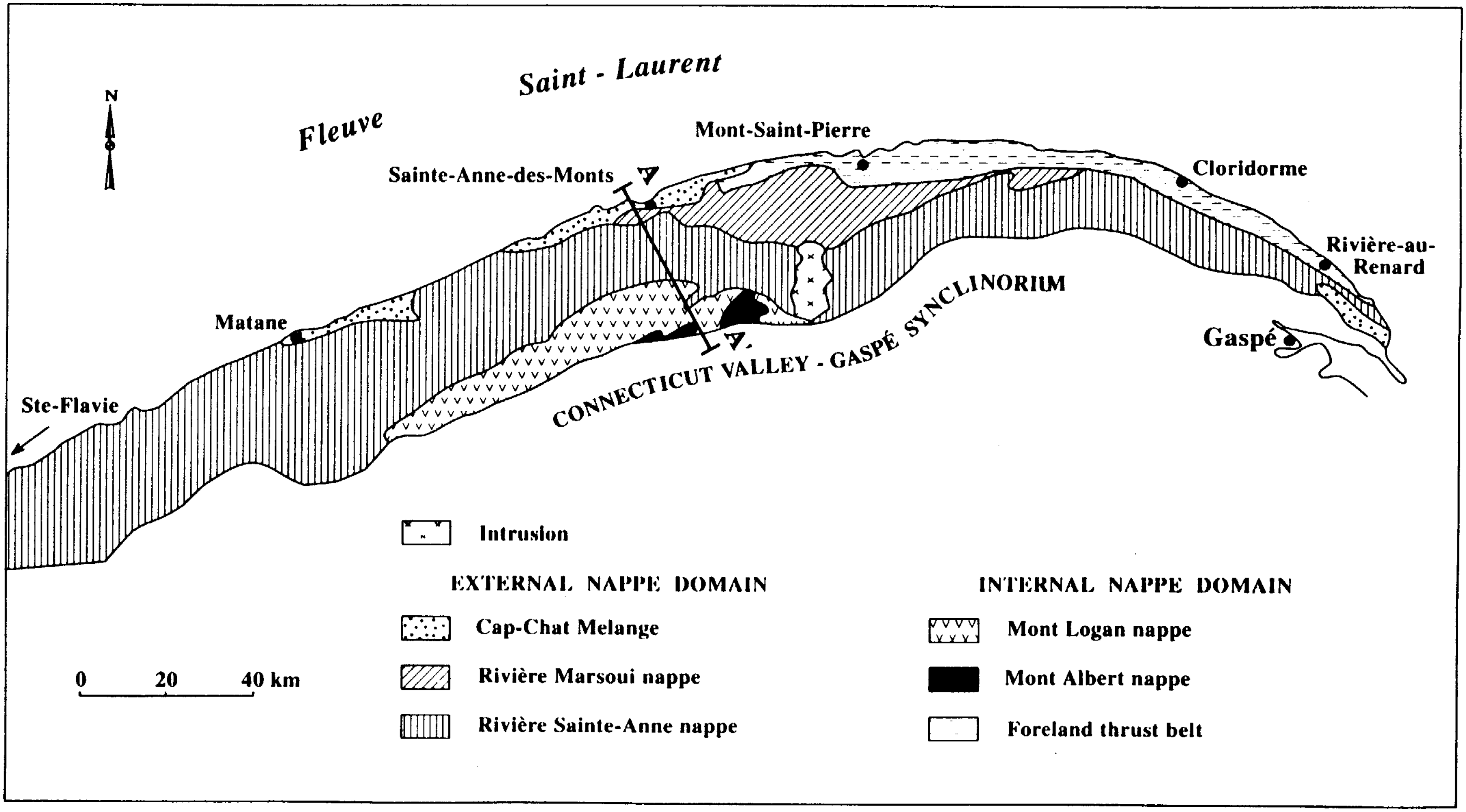

Figure 5.11. Tectonostratigraphic zones of the Humber Zone in the Gaspé Peninsula. From Slivitzky et al. (1991).

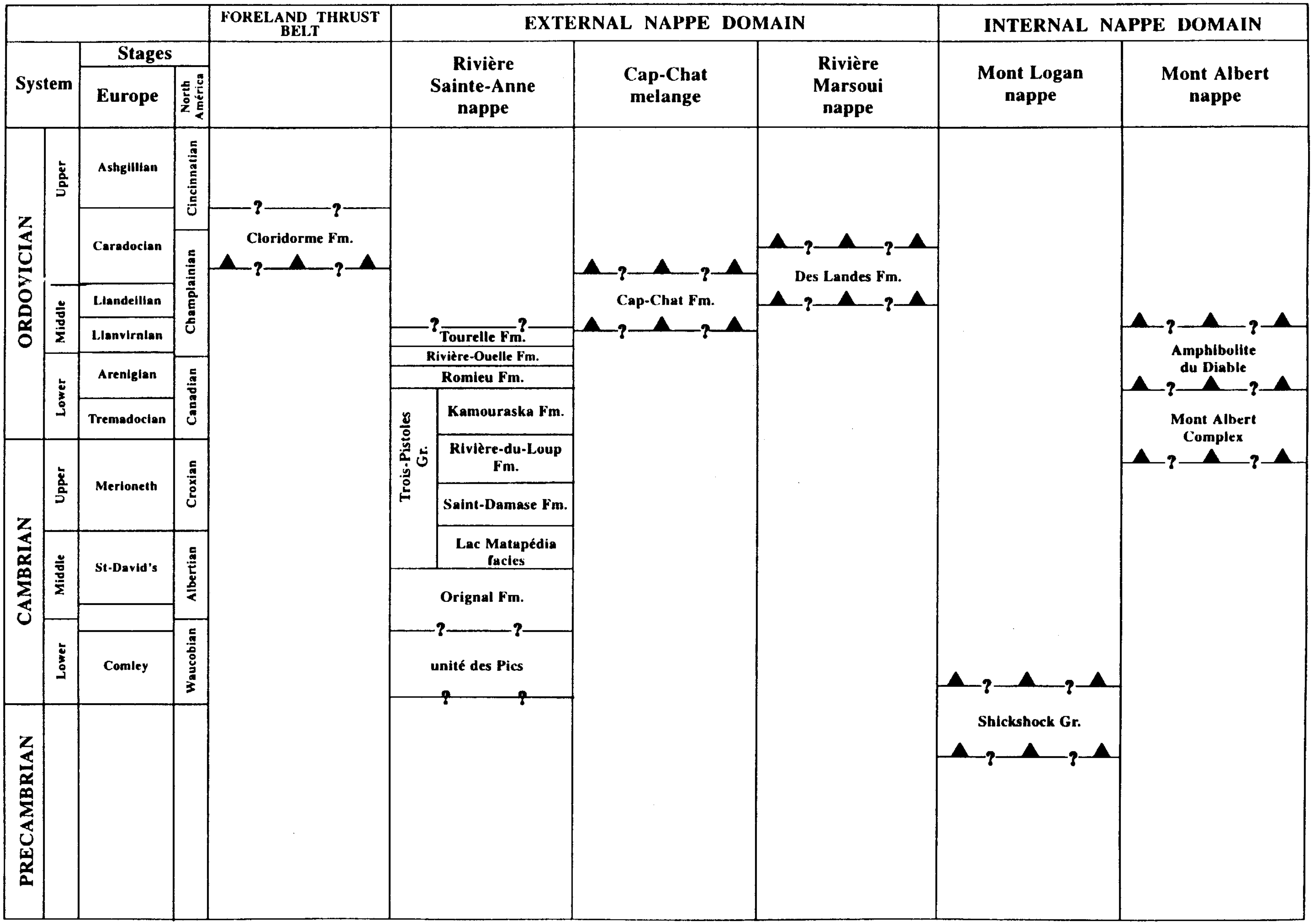

Figure 5.12. Correlation chart of Cambro-Ordovician rocks of the Humber Zone in northern Gaspé Peninsula. Modified from Slivitzky et al. (1991).

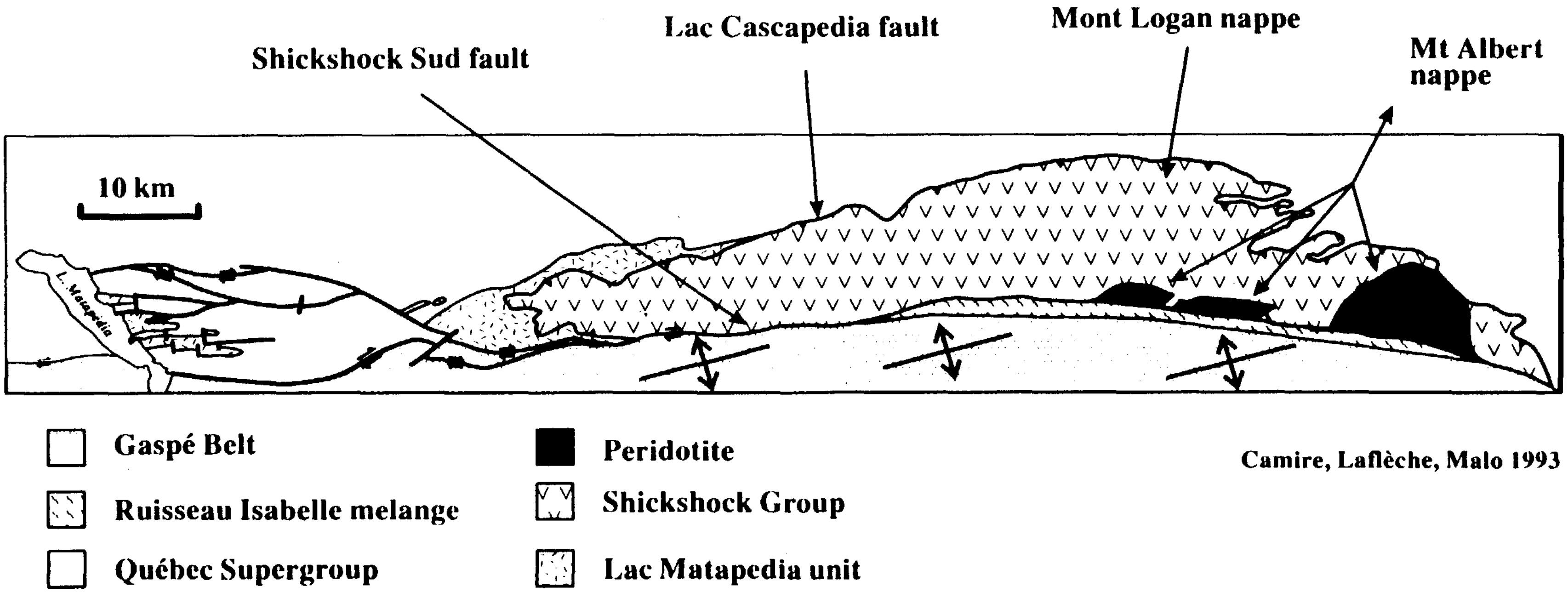

Figure 5.13. Geology of the internal nappe domain of the Humber Zone in the Gaspé Peninsula. Modified from Camiré et al. (1993).

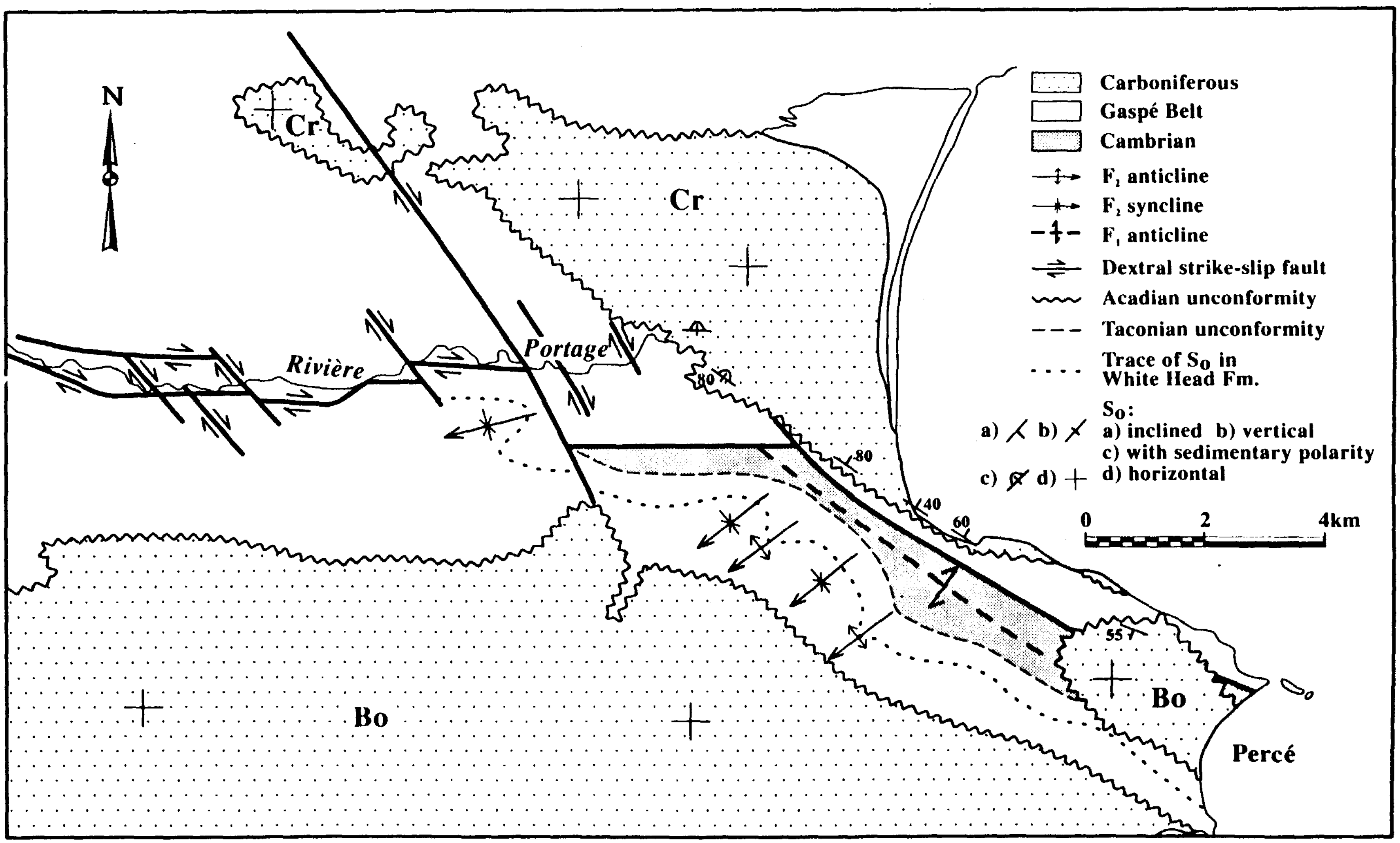

Figure 5.14. Geology of the Percé area. Modified from Kirkwood (1989). Bo: Bonaventure Formation, Cr: Cannes de Roches Formation.

represents the basal part of an ophiolitic complex which is composed mainly of harzburgites with podiform lenses of dunite and small veins of orthopyroxenite (Beaudin, 1984). The Amphibolite du Diable is constituted of different amphibolite facies derived from volcanic and sedimentary rocks (Gagnon and Jamieson, 1986).

The Lower Cambrian (Upper Hadrynian?) Shickshock Group constitutes the Mont Logan nappe (Fig. 5.13). It is composed mainly of mafic volcanic rocks with minor amount of sedimentary rocks (arkose, pelite, conglomerate and marble). All these rocks have been regionally metamorphosed to greenschist and middle amphibolite grades during the Taconian orogeny (St-Julien et al., 1990; Camiré et al., 1993a; Camiré, 1995). The Mont Albert and Mont Logan nappes constitute the internal nappe domain of the Humber Zone in northern Gaspé Peninsula. The Maquereau Group in southern Gaspé has been correlated with the Shickshock Group (De Broucker, 1987; Slivitzky et al., 1991) and is also included in the internal nappe domain. The Maquereau Group consists of feldspathic sandstones and pelites interbedded with conglomerate and mafic volcanic rocks (De Broucker, 1987).

The Rivière Sainte-Anne nappe is constituted of Middle Cambrian to Middle Ordovician sedimentary units with some minor amount of volcanic rock assemblages, which are, from bottom to top (Fig. 5.12): Orignal Formation., Trois-Pistoles Group, Romieu, Rivière-Ouelle and Tourelle formations, the Lac Matapédia facies and the unité des Pics. The Orignal Formation consists of a greenish-grey to red mudrock lithofacies, a red to grey mudrock and limestone lithofacies, and grey mudrocks and sandstone lithofacies. The Trois-Pistoles Group comprises three formations, from bottom to top: Saint-Damase, Rivière-du-Loup and Kamouraska. The Saint-Damase is composed of sandstones rich in quartz and feldspars, polygenic conglomerates, orthoquartzites, green claystones and siltstones. The Rivière-du-Loup is constituted of black to grey shales and mudstones with local interbeds of siltstones and quartzites. The Kamouraska is characterized by pure white orthoquartzite with shale and dark grey mudstones. The Lac Matapédia facies is composed of mafic volcanic rocks with arkose and red mudslates. These volcanic rocks were included in the Shickshock Group (Slivitzky et al., 1991), but they are now considered to be a distinct volcanic rock assemblage (Camiré et al., 1993b). The basalts of the Lac Matapédia facies are neither chemically nor petrogenetically associated with the metabasalts of the Shickshock Group (Camiré et al., 1993b). The structural context of the Lac Matapédia facies suggest that the basalts are part of the Trois Pistoles Group. Other volcanic rock assemblage caught up in thrust slices within the Rivière Sainte-Anne nappe (e.g. unité des Pics, Brisebois et al., 1991) can be lithologically and geochemically correlated with the Lac Matapédia facies but the unité des Pics might be older than the Lac Matapédia facies. The Romieu Formation is a calcareous shale, with calcilutite and prismatic calcite interbeds. The Rivière Ouelle Formation is characterized by a great variety of lithologies (Slivitzky et al., 1991), including mudstone, mudshale, siltstone, calcilutite, calcarenite, conglomerate limestone and orthoquartzite. The Tourelle Formation (Slivitzky et al., 1991) is made up of mainly thick-bedded, coarse- to medium-grained lithic wacke and thinner beds of siltstone. Locally graded-bedding, load and flute casts are found, as well as conglomeratic beds composed of terrigenous, volcanic and limestone rock fragments, and clasts of chert. Provenance study of sandstones indicates that they derived from an orogenic belt (Hiscott, 1978). The source area of other Middle Cambrian to Middle Ordovician sedimentary rocks of the Rivière Sainte-Anne nappe is believed to be the Grenville basement to the north (St-Julien et al., 1993). Limestone conglomerates of the Rivière Ouelle Formation were derived from an unknown Cambrian-Lower Ordovician platform, to the north, which was suffering from local erosion during the Early Paleozoic.

The Rivière Marsoui nappe is constituted of the Middle Ordovician Des Landes Formation (Fig. 5.11), which is composed of greenish-grey chert with black siliceous mudstone and siltstone at the base followed by a sequence of turbidites made up of clayshale, calcilutite beds, arenaceous calcarenite and calcareous arenite. Arenite beds show numerous internal sedimentary structures such as graded bedding, parallel- and cross laminations.

The Cap-Chat mélange is a Middle Ordovician chaotic unit constituted of blocks of different sizes in an argillaceous matrix (Slivitzky et al., 1991). The Rivière Ouelle, Tourelle and Des Landes formations can be recognized in these blocks.

The Caradocian Cloridorme Formation is the only stratigraphic unit found in the foreland thrust belt (Fig. 5.12). It is composed of different shales and sandstones. The principal lithologies are lithic wacke, calcareous fined-grained wacke, calcareous lithic arenite, silty limestone, calcareous and non-calcareous mudstone, dolomitic mudstone and clayshale, silty claystone and conglomeratic mudstone. The sandy lithologies exhibit all the internal sedimentary structures typical of turbidites deposits. Provenance study indicates that the Cloridorme Formation derives from a recycled orogenic source (Ko, 1985).

Structural geology and structural style of the Humber Zone

The most striking structural features within the Humber Zone are the regional thrust faults that can be mapped from western to eastern parts the Humber Zone of the Gaspé Peninsula (Fig. 5.11). Thrust faults dip gently to the south and regional folds are overturned to the NW (Fig. 5.15). Four phases of folding are recognized within the Cambro-Ordovician rocks of the Humber Zone (Slivitzky et al., 1991). F1 folds are E- to NE-trending, recumbent or highly overturned to the N or the NW. There is no axial planar cleavage with these F1 folds in the external nappe domain, whereas a S1 schistosity is well developed within the Shickshock Group. F2 folds are NE-trending and overturned to the NW. A good axial planar cleavage is developed with F2 folding. The first two phases of folding are ascribed to the Taconian orogeny (Slivitzky et al., 1991). F3 and F4 folds are open, NE to NNE-trending, and usually upright. They are interpreted to be Acadian (Slivitzky et al., 1991).

The Mont Albert nappe is at the highest structural level of the nappe pile (Figs. 5.13, 5.15). The Mont Albert and the Mont Logan nappes, the internal nappe domain, which comprised the oldest rock unit of the Shickshock Group, overthrust the Rivière Sainte-Anne nappe of the external

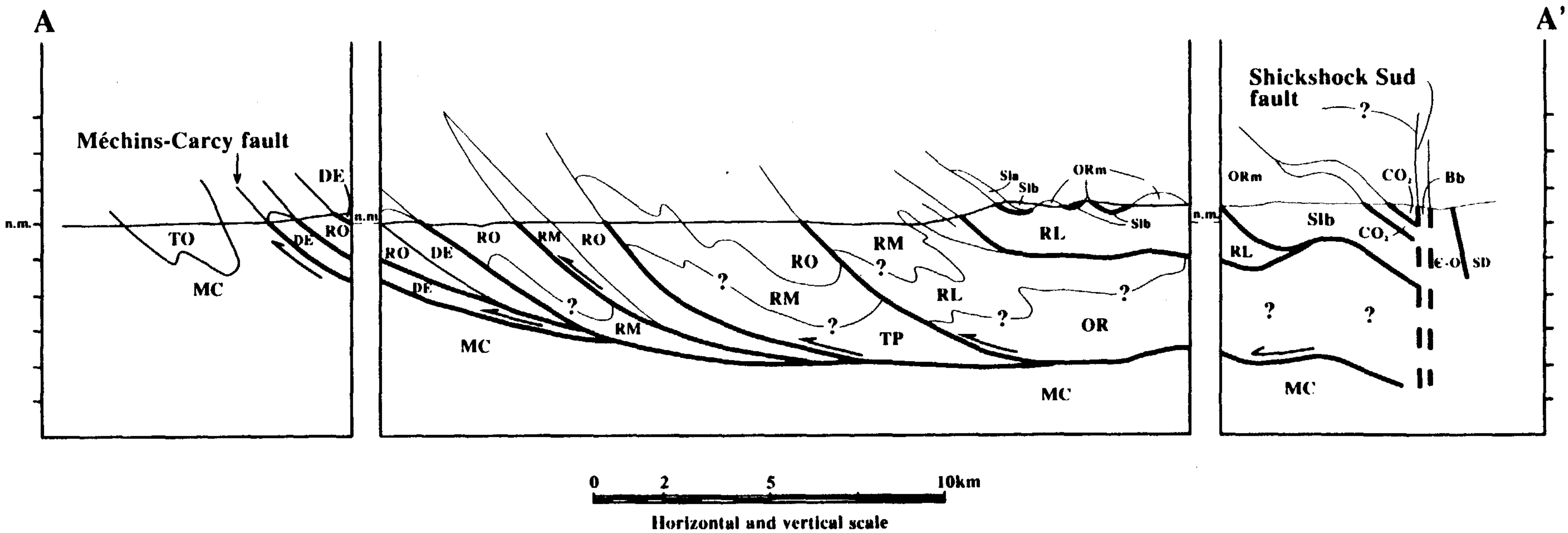

Figure 5.15. Structural cross-section AA' across the Humber Zone. Localization on figure 5.11. BB: equivalent to the Ruisseau Isabelle Mélange, C-O: Cambro-Ordovician, DE: Des Landes Fm., MC: Cap-Chat Mélange, Orm: Orignal Fm. (metamorphic), RL: Rivière-du-Loup Fm., RM: Romieu, RO: Rivière Ouelle Fm., SD: Siluro-Devonian, Sla: Shickshock Gr. (arkose), Slb: Shickshock Gr. (basalt), TO: Tourelle Fm., TP: Trois-Pistoles Gr. From Slivitzky et al. (1991).

nappe domain. This piggy-back sequence of thrusting, older rocks over younger rocks, is recognized between each nappe from the Mont Logan nappe to the north and seems to be the rule in the Humber Zone of the Gaspé Peninsula. However, in some places the Cap-Chat mélange is thrusted by the Cloridorme Formation, the youngest stratigraphic unit of the Humber Zone. It is explained by a late (Acadian) out-of sequence thrusting (Slivitzky et al., 1991).

Tectonostratigraphy of the Dunnage Zone

In the northern Gaspé Peninsula, most of the Dunnage Zone is concealed by the overlying Upper Ordovician to Middle Devonian rocks, except along the Shickshock-Sud fault and in the Mont Serpentine inlier (Figs. 5.6, 5.10, 5.13) where rocks that can be ascribed to the Dunnage Zone crop out. In the southern Gaspé Peninsula (Figs. 5.6, 5.9, 5.14), the Mictaw Group of the Maquereau-Mictaw inlier and the Rivière Port-Daniel mélange (De Broucker, 1987), just southwest of the Rivière Port-Daniel fault, the Nadeau ophiolitic mélange (De Broucker, 1987), the Arsenault Formation and the McCrea mélange along the Grand Pabos fault (Malo et al., 1993) are considered to belong to the Dunnage Zone (Tremblay et al., 1995). Rocks of the Dunnage Zone in the Gaspé Peninsula can be included in the mélange and fore-arc basin domains, whereas the volcanic arc domain is absent.

Mélange units and serpentinite bodies mapped in the Gaspé Peninsula mark the BBL as in the Estrie-Beauce region. These are, from northwest to southeast, the Ruisseau Isabelle mélange, the Lady Step complex, the Rivière Port-Daniel mélange, the Nadeau ophiolitic mélange and the McCrea mélange (Figs. 5.6, 5.16). The Ruisseau Isabelle mélange (Fig. 5.13) contains graphitic and graptolitic shales, dolomitized limestone, serpentinite and dolomitized serpentinite in a chaotic shaly matrix of pebbly mudstone with a phacoidal cleavage (St-Julien et al., 1990). The Ruisseau Isabelle mélange, located in the fault zone of the Shickshock-Sud fault, is in fault contact, to the north, with the volcanics of the Cambrian Shickshock Group. To the south, the mélange-type rocks are either in fault contact or unconformably overlain by Silurian strata of the Gaspé Belt.

The Lady Step complex crops out at the Mont Serpentine inlier, northeast of Gaspé (Figs. 5.6, 5.10). The Lady Step complex comprises serpentinized ultramafic, metaarkoses and metagreywacke, metabasalts, amphibolitized gabbros, pyroxenite, granitic blocks and gneiss, chlorite schists and metamorphic schists (Berger and Ramsay, 1993; De Broucker, 1987; Béland, 1980). The matrix is a sheared and schistose serpentinite and most of the fragments are brecciated, whereas metagreywackes and metaarkose exhibit a cataclastic textures. De Broucker (1987) interpreted this breccia as an ophiolitic mélange, like the Nadeau ophiolitic mélange to which it is equivalent. To the north, the Bassin Nord-Ouest fault separates the Lady Step complex from the Lower Devonian unit of the Gaspé Belt, whereas, to the south, the mélange is partly unconformably overlain by Upper Silurian units or is in fault contact the Lower Devonian strata (Berger and Ramsay, 1993).

The Rivière Port-Daniel mélange is an olistostromal mélange made up of igneous and sedimentary blocks in a sedimentary matrix. Blocks are composed of serpentinite, basic volcanic rocks, chert,

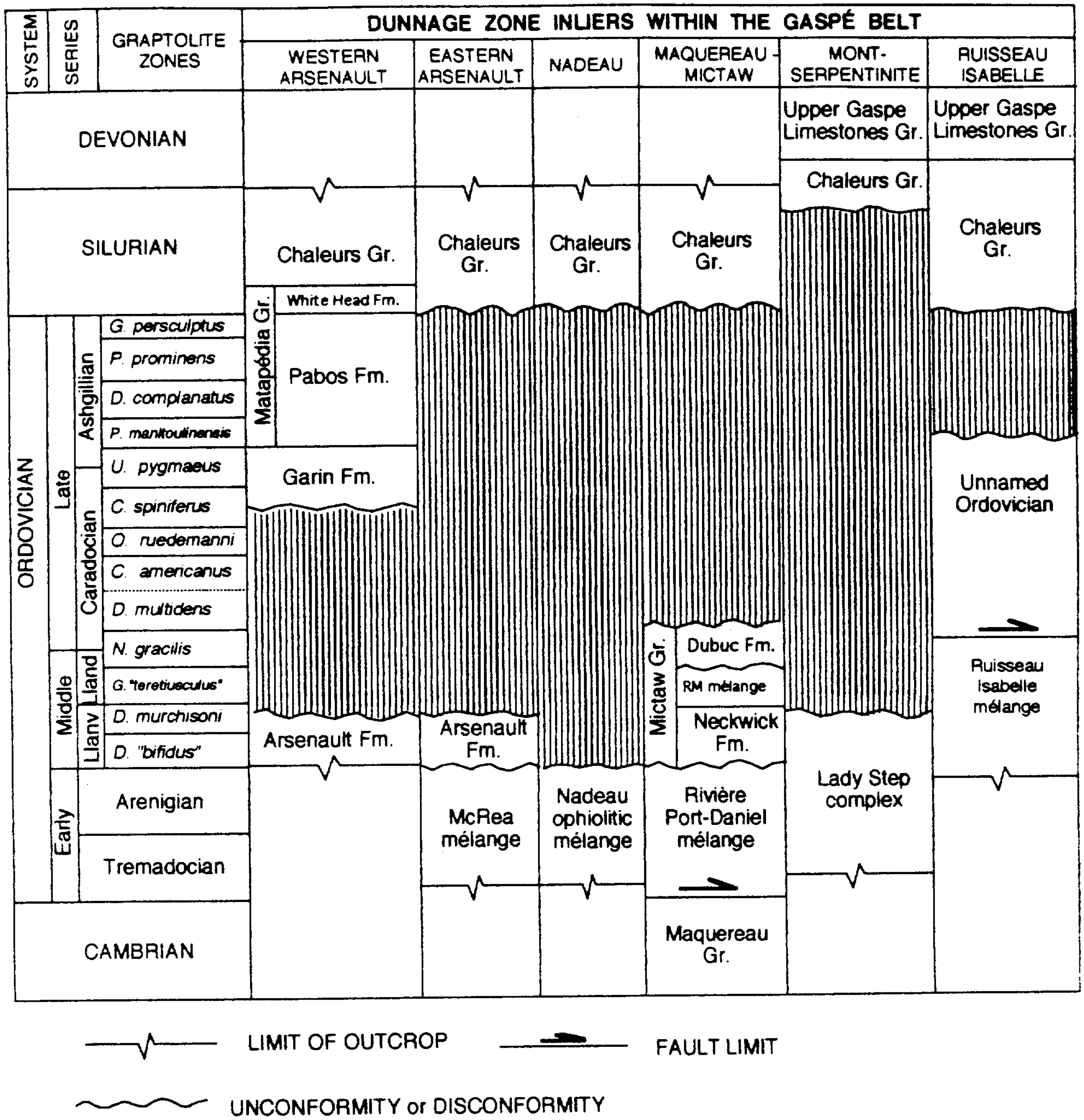

Figure 5.16. Correlation chart of Cambro-Ordovician rocks of the Dunnage Zone in the Gaspé Peninsula.

granitoid, metagreywacke, silty limestone, dolomite, red mudstone and rare metasandstone (De Broucker, 1987, Williams and St-Julien, 1982). The matrix varies from a green to black mudshale to a black pebbly mudstone which exhibits phacoidal cleavage, and to a polygenic conglomerate with radiolarite, chert and sandstone in which are incorporated various types of blocks (De Broucker, 1987). The mélange is intruded by large tholeiitic diabase sill near its upper contact with the Neckwick Formation. The Rivière Port-Daniel mélange is bordered to the east by the Rivière Port-Daniel fault and further east by the Cambrian Maquereau Group of the Humber Zone (De Broucker, 1987; Williams and St-Julien, 1982). To the west, the mélange is unconformably overlain by the Llanvirnian Neckwick Formation of the Mictaw Group, indicating a pre-Middle Ordovician or an Early Ordovician age for the mélange (Fig. 5.16).

The Nadeau ophiolitic mélange (Fig. 5.9) contains decimetric to hectometric blocks of serpentinized tectonic peridotite, amphibolite, tuffaceous metagreywacke with a cataclastic texture, quartzite, granite and granodiorite in a matrix of schistose serpentinite (De Broucker, 1987; Williams and St-Julien, 1982). Tuffaceous metagreywacke and amphibolite have been correlated with some facies of the Chain Lakes Massif (De Broucker, 1987). The Nadeau ophiolitic mélange is surrounded by Silurian units of the Gaspé Belt in an anticline. The contact with these younger rocks is either a fault or and unconformity (De Broucker, 1987). The unconformity gives a pre-Silurian age for the mélange but it is believed to be pre-Middle Ordovician like the Rivière Port-Daniel mélange (Fig. 5.16) (De Broucker, 1987).

The McCrea mélange is located along the Grand Pabos fault, northwest of the Maquereau-Mictaw inlier, on strike with the Rivière Port-Daniel and the Nadeau ophiolitic mélanges (Fig. 5.9). The McCrea mélange contains blocks of granitic rocks, basic to intermediate volcanic rocks, red and green slate, sandstone, calcareous siltstone, dolomitized serpentinite and serpentinized peridotite (Malo et al., 1993). One of the silty limestone yielded Late Cambrian conodonts. The matrix is a black pebbly mudstone which exhibits a phacoïdal cleavage. The mélange is intruded by a large gabbroic sill, which shows chemical resemblance to normal mid-ocean ridge basalts (N-MORB, Bédard, 1986). The McCrea mélange is bordered to the north by the Grand Pabos fault which separates the mélange from the Upper Ordovician to Lower Silurian rocks of the Gaspé Belt. To the south, an easterly trending fault partially bounds the mélange and represents the eastern contact with the Lower Silurian terrigenous units of the Chaleurs Group and the western contact with the Middle Ordovician greywackes of the Arsenault Formation (Fig. 5.9). In its central part, an unconformity is observed between the mélange and the Arsenault Formation (Fig. 5.9). Since the McCrea mélange is unconformably overlain by the Llanvirnian Arsenault Formation and contains Late Cambrian limestone blocks, it is considered to be Lower Ordovician (Fig. 5.16).

The Mictaw Group is composed of three stratigraphic units: the Neckwick Formation, a Llanvirnian flysch sequence; the Rivière du Milieu mélange, a sedimentary mélange, and the Llandeilian to Caradocian turbidites of the Dubuc Formation (Fig. 5.9). The Neckwick Formation is composed mainly of sandstone and shale with minor interbeds of felsic tuff and microconglomerate (De Broucker, 1987). Sandstones are greenish-grey lithic wacke, medium- to coarse-grained, 10 cm to 10 m thick-bedded. Most of the beds are massive, but graded bedding and load and flute casts are observed. Lithic fragments are mostly volcanic with minor amount of sedimentary, plutonic, metamorphic and ophiolite-derived rock fragments. Shales are green to dark grey. Microconglomerate beds are 50 to 100 cm thick and contain mainly lithic fragments with quartz and feldspath. Tuffs are yellowish-grey, very fine-grained, 1 to 5 m thick bedded and show a vitroclastic texture in thin sections. These are felsic tuffs with a high $SiO2$ content (70 to 80%; De Broucker, 1987). Diabase sills are found in the lower part of the formation, they have a tholeiitic affinity (Low-K tholeiite) like the diabase sill found in the underlying Rivière Port-Daniel mélange (see above). A petrographic provenance study (De Broucker, 1987) of sandstones and microconglomerates indicates that they derived from a recycled orogen and an orogenic arc (Dickinson and Suczeck, 1979). Paleocurrent analysis based on flute casts suggests that the source area was to the south of the actual Neckwick Formation (De Broucker, 1987). The Neckwick Formation unconformably overlies the Rivière Port-Daniel mélange and the Maquereau breccia. The upper contact with the Rivière du Milieu mélange is faulted (Fig. 5.9). The Lower Silurian Chaleurs Group also rest unconformably on the Neckwick in the southeastern part of the formation (Fig. 5.9).

The Rivière du Milieu mélange is a chaotic unit containing blocks in a sedimentary matrix. The matrix is a green to black mudshale with a phacoïdal cleavage which contains blocks of sedimentary origin, calcareous to dolomitic siltstone and sandstone. Sandstone blocks are argillaceous lithic wacke similar to the greywacke of the Neckwick Formation. The contact between the Rivière du Milieu and the Neckwick Formation is believed to be a thrust fault, whereas an unconformity is observed between the Dubuc Formation and the mélange (De Broucker, 1987).

The Dubuc Formation comprises two facies: a shale sequence, in the lower part of the formation, and a turbidite sequence with more sandstone in the upper part (De Broucker, 1987). Black graptolitic shale of the lower Dubuc contains few beds of sandstone and conglomerate, and calcareous concretions aligned in the bedding plane. Conglomerate beds are polygenic and comprise rock fragments from the underlying Rivière du Milieu mélange. The turbidite is a typical rhythmic sequence of sandstone and shale, with few conglomerate beds. Sandstones are grey, 10 to 100 cm thick, very fine- to coarse grained, and are composed mainly of quartz with lesser amounts of lithic fragments and feldspars. Sedimentary and volcanic clasts are rare, whereas the metamorphic clasts are the most abundant rock fragments in the sandstones. Conglomerates are composed of sedimentary and metamorphic rocks fragments: greenish-grey lithic wacke, calcareous to dolomitic siltstone, green and black mudshale, metasandstone, milky quartz, metamorphic schists and quartzitic mylonites. A petrographic provenance study (De Broucker, 1987) of sandstones and microconglomerates indicates that they derived from a recycled orogen (Dickinson and Suczeck, 1979) of high-grade metamorphism. The Dubuc Formation is unconformably overlain by the Lower Silurian part of the Chaleurs Group (Figs. 5.9, 5.16).

The Arsenault Formation (Fig. 5.9) is correlated lithologically to the Neckwick Formation of the Mictaw Group (Malo, 1986; De Broucker, 1987). It is composed of thick-bedded, greenish-grey lithic wacke with black to olive-green claystone, minor grey to black fine-grained tuff interbeds and a few gabbroic sills. Petrography of the sandstones shows the same composition than those of the Neckwick Formation. They are composed mainly of volcanic rock fragments with minor amount of sedimentary, plutonic, metamorphic and ophiolite-derived rock fragments. As for the Neckwick, petrographic analysis of sandstones (Malo, 1986) indicates that they derived from a recycled orogen and an orogenic arc (Dickinson and Suczek, 1979). Tuff interbeds and gabbroic sills of the Arsenault have a chemical composition similar to the felsic tuffs and gabbroic intrusive at the base of the Neckwick Formation (De Broucker, 1987). In the eastern Arsenault area (Fig. 5.9), the Llanvirnian Arsenault Formation rests unconformably on the McCrea mélange. The Arsenault resting on the McCrea mélange is in turn overlain unconformably by the Chaleurs Group. This situation is identical to that occurring 15 km to the southeast where the Neckwick rests unconformably on the Rivière Port-Daniel mélange and is in turn overlain unconformably by the Chaleurs Group, in its southeastern outcropping area (Fig. 5.9). The Rivière Port-Daniel - Neckwick assemblage is considered to be equivalent to the McCrea-Arsenault one. The unconformity between the Mictaw in a whole and the Chaleurs is also present 15 km to the north between the Arsenault Formation and the Chaleurs Group (Fig. 5.9).

Structural geology and structural style of the Dunnage Zone

The most significant structural feature of the Dunnage Zone is its northern limit with the Humber Zone, the BBL. In the Gaspé Peninsula, the BBL, a Taconian feature, has been used by Middle Devonian Acadian strike-slip faults (Malo et al., 1992) and shows a complex history of faulting. The main deformation of the Dunnage Zone in the Mictaw Group, the NE-trending structures, folds and associated penetrative cleavage, are related to the Middle Devonian Acadian deformation that affects the Gaspé Belt. However, NW-trending pre-Acadian folds are recognized in the Mictaw Group (De Broucker, 1987). The angular unconformity between the Silurian strata of the Chaleurs Group and the northwesterly folded Middle Ordovician Mictaw Group implies folding during Middle to Late Ordovician time. De Broucker (1987) interpreted the deformation related to these northwesterly folds as a late Ordovician event probably contemporaneous with the last nappe emplacement in the Humber Zone. The formation of the Rivière du Milieu mélange and the large NW-trending fault at the base of the mélange are related to this tectonic event (De Broucker, 1987).

In the McCrea mélange and Arsenault Formation, the penetrative cleavage is E-NE and associated with the regional Middle Devonian Acadian deformation of the Gaspé Belt (Malo et al., 1993). Fabrics found in the mélange along the Grand Pabos fault are all indicative of a dextral strike-slip movement which is also Acadian-related (Kirkwood and Malo, 1993). In the McCrea-Arsenault area, the Acadian deformation related to the Grand Pabos fault has obliterated the Ordovician-related deformation. Except the phacoidal cleavage in the matrix of the mélange that can be attributed to Ordovician tectonism in the Dunnage Zone like it has been suggested for the other mélange units of the Gaspé subzone, no evidence of pre-Acadian deformation has survived.

5.3.2 THE GASPÉ BELT

Stratigraphy

The most complete succession of the Gaspé Belt is found in the Gaspé Peninsula where the four broad temporal and lithological rock assemblages are well developed. The older rock assemblage (1) of Upper Ordovician-lowermost Silurian deep water fine-grained siliciclastic and carbonate facies, which is constituted of the Honorat and Matapédia groups, crops out mainly in the APA and the Matapédia Group occurs in some anticlines in the CVGS and CBS (Figs. 5.7, 5.17). The second rock assemblage (2) of Silurian-lowermost Devonian shallow to deep water shelf facies is comprised only of the Chaleurs Group occurring in the CVGS and CBS (Figs. 5.7, 5.17). The third rock assemblage (3) of Lower Devonian mixed siliciclastic and carbonate fine-grained deep shelf and basin facies comprises the Upper Gaspé Limestones and Fortin groups cropping out only in the CVGS (Fig. 5.7). The youngest rock assemblage (4) of Lower to Middle Devonian nearshore to terrestrial coarse-grained facies is constituted of the Gaspé Sandstones Group occurring in the CVGS (Figs. 5.7, 5.17). The La Garde and Pirate Cove formations in the western CBS (Fig. 5.17, locality J) are equivalent of the Gaspé Sandstones Group.

Rock assemblage 1 - Honorat and Matapédia groups - The first rock assemblage of the Gaspé Belt is composed of a lower siliciclastic assemblage (Honorat Group and part of the Matapédia Group) and an upper carbonate assemblage (upper part of the Matapédia Group) (Fig. 5.18). The lower siliciclastic assemblage is Late Ordovician in age and the carbonate assemblage is mainly Late Ordovician to Early Silurian.

The Honorat Group (Garin Formation; Malo, 1988a) is made up of various, chiefly terrigenous rocks: black claystone, non-calcareous grey mudstone, greenish-grey siltstone, calcareous siltstone, calcareous quartz-wacke, lithic wacke, conglomerate and silty dolomitic limestone. The sandstones exhibit numerous sedimentary structures (graded bedding, parallel and cross-laminations, load and flute casts).

The lower part of the Matapédia Group (Pabos Formation) consists of laminated calcareous mudstone at its base, followed by a sequence of calcareous rocks: calcareous mudstone, argillaceous limestone, calcareous siltstone, silty limestone, calcareous sandstone, calcareous conglomerate, and sandy calcarenite and calcilutite. Siltstone and sandstone are thin to medium-bedded and exhibit parallel and cross-lamination as well as flute casts. Calcareous conglomerates are thick bedded and contain clasts composed of Pabos and Honorat lithologies together with exotic clasts of sericite and chlorite schists, milky quartz and foliated sandstone. The upper part of the Matapédia Group (White Head Formation) is composed of thin-bedded grey or brown calcilutites with thinner interbeds of calcareous mudshales and a few thin beds of calcarenites, dark green calcareous mudstones, and thinly bedded silty and argillaceous limestone, calcareous shale and lenticular calcarenite with local limestone conglomerate, calcarenite, calcilutite and sandy limestone in thin to very thick beds.

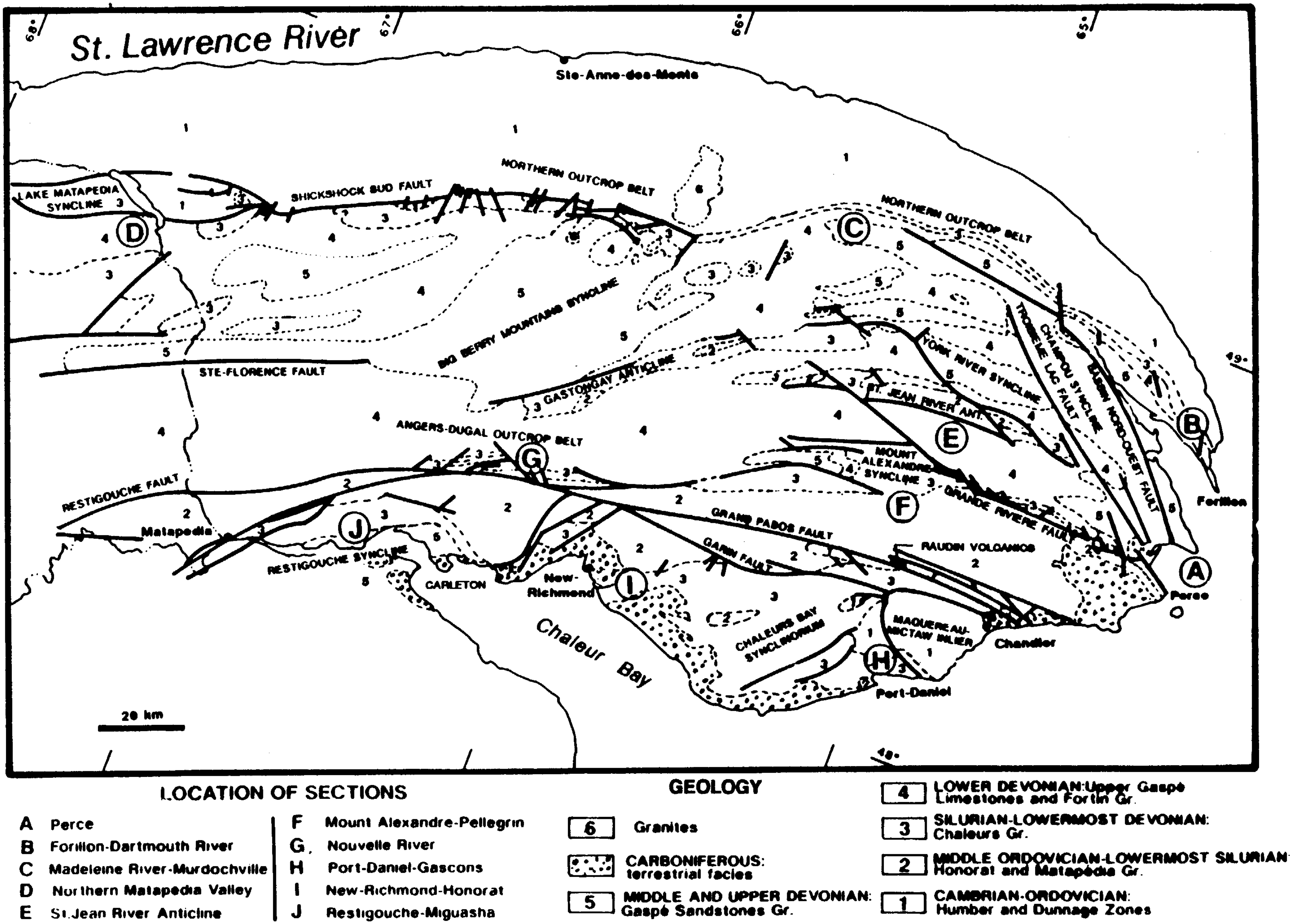

Figure 5.17. Geological map of Gaspé Belt in the Gaspé Peninsula. Letters in circles refer to location of stratigraphic sections of figure 5.18. From Malo and Bourque (1993).

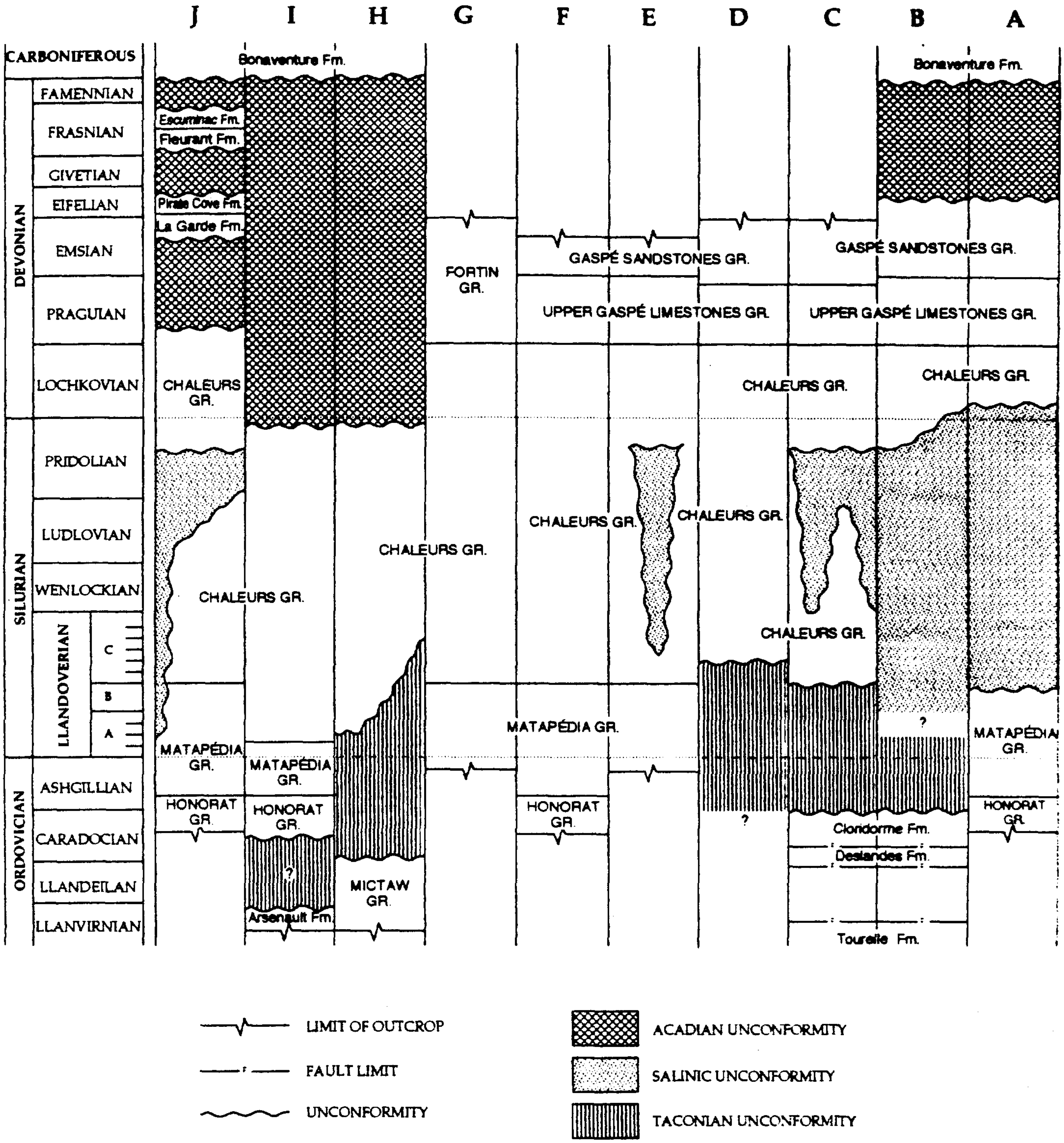

Figure 18. Correlation chart of Middle Paleozoic rocks of Gaspé Belt in Gaspé Peninsula and stratigraphic range of unconformities. From Malo and Bourque (1993).

Rocks assemblage 2 - Chaleurs Group - The stratigraphy of the Chaleurs Group in the eastern CBS consists of three broad assemblages (Bourque et Lachambre, 1980; Bourque et al., 1986; Bourque et al., 1993): (1) a lower siliciclastic assemblage, ranging from fine- to coarse-grained (Clemville, Weir and Anse Cascon formations); (2) a distinctive middle limestone assemblage (Anse à Pierre-Loiselle and La Vieille formations); and (3) an upper fine-grained siliciclastic *Zoophycos*-rich assemblage (Gascons and Indian Point formations) with intervening reef limestones and redbeds (West Point Formation) and mafic lava flows (Restigouche and Black-Cape volcanites).

Towards the west, the Chaleurs Group in the Restigouche syncline (Fig. 5.17 and column J, Fig. 5.18) is separated into two entities by the Salinian unconformity (Bourque and Lachambre, 1980). The succession between the Matapédia Group and the unconformity is composed of three rock assemblages. The lower assemblage (Mann Formation) consists of grey, structureless, fine-grained siliciclastites with intercalated thinly bedded parallel and convolute-laminated bioturbated fine-grained sandstones, and minor nodular calcilutites and calcarenites. It is locally rich in shallow shelf brachiopods. It correlates with the lower siliciclastic assemblage of the Chaleurs Group in the eastern CBS. The overlying assemblage (Anse à Pierre-Loiselle and La Vieille formations) is the same limestone assemblage as in the eastern CBS. It is composed of nodular limestones, with locally abundant large smooth-shelled pentamerid brachiopods, and biohermal limestones. Mafic volcanic rocks (Restigouche volcanites) occur within and above the limestone assemblage. They consist of basic lava flows, tuffs and volcanic breccias. That part of the Chaleurs Group beneath the unconformity was affected by folding before Late Silurian erosion that has stripped off locally all units of the Chaleurs Group and part of the Matapédia Group. Beds under the unconformity are no younger than early Ludlovian. The Chaleurs Group above the Salinian unconformity consists of two units. It starts with thick basal conglomerate (New Mills Formation) whose lithology is laterally variable. In the western part of the syncline, it consists mainly of pebbles and boulders of dark mafic volcanic rocks in a volcanic sandy matrix, while in the central part, pebbles and boulders (up to 1 m) are dark grey calcilutite, contained in red fine-grained sandstone. The limestone conglomerate forms very thick beds interlayered with red sandstones. Minor pink felsic volcanic rocks occur in the western part of the syncline. The conglomerate unit disappears towards the east. The second unit is a very thick sequence (Dalhousie Formation) of sedimentary and volcanic rocks. In the western part of the syncline, thin- to medium-bedded dark grey parallel-laminated argillaceous fine-grained sandstones interbedded with mudstones underlie mafic and minor felsic volcanic rocks. In the eastern part of the syncline, sedimentary units are more massive, muddier and more calcareous, and alternate regularly with the volcanic units. The volcanic rocks are vesicular and massive, or brecciated lava flows and pyroclastic rocks varying in composition from basaltic to rhyolitic (Bélanger, 1982; Laurent and Bélanger, 1984); andesites predominate. The pyroclastic rocks occur as thin layers of well-bedded pumice or scoria and ash deposits, and as thick units of unsorted block and ash deposits. Consanguineous intrusive bodies are few and always of small size. Fossils of that unit in both Québec and New Brunswick indicate a Lochkovian-Pragian age interval.

At the western extremity of the Restigouche syncline (Fig. 5.17), a structural slice (Sellarsville slice) contains sedimentary rocks of Ludlovian to Lochkovian age, consisting of mudcracked red and green fine-grained siliciclastics, minor limestone conglomerates with marine fossils, and at top of the sequence, small stromatoporoid bioherms and biostromes. The redbeds, as well as the bioherms and biostromes, correspond in age and lithology to the reefs and redbeds of the upper assemblage of the Chaleurs Group in the eastern CBS. Massively bedded greenish grey calcareous fine-grained siliciclastic rocks, locally rich in brachiopods, are found above that sequence. The sequence of the Sellarsville slice is equivalent in time to the unconformity and the New Mills conglomerate formation of the nearby Restigouche syncline, indicating the occurrence of local basins in which accelerated sedimentation took place in response to local uplift.

The most complete succession of the Chaleurs Group in the CVGS occurs in the Mount Alexandre-Pellegrin and Nouvelle River areas (Fig. 5.17 and columns F and G, Fig. 5.18) where the group rests conformably on the Matapédia Group of the APA and is overlain also conformably by the Upper Gaspé Limestones or Fortin groups. Along the northern edge of the CVGS (Northern Outcrop Belt and Lake Matapédia syncline; columns B, C and D, Fig. 5.18), in the Percé area (column A, Fig. 5.18) and in the rivière Saint-Jean anticline (column E, Fig. 5.18), the Chaleurs Group succession is more or less complete, since the group lies unconformably on older rocks and since parts of it have been stripped off by local erosion during Ludlovian time. The Chaleurs Group is therefore best described in terms of two sequences: (1) a northern shallow water sequence, including the Northern Outcrop Belt and Matapédia syncline, the Percé area and the eastern tip of the rivière Saint-Jean anticline; and (2) a southern deeper water sequence, comprising the western part of the rivière Saint-Jean anticline, the Gastonguay anticline, the Mount Alexandre syncline and the Angers-Dugal Outcrop Belt (Fig. 5.17).

The Chaleurs Group of the northern CVGS (Northern outcrop belt) (Bourque, 1975 and 1977; Lachambre, 1987; Bourque et al., 1993) is composed predominantly of siliciclastic facies, from bottom to top: (1) a claystone (Awantjish and Burnt Jam Brook formations) or calcilutite (Sources Formation) horizon; (2) a thin quartzarenite unit (Val-Brillant Formation); (3) a nodular and biohermal limestone horizon (Sayabec Formation) correlating with the middle limestone assemblage of the Chaleurs Group in the CBS; and (4) a thick fine-grained siliciclastic unit (Gascons, Indian Point and Roncelles formations) correlating with the upper fine-grained siliciclastic assemblage of the Chaleurs Group in the CBS. The last unit contains local reef limestone bodies (West Point Formation) and conglomerate lenses (Griffon Cove River and Owl Capes Members). As in the Restigouche syncline, a mappable unconformity occurs within the Chaleurs Group. In the eastern part of the rivière Saint-Jean anticline (column E, Fig. 5.18), the unconformity is local and overlain by a distinctive thick-bedded coarse-grained petromictic conglomerate (Owl Capes Member). In the Madeleine River area (column C, Fig. 5.18), the erosion has stripped off variable portions of the Chaleurs Group. Reef limestone bodies (West Point Formation) occur above the unconformity (Bourque et al., 1986; Lachambre, 1987). In the easternmost part of the Northern Outcrop Belt (column B, Fig. 5.18), lenses of pebble and cobble petromictic conglomerate (Griffon Cove River Member) occur associated with mudcracked redbeds above the unconformity. This conglomerate-redbed association correlates in age and lithology with that of the Restigouche syncline above the unconformity (New Mills Conglomerate).

The Chaleurs Group of the southern CVGS (Central outcrop belt) is more uniform in composition than in the northern sequence. It is composed mostly of fine-grained siliciclastic rocks (Burnt Jam Brook and Saint-Léon formations), with the exception of a local thin lithoclastic and quartz sandstone and conglomerate unit (Laforce Formation) of Wenlockian-early Ludlovian age, and mafic volcanic rock bodies (Baldwin volcanites) occurring in the upper portion of the group.

Rock assemblage 3 - Upper Gaspé Limestones and Fortin groups - The Upper Gaspé Limestones Group is composed of three lithologic assemblages (Lespérance, 1980a and b; Rouillard, 1986): (1) a lower monotonous sequence of more or less shaly, dolomitic and siliceous calcilutite or limy mudstone (Forillon Formation), it is more calcareous and more siliceous in the eastern part of the area; (2) a middle sequence of thinly to very thickly bedded siliceous and dolomitic limestone and mudstone, with minor calcarenite, sandstone and bentonite beds (Shiphead Formation), containing in the southern half of the area, units of coarse-grained sandstone and mudstone with numerous slump structures, a lithology very similar to that of the Fortin Group of the Assémetquagan River area (Fig. 5.17); (3) an upper homogeneous sequence of thin to medium-bedded cherty to siliceous or silty calcilutite (Indian Cove Formation). Bimodal alkaline volcanic rocks consisting of basalts, rhyolites, volcaniclastites are interbedded with limestones.

The Fortin Group in the southwestern portion of the CVGS in Gaspé Peninsula is a thick distinctive dark mudstone and fine to medium-grained sandstone sequence (McGerrigle, 1946; Dalton, 1987; Hesse and Dalton, 1989). It conformably overlies the Chaleurs Group in the Nouvelle River area (column G, Fig. 5.18). Mafic volcanic rocks consisting of pyroclastites and lavas are found in the western part of the Fortin Group along the Sainte-Florence fault (Berger, 1993).

Rock assemblage 4 - Gaspé Sandstones and equivalent - The Gaspé Sandstones of the CVGS (columns A to F, Fig. 5.18) comprise four conformably superposed sandstone and conglomerate assemblages (McGerrigle, 1950). The York Lake Formation, at the base, consists of alternating siliceous calcilutites with minor quartz arenites and wackes, and greenish grey medium-grained feldspathic wackes, constituting a transition between the Upper Gaspé Limestones and Gaspé Sandstones groups. The overlying York River Formation is composed of a lower mudstone-siltstone-sandstone assemblage with a few calcarenites and an upper sandstone assemblage with minor mudstones, the sandstones being medium to thick-bedded, greenish grey, medium to coarse-grained, feldspathic and lithic wackes with large-scale cross-bedding. The Battery Point Formation consists at the base of a number of superposed fining upward sequences of conglomeratic sandstone, medium to coarse-grained sandstone, and minor siltstone and mudstone (Cant and Walker, 1976), overlain by another assemblage of fining-upward sequences in which red mudstone and siltstone are abundant (Rust, 1981; Walker and Cant, 1979), overlain in turn by coarser sandstone with less clearly defined fining upward sequences, and ending with a red unit of sandstone, siltstone and mudstone. The upper unit, the Malbaie Formation, is composed of very thick-bedded conglomerate composed of pebbles and cobbles of limestone, siliciclastic and volcanic rock fragments derived from the older Matapédia and Chaleurs groups, interbedded with medium to coarse-grained red sandstone (Rust, 1976, 1981). The Gaspé Sandstones are unconformably overlain by Carboniferous rocks. In the central CVGS, bimodal alkaline volcanic rocks consisting of basalts, rhyolites, volcaniclastites are interbedded with the sandstones.

Coarse-grained Emsian to Frasnian terrestrial deposits equivalent to the Gaspé Sandstones occur in the core of the Restigouche syncline. The sequence is divided into four units (Alcock, 1935; Williams and Dineley, 1966): the La Garde, Pirate Cove, Fleurant and Escuminac formations (column J, Fig. 5.18). The La Garde Formation (Alcock, 1935; Béland, 1958; Dineley and Williams, 1968) is believed to lie disconformably on the Chaleurs Group. It is composed of thick beds of well-rounded pebble and cobble conglomerates interlayered with grey or greenish-grey coarse to fine-grained cross-bedded sandstone and a few mudstone beds. Clasts of Matapédia Group limestone were found in conglomerates in the eastern part of the outcrop area. The sequence coarsens upward and contains very few fossils. The thickness of the unit is estimated to be less than 1500 m (Dineley and Williams, 1968; Rust, 1989). The conformably overlying Pirate Cove Formation (Alcock, 1935; Dineley and Williams, 1968; Zaitlin and Rust, 1983) consists predominantly of red sandy siltstone and mudstone. The most striking lithology is limestone conglomerate whose clasts were derived predominantly from the Matapédia Group outcrop area to the north (Fig. 5.17). Clasts of the underlying Devonian units also occur. Except for the occurrence of palynomorphs, the unit is unfossiliferous.

Structural geology and structural style
The major structural trend of the Upper Ordovician to Middle Devonian rocks of the Gaspé Belt is oriented roughly NE-SW. This structural trend is transected by major E-trending strike-slip faults in the southeastern Gaspé and NW-trending strike-slip faults in the northeastern Gaspé (Fig. 5.7). The dominant trend of Acadian faults is used to divide the Gaspé Belt into three regions. The western region, which comprises the western and central parts of the CVGS, the western APA and the Restigouche syncline, is characterized by NE-trending faults (Fig. 5.7); the southeastern region, which comprises the eastern APA and the CBS, is characterized by E-trending faults (Fig. 5.7); and the northeastern region, which comprises the northeastern CVGS, is characterized by NW-trending faults (Figs. 5.7, 5.19).

Folds - Regional Acadian folds and cleavage in the Gaspé Peninsula are denoted F_R and S_R respectively. In the APA, the NE-trending F_R folds are doubly-plunging (Fig. 5.20). F_R folds are open and upright in the core of the anticlinorium, but tight, upright and inclined to the NE or the SW near the major faults (Fig. 5.21A). The NE-trending F_R folds are oblique to the major E-trending strike-slip faults (Fig. 5.20). The coeval regional NE-trending S_R cleavage is well developed throughout the APA and is usually rotated toward an easterly direction in structural domains that border the Grande Rivière and Grand Pabos faults (Malo and Béland, 1989). Within

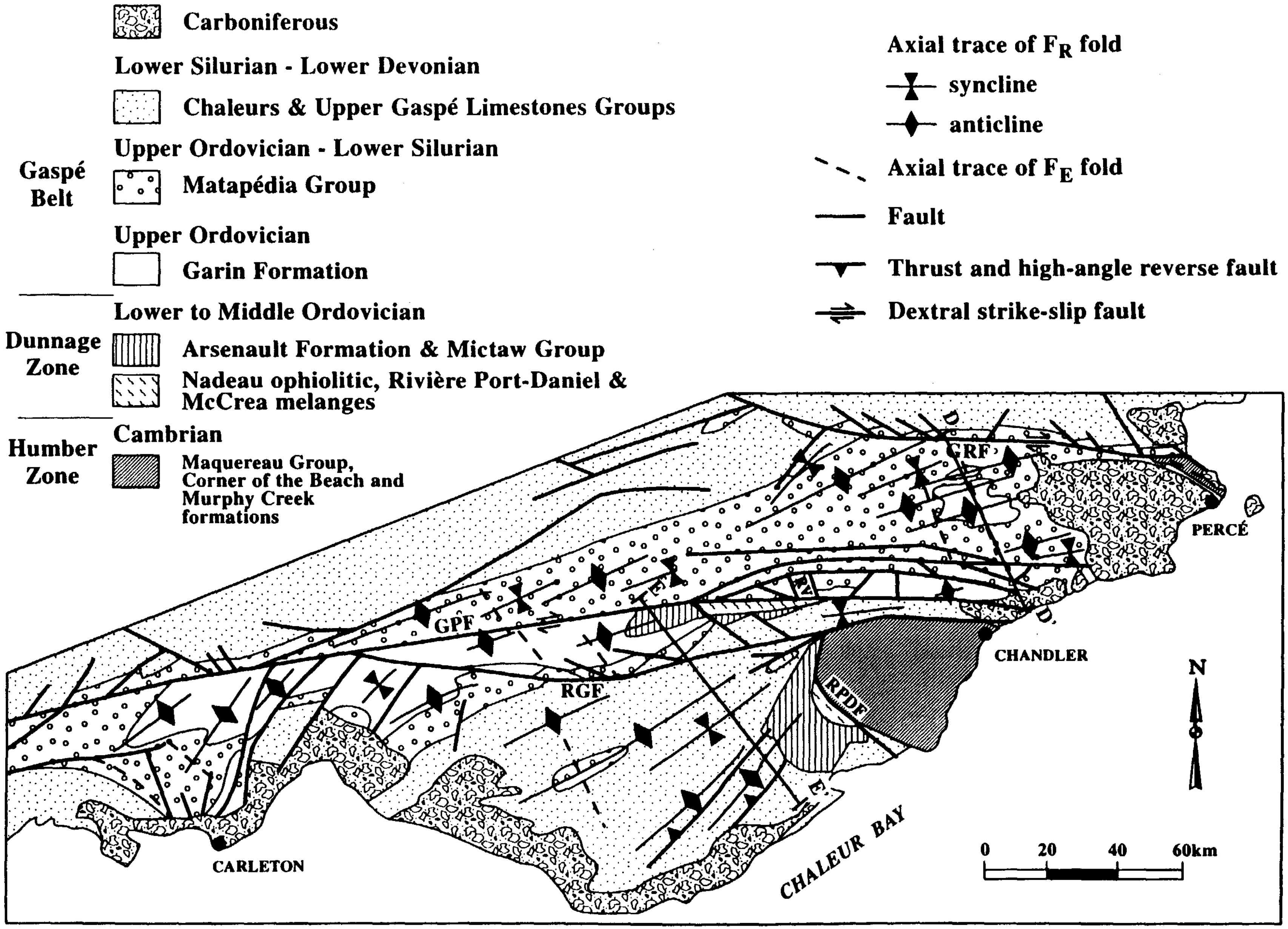

Figure 5.20. Geology of the southern Gaspé Peninsula. Modified from Brisebois et al. (1991).

A)

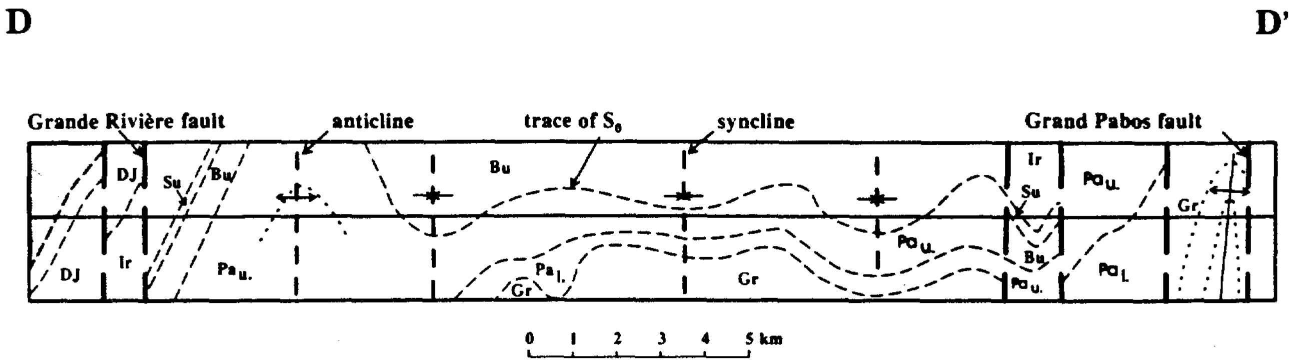

B)

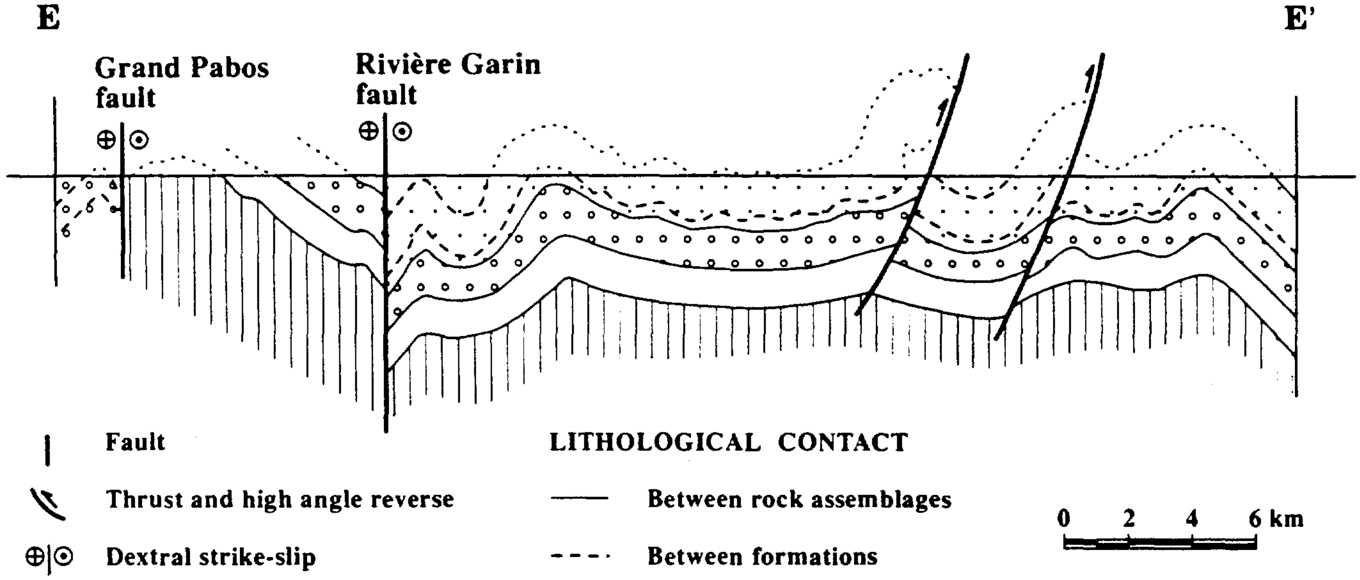

Figure 5.21. Structural cross-sections: A) DD' in the Aroostook-Percé anticlinorium, north of the Grand Pabos fault. Localization on figure 5.20. From Malo (1988b). BU: Burmingham Mb., DJ: Des Jean Mb., Gr.: Garin Fm., IR: L'Irlande Mb., Pal: lower Pabos Fm., Pau: upper Pabos Fm., Su: Côte de la Surprise Mb.r, B) EE' in the Aroostook-Percé anticlinorium and the Chaleurs Bay synclinorium, south of the Grand Pabos fault. Localization on figure 5.20.

zones bordering the major faults, the S_R cleavage is deformed by late riedel-shear fabrics in the semi-brittle to brittle deformation zone, whereas some C-S fabrics and shear bands are well developed in the ductile deformation zone.

In the western CVGS, the Acadian regional folds are NE-trending (e.g. Gastonguay anticline, Fig. 5.7). From the Gastonguay fault to the east, regional folds tends to become more easterly oriented (e.g. rivière Saint-Jean anticline, Fig. 5.7) and NW-trending folds are recognized close to the Bassin Nord-Ouest faults (Fig. 5.7). In most of the CVGS, Acadian F_R folds are characterized by large, low-amplitude, generally open and upright synclines of Devonian rocks (Gaspé Sandstones), and narrow and tighter anticlines of Silurian-lowermost Devonian (Chaleurs Group) (Figs. 5.22, 5.23, 5.24). F_R have subhorizontal hinge lines and several anticlines are asymmetrical, with their northern limbs slightly steeper than their southern limbs (Figs. 5.22, 5.23). In western Gaspé, the CVGS is bounded by the Shickshock-Sud fault, to the north, and by the Restigouche fault, to the south (Fig. 5.7). In this area, the Sainte-Florence fault divides two tectonostratigraphic domains: (1) a northern domain consisting of platformal limestones (Upper Gaspé Limestones) gently folded, the Gaspé Folded Belt, and (2) a southern domain constituted by Fortin Group flysch with similar folds, the Gaspé Through (Figs. 5.22). These two domains of the CVGS are also recognized in the central Gaspé Peninsula (Fig. 5.23), but become unrecognizable in the eastern part of the peninsula. The southern domain is part of the Early Devonian "slate belt" of the CVGS (Boucot, 1970). In this western CVGS, the intensity of Acadian deformation increases southward across the Sainte-Florence fault. In the Gaspé Folded Belt, rocks are gently folded (class 1B folds, Ramsay, 1967) and the S_R cleavage is only slightly developed, whereas south of the fault and of the Big Berry Mountains syncline (Figs. 5.7, 5.23), the rocks are tightly folded (class 2 folds, Ramsay, 1967) and contain a penetrative slaty S_R cleavage (Kirkwood et al., 1995). The Gastonguay anticline, which is bounded by faults, is tighter and inclined to the NW (Fig. 5.23). In the northeastern CVGS, the F_R fold trend varies from NE to nearly E (Fig. 5.19). On McGerrigle's (1950) cross-sections (Fig. 5.24), we recognize the same structural style of folding as the one observed in the western CVGS with large open synclines of Devonian rocks (unit 9, York River Formation) and tight anticlines of older Silurian rocks (units 2 and 4, White Head Formation and undifferentiated Siluro-Devonian rocks).

F_R folds of the CBS are NE-trending (Fig. 20), open to moderate with subhorizontal hinge lines (Fig. 5.21B). Generally F_R folds are upright but some F_R folds are inclined to the SE (Fig. 5.21B). Axial-plane cleavage is not a penetrative fabric in the rocks of the Chaleurs Group within the synclinorium, except for the northeastern most tip of the CBS, the Raudin syncline (Fig. 5.19), where a strong penetrative cleavage is well developed.

A NW-trending folding, with no penetrative cleavage, precedes the F_R NE-trending folding (Malo and Béland, 1989). These transverse NW-trending folds are denoted F_E because they are the earliest folds recognized in the Gaspé Belt rocks. The result of the two successive phases of folding produces dome and basin interference patterns which is well illustrated in the area north of Chandler where the core of the anticlinorium is occupied by a large dome of the oldest rocks of

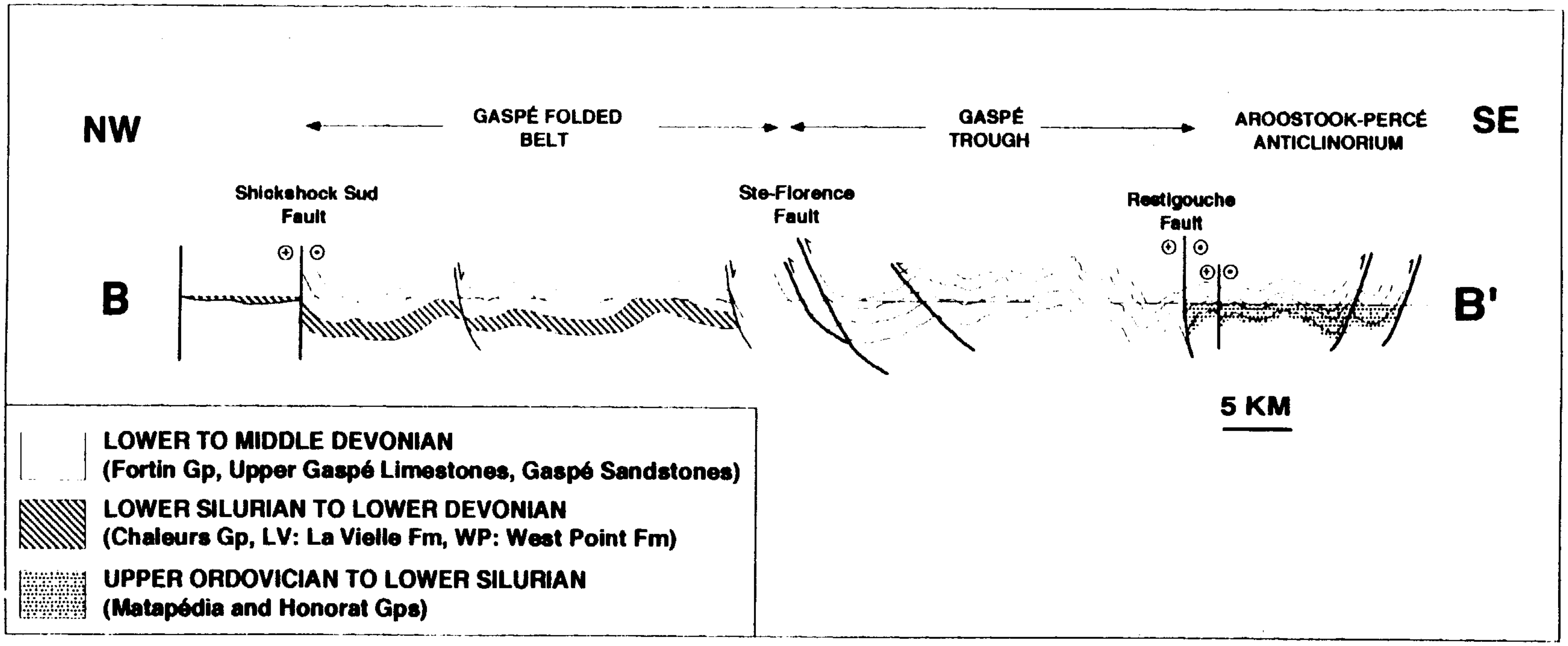

Figure 5.22. Structural cross-section BB' in the western part of the Gaspé Belt, along the Matapédia River. Localization on figure 5.7. Modified from Kirkwood (1993).

zones bordering the major faults, the S_R cleavage is deformed by late riedel-shear fabrics in the semi-brittle to brittle deformation zone, whereas some C-S fabrics and shear bands are well developed in the ductile deformation zone.

In the western CVGS, the Acadian regional folds are NE-trending (e.g. Gastonguay anticline, Fig. 5.7). From the Gastonguay fault to the east, regional folds tends to become more easterly oriented (e.g. rivière Saint-Jean anticline, Fig. 5.7) and NW-trending folds are recognized close to the Bassin Nord-Ouest faults (Fig. 5.7). In most of the CVGS, Acadian F_R folds are characterized by large, low-amplitude, generally open and upright synclines of Devonian rocks (Gaspé Sandstones), and narrow and tighter anticlines of Silurian-lowermost Devonian (Chaleurs Group) (Figs. 5.22, 5.23, 5.24). F_R have subhorizontal hinge lines and several anticlines are asymmetrical, with their northern limbs slightly steeper than their southern limbs (Figs. 5.22, 5.23). In western Gaspé, the CVGS is bounded by the Shickshock-Sud fault, to the north, and by the Restigouche fault, to the south (Fig. 5.7). In this area, the Sainte-Florence fault divides two tectonostratigraphic domains: (1) a northern domain consisting of platformal limestones (Upper Gaspé Limestones) gently folded, the Gaspé Folded Belt, and (2) a southern domain constituted by Fortin Group flysch with similar folds, the Gaspé Through (Figs. 5.22). These two domains of the CVGS are also recognized in the central Gaspé Peninsula (Fig. 5.23), but become unrecognizable in the eastern part of the peninsula. The southern domain is part of the Early Devonian "slate belt" of the CVGS (Boucot, 1970). In this western CVGS, the intensity of Acadian deformation increases southward across the Sainte-Florence fault. In the Gaspé Folded Belt, rocks are gently folded (class 1B folds, Ramsay, 1967) and the S_R cleavage is only slightly developed, whereas south of the fault and of the Big Berry Mountains syncline (Figs. 5.7, 5.23), the rocks are tightly folded (class 2 folds, Ramsay, 1967) and contain a penetrative slaty S_R cleavage (Kirkwood et al., 1995). The Gastonguay anticline, which is bounded by faults, is tighter and inclined to the NW (Fig. 5.23). In the northeastern CVGS, the F_R fold trend varies from NE to nearly E (Fig. 5.19). On McGerrigle's (1950) cross-sections (Fig. 5.24), we recognize the same structural style of folding as the one observed in the western CVGS with large open synclines of Devonian rocks (unit 9, York River Formation) and tight anticlines of older Silurian rocks (units 2 and 4, White Head Formation and undifferentiated Siluro-Devonian rocks).

F_R folds of the CBS are NE-trending (Fig. 20), open to moderate with subhorizontal hinge lines (Fig. 5.21B). Generally F_R folds are upright but some F_R folds are inclined to the SE (Fig. 5.21B). Axial-plane cleavage is not a penetrative fabric in the rocks of the Chaleurs Group within the synclinorium, except for the northeastern most tip of the CBS, the Raudin syncline (Fig. 5.19), where a strong penetrative cleavage is well developed.

A NW-trending folding, with no penetrative cleavage, precedes the F_R NE-trending folding (Malo and Béland, 1989). These transverse NW-trending folds are denoted F_E because they are the earliest folds recognized in the Gaspé Belt rocks. The result of the two successive phases of folding produces dome and basin interference patterns which is well illustrated in the area north of Chandler where the core of the anticlinorium is occupied by a large dome of the oldest rocks of

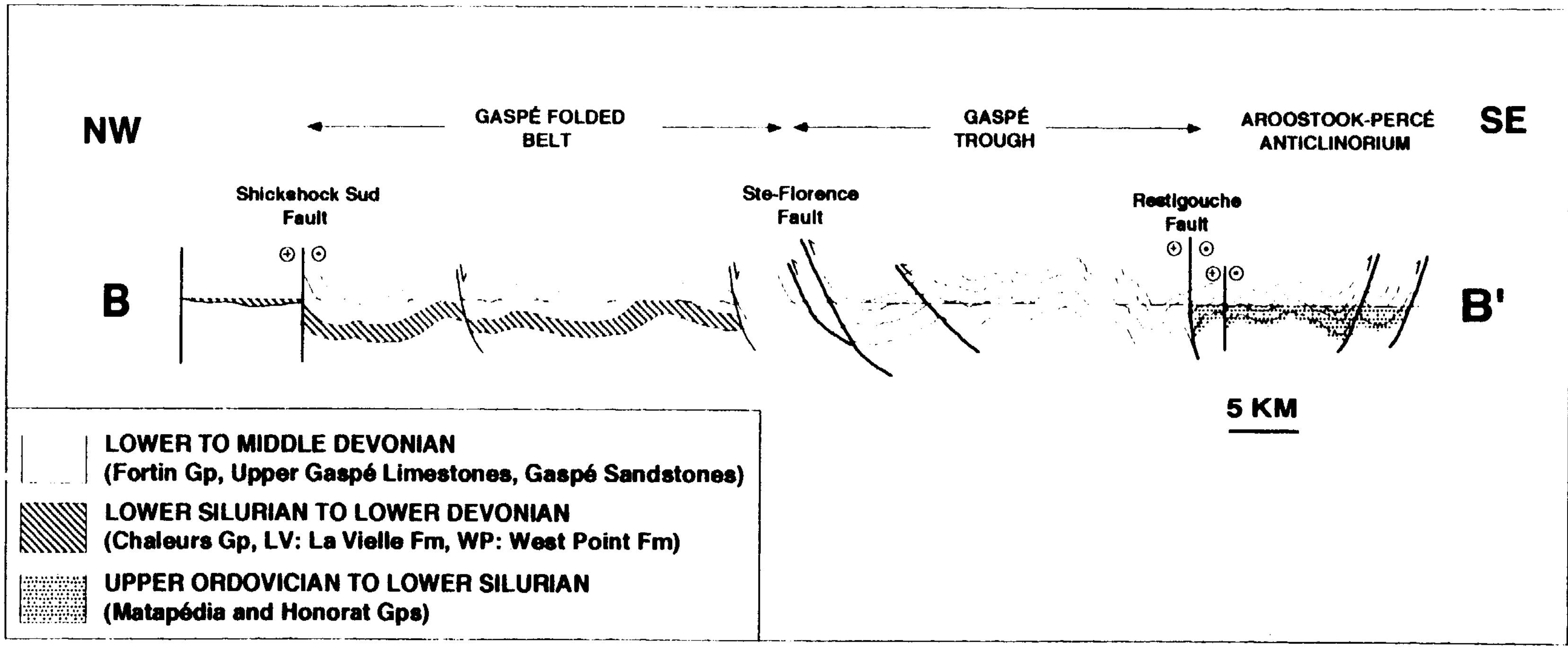

Figure 5.22. Structural cross-section BB' in the western part of the Gaspé Belt, along the Matapédia River. Localization on figure 5.7. Modified from Kirkwood (1993).

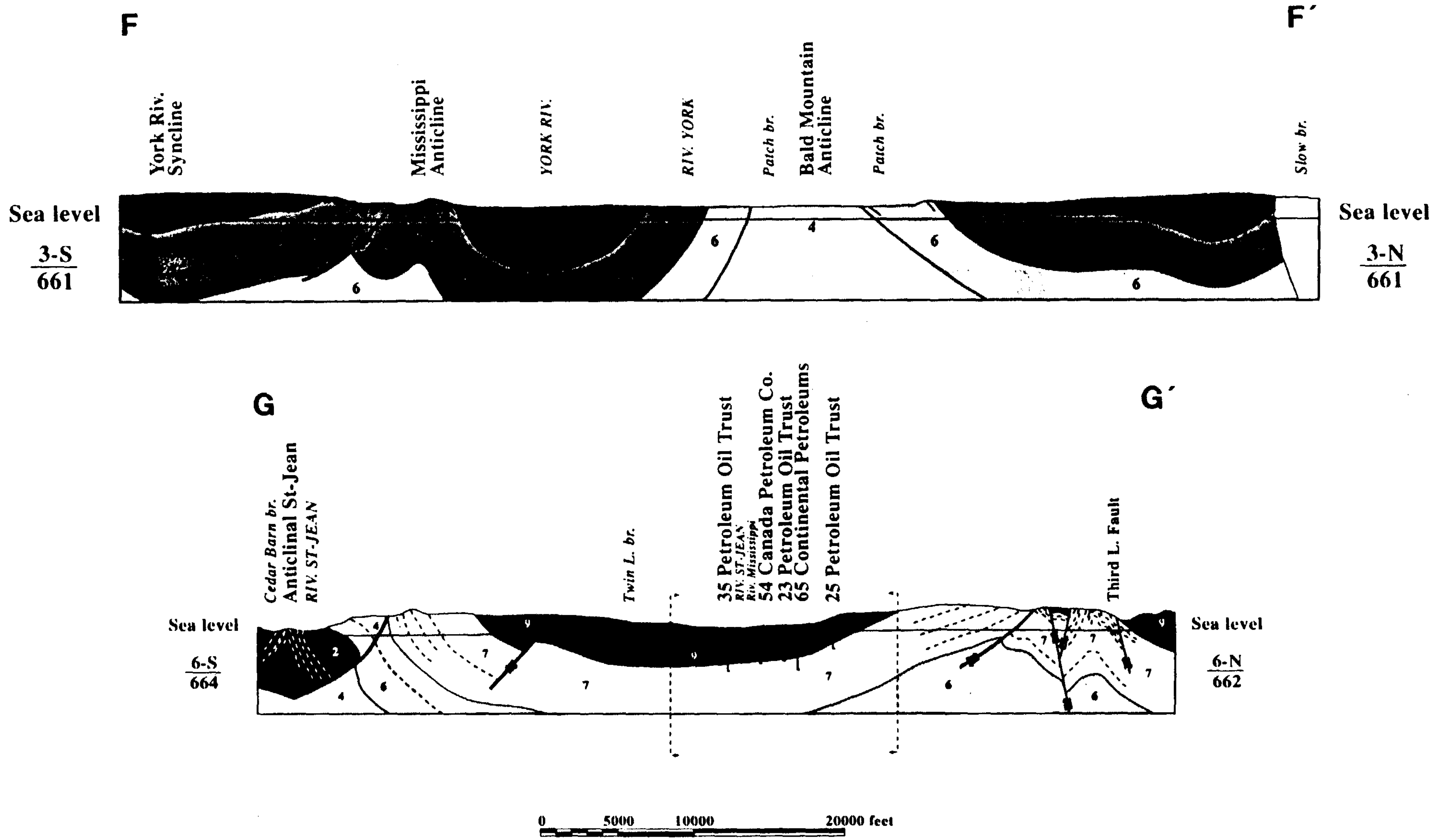

Figure 5.24. Structural cross-sections FF' and GG' in the eastern part of the Connecticut Valley-Gaspé synclinorium. Localisation on figure 5.19. From McGerrigle (1950).

the Gaspé Belt, the Honorat Group (Fig. 5.20). In the eastern APA, F_E folds are large open structures with wavelength of 15 to 20 km (Malo, 1986), whereas, in the Matapédia, they are upright to slightly inclined, open to tight, with wavelengths ranging from 2 to 6 km (Théberge, 1979). The fact that the S_R cleavage remains unaffected by this folding clearly indicates the succession of events. The transverse F_E folding is observed throughout the APA (Kirkwood, 1989; Gauthier, 1986; Malo, 1988b; Simard, 1986; Théberge, 1979; Vennat, 1979). In the Restigouche syncline, earlier or pre-F_R folds of indeterminate trend occur in the Chaleurs Group under the Salinian unconformity. Since NW-trending F_E folds affected the Chaleurs Group (Simard, 1986) in the Carleton area (Fig. 5.20), which is the eastern part of the Restigouche syncline, it is believed that the earlier folds of the Restigouche syncline belong to the F_E folding episode. The earlier F_E folding is also observed in the northeastern CVGS (Fig. 5.7), for example NW-trending fold between the Troisième Lac and Bassin Nord-Ouest faults (Fig. 5.19). Statistical analysis of S_0 along the Bassin Nord-Ouest fault indicate that some structural domains are characterized by WNW-trending folds (Berger and Ramsay, 1993).

Faults - Information concerning the kinematics and displacement history of major faults is essential to unravel the tectonic history of an orogen. In the following analysis, we will analyse the major Acadian faults in the already defined three regions of the Gaspé Belt. We will also pay attention to the relationship of Acadian faults to the Baie Verte-Brompton Line (BBL) in order to better constrain the tectonic history of the Gaspé Peninsula from the Taconian to Acadian times. The CVGS has been interpreted as a fault-bounded, subsided trough that originated after the emplacement of the Taconian allochthon in northern Gaspé (Beaudin, 1980, 1984; Rogers, 1970). This regime of normal faulting, which was probably active during the sedimentation of the whole Gaspé Belt, was followed by strike-slip movements along the same faults during the Acadian orogeny. Some Acadian faults may also have used older Taconian faults and their history can be very complex.

In the western region, the major faults trend is NE (Fig. 5.7). These faults, subparallel to the regional folding, are thrust or high-angle reverse faults. Acadian thrusting are NW-directed to the north of the APA whereas they are SE-directed to the south (Fig. 5.7). In the middle part of the CVGS (Fig. 5.7, the Sainte-Florence fault could represent the northeastern extension of the La Guadeloupe fault of the Québec Eastern Townships, which is a NW-directed Acadian thrust fault (Cousineau and Tremblay, 1993; Tremblay et al., 1989). The Sainte-Florence fault shows two episodes of faulting. Vertical stretching lineations (Kirkwood and St-Julien, 1987; Chen, 1994) within the fault zone suggest a NW-directed reverse movement along the fault. Mesoscopic Riedel-type vertical shears and vertical mineralized veins compatible with brittle-ductile dextral strike-slip motion along the fault (Berger, 1993; Chen, 1994) clearly overprint the vertical stretching lineation. Ductile and brittle fabrics are observed in rocks of the Lower Devonian Fortin Group indicating that the two episodes of faulting are post-Early Devonian. In the central part of the CVGS, the Marcil Nord fault, just south of the Big Berry Mountain syncline (Fig. 5.23), is also interpreted as a NW-directed high-angle reverse fault (Carbonneau, 1959). The Marcil Sud fault could be interpreted as a back-thrust of the Marcil Nord Fault (Fig. 5.23).

Farther south, the Restigouche fault is a longitudinal fault that separates the CVGS and the APA. The Restigouche fault continues to the south in New Brunswick (St. Peter, 1977), where it trends N-NE compared with an E-NE trend in the Matapédia area and an E trend for its prolongation into the eastern Gaspé, the Grand Pabos fault (Fig. 5.7). This different direction of the Grand Pabos-Restigouche fault suggests that the movement, in its western end, could be vertical as opposed to the horizontal strike-slip movement in its eastern end (see below). The Restigouche fault was described as a NW-directed high-angle reverse fault in the Matapédia area (Lachance, 1979) and northern New Brunswick (St. Peter, 1977). In the Matapédia area, subvertical C-S fabrics in the fault zone indicate a dextral strike-slip component of movement, and the fault is there interpreted as a dextral oblique-slip fault (Kirkwood and St-Julien, 1987). In the southwestern Gaspé Peninsula (Fig. 5.7), the southern limit of the APA is the Sellarsville fault which separates the anticlinorium from the Restigouche syncline. This fault was considered as a SE-directed thrust fault (Bourque and Lachambre, 1980). The study of mesoscopic brittle faults and shear-sense indicators along the Sellarsville fault zone confirms that this fault is a high-angle reverse faults with a movement to the southeast (Trudel and Malo, 1993). We should also note that, farther east, other southeastward-directed high-angle reverse faults are present in the CBS (Fig. 5.20).

Still in the western region, in the central CVGS, the Shickshock-Sud fault is an example of a complex fault which was active during both the Taconian and Acadian orogenies. The BBL follows the Shickshock-Sud fault (Fig. 5.6), a complex fault zone which comprises sheared and brecciated rocks of different ages. Cambro-Ordovician rocks of the Humber Zone, Middle to Late Ordovician Ruisseau Isabelle mélange and Siluro-Devonian rocks of the Gaspé Belt are all affected by the Shickshock-Sud fault (Fig. 5.13). Based on stratigraphic relationships, the movement along the Shickshock-Sud fault was interpreted by Beaudin (1980) as normal during the Silurian and Early Devonian, and reactivated subsequently as a high angle reverse fault during the Acadian deformation. Berger (1985) and Lebel (1985) however, studied the brittle deformation features within the Siluro-Devonian rocks along the Shickshock-Sud fault and deduced a dextral strike-slip component of movement along the fault in post-Early Devonian time. Recent works along the Shickshock-Sud fault suggest that there are at least two episodes of faulting (Sacks and Malo, 1994, 1995). On the north side of the fault, high temperature mylonites occur in the Cambrian metavolcanic rocks of the internal nappe domain of the Humber Zone (Shickshock Group) and in the amphibolites of the Amphibolite du Diable, at the base of the Mont-Albert nappe. The mylonitic foliation dips moderately to strongly to the SE and the stretching lineation plunges E-SE. Shear bands, asymmetric porphyroblasts, and asymmetric folds indicate oblique dextral strike slip and a NW-directed reverse motion (Sacks and Malo, 1994). These ductile deformation features are absent within Early Silurian rocks of the Gaspé Belt on the south side of the fault. Vertical brittle-ductile shear zones, indicating horizontal dextral strike-slip movement, are present on both sides of the fault and are superimposed on the ductile mylonites. These observations imply that ductile deformation in Cambrian rocks are related to pre-Silurian movement whereas the superimposed brittle-ductile deformation is associated with post-Early Devonian strike-slip movement.

In the southeastern region, the major faults are the E-trending Grand Pabos, Grande Rivière and Rivière Garin faults the Grand Pabos fault system (Fig. 5.7). These dextral strike-slip faults are characterized by ductile high strain zones bordered by brittle-ductile, low strain zones (Kirkwood and Malo, 1993). Shear-sense indicators and offsets of stratigraphic markers indicate a horizontal dextral displacement of more than 100 km in southern Gaspé Peninsula along the Grand Pabos fault system (Malo and Béland, 1989). Microscopic and mesoscopic fabrics indicating dextral strike-slip motion are observed in the Middle Ordovician rocks of the Dunnage Zone, in the Upper Ordovician-Lower Silurian rocks of the APA, and in the Silurian-Early Devonian rocks of the CVGS and CBS along the Grand Pabos fault system (Figs. 5.6, 5.7), implying a post-Early Devonian age for movement along the fault system. The NE-trending faults, subparallel to the regional F_R folding, are high-angle reverse and oblique faults (Figs. 5.20, 5.21B). Acadian reverse faulting is mainly NW-directed in the Gaspé Belt, with minor SE-directed movement in the southern part of the peninsula, in the CBS (Figs. 5.20, 5.21B). In western Gaspé Peninsula, some of the NE-trending faults are lateral equivalents of major strike-slip faults to the east (*i.e.* Restigouche and Grand Pabos faults; Figs. 5.6, 5.7). Both NW- and SE-directed transport along the reverse faults in southern Gaspé Peninsula are related to a dextral transpressive regime during the strike-slip motion along the Grand Pabos fault system.

Still in the southeastern region, we find a major NW-trending fault within the Maquereau-Mictaw inlier, the Rivière Port-Daniel fault (Figs. 5.6, 5.9), which also affect the Gaspé Belt rocks of the CBS (Fig. 5.9). The Rivière Port-Daniel fault is interpreted to be the BBL in southern Gaspé Peninsula (Williams and St-Julien, 1982). It is a composite structure, that was active from Late Cambrian to Middle Devonian time (De Broucker, 1987). A strain gradient has been observed in Cambrian rocks of the internal nappe domain of the Humber Zone (Maquereau Group) nearing the Rivière Port-Daniel fault (De Broucker, 1987); the cleavage intensifies and changes gradually into a well-developed foliation near the fault. Over a distance of a few hundred metres, a mylonitic foliation develops, evolving from cataclastic textures to proto-mylonites and ultra-mylonites. The stretching lineation and shear-sense indicators in the mylonites indicate horizontal dextral strike-slip motion (De Broucker, 1987). This movement is Late Cambrian to Early Ordovician in age because comparable structures and textures are not found in rocks of the Lower to Middle Ordovician Rivière Port-Daniel mélange (Dunnage Zone). Tectonic breccia in the Maquereau Group and the Rivière Port-Daniel mélange (Williams and St-Julien, 1982) as well as NE-verging thrust faults in the Middle Ordovician rocks of the Dunnage Zone (Mictaw Group) suggest post-Middle Ordovician movements along the Rivière Port-Daniel fault (De Broucker, 1987). These movements are part of a complex faulting history with normal and thrust motion during the accretion of the Rivière Port-Daniel and Nadeau ophiolitic mélanges (Dunnage Zone) with the Maquereau Group (Humber Zone) (De Broucker, 1987). Finally, post-Silurian (Devonian) movement is indicated by reverse and normal faults in Silurian rocks of the Gaspé Belt exposed along Chaleurs Bay (Fig. 5.9).

The northeastern region, the eastern CVGS, is characterized by NW-trending faults (Figs. 5.7, 5.19). The most important ones are the Bassin Nord-Ouest, the Troisième Lac, and the

Gastonguay faults. These three faults have been used by many to delimit tectonic blocks within the CVGS (Roksandic and Granger, 1981; Héroux et al., 1983; Amyot, 1984; Bertrand, 1987; St-Julien and Bourque, 1990; Lavoie, 1992; Berger and Ramsay, 1993). All these authors have recognized the same blocks: a northern block, north of the Bassin Nord-Ouest fault, a central block, between the Bassin Nord-Ouest and the Troisième Lac faults, and a southern block, south of the Troisième Lac fault. This latter southern block is limited to south by the Grande-Rivière fault and to the west by the Gastonguay fault. The structural study of outcrops along the Bassin Nord-Ouest and Troisième Lac faults (Béland, 1980; Berger and Ramsay, 1993) shows that these are Acadian dextral strike-slip faults with a vertical component of movement. This dextral strike-slip movement probably corresponds to the last Acadian movement in the northeastern Gaspé Belt. For instance, in the Percé area, it has been shown that the southern extension of the Troisième Lac fault crosscuts E-trending faults associated to the Grande Rivière fault (Kirkwood, 1989).

The NW-trending faults are probably older than late Acadian and were active during sedimentation of the Silurian and Lower Devonian facies of the Gaspé Belt. Facies variations in rocks of the Upper Silurian Chaleurs Group and Lower Devonian Upper Gaspé Limestones Group related to movement along the Bras Nord-Ouest and Troisième Lac faults (Lavoie, 1992) (Fig. 5.25) as well as significant wedging of these rocks towards the faults (Fig. 5.25), as observed on seismic reflection profiles that crosscut the two faults (Roksandic and Granger, 1981), strongly suggests synsedimentary movement along the faults. Other sedimentological analysis of the Gaspé Sandstones (Rust, 1981; Amyot, 1984), the Upper Gaspé Limestones (Amyot, 1984; Lavoie, 1992), and of the Chaleurs Group (Bourque et al., 1993, 1995, 1996 submitted), as well as thermal maturation studies of the northeastern Gaspé Peninsula (Héroux et al., 1983; Bertrand, 1987) also suggest synsedimentary movements along the faults (see also part 1 of this report by Bourque and Malo). These movements may have started in Llandoverian and continue until the Pragian. The Gastonguay and Grande Rivière faults were active during the sedimentation of the Burnt Jam Brook, whereas the Bassin Nord-Ouest fault was active during the deposition of the Gaspé Sandstones (Rust, 1981; Amyot, 1984).

There is also evidence for a pre-Silurian motion along the Bassin Nord-Ouest fault, before normal motion during sedimentation of the Siluro-Devonian rocks (Béland, 1980; Berger and Ramsay, 1993). In the Mont Serpentine inlier (Fig. 5.10), Cambro-Ordovician rocks of the Dunnage Zone (Lady Step complex) are affected by a well developed NW-trending foliation which contains subhorizontal mineral lineations (Béland, 1980; Berger and Ramsay, 1993). These ductile fabrics are not observed in the unconformably overlying Upper Silurian and Lower Devonian strata to the south. Small-scale brittle faults affect the Siluro-Devonian rocks and crosscut earlier structural elements in the Lady Step complex (Béland, 1980). These relationships suggest that there has been pre-Silurian ductile strike-slip motion along the northern part of the Bassin Nord-Ouest fault, and with a dextral sense of shear according to Berger and Ramsay (1993). This pre-Silurian motion can be attributed to the Taconian orogeny (Malo and Kirkwood, 1996) and the Bassin Nord-Ouest fault corresponds to the trace of the BBL in northeastern Gaspé Peninsula (Malo et

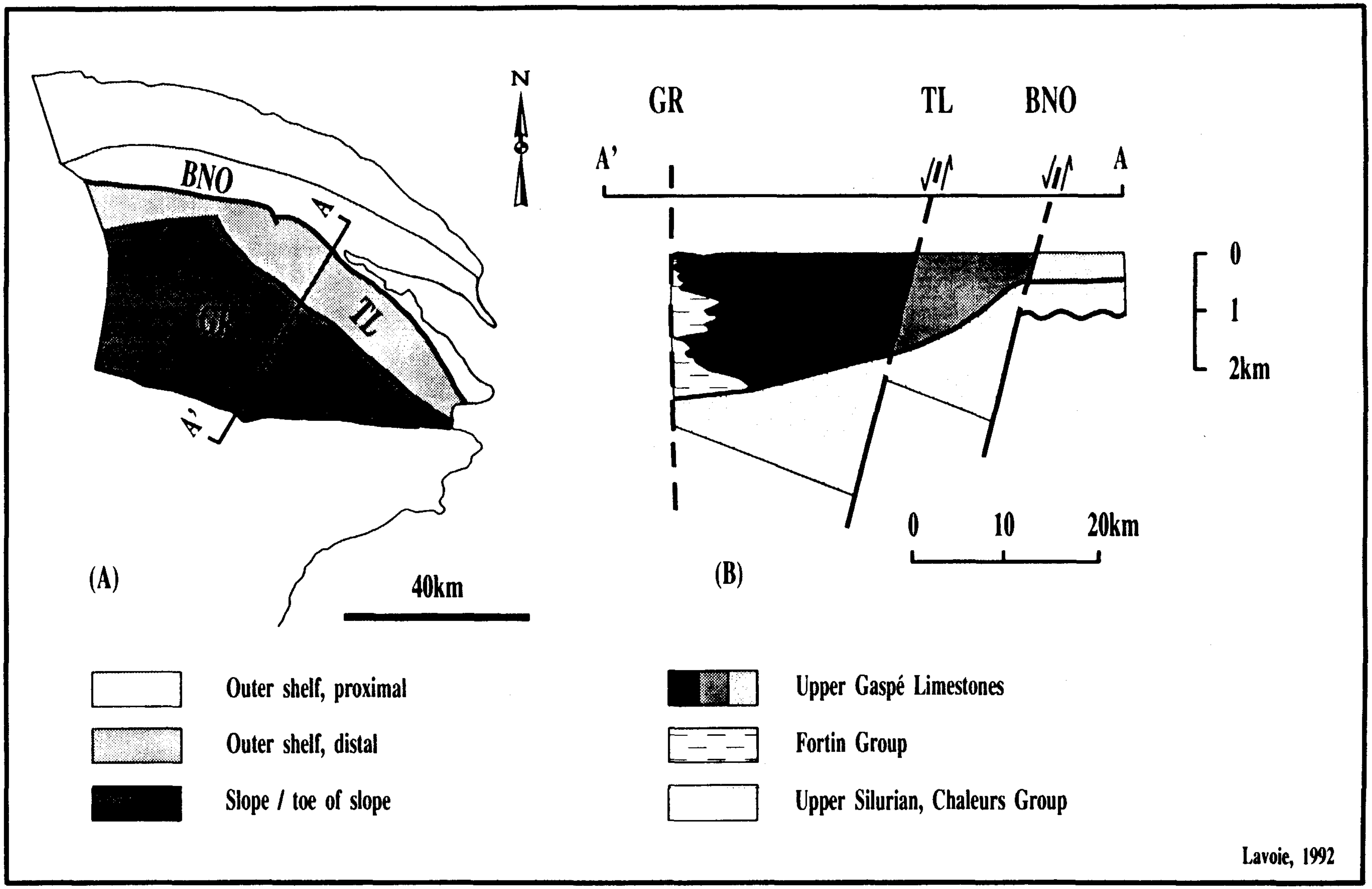

Figure 5.25 A) Paleoenvironmenttal interpretation of lithotectonic domains of the Upper Gaspé Limestones. B) Simplified cross-section, based on Roksandic and Granger (1981) interpretation of seismic profile, showing the relation between synsedimentary faulting and the distribution of lihofacies. BNO: Bassin Nord-Ouest fault, TL: Troisième Lac fault, GR: Grande Rivière fault. From Lavoie (1992).

al., 1992). Continued motion, as normal faulting during the sedimentation, along the NW-trending faults of the northeastern region of the Gaspé Belt was inverted in Late Devonian time by the Acadian transpression (strike-slip with high-angle reverse motion). The overprinting small-scale brittle faults are related to this post-Early Devonian dextral motion along the Bassin Nord-Ouest fault (Berger and Ramsay, 1993).

Faulting and folding relationship - The oblicity of F_R NE-trending folds to major E-trending faults in southeastern Gaspé Peninsula suggests that the folds possibly originate from the dextral strike-slip movement along the faults. In the APA (Fig. 5.20), major strike-slip faults, subsidiary faults, low-angle synthetic and high-angle antithetic faults with respect to the master strike-slip faults, rotated oblique regional folding (F_R), and regional cleavage (S_R), and late shear fabrics are all related to the same Acadian regional deformation event consistent with a classical strike-slip tectonics model (Malo and Béland, 1989). The oblicity of F_R folds with Acadian strike-slip faults is also observed along the Shickshock-Sud fault (Figs. 5.7, 5.13). F_R are open and upright which is typical of folds in a wrench tectonics environment (Wilcox et al., 1973). Since the D_R deformation implies horizontal shortening (F_R folds, S_R cleavage and high-angle reverse faults) across the Gaspé Belt accompanied by transcurrent motion along major strike-slip faults, it is believed that the D_R deformation is the result of a transpressional regime (Sanderson and Marchini, 1984) during post-Middle Devonian time.

In the northeastern region, the spatial relationship between NW-trending folds and faults is evident and it is likely that there is a genetic link between the development of both type of structures. Like those of the eastern CVGS, the early NW-trending folds elsewhere in the Gaspé Belt are sometimes spatially associated to NW-trending faults (e.g. Percé and Carleton areas in the APA, Fig. 5.20). They are interpreted as drape folds in response to Salinian block faulting. Berger and Ramsay (1993) believed that NW-trending folds are the regional E-trending folds of northeastern CVGS that have rotated clockwise within the dextral strike-slip faults system of the Troisième Lac and Bassin Nord-Ouest faults.

Strain analysis - The incremental strain analysis performed within rocks of the Gaspé Belt in western Gaspé Peninsula helped to determine the regional progressive deformation history (D_R) in this part of the Appalachians (Kirkwood et al., 1995). The incremental extension history was deduced by studying the growth of syntectonic fibres within pyrite pressure shadows in three mutually perpendicular sections (Kirkwood, 1995). The three dimensional fibre geometry reveals a complex extension history during the regional Acadian progressive deformation. The incremental extension direction was initially oriented vertically within the cleavage plane and changed abruptly to subhorizontal within the cleavage plane (S_R) parallel to the regional fold axes (F_R). The fibres were genetically divided into five sections which record distinct structural stages during D_R. The growth patterns indicate that layer-parallel shortening, folding and cleavage development associated with vertical extension occurred during regional coaxial deformation (Fig. 5.26A, stage I). During the last structural stage, deformation resulting from regional simple shear was responsible for orogen parallel extension and produced further development of cleavage

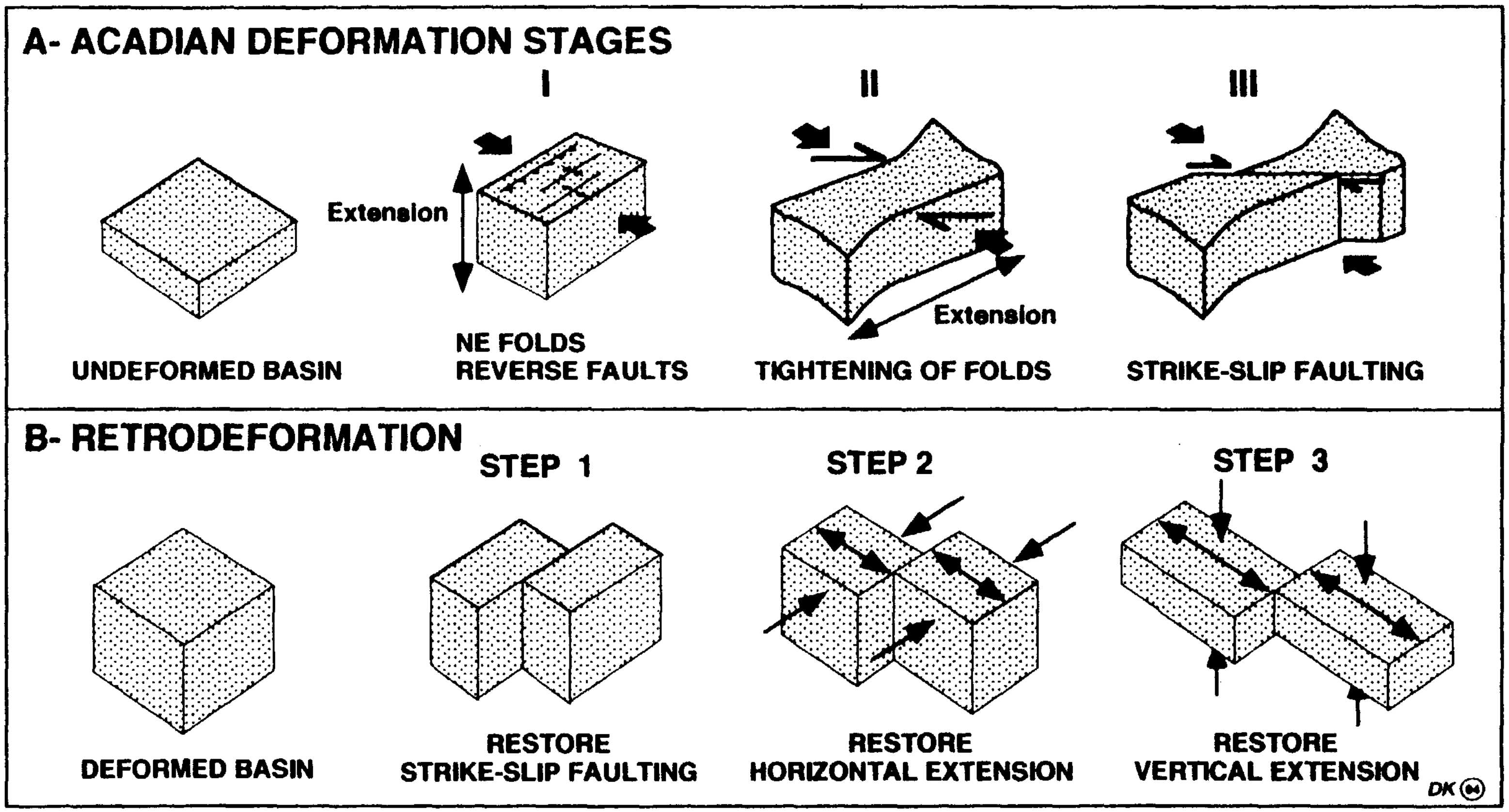

Figure 5.26. A: The three main Acadian deformation stages: 1 - folding and reverse faulting, 2 - tightening of folds and initiation of strike-slip faulting, 3 - slip along strike-slip faults. Modified from Kirkwood (1994). B: The three retrodeformation steps: 1 - restoration of slip along strike-slip faults, 2 - restoration of horizontal extension, 3 - restoration of vertical extension. From Malo and Kirkwood (1996).

planes and fold tightening (Fig. 5.26A, stage II). Assuming plane strain, strain data indicate vertical extensions up to 160%, fold-axis parallel extensions up to 110% and an average horizontal shortening across the cleavage of 77% for the Lower Devonian rocks of the Fortin Group within the Gaspé trough of the CVGS and of 65% for the Upper Ordovician to Lower Silurian rocks of the APA (Kirkwood, 1995).

The western part of the peninsula is crosscut by three major faults: the Shickshock Sud fault in the north, the Ste-Florence fault and the Grand Pabos fault in the south (Fig. 5.7). Fibres within rocks of the Gaspé Trough and the APA record the complex structural history of the Gaspé Belt which evolved from an essentially pure shortening deformation to a dominantly simple shear deformation within a transpressive setting (Kirkwood et al., 1995). The two major incremental extension directions (early vertical and late horizontal) resulted from a continuous progressive deformation during the Acadian orogeny (Fig. 5.26A, stages I and II). Timing of this deformation event in the Gaspé Peninsula is restricted to the Devonian since the youngest rocks that record this extension history are the Lower Devonian slates of the Fortin Group within the CVGS between the Sainte-Florence and Restigouche faults (Fig. 5.7). The first part of the Acadian progressive deformation is characterized by the sequential development of folds, cleavage and reverse faulting along the Ste-Florence fault (Kirkwood, 1995). Shortening related to the vertical extension during these structural stages accounts for approximately 70% of the total shortening (Kirkwood, 1995). The last part of the progressive deformation within the belt is recorded by fold-axis parallel extension and contributed to further flattening of the folds. This event reflects the strain imposed on the rocks during regional dextral transcurrent shearing along the major strike-slip faults.

Palinspastic reconstruction of the Gaspé Belt basin

Previously, the paleogeographic interpretation of the basin presented many inconsistencies when portrayed on the present geographic map of the Gaspé Peninsula. The palinspastic map presented in Fig. 5.27 is a much more appropriate base map for the basin and allows for a more realistic paleogeographic interpretation for the Gaspé Belt basin (see Bourque et al., 1993; and part 1 of this report by Bourque and Malo). However, we should mention that this restoration does not consider deformation related to the Salinian disturbance and thus is intended to reflect the pre-Middle Devonian geometry of the basin. In order to retrodeform a given area, one must have precise knowledge of the displacement paths imposed during deformation. The kinematic history of the Gaspé Belt determined by the detailed analysis of structural features such as folds, faults and cleavage combined with regional and local finite strain analysis (Kirkwood, 1995) provides us with the sequential development of the structural features in the Gaspé Belt. The chronological development of the Acadian deformation stages during D_R is presented in Fig. 5.26A. The three main Acadian deformation stages are: 1 - layer-parallel shortening followed by folding, cleavage development and reverse faulting, 2 - tightening of folds du to enhanced cleavage development and initiation of strike-slip faulting, and 3 - slip along strike-slip faults (Kirkwood, 1995). Based on these three regional deformation stages, the retrodeformation of rocks of the Gaspé Belt can thus be performed by a step-by-step method such as indicated in Fig. 5.26B (Kirkwood, 1993).

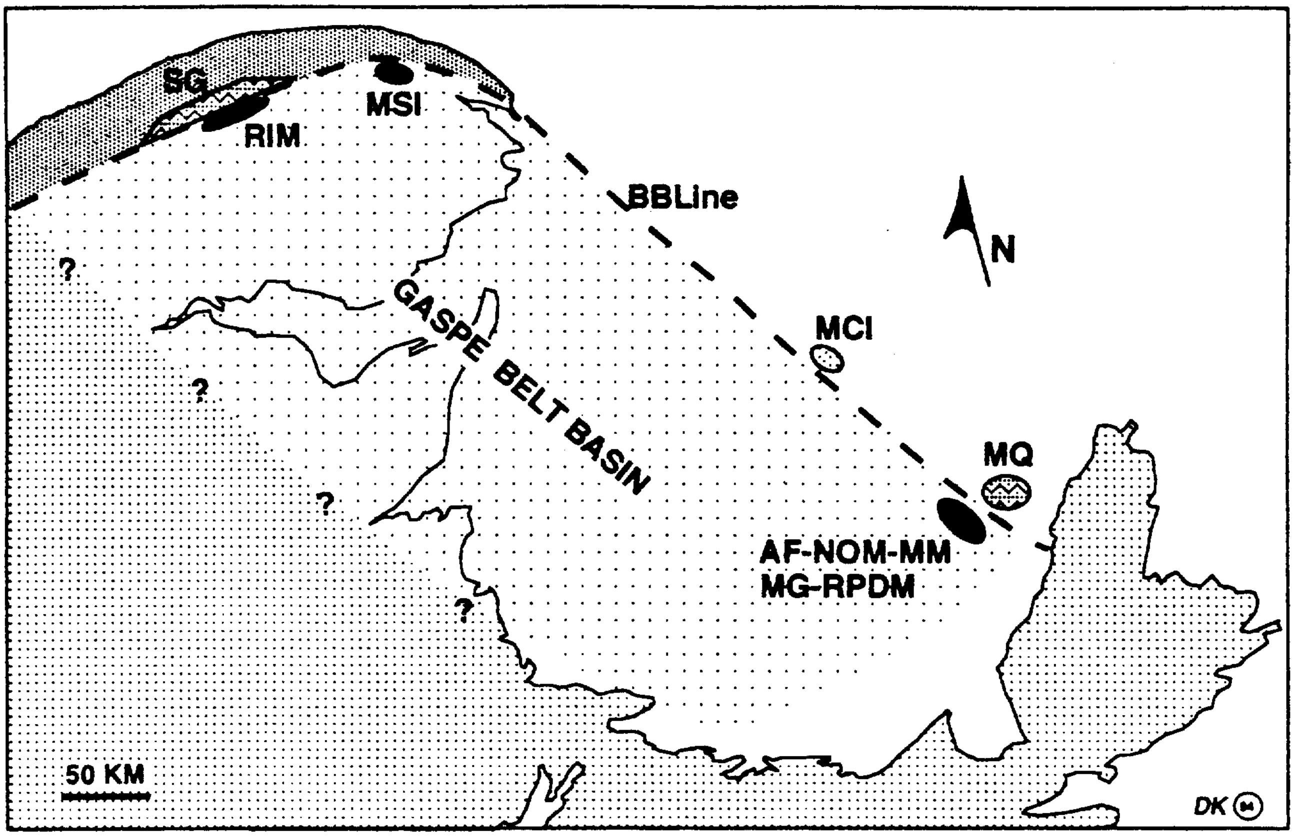

Figure 5.27. Palinspastic reconstruction of the Gaspé belt basin after the three retrodeformation steps using the BBL (Baie Verte-Brompton line) and the approximate location of Cambrian-Ordovician terrains as spatial markers plotted on a present-day geographic map of the Maritimes provinces. AF: Arsenault Formation, CBI: Cape Breton Island, MCI: Murphy Creek inlier, MG: Mictaw Group, MM: McCrea mélange, MQ: Maquereau Group, MSI: Mont Serpentine inlier, NOM: Nadeau ophiolitic Mélange, RPDM: Rivière Port-Daniel Mélange, RIM: Ruisseau Isabelle mélange, SG: Shickshock Group. For patterns see figure 5.34. From Malo and Kirkwood (1996).

Three retrodeformation steps are defined, starting by the restoration of the last deformation stage and working back to the first deformation stage. The first step is to restore the slip along the Acadian strike-slip faults, the second step is to restore the horizontal extension and shortening related to the Acadian regional simple shear event and the third step is to restore the vertical extension (and related Acadian horizontal shortening) by unfolding, removing internal strain associated to cleavage development and restoring slip along the reverse faults.

In southern Gaspé Peninsula, the inferred NW-trending trace of the BBL is cut by the E-trending faults of the Grand Pabos fault system (Fig. 5.6), all of which are Middle Devonian Acadian dextral strike-slip structures (Malo and Béland, 1989). Malo et al. (1992) presented a partial restoration of the Gaspé Belt by removing the apparent known dextral displacements along these faults (Fig. 5.28). Consequently, the BBL was displaced towards the east in order to restore it to its pre-Middle Devonian position (Fig. 5.28). This restoration corresponds to the first step of the retrodeformation of the basin. Details concerning the step-by-step restoration of the Gaspé Belt are presented in Kirkwood (1993, 1994) and only the complete restoration of the Gaspé Belt basin is presented here (Fig. 5.27). This restoration shows the undeformed dimension of the Gaspé Belt basin in pre-Devonian times and the approximate location of Cambrian-Ordovician terranes and the trace of the BBL on a present-day geographic map of the Maritimes (Fig. 5.27). The paleogeographic map clearly shows that the Gaspé Belt basin was much larger than its present size and extended as far as the present-day location of the Cape Breton Island. This restoration gives a more realistic picture of the geometry of the post-Taconian successor basin located in the Québec Reentrant at the southwest margin of the St. Lawrence Promontory than the one reflected by the present-day geological map of this part of the orogen.

5.3.3 UPPER DEVONIAN TO CARBONIFEROUS

Two Upper Devonian rock units occur in the southwestern Gaspé Peninsula, in the Restigouche syncline (Fig. 5.17), the Fleurant and Escuminac formations (Fig. 5.18, locality J), whereas two lithostratigraphic units of Carboniferous age are found along the Chaleurs Bay in Gaspé Peninsula (Fig. 5.7), the Bonaventure and Cannes de Roche formations. The Cannes de Roche is restricted to the northeastern Gaspé Peninsula and is considered to be a lateral equivalent of the Bonaventure (Fig. 5.14). Carboniferous strata of the Chaleurs Bay are part of the Restigouche basin (van de Pool, 1995) which is integrated in the larger Maritimes Basin of the Maritime provinces (Fig. 5.4). Rocks of the Maritime Basin are found in the Gulf of St. Lawrence and crop out in the Gaspé Peninsula, New Brunswick, Nova Scotia, Prince Edward Island and Newfoundland.

Stratigraphy

The Frasnian Fleurant Formation (Alcock, 1935; Dineley and Williams, 1968; Zaitlin and Rust, 1983) lies unconformably upon the Eifelian Pirate Cove Formation (Fig. 5.18). It is a grey, well-rounded pebble and cobble conglomerate, whose clasts are dominantly limestone, with lesser amounts of volcanics and sandstones, and minor plutonic rocks (Rust, 1982). The unit is 18 m

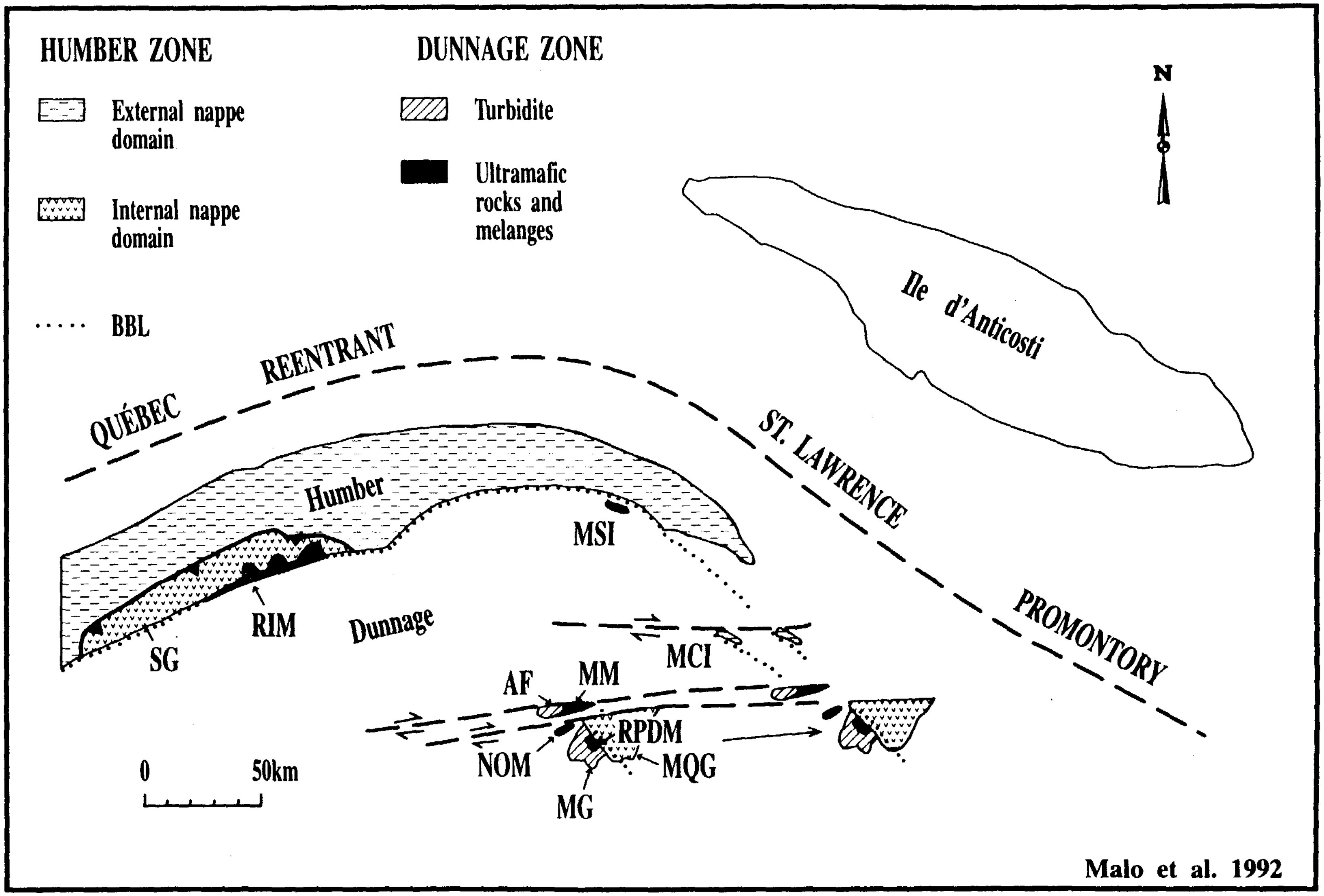

Figure 5.28. Restoration of the Baie-Verte - Brompton Line and Cambro-Ordovician features before Middle Devonian strike-slip faulting in southern Gaspé Peninsula. AF: Arsenault Fm., MG: Mictaw Gr., MM: McRea Mélange, MQG: Maquereau Gr., MCI: Murphy Creek inlier, MSI: Mount Serpentine inlier, NOM: Nadeau ophiolitic Mélange, RIM: Ruisseau Isabelle Mélange, RPDM: Rivière Port-Daniel Mélange, SG: Shickshock Gr. From Malo et al. (1992).

thick and unfossiliferous. The overlying Escuminac Formation rests conformably upon the Fleurant. It consists of greenish grey thin to thick-bedded sandstone, siltstone and laminated shale. Sandstones and siltstones exhibit abundant sole marks, as well as parallel lamination and current ripples. Fossil fishes and plants are common and have been the subject of several paleontological studies.

The Bonaventure Formation consists of coarse clastic red rocks. Conglomerate beds contain boulders up to 50 cm in diameter of heterogeneous lithologies that can be matched with the underlying units of the Gaspé Belt. The Cannes de Roches is comprised also of red conglomerates overlain by a 30 meter thick sequence of red and green sandstones and mudstones, followed by grey conglomerates, sandstones and mudstones (Rust, 1981). The age of the two formations is not precise but believed to be early-Middle Carboniferous (van de Pool, 1995).

Structural geology and structural style

In general, Upper Devonian and Carboniferous rocks of the Chaleurs Bay are horizontal, undisturbed, and not affected by penetrative deformation, although minor normal faults have been observed in the Carleton and Percé areas (Bernard and St-Julien, 1986; Kirkwood, 1989). The Acadian fault system was reactivated in the southern part of the peninsula during post-Carboniferous time, since the Grand Pabos fault offsets Carboniferous strata at its east end (Fig. 5.7). This post-Carboniferous movement, however, is small compared to the 85 km of dextral displacement of pre-Carboniferous rocks to the west (Malo and Béland, 1989).

On air photos, in the Escuminac and Carleton area, we can locally observe ridges of Carboniferous strata that are subvertical. Away from the ridges, where Carboniferous rocks are nearly vertical, strata become horizontal. Bernard and St-Julien (1986) related this tilting of the usually horizontal strata to normal faults; they have estimated a vertical throw of 600 m on one these normal fault in the Carleton area (Fig. 5.29). In the Chandler area, vertical strata of the Bonaventure Formation near the Grand Pabos fault is interpreted to be related to a post-Carboniferous normal movement along the Acadian dextral strike-slip fault. Subvertical strata of the Cannes de Roche and Bonaventure formations in the Percé area (Fig. 5.14) are also interpreted to be related to normal faulting (Kirkwood, 1989).

5.4 TECTONIC EVOLUTION

5.4.1 HUMBER AND DUNNAGE ZONES AND THE TACONIAN OROGENY

The Taconian orogeny is interpreted as a result of a collision between the Early Paleozoic passive continental margin, the Humber Zone, and an outboard microcontinent or continental magmatic arc above an east-dipping subduction zone (St-Julien and Hubert, 1975; Williams, 1979; Stanley and Ratcliffe, 1985; de Broucker, 1987). The Nadeau ophiolitic mélange and the Lady Step complex contains large blocks of metamorphic rocks similar in lithology and age to the Chain Lakes Massif in Maine (Fig. 5.5) which suggests that Chain Lakes Massif-type rock was part of

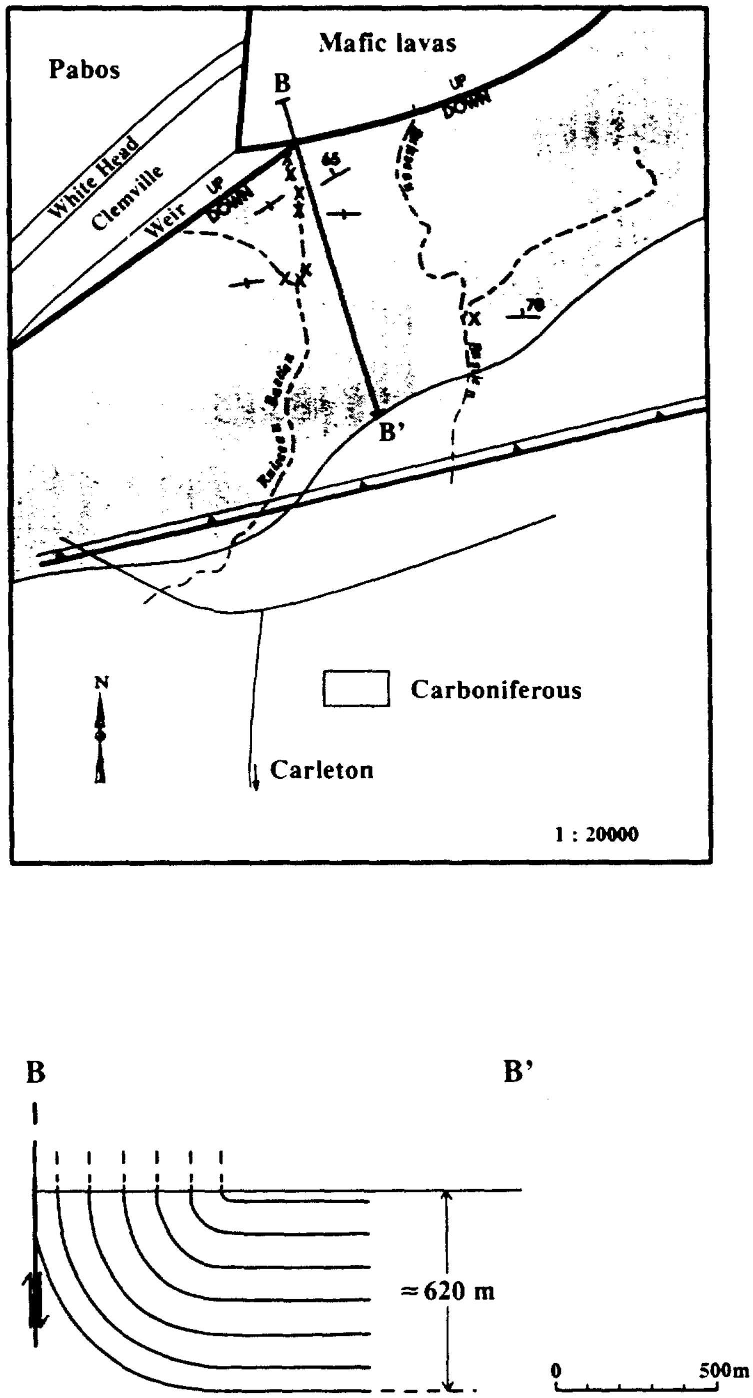

Figure 5.29. Structural cross-section across the Bonaventure ridge in the Carleton area. From Bernard et St-Julien (1986)

the microcontinent or terrane accreted to the North-American miogeocline or Laurentia (De Broucker, 1987).

Rocks of the Shickshock and Trois-Pistoles groups, Orignal, Romieu and Rivière Ouelle formations represent the ancient passive continental margin of North America (Laurentia). They were deposited on the eastern margin of Laurentia, the western side of the Iapetus ocean, from Early Cambrian (Hadrynian?) to Early Ordovician time. Middle to Upper Ordovician rocks of the Tourelle, Des Landes, and Cloridorme formations, as well as those of the Cap-Chat mélange are synorogenic deposits formed in the Taconian foreland region. Middle Ordovician mélange units of the Dunnage Zone (Nadeau ophiolitic mélange, Rivière Port-Daniel, Ruisseau Isabelle and McCrea mélanges, and Lady Step complex) are viewed as part of an accretionary prism over a southeasterly dipping subduction zone under the continental magmatic arc. The Middle Ordovician flyschs (Arsenault, Neckwick, Dubuc formations) and Rivière du Milieu mélange represent synorogenic deposits in the fore-arc basin over the accretionary prism and the subduction through (Fig. 5.30). Peridotites of the Mont Albert and the underlying Amphibolite du Diable are vestiges of the oceanic crust obducted on the continental margin of the Humber Zone.

Early Cambrian
Mafic volcanic rocks of the Shickshock and Maquereau groups, as well as those of the Lac Matapédia facies and of the unité des Pics, are related to the continental break-up of Laurentia in Late Hadrynian to Early Cambrian time (Camiré et al., 1995; Bédard and Wilson, in press). Arkosic sandstones and conglomerates of the Shickshock and Maquereau groups associated with the mafic volcanic rocks were deposited during the rifting stage which created the Iapetus ocean (Fig. 5.30A).

Middle Cambrian to Early Ordovician
The Orignal, Romieu and Rivière Ouelle formations, and the Trois-Pistoles Group are slope and rise deposits which record the development of the passive continental margin from Middle Cambrian to Early Ordovician time (Fig. 5.30B). Mudrocks of the Orignal Formation, mudstones of the Rivière-du-Loup Formation, calcareous shale of the Romieu and mudrocks of the Rivière-Ouelle have been deposited in a deep marine environment. Sandstones of the Saint-Damase and Kamouraska formations are proximal turbidites deposited on the continental slope. The conglomerates limestones of the Rivière Ouelle are found in channels and are associated with proximal limy turbidites (Slivitzky et al., 1991). They originate from a Cambrian - Lower Ordovician platform located to the north during the deposition of the Rivière Ouelle Formation.

Peridotites of the Mont Albert complex is considered to be the remnant of the Iapetus oceanic crust (Fig. 5.30B) (Beaudin, 1984). The Amphibolite du Diable is interpreted as an oceanic basalt that was metamorphosed to amphibolite facies during the obduction of the Mont Albert complex. This obduction is dated at 456 ± 3 Ma (Lux, 1986).

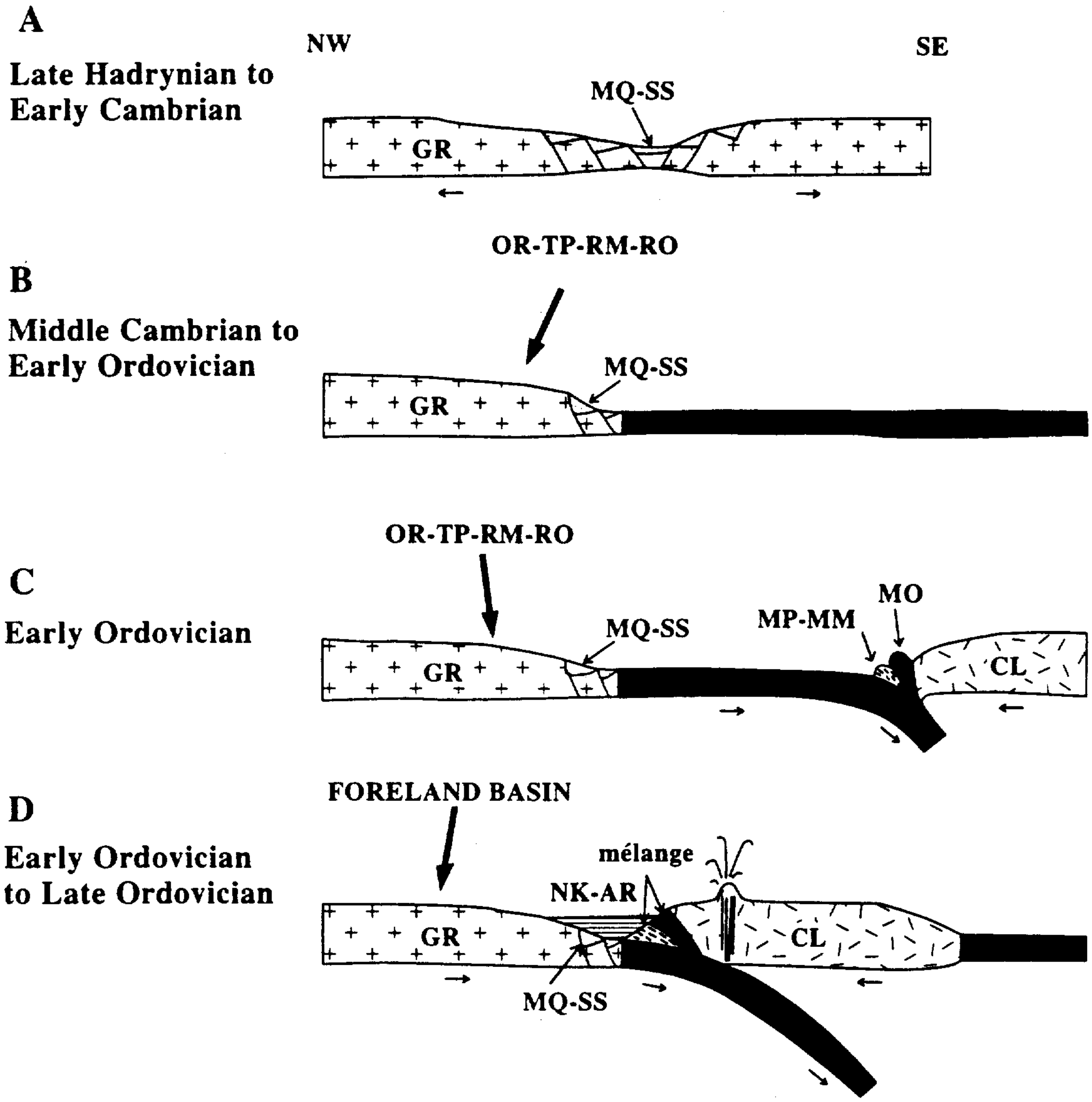

Figure 5.30. Tectonic evolution of the Humber and Dunnage from Cambrian to Late Ordovician time. CL: Chain Lake Massif, GR: Grenville, MP-MM: Rivière Port-Daniel and McRea mélanges, MQ-SS: Maquereau-Shickshock groups, NK-MM: Neckwick-Arsenault formations, OR-TP-RM-RO: Orignal Fm.-Trois-Pistoles Gr.-Romieu Fm.-Rivière-Ouelle Fm., Modified from De Broucker (1987).

South of the Humber Zone, mélanges of the Dunnage Zone were formed in the accretionary prism over the subduction zone in front of the volcanic arc (Fig. 5.30C).

Middle Ordovician to Late Ordovician

The synorogenic Ordovician flyschs of the Tourelle, Des Landes and Cloridorme formations are interpreted to be part of the foreland basin in front of the advancing Taconian thrust sheets (Fig. 5.30D) (Hiscott et al., 1986). The presence of chromite grains and spinels in the sandstones suggests that the obduction of the ultramafic rocks of the oceanic crust started in the early Middle Ordovician. Sandstones of the Tourelle Formation represent mid-fan proximal turbidites (Hiscott, 1980). The Des Landes and Cloridorme are classical turbidites deposited in a more distal environment. They are contemporaneous with the external nappes transport towards the NW (Slivitzky et al., 1991). The Cap-Chat mélange is interpreted as a tectonic olistostromal mélange (Slivitzky et al., 1991).

The development of the foreland basin marks the beginning of the Taconian thrusting in the external nappes domains whereas the Taconian unconformity in the northeastern Gaspé may represent the end of the Taconian tectonism. It is also possible that some deformation occurred in the internal nappes domain (Shickshock and Maquereau groups) in the Late Cambrian to Early Ordovician time (Hibbard et al., 1995).

To the south, in the Dunnage Zone, turbidites were deposited in fore-arc basins of the Dunnage Zone (Arsenault, Neckwick, Dubuc formations) during Middle Ordovician. Following deposition of these flyschs, basin inversion produced an unconformity with a hiatus spanning the Llandeilian to the late Caradocian time (Fig. 5.16). This hiatus might be due to an uplift related to Ordovician tectonic activity in the Dunnage Zone to the south, in New Brunswick (Fig. 5.31A) (van Stall, 1994).

Large gabbroic intrusions in the Rivière Port-Daniel and McCrea mélanges, as well as the gabbroic sills in the Neckwick and Arsenault formations, the Pabos suite of Bédard (1986), are all cogenetic and comagmatic, and bear geochemical characteristics with N-MORB (Bédard 1986). Since these tholeiites intrude the Llanvirnian Neckwick and Arsenault formations and some blocks of these gabbro are found in a conglomerate at the base of the Silurian Chaleurs Group resting unconformably on the Arsenault Formation, they are post-Llanvirnian to pre-Silurian. They suggest a local tensional or rifting event between the Taconian and Acadian orogenies (Bédard 1986). De Broucker (1987) interprets these tholeiites as the product of a tensional event in the fore-arc basin during Middle Ordovician time.

Except the phacoidal cleavage in the matrix of the mélange that can be attributed to Ordovician tectonism in the Dunnage Zone, no evidence of pre-Acadian deformation has survived. The main deformation of the Dunnage Zone in the Mictaw Group, the northeasterly trending structures, folds and associated penetrative cleavage, are related to the Middle Devonian Acadian deformation that affects the Gaspé Belt.

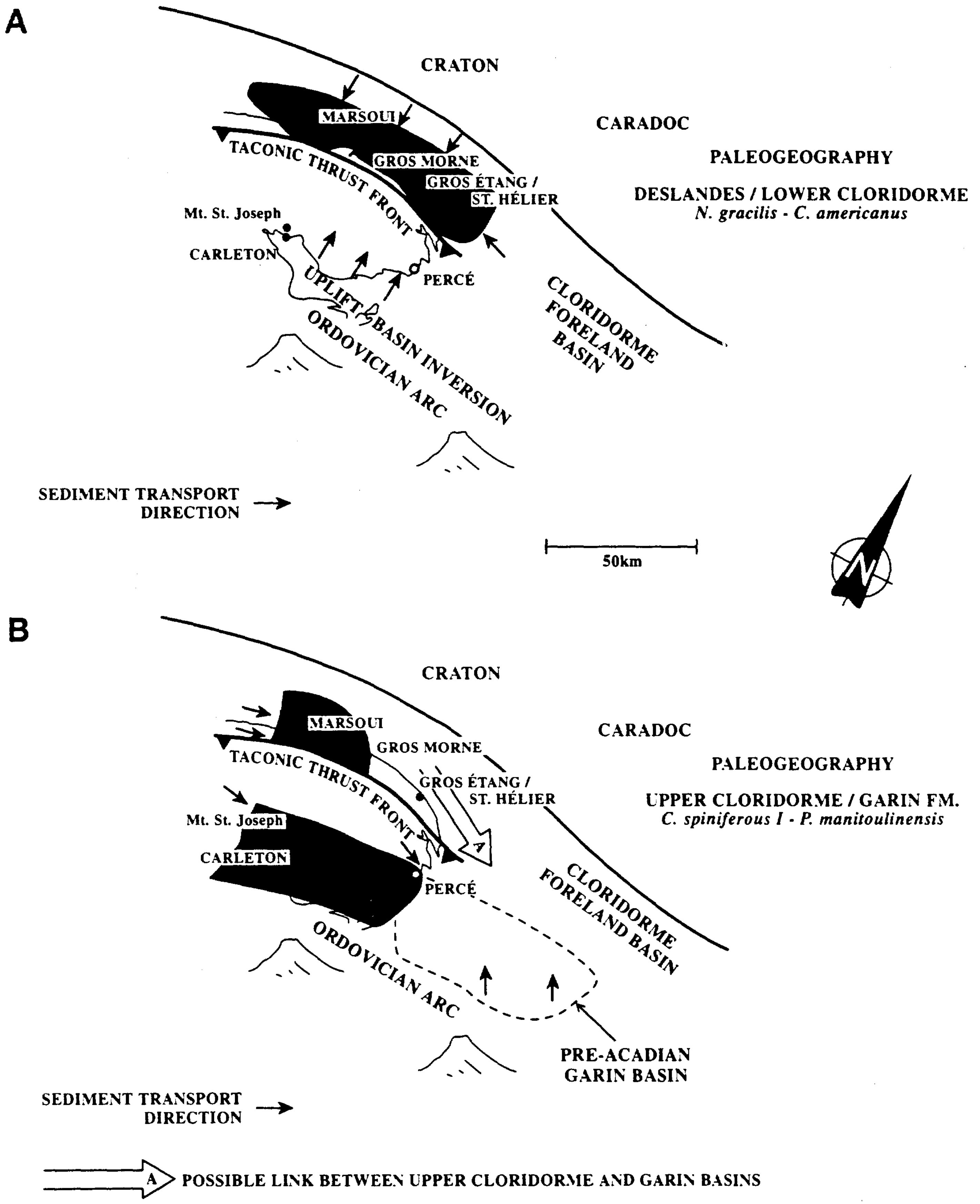

Figure 5.31: A: Tectonic setting of Des Landes and Cloridorme formations in early Caradoc. Gray area denotes inferred extent of foreland basin fill. From Kessler et al. (1996). B: Tectonic setting of upper Cloridorme and Garin formations in late Caradoc. Gray area denotes inferred extent of the two basins fill. From Kessler et al. (1996).

In Late Caradocian time, the final stage of filling of the Taconian foreland basin is represented by the upper Cloridorme Formation in the Humber Zone. In the same time, the sedimentation of the Garin Formation (Honorat Group) of the Gaspé Belt basin was initiated, to the south, over rocks of the Dunnage Zone (Fig. 5.31B). Similarities in graptolite zonation, provenance setting, and sediment transport direction suggest the upper Cloridorme and Garin formations were deposited in the same or adjacent flysch basins (Fig. 5.31B) (Kessler et al., 1995). On a more regional pre-Devonian palinspastic map, it is noteworthy that the northeastern part of the actual Gaspé Peninsula was a region of flysch sedimentation during the *C. spiniferus* time (Fig. 5.32). Distal turbidites and black shales were deposited in the Taconian foreland basin (upper Cloridorme Formation), in the successor Gaspé Belt basin (Garin Formation) and also on the platform in the Anticosti Island area (Macasty Formation).

5.4.2 GASPÉ BELT: THE SALINIAN DISTURBANCE AND THE ACADIAN OROGENY

Three distinctive unconformities occur in the sequence of the Gaspé Belt (Fig. 5.33). The oldest unconformity at the base of the sequence is the Taconian unconformity in northern Gaspé, where rocks of the Gaspé Belt overly those of the Humber Zone, and an Ordovician hiatus or unconformity in southern Gaspé, where rocks of the Gaspé Belt overly those of the Dunnage Zone (Fig. 5.7). The second unconformity, located within the Chaleurs Group, is dated as Late Ludlovian-Early Pridolian, and corresponds to the Salinian disturbance. The third unconformity is angular and occurs between Middle or Late Devonian and Carboniferous rocks. It corresponds to the Acadian orogeny. Major regression-transgression cycles in the Gaspé Belt occurred more or less in response to the three tectonic pulses recorded by the unconformities, the Taconian orogeny, the Salinian disturbance and the Acadian orogeny. Fig. 5.33 shows the main tectonic events with respect to sedimentary evolution of the Gaspé Belt. Shallowing phase I corresponds to infilling of the successor basin left after the Taconian orogeny, whereas shallowing phase II culminated with the Salinian disturbance. Shallowing phase III is a response to general uplifting of the basin that preceded the main Acadian deformation.

Since the paleogeographic evolution based on facies distribution of the Gaspé Belt basin is discussed in the first part of this report by Bourque and Malo, the tectonic evolution of the Gaspé Belt will be discuss according to the faulting and progressive deformation histories. The palinspastic geometry of the Gaspé Belt basin (Fig. 5.27) will be used to summarize our observations concerning the movement history along the major faults of the Gaspé Peninsula.

Pre-Silurian Time: Taconian-Related Structures

The complex faulting history within the Shickshock-Sud, Port-Daniel and Bassin Nord-Ouest fault zones, which are parallel to the trace of the BBL (Fig. 5.6), reveals that a first episode of faulting involved ductile deformation in pre-Silurian time. Cambrian rocks of the internal nappe domain of the Humber Zone along the Shickshock-Sud fault record oblique motion (thrusting to strike-slip) (Fig. 5.34A). Subhorizontal lineations in the Cambro-Ordovician rocks of the Dunnage Zone within the Mont Serpentine inlier, along the Bassin Nord-Ouest fault, indicate

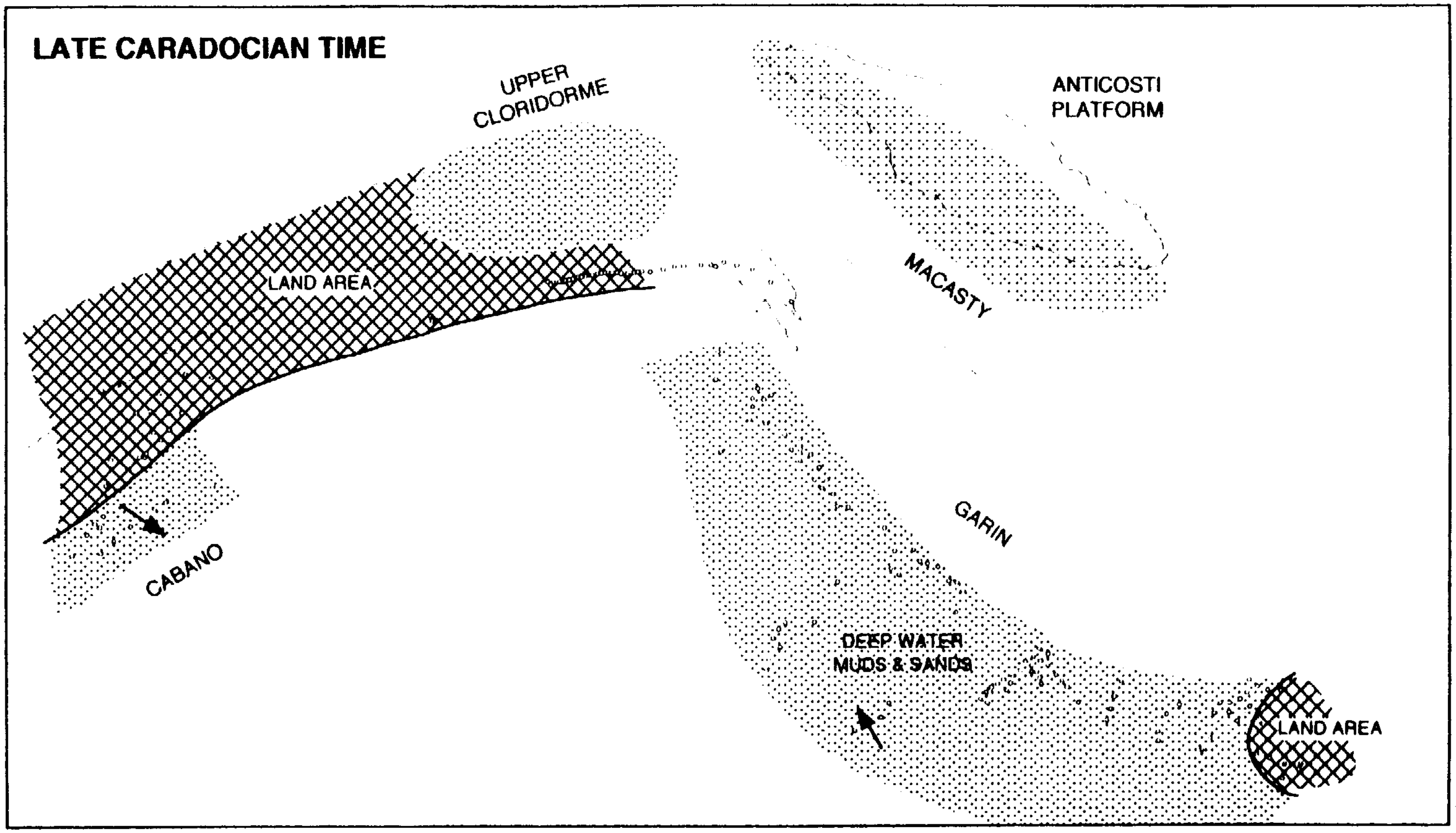

Figure 5.32. Paleogeography of the Gaspé Peninsula during the Late Ordovician time (*C. spiniferus* zone) showing deposition of tubidites and black shale facies. Modified from Bourque et al. (submitted, 1996).

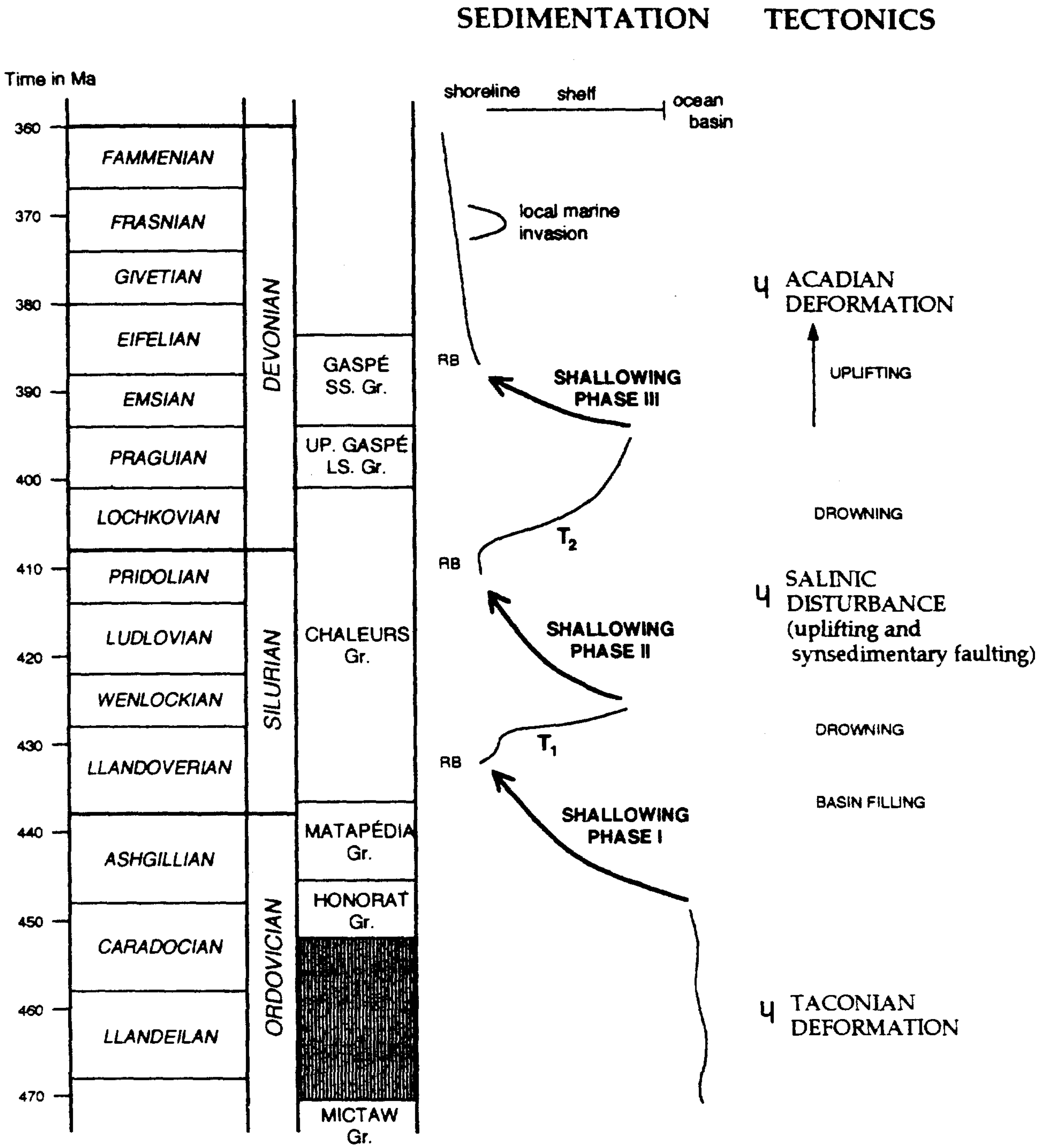

Figure 5.33. Summary of sedimentary and tectonic evolution of Middle Ordovician to Late Devonian sequence of Gaspé Belt in Gaspé Peninsula, Québec Appalachians. T1 and T2 are transgression phases. RB indicates occurrence of red beds. Minor local marine invasion occurred during Frasnian time. From Malo and Bourque (1993).

strike-slip motion and Cambrian rocks of the internal nappe domain of the Humber Zone in the Rivière Port-Daniel fault zone also record horizontal dextral movement (Fig. 5.34A) occurring during the Late Cambrian and Middle Ordovician time interval (De Broucker, 1987). Adding this information to the pre-Devonian palinspastic map shows that dextral strike-slip faulting occurred along the St. Lawrence Promontory parallel to the BBL, whereas a combined dextral strike-slip and NW-directed thrust motion occurred along the Shickshock-Sud fault in northern Gaspé Peninsula. Because these ductile deformation features are only recorded in Cambrian-Ordovician rocks, we attribute this pre-Silurian motion along the BBL to accretionary processes related to the extrusion of rocks of the northern Appalachians in the Québec Reentrant during the Taconian orogeny (Fig. 5.34A). The fault zone parallel to the St. Lawrence Promontory which was active during the opening of the Iapetus ocean in Late Precambrian to Early Cambrian time (Thomas, 1977) was first reactivated during the collision of outboard terranes in Ordovician time.

Late Silurian-Early Devonian Time: Salinian Disturbance
During the sedimentation of the Gaspé Belt, brittle extensional faulting occurred parallel to the St. Lawrence Promontory in northeastern Gaspé Peninsula (Fig. 5.34B). Sedimentological analysis of the Gaspé Belt rocks in the northeastern part of the Gaspé Peninsula and seismic refection data (Roksandic and Granger, 1981) suggest that the Bassin Nord-Ouest and Troisième Lac faults were active as normal faults during the Late Silurian to Early Devonian sedimentation. The Late Silurian-Early Devonian time interval corresponds to the Salinian unconformity well recorded in the Gaspé Belt basin (Bourque et al., 1995, 1993; Malo and Bourque, 1993), the unconformity resulting from the episode of synsedimentary faulting. The NW-trending F_E folds are spatially associated to the NW-trending faults (Figs. 5.7 and 34B; southwest of the Bassin Nord-Ouest fault in the CVGS, and the Percé and Carleton areas in the APA) (Kirkwood, 1989; Simard, 1986). On the pre-Devonian palinspastic map (Fig. 5.34B), the F_E folds are located mainly in the eastern part of the Gaspé Belt basin along the St. Lawrence Promontory. They are interpreted as extensional forced folds (Withjack et al., 1990) which formed over faulted blocks delineated by Late Silurian-Early Devonian extensional faults. Late Silurian extensional faults are also recognized at the margin of the basin in the Témiscouata area, west of the Gaspé Peninsula (Bourque et al., 1993). It should be pointed out that volcanism also occurred during the Late Silurian-Early Devonian time interval in the Gaspé Belt basin consisting of within-plate continental tholeiitic basalts, alkali basalts and andesites (Laurent and Bélanger, 1984; Bédard, 1986; Doyon, 1992; Dostal et al., 1993; Doyon and Dalpé, 1993). Doyon (1992) and Dostal et al. (1993) associated this period of volcanism to rifting related to the collision of Gondwana-related terranes (Avalon) to Laurentia. All these events suggest that the Late Silurian to Early Devonian period corresponded to an episode of regional extension in the Gaspé Peninsula. Extensional phases are well documented in many other compressional orogens (Malavieille, 1987; Dewey, 1988; Platt and Vissers, 1989; Carmignani and Kligfield, 1990) and can be related to extensional collapse of the orogen induced by excessive topographic elevation, as recently postulated for the northern New Brunswick part of the Appalachian orogen by de Roo and van Staal (1994). Extension can also be locally manifested in the Québec Reentrant by rifting parallel to the St. Lawrence Promontory at the onset of orogen-scale transcurrent motion between

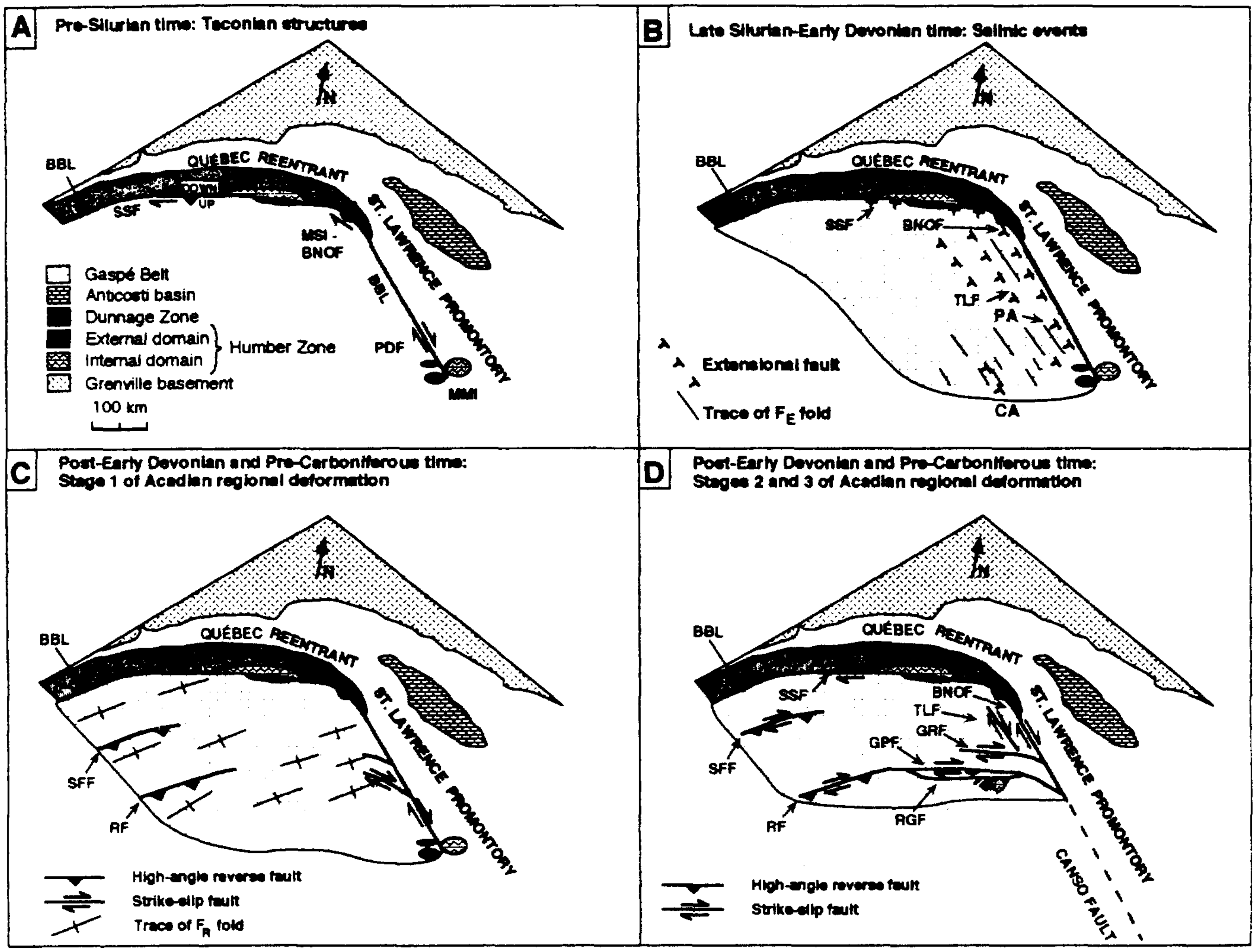

Figure 5.34. Chronological tectonic evolution of mid-Paleozoic deformation events in the Gaspé Appalachians. A: Pre-Silurian time: ductile faulting along the BBL. B: Late Silurian-Early Devonian time: brittle extensional faulting in northeastern part of the Gaspé belt basin. C: Post-Early Devonian and pre-Carboniferous time - Stage 1 of DR : Initiation of major faults at depth and ductile faulting contemporaneous with development of regional NE-trending FR folds in the sedimentary cover rocks of the Gaspé belt. D: Post-Early Devonian and pre-Carboniferous time - Stages 2 and 3 of DR : Brittle-ductile strike-slip faulting and slip along major strike-slip faults. BBL: Baie Verte-Brompton Line, BNOF; Bras Nord-Ouest fault, CA: Carleton area, GPF: Grand Pabos fault, GRF: Grande Rivière fault, MMI: Maquereau-Mictaw inlier, PA: Percé area, PDF: Port-Daniel fault, RF: Restigouche fault, RGF: Rivière Garin fault, MSI: Mont Serpentine inlier, SFF: Sainte-Florence fault, SSF: Shickshock-Sud fault, TLF: Troisième Lac fault. From Malo and Krkwood (1996).

Gondwana-related terranes (Avalon) and Laurentia as recently proposed by Keppie and Dostal (1994). Thermal uplift during rifting may have caused stretching of the crust, intraplate volcanism and synsedimentary blocks faulting. However, dextral transpression is only recorded during the Early to Middle Devonian throughout the northern Appalachians (Hibbard, 1994) while volcanism in the Québec Reentrant began earlier during the Silurian. Alternatively, extensional faults such as those developed during the Late Silurian-Early Devonian time interval in the Gaspé Peninsula, could also have formed at the margin of the basin during subsidence due to the weight of onlapping nappes further south. Late Silurian to Early Devonian overthrusting has been documented by van Staal and de Roo (1996) in New Brunswick, Lin and others (1994) in Cape Breton, and Cawood (1993) and Stockmal and Waldron (1993) in Newfoundland. In northern New Brunswick, overthrusting was followed by extensional collapse which might have help to induce extension in the Gaspé Belt basin farther north.

Post-Early Devonian and Pre-Carboniferous Time: Acadian Orogeny

The Acadian progressive deformation history (D_R) is separated into three deformation stages which define the sequential development of structural features (Fig. 5.26). During the first stage (Fig. 5.34C), layer-parallel shortening was followed by folding and cleavage development. Reverse motion along the Ste-Florence fault, and possibly along other fold-parallel reverse faults, is also related to this first deformation stage which is characterized by vertical extension (Fig. 5.34C). Continued shortening was accommodated by further development of cleavage resulting in tightening of pre-existing folds. During this second stage (Fig. 5.34D), the incremental extension direction abruptly changed from subvertical to subhorizontal and reflecting the dominance of the simple shear component over the pure shear component in the bulk transpressive regime affecting this part of the northern Appalachians. The last deformation stage is characterized by the development of the strike-slip fault systems in the cover rocks which crosscut the previously formed structures (Fig. 5.34D).

Post-Early Devonian strike-slip motion along the Grand Pabos fault system (Grande Rivière, Grand Pabos, Rivière Garin faults) is characterized by the development of plastic and brittle-ductile to brittle structures (Malo and Béland, 1989). Structural analysis of these fault zones indicates that the ductile part of the deformation was followed by the development of brittle-ductile and brittle structures (Kirkwood and Malo, 1993). Both ductile and brittle-ductile deformation features along the E-trending faults of the Grand Pabos fault system were initiated during post-Early Devonian time and are related to the same regional dextral strike-slip motion (Fig. 5.34D). The Sainte-Florence fault also shows evidence of brittle deformation superimposed on earlier ductile deformation. As for the Grand Pabos fault system, ductile and brittle deformations are post-Early Devonian, although the early ductile deformation is related to a reverse motion along the fault whereas the late brittle deformation features indicate a dextral strike-slip motion (Figs. 5.34C, 5.34D).

Brittle structures within the NW-trending Troisième Lac and Bassin Nord-Ouest faults indicate dextral movement with a slight vertical component during Middle to Late Devonian time

(Kirkwood, 1989; Berger and Ramsay, 1993). Post-Early Devonian dextral motion is also recorded along the Shickshock-Sud fault and is characterized by the development of brittle-ductile shear zones (Berger, 1985; Lebel, 1985). Structural evidence from the Shickshock-Sud fault zone does not shed any light on its interplay with other post-Early Devonian faults in northeastern and southern Gaspé Peninsula. However, the development of essentially brittle-ductile structures along the Shickshock-Sud fault in post-Early Devonian time seems to be contemporaneous with brittle-ductile movement along the Grand Pabos fault system in southern Gaspé Peninsula, the Sainte-Florence fault in western Gaspé Peninsula, and the Troisième Lac and Bassin Nord-Ouest faults in northeastern Gaspé Peninsula (Fig. 5.34D). Structural relationships in the Percé area suggest that dextral motion along the Troisième Lac fault persisted for a longer period of time in northeastern Gaspé Peninsula since faults parallel to the Troisième Lac fault offset the E-trending Grande Rivière fault (Kirkwood, 1989).

Discussion on the Salinian disturbance and the Acadian orogeny

The Devonian Acadian orogeny is the most widespread orogenic event in the northern Appalachians (Roy and Skehan, 1993; Williams, 1993). The docking of the Avalon terrane is generally viewed as the cause of the Devonian Acadian orogeny throughout the northern Appalachians (Bradley, 1983; Williams and Hatcher, 1983; Osberg et al., 1989). In a Paleozoic plate tectonic scenario, the Acadian orogeny corresponds to the collision of the Appalachian margin of Laurentia with Gondwana and the peri-Gondwanide terranes, including the Avalon terrane (Van der Voo, 1988). The geological record of peri-Gondwanide terranes, which is well preserved in the Central Mobile Belt of the northern Appalachians (van der Pluijm and van Staal, 1988), shows a complex tectonic history of accretion during the Late Ordovician and Silurian (van Staal, 1994). A two-phase scenario has been proposed for the Acadian orogeny (Cawood, 1993; Williams, 1993; Hibbard, 1994). These authors argue that both phases form a chronologically continuous deformation scheme spanning from the Late Silurian to the Middle Devonian. Conversely, some workers have separated the tectonic pulses into two distinct orogenic phases, thereby introducing the Late Silurian Salinian orogeny (Dunning et al., 1990; Lin et al., 1994; van Staal and de Roo, 1996). Nevertheless, these two phases are also recognized in the Gaspé part of the orogen and are recorded as a first phase of extensional faulting, minor folding and a resulting unconformity clearly dated as Late Silurian followed by a second phase of dextral transpression during the Middle Devonian. Stratigraphic analysis shows that the first phase is followed by a transgressive episode (T2 on Fig. 5.33) and a successive shallowing-upward phase (phase III on Fig. 5.33) leading into the second Middle Devonian deformation phase, with 20 to 25 million years separating the two pulses (Malo and Bourque, 1993).

During the Devonian continental collision, the St. Lawrence Promontory acted as an indentor on Gondwana-related terranes. The continental convergence created large-scale dextral shearing within Gondwana-related terranes, parallel to the southwestern wall of the St. Lawrence Promontory along the Canso fault (Stockmal et al., 1987) and brought about lateral extrusion or tectonic escape of these outboard terranes into the Québec Reentrant. The NW-directed motion of advancing Gondwana-related terranes closed the Gaspé Belt basin while lithospheric delamination apparently occurred at the St. Lawrence Promontory in Newfoundland (Stockmal et al., 1987; 1990). The inherited geometry of the Appalachian margin of Laurentia caused suborthogonal convergence in southern Québec which induced major thrusting, and oblique convergence in the Gaspé Peninsula resulting in strike-slip faulting and transpression.

Analysis of Acadian structures in the Québec Appalachians suggests a NW-SE directed principal shortening axis. The NE-trending F_R folds and regional cleavage formed in the supracrustal rocks during initial closure of the Gaspé Belt basin, in response to convergence between Laurentia and Gondwana (Fig. 5.35A). Although the exact relative motion between the plates is unknown, the geometry of the southern limit of Laurentia suggests that, for a NW-directed convergence, the relative movement between Laurentia and Gondwana was predominantly transcurrent along the edge of the St. Lawrence Promontory and parallel to the Canso fault, oblique in southern Gaspé Peninsula and progressively more orthogonal southwestward in southern Québec (Fig. 5.35A). Folding preceded faulting in the Gaspé (Fig. 5.35A) which is to be expected in strike-slip terranes (Wilcox et al., 1973). Major dextral strike-slip faults probably formed later when Gondwana-related terranes collided with Laurentia (Fig. 5.35B).

The Acadian faulting and penetrative deformation in the Gaspé Peninsula represent the supracrustal manifestation in the external zone of a continental collision (Laurentia and Gondwana) which took place further southeast. The development of strike-slip faults and the transpressive deformation in the Gaspé Peninsula indicates that the collision was oblique in this part of the Québec Reentrant where large-scale lateral displacements affected the supracrustal sequence (Humber and Dunnage Zones, and Gaspé Belt) (Malo and Béland, 1989; Malo et al., 1992). Seemingly however, this part of the orogen did not close until the Early Devonian because rocks deposited within the post-Taconian successor basin covering the Quebec reentrant were undeformed prior to the Early Devonian (excluding the minor folding (F_E) related to the Salinian disturbance), a hypothesis strongly supported by the palinspastic geometry of the Gaspé Belt basin shown on Fig. 5.28. The approach of the Acadian hinterland recorded by the rising of mountainous terrains immediately south of the Gaspé Belt basin is documented by the sedimentation of Middle Devonian molasse-type deposits (Malbaie Formation) in the southern part of the basin (Rust, 1981). The sedimentological record also shows that development of newly uplifted terrains proceeded towards the W-NW. Miramichi terrain (hinterland) most probably progressed northwestward within the Québec Reentrant, parallel to the St. Lawrence Promontory, and was extruded laterally towards the west along major dextral strike-slip faults such as the Rocky Brook Millstream and Catamaran faults.

Taconian ductile strike-slip and oblique-slip faults, the Late Silurian-Early Devonian tectonic activity (NW-trending F_E folding, Salinian unconformity, NW-trending synsedimentary faults, intraplate volcanism) and large-scale dextral Acadian strike-slip faults are not recognized in the southern part of the Québec Appalachians (St-Julien and Hubert, 1975), where major Taconian and Acadian deformation features are thrust faults related to a global NW tectonic transport (Tremblay and Pinet, 1994). The mid-Paleozoic tectonic events particular to the northeastern part

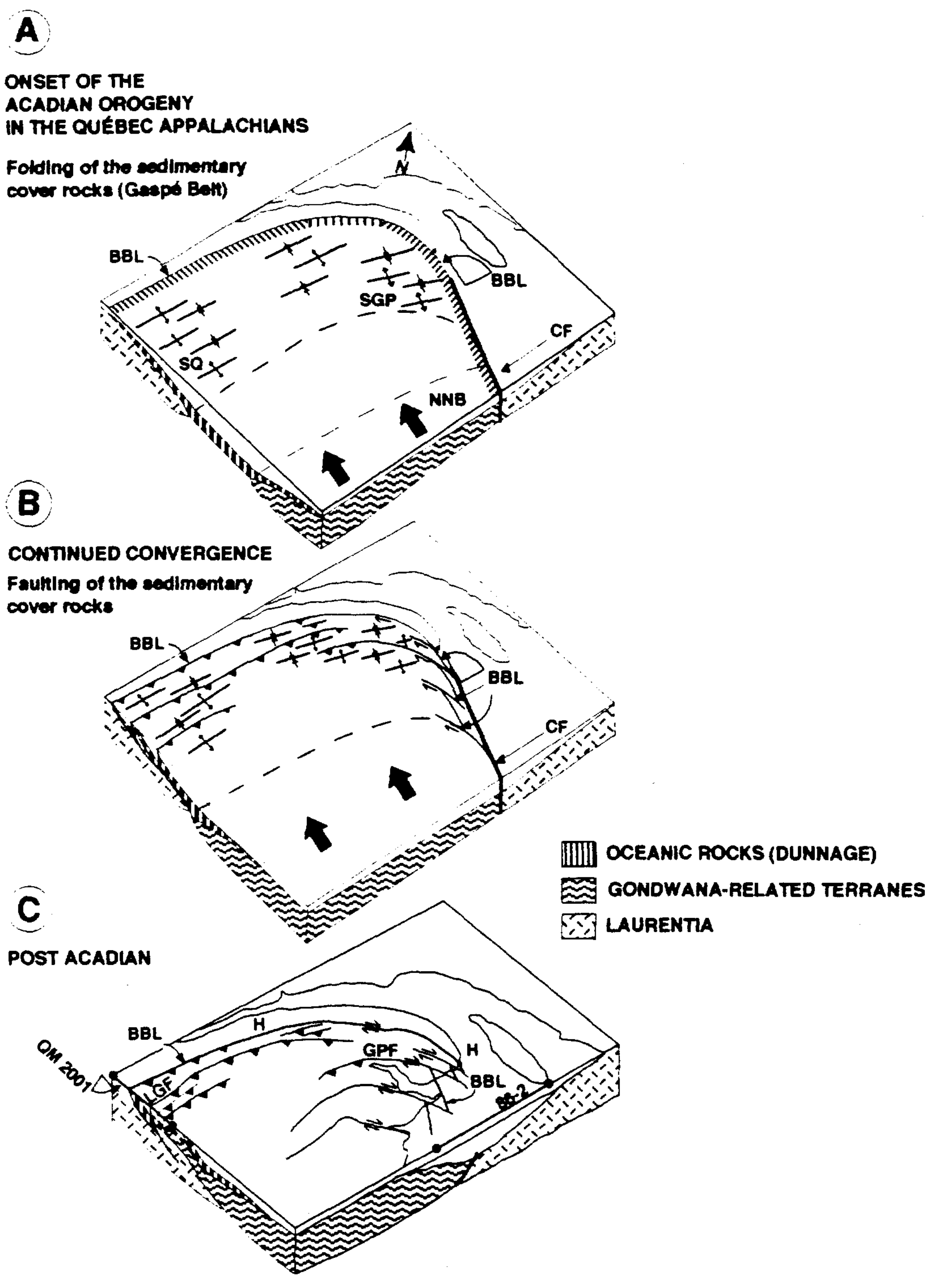

Figure 5.35. Structural evolution of the external zone of the Acadian orogen in the Québec Appalachians. Taconian deformation in the Québec Appalachians and deformation features in the supracrustal rocks over the composite Central/Avalon are not shown. H: Humber Zone, GPF: Grand Pabos fault, LGF: La Guadeloupe fault, NNB: northern New Brunswick, QM 2001-Québe-Maine seismic line, SGP: southern Gaspé Peninsula, SQ: southern Québec, 86-2: marine seismic line.

of the Québec Reentrant and well documented in the Gaspé Peninsula, are recorded in rocks located close to the NW-trending margin of St. Lawrence Promontory, within one of the most important reentrants in the Appalachians mountain belt (Thomas, 1977). As suggested by others (Stockmal et al., 1987; Stockmal et al., 1990; Keppie and Dostal, 1994; van Staal, 1994), the irregular geometry of the collision zone has played a local, but significant role in the kinematics of mid-Paleozoic deformation in the Gaspé Peninsula. This is reflected by the limited effect of the Salinian disturbance on rocks of the Gaspé Belt basin which were more or less sheltered from intense deformation by their position deep within the Québec Reentrant. The Salinian disturbance, which is manifested by the development of folds, cleavage, faults and ductile shear zones in Maine, New Brunswick, Nova Scotia and Newfoundland, has produced only a minor episode of folding and extensional faulting in the Gaspé Peninsula. The size and extent of the undeformed Gaspé Belt basin also suggests that the locus of intense Salinian deformation must have been located much farther southeast.

5.4.3 Post-Carboniferous time - Alleghanian Related-Faults

In the Chandler area, the Grand Pabos fault affect the Bonaventure Formation indicating that the Acadian fault system was reactivated in southern Gaspé Peninsula. Other minor faults recognized in the Carboniferous rocks can be interpreted as normal. This normal faulting is probably related to the formation of the Carboniferous Maritimes Basin. Striations on fault planes indicate that the fault have experienced more than one movement. The paleostress analysis using striated Carboniferous fault planes along the Chaleurs Bay shows that the Bonaventure Formation have experienced horizontal compression that can be related to the Alleghanian orogeny (Faure, 1995).

5.5 Recommendation for Future Works

5.5.1 Phase 2 (December 1, 1996)

1- Initiation of detailed field work to study fracture enhancement of porosity and permeability in the limestone units.

2- Re-interpretation of structural cross-sections in NE Gaspé made by McGerrigle (1950) in the light of the new geological map of Brisebois et al (1991) and new idea on tectonic evolution of this part of the Gaspé Peninsula.

5.5.2 Next Year

1 - Salinian and Acadian structural style in NE Gaspé

This project deals with structural geology of the northeastern Gaspé Peninsula with a focus on regional Salinian folding and faulting. Particular attention will be focused on the structural features related to the development of the Salinian disturbance.

In part 1 of this report, we have shown that extensional faulting played a major role for reef settlement and development. Our model of block faulting suggests a domino-style of extension and illustrates only the upper part of such a system. With the seismic data available, we do not have any constraints to see if the near-vertical fault merge at depth with a major subhorizontal (listric) detachment dipping to the SW. Our figure 1.17 also shows that the southwestern side of Bassin Nord-Ouest, Troisième Lac and Gastonguay faults dropped down which is in good agreement with a domino-style of faulting, but we cannot rule out that other type of extension such as hort and grabben may have been active during Late Silurian-Early Devonian time in NE Gaspé. However, a late inversion is needed in order to explain the actual geometry of stratigraphic units along the Bassin Nord-Ouest fault. Older rocks of the Indian Cove, York Lake and York River formations, on the SW side of the fault, as opposed to the younger Battery Point Formation, on the NE side, suggest a reverse motion to the NE. We also know that mesoscopic structural elements, particularly those related to faulting (vein, fracture, etc), as well as the map pattern, suggest a dextral strike-slip motion for the Bassin Nord-Ouest and Troisième Lac faults (Béland, 1980; Berger and Ramsay, 1993). Tectonic evolution of the NE Gaspé is very complex and need to be re-evaluated according to new concepts on faulting history of this part of the Québec Appalachians.

Questions to address

- If NW-trending folds of the Gaspé Belt are related to normal faulting, what is the nature of these NW-trending longitudinal folds; are they drag folds, reverse-drag folds or rollover folds (Schlische, 1995)?

- What is the mode of extension during the Salinian normal faulting, domino-style extensional faulting over a listric normal fault or a horst and grabben type of extension? Did the extensional faulting create fault traps?

- With the exception of regional NW-trending faults and longitudinal folds, do we find other structural elements that can be ascribed to Salinian deformation? If yes, what is the influence of Salinian fracturing on the development of the porosity and permeability?

- Can we apply the strike-slip tectonics model of southern Gaspé to northeastern Gaspé Peninsula?

- What is the relationship between E-trending and NW-trending folds?

- The extensional Late Silurian-Early Devonian Gaspé Belt basin was inverted by a Acadian transpression in northeastern Gaspé Peninsula. Basin inversion can cause remigration of hydrocarbons, and it can also create structural traps. What are the implications of this Acadian tectonic inversion for petroleum exploration?

2- Fracture enhancement of porosity and permeability in the Silurian and Devonian section of NE Gaspé

The principle objective of this project is to focus attention on the brittle structures, i.e. the faults and related shear-fractures, genetically related to the two major tectonic events that affected the Silurian-Devonian section of NE Gaspé, the Salinian Disturbance and the Acadian Orogeny. Such structures might have contributed significantly to the porosity and permeability of the rocks, i.e., to the development of conduits and of petroleum reservoirs in NE Gaspé. Isotope geochemistry and fluid inclusion microthermometry of vein material will characterize fluids associated to the main tectonic events, and ultimately will allow parentage with main diagenetic phases.

Questions to address

- Can we determine the genetic link of fracture sets with geological events such as early overpressuring within the basin, Salinian extension and/or Acadian compression?

- Are the fractures within the Silurian-Devonian section important positive contributors to the reservoir storage capacity or permeability?

- Did fracture development enhance the porosity of reservoir rocks and rock permeability in specific carrier beds?

- Can we characterize the chemistry of the fluids that circulated within the fractures and establish a time-integrated model of fluid flow within the Silurian-Devonian section?

- Did oil-rich fluids migrate along the fractures and if so when did they circulate?

References

Alcock, F.J., 1935, Geology of Chaleurs Bay region. Geological Survey of Canada Memoir 183,146 p.

Amyot, G., 1984, Lithostratigraphie de sous-surface de l'est de la Gaspésie. Ministère de l'Énergie et des Ressources du Québec, ET 83-11, 75 p.

Armstrong, T.R., Tracy, R.J., and Hames, W.E., 1992. Contrasting styles of Taconian, Eastern Acadian and Western Acadian metamorphism, central and western New England. Journal of Metamorphic Geology, **10**, 415-426.

Beaudin, J., 1980, Région du Mont-Albert et du Lac Matapédia. Ministère de l'Énergie et des Ressources du Québec, Rapport intérimaire DPV-705, 83 p.

Beaudin, J., 1984. Analyse structurale du Groupe de Shickshock et de la péridotite du mont Albert, Gaspésie. Ph.D. thesis, Université Laval, 241 p.

Bédard, J.H., 1986, Pre-Acadian magmatic suites of the southeastern Gaspé Peninsula. Geological Society of America Bulletin, **97**, 1177-1191.

Bédard, J.H., and Wilson, C., (in press). Fractionation and contamination fo Maquereau Group lavas, southern Gaspé, Québec Appalachians. In The nature of magmatism in the Appalachians orogen, ed. A.K. Sinha. Geological Society of America Memoir.

Béland, J., 1958, Oak Bay map-area: Québec, Department of Mines, Preliminary Report 375, 12 p.

Béland, J., 1980, Faille du Bassin Nord-Ouest et faille du Troisième Lac dans la partie est de la Gaspésie. Ministère de l'Energie et des Ressources du Québec, Rapport intérimaire DP-740, 20 p.

Bélanger, J., 1982, Roches volcaniques dévoniennes de la bande de Restigouche. Ministère de l'Energie et des Ressources du Québec, Rapport intérimaire DP-939, 13 p.

Berger, J., 1985, Analyse structurale de la faille Shickshock-Sud en Gaspésie occidentale, Québec. M.Sc. memoir, Montréal, Université de Montréal, 29 p.

Berger, J., 1993, Étude structurale et gîtologique de la faille de Sainte-Florence, Gaspésie. Ministère de l'Énergie et des Ressources du Québec, Rapport final MB 93-01, 48 p.

Berger, J., and Ramsay, E., 1993, Etude structurale et pétrologique de la région du mont de la Serpentine. Ministère de l'Énergie et des Ressources du Québec, Rapport final MB 93-22, 44 p.

Bernard, D., and St-Julien, P., 1986, Analyse structurale du Silurian-Dévonien du centre de la Gaspésie et du Carbonifère du sud et de l'est de la Gaspésie. Ministère de l'Énergie et des Ressources du Québec, Rapport intérimaire MB 86-36, 33 p.

Bertrand, R., 1987, Maturation thermique et potentiel pétroligène des séries post-taconiennes du nord-est de la Gaspésie et de l'Île d'Anticosti. D.Sc. thesis, Université de Neufchâtel, Suisse, 647 p.

Boucot, A.J., 1962, Appalachian Silurian-Devonian, *in* Coe, K., ed., Some aspects of the Variscan fold belt. Manchester University Press, Manchester, 155-163.

Boucot, A.J., 1970. Devonian slate problems in the Northern Appalachians. Maine Geological Survey Bulletin, **23**, 42-48.

Bourque, P.A., 1975, Lithostratigraphic framework and unified nomenclature for Silurian and basal Devonian rocks in eastern Gaspé Peninsula, Québec. Canadian Journal of Earth Sciences, **12**, 858-872.

Bourque, P.A., 1977, Silurian and basal Devonian of northeastern Gaspé Peninsula. Ministère de l'Energie et des Ressources du Québec, Etude spéciale ES-29, 232 p.

Bourque, P.A., and Lachambre, G., 1980, Stratigraphie du Silurien et du Dévonien basal du Sud de la Gaspésie. Ministère de l'Energie et des Ressources du Québec, Etude spéciale ES-30, 123 p.

Bourque, P.A., Amyot, G., Desrochers, A., Gignac, H., Gosselin, C., Lachambre, G., and Laliberté, J.Y., 1986, Silurian and Lower Devonian reef and carbonate complexes of the Gaspé Basin, Québec - A summary. Bulletin of Canadian Petroleum Geology, **34**, 452-489.

Bourque, P.A., Gosselin, C., Kirkwood, D., Malo, M., and St-Julien, P., 1993, Le Silurien du segment appalachien Gaspésie-Matapédia-Témiscouata, Québec: Stratigraphie, géologie structurale et paléogéographie, Ministère de l'Énergie et des Ressources du Québec, Rapport final MB 93-25, 115 p.

Bourque, P.A., Brisebois, D., and Malo, M., 1995, Gaspé Belt, *in* Williams, H., ed., Geology of the Appalachian/Caledonian Orogen in Canada and Greenland: Geological Survey of Canada, Geology of Canada, v. 6, *also* Geological Society of America, The Geology of North America, **F-1**, 316-351.

Bourque, P.A., Malo, M., and Kirkwood, D., (Submitted, 1996), Sea-level changes, paleogeography and tectono-sedimentary history at margin of Laurentia during Silurian-Early Devonian time: the Gaspé Belt, Québec. Geological Society of America Bulletin.

Bradley D.C., 1983, Tectonics of the Acadian orogeny in New England and adjacent Canada: Journal of Geology, **91** 381-400.

Brisebois, D, Lachambre, G., and Piché, G., 1991. Carte géologique, Péninsule de la Gaspésie, Carte 2146. Ministère de l'Énergie et des Ressources du Québec, DV 91-21.

Camiré, G.E., 1995. Development of inverted metamorphic gradient in the internal domain of the Taconian belt, Gaspé Peninsula. Canadian Journal of Earth Sciences, **32**, 37-51.

Camiré, G.E., Malo, M., and Tremblay, A., 1993a, Étude structurale et métamorphique du Groupe de Shickshock, Gaspésie septentrionale, Québec. Commission géologique du Canada, Étude 93-1D, 155-160.

Camiré, G., La Flèche, M.R., and Malo, M., 1993b, Géochimie des roches volcaniques cambro-ordoviciennes du Groupe de Shickshock: incidences sur la stratigraphie et le contexte géotectonique de la Gapésie septentrionale. Commission géologique du Canada, Étude 93-1E, 281-290.

Camiré, G., La Flèche, M.R., and Jenner, G.A., 1995, Geochemistry of pre-Taconian mafic volcanism in the Humber Zone of the northern Appalachians, Québec, Canada. Chemical Geology, **119**, 55-77.

Cant, D.J., and Walker, R.G., 1976, Development of a braided-fluvial facies model for the Devonian Battery Point Sandstone, Québec. Canadian Journal of Earth Sciences, **13**, 102-119.

Carbonneau, C., 1959, Région de Richard-Gravier, Péninsule de Gaspé. Ministère des Richesses Naturelles du Québec, Rapport Géologique 90, 75 p.

Carrara, A., and Fyson, W.F., 1973. Taconian and Acadian folds in northern and western Gaspé Peninsula, Québec. Canadian Journal of Earth Sciences, **10**, 498-509.

Carmignani, L., and Kligfield, R., 1990, Crustal extension in the northern Apennines: the transition from compression to extension in the Alpi Apuane complex. Tectonics, **9**, 1275-1303.

Cawood, P.A., 1993, Acadian Orogeny in West Newfoundland, *in* Roy, D.C. and Skehan, S.J., eds., The Acadian Orogeny: Recent Studies in New England, Maritime Canada, and the Autochtonous Foreland: Geological Society of America, Special Paper 275, 135-152.

Chen, L.Z., 1994, Étude métallogéniquede la minéralisation aurifère associée à la faille de Sainte-Florence, vallée de Matapédia, Gaspésie, Canada. M.Sc. memoir, Sainte-Foy (Québec), Canada, Institut national de la recherche scientifique, Université du Québec, 83 p.

Cousineau, P.A., 1990, Le Groupe de Caldwell et le domaine océanique entre St-Joseph-de-Beauce et Ste-Sabine. Ministère de l'Énergie et des Ressources du Québec, MM 87-02, 165 p.

Cousineau, P.A., 1991, The Rivière des Plante ophiolitic Mélange: Tectonic setting and mélange formation in the Québec Appalachians. Journal of Geology, **99**, 81-96.

Cousineau, P, and Tremblay, A., 1993, Acadian deformations in the southwestern Québec Appalachians, *in* Roy, D.C. and Skehan, S.J., eds., The Acadian Orogeny: Recent Studies in New England, Maritime Canada, and the Autochtonous Foreland. Geological Society of America, Special Paper 275, 85-99.

Dalton, E., 1987, Sedimentary facies and diagenesis of the Lower Devonian Temiscouata and Fortin Formations, Northern Appalachians, Québec and New Brunswick. M.Sc. thesis, Montréal, McGill University, 228 p.

David, J., 1994, Évolution géologique du segment nord de l'orogène appalachien à la transition des épisodes de déformation Taconien et Acadien: Exemples des régions de Témiscouata-Rimouski, Québec, et de Woodstock, Nouveau-Brunswick.Ph.D. thesis, Université de Montréal, Montréal.

De Broucker, G., 1987, Stratigraphie, pétrographie et structure de la boutonnière de Maquereau-Mictaw (Région de Port-Daniel, Gaspésie). Ministère de l'Énergie et des Ressources du Québec, Mémoire MM 86-03, 160 p.

Desjardins, C., Paradis, S., and Tremblay, A., 1994, Petrological and geochemical characteristics of volcanic rocks of the Frontenac and clinton formations, southern Québec Appalachians. Geological Society of America, Abstracts with programs, **26**, 14-15.

de Roo, J.A., and van Staal, C.R., 1994, Transpression and recumbent folding: Steep belts and flat belts in the Appalachian Central Mobile Belt of northern New Brunswick, Canada. Geological Sociery of Amerca Bulletin, **106**, 541-552.

Dewey, J.F., 1988, Extensional collapse of orogens. Tectonics, **7**, 1123-1139.

Dickinson, W.R., and Suczeck, C.A., 1979, Plate tectonics and sandstone composition. American Association of Petroleum Geologists Bulletin, **63**, 2164-2182.

Dineley D.L., and Williams B.P.J., 1968. The Devonian continental rocks of the lower Restigouche River, Québec. Canadian Journal of Earth Sciences, **5**, 945-953.

Dostal, J.R., Laurent, R., and Keppie, J.D., 1993, Late Silurian-early-Devonian rifting during dextral transpression in the southern Gaspé Peninsula (Québec): petrogenesis of volcanic rocks. Canadian Journal of Earth Sciences, **30**, 2283-2294.

Doyon, M., 1992. Géochimie et environnement tectono-stratigraphique des roches volcaniques du centre nord de la Gaspésie, Québec. Ph.D. thesis, Université de Montréal, Montréal, Canada, 254 p.

Doyon, M., and Dalpé, C., 1993, Roches magmatiques Silurian-Dévoniennes de la Gaspésie. Ministère de l'Énergie et des Ressources du Québec, Rapport final MB 93-16, 128 p.

Dunning, G.R., O'Brien, S.J., Colman-Sadd, S.P., Blackwood, R.F., Dickson, W.L., O'Neill, P.P., and Krogh, T.E., 1990, Silurian orogeny in the Newfoundland Appalachians. Journal of Geology, **98**, 895-913.

Faure, S., 1995, Reconstitution des paléocontraintes tectoniques dans les Basses-Terres du Saint-Laurent et les Appalaches du Québec et du nord du Nouveau-Brunswick. Ph.D. thesis, INRS-Géoressources, Université du Québec, Sainte-Foy, 259 p.

Gagnon, Y.D., and Jamieson, R.A., 1986. Étude de la semelle métamorphique du complexe du Mont Albert, Gaspésie, Québec. Commission géologique du Canada, Étude 86-1B, 1-10.

Gauthier, L., 1986, Analyse stratigraphique et structurale de l'anticlinorium d'Aroostook-Percé, au nord de Port-Daniel. M.Sc. memoir, Université de Montréal, Montréal, 89 p.

Hall, J., 1859. Description and figures of organic remains of the lower Helderberg Group and the Oriskany Sandstone. New York Geological Survey, Natural History of New York, pt. 6, Paleontology, **3**, 532 p.

Hesse, R., and Dalton, E., 1989, The Devonian Fortin Formation, *in* Bourque, P.A., Hesse, R., and Rust, B., eds., Sedimentology, paleoenvironments and paleogeography of the Taconian to Acadian rock sequence of Gaspé Peninsula. Geological Association of Canada, Guidebook to Field Trip B8, 57-69.

Hesse, R., and Dalton, E., 1991, Diagenetic and low-grade metamorphism terranes of the Gaspé Peninsula related to the geological structure of the Taconian and Acadian orogenic belts, Québec Appalachians. Journal of Metamorphic Geology, **9**, 775-790.

Héroux, Y., Bertrand, R., Achab, A., and Chagnon, A., 1983, Évolution thermique de l'extrémité orientale de la péninsule de Gaspé, en relation avec les déformations tectoniques. Ministère de l'Énergie et des Ressources du Québec, DP 83-23, 85 p.

Hibbard, J.P., 1994, Kinematics of Acadian deformation in the Northern and Newfoundland Appalachians. Journal of Geology, **102**, 215-228.

Hibbard, J.P., Trzcienski, W.E., Jr., and St-Julien, 1995, Humber Zone internal, *in* Williams, H., ed., Geology of the Appalachian/Caledonian Orogen in Canada and Greenland. Geological Survey of Canada, Geology of Canada, v. 6, *also* Geological Society of America, The Geology of North America, **F-1**, 114-139.

Hiscott, R.N., 1978, Provenance study of deep-water sandstones, Tourelle Formation, Québec, and implications for initiation of the Taconic Orogeny. Canadian Journal of Earth Sciences, **15**, 1579-1597.

Hiscott, R.N., 1980, Depositional framework of sandy mid-fan complexes of Tourelle Formation, Ordovician, Québec. American Association of Petroleum Geologists Bulletin, **64**, 1052-1077.

Hiscott, R.N., Pickering, K.T., and Beeden, D.R., 1986. Progressive filling of a confined Middle Ordovician foreland basin associated with the Taconic Orogeny, Québec. *In* Homewood, P., and Allen, P.A., (eds.), Foreland Basins. International Association of Sedimentologists, Special publication 8, 309-325.

Howie, R.D., and Barss, M., 1975. Upper Paleozoic Rocks of the Atlantic provinces, Gulf of St. Lawrence and adjacent continental shelf. *In* W.J.M. Van der Linden and J.A. Wade, (eds.), Offshore Geology of Eastern Canada, Vol. 2, Regional Geology. Geological Survey of Canada, Paper 74-30, 2: 35-50.

Kay, M., 1951. North American Geosynclines. Geological Society of America Memoir 48, 143 p.

Keen, C.E., Keen, M.J., Nichols, B., Reid, I., Stockmal, G.S., Colman-Sadd, S.P., O'Brien, S.J., Miller, H ., Quinlan, G., Williams, H., and Wright, J., 1986, A deep seismic reflection profile across the northern Appalachians. Geology, **14**, 141-145.

Keppie, J.D., and Dostal, J., 1994, Late Silurian-Early Devonian transpressional rift origin of the Quebec Reentrant, northern Appalachians: Constraints from geochemistry of volcanic rocks. Tectonics, **13**, 1183-1189.

Kessler, L.G. II, Prave, A.R., Malo, M., and Bloechl, W.V., 1995, Mid-Upper Ordovician flysch deposition, northern Gaspé Peninsula, Québec: A synthesis with implications for foreland and successor basin evolution in the northern Appalachians orogen. In Cooper, J.D., Droser, M.L., and Finney, S.C., (eds.), Ordovician Odyssey: Short Papers for the Seventh International Symposium on the Ordovician System. Society for Sedimentary Geology (SEPM), Pacific Section, 7, 251-255.

Kirkwood, D., 1989, Géologie structurale de la région de Percé. Ministère de l'Energie et des Ressources du Québec, Etude ET 87-17, 42 p.

Kirkwood, D., 1993, Étude qualitative et quantitative de la déformation acadienne du bassin Silurian-Dévonien de la péninsule gaspésienne, Appalaches du nord. Ph.D. thesis, Université Laval, Québec, Canada, 178 p.

Kirkwood, D., 1994, Quantification de la déformation acadienne dans les roches du bassin siluro-dévonien de la péninsule gaspésienne. Association professionnelle des géologues et des géophysiciens du Québec, La Revue géologique du Québec, **1**, 24-27.

Kirkwood, D., 1995, Strain partioning and progressive deformation history of a transpressive belt, northern Appalachians. Tectonophysics, **231**, 15-35.

Kirkwood, D., and St-Julien, P., 1987. Analyse structurale du Siluro-Dévonien dans la vallée de la Matapédia. Ministère de l'Energie et des Ressources du Québec, Rapport intérimaire MB 87-33, 17 p.

Kirkwood, D., and Malo, M., 1993, Across strike geometry of the Grand Pabos fault zone: evidence for Devonian dextral transpression in the Québec Appalachians. Canadian Journal of Earth Sciences, **30**, 1363-1373.

Kirkwood, D., Malo, M., St-Julien, P., and Therrien, P., 1995. Vertical and fold-axis parallel extension within a slate belt in a transpressive setting, northern Appalachians. Journal of Structural Geology, **17**, 329-343.

Ko, J., 1985, Controls on greywacke petrology in Middle Ordovician Cloridorme Formation: tectonic settings of source provenance areas versus diagenesis. M.Sc. thesis, McGill University, Montréal, 236 p.

Lachambre, G., 1987, Le Silurien et le Dévonien basal du Nord de la Gaspésie. Ministère de l'Energie et des Ressources du Québec, Etude ET 84-06, 83 p.

Lachance, S., 1979, Géologie de la région de Saint-André-de-Ristigouche. Ministère des Richesses Naturelles du Québec, Rapport intérimaire DPV-667, 19 p.

Laurent, R., and Bélanger, J., 1984, Geochemistry of Silurian-Devonian alkaline basalt suites from the Gaspé Peninsula, Québec Appalachians. Maritime Sediments and Atlantic Geology; **20**, 67-78.

Lavoie, D., 1992, Carbonate sedimentation in an extensional tectonic regime: The Lower Devonian Upper Gaspé Limestones, Québec Appalachians. Canadian Journal of Earth Sciences, **29**, 118-128.

Lavoie, D., and Bourque, P.A., 1992. Stratigraphy, paleoenvironmental evolution and regional significance of the Silurian Lake Aylmer-Lake Saint-François belt, Eastern Townships, Québec. Atlantic Geology, **28**, 243-255.

Lebel, D., 1985, Analyse structurale de la déformation acadienne, principalement la faille de Shickshock Sud dans la région de Rimouski-Matapédia. M.Sc. memoir, Université de Montréal, Montréal, Canada, 130 p.

Lespérance, P.J., 1980a, Calcaires Supérieurs de Gaspé. Les aires-types et le prolongement vers l'ouest. Ministère de l'Energie et des Ressources du Québec, Rapport intérimaire DPV-595, 92 p.

Lespérance, P.J., 1980b, Les Calcaires Supérieurs de Gaspé (Dévonien Inférieur) dans le nord-est de la Gaspésie. Ministère de l'Energie et des Ressources du Québec, Rapport intérimaire DPV-751, 35 p.

Lin, S., van Staal, C.R., and Dubé, B., 1994, Promontory-promontory collision in the Canadian Appalachians. Geology, **22**, 897-900.

Lux, D.R., 1986, 40AR/39AR ages for minerals from the amphibolite dynamothermal aureole, Mont Albert, Gaspé, Québec. Canadian Journal of Earth Sciences, **23**, 21-26.

Malavieille, J., 1987, Kinematics of compressional and extensional ductile shearing deformation in a metamorphic core complex of the northeastern Basin and Range. Journal of Structural Geology, **9**, 541-544.

Malo, M., 1986, Stratigraphie et structure de l'anticlinorium d'Aroostook-Percé en Gaspésie, Québec. Ph.D. thesis, Université de Montréal, Montréal, 280 p.

Malo, M., 1988a, Stratigraphy of the Aroostook-Percé Anticlinorium in the Gaspé Peninsula, Québec. Canadian Journal of Earth Sciences, **25**, 893-908.

Malo, M., 1988b, L'anticlinorium d'Aroostook-Percé de l'est de la Gaspésie. Ministère de l'Energie et des Ressources du Québec Etude ET 87-06, p.

Malo, M., and Béland, J., 1989, Acadian strike-slip tectonics in the Gaspé region, Québec Appalachians. Canadian Journal of Earth Sciences, **26**, 1764-1777.

Malo, M., Kirkwood D., De Broucker, G., and St-Julien, P., 1992, A reevaluation of the position of the Baie Verte - Brompton Line in the Quebec Appalachians: the influence of Middle Devonian strike-slip faulting in Gaspé Peninsula. Canadian Journal of Earth Sciences, **29**, 1265-1273.

Malo, M., and Bourque, P.A., 1993, Timing of the deformation events from Late Ordovician to mid-Devonian in the Gaspé Peninsula, *in* Roy, D.C. and Skehan, S.J., eds., The Acadian Orogeny: Recent Studies in New England, Maritime Canada, and the Autochtonous Foreland. Geological Society of America, Special Paper 275, 101-122.

Malo, M., Moritz, R., Chagnon, A., and Roy, F., 1993, Géologie et métallogénie du segment oriental de la faille du Grand Pabos, Gaspésie. Ministère de l'Énergie et des Ressources du Québec, Rapport final MB 93-55, 123 p.

Malo, M., Tremblay, A., Kirkwood, D., and Cousineau, P., 1995, Along-strike structural variations in the Quebec Appalachians: consequence of a collision along an irregular margin. Tectonics, **14**, 1327-1338.

Malo, M., and Kirkwood, D., 1996, Faulting and progressive strain history fo the Gaspé Peninsula in Post-Taconian time: A review, *in* Hibbard, J.P., van Staal, C.R, and Cawood, P.A., eds., Current Perspectives in the Appalachians-Caledonian Orogen. Geological Association of Canada, Special Paper 41, 267-282.

Marillier, F., Keen, C.E., Stockmal, G.S., Quinlan, G., Williams, H., Colman-Sadd, S.P., and O'Brien, S.J., 1989, Crustal structure and surface zonation of the Canadian Appalachians: implications of deep seismic data. Canadian Journal of Earth Sciences, **26**, 305-321.

McGerrigle, H.W., 1946, A revision of the Gaspé Devonian. Transaction Royal Society of Canada, 3th Ser., sec. IV, **XL**, 41-54.

McGerrigle, H.W., 1950, The geology of eastern Gaspé: Québec, Department of Mines, Geological Report 35, 168 p.

Naylor, R.S., Boone, G.M., Boudette, E.L., Ashende, D.D., and Robertson, P., 1973, Precambrian rocks in the Bronson Hill and Boundary Mountain anticlinoria. EOS, **54**, 495.

Osberg, P.H., Tull, J.F., Robinson, P., Hon, R., and Butler, J.R., 1989, The Acadian orogen, *in* Hatcher, R.D.Jr., Thomas, W.A. and Viele, G.W., eds., The Appalachian-Ouachita Orogen in the United States. Geological Society of America, The Geology of North America Volume F-2, 179-232.

Pavlides, L., Boucot, A.J., and Skidmore, W.B., 1968, Stratigraphic evidence for the Taconic Orogeny in the Northern Appalachians, *in* Zen, E-an, White, W.S., Hadley, J.B. and Thompson, J.B. Jr, eds., Studies of Appalachian geology: northern and maritime. Billing volume, 61-82.

Pinet, N., and Tremblay, A., 1995, Tectonic evolution of the Québec-Maine Appalachians: From oceanic spreading to obduction and collision in the Northern Appalachians. American Journal of Science, **295**, 173-200.

Platt, J.P., and Vissers, R.L.M., 1989, Extensional collapse of thickened continental lithosphere: A working hypothesis for the Alboran Sea and Gibraltar arc. Geology, **17**, 540-543.

Ramsay, J.G., 1967, Folding and fracturing of rocks. McGraw Hill, 568 p.
Rogers, J., 1970, The tectonics of the Appalachians. John Wiley and Sons, New York, 271 p.
Roksandic, M.M., and Granger, B., 1981, Structural styles of Anticosti Island, Gaspé Passage, and eastern Gaspé Peninsula inferred from reflection seismic data, *in* Lespérance, P.J., ed., Field meeting, Anticosti-Gaspé, 1981. Vol. II: Stratigraphy and paleontology: IUGS Subcommission on Silurian Stratigraphy and Ordovician-Silurian Boundary Working Group, Département de géologie, Université de Montréal, 211-221.
Rouillard, M., 1986, Les Calcaires Supérieurs de Gaspé (Dévonien inférieur), Gaspésie. Ministère de l'Energie et des Ressources du Québec, Rapport intérimaire MB 86-15, 94 p.
Roy, D.C., and Skehan, S.J., 1993, Preface, *in* Roy, D.C. and Skehan, S.J., eds., The Acadian Orogeny: Recent Studies in New England, Maritime Canada, and the Autochtonous Foreland. Geological Society of America, Special Paper 275, V-VI.
Rust, B.R., 1976, Stratigraphic relationships of the Malbaie Formation (Devonian), Gaspé, Québec. Canadian Journal of Earth Sciences, **13**, 1556-1559.
Rust, B.R., 1981, Alluvial deposits and tectonic style: Devonian and Carboniferous successions in Eastern Gaspé, *in* Miall, A.D., ed., Sedimentology and tectonics in alluvial basins. Geological Association of Canada, Special Paper **23**, 49-76.
Rust, B.R., 1982, Continental Devonian and Carboniferous sedimentation of eastern Gaspé Peninsula, *in* Hesse, R.E., Middleton, G.V. and Rust, B.R., eds., Paleozoic continental margin sedimentation in the Québec Appalachians. International Association of Sedimentologists, 11th International Congress, Hamilton, Ontario, Guidebook to field Excursion 7B, 107-125.
Rust, B.R., 1989, Proximal gravelly braidplain deposit of the La Garde Formation, Highway 132, Ristigouche, Stop 1.3, *in* Bourque, P.A., Hesse, R. and Rust, B., eds., Sedimentology, paleoenvironments and paleogeography of the Taconian to Acadian rock sequence of Gaspé Peninsula. Geological Association of Canada-Mineralogical Association of Canada, Guidebook to Field Trip B8, 75-77.
Sacks, P., and Malo, M., 1994, Taconian and Acadian transpressional faulting, Mont Albert and Mont Logan nappes and along the Shickshock sud fault, Gaspé Appalachians, Quebec [abstract]. Geological Society of America, Abstracts with programs, Annual Meeting 1994, Seattle, A196.
Sacks, P., and Malo, M., 1995, Kinematics and strain patterns of Acadian strike-slip deformation along the Shickshock Sud fault, Gaspé Appalachians, Québec, Canada. Geological Society of America, Annual Meeting, New Orleans, Abstracts with program, **27**, A221.
Sanderson, D.J., and Marchini, W.R.D., 1984, Transpression. Journal of Structural Geology, **8**, 449-458.
Schlische, R.W., 1995, Geometry and origin of fault-related folds in extensional settings. American Association of Petroleum Geologists Bulletin, **79**, 1661-1678.
Sikander, A.H., and Fyson, W.K., 1969. Structural development of the Paleozoic rocks of western Gaspé, Québec. Canadian Journal of Earth sciences, **6**, 1113-1127.
Simard, M, 1986, Géologie et évaluation du potentiel minéral de la région de Carleton. Ministère de l'Énergie et des Ressources du Québec, Étude ET 84-11, 27 p.

Simonetti, A., and Doig., R., 1990. U-Pb and Rb-Sr geochronology of Acadian plutonism in the Dunnage Zone of the southern Québec Appalachians. Canadian Journal of Earth Sciences, **27**, 881-892.

Slivitzky, A., and St-Julien, P., 1987, Compilation géologique de la région de l'Estrie-Beauce. Ministère de l'Énergie et des Ressources du Québec, MM 85-04, 40 p.

Slivitzky, A., St-Julien, P., and Lachambre, G., 1991, Synthèse géologique du Cambrian-Ordovicien du nord de la Gaspésie. Ministère de l'Énergie et des Ressources du Québec, Étude ET 88-14, 61 p.

Stanley, R.S., and Ratcliffe, N.M., 1985, Tectonic synthesis of the Taconian Orogeny in western New England. Geological Society of America Bulletin, **96**, 1227-1250.

St-Julien, P., and Hubert, C., 1975, Evolution of the Taconian Orogen in the Québec Appalachians. American Journal of Science, **275-A**, 337-362.

St-Julien, P., Slivitzky, A., and Feininger, T., 1983, A deep structural profile across the Appalachians of southern Québec Appalachians, *in* Hatcher, R.D.Jr., Williams, H., and Zietz, I., eds., Contributions to tectonics and geophysics of mountains chains. Geological Society of America, Memoir 158, 103-112.

St-Julien, P., Trzcienski, W.E., and Wilson, C., 1990, A structural, petrological and geochemical traverse of the Shickshock Terrane, Gaspésie, *in* Trzcienski, W.E., ed., Guidebook for field trips in La Gaspésie, Québec. New England Intercollegiate Geological Conference, 82nd annual meeting, Gîte du Mont Albert, Gaspésie, Québec, 248-285.

St-Julien, P., and Bourque, P.A., 1990, Rapport d'évaluation géologique et géophysique de la région de Malbaie-Fortin-York, Gaspésie (Permis 842-843-844). Ministère de l'Énergie et des Ressources du Québec, Rapport statutaire, permis 842-843-844, rapport 89TS842+, 46 p.

St. Peter, C.J., 1977, Geology of parts of Restigouche, Victoria and Madawaska Counties, Northwestern New Brunswick. Mineral Resources Branch, New Brunswick Department of Natural Resources Report of Investigation 17, 69 p.

Stockmal, G.S., Colman-Sadd, S.P., Keen, C.E., O'Brien, S.J., and Quinlan, G., 1987, Collision along an irregular margin: a regional plate tectonic interpretation of the Canadian Appalachians. Canadian Journal of Earth Sciences, **24**, 1098-1107.

Stockmal, G.S., Colman-Sadd, S.P., Keen, C.E., Marillier, F., O'Brien, S.J., and Quinlan, G., 1990, Deep seismic structure and plate tectonic evolution of the Canadian Appalachians. Tectonics, **9**, 45-62.

Stockmal, G.S., and Waldron, J.W.F., 1993, Structural and tectonic evolution of the Humber zone, western Newfoundland, 1. Implications of balanced cross sections through the Appalachian structural front, Port au Port peninsula. Tectonics, **12**, 1056-1075.

Théberge, R., 1979, Etude tectono-stratigraphique des roches ordoviciennes et siluriennes de l'anticlinorium d'Aroostook-Percé à Matapédia. M.Sc. memoir, Université de Montréal, Montréal, 63 p.

Thomas, W.A, 1977, Evolution of Appalachian-Ouachita salients and recesses from reentrants and promontories in the continental margin. American Journal of Science, **277**, 1233-1278.

Tremblay, A., St-Julien, P., and Labbé, J.Y., 1989, Mise à l'évidence et cinématique de la faille de La Guadeloupe, Appalaches du sud du Québec. Canadian Journal of Earth Sciences, **26**, 1932-1943.

Tremblay, A., and St-Julien, P., 1990. Structural style and evolution of a segment of the Dunnage Zone form the Québec Appalachians and its tectonic implications. Geological Society of America Bulletin, **102**, 1218-1229.

Tremblay, A., 1992, Tectonic and accretionary history of Taconian oceanic rocks of the Québec Appalachians. American Journal of Science, **292**, 229-252.

Tremblay, A., and Pinet, N., 1994, Distribution and characteristics of Taconian and Acadian deformation, southern Québec Appalachians. Geological Society of America Bulletin, **106**, 1172-1181.

Tremblay, A., Malo, M., and St-Julien, P., 1995, Dunnage Zone - Québec. Canadian Appalachians Region, *in* Williams, H., ed., Geology of the Appalachian/Caledonian Orogen in Canada and Greenland. Geological Survey of Canada, Geology of Canada, v. 6, *also* Geological Society of America, The Geology of North America, **F-1**, 179-197.

Trudel, C., and Malo, M., 1993. Analyse des contraintes par méthodes graphiques dans une zone de coulissage: exemple de la région de Matapédia, Gaspésie, Appalaches du Québec. Canadian Journal of Earth Sciences, **30**, 591-602.

van de Poll, H.W., 1995, Upper Paleozoic rocks: New Brunswick, Prince Edward Island, and Îles de la Madeleine, *in* Williams, H., ed., Geology of the Appalachian/Caledonian Orogen in Canada and Greenland. Geological Survey of Canada, Geology of Canada, v. 6, *also* Geological Society of America, The Geology of North America, **F-1**, 455-492.

van der Pluijm, B.A., and van Staal, C.R., 1988, Characteristics and evolution of the Central Mobile Belt, Canadian Appalachians. Journal of Geology, **96**, 535-548.

van der Voo, R., 1988, Paleozoic paleogeography of North America, Gondwana and intervening displaced terranes. Comparisons of paleomagnetism with paleo-climatology and biogeographical pattern. Geological Society of America Bulletin, **100**, 311-324.

van Staal, C.R., 1994, Brunswick subduction complex in the Canadian Appalachians: Record of the Late Ordovician to Late Silurian collision between Laurentia and the Gander margin of Avalon. Tectonics, **13**, 946-962.

van Staal, C.R., and de Roo, J.A., 1996, Post-Ordovician structural history of the Central Mobile Belt of the northern Appalachians: collision, Salinic uplift, extensional collapse and the Acadian orogeny, *in* Hibbard, J.P., van Staal, C.R, and Cawood, P.A., eds., Current Perspectives in the Appalachians-Caledonian Orogen. Geological Association of Canada, Special Paper 41, 367-390.

Vennat, G., 1979, Structure et stratigraphie de l'anticlinorium d'Aroostook-Percé dans la région de Saint-Omer - Carleton, Gaspésie, Appalaches du Québec. M.Sc. memoir, Université de Montréal, Montréal, 67 p.

Walker, R.G., and Cant, D.J., 1979, Facies model 3. Sandy fluvial systems, *in* Walker, R.G., ed., Facies models. Geoscience Canada Reprint Series 1, 23-31.

Whalen, J.B., 1993, Geology, petrography, and geochemistry of Appalachian granites in New Brunswick and Gaspésie. Geological Survey of Canada Bulletin 436, 124 p.

Wilcox, R.E., Harding, T.P., and Seeley, D.R., 1973. Basic wrench tectonics. Bulletin of American Association of Petroleum Geologists, **57**, 74-96.

Williams, B.P.J., and Dineley, D.L., 1966. Studies of the Devonian strata of Chaleurs Bay, Québec. Maritime Sediments, **2**, 7-10.

Williams, H., 1979, Appalachian Orogen in Canada. Canadian Journal of Earth Sciences, **16**, 792-807.

Williams, H., 1984. Miogeocline and suspect terranes of the Caledonian-Appalachian Orogen: tectonic patterns in the North-Atlantic region. Canadian Journal of Earth Sciences, **21**, 887-901.

Williams, H., 1993, Acadian Orogeny in Newfoundland, *in* Roy, D.C. and Skehan, S.J., eds., The Acadian Orogeny: Recent Studies in New England, Maritime Canada, and the Autochtonous Foreland. Geological Society of America, Special Paper 275, 123-134.

Williams, H., 1995, Temporal and spatial divisions. Chapter 2 *in* Geology of the Appalachian-Caledonian orogen in Canada and Greenland. *Edited by* H. Williams. Geological Survey of Canada, Geology of Canada, No. 6., 21-44 (also Geological Society of America, The Geology of North America, v. F-1).

Williams, H., and St-Julien, P., 1982, The Baie Verte-Brompton Line: an Early Paleozoic continent ocean interface in the Canadian Appalachians, *in* St-Julien, P., and Béland, J., eds., Major Structural Zones and Faults of the Northern Appalachians. Geological Association of Canada Special Paper 24, 177-208.

Williams, H., and Hatcher, R.D., Jr., 1982, Suspect terranes and accretionary history of the Appalachian orogen. Geology, 10: 530-536.

Williams H., and Hatcher, R.D., Jr., 1983, Appalachian suspect terranes, *in* Hatcher, R.D.Jr., Williams, H., and Zietz, I., eds., Contributions to tectonics and geophysics of mountains chains. Geological Society of America, Memoir 158, 33-53.

Wilson, J.T., 1966, Did the Atlantic close and then re-open? Nature, **211**, 676-681.

Withjack, M.O., Olson, J., and Peterson, E., 1990. Experimental models of extensional forced folds. American Association of Petroleum Geologists Bulletin, **74**, 1038-1054.

Zaitlin, B.A., and Rust, B.R., 1983. A spectrum of alluvial deposits in the Lower Carboniferous Bonaventure Formation of western Chaleurs Bay area, Gaspé and New Brunswick, Canada. Canadian Journal of Earth Sciences, **20**, 1098-1110.